An Experimental Study on Soil Water Characteristics and Hydraulic Conductivity of Compacted Soils

Faik Cuceoglu

Thesis submitted to the faculty of Virginia Polytechnic Institute and State University
in partial fulfillment of the requirements for the degree of

MASTER OF SCIENCE
in
CIVIL ENGINEERING

C. Guney Olgun, Chair
Theresa Wynn Thompson, Co-chair
Adrian Rodriguez-Marek

August 5, 2016
Blacksburg, Virginia

Keywords: compacted soils, unsaturated soil mechanics, soil-water characteristic curve, hydraulic conductivity function, transient analysis, hysteresis

An Experimental Study on Soil Water Characteristics and Hydraulic Conductivity of Compacted Soils

by Faik Cuceoglu

ABSTRACT

The importance of applying unsaturated soil mechanics concepts to geotechnical engineering design has been widely recognized. Soil water characteristic curve (SWCC) and hydraulic conductivity function (HCF) are vital soil properties that govern engineering behavior of unsaturated soils. In this study, a transient water release and imbibitions method (TRIM) is used to measure the SWCC and HCF under drying and wetting states, which accommodates integrated experimental and modeling techniques. The results of saturated hydraulic conductivity tests through flexible wall method are then used as input parameters for simulating experimental data. In general, the model provides a satisfactory fit to experimental data.

Soil water characteristic curves (SWCCs) and hydraulic conductivity functions (HCFs) are presented for a variety of soils that were prepared at different molding water contents and compactive efforts. The influences of dry density, molding water content, and hysteresis have been investigated. Dry density affects soil-water characteristic in terms of its air-entry value (AEV), rate of drying, and size of the hysteresis loop. The test results indicate that the SWCC and HCF obtained in terms of volumetric water content is more sensitive to the changes in dry density than molding water content. Based on cohesive soil results, some statistical relations are proposed to estimate wetting-path SWCC and HCF parameters from more easily measured drying curves. Changes in the van Genuchten's fitting parameters and residual volumetric water content are investigated for both drying and wetting conditions, with changes in the kaolin clay content.

An Experimental Study on Soil Water Characteristics and Hydraulic Conductivity of Compacted Soils

by Faik Cuceoglu

GENERAL AUDIENCE ABSTRACT

Traditional soil mechanics practice has experienced considerable changes during the past few decades. Within that period, the necessity of unsaturated soil mechanics has gradually emerged and become a part of geotechnical engineering practice. Soil water characteristic curve (SWCC) and hydraulic conductivity function (HCF) are very important properties in the assessment of unsaturated soil behaviors. A transient water release and imbibitions method (TRIM) is used to investigate unsaturated soil properties of a variety of test soils under laboratory conditions. TRIM integrates a testing program and a modeling technique to measure SWCC and HCF concurrently for both drying (water release upon matric suction increase) and wetting (water imbibition upon matric suction decrease) conditions.

Compaction, which is a classical application involving unsaturated soil, has the preferred practice for improving the mechanical and hydraulic properties of a soil. The structure and fabric of compacted material is very dependent on the compacted conditions, including compactive effort and molding water content. This paper evaluates the influence of such mentioned factors on the SWCC and HCF. The test results indicate that the SWCC and HCF obtained in terms of volumetric water content is more sensitive to the changes in compactive effort than molding water content. Hysteresis phenomena, the difference in the relationship between the water content of the soil and the corresponding water potential under drying and wetting path, is investigated. Based on cohesive soil results, some statistical relations are proposed to estimate wetting-path SWCC and HCF parameters from more easily measured drying curves.

ACKNOWLEDGMENTS

I would like to express my sincere appreciation to my advisor Dr. C. Guney Olgun for his ultimate support and invaluable guidance throughout my research. I also would like to present my deepest gratitude to my co-advisor Dr. Thompson and committee member Dr. Rodriguez-Marek for their contributions and feedback to this work.

I wish to greatly acknowledge the support of Turkish State Hydraulic Works, for the full scholarship funding. This scholarship provided me with the great opportunity to become a member of the Virginia Tech family and to expand my knowledge in geotechnical engineering by interacting with distinguished Virginia Tech faculty members.

I owe a special debt to Dr. Brandon for letting me work at the W. C. English Laboratory. After long working hours on my research project, I recognized the English laboratory as my second home in Blacksburg. Also, I feel that the English laboratory fueled me with a strong inspiration to establish my own geotechnical laboratory in the future.

Furthermore, I am indebted to my family and friends for their unconditional support and constant encouragement to pursue my interests. I took a great pleasure in writing this thesis. I hope all readers will enjoy and benefit from it.

TABLE OF CONTENTS

LIST OF FIGURES

LIST OF TABLES

1. INTRODUCTION

1.1. Background and Motivations

Unsaturated soil mechanics is a branch of traditional soil mechanics that takes into account the effects of the pore air phase when dealing with three general phenomena, specifically, permeability, shear strength and volume change. Soil-water characteristic curves (SWCCs) and hydraulic conductivity functions (HCFs) demonstrated an important relationship to each of the unsaturated soil properties (Croney and Coleman 1954). These properties are vital when coping with issues involving unsaturated soils. Many of the traditional geotechnical engineering concerns fall wholly or partially into the category of unsaturated soil mechanics. Geotechnical engineering applications involving unsaturated soils include waste containment systems (landfills), embankment dams, slope stability, surficial drainage system, roadway pavements, reinforced soil walls, foundations on expansive soils and so on. Constitutive relationships that utilize the concepts of unsaturated soils have been proposed for the particular areas of interest to geotechnical engineering. Moreover, the implementation into engineering practice has been rather slow. One of the main reason of this delay in the application of unsaturated soil mechanics stem from the long testing duration required for the determination of the SWCC in the laboratory, and also the specialized equipment and training needed.

Initially, the constitutive behavior focused on the study of seepage, shear strength, and volume change problems. The increased complexity of unsaturated soil behavior extended from the laboratory to theoretical formulations and solutions. The 1980s decade was a period when boundary value problems were solved using numerical models. With the advent of computing technology, the increased computer power was integrated with iteration process and numerical models (Thieu et al. 2001).

Many of the existing laboratory techniques aim to measure either SWCC or HCF determination under a limited suction or water content range. In addition to that, they more often are able to measure SWCC only under drying conditions. This is a challenge for measuring wetting process and HCF under laboratory conditions. For example; instantaneous profiles methods usually requires extensive time, and the use of additional sensors and their instrumentations is impractical in

undisturbed soils. Several researchers have proposed techniques to predict or estimate the key parameters of SWCC for a variety of soils through conventional laboratory tests such as grain-size distribution (GSD), void ratio, and Atterberg limits (Tinjum et al. 1997; Vanapalli et al. 1999; Fredlund et al. 2002; Marinho 2005). The estimation techniques are attractive for practicing engineers as they reduce costs and duration associated with direct measurement of the SWCC, but still require a confirmation with laboratory or field tests.

Several experimental instruments under the axis translation technique were developed for measuring SWCC in a wide-range suction. The recent contribution to this technique was made by Wayllace and Lu (2012) with a Transient Release and Imbibitions Method (TRIM). TRIM integrates a systematic testing program and a modeling technique to measure SWCC and HCF concurrently. Compared to the previous experimental methods, TRIM presents many advantages, for example; simple and fast measurement of SWCC under drying and wetting conditions, applicability on remolded and undisturbed samples, and a robust inverse modeling algorithm. Taking into account the recent publications affiliated with TRIM, the validity, application and repeatability of this method have been verified by only a few researchers.

Compaction, which is a classical application involving unsaturated soils, has been a routine practice for improving the mechanical and hydraulic properties of soils since far before the formation of civil engineering. Compacted soil comprising of many earthworks constructed all over the world is most appropriately considered as an unsaturated soils framework. An understanding of the effects of compaction on soil fabric and structure is the key when investigating compacted fine-grained materials. Materials compacted at dry of optimum water content exhibit flocculated structures, whereas materials compacted at wet of optimum have dispersed structures (Holtz and Kovacs 1981). The preliminary experimental results point out that the distinguishing features of SWCC depend on several factors, including soil structure, molding water content, void ratio, dry density, type of soil, texture, mineralogy, specific surface, stress history, and method of compaction. The structure of compacted material is very dependent on the compaction conditions such as molding water content and compactive effort, which also directly influence the engineering properties of soil. However, there is still limited published data available to clarify the effect of those reasons on the SWCC and HCF.

1.2. Research Objectives

The motivation for this research emerges from the premises outlined above. This study forms part of an integrated experimental program that paves the way for further research. The main objective of performing this research is to investigate the effects of dry density or relative compaction and molding water content and kaolin clay content on the SWCC and HCF.

The specific objectives of this study are to:

- Review the terminology and basic concepts governing the hydraulic behavior of unsaturated soils.
- Review the experimental techniques that have been used to determine hydraulic properties of unsaturated soils.
- Review the SWCC and HCF models that have been proposed, and compare their strengths and weaknesses.
- Perform some preliminarily laboratory tests to determine the engineering properties of test materials.
- Prepare a schedule for each tested soil, in which specimens will be compacted at a targeted dry density and molding water content.
- Perform TRIM tests and saturated hydraulic conductivity tests through flexible wall method in the laboratory.
- Analyze the TRIM test data and determine SWCC and HCF using HYDRUS-1D finite element package during drying and wetting conditions.
- Investigate the influence of dry density and molding water content on the features of SWCC and HCF such as air-entry value and residual water content.
- Plot hysteretic SWCCs and HCFs along an initial drying path followed by a main wetting path.
- Determine which factors control the hysteresis on these curves and suggest some simple ratios based on test results.
- Investigate the influence of kaolin clay effect on van Genuchten's fitting parameters and residual volumetric water contents.
- Examine the response of TRIM's applicability and validity over a variety of soil tests.
- Finally, make recommendations based on test results for further research.

2. LITERAURE REVIEW

2.1. Introduction

Considering the main objectives of this study, it is convenient to begin with a brief description and background of key concepts relating to unsaturated soil mechanics such as SWCC and HCF. Then, suction and hydraulic conductivity measurement methods will be described. In this section, the emphasis will be placed on axis translation technique and outflow methods, which are strongly related to the working principles of TRIM. The next section will be continued with a detailed description of suction and hydraulic conductivity models. Here, the emphasis will be given to commonly used prediction methods based on mathematical models for SWCC, and empirical and macroscopic models for HCF.

2.2. Soil Water Characteristic Curve

2.2.1. Soil Suction

Soil suction or soil water potential is one of the fundamental physical properties used to describe the mechanical behavior of unsaturated soils. In general, soil suction is defined as the measure of free energy or stress that attracts and holds water in the pores of an unsaturated soil mass. Soil suction is the general term which may refer to matric suction, osmotic suction, or total suction. Total soil suction is defined in terms of the free energy or the relative vapor pressure (relative humidity) of the soil moisture (Fredlund et al. 2012) . Total suction (ψ) is composed by two major components: matric suction ($u_a - u_w$) and osmotic suction (π).

$$\psi = (u_a - u_w) - \pi \tag{2.1}$$

where u_a is the pore-air pressure, and u_w is the pore-water pressure. Suction arising from the presence of dissolved ions in water is referred to as osmotic suction. The matric component of suction is associated with capillary phenomenon, texture, and surface adsorptive forces of soil. The capillary phenomenon is usually demonstrated by the rise of water level in a capillary tube. The water rises up in the tube due to both the surface tension in the contractile skin and the tendency of water to wet the surface of the glass tube. The capillary water has a negative pressure with respect to the

air pressure, which is generally atmospheric pressure (u_a=0). The pore pressure is sometimes highly negative at low degrees of saturation as a result of the absorptive forces between soil particles and water.

2.2.2. Fundamentals of Soil Water Characteristic Curve

The soil-water characteristic curve (SWCC) is very important for estimating the hydro-mechanical behavior of unsaturated soils such as volume change, shear strength, and hydraulic conductivity (Fredlund 2000). The SWCC defines the constitutive relationship between the matric suction, and the amount of water in the soil at equilibrium, which is represented by the gravimetric water content (w) or volumetric water content (θ) or the degree of saturation (S). Volumetric water content and degree of saturation is easily related to each other through the porosity of the soil (n):

$$\theta = S * n \tag{2.2}$$

Figure 2.1 shows an idealized soil-water characteristic curve with some of its key features, including air-entry value, residual water content, and the hysteresis between the drying and wetting curves. At zero suction, the volumetric water content is called the saturated volumetric water content (θ_s) and is representative of the total capacity of the soil pores. In a fully saturated state, the degree of saturation is equal to 1, thus the saturated volumetric water content is substituted with the porosity term.

The air-entry value (AEV) is the point at which air enters the pore space. The air-entry value represents the matric suction value needed to cause water to be drawn from the largest pore space within the soil. The residual water content (θ_r) is considered to be the water content at which an increasingly large suction change is required to remove additional water from the soil (Vanapalli et al. 1999). Under this condition, the pore-water is usually absorbed around the particles.

The SWCC has three stages that describes the process of desaturation of a soil with the increase of suction. These are outlined below starting with saturation conditions in the soil (Vanapalli 1994).

1. The boundary effect zone where the pore-water is in tension but soil remains saturated. This stage continues until the air-entry value, where the applied suction overcomes the capillary water forces in the soil.

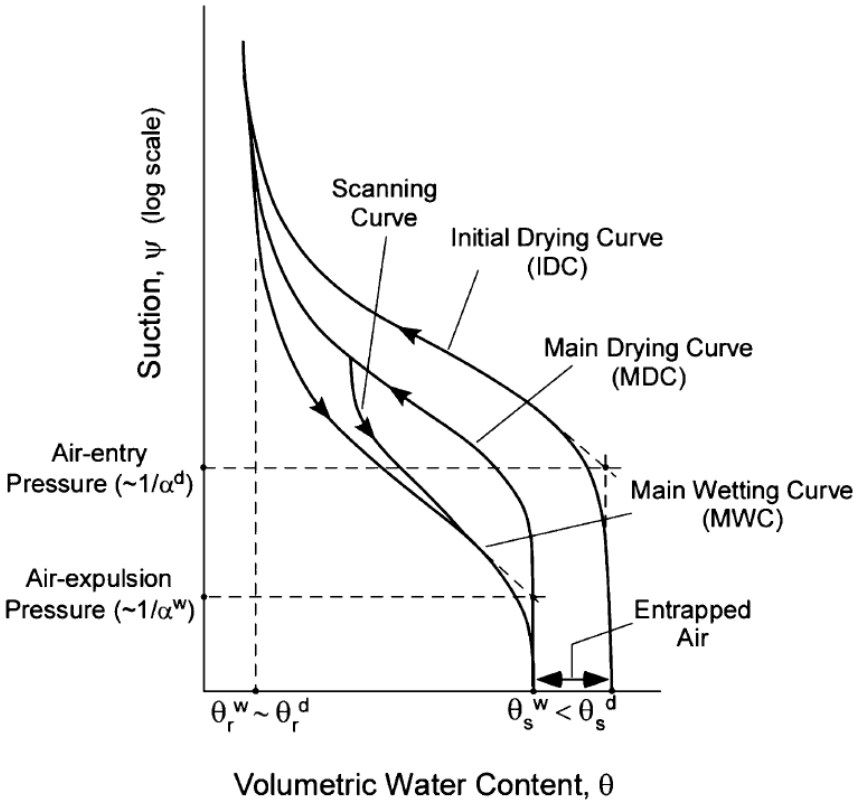

Figure 2.1. Schematic of typical SWCC after Likos et al. (2013)(with permission from ASCE)

2. The transition stage where the water within the pores is increasingly displaced from the soil by the suction rise. The stage starts with the air-entry value and ends with the residual water content.
3. The residual stage where the water is firmly absorbed by soil particles and flow occurs in the form of vapor. A very slow decrease in water content as suctions are highly increased.

2.2.3. Hysteresis in the Soil-Water Characteristic Curve

Hysteresis in soil is defined as the difference in the relationship between the water content of the soil and the corresponding water potential obtained under drying and wetting path. There is no unique equilibrium between water content and soil suction. Looking at the Figure 2.1, the drying curve always overlies the wetting curve and the ending point of the wetting curve differs from the initial saturation water content. The main drying and wetting curves are essentially the extremities of the SWCC for a given soil. The region between these main curves is called hysteresis loop, which

has infinite number of scanning curves inside of it. Numerous models describing soil water hysteresis have been developed. These models are either conceptual or empirical models. The conceptual models are based on domain theory of soil water hysteresis and assumes that each domain wets at a characteristic water pressure (or suction) and dries at a water pressure, regardless of the neighboring domains (Maqsoud et al. 2004). Empirical models are mainly related to the analysis of the shape and properties of SWCC.

Because of experimental difficulties inherent in measuring the wetting curve, usually only the drying portion of the curve is measured (Hillel 1980). Hysteresis introduces great difficulties in the application of SWCC in unsaturated soil mechanics. Hysteresis of SWCC is caused by the following reasons (Tindall et al. 1999):

- Geometric Pore Non-Uniformity: Variations in the geometric size and shapes of soil pores causes geometric hysteresis. Soil pores are generally irregular and connected to by narrow passageways of various sizes. This is also known as ink-bottle effect (Haines 1930).
- Contact Angle Effect: The contact angle and radius of curvature of the soil-water on the pore wall is greater in an advancing (wetting) meniscus than in a receding (drying) meniscus.
- Entrapped Air: The encapsulation of air in "dead-end" or "occluded" pores when the soil suction is increasing or decreasing. The presence of entrapped air reduces the water content of a newly wetted soil and accentuates the hysteresis effect.
- Shrinkage, Swelling, or Aging: These phenomena are able to result in differential changes of soil structure, accompanied by changes in pore space, depending on the wetting and drying history of the soil.

Although the exact roles and relative importance of the above factors remain unclear for a wide-range of soil types and water content regimes, the first factor has great importance in creating hysteresis.

2.3. Hydraulic Conductivity Function

2.3.1. Fundamentals of Hydraulic Conductivity Function

Permeability is a property of a soil that permits the transmission of fluids. This property is denoted by K, and is also called intrinsic permeability. K has units of length squared (m^2) and is dependent

only on pore-size, pore geometry and pore-size distribution. The permeability is related to the hydraulic conductivity (k) by the relation given in Equation 2.3:

$$k = \frac{\rho g}{\mu} K \tag{2.3}$$

where ρ is the fluid specific mass, g is the gravitational acceleration, μ is the dynamic viscosity.

The hydraulic conductivity of unsaturated soil is a function of material variables describing the pore structure (e.g., void ratio and porosity), the pore fluid properties (e.g., density and viscosity), and relative amount of pore fluid in the system (e.g., water content and degree of saturation). The hydraulic conductivity is typically described in terms of matric suction head $k(h_m)$, matric suction $k(\psi)$, degree of saturation $k(S)$, or volumetric water content $k(\theta)$. The air-filled pores are considered to be non-conductive channels to the flow of water. Therefore, the available pathways for water flow in an unsaturated soil decrease as the moisture content decreases. Figure 2.2 presents examples of typical $k(\theta)$ and $k(h_m)$ curves for relatively coarse, medium and fine textured soils. Notice that the coarse-grained materials (gravel, sand and geotextiles) have high hydraulic conductivity near saturation, while the fine-grained materials (silt and clay) have lower hydraulic conductivity. Also notice that the hydraulic conductivity decreases very significantly as the soil becomes unsaturated. Coarse-grained materials experience much more dramatic decrease than fine-grained materials because fine-grained materials can retain more water under high suctions. The residual water content is where the hydraulic conductivity asymptotically approaches zero.

2.3.2. Hysteresis in the Hydraulic Conductivity Function

Hydraulic conductivity function is directly related to SWCC so that hysteresis becomes evident when hydraulic conductivity is plotted as a function of matric suction or volumetric water content. As seen in Figure 2.3, hydraulic conductivity is generally greater along a drying curve than for the same magnitude of suction along the wetting curve. It is worthwhile to note that the $k(\psi)$ relationship displays a considerable hysteresis, therefore, it is favorable to use $k(\theta)$ as this relationship is less sensitive to hysteresis and in principle better adapted for solution of the unsaturated flow equation (Topp and Miller 1966). This observation is attributed to the fact that hydraulic conductivity is directly related to the volume fraction of pore space available for fluid flow (Lu and Likos 2004).

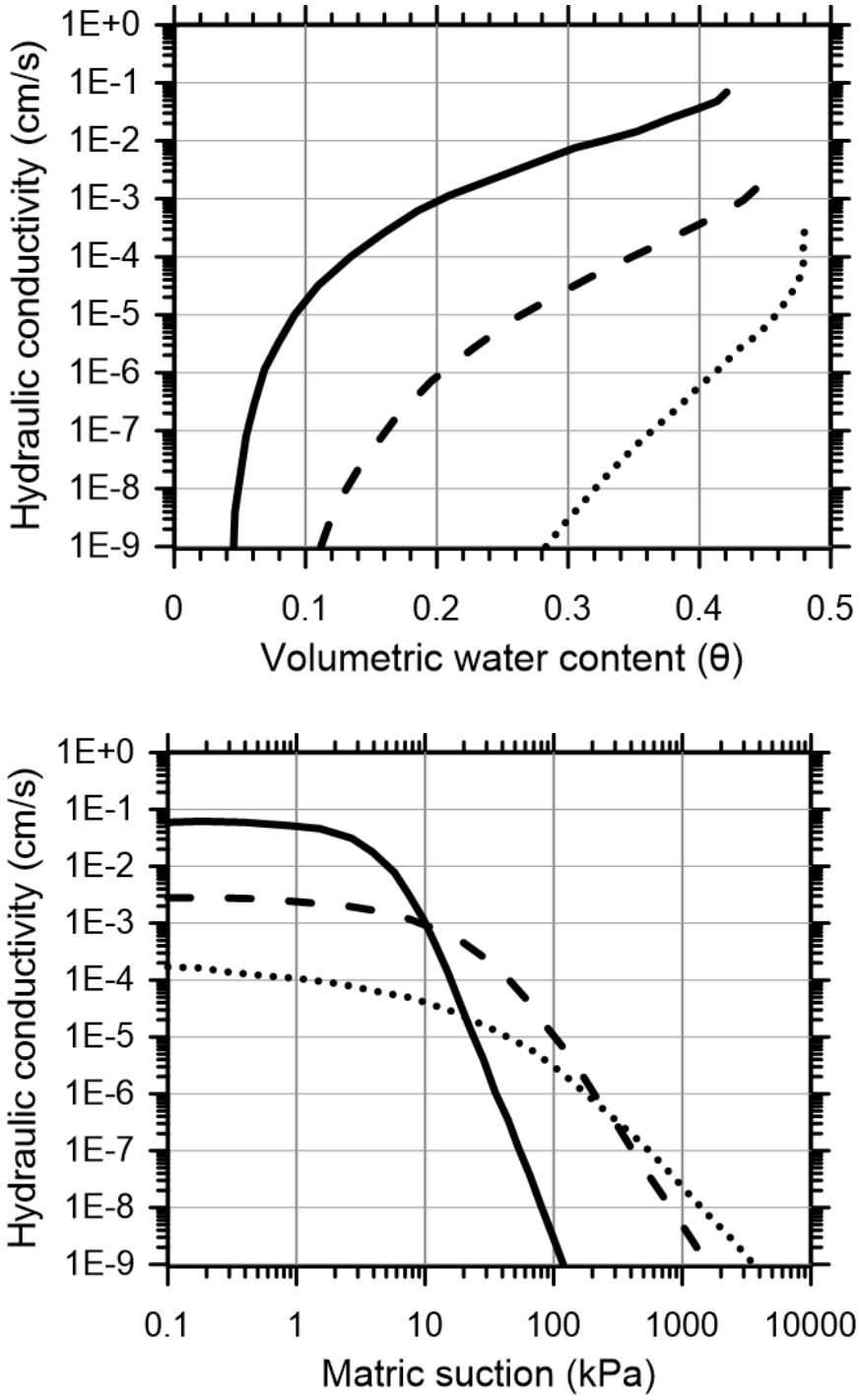

Figure 2.2. Typical curves of the hydraulic conductivity, as a function of the water content (above), and pressure head (below) for coarse- (solid line), medium- (dashed line), and fine-textured (dotted line) soils after van Genuchten and Pachepsky (2011)(with permission from Springer)

It is possible that the filled pores during drying might be different in size and shape than those that are filled during wetting, resulting in a different suction for the same moisture content upon drying and wetting.

The hydraulic conductivity of a saturated soil is important for the HCF. In practice, this is usually the only value that is experimentally obtained from the HCF, the rest of HCF is predicted by empirical, macroscopic and statistical models. These models will be discussed on the following pages.

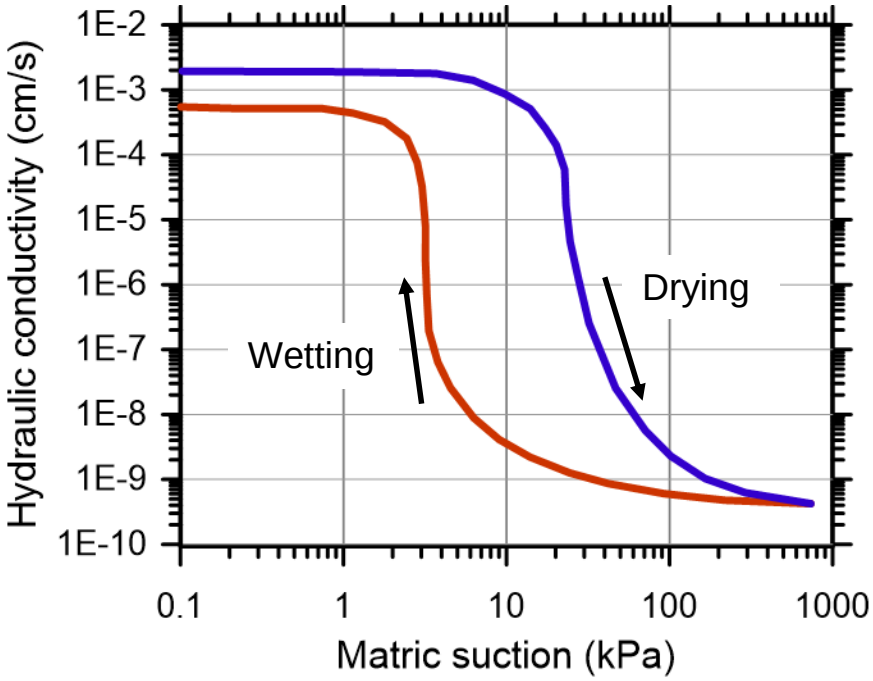

Figure 2.3. Hysteresis in HCF after Lu and Likos (2004)(with permission from John Wiley & Sons)

2.3. Suction Measurement Techniques

2.3.1. Overview of Suction Measurement Techniques

The determination of the soil-water characteristic curve becomes essential when dealing with unsaturated soils. Several laboratory and field measurement techniques are currently available. In terms of their measured suction component, approximate measurement range, applicability in laboratory or field, these techniques are summarized in Table 2.1. A brief description of some of the common methods is presented in the following sections.

Table 2.1. A summary of soil suction measurement techniques after Lu and Likos (2004)(with permission from John Wiley & Sons)

Suction Component Measured	Technique/Sensor	Approximate Suction Range (kPa)	Laboratory/Field	References
Matric Suction	Tensiometers	0-100	Laboratory and field	Cassel and Klute (1986); Stannard (1992)
	Axis translation techniques	0-1,500	Laboratory	Hilf (1956); Bocking and Fredlund (1980); Wayllace and Lu (2012)
	Electrical/thermal conductivity sensors	0-400	Laboratory and field	Johnston (1942); (Phene et al. (1971a); Phene et al. (1971b)) ; Fredlund and Wong (1989)
	Contact filter paper method	Entire range	Laboratory and field	El-Ehwany and Houston (1990); Houston et al. (1994)
Total Suction	Thermocouple	100-8,000	Laboratory and field	Spanner (1951)
	Chilled-mirror hygrometers	1,000-450,000	Laboratory	Gee et al. (1992); Wiederhold (1997)
	Resistance/capacitance sensors	Entire range	Laboratory	Wiederhold (1997); Albrecht et al. (2003)
	Isopiestic humidity control	4,000-400,000	Laboratory	Young (1967)
	Two-pressure humidity control	10,000-600,000	Laboratory	(Likos and Lu (2001); Lu and Likos (2003))
	Non-contact filter paper method	1,000-500,000	Laboratory and field	Fawcett and Collis-George (1967); McQueen and Miller (1974); Houston et al. (1994); Likos and Lu (2002)

2.3.2. Tensiometers

A tensiometer measures the negative pore-water pressures in a soil. The tensiometer, introduced by Richards and Gardner (1936), has experienced many modification for specific purposes. As illustrated in Figure 2.4, a tensiometer basically consists of a high-air entry, porous ceramic cup connected to a pressure sensor by a water-filled conduit. The porous cup is inserted into the unsaturated soil, then the soil sucks the water along the cup wall until equilibrium is achieved between the soil and the water tension inside the cup. At that time, the negative pressure is read. Due to the cavitation of the water in the tensiometer tube, the pore-water pressure is measured effectively until negative 100 kPa is reached (Stannard 1986; Take and Bolton 2003). Tensiometers are recognized as the best measuring method for the low-range of suction.

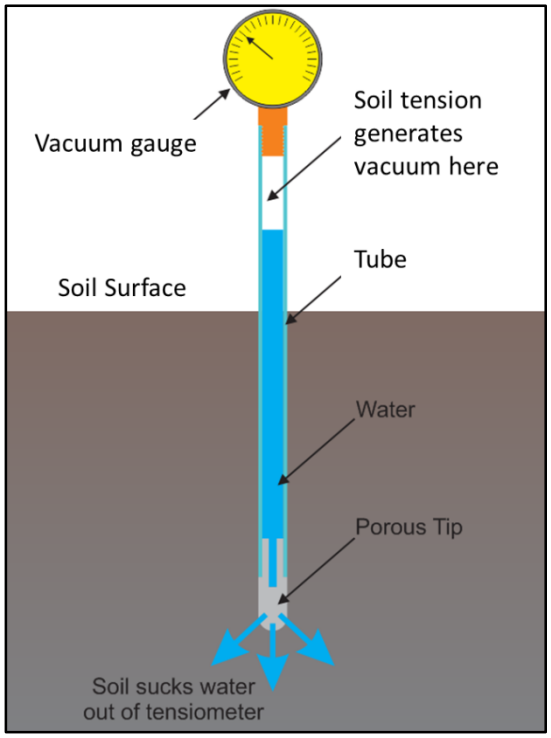

Figure 2.4. A tensiometer example

2.3.3. Axis Translation Techniques

Hilf (1956), the father of axis translation techniques, demonstrated that pore-water pressure increases if the ambient pressure is increased. Axis translation technique is commonly used to measure the matric suction of undisturbed and remolded soil samples. Axis translation is achieved by separating the air and water phases through the pores of a saturated high air-entry material

(HAE) (Bocking and Fredlund 1980). This is a useful laboratory technique that measures testing specimens with suction values that are greater than 100 kPa without any problems associated with cavitation. The air-entry value of the disk must be higher than the matric suction to be measured. With the availability of high air-entry disks, with maximum air-entry values up to 1500 kPa, suction measurement ranges of axis translation technique are extended to very high pressure limits (Fredlund and Rahardjo 1993).

2.3.3.1. Pressure Plates

By far the most common use of the translation technique is in the pressure plate apparatus. A soil sample is placed within the chamber onto a HAE plate that only permits the flow of water through the saturated pore spaces and prevents air passing up to the air-entry value (Lu and Likos 2004). The pressure plate technique is performed by increasing the soil matric suction in different steps and measuring the water content of soil sample at the end of each increment. Thus, the water content of each particular specimen provides a single point on the SWCC. It is recommended to repeat this process with as many specimens to obtain a better SWCC. Figure 2.5 illustrates a typical pressure plate apparatus.

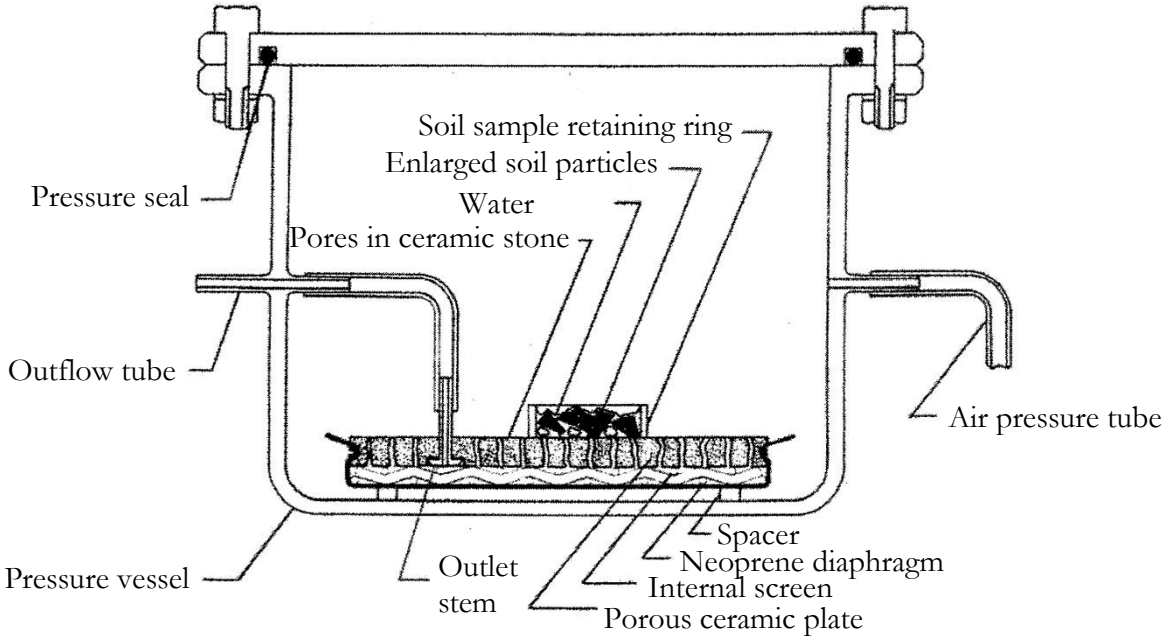

Figure 2.5. Schematic drawing of a typical pressure plate after Lu and Likos (2004)(with permission from John Wiley & Sons)

2.3.3.2. Tempe Pressure Cells

Tempe pressure cells are similar in concept and apparatus compared with the pressure plate systems. A known amount of fully-saturated soil specimen is placed in a cell and a series of increasing increments of air pressure is applied to the sample. The equilibrium water content is determined for each pressure increment, and the change in water content is determined by measuring the weight of the tempe pressure cell. After the highest desired value of air pressure is applied to the sample, the device is disassembled and the water content of the soil sample is determined. Based on this water content and the weights from previous measurements, the SWCC is constructed. Figure 2.6 shows the components of a tempe pressure cell.

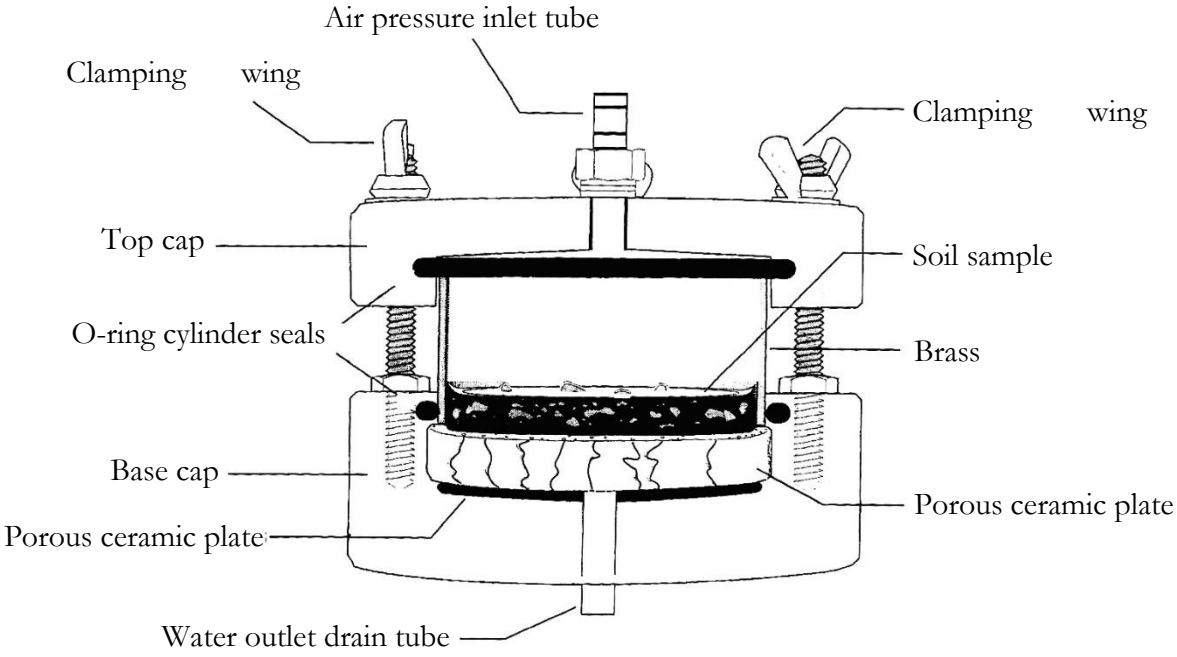

Figure 2.6. Schematic drawing of a typical Tempe cell pressure after Lu and Likos (2004)(with permission from John Wiley & Sons)

2.3.4. Filter Paper Techniques

This technique covers the measurement of the soil suction by filter paper, a method that is used in agriculture and soil science applications. Filter paper techniques offer significant advantages such as relative simplicity, low cost, and improved accuracy over other testing techniques (Likos and Lu 2002). Filter paper methods have been used and investigated by numerous researchers (Fawcett and

Collis-George 1967; Al-Khafaf and Hanks 1974; McQueen and Miller 1974; Hamblin 1981; Chandler and Gutierrez 1986; Houston et al. 1994; Swarbrick 1995).

The ASTM standard D5298 (2010) describes the calibration curve (a combination of both drying and wetting curves) and test procedures for the measurement of either matric suction through contact filter paper or total suction through non-contact. In contact filter paper method, the water content of an initially dry filter paper increases due to a flow of water transferred from soil to filter paper until both come into equilibrium. The matric suctions inferred from filter paper measurements depend on a calibration between the water content of the filter paper and suction. Houston et al. (1994) developed two different calibration curves, one for total suction and one for matric suction measurements. In addition, Bulut et al. (2001) reported an evaluation on both drying and wetting filter paper suction calibration. Figure 2.7 shows a general testing configuration for filter paper testing.

2.4. Hydraulic Conductivity Measurement Techniques

2.4.1. Overview of Hydraulic Conductivity Measurement Techniques

There are many different types of hydraulic conductivity tests that are suited for different types of soils, testing time scales, and laboratory or field setups. Laboratory tests are preferred because they are less expensive than field tests, and the hydraulic boundary and stress conditions are better controlled. However, field tests provide a more valuable data set, allowing to test larger masses of soil, and test the effects of soil fabric and stress conditions. All current hydraulic conductivity measurement techniques are categorized under two main approaches, including steady-state and transient methods. Steady-state techniques assume that the flux, gradient, and water content of the soil-water system are constant with time throughout the entire domain. Conversely, transient techniques consider the magnitude and direction of the flow changing with time. Both the hydraulic conductivity testing techniques and their application to unsaturated soils are described and summarized in Table 2.2.

2.4.2. Steady State Measurement Techniques

Steady-state methods rely on the validity of Darcy's law, which states that the coefficient of hydraulic conductivity is the ratio of the flow rate to the hydraulic gradient. Most of the steady-state methods used to measure unsaturated hydraulic conductivity are similar to those used for saturated

hydraulic conductivity. The constant-head method, constant-flow method and centrifuge method are described under this technique.

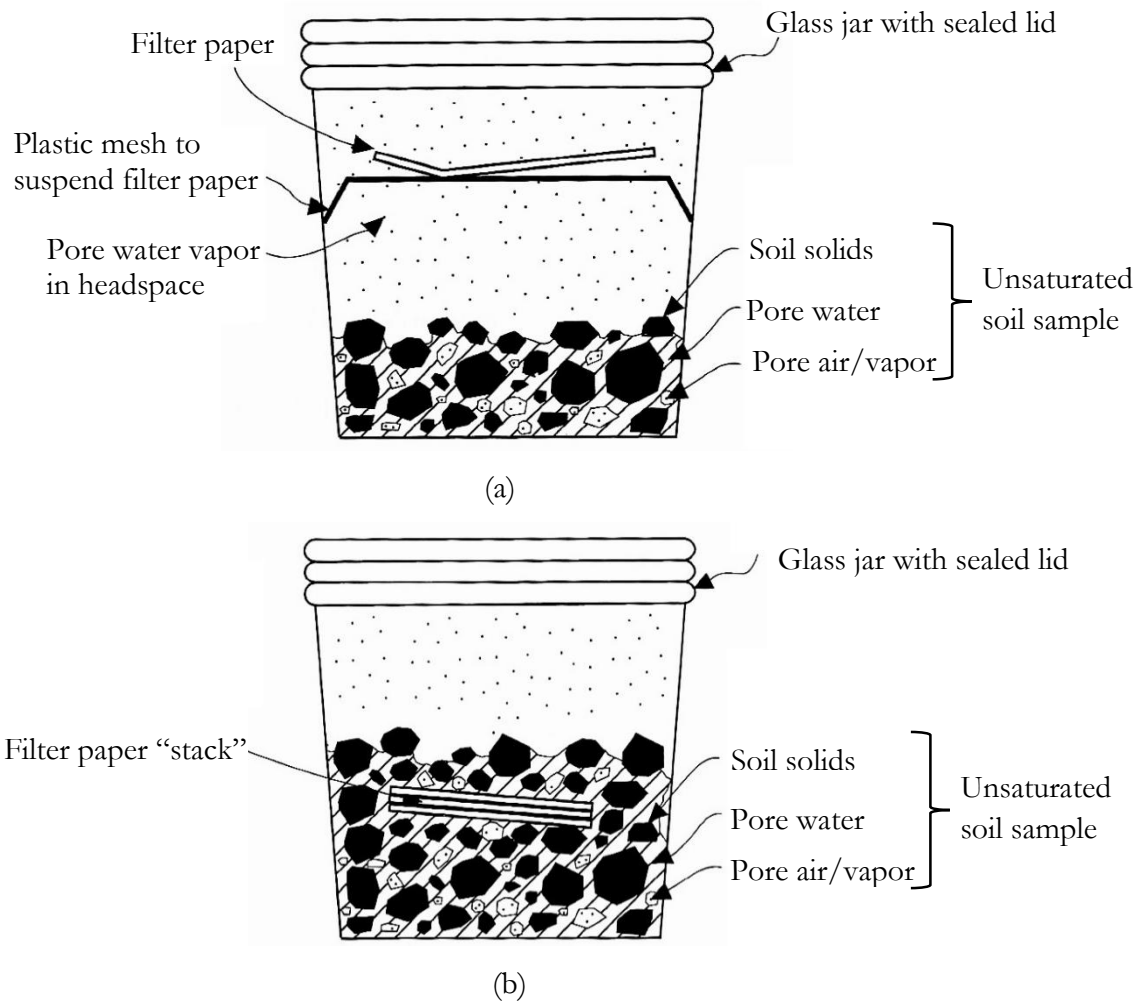

Figure 2.7. General testing configurations for filter paper testing: a) non-contact method, and b) contact method after Lu and Likos (2004)(with permission from John Wiley & Sons)

Table 2.2. Laboratory methods for measuring the HCF after Masrouri et al. (2009)(with permission from Springer)

Techniques	Test Methods	Advantages	Disadvantages	Relative Cost
Steady State (SS)	Constant Head	• Simplicity • Able to control stress state	• Costly, tedious and lengthy in low permeability materials	Low
	Constant Flow	• Simplicity • Able to control stress state • Faster and higher resolution than constant head • Yields SWCC and HCF	• Flow pump required	Moderate initial equipment cost
	Centrifuge	• Shor time for measuring low hydraulic conductivity	• Centrifuge required	High initial equipment cost
Transient	Outflow	• Faster than steady state • Good control on mass • Simplicity	• Few reliable and favorable comparisons with other methods	Low
	Instantaneous profile	• Simplicity • Yields HCF and SWCC • Good for clays (30%-90% saturation) and sands (<50% saturation)	• Poor mass control • No control on stress state • Possibility of errors when fully saturation is approached	Moderate to high initial equipment cost

2.4.2.1. Constant-Head Method

This is one of the oldest and most common laboratory techniques, which is a direct application of Darcy's law under steady-state flow conditions (Corey 1957). A constant head of water at a constant pressure is maintained across the vertical soil column when the ends are fitted with high air-entry disks. Matric suction is applied, and the flow rate is measured during testing. When the flow process reaches a steady-state condition, the hydraulic conductivity is calculated for that particular imposed suction value. This test needs to be repeated under different suction values to obtain a HCF curve. One of the key differences between unsaturated and saturated hydraulic conductivity measurement apparatuses is the porous plates at the ends, which maintain matric suction during testing (Benson and Gribb 1997). This testing is mostly used for coarse-grained soils and longer testing times are required. A number of modified experimental systems under constant-head testing technique have been introduced (Corey 1957; Barden and Pavlakis 1971; Klute 1972; Klute and Dirksen 1986; Huang et al. 1998b).

2.4.2.2. Constant-Flow Method

The constant-flow is a laboratory testing technique that has been used in the past to measure the hydraulic conductivity of saturated or unsaturated soils (Olsen et al. 1991). Instead of applying a constant-head on one end of a specimen, a constant flow is either pumped into or withdrawn from a soil specimen at a controlled rate using a multispeed syringe pump and measuring the pressure difference induced across the specimen with a differential pressure transducer (DPT). This procedure eliminates the errors in conventional techniques, the difficulties in measuring extremely low flow rates, and the necessity to apply excessive gradients (Olsen et al. 1988; Lu et al. 2006). Flow rates ranging from 10^{-7} to 10^{-1} cm^3/s are obtained with flow pumps which makes this method suitable for all types of soils (Olsen et al. 1994). For determination of unsaturated hydraulic conductivity, positive air pressure is applied from the top cap and a known volume of water is withdrawn from the sample through the base cap. Once a steady-state condition is achieved, the corresponding matric suction is recorded from the transducer and then the water content of specimen is calculated relative to the initially saturated condition. The testing procedure continues by incrementally decreasing the water volume of the specimen. At each water content increment, matric suction and hydraulic conductivity are determined in order to establish SWCC and HCF.

2.4.2.3. Centrifuge Method

The combination of centrifugal force and steady flow provides a great opportunity for the measurement of saturated and unsaturated hydraulic properties (Nimmo et al. 1987; Nimmo and Akstin 1988; Caputo and Nimmo 2005). This is a relatively recent laboratory technique that rapidly establishes a steady-state flow condition in a soil specimen spinning in a centrifuge. Steady-state conditions require a constant flow rate and a constant centrifugal force to keep both the water content and the water flux (q) constant (Nimmo et al. 2002). At sufficiently high rotational speeds, the gradients due to matric potential are negligible compared to those imposed by the rotation. Under this circumstance, the water flow through the sample is governed by two driving gradients: (1) the suction gradient acting through the sample, and (2) the centrifugal gravity gradient. Once the steady-state conditions are satisfied, hydraulic conductivity is computed using a form of Darcy's equation (2.4) which takes into account both suction and centrifugal forces.

$$q = k(\psi)\rho_w \omega^2 r \tag{2.4}$$

where ρ_w is the density of water, ω is the rotation speed, and r is the radius from the axis of rotation. This method permits the association of the water content of sample and suction values with the measured hydraulic conductivity. Repeated measurements with different centrifugal speeds give additional data points needed to define the HCF. The method works well when testing dense specimens with a pore structure insensitive under stress conditions.

2.4.3. Transient Measurement Techniques

In pursuit of obtaining useful unsaturated hydraulic conductivity data in a short span of time, a variety of transient methods have been proposed. They are rapid compared to the steady-state methods and provide better mass control. Transient techniques rely on solving the governing transient fluid flow equation in one-dimension under controlled initial and boundary conditions from measurement of flux or water content profiles at known locations and times. The governing equation for transient water flow in soil is derived by applying the principle of mass conservation. The principle states that for a given elemental volume of soil, the rate of water gain or loss is conservative and is equal to the net flux in or out of the element. The majority of transient techniques and associated analysis models assume that the soil matrix does not undergo a significant deformation with the changes in matric suction or water content. Laboratory and field instantaneous

profile methods, outflow methods, the Bruce-Klute method, ultracentrifuge, and thermal method are recognized as transient techniques. Outflow methods underpin this research study, and hence only outflow methods will be discussed herein.

2.4.3.1. Outflow Methods

Outflow methods are widely used laboratory techniques that concurrently measure HCF and SWCC. The procedure is typically conducted in an apparatus using a conventional axis translation technique such as pressure plate and tempe pressure cells. The underlying principle is to force water out of a soil under a single or a series of pressure increments, and determine hydraulic diffusivity by recording water outflow over time. The outflow methods are prolific because the laboratory measurements are relatively quick, and they are carried out in controlled boundary conditions (Van Dam et al. 1990). Outflow techniques are generally limited to relatively coarse-grained soil where drainage occurs relatively rapid. The outflow methods are classified under four general approaches: one-step, multi-step, multi-step direct, and continuous outflow.

2.4.3.1.1. One-Step Outflow Method

The one-step outflow method represents an attractive and routinely used laboratory measurement technique (Gardner 1962; Valiantzas et al. 1988; Toorman et al. 1992). The determination of the suction and water content relationship is obtained from the outflow results when only one big pressure increment is applied to the soil sample. The outflow data are then analyzed to obtain the hydraulic diffusivity function for a broad range of water contents. Doering (1965) derived the equation of Gardner (1956) to calculate hydraulic diffusivity from instantaneous rates of outflow and average water content:

$$D[\theta] = \frac{-4L^2}{\pi^2(\theta - \theta_f)} \frac{\partial \theta}{\partial t} \tag{2.5}$$

where L is the length of the soil sample, θ is the average water content when the outflow rate is $\partial\theta/\partial t$, and θ_f is the final water content. Gupta et al. (1974) showed that the analysis of one-step flow outflow data leads to an error of factor 3. Gupta et al. (1974) developed a more accurate and sophisticated method, based on the determination of an effective mean hydraulic diffusivity. Two years later, Passioura (1977) presented another version of one-step outflow, based on the assumption that $\partial\theta/\partial t$ is effectively constant throughout the draining soil core sample at any given

time. Kool et al. (1985) evaluated one-step outflow experiments by inverse solution, and suggested an iterative procedure using computer simulations to solve flow equation.

The primary advantage of the one-step method is that this method is faster than the multi-step outflow method and HCF can be obtained in much less time. A major problem of the one-step outflow method has always been that the quick change of the boundary condition does not represent natural conditions.

2.4.3.1.2. Multi-Step Outflow Method

Multi-step outflow method basically consists of subjecting a soil specimen to small incremental steps in matric suction, while monitoring the rate of pore water outflow and total outflow during each step. This method is a valid alternative to the one-step outflow method in order to deal with the non-uniqueness of the solution. The data is analyzed by making several assumptions (Benson and Gribb 1997): (1) hydraulic conductivity is constant over each suction increment, (2) suction is linearly related to water content over the suction increment, (3) the high-air entry disk provides no impedance to flow, (4) flow is one-dimensional, (5) flow due to gravity is negligible, (6) the specimen is homogenous and rigid. Giving these assumptions, and adding initial and boundary conditions, the hydraulic conductivity ($k_{\psi_{avg}}$) corresponding to the average suction is written as:

$$k_{\psi_{avg}} = D\frac{\Delta\theta}{\Delta\psi} \tag{2.6}$$

where the hydraulic diffusivity D is assumed to be a constant over the small increment in applied suction, and $\Delta\theta$ is the change in water content as a result of applied suction increment ($\Delta\psi$).

Early investigations confirmed that the outflow data of multi-step experiments contain adequate information for unique estimates of soil hydraulic functions (Mous 1993; van Dam et al. 1994). However, the results from Eching and Hopmans (1993) and Crescimanno and Iovino (1995) showed that additional measurements were needed even when multi-step experiments were performed. The multi-step method is also explained by inverse solution. Based on results of parameter optimizations of simulated outflow data, Zurmühl and Durner (1998) deduced that the multi-step method, using outflow data in the objective function, provides sufficient information for a unique and simultaneous estimation of all van Genuchten (1980) and Mualem (1976) parameters.

2.5. Suction and Hydraulic Conductivity Models

2.5.1. Soil Water Characteristic Curve Models

Many effective laboratory apparatuses are utilized over the years to establish a relationship between soil suction and volumetric/gravimetric water content. All experimental tests intend to obtain several pairs of suction and moisture data and then generate a complete SWCC. Unfortunately, most of them are costly and may take several days or longer to obtain a decent SWCC. In order to cope with those problems, alternatives to direct measurements are required.

Several mathematical approaches and prediction methods have been proposed to represent SWCC. The use of mathematic models has several advantages such as an efficient representation and comparison of the hydraulic properties of different soils and soil horizons (van Genuchten et al. 1991). Most of the equations are empirical in nature and are derived from the shape of the SWCC. Three of the most frequently used models and their equations in geotechnical filed, namely Brooks and Corey (1964), van Genuchten (1980) and Fredlund and Xing (1994a) models, are elaborately discussed in this section with their attributes and limitations. Also, Leong and Rahardjo (1997a), Singh (1997) and Ridley and Wray (1995) provided an excellent review and analyses of these models.

Another approach, based on pedotransfer functions (PTFs) and "knowledge-based" systems that emerged as a consequence of estimating the coefficients in these various models, remains difficult and time-consuming. They are called indirect measurement methods which predict hydraulic properties using limited (textural classes only) to more extended (grain-size distribution, Atterberg limits, texture, dry bulk density, porosity and one or two water retention points) input data (Ghanbarian-Alavijeh et al. 2010). These methods are not discussed here. If it is requested, Arya and Paris (1981), Haverkamp and Parlange (1986), Fredlund et al. (2002), and Haverkamp et al. (2005) presented a comprehensive description for these methods.

Parameter identification by inverse simulation of transient outflow/inflow experiments under known boundary conditions is an attractive alternative to determine SWCC (Durner et al. 1999). This method will be discussed in-depth in the Materials and Research Method chapter.

2.5.1.1. Brooks and Corey (BC) Model

The Brooks and Corey (1964) model is recognized as one of the earliest models to propose an equation for SWCC. The equation is in the form of power-law relationship given as:

$$\Theta = S_e = \begin{cases} 1 & \psi < \psi_b \\ \left(\frac{\psi_b}{\psi}\right)^{\lambda} & \psi \geq \psi_b \end{cases} \tag{2.7}$$

where ψ_b is the air-entry pressure of soil, λ is the pore size distribution index. For modeling purposes, a dimensionless water content variable, Θ, may be defined by normalizing volumetric water content with its saturated and residual values as:

$$\Theta = \frac{\theta - \theta_r}{\theta_s - \theta_r} \tag{2.8}$$

If the residual volumetric water content (θ_r) is equal to zero, then the normalized water content is equal to the degree of saturation (S). The effective degree of saturation (S_e) may also be normalized by fully saturated condition ($S = 1$) and the residual saturation degree (S_r) in a similar manner:

$$S_e = \frac{S - S_r}{1 - S_r} \tag{2.9}$$

Based on the Equation (2.7), the SWCC is assumed to be an exponentially decreasing function of water content at soil suctions greater than the air-entry pressure and remains constant for suctions less than the air-entry value. Theoretically, pore-sized distribution index approaches infinity for soils with a uniform pore-size distribution, whereas it quickly comes closer to zero for soils with a wide-range of pore sizes.

The BC model has been verified by several studies (Gardner 1970; Gardner et al. 1970; Rogowski 1971; Campbell 1974; Clapp and Hornberger 1978; Williams et al. 1983; Timlin et al. 1999). In light of preliminary experimental results, the BC model promises more suitable results for coarse-grained soils than for fine-grained soils (van Genuchten and Nielsen 1985; Milly 1987). Moreover, the BC model has a few drawbacks, for instance, losing applicability at high suction ranges and the absence of an inflection point.

2.5.1.2. van Genuchten (VG) Model

Based on the Mualem's theory (Mualem 1976), van Genuchten (1980) proposed an empirical SWCC model which assumes more or less sigmoidal shape and includes three fitting parameters. The VG model is given as:

$$\Theta = S_e = \left[\frac{1}{1 + (\alpha\psi)^n}\right]^m \tag{2.10}$$

where α, n and m are fitting parameters pertaining to air-entry pressure, pore-size distribution, and overall symmetry of the curve, respectively. In the above equation, the suction term (ψ) are expressed in either units of pressure (commonly kilopascal, kPa) or head (commonly meter or centimeter) (Lu and Likos 2004). If suction term is expressed in units of kPa, the air-entry pressure parameter must be expressed in units of kPa^{-1}.

Increasing the number of free parameters certainly allows more flexibility in the fitting of SWCCs, but constraining the m parameter provides great stability during parameter optimization and permission of a closed-form equation of the SWCC (van Genuchten et al. 1991; Kosugi et al. 2002). Instead of committing a constant m value and in an attempt to establish a closed-form expression, van Genuchten (1980) proposed the relationships of $m = 1 - 1/n$ ($n > 1, 0 < m < 1$). Overall, the VG model has more considerations and advantages than the BC model, for example, taking account an inflection point, applicability on a variety of soil types, and great flexibility within a wide-range of suction.

2.5.1.3. Fredlund and Xing (FX) Model

Fredlund and Xing (1994a) suggested the Equation (2.9) for estimating the soil-water characteristic curve based on the assumption that the shape of the SWCC is dependent of the pore-size distribution of soil;

$$\theta = C(\psi)\theta_s \left[\frac{1}{ln[e + (\psi/\alpha)^n]}\right]^m \tag{2.11}$$

where ψ is the matric suction of the soil at a given water content (kPa), and e is the natural logarithmic constant. The model fitting parameters (α, n, and m) have the same meaning as

mentioned in the VG model. The $C(\psi)$ is a correction factor that forces model through a prescribed suction value of 10^6 kPa at zero water content and is given by:

$$C(\psi) = \left[1 - \frac{\ln(1 + \psi/\psi_r)}{\ln(1 + 10^6/\psi_r)}\right] \tag{2.12}$$

where ψ_r is the suction value (kPa) at the residual condition.

A graphical estimation of three parameters (α, n, and m) are obtained from inflection points located on the SWCC drawn in a semi-log plot. The detailed studies from Leong and Rahardjo (1997a), Zapata et al. (2000) and Sillers et al. (2001) showed that the Fredlund and Xing (1994a) model fits very-well for a variety of soils over a wide range of suction.

2.5.2. Hydraulic Conductivity Models

Hydraulic conductivity of unsaturated soils is a relatively unique function that can be varied with the degree of saturation (Richards 1931; Childs 1940; Gardner 1956; Gillham et al. 1976; Ahuja et al. 1988; Assouline 2001; Sheng 2011). Several mathematical models have been developed to determine HCF through experimental data set. It is desirable to determine all necessary data by direct measurements, however, it is not always easy to perform the necessary experiments due to high costs, time (especially for low water content conditions), hysterical nature of hydraulic properties, and also the available experiment data sometimes cannot represent the complete relationships describing the hydraulic properties (Mualem 1986). Numerous attempts have been made to predict the hydraulic conductivity function through the use of the relationship between water content and pore-water pressure, most notably the SWCC. Brutsaert (1967), Mualem (1978), Fredlund et al. (1994b), and Leong and Rahardjo (1997b) provide detailed summaries of several hydraulic conductivity models and modeling techniques. HCF models are categorized under three major approaches, namely empirical, macroscopic, and statistical models.

2.5.2.1. Empirical Models

Empirical models typically consist of fitting simple mathematical formulas that consider saturated hydraulic conductivity and various curve fitting parameters. As mentioned before, the curve fitting parameters are related to the shape of the SWCC. By establishing a curve-fitting optimization on the

available experimental data, the following relationships between the hydraulic conductivity and the water content (θ) or suction (ψ) are derived as:

$$k = f(\theta) \quad \text{or} \quad k = f(\psi) \tag{2.13}$$

The SWCC and the HCF usually represent similar curve shapes. This resemblance is a natural and expected result because water only flows through the water phase in the soil (Leong and Rahardjo 1997b).

One of the earliest models was suggested by Richards (1931), as a simple linear function involving two fitting parameters, a and b, that are the intercept and slope of the HCF in the k-ψ graph, respectively.

$$k(\psi) = \alpha\psi + b \tag{2.14}$$

Davidson et al. (1969) proposed a modified form to express hydraulic conductivity as a function of water content:

$$k(\psi) = \exp(-\alpha\psi) \tag{2.15}$$

where a is a dimensionless empirical constant. A number equations for the HCF have been suggested and some of them are summarized in Table 2.2. Empirical hydraulic conductivity models are conveniently applied in engineering design, especially for geotechnical engineers with limited theoretical backgrounds.

2.5.2.2. Macroscopic Models

Macroscopic models aim to derive an analytical expression for the HCF, based on physical consideration such as similarity between laminar flow (microscopic level) and flow in porous media (macroscopic level) (Huang et al. 1998a). All these models have the following general form of a power function:

$$k(S) = k_s S_e^n \quad \text{or} \quad k(\Theta) = k_s \Theta^n \tag{2.16}$$

Averjanov (1950) and Yuster (1951) suggested the exponent constant (n) equal to 3.5 and 2.0, respectively, by using the model of parallel, uniform, cylindrical capillary tubes, and some mathematical approximations. Irmay (1954) derived a theoretical value of $n = 3$, and Corey (1954) suggested $n = 4$. These researchers suggested their estimations depending on experiments performed with various soils. It concludes that the exponent value needs to be updated for each soil type. Also, Brooks and Corey (1964) criticized researchers who estimated the exponent constant without taking into account the effect of pore-size distribution. To consider the effect of pore-size distribution on hydraulic conductivity, Brooks and Corey (1964) proposed a macroscopic model which defines a relationship between hydraulic conductivity and suction as follows:

$$k(\psi) = S_e = \begin{cases} k_s & \psi < \psi_b \\ k_s \left(\frac{\psi_b}{\psi}\right)^{\eta} & \psi \geq \psi_b \end{cases} \tag{2.17}$$

where ψ_b is the air-entry pressure of soil, and the exponent η is related to the BC pore size distribution index λ by the equation:

$$\eta = 2 + 3\lambda \tag{2.18}$$

Using the experimental data of 50 soils, Mualem (1976) suggested that $n = 3 - 2m$ where m is a soil-water parameter being positive for granular material and negative for unstructured soils of fine texture. Mualem (1976) found that n varies from 2.45 to 24.5. The varying exponent value in the models of Brooks and Corey (1964) and Mualem (1976) provides a wider applicability than the other models.

2.5.2.3. Statistical Models

Statistical models have shown to be the most rigorous methods for indirect determination of the unsaturated hydraulic conductivity (Mualem 1986; Leong and Rahardjo 1997b). The statistical approach relates the hydraulic conductivity of a soil to the information obtained from its measurements or models of the SWCC. Numerical statistical models have been developed to explain

the pore-size distribution function in soil (Childs and Collis-George 1950; Burdine 1953; Brutsaert 1967; Mualem 1976; Mualem and Dagan 1978). The methodology of the statistical models are based on the following common assumptions (Mualem 1986):

a. The soil is assumed to be a system consisting of a set of interconnected, randomly distributed pores characterized by pore radius (r) and described by a statistical pore distribution $f(r)$.
b. The Hagen-Poiseuille equation is valid at the level of a singular pore channel.
c. Based on the Kelvin's capillary law, the soil-water characteristic curve is a representation of the pore-size distribution function.

Table 2.3. Empirical and macroscopic equations for modeling unsaturated hydraulic conductivity function after Lu and Likos (2004)(with permission from John Wiley & Sons)

Type	Function	Reference
$k(\theta)$ or $k(S)$	$k(\theta) = k_s \Theta^n$	Averjanov (1950)
	$k(\theta) = k_s S_e^n$ $k(\theta) = k_s \exp[\alpha(\theta - \theta_s)]$	Davidson et al. (1969)
	$k(\theta) = k_s \left(\frac{\theta}{\theta_s}\right)^n$	Campbell (1973)
$k(\psi)$ or $k(h)$	$k(\psi) = \alpha\psi + b$	Richards (1931)
	$k(\psi) = \alpha\psi^{-n}$	Wind (1955)
	$k(\psi) = \exp(-\alpha\psi)$ $k(\psi) = \frac{k_s}{1 + \alpha\psi^n}$	Gardner (1958)
	$k(\psi) = k_s$ for $\psi \leq \psi_{aev}$ $k(\psi) = k_s \left(\frac{\psi_b}{\psi}\right)^\eta$ for $\psi > \psi_{aev}$	Brooks and Corey (1964)

3. MATERIALS & RESEARCH METHOD

3.1. Introduction

In order to determine the engineering properties of the test materials, a series of laboratory tests were performed. All laboratory tests have been successfully completed and significant results have been obtained. For each laboratory test conducted, a brief description is given and its importance is explained. In the research method section, the working principles of TRIM and inverse modeling is explained with a short literature review.

3.2. Materials

Three natural soils (from sandy to clay-dominated) and artificial sand-clay mixtures in varying proportions are employed as test materials. The natural soils were sampled from different locations along the streambanks of the New River in the Blacksburg area, in Virginia.

In this study, the natural soils were named with their location from where they were taken, stated below. Also, two initials were assigned for these soils to entitle the test numbers shortly. They were initially air-dried, and then run through a 2 mm (#10) mesh before testing.

- Whitehorne soil (WH) was acquired from the top 10-40 cm of a river terrace located next to the New River at Whitehorne near Blacksburg, VA.
- Stroubles Creek soil (SC) was acquired from along the Stroubles Creek near Blacksburg, VA.
- Toms Creek soil (TC) was obtained from the banks of Toms Creek river near Blacksburg, VA (N 37 12.349' E 80 33.895').

The sand-clay mixtures used in this study consist of mixtures of play sand and Wilco LPC kaolin clay, which are commercially available. The play sand is a specially graded sand that has been washed, dried and screened before packaging. Wilco LPC clay is a relatively coarse-grained kaolin clay designed for drain and pressure casting applications. Sand was mixed with clay at two different weight percentages in dry state, such as mixtures containing 15%, and 25% kaolin clay. They were mixed thoroughly for 5 to 10 minutes by hand.

Before moving to the main testing program, the basic properties of test materials were characterized with a series of laboratory tests, including the determination of mineral composition, specific gravity, Atterberg limits, grain-size distribution, and standard proctor compaction tests. All tests were performed in accordance with the pertinent ASTM standard.

3.2.1. Mineral Composition

Minerals are naturally formed crystal structures that include one or more chemical elements. Quartz and clay minerals are common products formed after chemical weathering of rock forming materials (Huat et al. 2007). Clays and clay minerals are mainly found on or near the surface of the Earth. Clay minerals are composed of planes of cations, arranged in layered silicates.

Table 3.1. Mineralogical analysis results of Whitehorne soil

Clay minerals	**% Layer Silicate**
Hydroxyl-interlayered Vermiculite	35%
Kaolinite	15%
Quartz	13%
Vermiculite	10%
Mica	10%
Chlorite	10%
Smectite	6%

The clay mineral composition has a considerable influence on the physical properties of soils. In many typical engineering project, the examination of clay minerals is not a routine consideration, however doing so provides a better understanding of the performance of clay soils in engineering use (Dumbleton and West 1966). The surface of a clay particle (negatively charged) attracts the positive ions of water molecules. This phenomena is known as the diffuse double layer (DDL) and it is highly dependent on the type of clay minerals. White (1949) studied the effect of different clay minerals on the Atterberg limits and indicated that the plastic limit results as attapulgite > montmorillonite > illite > kaolinite. The clay mineral composition of natural soils in this study was investigated through mineralogical analysis tests. The analysis results are tabulated below for each natural soil.

Table 3.2. Mineralogical analysis results of Stroubles Creek soil

Clay minerals	% Layer Silicate
Kaolinite	35%
Montmorillonite	25%
Mica/Illite	20%
Hydroxyl-interlayered Vermiculite	15%
Chlorite	3%
Quartz	2%

Table 3.3. Mineralogical analysis results of Toms Creek soil

	Major (>30%)	Minor (2%-10%)	Trace (<2%)
Minerals	Quartz	Illite	Kaolinite, illite, chlorite, montmorillonite

Montmorillonite (approximately 25%) is the dominant mineral of Stroubles Creek soil. For Whitehorne soil, vermiculite is the dominant clay mineral. Based on X-Ray diffraction results, the overwhelming majority of Toms Creek soil is quartz minerals. The kaolin clay in the mixture samples, as the name implies, is composed primarily of kaolinite (>90%), mica and quartz (<10%), based on product information supplied by the Old Hickory Company.

3.2.2. Specific Gravity

Specific gravity (G_s) of solid particles is defined as the ratio of mass of a given volume of solids to the mass of an equal volume of water at 20°C. The testing procedure conformed to ASTM Standard D584 (2014). Specific gravity tests were performed only for natural soils. The specific gravity of sand and clay mixtures was assumed to be 2.65 Mg/m^3 by considering the specific gravity determinations delivered from suppliers. The test results are found in Table 3.4.

3.2.3. Atterberg Limits

Atterberg limits are the most important references in the description of fine-grained soils such as liquid limit (LL), plastic limit (PL), plasticity index (PI), and shrinkage limit. The water content level is capable of making a great difference on the engineering behavior and consistency of soils. The liquid limit is a stage where the soil passes from a plastic state to liquid state by changing moisture content of the soil. The plastic limit is defined as the moisture content at the boundary between the plastic and semisolid states of consistency. The liquid and plastic limit test procedures are given in ASTM standard D4318 (2003). Method B of this standard on soils passing the 425 μm (sieve No. 40) was used.

Liquid limits were determined by using Casagrande's liquid limit device. To determine the plastic limit, the soil was rolled by hand until the soil started to crumble at a diameter of 1/8 inches. Liquid limit and plastic limit are the water contents at which all test materials exhibited both liquid and plastic nature, respectively. The test results are given in Table 3.4.

3.2.4. Grain Size Distribution

Atterberg limits are usually not enough to justify the classification of a particular soil accurately. Therefore, a grain-size distribution (GSD) test was performed for all test materials. The effective diameter of the soil particles strongly effect the uniformity characteristics of the soil mass. The GSD was determined by following the ASTM standard specification D422 (2007) and C136 (2006). The sieve test determines particle sizes larger than 75 μm (retained on the No. 200 sieve), while hydrometer analysis determines the particle sizes below 75 μm. All test soils contained fine to coarse sized particles, therefore a combined analysis was employed.

3.2.4.1. Sieve Analysis

The air-dried soil samples were oven-dried at a temperature of 110°C. The amount taken from each soil conformed to the criterion established by ASTM standard C136 (2006). The test soils were placed in the stacked sieves, and then shaken on a mechanical sieve shaker for approximately 15 mins. In addition to these tests, a wet sieve analysis was performed for Wilco LPC kaolin clay by running the soil through a #200 mesh in accordance to the ASTM standard D1140 (2014). It is confirmed that Wilco LPC kaolin clay has no particles greater than 75 μm.

3.2.4.2. Hydrometer Analysis

After the sieve analysis, the soil retained on the pan included silt and clay particles. The grain-size distribution for this fraction of soil was determined by a hydrometer analysis, also known as sedimentation method, in accordance of ASTM D422 (2007). The principle of hydrometer analysis is based on an application of Stoke's law to a soil and water suspension and periodic measurement of the density of suspension. The retained soil was added to a solution of water and dispersion of sodium metaphosphate ($NaPO_3$) to break the bonds of clay particles. The temperature correction (F_T), specific gravity correction (a), zero correction (F_Z), and specific gravity corrections were applied to the hydrometer readings.

Based on the soil retained on each sieve, and hydrometer analysis, the particle size distribution graphs of all test soils were generated, shown in Figure 3.1-3.5.

3.2.5. Standard Proctor Compaction Test

Compaction means pressing the soil particles close to each other through a mechanical method. Laboratory compaction tests create guidelines that are generally used to justify the compaction levels performed in the field. Standard proctor and modified proctor are common laboratory compaction tests. Standard Proctor compaction tests were conducted according to ASTM standard D698 (2003) to establish the compaction moisture content and dry unit weight relationships, and also to determine the optimum moisture content (w_{opt}) of a given soil under a particular compactive effort. Compactive effort is a measure of the mechanical energy applied to a soil mas.

The test soils were firstly dried in the oven. Bearing in mind that the optimum water content is typically slightly lower than the plastic limit, enough amount of water was added to the oven-dried soil and mixed thoroughly. Soil was covered with plastic and kept overnight for proper mixing of water. Soil samples were compacted in three layers and tamped with 25 hammer blows for each layer which corresponds to a total energy of 12,400 ft-lbf/ft^3. After each compaction trial, a small amount of soil was kept for water content determination and then water was added to soil sample. At the optimum moisture content, the dry density does not increase any further and it starts to decrease with the increase of water content. Several trials were performed, as necessary, at different water contents to determine a precise compaction curve. The maximum dry density $(\gamma_d)_{max}$ and optimum water content (w_{opt}) for each test soil are given in Table 3.4. Figures 3.6-3.10 demonstrate

the maximum dry density$(\gamma_d)_{max}$, optimum water content (w_{opt}), zero-air voids (ZAV) and the compaction curve obtained for each soil specimen.

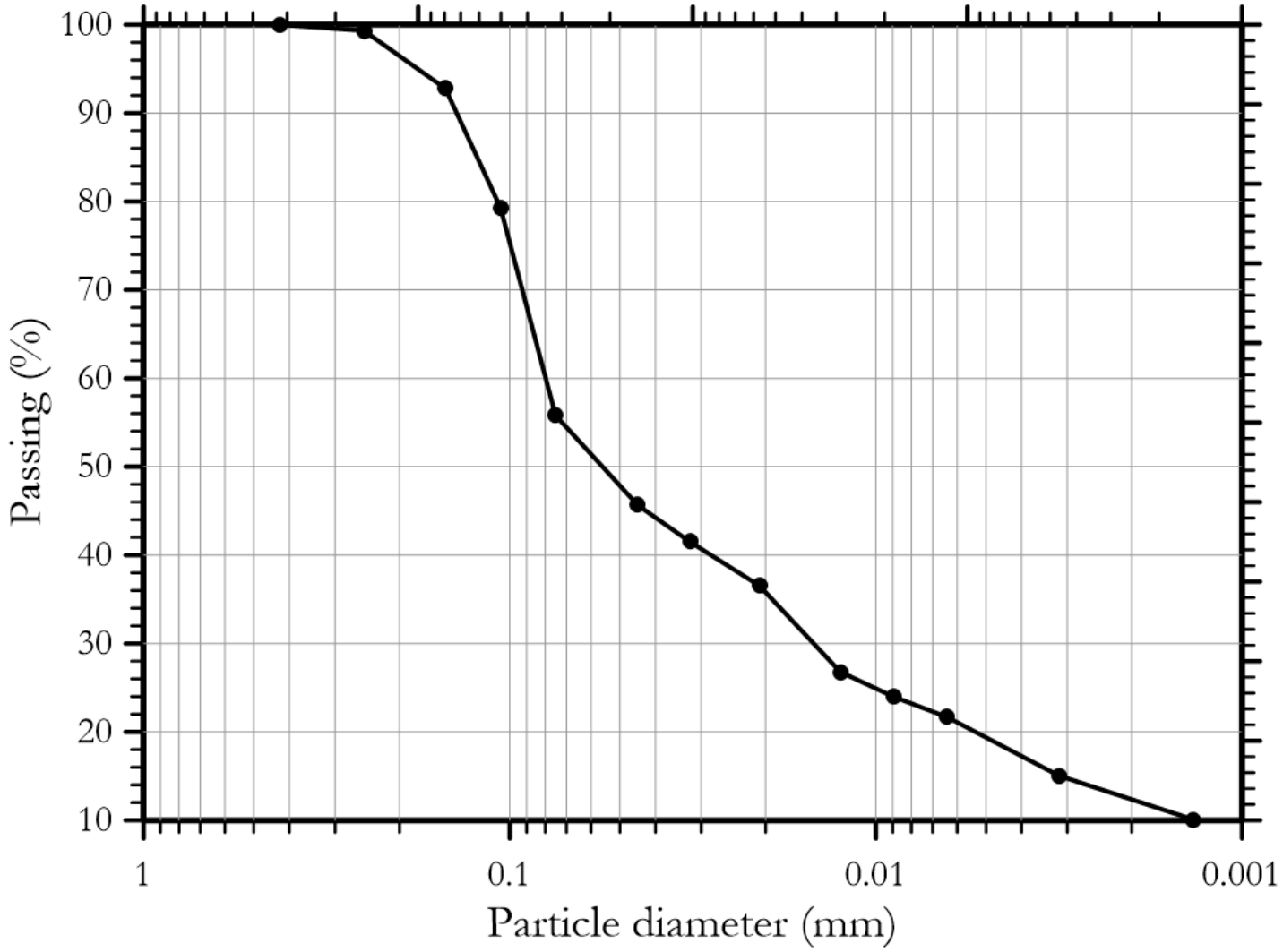

Figure 3.1. The grain-size distribution of Whitehorne soil

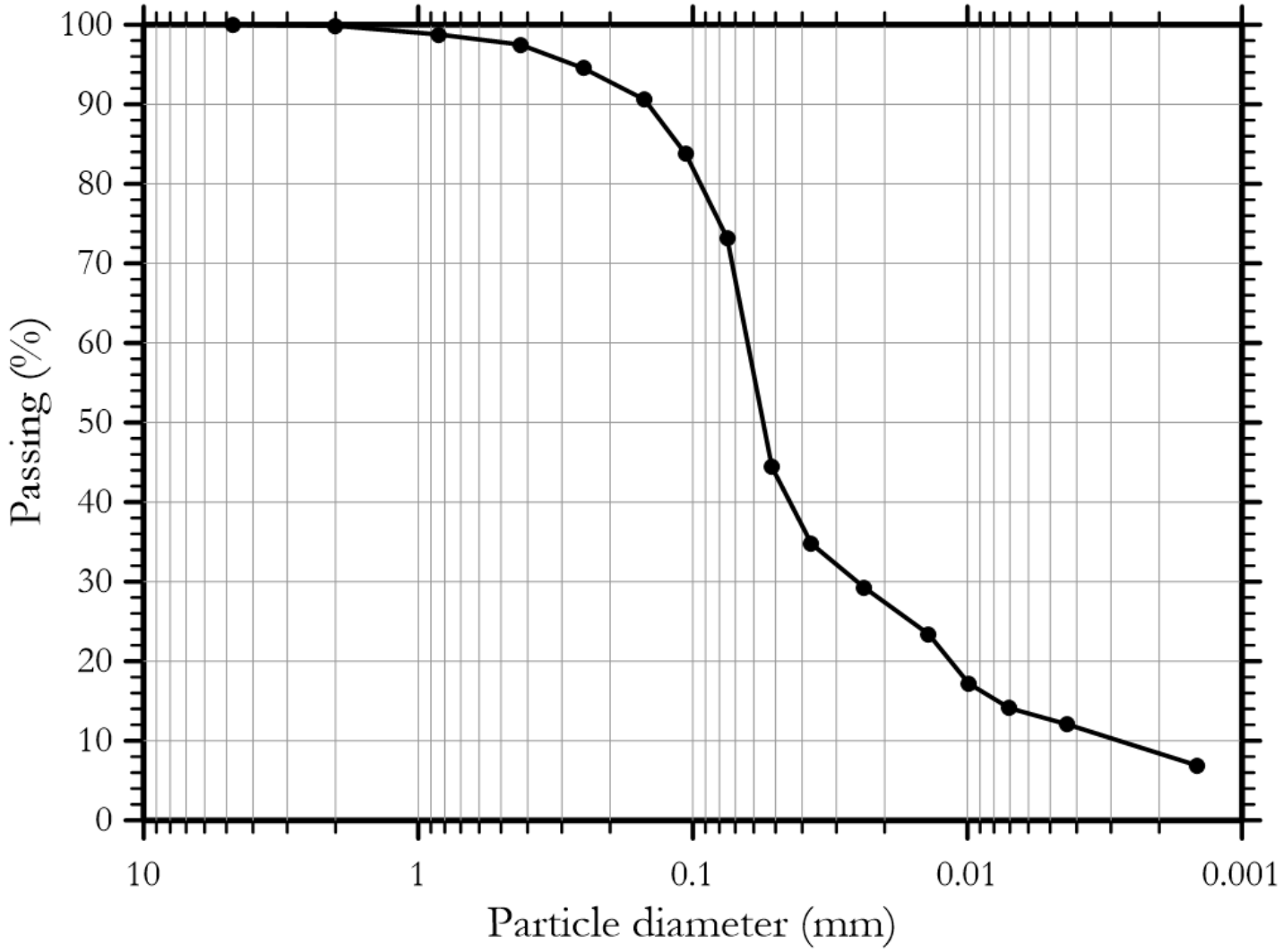

Figure 3.2. The grain-size distribution of Stroubles Creek soil

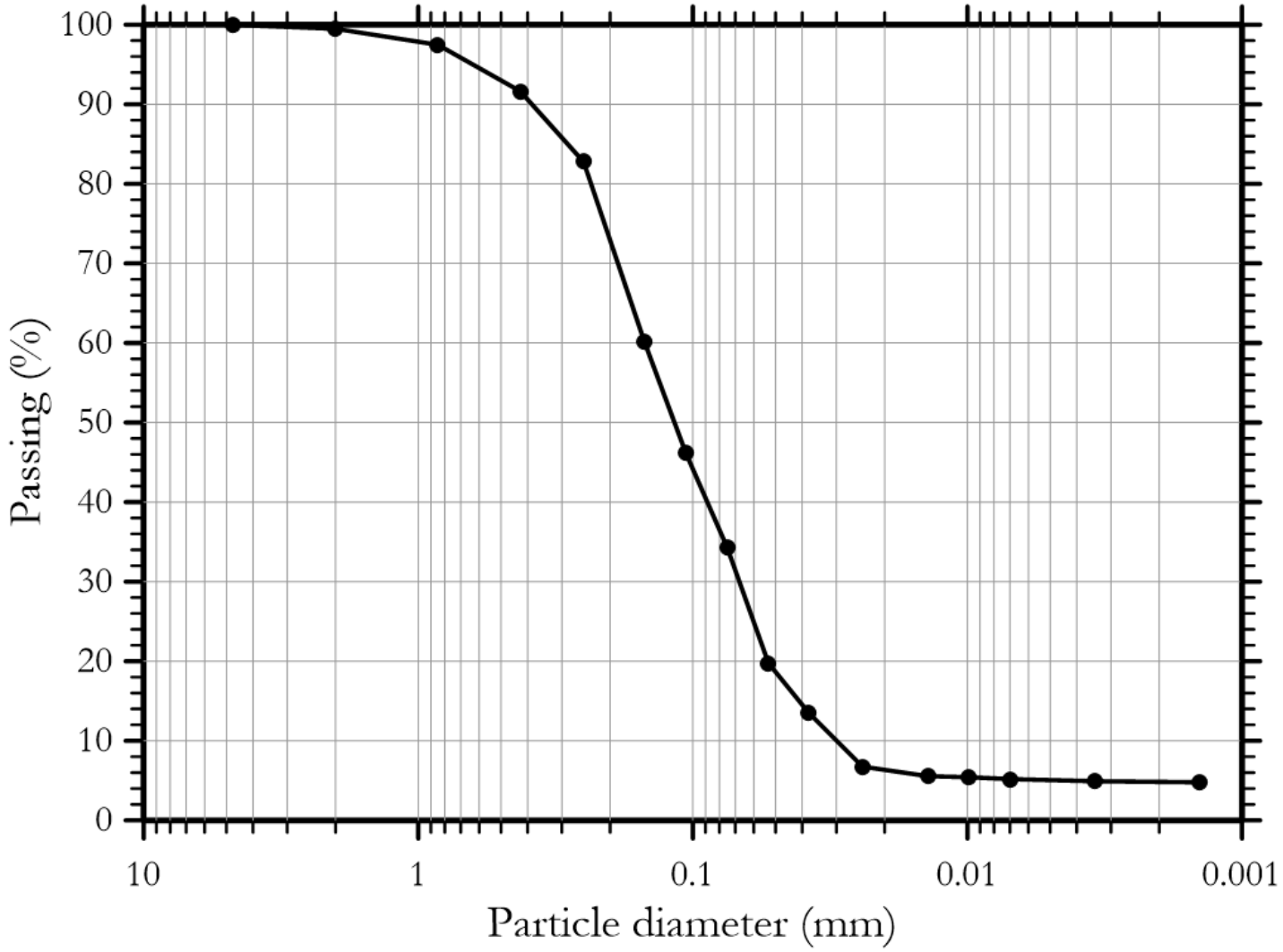

Figure 3.3. The grain-size distribution of Tom's Creek soil

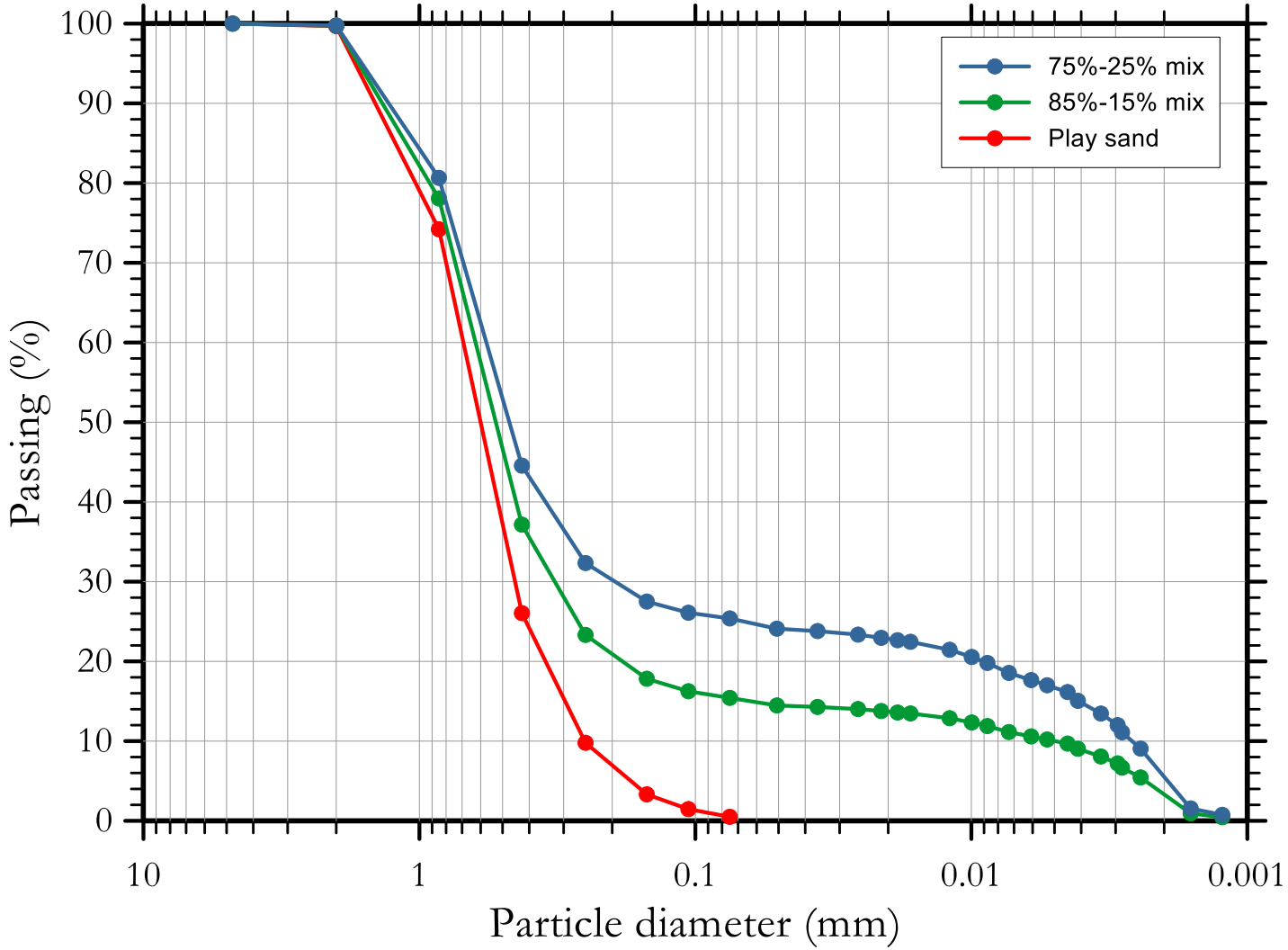

Figure 3.4. The grain-size distribution of sand-clay mixtures and play sand

Table 3.4. The summary of test results of the investigated soils

Test Soil	USCS Soil Classification	Specific Gravity, Gs (Mg/m^3)	Liquid Limit, LL (%)	Plastic Limit, PL (%)	Plasticity Index, PI (%)	Maximum Dry Density, $\gamma_{d_{max}}$ (g/cm^3)	Optimum water content, w_{opt} (%)
Whitehorne	Lean Clay (CL)	2.61	44.15	31.62	12.53	1.375	29.9
Stroubles Creek	Fat Clay (CH)	2.59	51.20	24.54	25.41	1.550	22.6
Toms Creek	Silty Sand (SM)	2.68	30.74	20.53	10.21	1.694	18.2
Sand – Clay mix (85%-15%)	Clayey Sand (SC)	2.65	20.96	12.81	8.15	1.937	9.4
Sand – Clay mix (75%-25%)	Clayey Sand (SC)	2.65	24.66	13.81	10.85	2.002	10.4
Play sand	Poorly Graded Sand (SP)	2.65	NP	NP	NP	1.727	-
Wilco LPC kaolin clay	Lean Clay (CL)	2.65	41.58	23.57	18.01	-	-

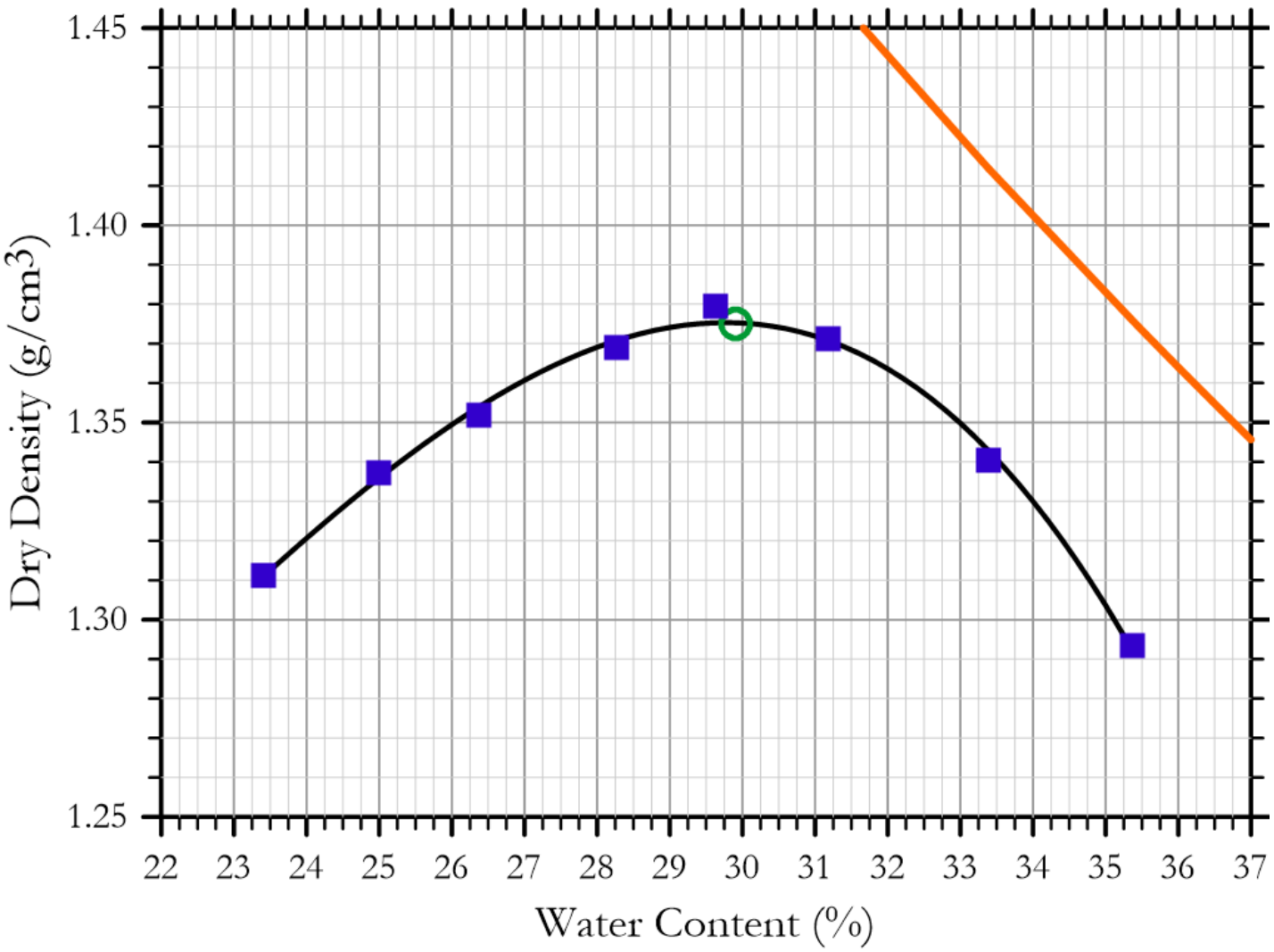

Figure 3.5. Compaction curve of Whitehorne soil

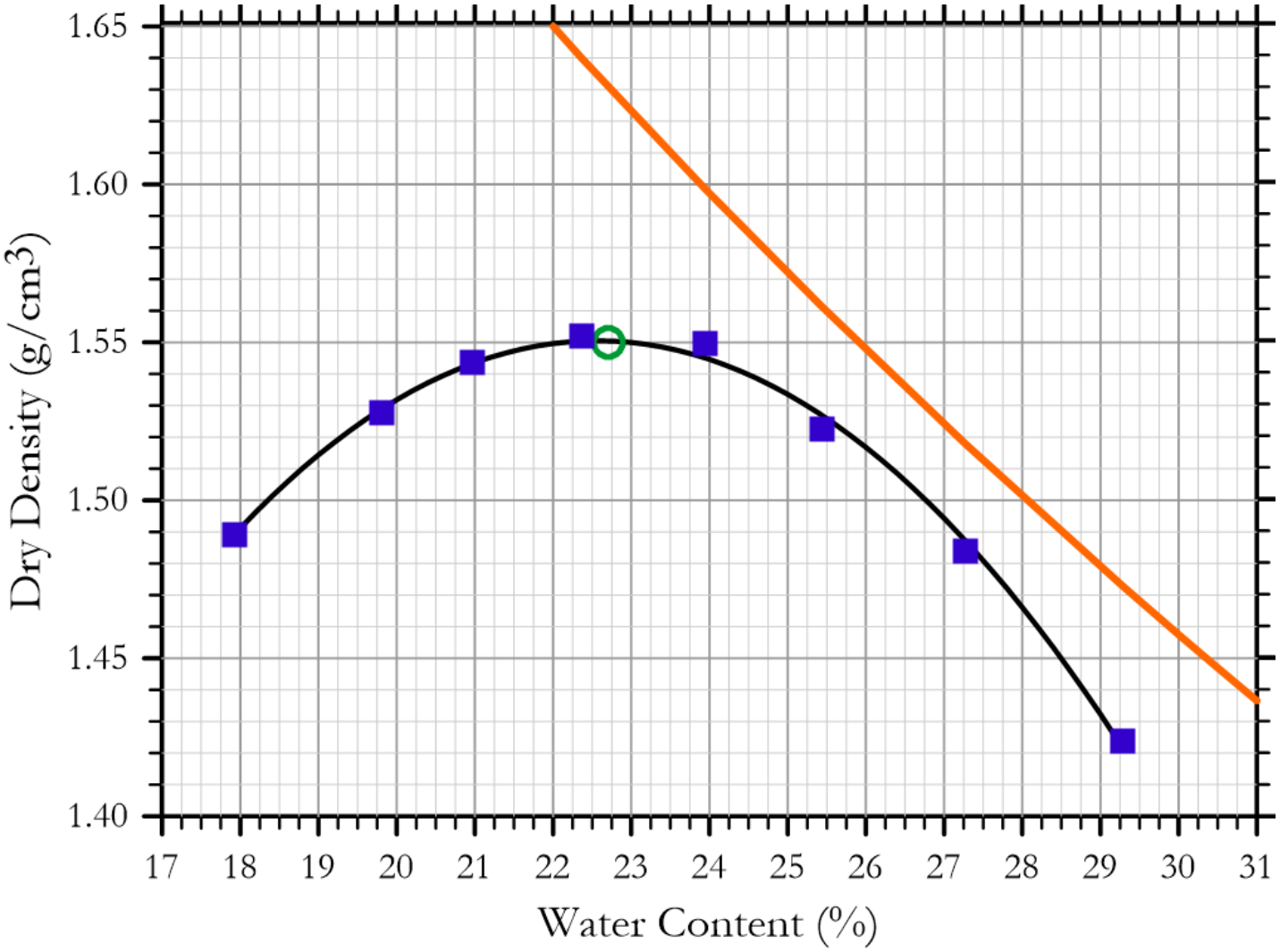

Figure 3.6. Compaction curve of Stroubles Creek soil

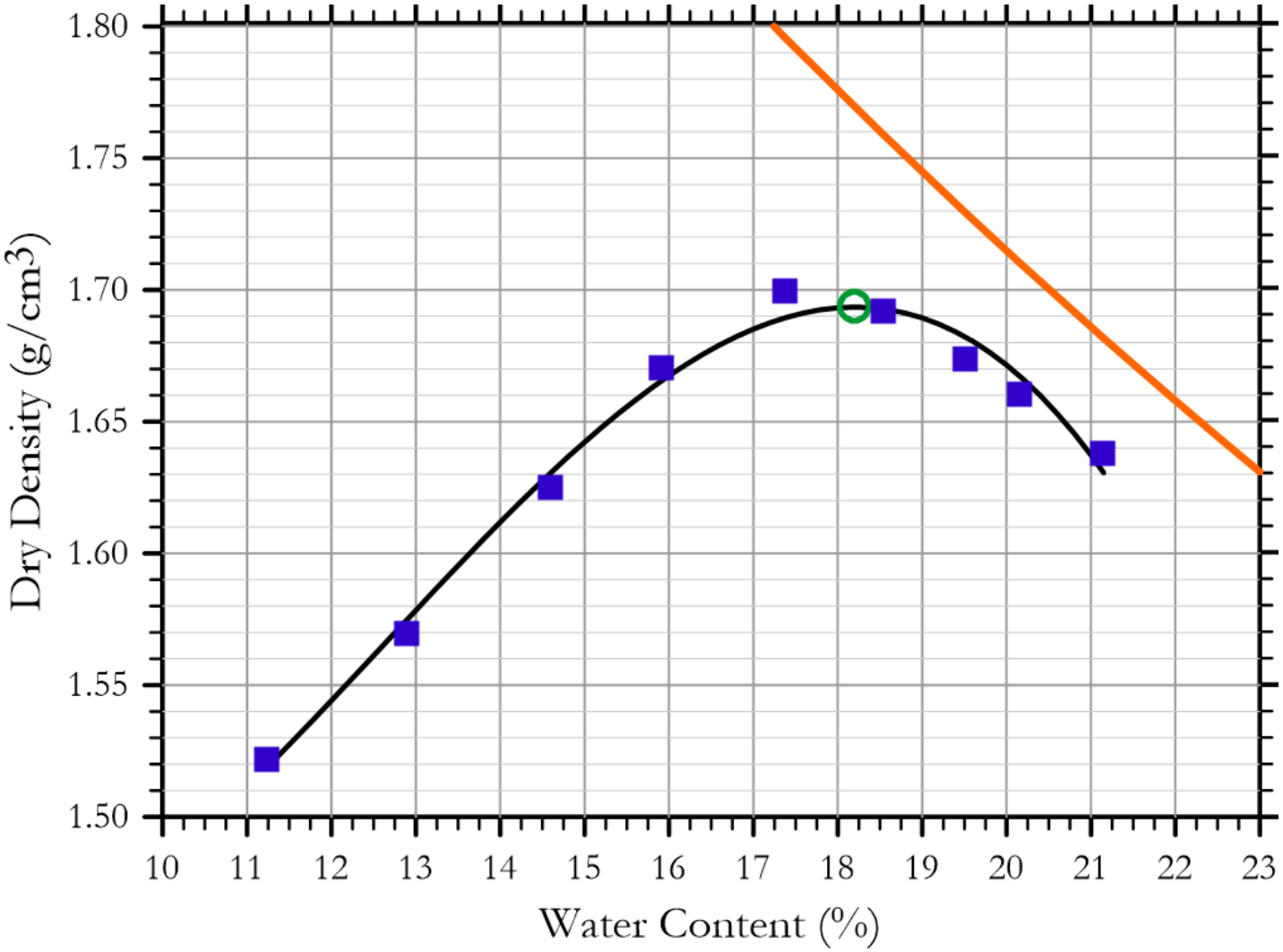

Figure 3.7. Compaction curve of Tom's Creek soil

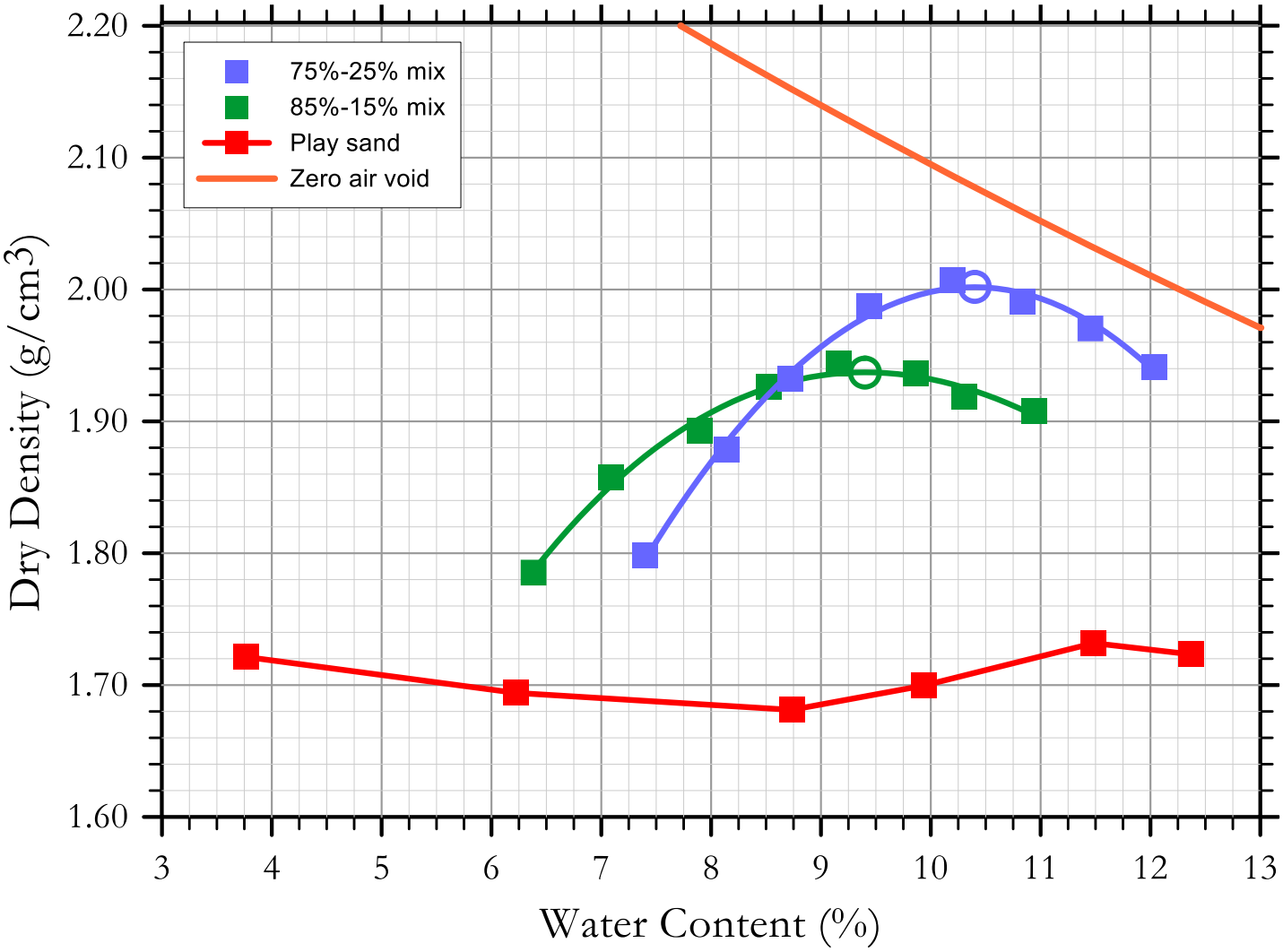

Figure 3.8. Compaction curves of sand-clay mixtures and play sand

3.3. Research Method

Transient release and imbibition method (TRIM) integrates an experiment program and a modeling technique to determine hydraulic properties of various types of soils in a simple, fast and reliable way (Likos et al. 2013; Lu et al. 2013; Dong et al. 2014). From a testing program perspective, TRIM shares a similar methodology with the suction measurement methods of tempe pressure cells and pressure plates. This method is categorized under axis translation techniques.

3.3.1. TRIM Working Principles

The soil sample on the HAE ceramic stone exposed to an instantaneous change in matric suction, responses through transient water outflow or inflow (Kool et al. 1985; Parker et al. 1985; Wildenschild et al. 1997). A sudden increase in suction results in water outflow through the soil sample which represents a drying state, in Figure 3.11. The other way round, a sudden decrease in suction results in water imbibition back into the soil sample which represents a wetting state, in Figure 3.12.

While maintaining the matric suction at a reference value through the pores of a saturated HAE ceramic stone, transient outflow or inflow response is continuously recorded by an electronic balance until steady state conditions at equilibrium. Measured transient water flow data, changes in water content with times series, is used as an objective function in the inverse model that solves Richards' equation in one dimension (Likos et al. 2013; Mavimbela and van Rensburg 2013). The hydraulic diffusivity of a soil sample is also controlled by HAE ceramic stone, so the assessment of transient response must be done by taking hydraulic properties and impedance of the ceramic stone into consideration.

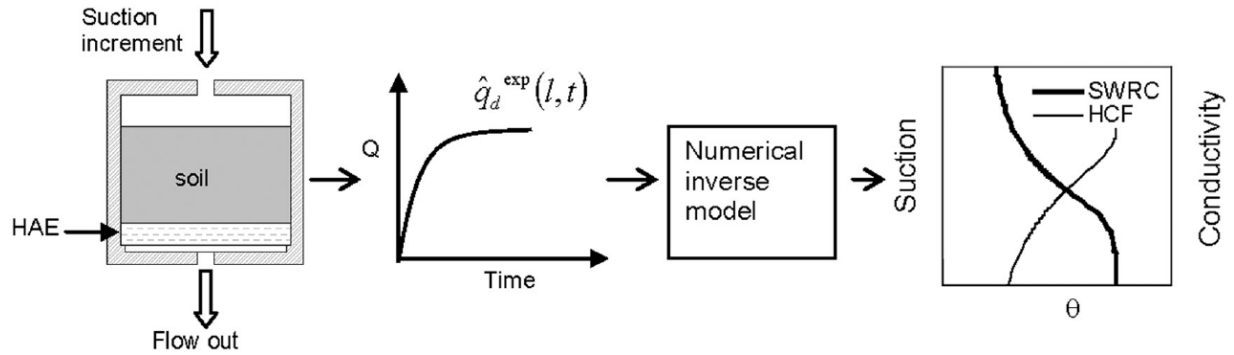

Figure 3.9. Illustration of TRIM method for drying state after Wayllace and Lu (2012)(with permission from ASTM International)

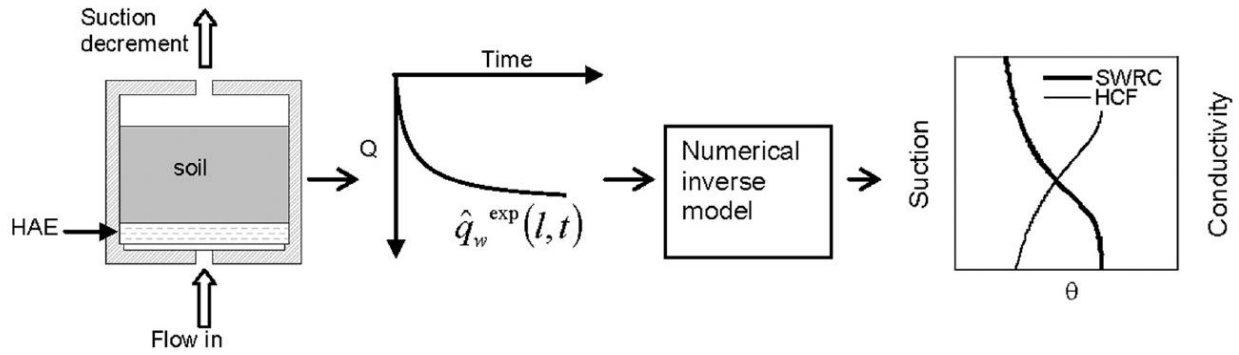

Figure 3.10. Illustration of TRIM method for wetting state after Wayllace and Lu (2012) (with permission from ASTM International)

3.3.2. Inverse Modeling Algorithm

Inverse theory is the mathematical process of predicting (or estimating) the numerical values (and associated statistics) of a set of model parameters of an assumed model, based on a set of data or observation. In this study, it is desired to obtain two-step water outflow $[\hat{q}_d{}^{exp}(l,t)]$ and single-step water inflow $[\hat{q}_w{}^{exp}(l,t)]$ data, as shown in Figure 3.13. The measured experimental time-series water flow data is a unique function for a given soil used as an objective function in inverse numerical model to derive estimates of hydraulic parameters using parameter optimization. The objective function (Φ) quantifies the discrepancy between observed flow variables and those simulated by a numerical model with initial hydraulic parameter input.

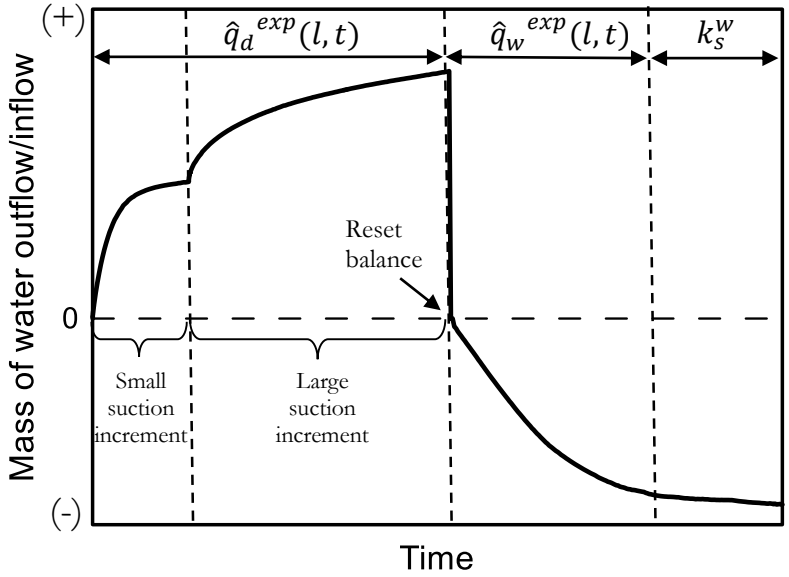

Figure 3.11. A complete transient flow data from a typical TRIM test

As mentioned earlier, two groups of methods are available to characterize a flow: steady-state flow conditions and transient flow. Steady state equations invert Darcy's equation, whereas transient methods invert Richards' equation. Inversion of Richards' equation allows more flexibility in experimental boundary conditions and improves a fast and accurate analysis compared with steady state methods (Hopmans et al. 2002).

Richards' flow equation governs transport of water through soil, in response to the forces of gravity or water pressure. The one dimensional form of Richards' equation is given as follows (Richards 1931):

$$\frac{\partial}{\partial z}\left[\begin{matrix}k(h)\\ \left(\frac{\partial h}{\partial z}+1\right)\end{matrix}\right]=\frac{\partial\theta(h)}{\partial h}\frac{\partial h}{\partial t} \tag{3.1}$$

where θ is volumetric soil water content [L^3L^{-3}], t is time [T], z is the vertical coordinate (from a reference level) [L], k is unsaturated hydraulic conductivity [LT^{-1}], and h is the water pressure head [L]. For drying state, initial and boundary conditions are defined as:

$$h(z,t=0)=0 \tag{3.2}$$

$$h(z=0,t>0)=h_d \tag{3.3}$$

$$\frac{\partial h(z=-l,t>0}{\partial z}=0 \tag{3.4}$$

where h_d is the applied increase in matric suction head, and l denotes total height which is the soil sample height (l_1) plus the thickness of HAE ceramic stone (l_2). For the wetting state, initial and boundary conditions are defined as:

$$h(z,t=t_d)=h(z) \tag{3.5}$$

$$h(z=0,t>t_d)=t_w \tag{3.6}$$

$$\frac{\partial h(z=-l, t>t_d)}{\partial z}=0 \tag{3.7}$$

where t_d is the termination time of drying state, and h_w signifies the applied decrease in matric suction. Finite-element and finite-difference techniques are used to numerically solve Equation (3.1) (Likos et al. 2013). Equation (3.4), the combination of Equation (3.1) and Equation (3.2), represents the drying state:

$$q(0,t)=k_s^c\frac{\partial h(z=0,t)}{\partial z}=\hat{q}_d(l,t) \tag{3.8}$$

where k_s^c is the saturated hydraulic conductivity of the HAE ceramic stone. For wetting state, it is written as:

$$q(0,t)=k_s^c\frac{\partial h(z=0,t)}{\partial z}=\hat{q}_w(l,t) \tag{3.9}$$

As illustrated in Figure 3.14, the inverse method is grouped under three interrelated functional steps (Hopmans et al. 2002):

1. Transient experiment: A controlled experimental time-series water flow data for which initial and boundary conditions are prescribed.
2. Numerical flow model: A numerical flow model that simulates experimental transient response.
3. Parameter optimization: An optimization algorithm that accomplishes the minimization of the objective function through an iterative solution of the transient flow equation.

Kool et al. (1985) recommend a prediction of reasonably close initial parameters and this allows for outflow measurement errors be small. In order to verify solution uniqueness, an iterative process might be rerun with different initial parameters and its convergence to the same or similar final results must be confirmed (Eching et al. 1994).

3.3.3. Inverse Modeling for Drying State

A fully implicit one-dimensional transient water flow constitutes two materials in the system, including a ceramic stone and a soil sample. A custom designed ceramic stone was used, so that the

hydraulic properties of the ceramic stone are always the same for drying and wetting states. Drying state takes into account two suction increments to construct a robust model and parameters obtained through inverse modeling.

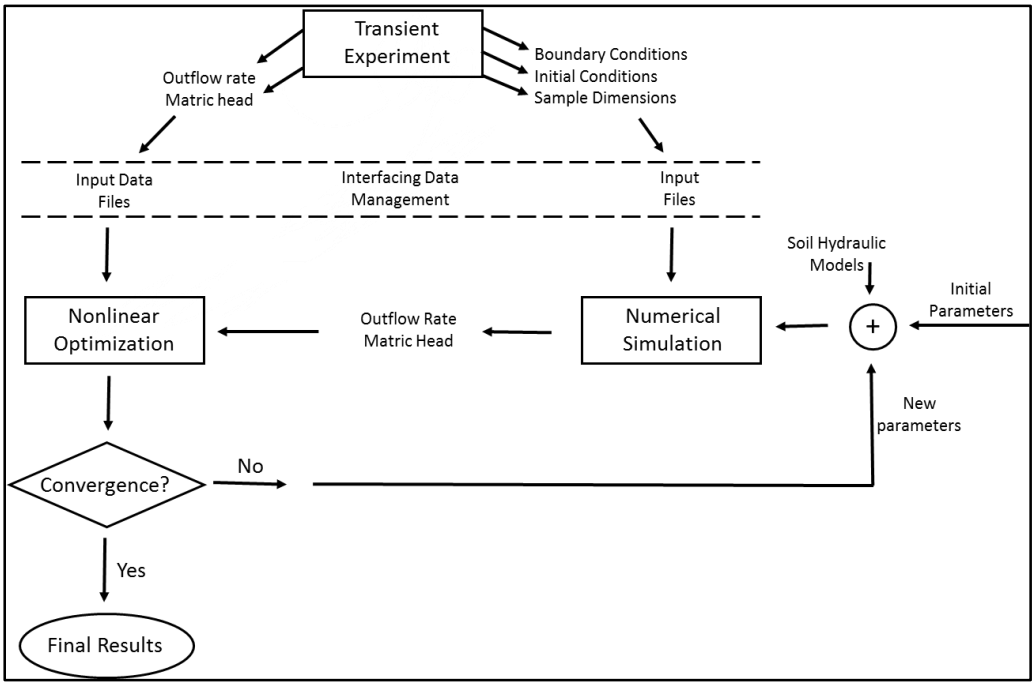

Figure 3.12. Flow chart of the inverse method

The van Genuchten (1980) soil hydraulic functions and the statistical pore-size distribution model of Mualem (1976) is used to define soil-water characteristic curves and hydraulic conductivity functions. The van Genuchten (1980) hydraulic model for drying state is expressed as:

$$S_e = \frac{\theta - \theta_r^d}{\theta_s^d - \theta_r^d} = \left[\frac{1}{1 + \left(\alpha^d (u_a - u_w)\right)^{n^d}}\right]^{m^d} \tag{3.10}$$

where θ_s^d is the saturated volumetric water content, θ_r^d is the residual volumetric water content, n is the pore-size distribution parameter, α is the inverse of air-entry pressure of the sample, and m equals $1 - 1/n^d$. The values m, n, and α are empirical fitting parameters used in the van Genuchten (1980)'s equation. The superscript d identifies drying state.

$$k^d = k_s^d \frac{\left\{1 - (\alpha^d * h)^{n^d - 1} * \left[1 + \left(\alpha^d (u_a - u_w)\right)^{n^d}\right]^{(1/2 - 1/2n^d)}\right\}^{(1-1/n^d)}}{\left[1 + \left(\alpha^d (u_a - u_w)\right)^{n^d}\right]^{(1/2 - 1/2n^d)}} \quad (3.11)$$

where k_s^d is the saturated hydraulic conductivity. These parameters are also depicted in Figure 3.15.

Upper and lower boundary conditions are defined as no flow on top and a specified pressure head at the bottom. Initial conditions are specified in terms of pressure heads and set to zero. The van Genuchten's closed form equation and the Mualem's fixed tortuosity parameter ($I = 0.5$) in conductivity function increases the uniqueness of optimized parameters by reducing the number of free parameter (Zurmühl and Durner 1996; Durner et al. 1999; Hopmans et al. 2002). The saturated volumetric water content (θ_s^d), which is also the porosity (n_p), of soil sample is independently calculated from the following equation:

$$n_p = 1 - \frac{m_s}{G_s * \rho_w * V_t} \quad (3.12)$$

where G_s is the specific gravity of sample, m_s is the mass of solids, V_t is the total volume of the specimen, and ρ_w is the density of water. Conversely, the saturated hydraulic conductivity (k_s^d) of the soil sample was measured from a hydraulic conductivity test using a flexible wall permeameter. An independently measured saturated hydraulic conductivity provide us an intuition into better estimating maximum and minimum initial constrains for an optimization process.

The objective function of the drying state was defined with at least 100 points. The inversed data set was weighted by standard deviation and the associated weighting coefficients for each point were equal to 1. After the minimum and maximum initial estimates are appropriately assigned, soil hydraulic properties such as residual volumetric water content (θ_r^d), fitting parameters (α^d, n^d), and saturated hydraulic conductivity (k_s^d) are determined as an output of inverse modeling. Wayllace and Lu (2012) recommend repeated optimization by narrowing the range between initial estimates and measured values.

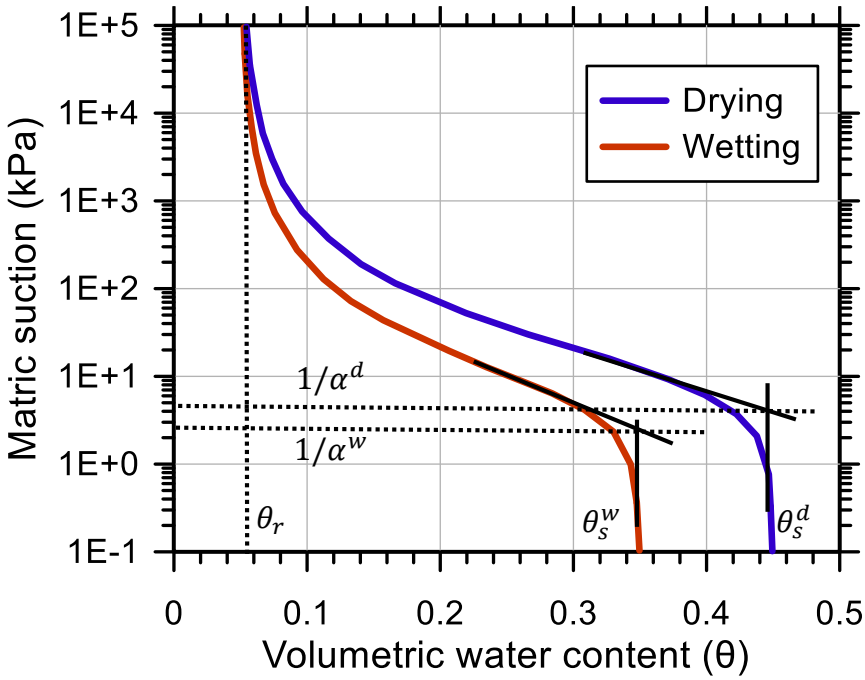

(a)

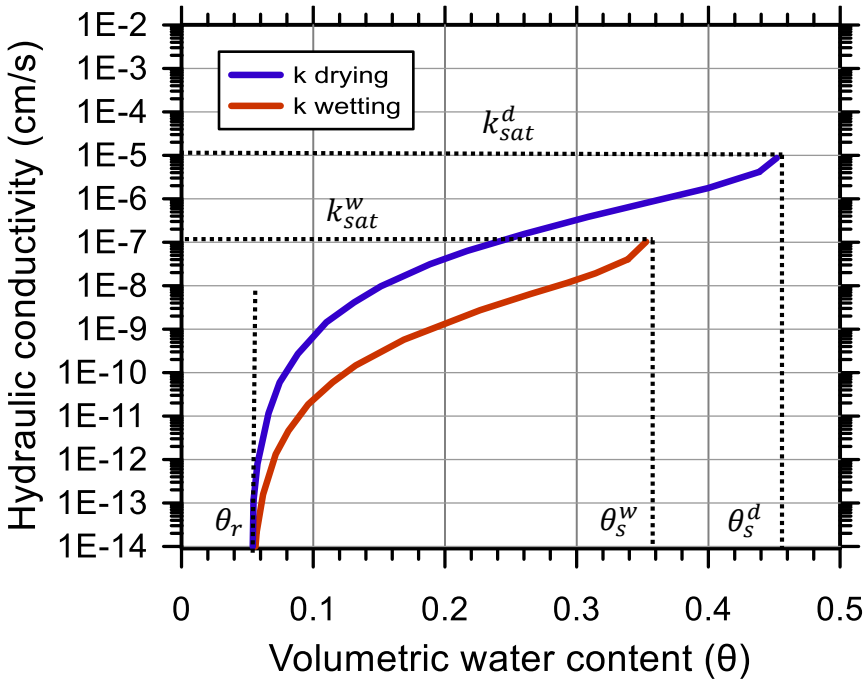

(b)

Figure 3.13. A graphical illustration of a) SWCC and b) HCF after Wayllace and Lu (2012)(with permission from ASTM International)

3.3.4. Inverse Modeling for Wetting State

Similar to the drying state, a one-dimensional flow for wetting state is modeled, which constitutes the soil sample and the ceramic stone. As indicated below, the Mualem (1976) and van Genuchten (1980) models are used to define hydraulic properties of soil;

$$S_e = \frac{\theta - \theta_r^w}{\theta_s^w - \theta_r^w} = \left[\frac{1}{1 + \left(\alpha^w (u_a - u_w)\right)^{n^w}}\right]^{m^w} \tag{3.13}$$

$$k^w = k_s^w \frac{\left\{1 - (\alpha^w * h)^{n^w - 1} * \left[1 + \left(\alpha^w (u_a - u_w)\right)^{n^w}\right]^{(1/2 - 1/2n^w)}\right\}^{(1 - 1/n^w)}}{\left[1 + \left(\alpha^w (u_a - u_w)\right)^{n^w}\right]^{(1/2 - 1/2n^w)}} \tag{3.14}$$

where the superscript w represents the wetting state. The same optimization algorithm is used to define soil hydraulic parameters ($\theta_s^w, \alpha^w, n^w, k_s^w$) in wetting state. These parameters are also graphically demonstrated in Figure 3.15. It is noted that, soil-water characteristic curves and hydraulic conductivity functions of drying and wetting states display a noticeable difference due to hysteresis phenomena. As a result of hysteresis, saturated water content and hydraulic conductivity for wetting states are lower compared to the drying states (Rassam and Williams 1999; Pham et al. 2005; Schneider et al. 2012).

Initial conditions for the wetting state are specified using the pressure head distribution at the completion time of drying state. Boundary conditions are specified as no water flow on top and a specified head at the bottom. The saturated hydraulic conductivity obtained through inverse modeling in wetting state is an equivalent hydraulic conductivity (k_{eq}) result of the entire system, including ceramic stone and soil sample. The saturated hydraulic conductivity of a soil sample is calculated using Darcy's law and the flow rate data at ($\theta = \theta_s^w$). The equivalent hydraulic conductivity equation given below considers the soil sample and ceramic stone as two individual horizontal layers with different thicknesses and hydraulic conductivities.

$$k_{eq} = \frac{l_s + l_c}{\frac{l_s}{k_s^w} + \frac{l_s}{k_s^c}} \quad 3.15$$

where k_s^c is the saturated hydraulic conductivity of the ceramic disk, l_s is the length of the soil sample, and l_c is the thickness of ceramic stone.

The objective function of wetting state was defined with at least 100 points. The inversed data set was weighted by standard deviation and the associated weighting coefficients for earlier data points were assigned between 0.5 and 1 for the remaining points. The residual volumetric water content for the wetting state is assumed to be equal to the residual volumetric water content obtained from the drying state. After the test is completed, the gravimetric water content of the sample is measured experimentally and then converted to volumetric water content that helps construct an initial estimate of saturated volumetric water content of a sample accurately for wetting state.

After the maximum and minimum initial estimates are appropriately assigned, soil hydraulic properties of wetting state such as saturated volumetric water content (θ_s^w), fitting parameters (α^w, n^w), and saturated hydraulic conductivity (k_s^w) are determined as an output of inverse modeling.

4. EXPERIMENTAL PROGRAM & DATA PROCESSING

4.1. Introduction

Transient Release and Imbibitions Method (TRIM) experimental set up is used to obtain SWCC and HCF. TRIM was presented and explained for the first time by Wayllace and Lu (2012). Since then, a few minor modifications have been made with respect to the testing apparatus. Currently, it appears that there is no available ASTM standard to assist this method either in testing program or data analysis. Besides TRIM tests, saturated hydraulic conductivity of specimens tested in TRIM was measured using a flexible wall permeameter. This chapter presents a detailed description of the entire laboratory testing program and data processing in cooperation with the HYDRUS-1D software program.

4.2. Experimental Program

4.2.1. TRIM Experimental Program

A brief description of TRIM components is required to understand the working mechanism of TRIM. The TRIM experimental program is explained in depth in this section.

4.2.1.1. Experimental Set Up and Machine Assembly

The machine assembly consists of 4 main components: the control panel, flow cell, effluent container and electronic balance, and a computer with an interface graphic software. The physical layout of the TRIM assembly with all components is shown in Figure 4.1.

4.2.1.1.1. Control Panel

The components of the control panel are grouped into 5 functions:

- A gage that displays the applied pressure in psi.
- Two air pressure regulators that are designed for low (0–15 kPa) and high (15–300 kPa) pressure ranges.
- A water reservoir that is used for the saturation of the thin water chamber underneath the ceramic stone, the bubble trap, and the plumbing.
- A bubble trap with one end connected to the line of flow cell and other end connected to the effluent container, and a vent cap on the top.

- Ports for vacuum, pressure and water supply to fill the water reservoir.

The component locations on the control panel are illustrated in the Figure 4.2.

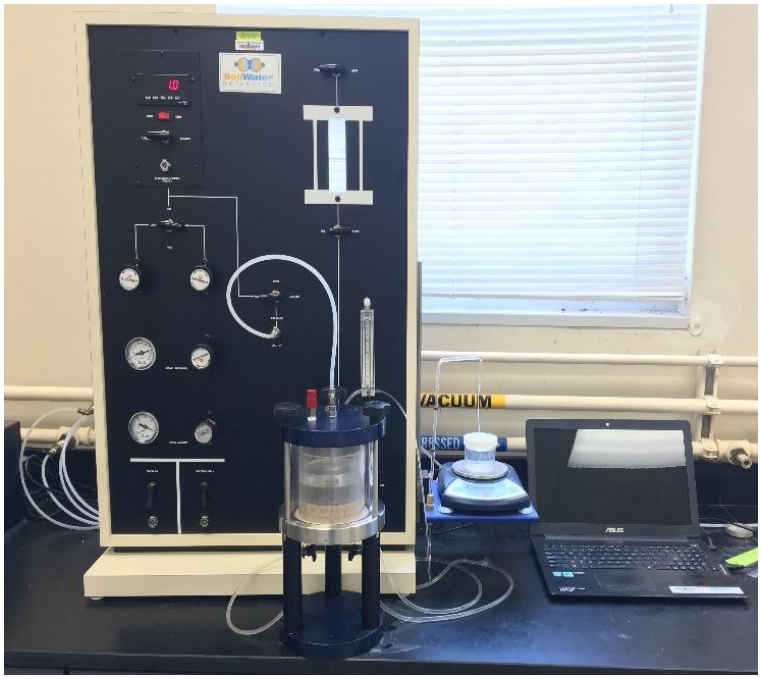

Figure 4.1. Physical layout of the TRIM assembly

4.2.1.1.2. Flow Cell

The flow cell is able to accommodate either undisturbed or remolded soil samples. It includes a ceramic stone, a circular O-ring, an aluminum cap, an acrylic wall for the soil sample, a stiff mesh, a spring top, and three threaded rods, as shown in Figure 4.3. The aluminum base of the flow cell hosts a small reservoir just under the ceramic stone, which has two separate outlets controlled with valves. The first outlet is connected to the water reservoir in the panel, the second outlet goes to the bubble trap and the effluent container. Vacuum and air pressure are applied through the top plate.

4.2.1.1.3. Effluent Container and Electronic Balance

A plastic water container and an electronic balance shown in Figure 4.4 are used to record water flow in or out of the soil sample. The electronic balance is capable of measuring 200 g with an accuracy of $\pm$0.01 g. A sliding board is attached to one side of the panel to allow adjusting of the

elevation of effluent container and electronic balance over the platform. The effluent container is filled with water in drying state and the accumulated water is supplied in wetting state.

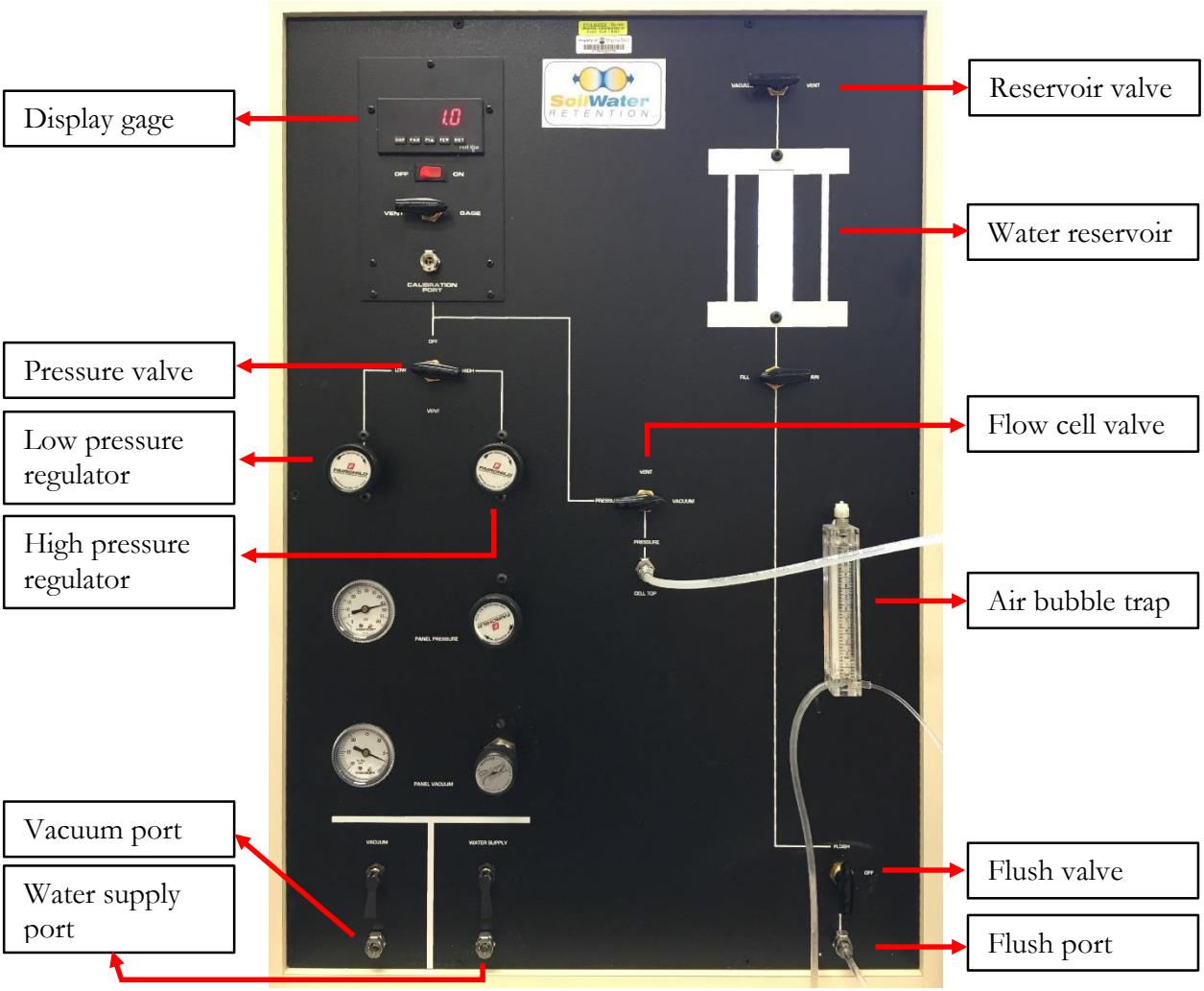

Figure 4.2. Control Panel and its main components

This water transportation in the effluent container is provided with a 1/16 in. tube that goes through a small hole (slightly larger than 1/16 in. diameter) in the middle of container lip to prevent evaporation.

Figure 4.3. Main components of flow cell

Figure 4.4. Effluent container and electronic balance

4.2.1.1.4. Software Interface: TRIM

The electronic balance is connected to the computer with a USB cable. A graphic interface software, called TRIM, logs and records the data throughout the test. Figure 4.5 shows the main screen of the TRIM data acquisition program, including a basic diagram of the hardware layout, a display of current balance reading, a graph of balance reading with time, a large "stop" button, and the path name of the data file on the progress. In addition, there are entry boxes on the main screen for air pressure, data logging intervals, and note to data file controlled by users. The applied air pressure and any specified comments for each state must be typed into their respective boxes at the beginning of each process. Data logging frequency for this experiment is set to 10 second intervals after any matric suction change on the soil sample. Once the process comes closer to the steady state, data logging intervals are increased to every 600 seconds.

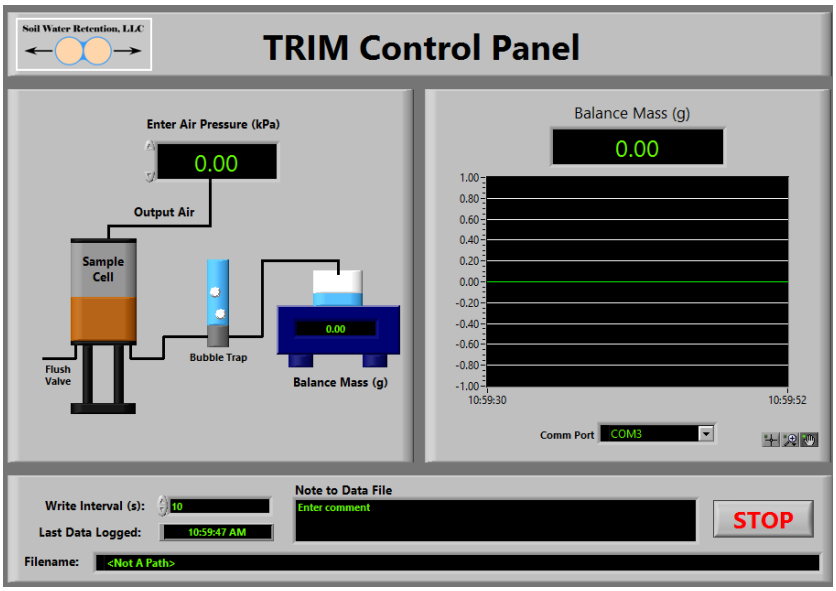

Figure 4.5. Main screen of the TRIM data acquisition program

4.2.1.2. HAE Ceramic Stone and System Saturation

Prior to testing, the entire system must be saturated, this includes the ceramic stone, the thin water chamber underneath the ceramic stone, the air bubble trap, and the tubing lines. In order to achieve system saturation, the water reservoir in the control panel should be filled with de-aired water. By positioning the water reservoir to "flush" and having both flow cell valves opened, the tubing, bubble trap and small reservoir underneath the ceramic stone are saturated. During this process, the

air bubble trap is filled with water up to the 0.5 ml position by opening the vent cap of the bubble trap. The next step is to achieve ceramic stone saturation in a glass desiccator or directly in the flow cell, basically both through the same concept. The way to saturate the ceramic stone in the flow cell used in the testing program, is to maintain a vacuum inside the flow cell at least for 24 hours when there is about 2 cm of ponded water on the ceramic stone. The ceramic stone is designed to withstand a full vacuum of 10 inches of mercury, this is the maximum recommended vacuum in the saturation phase.

4.2.1.3. Sample Preparation and Saturation

Prior to compaction, the soil was mixed with water to achieve the desired moisture content. The moistened soil was kept at least 16 hours to allow time for the soil particles to hydrate as recommended by ASTM Standard D698 (2003). The specimen of a given weight was prepared and dynamically compacted layer by layer in the acrylic mold to a target dry density (g/cm^3) or relative compaction (%) using a 1.4 inch diameter foot-tamper. The samples at low relative compaction levels were compacted directly into the flow cell. However, samples at high relative compaction levels were compacted outside the flow cell, then transferred to the flow cell because the ceramic stone could be damaged with hammer blows during compaction. For a good homogeneity and perfect compaction, the distribution of blows over the sample was carried out with great care. The final height reading of the sample is measured by using a digital caliper to the nearest 1000^{th} of an inch.

The saturation of samples is accomplished by applying vacuum on top of the sample while de-aired water in the effluent container flows through the ceramic stone to the sample. In order to diminish swelling or volume change in the sample, a stiff mesh and a spring is placed on top of the sample. To verify the full saturation of the sample, the sample weight and height, as shown in Figure 4.6, is measured after saturation. The amount of imbibed water to the sample must be equal to or slightly greater than the amount of water required to saturate the sample calculated through the known soil parameters such as porosity, sample volume, and initial moisture content.

4.2.1.4. Drying State Procedure

Drying state consists of two steps, these are the application of small and large suction increments. As mentioned in the Materials and Research Method chapter, the inverse modeling of drying state

takes into account the combination of data sets compiled from both steps. While the drying state is in progress, the ceramic stone and effluent container are always kept at the same level because a positive or negative pressure head is not requested.

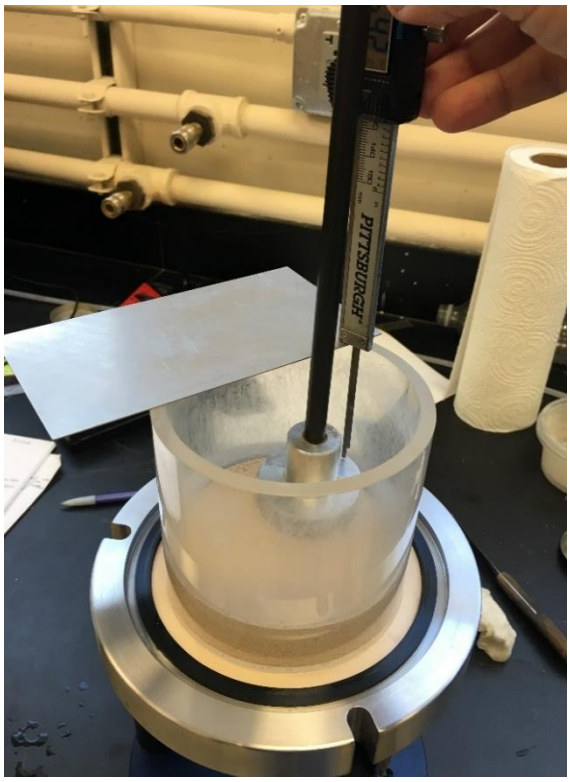

Figure 4.6. Height measurement of the specimen with a digital caliper

4.2.1.4.1. Application of Small Suction Increment

First, a small increment of air pressure, known as matric suction, slightly larger than the air-entry pressure should be applied to the soil sample. The small suction pressure in the range of 0 – 15 kPa is maintained by the low pressure regulator. The "small increment" must be written under the comment box. The great benefit of small suction process is approaching the air-entry pressure of soil samples closely by setting the pressure in particular levels. Wayllace and Lu (2012) recommends 1 to 2 kPa for sands and 6 to 8 kPa for silty materials, and it is common to increase these pressures in the presence of clay material. During the application of small suction increment, water outflow is recorded and monitored until near steady state conditions, when the water outflow rate is 0 or negligibly small. This step is usually completed in 24 hours.

4.2.1.4.2. Application of Large Suction Increment

The second and final step of the drying state is the application of large suction increment. Firstly, "Large increment" comment is typed into the note box. The magnitude of large suction pressure is limited by the air-entry pressure of ceramic stone. In our testing program, a 3 bar HAE ceramic stone is used so the maximum suction is always set to 290 kPa through the high pressure regulator. This suction increment is applied for about 48 hours and water outflow is monitored and recorded until getting to near steady state conditions.

4.2.1.5. Quantification of Diffused Air through Ceramic Disk

The proper execution of this step is significant in order to accurately measure the water mass changes on the electronic balance. At the end of the large suction step, some water in the tubes and small reservoir underneath the ceramic stone is displaced because of the air bubbles. Any diffused air must be quantified to precisely measure the volumetric water content of soil. As a comment, "flushing air bubbles" must be typed into the note box in the software. Flushing air bubbles is accomplished by turning on the flow cell valve connected to water reservoir. It is also recommended to tilt the flow cell on its side and gently tap to ensure all air bubbles are out of the TRIM system and locked in the air bubble trap, so that the system remains saturated just before the wetting state. The water level in the air bubble trap should be recorded before and after the drying state. The amount of diffused air is strongly related with the volume of soil and the air pressure applied. The application of 290 kPa air pressure for 48 hours often ends up with between 1 to 3 cm^3 of diffused air. It is presumed that the rate of diffused air (g/g) is constant for drying state, and is calculated by dividing the volume of diffused air by the water mass change during the drying state. The constant rate of diffused air is a required parameter to calculate the real outflow data in the inverse modeling afterwards. The processing time for this step is approximately 20 minutes.

4.2.1.6. Wetting State Procedure

All diffused air is removed from the system in the previous step, and now the electronic balance is reset to zero. Air pressure is decreased to zero and then flow cell is vented to the atmosphere. The comment "wetting" must be typed into the note box. Once the matric suction is zero, the high suction potential of the soil specimen claims the water back from the effluent container and water flows into the flow cell through the ceramic stone until equilibrium is reached. Likewise, in the drying state process, the mass of water inflow is monitored and stored. If requested, a positive

hydraulic gradient is created at the bottom of the soil sample by elevating the effluent container on the electronic balance relative to the flow cell. If a positive pressure head is not preferred, they are always kept at the same level. By doing so, the bottom boundary condition (the pressure head at the base of ceramic stone) for wetting state is assumed to be 0. The only drawback of this choice might be a slight rise in the completion time of the wetting state process. The rate of water inflow to the sample is at first larger, and as the total head distribution is constant, steady state conditions are reached. Depending on the soil type and the volume of the specimen, the completion of this step may take 24 to 48 hours. The testing time required to complete each step is compiled in Table 4.1.

Table 4.1. Time required to complete TRIM testing program

Step	Time Required (h)
Specimen preparation	2 - 4
Saturation of the system and ceramic stone	24
Specimen saturation	6 - 12
Application of small suction increment	12 - 24
Application of large suction increment	48
Quantification of diffused air	0.4
Application of wetting conditions	24 - 48
Total	122 - 146

4.2.2. Hydraulic Conductivity Experimental Program

Another aim is to measure the saturated hydraulic conductivity of the samples tested in TRIM. Unfortunately, the same test specimens cannot be used for both TRIM and hydraulic conductivity tests. Identical TRIM samples at the same water contents, and the relative compactions were prepared separately for hydraulic conductivity tests. The relative compaction of samples changed at the end of the test. Due to this reason, instead of focusing on a particular relative compaction, a series of tests were performed at different relative compactions and an approximate curve was obtained for each soil.

4.2.2.1. Overview of the Flexible Wall Hydraulic Conductivity Method

Laboratory determinations of hydraulic conductivity for materials with a hydraulic conductivity less than or equal to 10^{-3} cm/s, are usually performed in a flexible wall permeameter. Flexible-wall permeameters were used according to these methods described in ASTM D5084 (2010). Flexible wall permeability tests were performed in modified triaxial cells. Interchangeable base pedestals and top caps permit the testing of specimens with diameters between 1.4 and 4 inches. Double drainage lines to both the top and the bottom of the specimen facilitate the flushing of air bubbles from hydraulic lines. Separate pressure controls maintain the cell pressure and the two pressures acting on the ends of the soil specimen. The flexible-wall permeameter provides some advantages over rigid-wall permeameters, for example, side-wall leakage does not occur (Lin and Benson 2000; Shackelford et al. 2000). This measurement method is most commonly used for commercial and research compatibility testing. Figure 4.7 shows the flexible-wall permeameter assembly used in the laboratory.

4.2.2.2. Sample Preparation

All samples were prepared using the preparation method commonly known as moist tamping. When using this method each sample is prepared at a specific water content. First, vacuum grease is applied to the bottom platen and a rubber membrane is placed over it. The two pieces of vacuum mold and membrane are positioned over the bottom platen. Filter paper is inserted between the mold and membrane to distribute the vacuum throughout the interior surface of the mold. Once the filter paper is in place, the top of the membrane is flipped over the top edge of the mold and vacuum is applied. The membrane lies smoothly and tightly against the surface of the mold. Figure 4.8 shows the complete set-up just before the compaction. A sample with a given weight was prepared and dynamically compacted layer by layer in the mold to a target density using a 1.4 inch diameter foot-tamper. Almost all samples were compacted in 4 layers and the approximate final height and diameter dimensions were 2" x 2.8" (51 x 71 mm). A slight pressure of vacuum was applied to the sample along the top platen in order to keep the whole sample together without distortion. The split mold was then carefully removed, and the specimen height and diameter were measured by using digital calipers and a pi tape.

4.2.2.3. Sample Saturation and Isotropic Consolidation

The pressure cell was filled with water and pressurized by a minimal cell pressure. Tap water was used for the saturation and permeation process. The drainage lines were flushed until no air bubbles were visible. For the specimens having a degree of saturation less than about 85%, ASTM D5084 offers an aid option to saturation process, called specimen soaking. Only the mixture samples in this project was subjected to this soaking stage. The specimens were soaked under partial vacuum applied to the top of the specimen in an attempt to purge air from the soil.

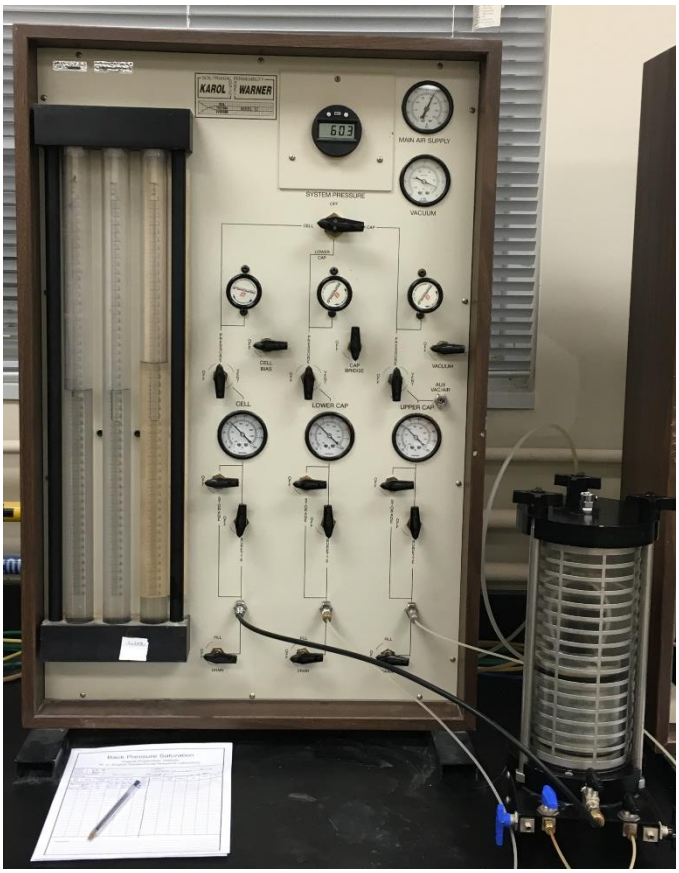

Figure 4.7. Pressure panel and permeameter

A back-pressure was applied to all the specimens using the permeant water at a particular effective stress to achieve a Skempton's coefficient (B) value of at least 0.95. A pressure transducer was also used to measure pore-water pressure response during the application of back-pressure. The pressure transducer system was not used in our testing program. In order to ensure full saturation of samples, the back pressure was often increased up to 60 psi, and headwater and tailwater burettes were

monitored when the change in the burettes corresponded to one back pressure increment of 0.1 ml or less. It is assumed that after a few days of back pressuring, any trapped air occupies volume too small to be considered. The back pressure and consolidation phases were generally completed concurrently.

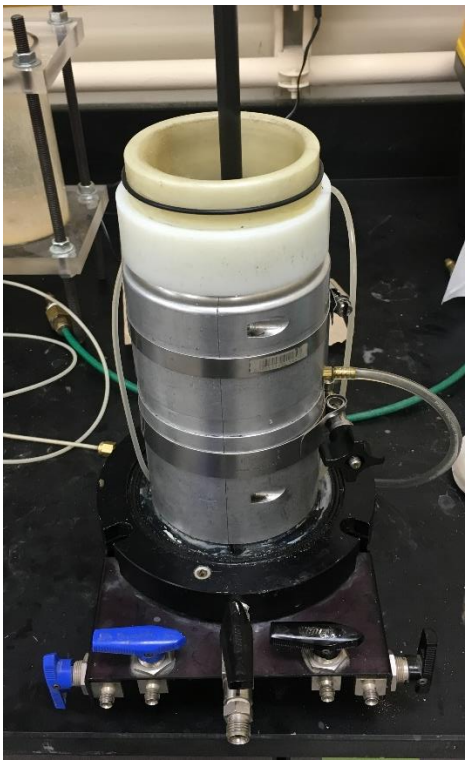

Figure 4.8. Compaction mold set-up

4.2.2.4. Permeation

The hydraulic conductivity testing followed Test Method C of ASTM D5084, which consists of falling headwater level and increasing tailwater level. In this case, headwater and tailwater are called inflow and outflow, respectively. Measuring from the downward flow is not favorable because they generally result in slightly smaller k values than actual (Bandini and Sathiskumar 2009). Tailwater flow was induced by applying a small back pressure differential between the bottom and top of the specimen. For each test, a hydraulic gradient was specified under the guidance of ASTM D5084. The quantity of inflow and outflow was recorded periodically. The tests were allowed to continue until hydraulic conductivity was steady and inflow and outflow rates were equal. The standard states for the inflow/outflow ratio of the permeameter should be in the range of 0.75 to 1.25. Once the

hydraulic conductivity was terminated, the permeameter was disconnected from the pressure panel. The height and diameter of the final specimen was measured. The specimen was oven dried and then the moisture content of sample was determined.

4.3. Data Processing

Many software packages are currently available that can simulate flow and transport in one-dimension (e.g., HYDRUS-1D, HP1, SOILCO2, and UNSATCHEM). These programs simulate the water flow in a relatively similar manner, different solute transport modules exist in the different codes (Šimůnek et al. 2007). This section summarizes a description of data processing following the test.

4.3.1. Hydrus-1D Software Program

Hydrus 1D is a Microsoft-based software package used to analyze one dimensional water flow, heat, and solute transportation in unsaturated, partially saturated or fully saturated porous media (Šimůnek et al. 2008a). All results presented in this thesis are obtained with the cooperation of the Hydrus-1D program that uses linear finite elements to numerically solve Richards' equation for saturated-unsaturated water flow. Hydrus-1D permits the use of five different mathematical models suggested by Brooks and Corey (1964), van Genuchten (1980), Vogel and Cislerova (1988), Kosugi (1996), and Durner (1994).

The program implements the Levenberg-Marquardt optimization algorithm to inversely predict unsaturated soil hydraulic properties for drying and wetting states, individually (Inoue et al. 2000). The Levenberg-Marquardt optimization curve-fitting method is basically a combination of the Gauss-Newton method and the gradient descent method to minimize the sum of the weighted squares of the errors between measured [$\hat{q}_d{}^{exp}\ (l,t)$ for drying state, and [$\hat{q}_w{}^{exp}\ (l,t)$ for wetting state] and curve-fitting functions [$\hat{q}_d\ (l,t)$ for drying state, and $\hat{q}_w\ (l,t)$ for wetting state]. The Levenberg-Marquardt method practices the gradient-descent method where there is large deviation between the measured and calculated solutions. When the solution calculated is close to the measured solution, it practices the Gauss-Newton method (Lourakis 2005; Gavin 2016).

Date	Time	Notes	Mass (g)	Uair (kPa)
6/30/2015	11:29:20 AM	small increment	0	15
6/30/2015	11:29:30 AM	small increment	0.66	15
6/30/2015	11:29:40 AM	small increment	1	15
6/30/2015	11:29:50 AM	small increment	1.13	15
6/30/2015	11:30:00 AM	small increment	1.19	15
6/30/2015	11:30:30 AM	small increment	1.4	15
6/30/2015	11:31:00 AM	small increment	1.48	15
6/30/2015	11:31:30 AM	small increment	1.58	15
6/30/2015	11:32:00 AM	small increment	1.66	15
6/30/2015	11:32:30 AM	small increment	1.76	15
6/30/2015	11:33:00 AM	small increment	1.88	15
6/30/2015	11:33:30 AM	small increment	1.99	15
6/30/2015	11:34:00 AM	small increment	2.1	15
6/30/2015	11:34:30 AM	small increment	2.21	15
6/30/2015	11:35:00 AM	small increment	2.31	15

Figure 4.9. A screen shot from the file of logged data

Parameter No.	Parameter Name in HYDRUS-1D	Input Value by the User	Hydrus window name for Jirka
1	State	drying	new parameter
2	Porosity	0.42	new parameter
3	Diameter D (cm)	10.16	new parameter
4	Sample (material 1) Height (cm)	7.62	new parameter
5	Ceramic (material 2) Thickness (cm)	0.3175	new parameter
6	Rate of Diffused Air Dair (g/g)	0.09	new parameter
7	Saturated k (cm/sec)	2.5e-05	new parameter
8	Minimum Qr	0.02	Water Flow Parameters, Material 1
9	Maximum Qr	0.12	Water Flow Parameters, Material 1
10	Minimum Qs	0.42	Water Flow Parameters, Material 1
11	Maximum Qs	0.42	Water Flow Parameters, Material 1
12	Minimum Alpha (1/cm)	0.015	Water Flow Parameters, Material 1
13	Maximum Alpha (1/cm)	0.1	Water Flow Parameters, Material 1
14	Minimum n	1.5	Water Flow Parameters, Material 1
15	Maximum n	2.5	Water Flow Parameters, Material 1
16	Minimum Ks (cm/sec)	2.5E-06	Water Flow Parameters, Material 1
17	Maximum Ks (cm/sec)	2.5E-04	Water Flow Parameters, Material 1
18	HAE Stone (Initial Estimate) Qr	0.07	Water Flow Parameters, Material 2
19	HAE Stone (Initial Estimate) Qs	0.34	Water Flow Parameters, Material 2
20	HAE stone (Initial Estimate) alpha	0.00015	Water Flow Parameters, Material 2
21	HAE Stone (Initial Estimate) n	7	Water Flow Parameters, Material 2
22	HAE Stone (Initial Estimate) Ks	2.50E-07	Water Flow Parameters, Material 2

Figure 4.10. A screen shot from "TRIM parameters" file

To start data processing, the logged file data recorded with the TRIM software during the test and the file with the name of "TRIM parameters", which contains information of the soil and ceramic stone used, are both required. They also must be located in the same folder. Figure 4.9 shows an example of the logged data recorded in a text file which has five columns: 1) date, 2) time, 3) notes (delivered comments), 4) water mass measured by the electronic balance, and 5) air pressure applied to the flow cell. The other file of "TRIM parameters" includes 22 parameters total, belonging to the soil and the ceramic stone, as seen in Figure 4.10. "Material 1" and "Material 2" refer to the soil sample and the ceramic stone respectively. The porosity, diameter, height, saturated hydraulic conductivity of soil sample, the predetermined water flow parameters of ceramic stone, and the calculated rate of diffused air are defined in that file.

4.3.2. Data Processing for Drying State

The Hydrus-1D program has an additional feature that can read the data output of TRIM tests. The file of logged data is converted for an inverse solution. Before running the program, some configurations must be applied such as hydraulic model, and upper and lower boundary conditions. These issues are explained in further depth in the research method section.

After running the simulation, a window screen will appear showing the different iterations for inverse modeling, as shown in Figure 4.11. This iterative process continues until a satisfactory degree of convergence is obtained such as when two successive iteration solutions differ less than the specified water and pressure head tolerance (Šimůnek et al. 2006). Almost all iterations were constructed on the assumption of a water content tolerance at 0.01 and head tolerance at 1 cm. The program also allows changing the maximum number of iterations during any time step. This option was set to 100.

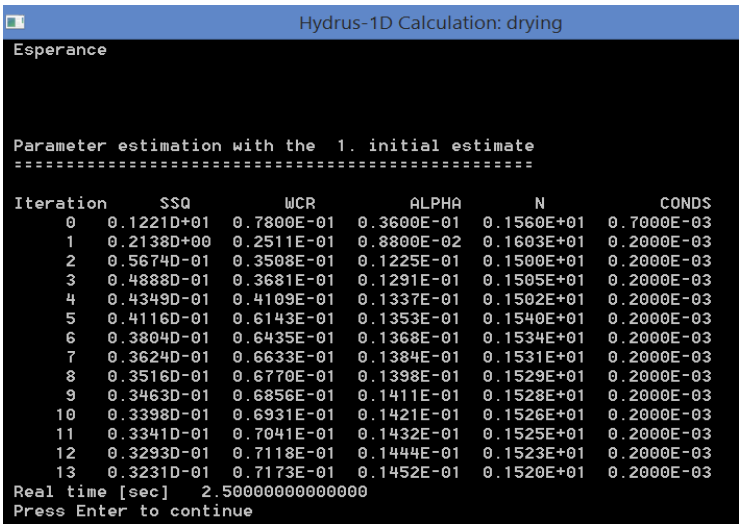

Figure 4.11. Window showing different iterations for inverse modeling at drying state

After the application has run, the results appear in the "Post-processing window". The modeled data must follow a similar trend with the objective function (experimental data). The comparison is checked by generating the graph "time" as a function of "cumulative bottom flux", as shown in Figure 4.12. The hollow circles and smooth line represent the experimental and modeled data, respectively. If the experimental data covers a narrow range of soil water contents or exhibits a considerable scatter relative to the modeled data, the specified maximum and minimum values under

the water flow parameters-material 1 window (Figure 4.13) must be updated before rerunning the program. It is also important to select meaningful initial estimates because Hydrus does not accept initial estimates that are out of the range.

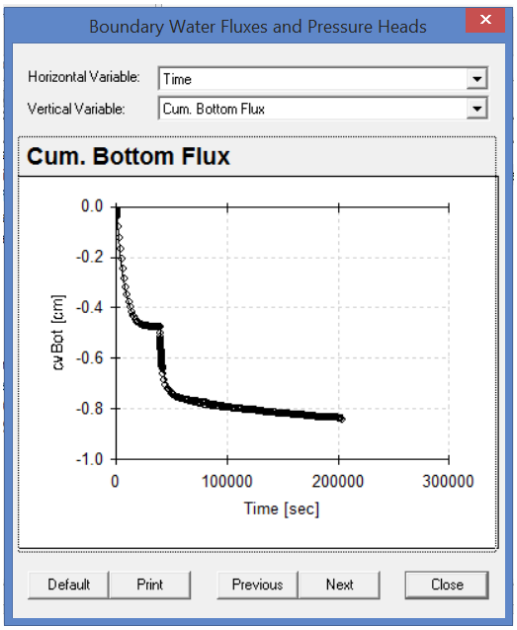

Figure 4.12. Plot comparing experimental and modeled data

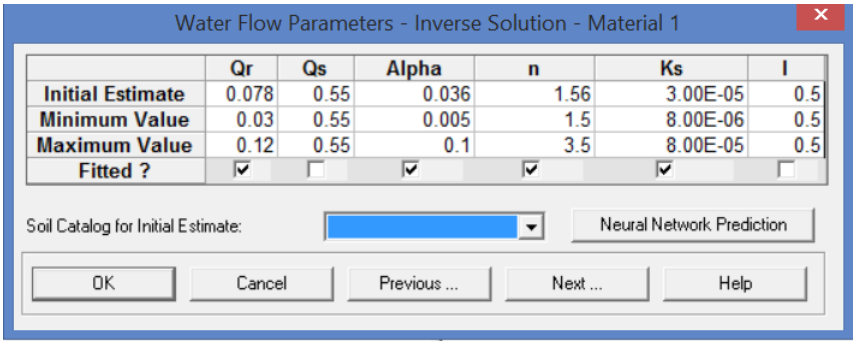

Figure 4.13. Water flow parameters of sample at drying state

The final estimates of the soil hydraulic parameters as a result of the inverse model; including the error of estimation, the confidence interval, the regression coefficient, and the final best fit, among other results are found under the "Inverse Solution Information" section (Figure 4.14).

4.3.3. Data Processing for Wetting State

Data processing for wetting state has a similar procedure as followed in data processing for drying state. First, residual volumetric water content ($\theta_r^d = \theta_r^w$) was updated with the value obtained from drying state. Next, the minimum and maximum value for saturated volumetric water content (θ_s^w) at wetting state was updated in consideration of the volumetric water content (the conversion of gravimetric water content to volumetric water content) obtained experimentally after wetting state was finished. Finally, fitting parameters (α, n) and saturated hydraulic conductivity (k_s^w) initial estimates, and maximum and minimum possible values were updated. As seen in Figure 4.15, the parameters that are checked for the "fitted" category are the parameters that are going to be iteratively optimized.

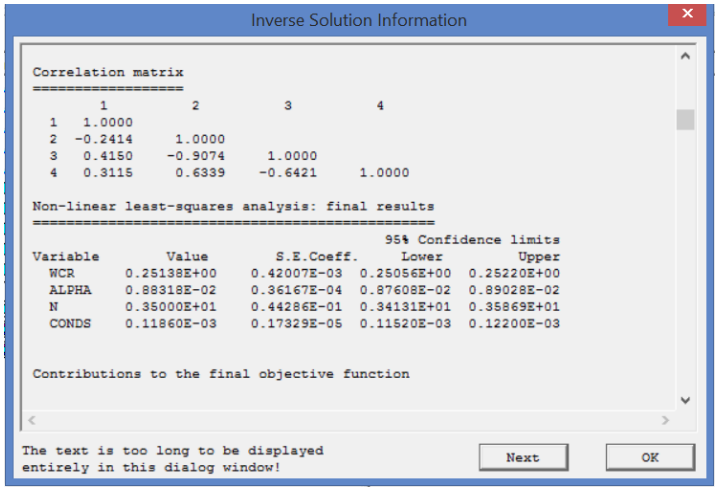

Figure 4.14. Final results of the drying state iteration

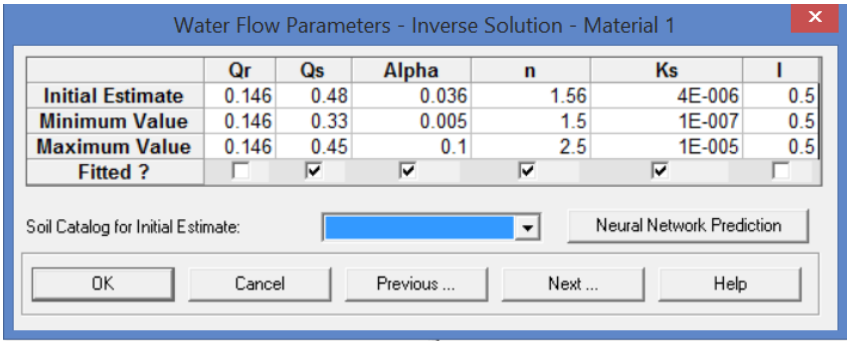

Figure 4.15. Water flow parameters of sample at wetting state

The initial conditions of the wetting state must be updated with the pressure head distribution of the last time step during drying state. The data with pressure head distribution obtained from the drying state was copied and then pasted into the soil profile summary window of wetting state, shown in Figure 4.16. The last head value was set to 0, that is the boundary condition applied to the system.

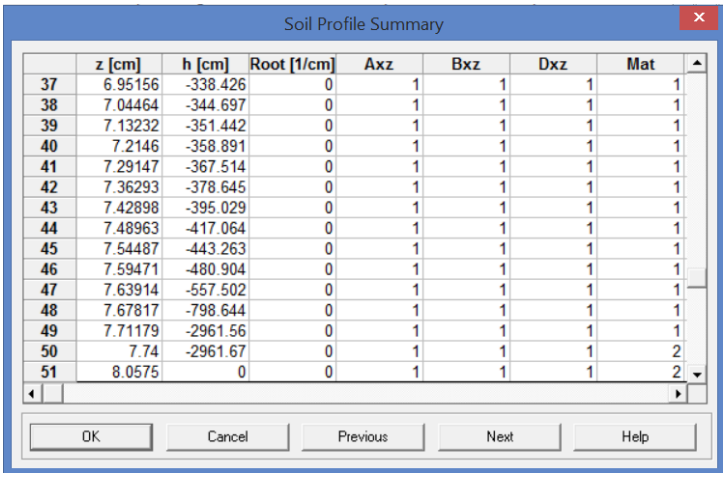

	z [cm]	h [cm]	Root [1/cm]	Axz	Bxz	Dxz	Mat
37	6.95156	-338.426	0	1	1	1	1
38	7.04464	-344.697	0	1	1	1	1
39	7.13232	-351.442	0	1	1	1	1
40	7.2146	-358.891	0	1	1	1	1
41	7.29147	-367.514	0	1	1	1	1
42	7.36293	-378.645	0	1	1	1	1
43	7.42898	-395.029	0	1	1	1	1
44	7.48963	-417.064	0	1	1	1	1
45	7.54487	-443.263	0	1	1	1	1
46	7.59471	-480.904	0	1	1	1	1
47	7.63914	-557.502	0	1	1	1	1
48	7.67817	-798.644	0	1	1	1	1
49	7.71179	-2961.56	0	1	1	1	1
50	7.74	-2961.67	0	1	1	1	2
51	8.0575	0	0	1	1	1	2

Figure 4.16. Soil profile summary window

After the simulation has successfully completed, the results appear in the "Post-processing window". The modeled and experimental data are compared by generating the graph "time" as a function of "cumulative bottom flux", as shown in Figure 4.18.

The final estimates of the soil hydraulic parameters, as a result of inverse model are found under "Inverse Solution Information" in the final results section, as shown in Figure 4.19. Hydraulic properties of soil sample for both drying and wetting conditions are now obtained.

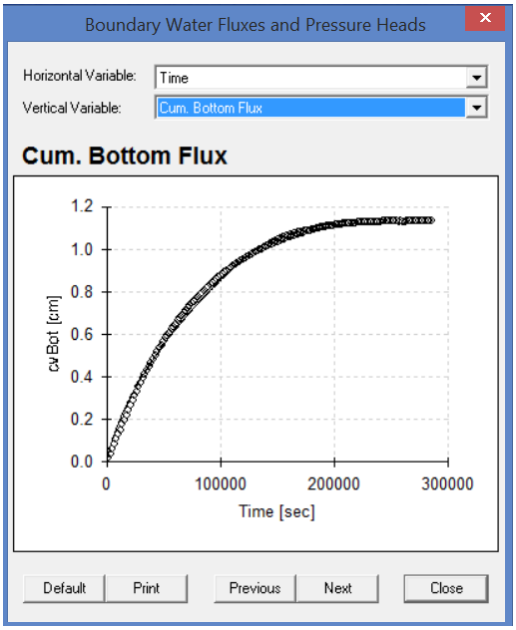

Figure 4.17. Plot comparing experimental and modeled data

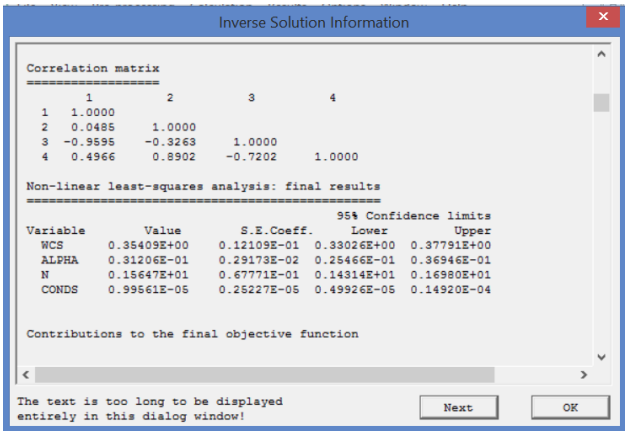

Figure 4.18. Final results of wetting state iteration

5. RESULTS & DISCUSSION

5.1. Introduction

This chapter presents the analysis of all test results obtained from TRIM and saturated hydraulic conductivity tests. The chapter also discusses the importance of separate hydraulic conductivity test results at the data processing stage. A TRIM test result and some saturated hydraulic conductivity test results are given for discussion. The graphs and tables are used in this chapter to summarize findings.

5.2. TRIM Tests

A total of 31 TRIM tests were performed for 5 types of soils at varied densities and molding water contents. In order to confirm the TRIM's applicability for a wide-range of soil types, and to understand the effects of kaolin clay content, three more tests were added to the schedule, 1 test on Play sand and 2 tests on Wilco LPC kaolin clay. All TRIM tests are summarized in Table 5.1. For each test, SWCC, HCF, mass water outflow, matric suction, and experiment and model data output plots are prepared to present the results. Also, the figures for all tests are gathered in Appendix A.

As an example, the test process of TRIMSC07 is explained in detail here. The test material of Stroubles Creek soil was previously classified as fat clay (CH). A few days before the test, the soil sample was molded at 19.60% water content (3% under the optimum water content). The test sample TRIMSC07 had a target dry density around 1.40 g/cm^3. The sample was initially compacted slightly over the target dry density, which is 1.42 g/cm^3 and placed directly into flow cell for saturation. During saturation, the air voids were filled with water. As a result of swelling, the actual final dry density after saturation process was calculated as 1.35 g/cm^3. The final volumetric water content was determined as 0.481 (cm^3/cm^3), with a total volume of 180.26 cm^3. After the sample was saturated, a suction of 3 kPa slightly above the air-entry value of soil sample was applied for 576 minutes resulting in a decrease of volumetric water content from 0.481 to 0.472 (4.01g of water release). A larger suction increment of 290 kPa was then applied for about 44 hours and resulted in around 44.20 g of water outflow. The large suction step reduced the volumetric water content to 0.227. The diffused air volume measured during drying conditions was 2.45 cm^3. Thus, the rate of diffused air (g/g) was calculated as 0.051.

Table 5.1. Summary of conducted TRIM tests

Soil Name	Molding Water Content (%)	Test No.	Test Ref.	Dry Density Before Saturation (g/cm^3)	Dry Density After Saturation (g/cm^3)	Std. Proctor Relative Compaction (%)
Stroubles Creek	19.60% (w_{opt} -3)	28	TRIMSC07	1.42	1.35	86.78
		4	TRIMSC03	1.35	1.30	83.96
	22.60% (w_{opt})	5	TRIMSC04	1.41	1.37	88.52
		3	TRIMSC02	1.24	1.23	79.22
	25.60% (w_{opt} +3)	R15	TRIMSC06	1.42	1.40	90.32
		7	TRIMSC05	1.33	1.32	85.15
Whitehorne	27.70% (w_{opt} -2)	27	TRIMWH11	1.35	1.32	96.09
		9	TRIMWH10	1.12	1.15	86.43
		R1	TRIMWH01	1.05	1.05	76.49
	29.70% (w_{opt})	R2	TRIMWH04	1.24	1.24	89.86
		1	TRIMWH06	1.07	1.05	76.62
	31.70% (w_{opt} +2)	6	TRIMWH09	1.34	1.33	96.41
		2	TRIMWH07	1.07	1.07	77.95
Tom's Creek	15.70% (w_{opt} -2.5)	8	TRIMTC06	1.65	1.60	94.21
		17	TRIMTC09	1.52	1.50	88.46
		13	TRIMTC08	1.42	1.40	82.52
	18.70% (w_{opt} +0.5)	10	TRIMTC07	1.60	1.58	93.16
		22	TRIMTC10	1.53	1.54	90.64

Soil Name	Molding Water Content (%)	Test No.	Test Ref.	Dry Density Before Saturation (g/cm^3)	Dry Density After Saturation (g/cm^3)	Std. Proctor Relative Compaction (%)
		24	TRIMTC11	1.40	1.40	82.62
Sand-Clay mix (75%-25%)	8.40% (w_{opt} -2)	20	TRIMM7X03	1.89	1.89	94.64
		12	TRIMM7X01	1.79	1.82	90.94
	9.90% (w_{opt} -0.5)	25	TRIMM7X05	1.83	1.85	92.19
		29	TRIMM7X06	1.71	1.70	84.56
	11.40% (w_{opt} +1)	21	TRIMM7X04	1.89	1.87	93.22
		16	TRIMM7X02	1.81	1.83	91.27
Sand-Clay mix (85%-15%)	8.10% (w_{opt} -1.3)	19	TRIMM8X04	1.86	1.83	94.34
		11	TRIMM8X01	1.70	1.74	89.72
	9.40% (w_{opt})	26	TRIMM8X05	1.83	1.81	93.63
		30	TRIMM8X06	1.71	1.69	87.25
	11.10% (w_{opt} +1.7)	18	TRIMM8X03	1.87	1.82	94.02
		14	TRIMM8X02	1.72	1.67	86.15
Play Sand	0	31	TRIMPS01	1.60	1.59	91.84
Wilco LPC Kaolin Clay	23.50% (PL)	32	TRIMKC01	1.31	1.26	-
		35	TRIMKC02	1.18	1.15	-

Data for the wetting state were obtained by applying matric suction to 0, which was accomplished by reducing the air pressure to 0 kPa and maintaining the effluent container on the balance and the ceramic stone in the flow cell at the same level. During the wetting state, a total of 35.84 g of water flowed into the sample. The wetting state was completed in about 27.5 hours. The mass water outflow and matric suction through these states are given in Figure 5.1. The transient water flow data for this test were used as the objective functions in inverse modeling to identify unsaturated hydraulic properties. As indicated in the previous chapter, cumulative bottom flux versus time plots and data generated by Hydrus-1D are used to confirm how well the experimental data fit the model. For a better demonstration, cumulative bottom flux data output for both states were converted to volumetric water content versus time data and plots. Figure 5.2 displays the change in volumetric water content of the soil sample as a function of time for both drying and wetting conditions; the dash lines are experimental data and the smooth blue lines are the predicted by the model. The objective functions were well fitted with the simulations, providing excellent inverse modeling results in parametric identifications. While setting up the inverse modeling, these considerations were taken into account:

(1) The lower limit for air-entry value was assigned to 2 kPa and the upper limit was set to 10 kPa. The air-entry value obtained for drying conditions was used as the maximum value while setting up the inverse modeling air-entry value parameter limits for wetting state.

(2) The lower and upper values for saturated hydraulic conductivity were assigned in terms of flexible-wall hydraulic conductivity test results of FXSC40 and FXSC10. The FXSC40 and FXCS10 provide a saturated hydraulic conductivity result for Stroubles Creek soil at 1.37 g/cm^3 and 1.33 g/cm^3 dry densities, respectively. For this TRIM sample at 1.35 g/cm^3 dry density, the test results can be used as upper and lower limits. The saturated hydraulic conductivity results of TRIMSC10 and TRIMSC40 were found to be 1.80E-05 cm/s (for maximum value) and 7.70E-06 cm/s (for minimum value), respectively. The saturated hydraulic conductivity of TRIM sample for drying state was calculated as 1.30E-05 cm/s after the inverse modeling simulation. As known, the hydraulic conductivity reduces as the water content reduces. Therefore, saturated hydraulic conductivity value must be less than 1.30E-05 cm/s, where k_{sat} of the wetting state is lower than k_{sat} of the drying state. The saturated hydraulic conductivity for wetting state was calculated as 9.50E-06 cm/s.

(3) The pore-size distribution value (n) is generally low for fine material samples. Therefore, n value was constrained between 1.5 and 2.0. The pore-size distribution results for drying and wetting states are 1.638 and 1.605, respectively.

(4) The experimentally measured gravimetric water content of the soil sample after the test was 32.5% and then converted to volumetric water content, calculated as 0.437, so the saturated volumetric water content was constrained to a narrow range close to this value.

Table 5.2 lists van Genuchten parameters for saturated hydraulic conductivity values of drying and wetting states for the TRIMSC07 identified by the inverse modeling analysis. The corresponding SWCC and HCF with the obtained soil parameters are shown in Figure 5.3. The hydrological soil properties obtained from inverse modeling for the rest of the tests are gathered in Tables 5.3-5.9.

Table 5.2. Hydrologic soil properties obtained from inverse modeling for TRIMSC07 (Stroubles Creek – 3% dry of optimum)

Molding Water Content (%)	Test No.	Test Ref.	State	θ_s	θ_r	α (1/kPa)	n	k_{sat} (cm/s)
19.60% (w_{opt} -3)	28	TRIMSC07	Drying	0.481	0.126	0.133	1.638	1.30E-05
			Wetting	0.440	0.126	0.217	1.605	9.50E-06

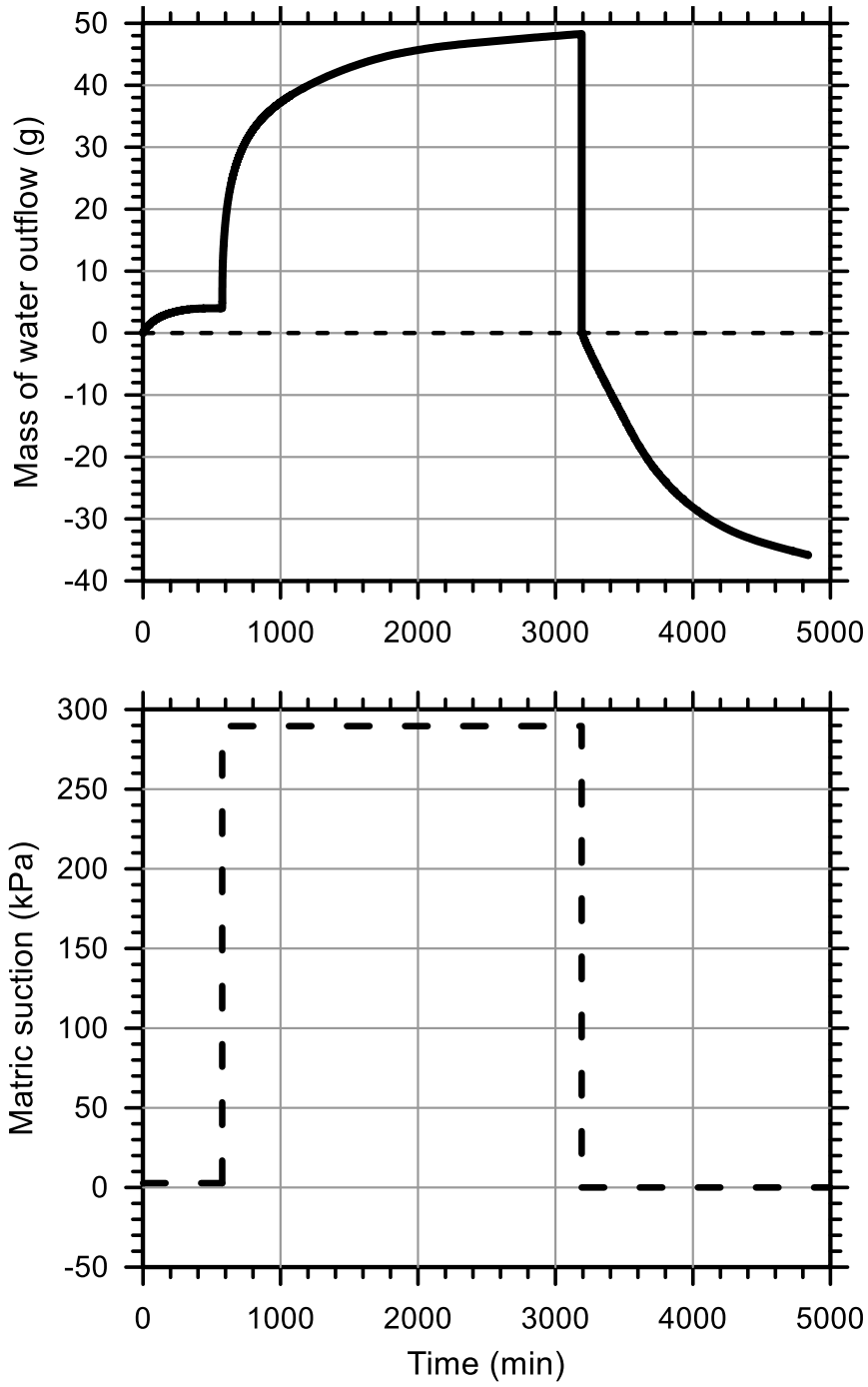

Figure 5.1. Transient water flow data and matric suction obtained from TRIMSC07 (Stroubles Creek - 3% dry of optimum) with complete drying and wetting states

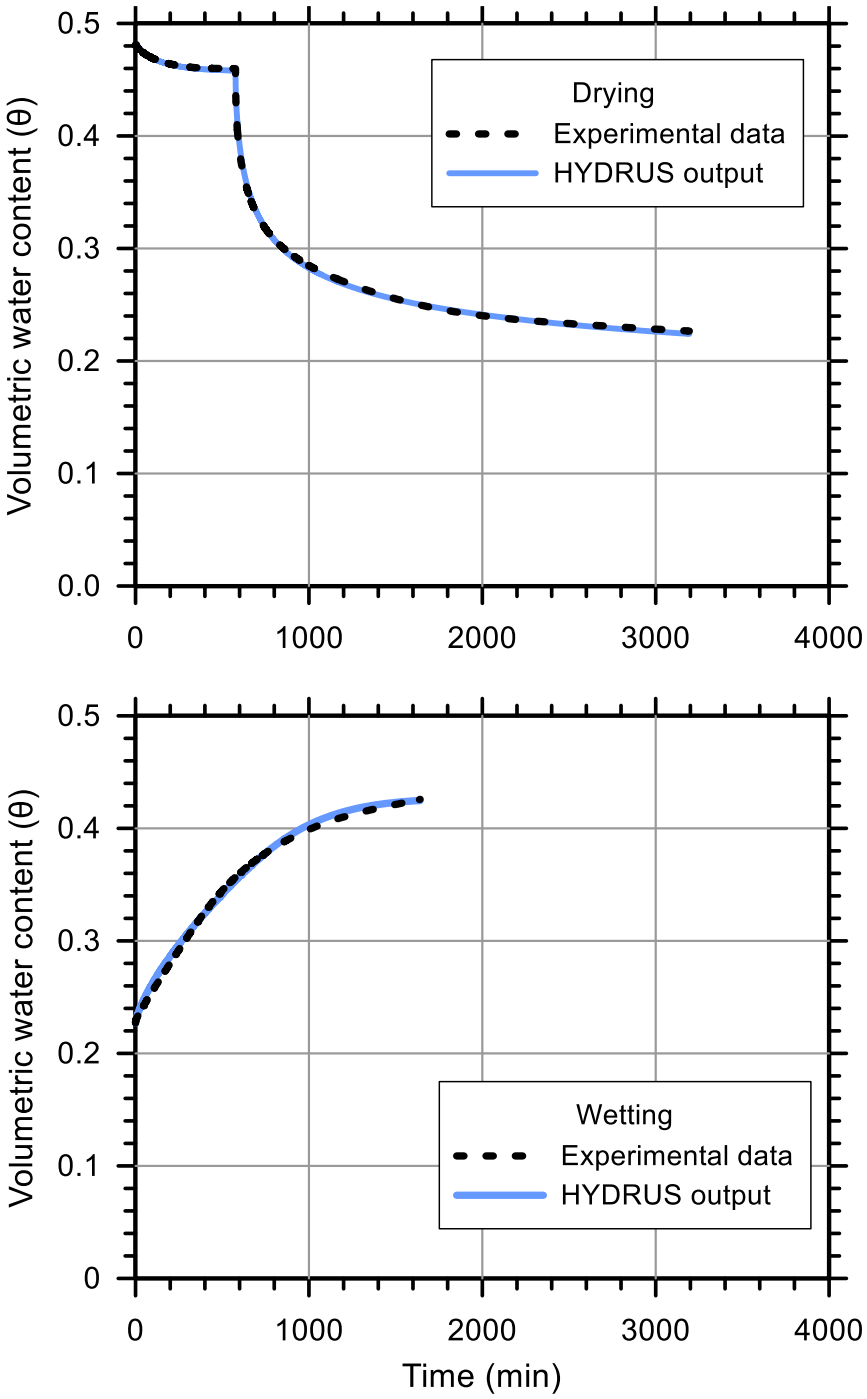

Figure 5.2. Comparison of experimental data and inverse modeling results of drying and wetting states for TRIMSC07 (Stroubles Creek - 3% dry of optimum)

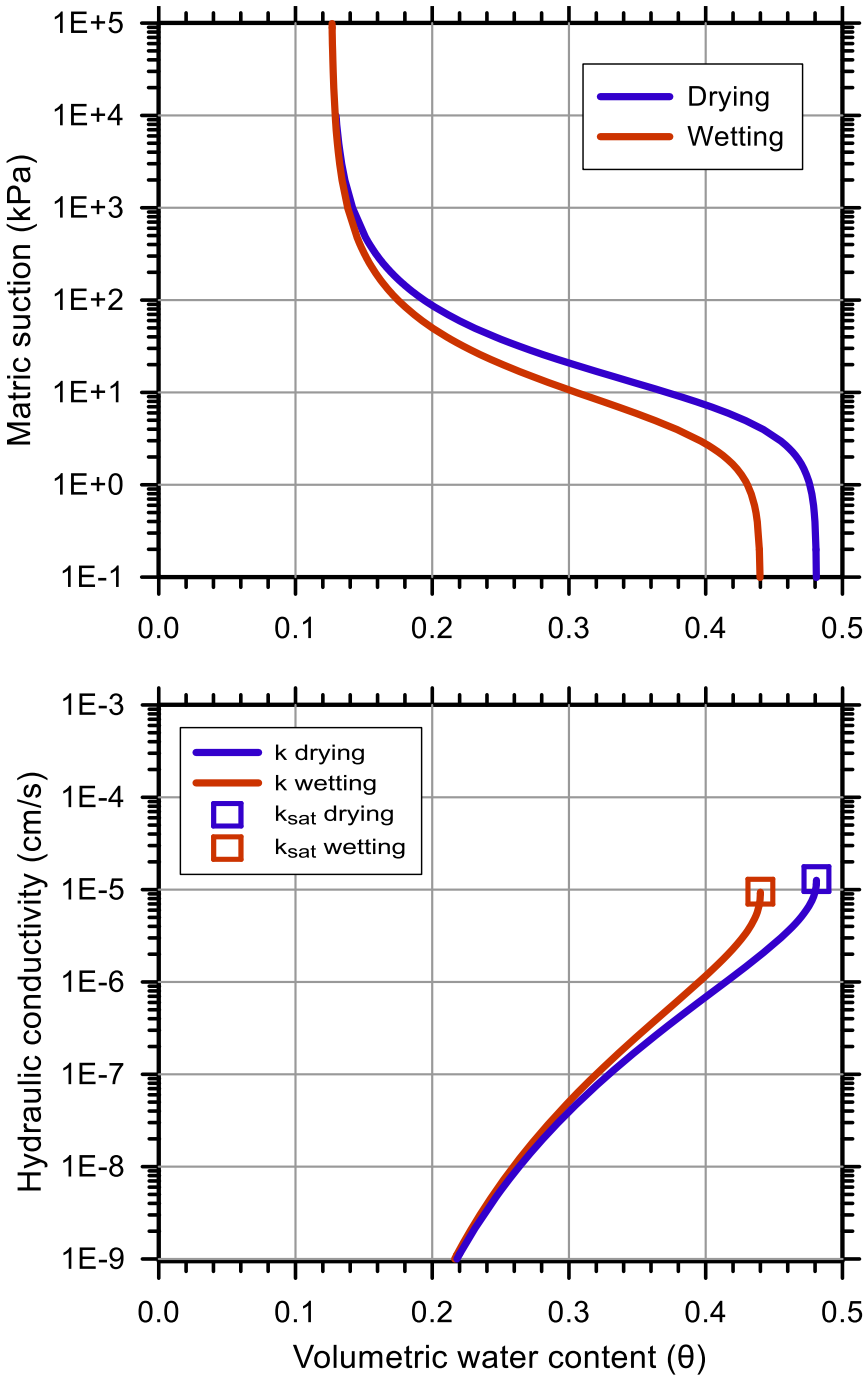

Figure 5.3. The SWCC and HCF of TRIMSC07 (Stroubles Creek - 3% dry of optimum)

Table 5.3. Hydrologic soil properties obtained from inverse modeling for Stroubles Creek soil

Stroubles Creek								
Molding Water Content (%)	Test No.	Test Ref.	State	θ_s	θ_r	α (1/kPa)	n	k_{sat} (cm/s)
19.60% (w_{opt} -3)	28	TRIMSC07	Drying	0.481	0.126	0.133	1.638	1.30E-05
			Wetting	0.440	0.126	0.217	1.605	9.50E-06
	4	TRIMSC03	Drying	0.498	0.096	0.151	1.522	3.50E-05
			Wetting	0.432	0.096	0.226	1.480	1.50E-05
22.60% (w_{opt})	5	TRIMSC04	Drying	0.470	0.145	0.172	1.497	9.66E-06
			Wetting	0.444	0.145	0.204	1.510	5.60E-06
	3	TRIMSC02	Drying	0.526	0.085	0.278	1.488	9.94E-05
			Wetting	0.425	0.085	0.428	1.380	7.50E-05
25.60% (w_{opt} +3)	15	TRIMSC06	Drying	0.459	0.120	0.248	1.855	6.00E-06
			Wetting	0.405	0.120	0.356	1.760	3.29E-06
	7	TRIMSC05	Drying	0.409	0.116	0.191	1.580	2.70E-05
			Wetting	0.435	0.116	0.224	1.550	1.40E-05

Table 5.4. Hydrologic soil properties obtained from inverse modeling for Whitehorne soil

Whitehorne								
Molding Water Content (%)	Test No.	Test Ref.	State	θ_s	θ_r	α (1/kPa)	n	k_{sat} (cm/s)
27.70% (w_{opt} -2)	27	TRIMWH11	Drying	0.507	0.173	0.143	1.850	1.50E-05
			Wetting	0.450	0.173	0.357	1.940	3.93E-06
	9	TRIMWH10	Drying	0.572	0.145	0.151	1.950	2.15E-04
			Wetting	0.459	0.145	0.194	1.850	8.51E-05
	R1	TRIMWH01	Drying	0.608	0.114	0.170	1.609	7.95E-04
			Wetting	0.492	0.114	0.415	1.570	4.50E-04
29.70% (w_{opt})	R2	TRIMWH04	Drying	0.539	0.166	0.124	1.760	5.63E-05
			Wetting	0.452	0.166	0.363	1.576	2.95E-05
	1	TRIMWH06	Drying	0.607	0.122	0.198	1.699	7.50E-04
			Wetting	0.488	0.122	0.418	1.580	3.50E-04
31.70% (w_{opt} +2)	6	TRIMWH09	Drying	0.505	0.184	0.117	1.800	2.21E-06
			Wetting	0.451	0.184	0.319	1.700	8.38E-07
	2	TRIMWH07	Drying	0.600	0.115	0.191	1.623	6.30E-04
			Wetting	0.478	0.115	0.410	1.500	2.90E-04

Table 5.5. Hydrologic soil properties obtained from inverse modeling for Tom's Creek soil

Tom's Creek								
Molding Water Content (%)	Test No.	Test Ref.	State	θ_s	θ_r	α (1/kPa)	n	k_{sat} (cm/s)
15.70% (w_{opt} -2.5)	8	TRIMTC06	Drying	0.386	0.125	0.140	1.600	7.50E-05
			Wetting	0.309	0.125	0.252	1.600	2.83E-05
	17	TRIMTC09	Drying	0.424	0.120	0.154	1.675	2.11E-04
			Wetting	0.320	0.120	0.173	1.620	1.00E-04
	13	TRIMTC08	Drying	0.463	0.115	0.390	1.601	6.10E-04
			Wetting	0.369	0.115	0.850	1.300	1.82E-04
18.70% (w_{opt} +0.5)	10	TRIMTC07	Drying	0.393	0.133	0.347	1.580	6.82E-05
			Wetting	0.325	0.133	0.342	1.282	4.00E-05
	22	TRIMTC10	Drying	0.410	0.125	0.487	1.619	1.09E-04
			Wetting	0.325	0.125	0.560	1.500	8.27E-05
	24	TRIMTC11	Drying	0.462	0.118	0.510	1.789	6.21E-04
			Wetting	0.375	0.118	0.703	1.528	3.32E-04

Table 5.6. Hydrologic soil properties obtained from inverse modeling for Sand-Clay (75%-25%) mix soil

Sand-Clay (75%- 25%)								
Molding Water Content (%)	Test No.	Test Ref.	State	θ_s	θ_r	α (1/kPa)	n	k_{sat} (cm/s)
8.40% (w_{opt} -2)	20	TRIMM7X03	Drying	0.285	0.137	0.231	1.921	2.18E-04
			Wetting	0.210	0.137	0.316	1.883	5.84E-05
	12	TRIMM7X01	Drying	0.313	0.108	0.430	2.200	4.00E-04
			Wetting	0.243	0.108	0.724	2.000	6.88E-05
9.90% (w_{opt} -0.5)	25	TRIMM7X05	Drying	0.304	0.121	0.280	2.071	3.70E-04
			Wetting	0.245	0.121	0.459	2.100	7.50E-05
	29	TRIMM7X06	Drying	0.361	0.084	0.499	2.252	8.04E-04
			Wetting	0.265	0.084	0.978	2.138	4.00E-04
11.40% (w_{opt} +1)	21	TRIMM7X04	Drying	0.296	0.130	0.234	1.800	2.50E-04
			Wetting	0.219	0.130	0.307	1.800	8.98E-05
	16	TRIMM7X02	Drying	0.311	0.111	0.423	2.484	4.19E-04
			Wetting	0.240	0.111	0.513	2.350	8.05E-05

Table 5.7. Hydrologic soil properties obtained from inverse modeling for Sand-Clay (85%-15%) mix soil

Sand-Clay (85%- 15%)								
Molding Water Content (%)	Test No.	Test Ref.	State	θ_s	θ_r	α (1/kPa)	n	k_{sat} (cm/s)
8.10% (w_{opt} -1.3)	19	TRIMM8X04	Drying	0.310	0.086	0.422	2.197	4.83E-04
			Wetting	0.265	0.086	0.605	2.123	2.18E-04
	11	TRIMM8X01	Drying	0.344	0.073	0.296	2.337	9.00E-04
			Wetting	0.257	0.073	0.416	2.243	7.00E-04
9.40% (w_{opt})	26	TRIMM8X05	Drying	0.316	0.085	0.438	2.200	5.50E-04
			Wetting	0.245	0.085	0.703	2.050	4.50E-04
	30	TRIMM8X06	Drying	0.362	0.072	0.509	2.350	2.19E-03
			Wetting	0.277	0.072	0.598	2.277	8.00E-04
11.10% (w_{opt} +1.7)	18	TRIMM8X03	Drying	0.313	0.087	0.301	2.390	2.31E-04
			Wetting	0.263	0.087	0.642	2.100	1.00E-04
	14	TRIMM8X02	Drying	0.371	0.066	0.709	2.500	2.27E-03
			Wetting	0.290	0.066	1.317	2.338	9.00E-04

Table 5.8. Hydrologic soil properties obtained from inverse modeling for Wilco LPC kaolin clay soil

Wilco LPC Kaolin Clay								
Molding Water Content (%)	Test No.	Test Ref.	State	θ_s	θ_r	α (1/kPa)	n	k_{sat} (cm/s)
23.50% (PL)	32	TRIMKC02	Drying	0.523	0.202	0.107	1.206	1.49E-03
			Wetting	0.439	0.202	0.137	1.208	1.00E-03
	35	TRIMKC02	Drying	0.567	0.178	0.265	1.215	2.21E-02
			Wetting	0.429	0.178	0.275	1.205	9.74E-03

Table 5.9. Hydrologic soil properties obtained from inverse modeling for Play sand soil

Play Sand								
Molding Water Content (%)	Test No.	Test Ref.	State	θ_s	θ_r	α (1/kPa)	n	k_{sat} (cm/s)
0	31	TRIMPS01	Drying	0.401	0.019	0.489	3.081	9.00E-03
			Wetting	0.298	0.019	1.019	3.160	3.00E-03

5.3. Flexible Wall Saturated Hydraulic Conductivity Tests

A total of 38 saturated hydraulic conductivity tests through flexible wall permeameter method were performed for 6 soil types at different densities and molding water contents. The results of all these tests are summarized in Table 5.10. For each test, volumetric flow ratio (outflow/inflow) and gradient change with time, and saturated hydraulic conductivity versus pore volumes of flow plots are generated to present results. The figures for all saturated hydraulic conductivity tests are given in Appendix B.

For a discussion and test description, the test FXSC40 is explained in detail in this section. In this test, Stroubles Creek soil was molded at 19.60% water content (3% dry of optimum). The soil sample was compacted to 1.28 g/cm^3 dry density or 82.86% standard proctor relative compaction. The initial and final values for TRIMSC40 are provided in Table 5.11. The flexible wall permeameter was used to conduct the falling head testing at different confining pressures and hydraulic gradients. First, the compacted sample was saturated by stepwise back pressure method. In the beginning, saturation was initiated with a small cell pressure to remove the entrapped air allowing water to flow at the top and bottom of the specimen. Moreover, the saturation process was continued with little back pressure increases at a time corresponding to an increased cell pressure level. During the saturation process, the sample consolidation was performed incrementally with 7 kPa, 14 kPa and finally 27.6 kPa effective stresses. Usually, the sample was kept for a day under each effective consolidation stress. After the saturation step, the consolidation cell pressure and consolidation back pressure were recorded as 441.3 kPa and 413.7 kPa, respectively. Flow was initiated by increasing the headwater pressure to 1.38 kPa (bottom to top flow). This pressure increase created an initial hydraulic gradient around 4. When the water flowed from bottom to top, the water level in headwater decreased and the water level in tailwater increased with time. This change caused the decrease of hydraulic gradient with time, as shown in Figure 5.4. Variations of water level in the headwater and tailwater glass pipes on the pressure control panel were regularly read during the experiment that took around 462 minutes. According to these readings, volumetric flow ratios of outlet to relative inlet (Q_{out}/Q_{in}) were calculated, as presented in Figure 5.4. During the entire testing duration, these ratios fluctuated between 0.75 and 1.25. In order to terminate the test, constant hydraulic conductivity values should be obtained or volumetric flow ratios should not vary significantly from unity. To evaluate the data, the calculated saturated hydraulic conductivity results

are plotted against the pore volumes of flow, as seen in Figure 5.5. In this test, a fluctuation in hydraulic conductivity results are noticed with decreasing hydraulic gradient. In such circumstances, instead of specifying a single saturated conductivity value, the results are evaluated in a limited range, for this test such as between 7.70E-06 cm/s and 4.61E-06 cm/s. After the test, specimen height and diameter were measured to determine final dry density. The effective consolidation stress of 27.6 kPa increased the dry density of the sample from 1.28 g/cm^3 to 1.37 g/cm^3. The final water content was measured in order to determine the degree of saturation. The degree of saturation was calculated as 99.73%.

The FXSC35 and FXSC10 were also conducted at the same molding water content (3% dry of optimum). Different effective consolidation pressures were chosen for these tests to target different dry densities. Figure 5.6 and Figure 5.7 show the hydraulic conductivity results of FXSC35 and FXSC10, respectively. For these tests, clear constant hydraulic conductivity results were obtained, so these were defined with only one hydraulic conductivity value.

In consideration of these three tests, a hydraulic conductivity trend with the dry density change was defined and then shown in Figure 5.8. Even under a slight effective consolidation pressure such as 6.90 kPa, the dry density of the soil sample reached to 1.33 g/cm, so a trend line becomes a necessity to roughly predict the saturated hydraulic conductivity values of TRIM tests that were conducted at low dry densities. For instance, the hydraulic conductivity result of TRIMSC03 was predicted this way. All tests conducted at 3% dry of optimum are compiled and shown in Figure 5.8.

Table 5.10. Summary of conducted flexible wall saturated hydraulic conductivity tests

Soil Name	Molding Water Content (%)	Test No.	Test Ref.	Effective Cons. Pressure (kPa)	Dry Density Before Saturation (g/cm^3)	Dry Density After Saturation (g/cm^3)	Std. Proctor Relative Compaction (%)
Stroubles Creek	19.60% (w_{opt} -3)	35	FXSC35	68.95	1.42	1.45	93.51
		40	FXSC40	27.85	1.28	1.37	88.12
		10	FXSC10	6.90	1.31	1.33	85.80
	22.60% (w_{opt})	36	FXSC36	68.95	1.40	1.46	94.03
		31	FXSC31	20.69	1.32	1.34	86.47
		32	FXSC32	5.52	1.20	1.30	83.66
	25.60% (w_{opt} +3)	50	FXSC50	68.95	1.42	1.47	95.07
		19	FXSC19	34.48	1.42	1.43	92.44
		20	FXSC20	27.58	1.31	1.37	88.63
		39	FXSC39	13.79	1.30	1.34	86.21
Whitehorne	27.70% (w_{opt} -2)	27	FXSC27	68.95	1.32	1.40	101.86
		9	FXSC09	27.58	1.22	1.26	91.59
		26	FXSC26	20.69	1.08	1.25	91.09
		18	FXSC18	3.45	1.21	1.20	87.11
	29.70% (w_{opt})	49	FXSC49	68.95	1.32	1.38	100.62
		17	FXSC17	34.48	1.32	1.33	96.82
		25	FXSC25	17.24	1.20	1.27	92.15
	31.70% (w_{opt} +2)	46	FXSC46	68.95	1.32	1.36	99.22
		11	FXSC11	34.48	1.04	1.32	96.22
		3	FXSC03	13.79	1.22	1.23	89.67
		28	FXSC28	3.45	1.15	1.20	87.23

Soil Name	Molding Water Content (%)	Test No.	Test Ref.	Effective Cons. Pressure (kPa)	Dry Density Before Saturation (g/cm^3)	Dry Density After Saturation (g/cm^3)	Std. Proctor Relative Compaction (%)
Tom's Creek	15.70% (w_{opt} -2.5)	47	FXSC47	34.48	1.40	1.64	96.68
		7	FXSC07	20.69	1.60	1.61	94.78
		48	FXSC48	6.90	1.60	1.55	90.95
	18.70% (w_{opt} +0.5)	51	FXSC51	68.95	1.62	1.69	99.59
		44	FXSC44	34.48	1.60	1.67	98.18
		24	FXSC24	6.90	1.45	1.57	92.26
Sand-Clay mix (75%-25%)	8.40% (w_{opt} -2)	45	FXSC45	27.58	1.87	1.91	95.63
		33	FXSC33	20.69	1.78	1.81	90.59
		38	FXSC38	13.79	1.68	1.77	87.76
	11.40% (w_{opt} +1)	43	FXSC43	41.37	1.90	1.94	96.89
Sand-Clay mix (85%-15%)	8.10% (w_{opt} -1.3)	42	FXSC42	34.48	1.83	1.85	95.71
		34	FXSC34	20.69	1.73	1.78	92.01
	11.10% (w_{opt} +1.7)	41	FXSC41	34.48	1.83	1.85	95.65
		37	FXSC37	17.24	1.71	1.76	91.08
Wilco LPC Kaolin Clay	23.50% (PL)	52	FXSC52	68.95	1.36	1.37	-
		53	FXSC53	20.69	1.21	1.34	-
		54	FXSC54	5.5	1.19	1.26	-

Table 5.11. Specimen information before and after the test TRIMSC40 (Stroubles Creek - 3% dry of optimum)

Property	Before Test	After Test
Total Mass (g)	310.00	348.19
Mass of Solids (g)	259.20	259.15
Mass of Water (g)	50.80	89.04
Total Volume (cm^3)	201.81	189.73
Volume of Solids (cm^3)	100.46	100.44
Volume of Water (cm^3)	50.80	89.04
Volume of Air (cm^3)	50.54	0.24
Water Content (%)	19.60	34.36
Volume of Voids (cm^3)	101.34	89.28
Void Ratio, e	1.009	0.889
Porosity, n (%)	0.502	0.471
Std. Proctor Relative Compaction (%)	82.86	88.12
Moist Density (g/cm^3)	1.54	1.84
Dry Density (g/cm^3)	1.28	1.37
Degree of Saturation (%)	50.13	99.73
Consolidation Cell Pressure (kPa)	441.3	
Consolidation Back Pressure (kPa)	413.7	
Effective Consolidation Pressure (kPa)	27.6	

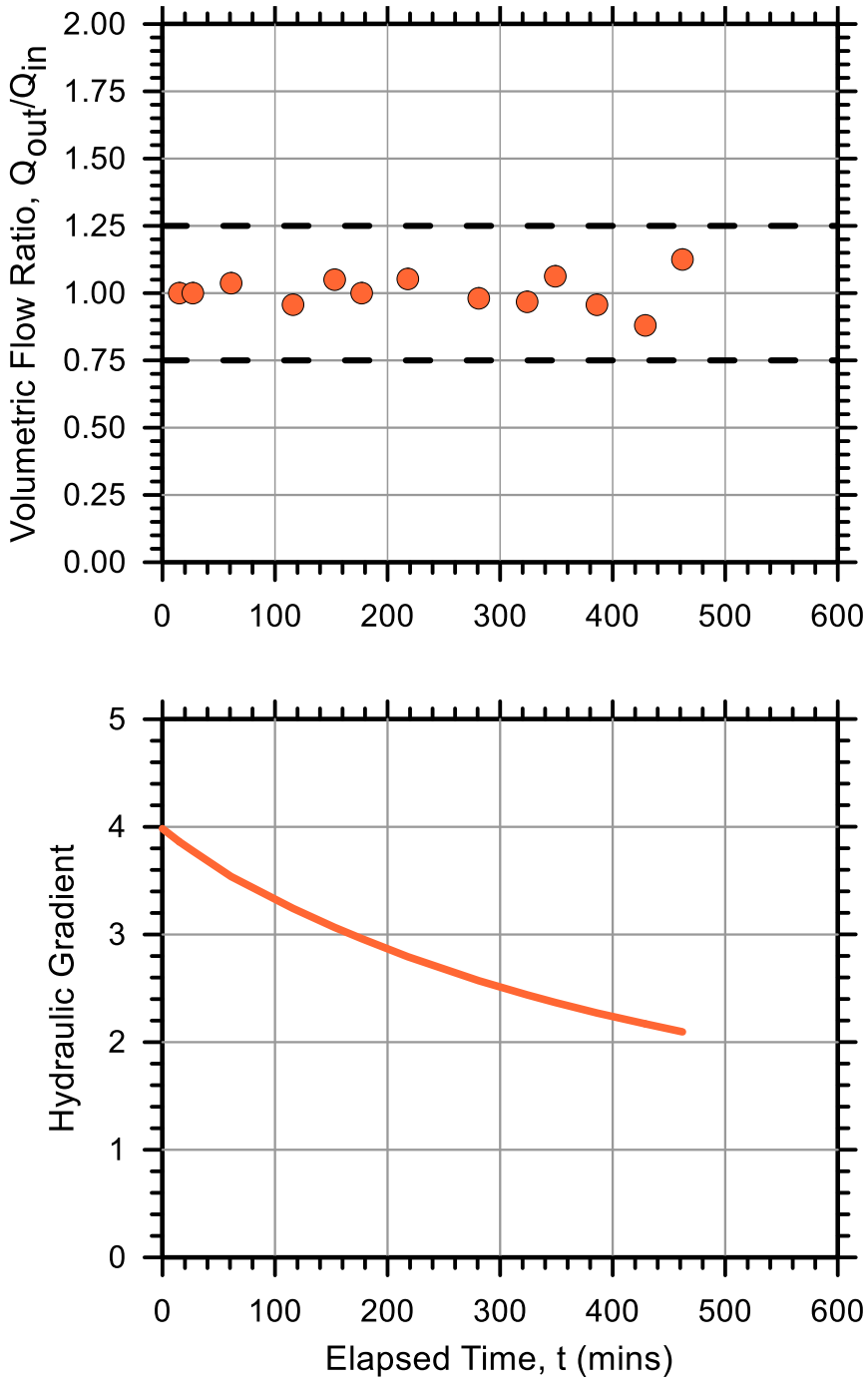

Figure 5.4. Volumetric flow ratio and hydraulic gradient as a function of time for FXSC40 (Stroubles Creek – 3% dry of optimum)

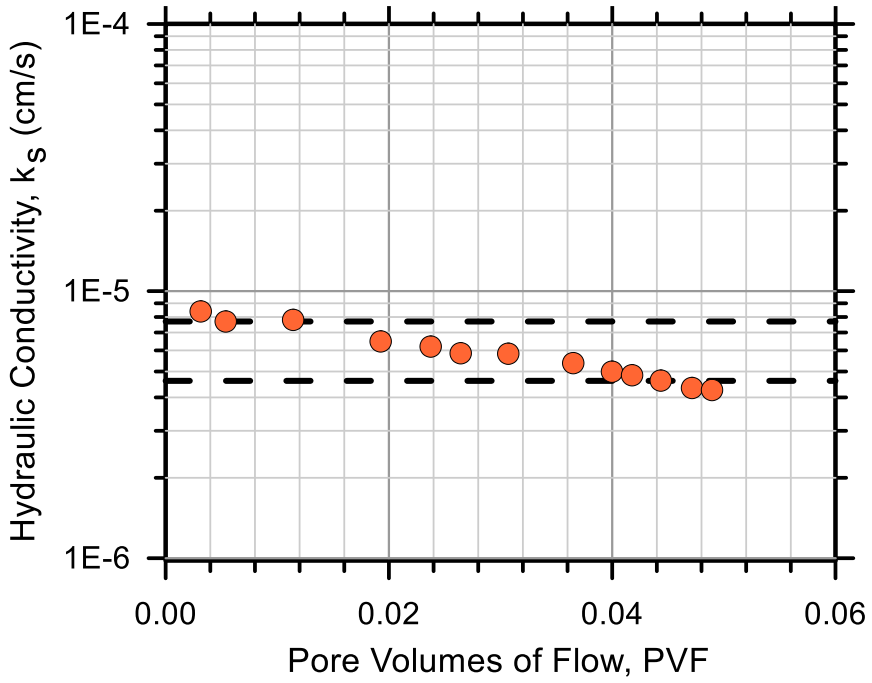

Figure 5.5. Hydraulic conductivity results of FXSC40 (Stroubles Creek – 3% dry of optimum)

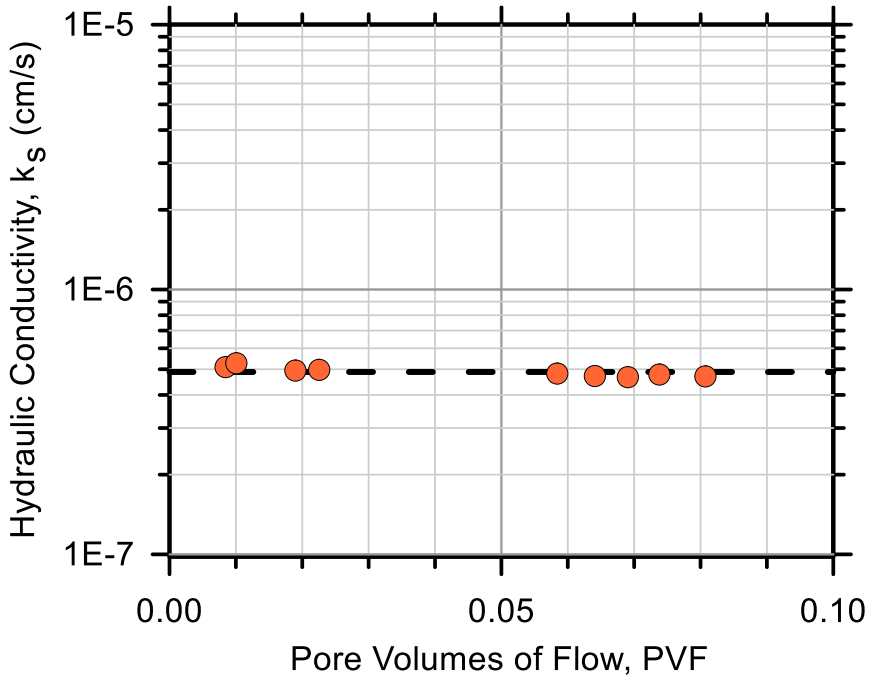

Figure 5.6. Hydraulic conductivity results of FXSC35 (Stroubles Creek – 3% dry of optimum)

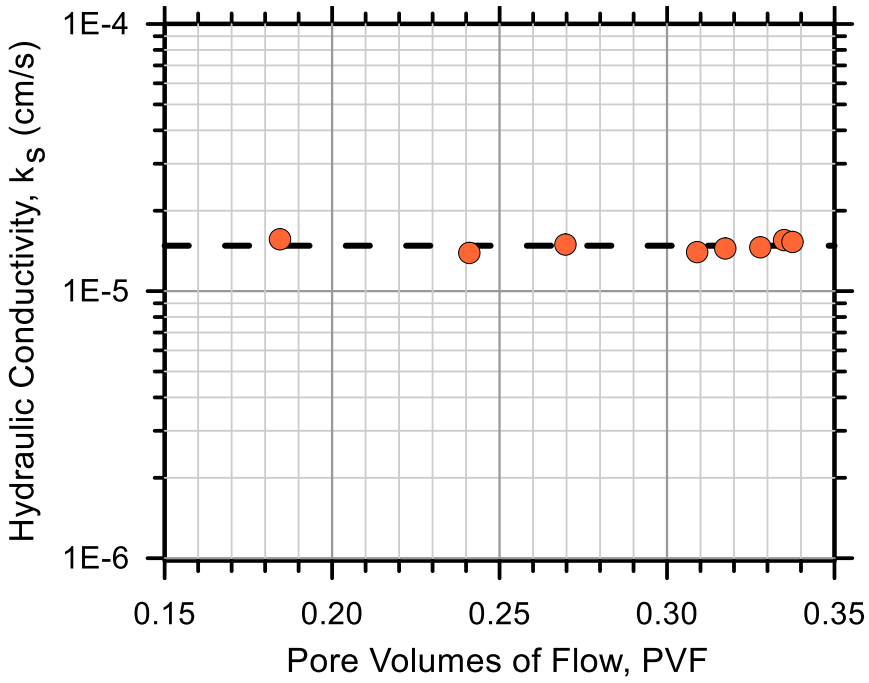

Figure 5.7. Hydraulic conductivity results of FXSC10 (Stroubles Creek – 3% dry of optimum)

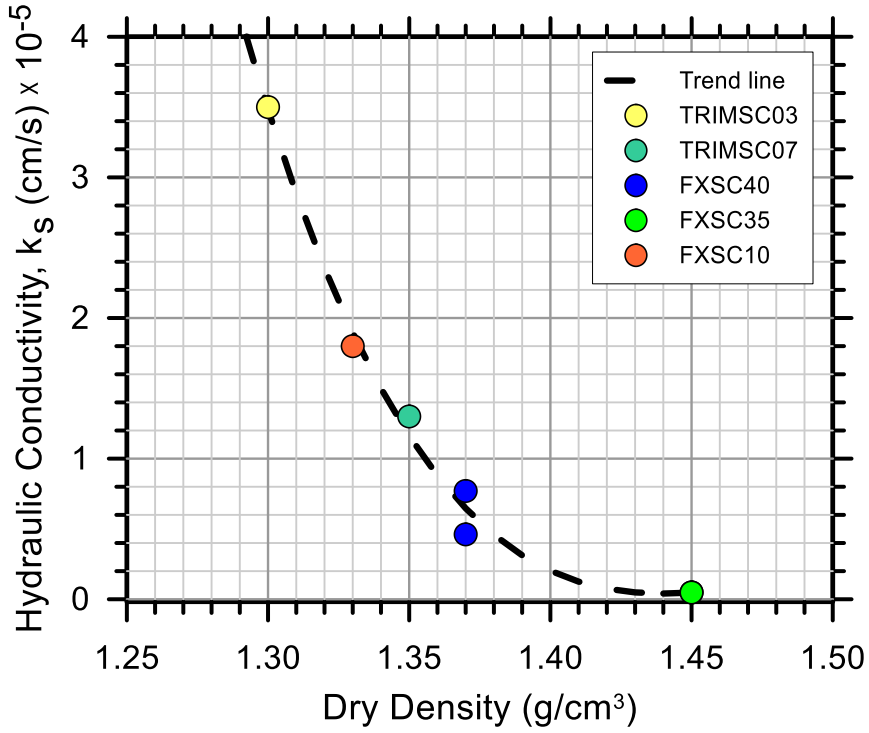

Figure 5.8. Hydraulic conductivity vs. dry density of all the Stroubles Creek tests at 3 % dry of optimum

5.4. Influence of the Molding Water Content

Specimens compacted at the same dry density but different initial water content under different compaction efforts are not considered as identical specimens. In spite of having the same texture and mineralogy, they can exhibit different soil properties when molded at different initial water contents. The influence of molding water content on the soil structure is well documented in the literature. Vanapalli et al. (1999) stated that the molding water content has a considerable influence on the resulting structure of fine-grained soils such as the clay till used in their research program. They noticed that the dry of optimum specimen exhibits a steeper SWCC when compared with specimens compacted at optimum and wet of optimum water contents. Tinjum et al. (1997) carried out drying tests on specimens compacted at the three different molding water contents. The results show that AEV of the specimen compacted dry of optimum is noticeably lower from those compacted on the wet side. The specimen compacted at a dry of optimum molding water content has relatively large pores occurring between the clods of the soil. On the contrary, those compacted at a wet of optimum molding water content have no visible relatively large interclod pores and are more homogenous.

The initial water contents traditionally selected for this study represent the dry of optimum, optimum, and wet of optimum conditions. The obtained optimum water content from standard proctor compaction test was used as a reference. Specimens were prepared and compacted at these particular water contents to determine how molding water content affects SWCC and HCF. Figure 5.9 shows the variation of the degree of saturation and unsaturated hydraulic conductivity with respect to matric suction, respectively. The specimen TRIMWH11 was prepared at 2% dry of optimum water content, while the specimen TRIMWH09 was prepared at 2% wet of optimum. The relationship between the degree of saturation and matric suction show that the drying curve of wet of optimum specimen closely lies over the dry of optimum specimen. The difference between drying curves molded at wet and dry of optimum water content diminishes as the matric suction increases. This finding is also valid for unsaturated hydraulic conductivity of those specimens. The unsaturated hydraulic conductivities at higher suctions were similar, because the largest pores will empty first and fill last under unsaturated conditions.

The resistance to water flow is relatively low in the dry of optimum specimens. Under relatively low suction values, removing water from large pores is very different from the large suction required to remove water from the microscopic pore spaces between soil particles within the clods of clay (Garcia-Bengochea et al. 1979; Acar and Olivieri 1989; Benson and Daniel 1990). As a result, a macro structure controls the initial drying of compacted specimens. The results suggest that AEV increases with an increase in the molding water content.

Unlike these mentioned results, which agree with most of previous studies, some results have not shown similar trends. In order to understand the whole picture, these conflicting results must be assessed by taking into account saturated hydraulic conductivity results measured through the flexible-wall method. Trend lines were defined for the tests at each molding water content. The change in hydraulic conductivity with dry density for different test soils are given in Figures 5.10-5.13. The slight increase of hydraulic conductivity for the Stroubles Creek samples at the dry optimum water content (w_{opt}-3) and the apparent difference in the results of Sand-Clay (85%-15%) samples are the only outcomes that have drawn attention. Apparently, the selected molding water contents slightly above or under the optimum water content do not have much considerable influence on the hydraulic conductivity results. It is difficult to come to a clear conclusion about the influence of molding water content in the light of these results.

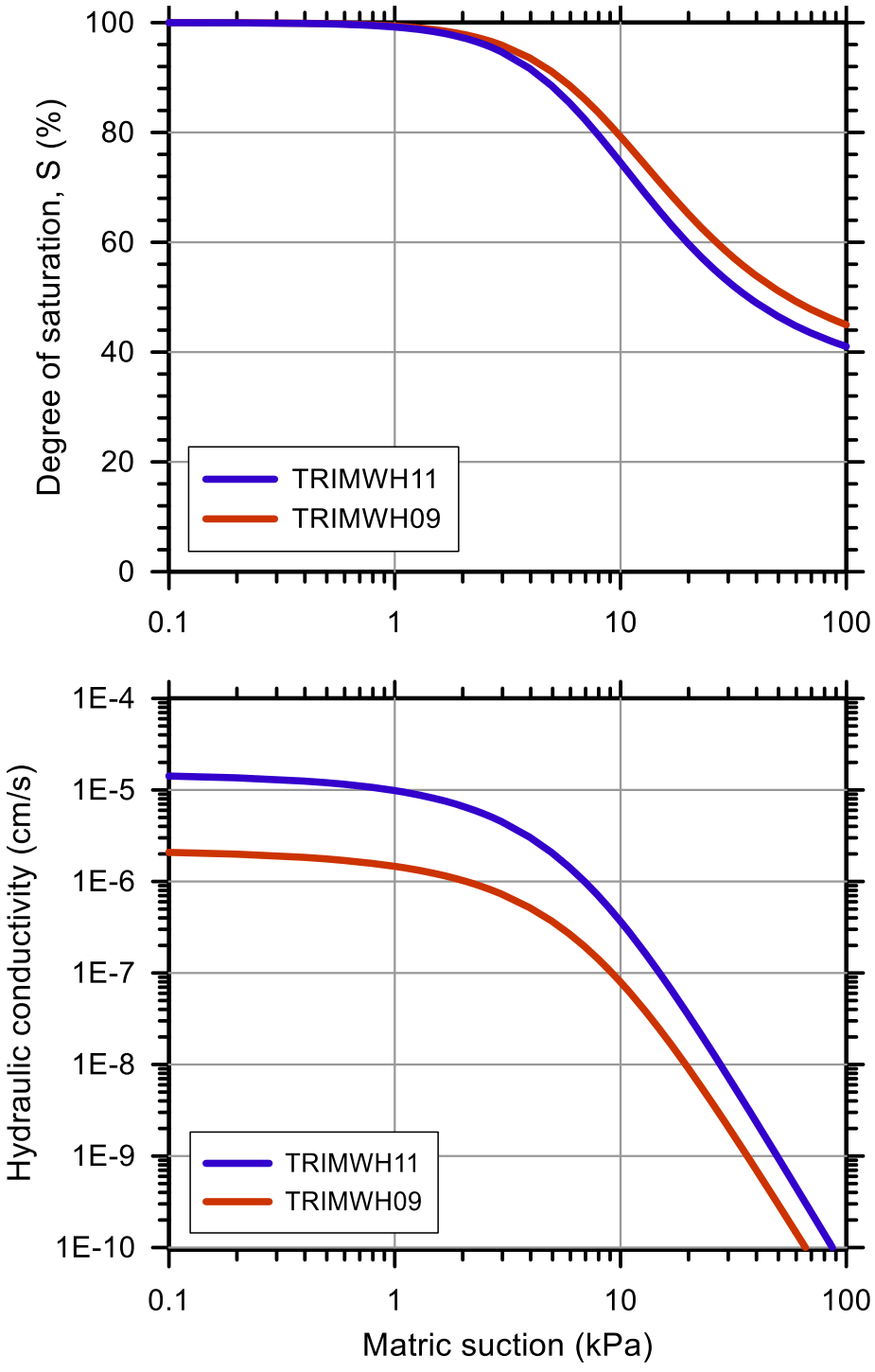

Figure 5.9. Degree of saturation and hydraulic conductivity vs. matric suction of TRIMWH11 (Whitehorne soil – 2% dry of optimum) and TRIMWH09 (Whitehorne soil – 2% wet of optimum) tests

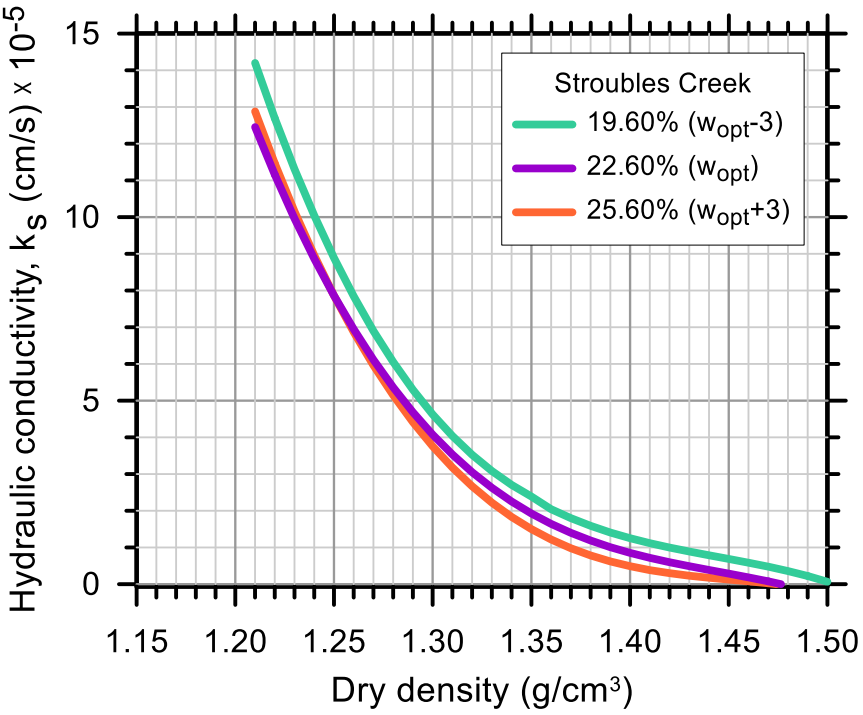

Figure 5.10. The determined hydraulic conductivity trend lines vs. dry density of Stroubles Creek soil at different molding water contents

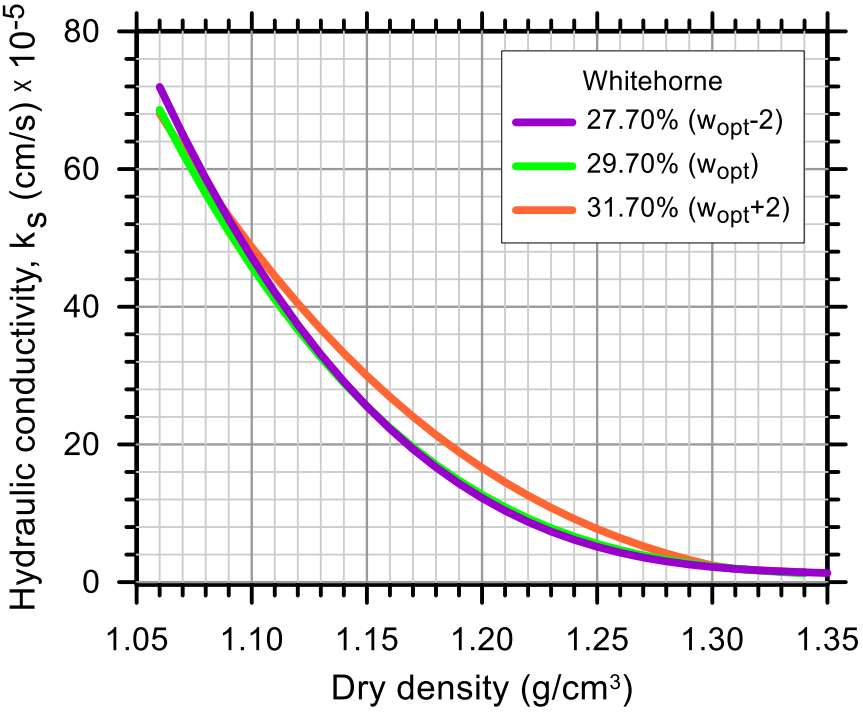

Figure 5.11. The determined hydraulic conductivity trend lines vs. dry density of Whitehorne soil at different molding water contents

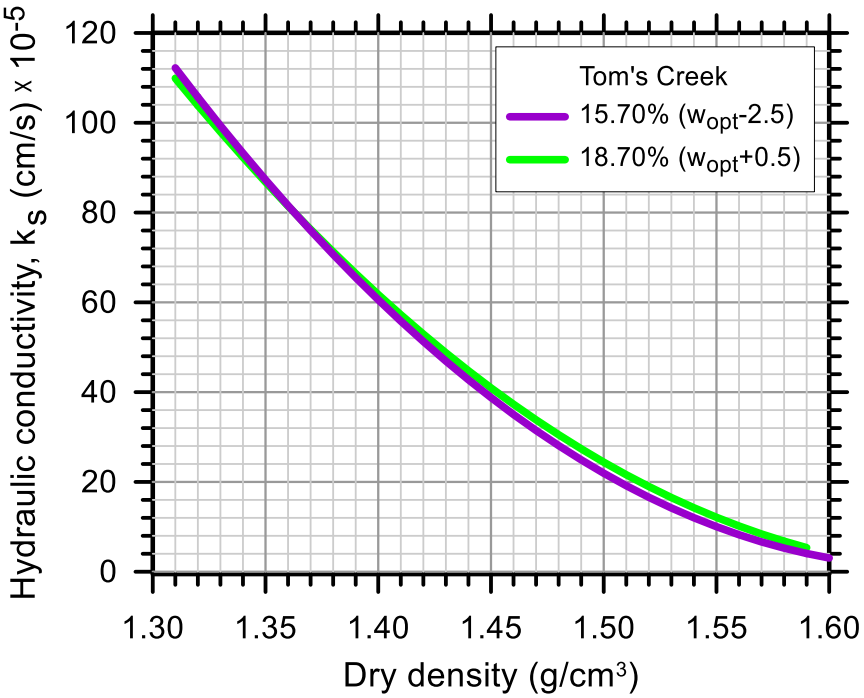

Figure 5.12. The determined hydraulic conductivity trend lines vs. dry density of Tom's Creek soil at different molding water contents

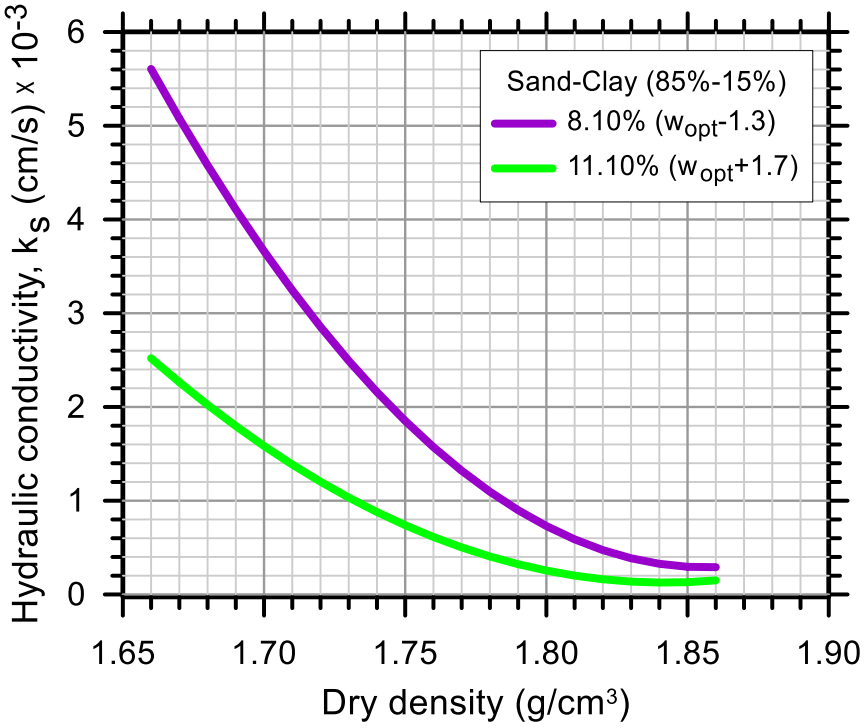

Figure 5.13. The determined hydraulic conductivity trend lines vs. dry density of sand-clay (85%-15%) mixture at different molding water contents

5.5. Influence of the Initial Dry Density

In the literature exist several researches related to the influence of soil density on the SWCC and HCF. In order to study the influence of the dry density on the SWCC, two or three different dry density targets at the same molding water content were selected for each soil. The compaction method was always the same, only the applied compactive effort was increased to reach high level of relative compaction. Increasing compactive effort results in smaller pores, and thus affect the shape of SWCC. Besides dry density, standard proctor relative compaction values are calculated with reference to the maximum dry density of standard proctor test results. Relative compaction is a useful parameters to assess all tests under a mutual scale.

For discussion, an example case is presented here and shown in Figure 5.14. The Stroubles Creek samples (TRIMSC04 and TRIMSC02) were compacted at the optimum water content. The final dry densities after saturation were 1.37 g/cm^3 for TRIMSC04 and 1.23 g/cm^3 for TRIMSC02. At the beginning of the test under zero suction, soil specimen with higher dry density or lower void ratio, as expected, exhibits a lower initial volumetric water content. Saturated volumetric water content at the beginning was 0.470 (cm^3/cm^3) for TRIMSC04 and 0.526 (cm^3/cm^3) for TRIMSC02. The point where the volumetric water content starts to decrease significantly indicates the air-entry value of the specimen. As the void ratio of specimen decreases, the average pore size reduces and the air-entry value of specimen increases. Air-entry value is one of the parameters of SWCC most influenced by dry density. Figure 5.15 and Figure 5.16 show that the air-entry values (AEVs) increase with an increase of dry density. The air-entry values of all tests for the Whitehorne soil in Figure 5.15 and Sand-Clay (75%-25%) mix in Figure 5.16 are gathered. The air-entry value is generally higher and the slope is slightly steeper for the specimen compacted with greater compactive effort. Once the air-entry value is overcome, this transition in water retention behavior reflects a limit of capillary tension that can be sustained by the soil. This limit varies conversely with the size of the pores and thus with the void ratio, and is the reason why the air-entry value decreases significantly when the void ratio increases. This result corroborates the trend drawn by several authors (Vanapalli et al. 1999; Kawai et al. 2000; Zhou and Yu 2005).

Croney and Coleman (1954) have reported that a silty sand, with a high initial compacted density, showed a higher air-entry value than that of a low initial compacted density. The rate of drying was

found to be less at higher initial density. It is seen that the soil specimen from TRIMSC04 with high dry density dries at a slower rate than the soil specimen from TRIMSC02 with lower dry density. This means that the dense soil specimen has greater ability to retain water. The residual volumetric water content change with an increase of dry density is presented in Figure 5.17 by providing the results from Sand-Clay (75%-25%) and (85%-15%) mixes. The water retention capacity significantly increases with the increase of dry density. Under a standard proctor relative compaction scale, all tests are brought together in Figure 5.18. Residual volumetric water content increases with the available fine content. The difference between Wilco LPC kaolin clay (very fine soil) and Play sand (granular soil) is tremendous. The slope of trend line becomes steeper for those where the presence of fine content is substantial.

Upon completion of the drying state, the tests were continued with the wetting state. As seen in Figure 5.14, there is a noticeable hysteresis between the drying and wetting curves. A general trend is shown, where the size of the hysteresis loop decreases as the dry density increases. This phenomenon will be discussed in-depth under the hysteresis section.

Several investigations have already proven that the specimen compacted with greater compactive effort had a lower saturated and unsaturated hydraulic conductivity because compaction with higher effort reduces the frequency of large pores and the average pore-size. These reductions in large pore frequency and average pore-size should result in lower hydraulic conductivity. Ren et al. (2014) discovered the relation between the hydraulic conductivity and the dry density of silty clay fit to a logarithmic curve. The TRIM tests for Stroubles Creek in Figure 5.19 and Tom's Creek in Figure 5.20 are presented to show the trend of saturated hydraulic conductivity with the change in dry density. It is noted that the format of trend line varies depending on the soil type. Apparently, the slope of trend lines become steeper as dry density decreases.

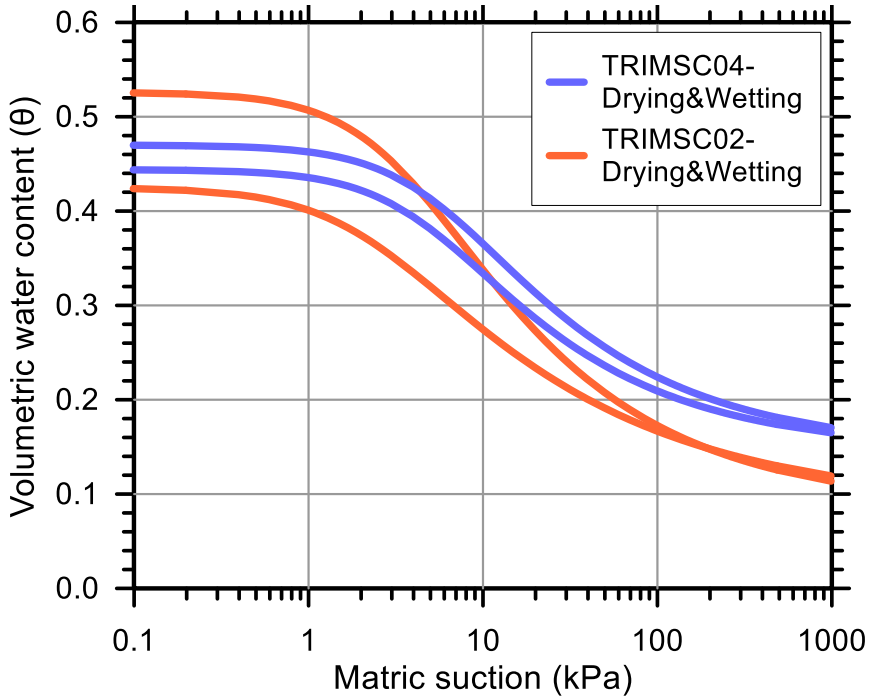

Figure 5.14. The SWCC of TRIMSC04 (high density Stroubles Creek specimen) & TRIMSC02 (low density Stroubles Creek specimen)

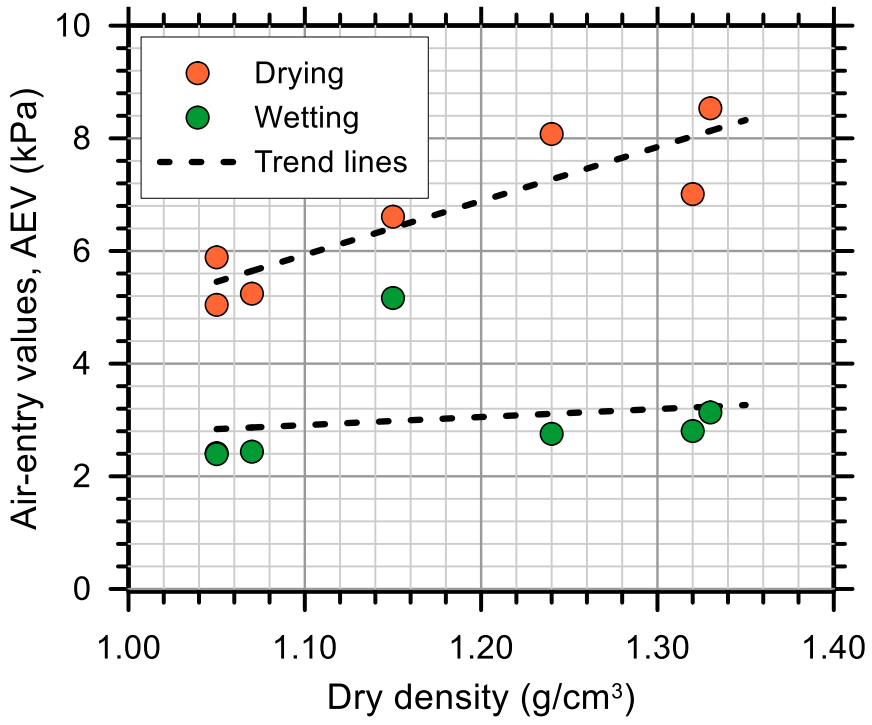

Figure 5.15. The variation of the air-entry value (AEV) with the dry density of Whitehorne soil

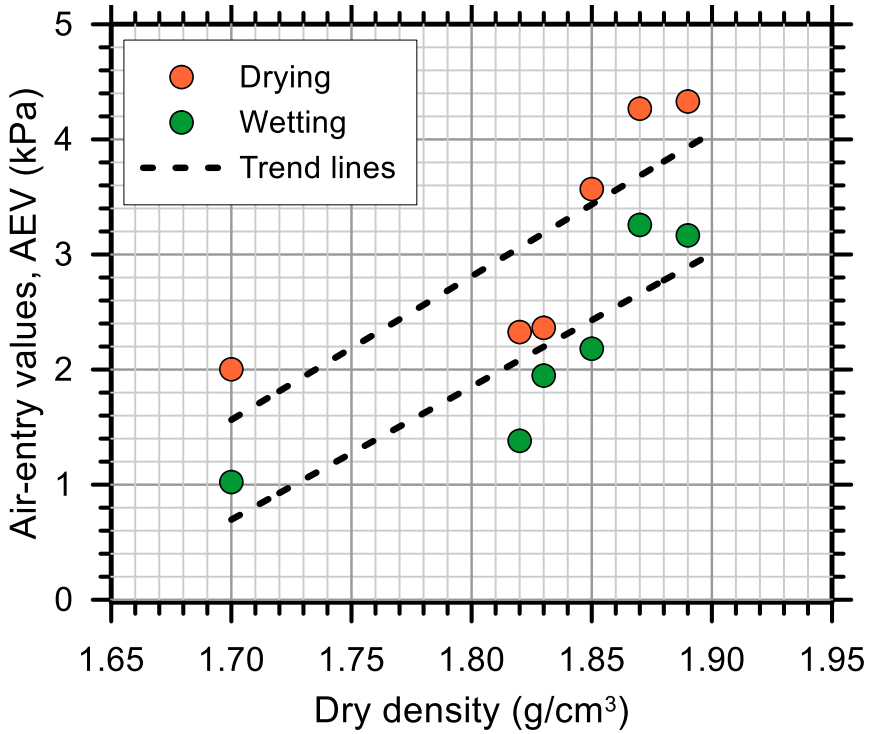

Figure 5.16. The variation of the air-entry value (AEV) with the dry density of Sand-Clay (75%-25%) mix

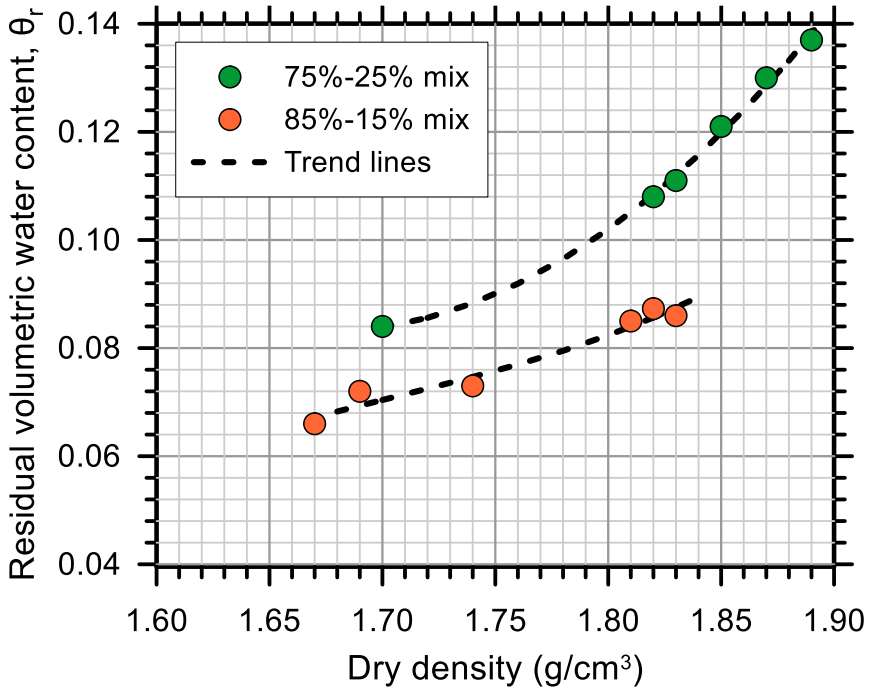

Figure 5.17. The variation of the residual volumetric water content with the dry density of Sand-Clay (75%-25%) and (85%-15%) mixes

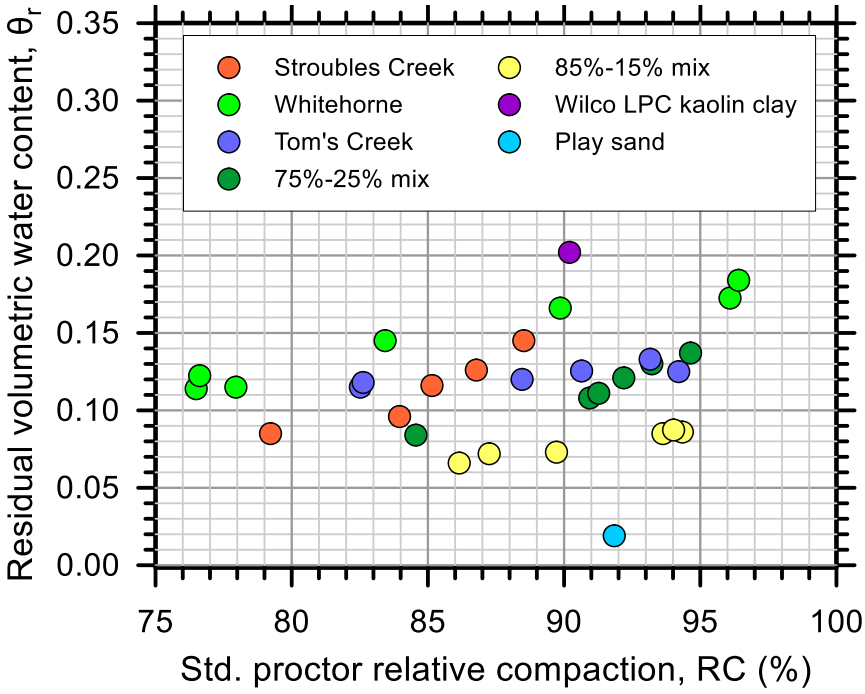

Figure 5.18. The variation of the residual volumetric water content with the std. proctor relative compaction for all tests

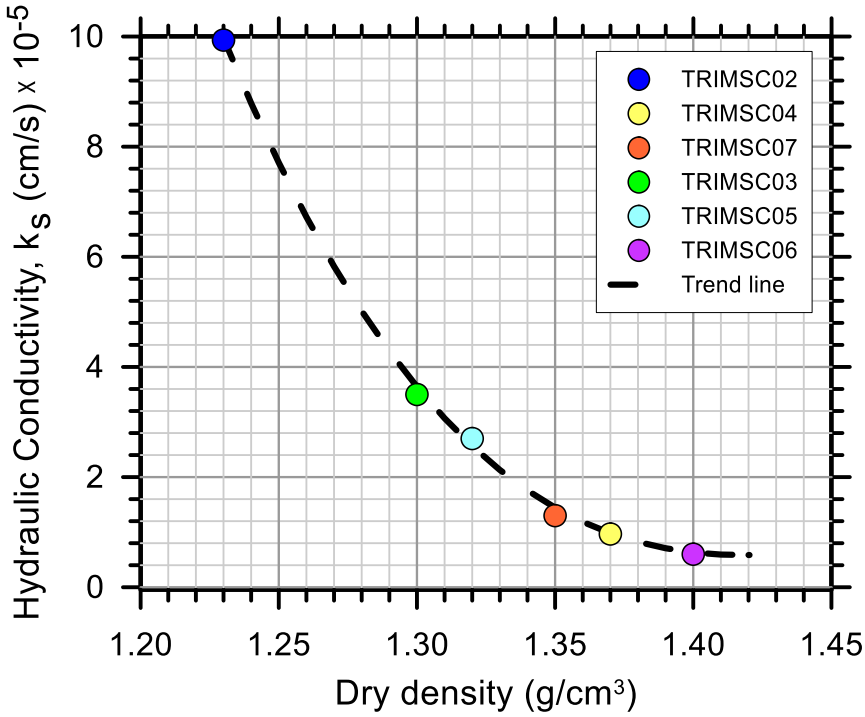

Figure 5.19. Hydraulic conductivity vs. dry density of all tests for Stroubles Creek soil

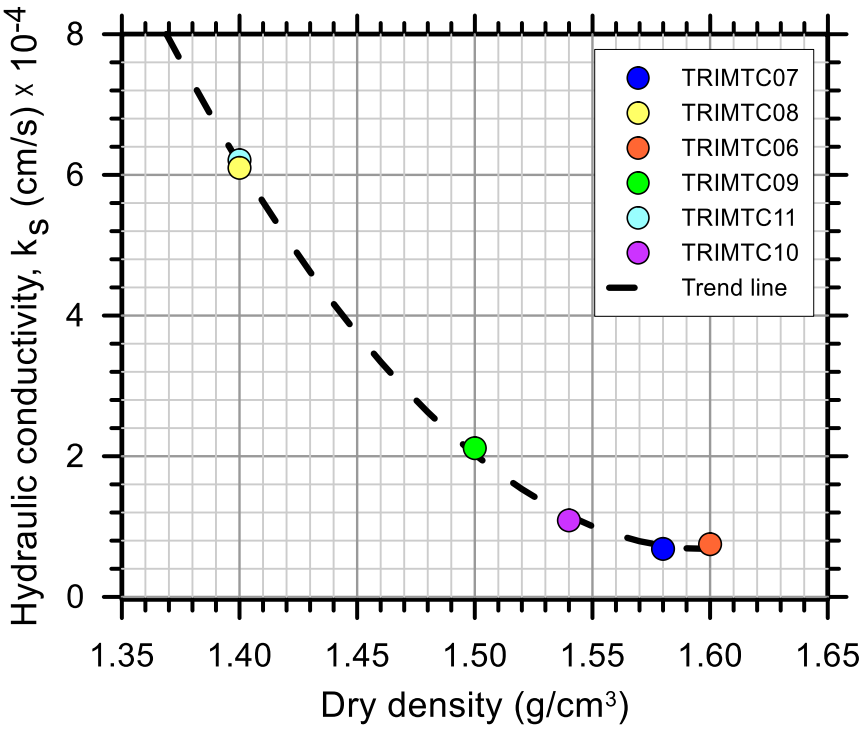

Figure 5.20. Hydraulic conductivity vs. dry density of all the tests for Tom's Creek soil

5.6. Hysteresis

The hysteresis is another significant effect that is attributed to several causes. The hysteresis between the drying and wetting SWCCs and HCFs was observed for all TRIM tests. The reasons underlying the hysteresis phenomena is likely to attributed to the ink-bottle effect, the contact angle effect, and entrapped air. The saturation of specimen after the drying process cannot be achieved through capillary action only due to these reasons. Therefore, none of the wetting curves reach full saturation at the end of wetting state. Also, previous research has revealed that swelling-shrinking or aging phenomena is unlikely to have significant effect on the observed hysteresis between drying and wetting SWCCs and HCFs. This repeated drying and wetting cycles can result in changing of the soil structure through shrinking and swelling.

The considerable effect of dry density on hysteresis has already shown in Figure 5.14. It is seen that the size of the hysteresis loop decreases as the dry density of sample increases. Similar results were pronounced by Croney and Coleman (1954) and Gallage et al. (2013). The ink-bottle effect is more prevalent for the loose soil specimen (large pores) than the in a dense soil specimen (small pores).

This effect is explained as different contact angles at the receding soil-water interface during drying and at the advancing soil-water interface during wetting. The reduction of porosity, in other words saturated volumetric water content, leads to the decrease of the radius of curvature of the meniscus and then generates a suction increase. It was found that the high-density specimen has a higher air-entry value and lower rate of saturation than the low-density specimen. In addition to that, a lean clay soil of Whitehorne and a clayey sand of Sand-Clay (85%-15%) compacted at just under 90% standard proctor relative compaction were examined to understand fines content effect on hysteresis. The specimen of TRIMWH04 with high fines content may have greater numbers of small pores (higher saturated volumetric water content) than the specimen of TRIMM8X01 with less fines content (lower saturated volumetric water content). As is seen in Figure 5.21, TRIMWH04 displays larger hysteresis than TRIMM8X01. The reason for this may be associated with the ink-bottle phenomenon and entrapped air. In addition, hydraulic conductivity functions of these tests are given in Figure 5.22 (hydraulic conductivity versus matric suction) and Figure 5.23 (hydraulic conductivity versus volumetric water content). A distinct difference exists between the drying and wetting curves for both specimens when the unsaturated hydraulic conductivity is stated as a function of matric suction. For a given suction, the unsaturated hydraulic conductivity is higher for the drying curve. This occurs due to the hysteresis in SWCC. At a reference suction, a soil undergoing a drying stage usually has a higher volumetric water content than soil undergoing wetting. The hysteresis is less discernable in the hydraulic conductivity versus volumetric water content plot. The drying and wetting hydraulic conductivity curves start off around the residual volumetric water content and follow a similar path. Fredlund and Xing (1994a) expressed that k-θ relationship is not hysteretic because the volume of water flow is a direct function of the volumetric water content.

Accurate estimates of soil hydraulic parameters representing drying and wetting paths are required for predicting hydraulic and mechanic responses. From cohesive soil respect, a comprehensive suite of laboratory tests are available in this research. Direct comparisons between drying and wetting parameters are plotted in Figures 5.24-5.27 for alpha, n, saturated volumetric water content, and saturated hydraulic conductivity, respectively. The ratios of α^w/α^d, n^w/n^d, θ^w/θ^d and k^w/k^d were calculated for all cohesive test soils. These values are presented as the mean (μ) ratio plus or minus the standard deviation (σ) about the mean ratio with coefficient of variation (σ/μ) in parentheses. Table 5.12 summarizes these results. Trend lines (dashed) represent the best curve fitting. The comparison of alpha for wetting and drying indicates that the scaling relation

α^w=1.66α^d holds on average, however there is a significant scatter due to the dependency on soil type. These results show a decent agreement with those of Likos et al. (2013) and Kool and Parker (1987), who studied cohesive soils and found a mean ratio α^w/α^d=1.73$\pm$0.94 (54) and α^w/α^d=1.88$\pm$0.40, respectively.

Table 5.12. Summary of measured drying and wetting parameter ratios

Ratio	$\mu \pm \sigma$ (COV%)
α^w/α^d	1.66$\pm$0.50 (30)
n^w/n^d	0.95$\pm$0.05 (6)
θ_s^w/θ_s^d	0.82$\pm$0.05 (7)
k_s^w/k_s^d	0.48$\pm$0.17 (37)

The comparison of pore-size distribution parameter (n) for drying and wetting states were examined. The n results do not show scatter depending on soil type. The scaling relation n^w/n^d=0.95$\pm$0.05 (6) was found for cohesive soils. Likos et al. (2013) provided additional evidence to strengthen the van Genuchten (1980) n parameter showing consistency for drying and wetting directions with close values to each other. In terms of cohesive soils, they noted the n^w/n^d ratio as 0.97$\pm$0.08 (8) with similar scatter about the mean.

Pham et al. (2005) manifested a comprehensive study about initial drying curves and main wetting curves. They revealed that air entrapment during wetting state corresponds approximately to 5-15% of total volume of specimen. An average of 10% air entrapment has been widely recognized in engineering practice. Likos et al. (2013) found a ratio of 0.87$\pm$0.11 (13) for cohesive soils. In this research, the ratio of θ_s^w/θ_s^d was reported as 0.82$\pm$0.05 (7).

A comparison between the saturated hydraulic conductivity at drying and end of the wetting tests was measured. The saturated hydraulic conductivity at the beginning of the initial drying curve was always greater than that obtained at the end of the main wetting curve. The saturated hydraulic conductivity at the beginning of the initial drying curve could be more than one order of magnitude greater than that obtained for wetting at the same water content. The drying and wetting saturated hydraulic conductivity results are graphed on a logarithmic scale in Figure 5.27. Even though, a

decent trend line was drawn, the coefficient of variation was calculated as 37, which is a reminder of the dependency to the soil type. The ratio of 0.48 roughly holds the general trend. The overall coefficient of variation of α^w/α^d (30) and k_s^w/k_s^d (37) was considerably greater than that for n^w/n^d (6) and θ_s^w/θ_s^d (7). Moreover, the results of k_s^w and k_s^d versus dry density for Stroubles Creek (Figure 5.28) and Whitehorne (Figure 5.29) are presented under a linear y scale after multiplying hydraulic conductivity results by 10^5. It is evident that hysteresis is not phenomenon that occurs randomly, it occurs in concordance with dry density change.

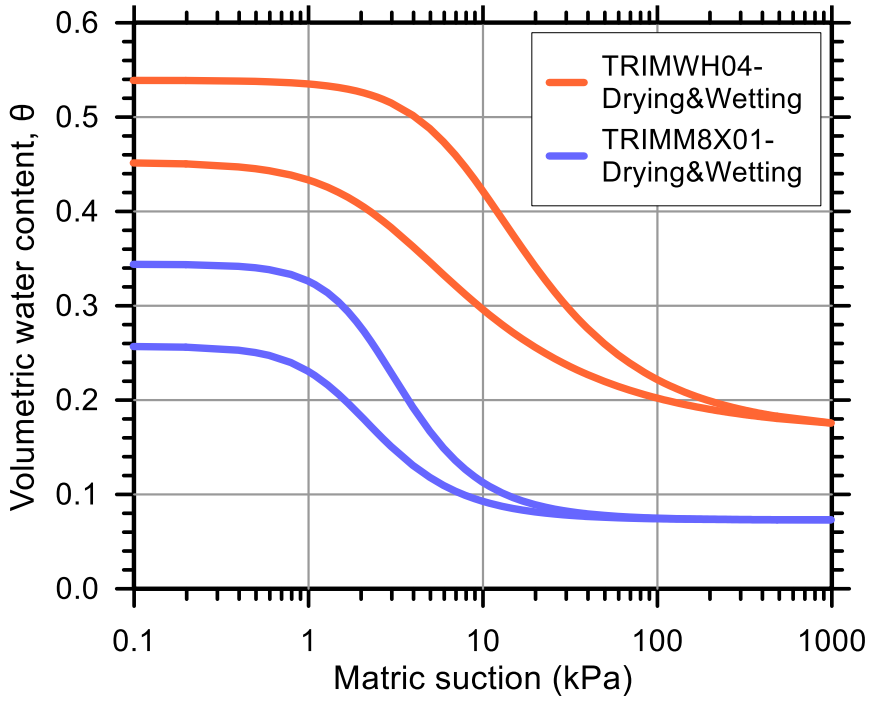

Figure 5.21. The SWCC of TRIMM8X01 (85%Sand-15%Clay specimen) & TRIMWH04 (Whiterhorne specimen)

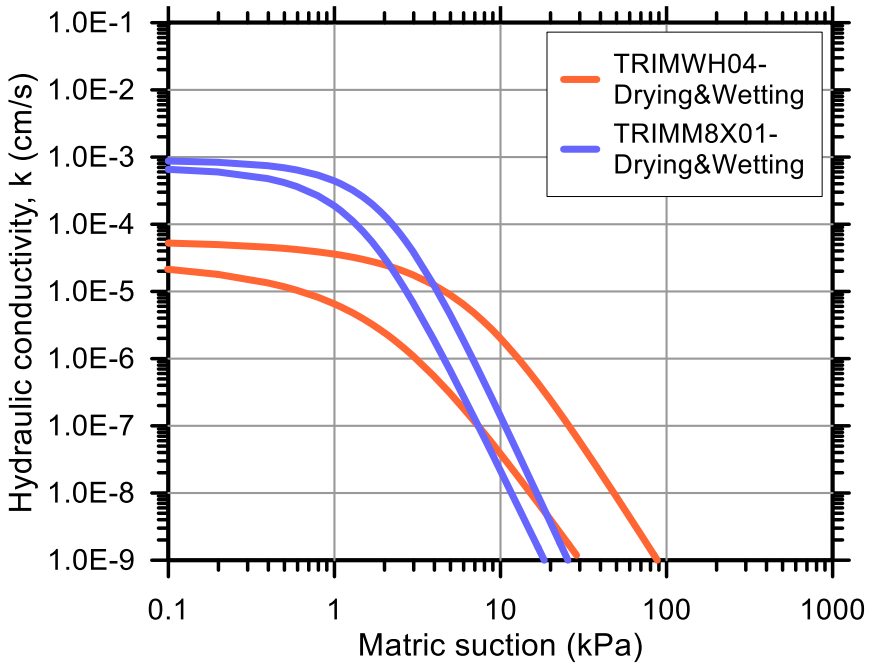

Figure 5.22. The HCF (k-ψ) of TRIMM8X01 (85%Sand-15%Clay specimen) & TRIMWH04 (Whiterhorne specimen)

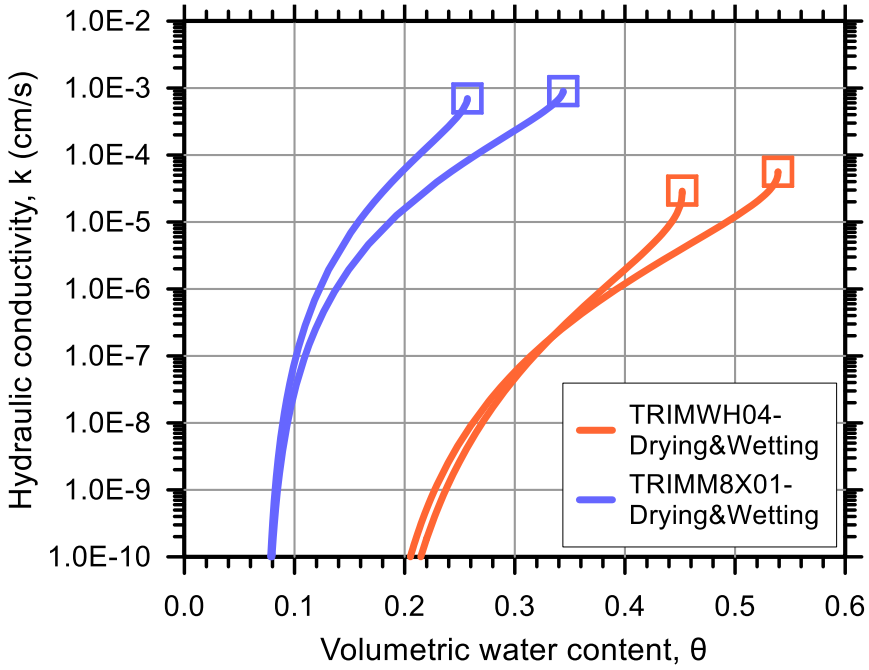

Figure 5.23. The HCF (k-θ) of TRIMM8X01 (85%Sand-15%Clay specimen) & TRIMWH04 (Whiterhorne specimen)

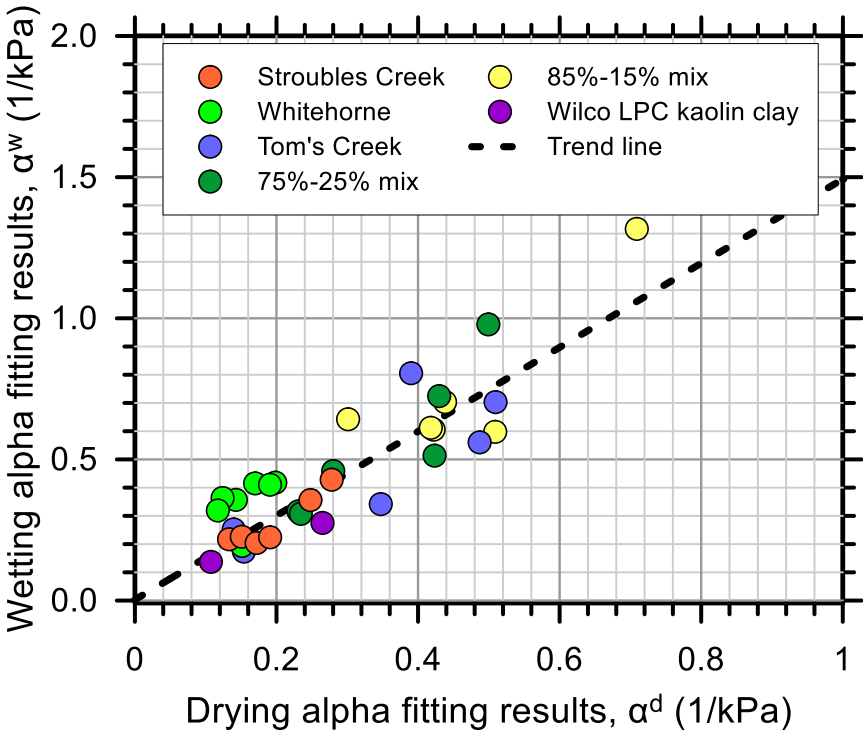

Figure 5.24. Comparison of wetting and drying alpha (α) parameters

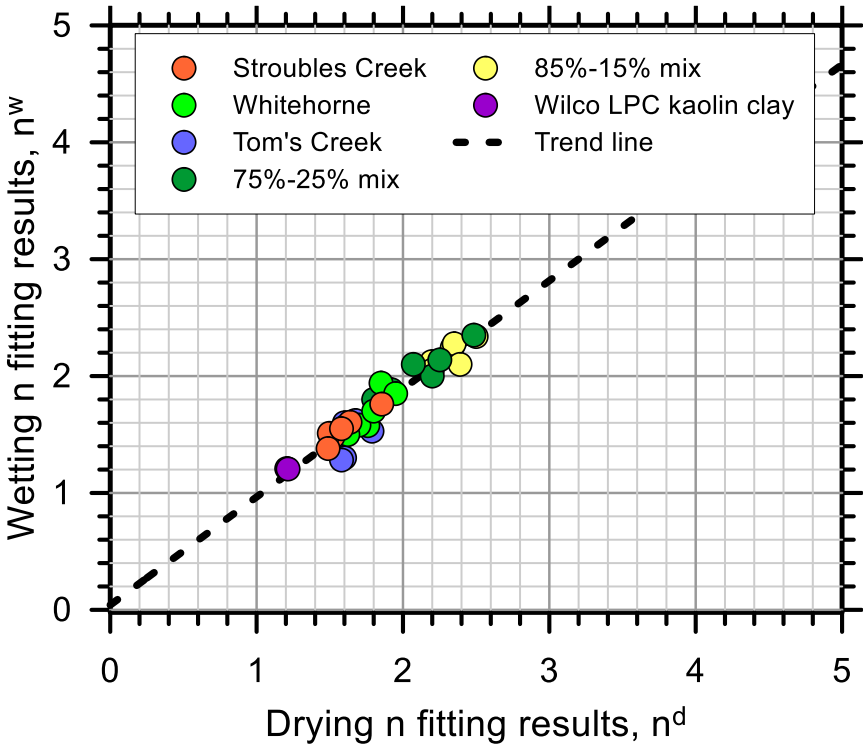

Figure 5.25. Comparison of wetting and drying pore-size distribution (n) parameters

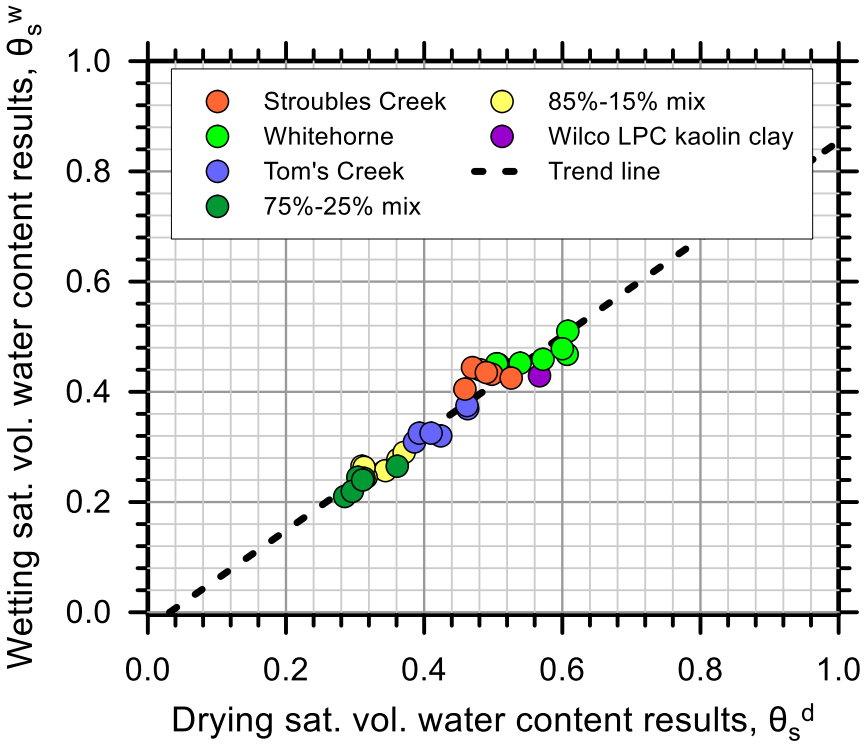

Figure 5.26. Comparison of wetting and drying saturated volumetric water content parameters

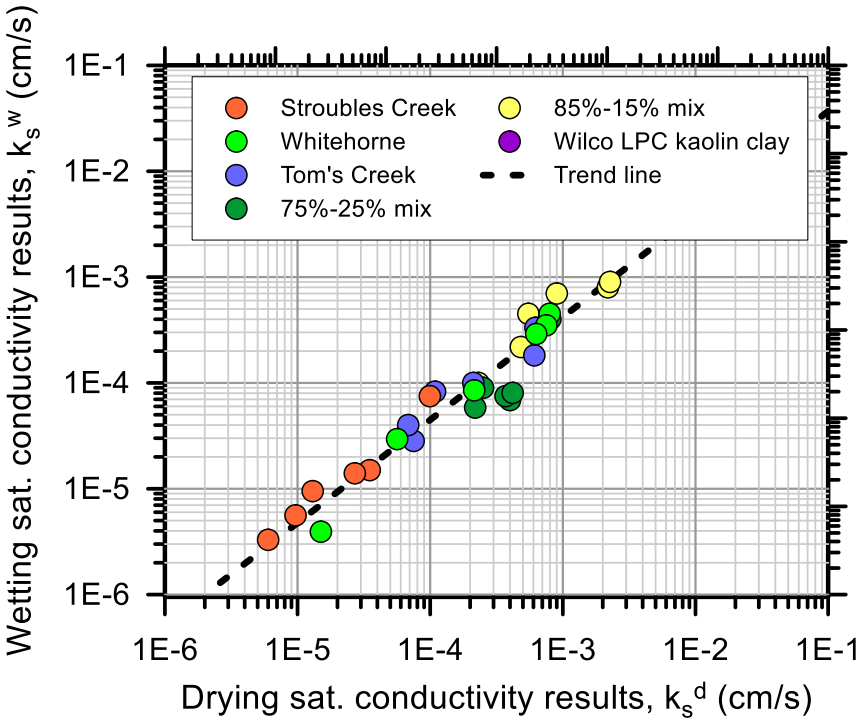

Figure 5.27. Comparison of wetting and drying saturated hydraulic conductivity results

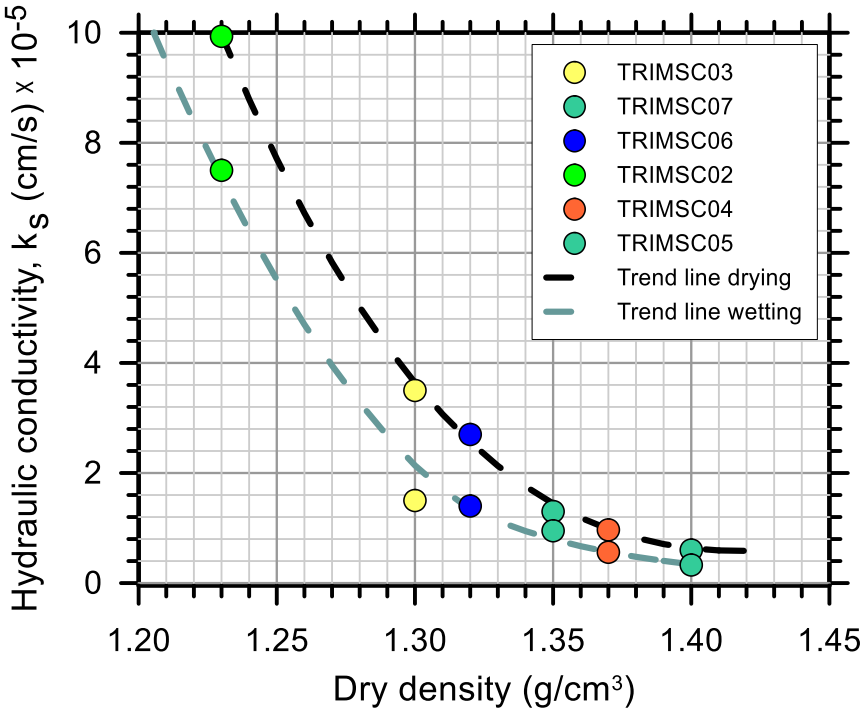

Figure 5.28. Hydraulic conductivity vs. dry density of Stroubles Creek TRIM tests

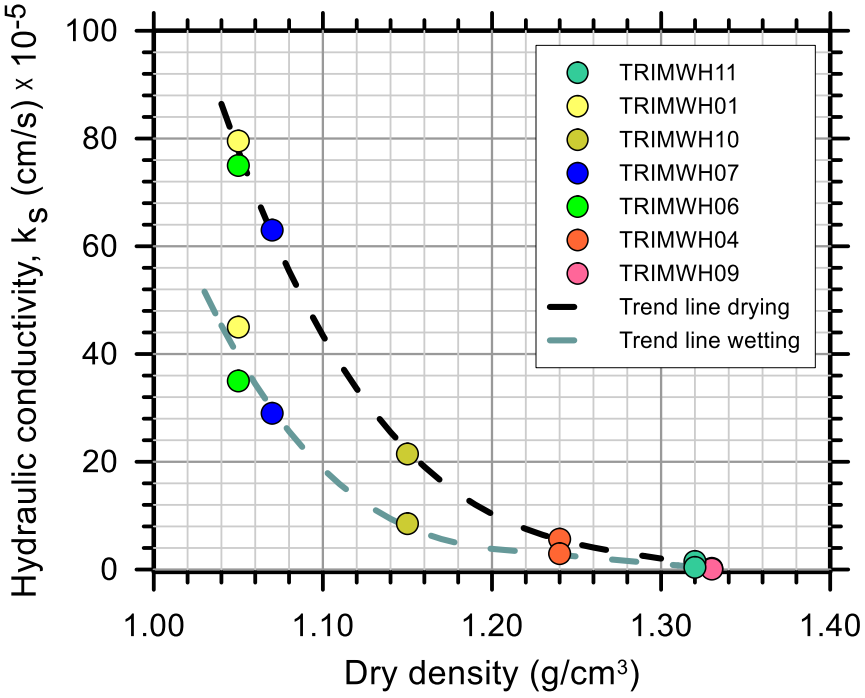

Figure 5.29. Hydraulic conductivity vs. dry density of Whitehorne TRIM tests

5.7. Influence of the Kaolin Clay Content

The variations of van Genuchten fitting parameters and residual volumetric water contents with kaolin clay content are shown in Figures 5.30-5.32. In order to enable a comparison for these parameters, the average values separately for drying and wetting conditions were calculated for all tests at each kaolin clay content. van Genuchten's alpha fitting parameter decreases with higher kaolin clay content, as shown in Figure 5.30. Fine materials such as silts and clays have greater specific surface area compared to granular materials such as sands and gravels. For example, the optimum water content of sand-clay (85%-15) mix at standard proctor compaction test was measured at 9.4%, while it was 10.4% for the sample of sand-clay (75%-25%). More fines in a specimen require more water for reaction. The low AEV is represented by smaller alpha fitting parameters. A large AEV is required for a soil with small pores and micro-scale structure dominated. The difference between drying and wetting narrows with an increase of kaolin clay content.

The pore-size distribution parameter (n) controls the slope of SWCC. As shown in Figure 5.31, n tends to decrease as the amount of kaolin contents in sand-clay mix increases. The average values for both drying and wetting have close values to each other, so a single trend line for both states was drawn.

The average residual volumetric water contents resulting from these test results are plotted versus kaolin clay content. As expected, residual volumetric water content increases with kaolin clay content. As shown in Figure 5.32, a tremendous difference is noted between the samples with 0% kaolin content (Play sand) and 100% kaolin clay content (Wilco LPC kaolin clay). Also, the slope of trend line decreases with increasing kaolin clay content.

The change of van Genuchten fitting parameter with increasing fines content was examined by several researchers. Osinubi et al. (2010) studied the effect of bagasse ash content on SWCC parameters. Except for the variation of n parameters, their findings have great agreement with our findings. Chiu and Shackelford (1998) worked on a very similar project to ours in a narrow range of kaolin clay content (between 0% and 30%). Their findings strongly support ours in terms of alpha and n fitting parameters and residual volumetric water content results.

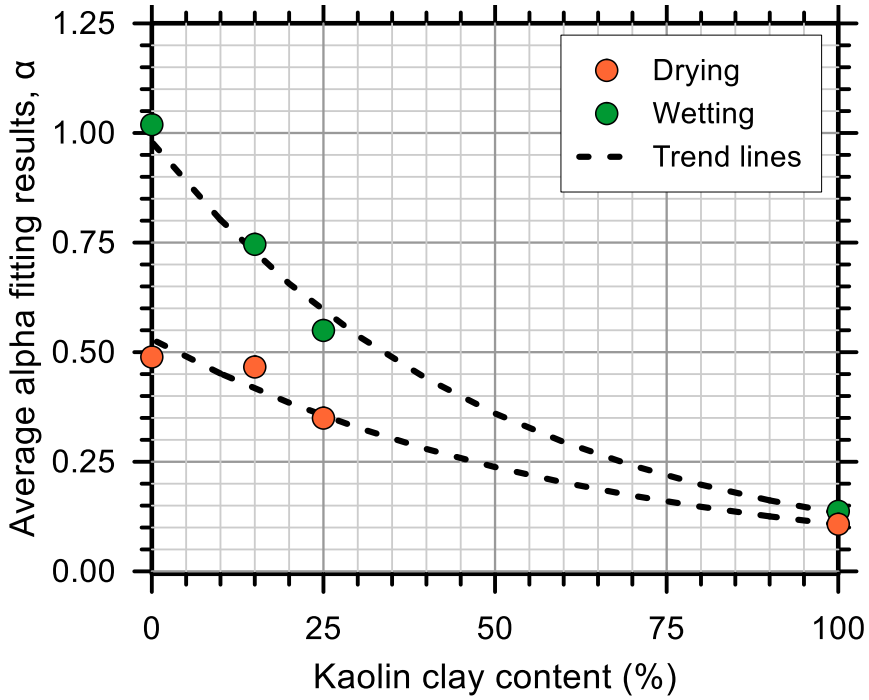

Figure 5.30. The variation of average alpha fitting parameters with kaolin clay content

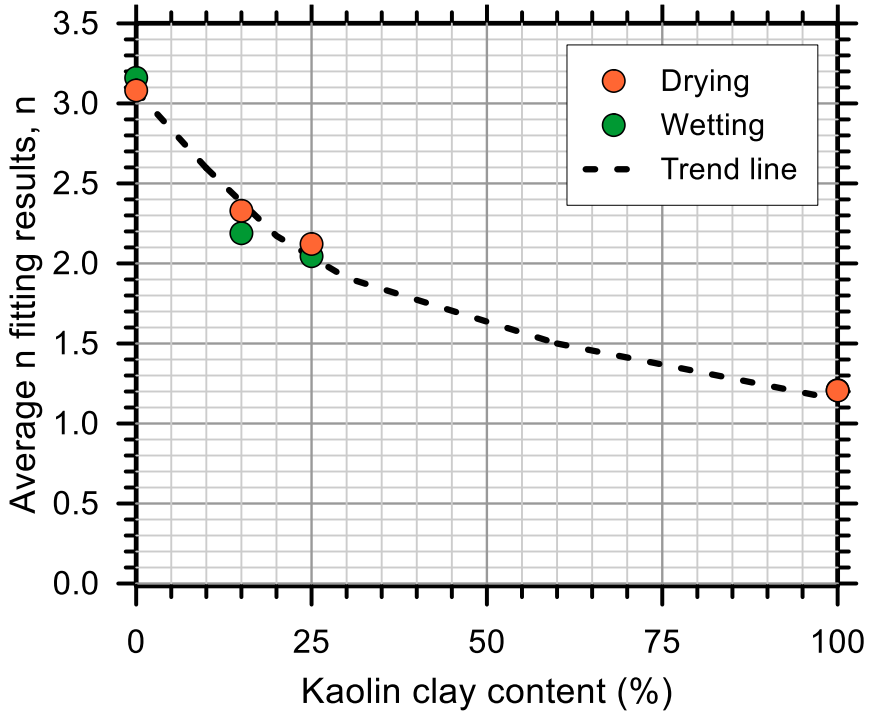

Figure 5.31. The variation of average n fitting parameters with kaolin clay content

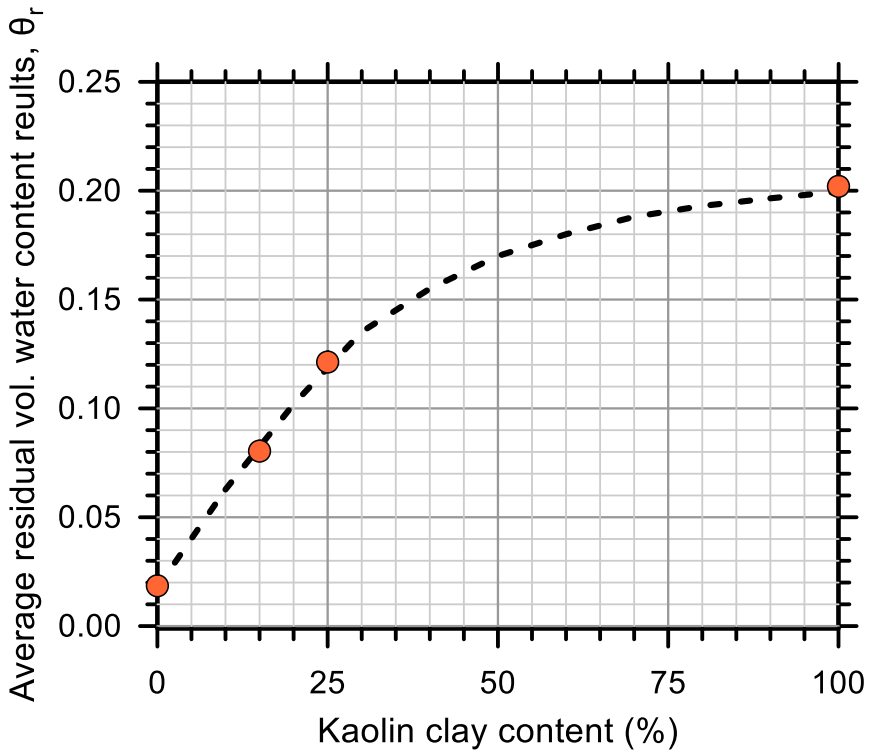

Figure 5.32. The variation of average residual volumetric water content results with kaolin clay content

5.8. Influence of the Cracking on TRIM Results

Drying of soils and its consequence of cracking is a crucial issue in geotechnical engineering. Cracks are also a significant threat for inception of failure surface at the top of the dams and embankments. The fact that soil cracks are particularly important for fine-textured clay soils during rainfall or irrigation is widely recognized. With studies related to experimental, theoretical and modeling, a substantial effort has been made to understand the effect of cracking on hydro-mechanics of unsaturated soils. In general, the problem of estimating the ground surface flux is a complicated problem, but the occurrence of cracks makes the problem even more sophisticated because of the numerous uncertainties arising from cracks.

Drying results from an initial thermodynamic imbalance between the soil moisture and its surroundings, which causes a transfer of liquids within the soil. Given the fundamental influence of water content in cracking, it is necessary to assess the partially saturated behavior. In a circumstance of cracking, the soil matric is divided into two components: (1) vertical infiltration through soil

surface and (2) lateral infiltration via soil cracks. The first component can be solved using 1-D Richards' equation as was done in this research. In order to consider the second component, the Green-Ampt approach can be used to calculate the horizontal infiltration from soil cracks into the soil matrix.

The serious simulation problems regarding kaolin clay TRIM tests are basically the consequence of cracking phenomena. For a discussion purpose, the mass water outflow data and volumetric water content change with time of TRIMKC01 are given in Figure 5.33. During the small suction pressure, a small amount of water outflow was monitored and a visible crack around the specimen was not noted. Just after the application of large suction, a rapid transient outflow and continuous large cracks through the soil specimen were recorded. Figure 5.34 shows the results of saturated hydraulic conductivity in change with dry density. As it is expected, the hydraulic conductivity is very low for this material. Taking into account these results, the maximum and minimum hydraulic conductivity values were set and an iteration process was applied. Although many trials were performed, a satisfactory convergence between model and experimental data was not obtained. As an attempt to achieve a best fitting, the range between maximum and minimum hydraulic conductivity value was extended and increased. A satisfactory convergence for hydraulic conductivity at the beginning of drying state was measured as 1.49E-03. This value is approximately three orders of magnitude greater than predicted value.

The measurement of the hydraulic conductivity for a cracked unsaturated soil is extremely difficult. Albrecht and Benson (2001) looked into the effect of desiccation on compacted natural clays. Hydraulic conductivity tests were conducted on the samples which experienced cracks after drying and wetting cycles. Hydraulic conductivity tests indicated that cracking of the specimen resulted in an increase in hydraulic conductivity, sometimes as large as three orders of magnitude. Lateral infiltration from the macropores into the soil greatly affects the fluid flow and should be included in water flow simulations of dry cracking soil (Greve et al. 2010). The difficulty in modeling to cracked soil is that the flow in both regions, one associated with macropores (the crack network) and the other with the less permeable matrix region, is described using Richards' equation, an assumption that is likely not applicable for flow in large drying cracks. If a soil contains cracks its physical behavior can be assumed to be bi-modal in character. Therefore, the inverse modeling of TRIM data must be improved for the soils susceptible to cracking.

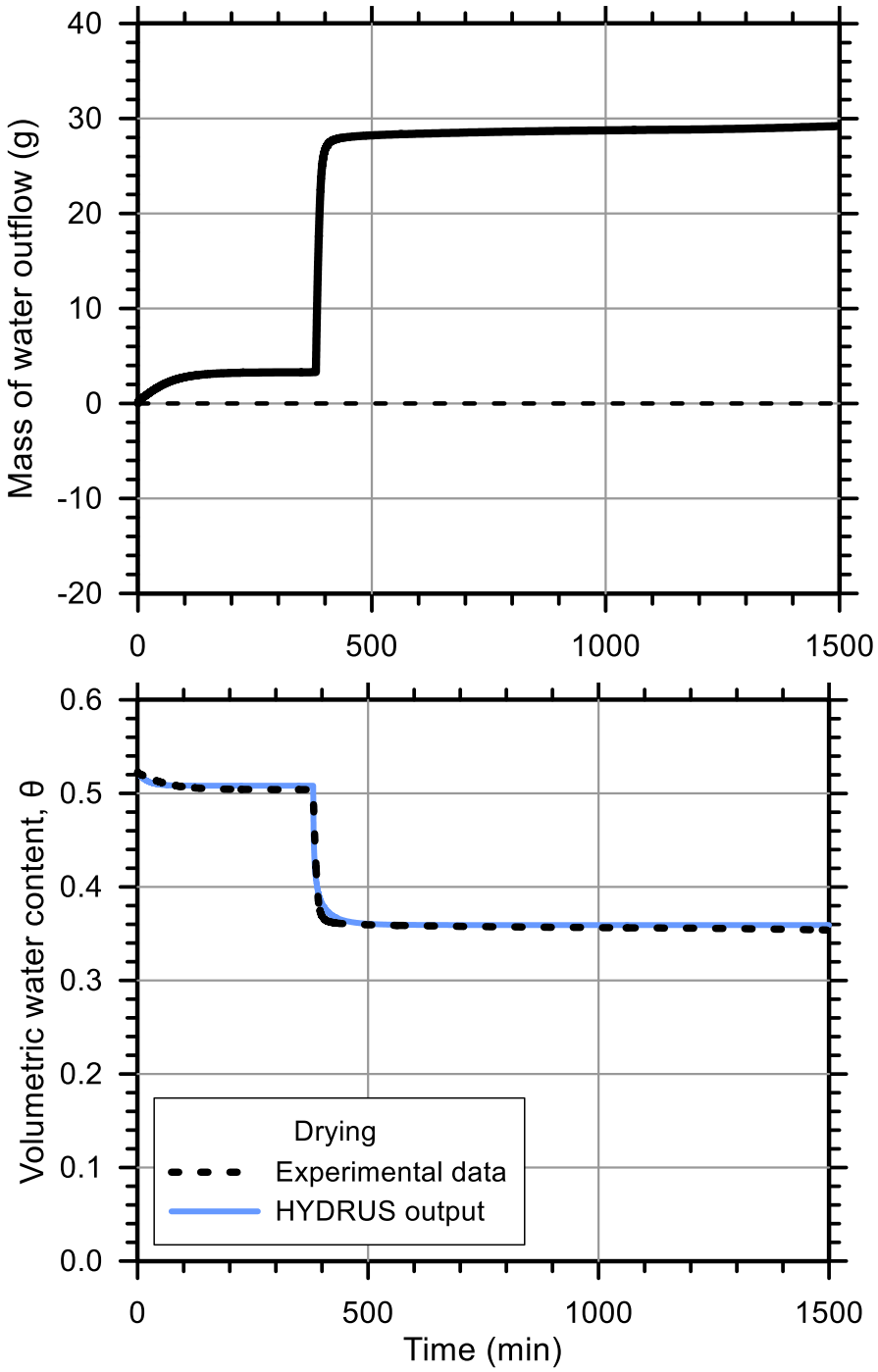

Figure 5.33. Mass water outflow and volumetric water content vs. time of TRIMKC01 test (Wilco LPC kaolin clay specimen)

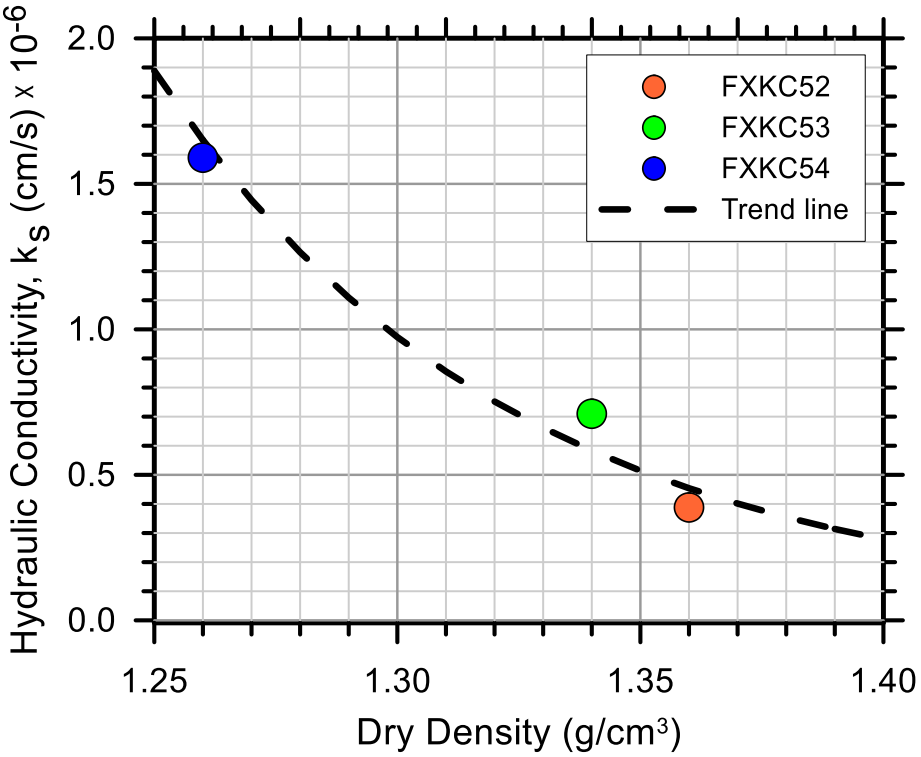

Figure 5.34. Hydraulic conductivity vs. dry density of Wilco LPC kaolin clay

6. SUMMARY & CONCLUSIONS

In order to have a fundamental understanding related to the hydrological properties of unsaturated soils under different conditions, a comprehensive experimental program was carried out. A series of TRIM tests and saturated hydraulic conductivity tests with the flexible wall method were performed to investigate the influences of several factors, including molding water content, initial dry density or relative compaction, hysteresis, and kaolin clay content. TRIM has capability to measure SWCC and HCF under wetting state. Therefore, the particular interest is not only on drying conditions, but also on wetting conditions of testing soils. This provides a strong tool to study hysteresis between the drying and wetting process in a soil profile. The unified drying and wetting testing protocol of TRIM provides a very simple and relatively rapid framework for experimental measurement. The results of saturated hydraulic conductivity through flexible wall method provided a crucial guidance in which maximum and minimum saturated hydraulic conductivity values are assigned during the drying iteration process. Data within this study are compared to findings presented by prior researchers in the area of unsaturated soil mechanics.

This study has provided valuable insights on the influence of certain factors on soil-water characteristics. Based on the experimental results, the following conclusions can be drawn:

1. Initial water content affects the soil structure which in turn has an influence on the soil-water characteristics of the tested soil. It is found that the soil specimen compacted at wet of optimum with relatively uniform pore-size distributions poses a large AEV, lower rate of desaturation, and a larger hysteresis loop than the dry of optimum soil specimen compacted at dry of optimum with relatively non-uniform pore-size distributions. The soil-water characteristics of the soil specimen compacted at optimum water content lies in between those of the specimens compacted at water contents that are dry and wet of optimum.
2. The soil specimens molded at the same water content, but with larger dry density yield a larger AEV and lower rate of drying process. AEV is one of the parameters of SWCC that is most influenced by dry density. Retaining water capacity (residual volumetric water content) of soil increases with an increase of dry density. Furthermore, hysteresis becomes less significant for the specimens compacted at high relative compaction levels.

3. The experimental results indicate that an increase in kaolin clay content results in an increase of residual volumetric water content, and a decrease in van Genuchten's fitting parameters (alpha and n).
4. Under the hysteresis framework, the fitting parameters for both drying and wetting conditions were used to quantitatively assess the differences and uncertainty for cohesive soils. Except for the Play sand test soil, all test soils are classified as cohesive soils. The results are reported as the mean ratio plus or minus the standard deviation about the mean ratio with coefficient of variation in parentheses. The relations of α^w/α^d=1.66$\pm$0.50 (30), n^w/n^d=0.95$\pm$0.05 (6), θ_s^w/θ_s^d=0.82$\pm$0.05 (7) and k_s^w/k_s^d=0.48$\pm$0.17 (37) are discovered. The relations of n^w/n^d and θ_s^w/θ_s^d confirmed that there is no significant dependency on nominal soil type, whereas, the relations of α^w/α^d and k_s^w/k_s^d show a significant scatter with the several of soil types.
5. The applicability of transient water analysis is questioned again for the soils which have a tendency to crack during drying process. The response of TRIM and data analysis for those soils is evaluated. Richards' equation is not sufficient to describe transient analysis in cracked soils. An improved model is required in order to evaluate cracked soil in a better and reliable way.
6. As a result of process iteration, a number of possible convergences are generated by HYDRUS 1-D. Therefore, it is necessary to assign logical maximum and minimum values for each parameter. At that point, particular results from saturated hydraulic conductivity values provided crucial guidance for the prediction of hydraulic conductivity result in drying and wetting states.

REFERENCES

Acar, Y. B., and Olivieri, I. (1989). "Pore fluid effects on the fabric and hydraulic conductivity of laboratory-compacted clay." *Transportation Research Record*(1219).

Ahuja, L. R., Ross, J. D., Bruce, R. R., and Cassel, D. K. (1988). "Determining unsaturated hydraulic conductivity from tensiometric data alone." *Soil Science Society of America Journal*, 52(1), 27-34.

Al-Khafaf, S., and Hanks, R. J. (1974). "Evaluation of the filter paper method for estimating soil water potential." *Soil Science*, 117(4), 194-199.

Albrecht, B. A., and Benson, C. H. (2001). "Effect of desiccation on compacted natural clays." *J Geotech Geoenviron*, 127(1), 67-75.

Albrecht, B. A., Benson, C. H., and Beuermann, S. (2003). "Polymer capacitance sensors for measuring soil gas humidity in drier soils." *Geotechnical Testing Journal, ASTM*, 26, 3-11.

Arya, L. M., and Paris, J. F. (1981). "A physicoempirical model to predict the soil moisture characteristic from particle-size distribution and bulk density data." *Soil Science Society of America Journal*, 45(6), 1023-1030.

Assouline, S. (2001). "A model for soil relative hydraulic conductivity based on the water retention characteristic curve." *Water Resources Research*, 37(2), 265-271.

Averjanov, S. (1950). "About permeability of subsurface soils in case of incomplete saturation." *English Collection*, 7, 19-21.

Bandini, P., and Sathiskumar, S. (2009). "Effects of silt content and void ratio on the saturated hydraulic conductivity and compressibility of sand-silt mixtures." *J Geotech Geoenviron*, 135(12), 1976-1980.

Barden, L., and Pavlakis, G. (1971). "Air and water permeability of compacted unsaturated cohesive soil." *Journal of Soil Science*, 22(3), 302-318.

Benson, C. H., and Daniel, D. E. (1990). "Influence of clods on the hydraulic conductivity of compacted clay." *Journal of Geotechnical Engineering*, 116(8), 1231-1248.

Benson, C. H., and Gribb, M. (1997). "Measuring unsaturated hydraulic conductivity in the laboratory and the field." *Unsaturated Soil Engineering Practice*, in S. Houston and D. G. Fredlund, ed., ASCE Special Technical Publication No. 68, 113-168.

Bocking, K. A., and Fredlund, D. G. (1980). "Limitations of the axis translation technique." *Proceedings of 4th International Conferance on Expansive Soils*, ASCE, 117-135.

Brooks, R. H., and Corey, A. T. (1964). "Hydraulic properties of porous media and their relation to drainage design." *Transactions of the ASAE*, 7(1), 26-0028.

Brutsaert, W. (1967). "Some methods of calculating unsaturated permeability." *Transactions of the ASAE*, 10(3), 400-0404.

Bulut, R., Lytton, R. L., and Wray, W. K. (2001). "Soil suction measurements by filter paper." *Proceedings of Expansive clay soils and vegetative influence on shallow foundations*, ASCE, 243-261.

Burdine, N. T. (1953). "Relative permeability calculations from pore size distribution data." *Journal of Petroleum Technology*, 5(03), 71-78.

American Society for Testing and Materials (ASTM) C136 (2006). "Standard Test Method for Sieve Analysis of Fine and Course." ASTM International, West Conshohocken, PA.

Campbell, G. S. (1974). "A simple method for determining unsaturated conductivity from moisture retention data." *Soil Science*, 117(6), 311-314.

Campbell, J. D. (1973). "Pore pressures and volume changes in unsaturated soils." Ph.D. Thesis, University of Illinois at Urbana-Champaign, IL.

Caputo, M. C., and Nimmo, J. R. (2005). "Quasi-steady centrifuge method for unsaturated hydraulic properties." *Water Resources Research*, 41(11).

Cassel, D. K., and Klute, A. (1986). "Water potential: tensiometry." *Methods of Soil Analysis: Part 1—Physical and Mineralogical Methods*, 563-596.

Chandler, R. J., and Gutierrez, C. I. (1986). "The filter-paper method of suction measurement." *Géotechnique*, 36(2), 265-268.

Childs, E. (1940). "The use of soil moisture characteristics in soil studies." *Soil Science*, 50(4), 239-252.

Childs, E. C., and Collis-George, N. (1950). "The permeability of porous materials." *Proceedings of the Royal Society of London A: Mathematical, Physical and Engineering Sciences*, The Royal Society, 392-405.

Chiu, T.-F., and Shackelford, C. D. (1998). "Unsaturated hydraulic conductivity of compacted sand-kaolin mixtures." *J Geotech Geoenviron*, 124(2), 160-170.

Clapp, R. B., and Hornberger, G. M. (1978). "Empirical equations for some soil hydraulic properties." *Water Resources Research*, 14(4), 601-604.

Corey, A. T. (1954). "The interrelation between gas and oil relative permeabilities." *Producer's monthly*, 19(1), 38-41.

Corey, A. T. (1957). "Measurement of water and air permeability in unsaturated soil." *Soil Science Society of America Journal*, 21(1), 7-10.

Crescimanno, G., and Iovino, M. (1995). "Parameter estimation by inverse method based on one-step and multi-step outflow experiments." *Geoderma*, 68(4), 257-277.

Croney, D., and Coleman, J. (1954). "Soil structure in relation to soil suction (pF)." *Journal of Soil Science*, 5(1), 75-84.

American Society for Testing and Materials (ASTM) D422 (2007). "Standard Test Method for Particle-Size Analysis of Soils." ASTM International, West Conshohocken, PA.

American Society for Testing and Materials (ASTM) D584 (2014). "Standard Test Methods for Specific Gravity of Soil Solids by Water Pycnometer." ASTM International, West Conshohocken, PA.

American Society for Testing and Materials (ASTM) D698 (2003). "Standard Test Method for Laboratory Compaction Characteristics of Soil Using Standard Effort (12,400 ft-lbf/ft 3 (600 kN-m/m 3))." ASTM International, West Conshohocken, PA.

American Society for Testing and Materials (ASTM) D1140 (2014). "Standard Test Methods for Determining the Amount of Material Finer than 75-μm (No. 200) Sieve in Soils by Washing." ASTM International, West Conshohocken, PA.

American Society for Testing and Materials (ASTM) D4318 (2003). "Standard Test Methods for Liquid Limit, Plastic Limit, and Plasticity Index of Soils." ASTM International, West Conshohocken, PA.

American Society for Testing and Materials (ASTM) D5084 (2010). "Standard Test Methods for Measurement of Hydraulic Conductivity of Saturated Porous Materials Using a Flexible Wall Permeameter." ASTM International, West Conshohocken, PA.

American Society for Testing and Materials (ASTM) D5298 (2010). "Standard Test Method for Measurement of Soil Potential Suction Using Filter Paper." ASTM International, West Conshohocken, PA.

Davidson, J. M., Stone, L. R., Nielsen, D. R., and Larue, M. E. (1969). "Field Measurement and Use of Soil-Water Properties." *Water Resources Research*, 5(6), 1312-1321.

Doering, E. J. (1965). "Soil-water diffusivity by the one-step method." *Soil Science*, 99(5), 322-326.

Dong, Y., Wayllace, A., Lu, N., and Smits, K. (2014). "Measurement of thermal conductivity function of unsaturated soil using a transient water release and imbibition method." *Geotechnical Testing Journal*, 37(6), 980-990.

Dumbleton, M. J., and West, G. (1966). "Some factors affecting the relation between the clay minerals in soils and their plasticity." *Clay Minerals*, 6(3), 179-193.

Durner, W. (1994). "Hydraulic conductivity estimation for soils with heterogeneous pore structure." *Water Resources Research*, 30(2), 211-223.

Durner, W., Priesack, E., Vogel, H.-J., and Zurmühl, T. (1999). "Determination of parameters for flexible hydraulic functions by inverse modeling." *Proceedings of the 1st International Workshop on Characterization and Measurement of the Hydraulic Properties of Unsaturated Porous Media*, 817-829.

Durner, W., Schultze, B., and Zurmühl, T. (1999). "State-of-the-art in inverse modeling of inflow/outflow experiments." *Proceedings of the 1st International Workshop on Characterization and Measurement of the Hydraulic Properties of Unsaturated Porous Media*, 661-681.

Eching, S. O., and Hopmans, J. W. (1993). "Optimization of hydraulic functions from transient outflow and soil water pressure data." *Soil Science Society of America Journal*, 57(5), 1167-1175.

Eching, S. O., Hopmans, J. W., and Wendroth, O. (1994). "Unsaturated hydraulic conductivity from transient multistep outflow and soil water pressure data." *Soil Science Society of America Journal*, 58(3), 687-695.

El-Ehwany, M., and Houston, S. L. (1990). "Settlement and moisture movement in collapsible soils." *Journal of Geotechnical Engineering*, 116(10), 1521-1535.

Fawcett, R. G., and Collis-George, N. (1967). "A filter-paper method for determining the moisture characteristics of soil." *Animal Production Science*, 7(25), 162-167.

Fredlund, D. G. (2000). "The 1999 RM Hardy Lecture: The implementation of unsaturated soil mechanics into geotechnical engineering." *Canadian Geotechnical Journal*, 37(5), 963-986.

Fredlund, D. G., and Rahardjo, H. (1993). *Soil mechanics for unsaturated soils*, John Wiley & Sons.

Fredlund, D. G., Rahardjo, H., and Fredlund, M. D. (2012). *Unsaturated soil mechanics in engineering practice*, John Wiley & Sons.

Fredlund, D. G., and Wong, D. K. H. (1989). "Calibration of thermal conductivity sensors for measuring soil suction." *Geotechnical Testing Journal, GTJODJ*, 12(3), 188-194.

Fredlund, D. G., and Xing, A. (1994a). "Equations for the soil-water characteristic curve." *Canadian Geotechnical Journal*, 31(4), 521-532.

Fredlund, D. G., Xing, A., and Huang, S. (1994b). "Predicting the permeability function for unsaturated soils using the soil-water characteristic curve." *Canadian Geotechnical Journal*, 31(4), 533-546.

Fredlund, M. D., Wilson, G. W., and Fredlund, D. G. (2002). "Use of the grain-size distribution for estimation of the soil-water characteristic curve." *Canadian Geotechnical Journal*, 39(5), 1103-1117.

Gallage, C., Kodikara, J., and Uchimura, T. (2013). "Laboratory measurement of hydraulic conductivity functions of two unsaturated sandy soils during drying and wetting processes." *Soils and Foundations*, 53(3), 417-430.

Garcia-Bengochea, I., Altschaeffl, A. G., and Lovell, C. W. (1979). "Pore distribution and permeability of silty clays." *Journal of the Geotechnical Engineering Division*, 105(7), 839-856.

Gardner, W. R. (1956). "Calculation of capillary conductivity from pressure plate outflow data." *Soil Science Society of America Journal*, 20(3), 317-320.

Gardner, W. R. (1958). "Some steady-state solutions of the unsaturated moisture flow equation with application to evaporation from a water table." *Soil Science*, 85(4), 228-232.

Gardner, W. R. (1962). "Note on the separation and solution of diffusion type equations." *Soil Science Society of America Proceedings*, 26, 404.

Gardner, W. R. (1970). "Post irrigation movement of soil water: II. Simultaneous redistribution tnd evaporation." *Water Resource Research*, 6, 1148-1153.

Gardner, W. R., Hillel, D., and Benyamini, Y. (1970). "Post-Irrigation Movement of Soil Water: I. Redistribution." *Water Resources Research*, 6(3), 851-861.

Gavin, H. P. (2016). "The Levenberg-Marquardt method for nonlinear least squares curve-fitting problems."Duke University, NC.

Gee, G. W., Campbell, M. D., Campbell, G. S., and Campbell, J. H. (1992). "Rapid measurement of low soil water potentials using a water activity meter." *Soil Science Society of America Journal*, 56(4), 1068-1070.

Ghanbarian-Alavijeh, B., Liaghat, A., Huang, G.-H., and Van Genuchten, M. T. (2010). "Estimation of the van Genuchten soil water retention properties from soil textural data." *Pedosphere*, 20(4), 456-465.

Gillham, R. W., Klute, A., and Heermann, D. F. (1976). "Hydraulic properties of a porous medium: Measurement and empirical representation." *Soil Science Society of America Journal*, 40(2), 203-207.

Greve, A., Andersen, M. S., and Acworth, R. I. (2010). "Investigations of soil cracking and preferential flow in a weighing lysimeter filled with cracking clay soil." *Journal of Hydrology*, 393(1), 105-113.

Gupta, S. C., Farrell, D. A., and Larson, W. E. (1974). "Determining effective soil water diffusivities from one-step outflow experiments." *Soil Science Society of America Journal*, 38(5), 710-716.

Haines, W. B. (1930). "Studies in the physical properties of soil. V. The hysteresis effect in capillary properties, and the modes of moisture distribution associated therewith." *The Journal of Agricultural Science*, 20(01), 97-116.

Hamblin, A. P. (1981). "Filter-paper method for routine measurement of field water potential." *Journal of Hydrology*, 53(3), 355-360.

Haverkamp, R., Leij, F. J., Fuentes, C., Sciortino, A., and Ross, P. J. (2005). "Soil water retention: I. Introdcution of a shape index." *Soil Science Society of America Journal*, 69(6), 1881-1890.

Haverkamp, R., and Parlange, J.-Y. (1986). "Predicting the water-retention curve from particle-size distribution: I. Sandy soils without organic matter." *Soil Science*, 142(6), 325-339.

Hilf, J. W. (1956). "An investigation of pore water pressure in compacted cohesive soils." Ph.D. Dissertation, University of Colorado.

Hillel, D. (1980). *Fundamentals of soil physics*, Academic press.

Holtz, R. D., and Kovacs, W. D. (1981). *An introduction to geotechnical engineering*.

Hopmans, J. W., Šimůnek, J., Romano, N., and Durner, W. (2002). "Inverse modeling of transient water flow." *Methods of Soil Analysis, Part 1, Physical Methods*, 963-1008.

Houston, S. L., Houston, W. N., and Wagner, A. (1994). "Laboratory filter paper suction measurements." *Geotechnical Testing Journal*, 17(2), 185-194.

Huang, S., Barbour, S. L., and Fredlund, D. G. (1998a). "Development and verification of a coefficient of permeability function for a deformable unsaturated soil." *Canadian Geotechnical Journal*, 35(3), 411-425.

Huang, S., Fredlund, D. G., and Barbour, S. L. (1998b). "Measurement of the coefficient of permeability for a deformable unsaturated soil using a triaxial permeameter." *Canadian Geotechnical Journal*, 35(3), 426-432.

Huat, B. B., Gue, S. S., and Ali, F. H. (2007). *Tropical residual soils engineering*, CRC Press.

Inoue, M., Šimůnek, J., Shiozawa, S., and Hopmans, J. (2000). "Simultaneous estimation of soil hydraulic and solute transport parameters from transient infiltration experiments." *Advances in Water Resources*, 23(7), 677-688.

Irmay, S. (1954). "On the hydraulic conductivity of unsaturated soils." *Eos, Transactions American Geophysical Union*, 35(3), 463-467.

Johnston, C. J. (1942). "Water-permeable jacketed thermal radiators as indicators of field capacity and permanent wilting percentage in soils." *Soil Science*, 54(2), 123-126.

Kawai, K., Kato, S., Karube, D., Rahardjo, H., Toll, D., and Leong, E. (2000). "The model of water retention curve considering effects of void ratio." *Proceedings of Unsaturated soils for Asia. Proceedings of the Asian Conference on Unsaturated Soils, UNSAT-Asia 2000, Singapore, 18-19 May, 2000.*, AA Balkema, 329-334.

Klute, A. (1972). "The determination of the hydraulic conductivity and diffusivity of unsaturated soils." *Soil Science*, 113(4), 264-276.

Klute, A., and Dirksen, C. (1986). "Hydraulic conductivity and diffusivity: laboratory methods." *Methods of Soil Analysis, Part I. Physical and Mineralogocal Methods,* Soil Science Society of America, Monograph No. 9, Madison, WI, 687-734.

Kool, J., Parker, J., and Van Genuchten, M. T. (1985). "Determining soil hydraulic properties from one-step outflow experiments by parameter estimation: I. Theory and numerical studies." *Soil Science Society of America Journal*, 49(6), 1348-1354.

Kool, J., and Parker, J. C. (1987). "Development and evaluation of closed-form expressions for hysteretic soil hydraulic properties." *Water Resources Research*, 23(1), 105-114.

Kosugi, K. (1996). "Lognormal distribution model for unsaturated soil hydraulic properties." *Water Resources Research*, 32(9), 2697-2703.

Kosugi, K., Hopmans, J. W., and Dane, J. H. (2002). "3. 3. 4 parametric models." *Methods of Soil Analysis: Part 4 Physical Methods*, 728-757.

Leong, E. C., and Rahardjo, H. (1997a). "Review of soil-water characteristic curve equations." *J Geotech Geoenviron*, 123(12), 1106-1117.

Leong, E. C., and Rahardjo, H. (1997b). "Permeability functions for unsaturated soils." *J Geotech Geoenviron*, 123(12), 1118-1126.

Likos, W., and Lu, N. (2001). "Automated measurement of total suction characteristics in high-suction range: Application to assessment of swelling potential." *Transportation Research Record: Journal of the Transportation Research Board*(1755), 119-128.

Likos, W., and Lu, N. (2002). "Filter paper technique for measuring total soil suction." *Transportation Research Record: Journal of the Transportation Research Board*(1786), 120-128.

Likos, W. J., Lu, N., and Godt, J. W. (2013). "Hysteresis and uncertainty in soil water-retention curve parameters." *J Geotech Geoenviron*, 140(4).

Lin, L.-C., and Benson, C. H. (2000). "Effect of wet-dry cycling on swelling and hydraulic conductivity of GCLs." *J Geotech Geoenviron*, 126(1), 40-49.

Lourakis, M. I. (2005). "A brief description of the Levenberg-Marquardt algorithm implemented by levmar." *Foundation of Research and Technology*, 4, 1-6.

Lu, N., Kaya, M., Collins, B. D., and Godt, J. W. (2013). "Hysteresis of unsaturated hydromechanical properties of a silty soil." *J Geotech Geoenviron*, 139(3), 507-510.

Lu, N., and Likos, W. J. (2003). "Automated humidity system for measuring total suction characteristics of clay." *Geotechnical Testing Journal, ASTM*, 26(2), 178-189.

Lu, N., and Likos, W. J. (2004). *Unsaturated soil mechanics*, J. Wiley, Hoboken, N.J.

Lu, N., Wayllace, A., Carrera, J., and Likos, W. J. (2006). "Constant flow method for concurrently measuring soil-water characteristic curve and hydraulic conductivity function." *Geotechnical Testing Journal*, 29(3), 256-266.

Maqsoud, A., Bussière, B., Mbonimpa, M., and Aubertin, M. (2004). "Hysteresis effects on the water retention curve: a comparison between laboratory results and predictive models." *Proceedings of the 57th Canadian Geotechnical Conference and the 5th Joint CGS-IAH Conference, Québec City, Que, Canada*, 24-27.

Marinho, F. A. M. (2005). "Nature of soil–water characteristic curve for plastic soils." *J Geotech Geoenviron*, 131(5), 654-661.

Masrouri, F., Bicalho, K. V., and Kawai, K. (2009). "Laboratory hydraulic testing in unsaturated soils." *Laboratory and Field Testing of Unsaturated Soils*, Springer, 79-92.

Mavimbela, S., and van Rensburg, L. (2013). "Estimating hydraulic conductivity of internal drainage for layered soils in situ." *Hydrology and Earth System Sciences*, 17(11), 4349-4366.

McQueen, I. S., and Miller, R. F. (1974). "Approximating soil moisture characteristics from limited data: empirical evidence and tentative model." *Water Resources Research*, 10(3), 521-527.

Milly, P. (1987). "Estimation of Brooks-Corey Parameters from water retention data." *Water Resources Research*, 23(6), 1085-1089.

Mous, S. L. J. (1993). "Identification of the movement of water in unsaturated soils: the problem of identifiability of the model." *Journal of Hydrology*, 143(1-2), 153-167.

Mualem, Y. (1976). "A new model for predicting the hydraulic conductivity of unsaturated porous media." *Water Resources Research*, 12(3), 513-522.

Mualem, Y. (1978). "Hydraulic conductivity of unsaturated porous media: generalized macroscopic approach." *Water Resources Research*, 14(2), 325-334.

Mualem, Y. (1986). "Hydraulic conductivity of unsaturated soils: Prediction and formulas." *Methods of soil analysis. Part 1. Physical and Mineralogical Methods*, 2nd edition A. Klute, Agronomy Monograph No. 9,, American Society of Agronomy, Madison, WI, 799-823.

Mualem, Y., and Dagan, G. (1978). "Hydraulic conductivity of soils: Unified approach to the statistical models." *Soil Science Society of America Journal*, 42(3), 392-395.

Nimmo, J. R., and Akstin, K. C. (1988). "Hydraulic conductivity of a sandy soil at low water content after compaction by various methods." *Soil Science Society of America Journal*, 52(2), 303-310.

Nimmo, J. R., Perksin, K. S., and Lewis, A. M. (2002). "Steady-state centrifuge." *Part 4. Physical Methods*, J. H. Dane, and C. Topp, eds.Methods of Soil Analysis. Soil Science Society of America, Madison, WI, 903-936.

Nimmo, J. R., Rubin, J., and Hammermeister, D. (1987). "Unsaturated flow in a centrifugal field: Measurement of hydraulic conductivity and testing of Darcy's law." *Water Resources Research*, 23(1), 124-134.

Olsen, H. W., Gill, J. D., Wilden, A. T., and Nelson, K. R. (1991). "Innovations in hydraulic-conductivity measurements." *Transportation Research Record*(1309).

Olsen, H. W., Morin, R. H., and Nichols, R. W. (1988). "Flow pump applications in triaxial testing." *Advanced Triaxial Testing of Soil and Rock*, ASTM International, 68-81.

Olsen, H. W., Willden, A. T., Kiusalaas, N. J., Nelson, K. R., and Poeter, E. P. (1994). "Volume-controlled hydrologic property measurements in triaxial systems." *in Hydraulic Conductivity and Waste Contaminant Transport in Soil*, ASTM International, 482-504.

Osinubi, K. J., Eberemu, A., Hoyos, L., Zhang, X., and Puppala, A. (2010). "Soil Water Characteristic Curve Parameters of Compacted Lateritic Soil Treated with Bagasse Ash." *Proceedings of Experimental and Applied Modeling of Unsaturated Soils*, ASCE, 79-87.

Parker, J. C., Kool, J. B., and Van Genuchten, M. T. (1985). "Determining soil hydraulic properties from one-step outflow experiments by parameter estimation: II. Experimental studies." *Soil Science Society of America Journal*, 49(6), 1354-1359.

Passioura, J. B. (1977). "Determining soil water diffusivities from one-step outflow experiments." *Soil Research*, 15(1), 1-8.

Pham, H. Q., Fredlund, D. G., and Barbour, S. L. (2005). "A study of hysteresis models for soil-water characteristic curves." *Canadian Geotechnical Journal*, 42(6), 1548-1568.

Phene, C. J., Hoffman, G. J., and Rawlins, S. L. (1971a). "Measuring soil matric potential in situ by sensing heat dissipation within a porous body: I. Theory and sensor construction." *Soil Science Society of America Journal*, 35(1), 27-33.

Phene, C. J., Rawlins, S. L., and Hoffman, G. J. (1971b). "Measuring soil matric potential in situ by sensing heat dissipation within a porous body: II. Experimental results." *Soil Science Society of America Journal*, 35(2), 225-229.

Rassam, D. W., and Williams, D. J. (1999). "Unsaturated hydraulic conductivity of mine tailings under wetting and drying conditions." *Geotechnical Testing Journal*, 22(2), 138-146.

Ren, J., Shen, Z.-z., Yang, J., Zhao, J., and Yin, J.-n. (2014). "Effects of Temperature and Dry Density on Hydraulic Conductivity of Silty Clay under Infiltration of Low-Temperature Water." *Arabian Journal for Science and Engineering*, 39(1), 461-466.

Richards, L. A. (1931). "Capillary conduction of liquids in porous mediums." *Journal Applied Physics*, 1, 318-333.

Richards, L. A., and Gardner, W. (1936). "Tensiometers for measuring the capillary tension of soil water." *Journal America Society Agronomy*, 28(1), 352-358.

Ridley, A. M., and Wray, W. K. (1995). "Suction measurement: A review of current theory and practices." *Proceedings of the 1st International Conference on Unsaturated Soils/*.

Rogowski, A. (1971). "Watershed physics: Model of the soil moisture characteristic." *Water Resources Research*, 7(6), 1575-1582.

Schneider, S., Mallants, D., and Jacques, D. (2012). "Determining hydraulic properties of concrete and mortar by inverse modelling." *Proceedings of MRS Proceedings*, Cambridge Univ Press, imrc11-1475-nw1435-p1460.

Shackelford, C. D., Benson, C. H., Katsumi, T., Edil, T. B., and Lin, L. (2000). "Evaluating the hydraulic conductivity of GCLs permeated with non-standard liquids." *Geotextiles and Geomembranes*, 18(2), 133-161.

Sheng, D. (2011). "Review of fundamental principles in modelling unsaturated soil behaviour." *Computers and Geotechnics*, 38(6), 757-776.

Sillers, W. S., Fredlund, D. G., and Zakerzadeh, N. (2001). "Mathematical attributes of some soil—water characteristic curve models." *Unsaturated soil concepts and their application in geotechnical practice*, Springer, 243-283.

Šimůnek, J., Sejna, M., Saito, H., and Sakai, M. (2008a). "The HYDRUS-1D software package for simulating the one-dimensional movement of water, heat, and multiple solutes in variably-saturated media." Department of Environmental Sciences, University of California, Riverside, CA.

Šimůnek, J., van Genuchten, M. T., and Sejna, M. (2006). "The HYDRUS software package for simulating two- and three-dimensional movement of water, heat, and multiple solutes in variably-saturated media." PC Progress, Prag, Czech Republic.

Šimůnek, J., van Genuchten, M. T., and Šejna, M. (2007). "Modeling subsurface water flow and solute transport with HYDRUS and related numerical software packages." *Proceedings of the Conference on Numerical Modelling of Hydrodynamic Systems*, CRC Press, 95.

Singh, V. P. (1997). *Kinematic wave modeling in water resources, Environmental hydrology*, John Wiley & Sons.

Spanner, D. C. (1951). "The Peltier effect and its use in the measurement of suction pressure." *Journal of Experimental Botany*, 145-168.

Stannard, D. I. (1986). "Theory, construction and operation of simple tensiometers." *Groundwater Monitoring & Remediation*, 6(3), 70-78.

Stannard, D. I. (1992). "Tensiometers—theory, construction, and use." *Geotechnical Testing Journal*, 15(1), 48-58.

Swarbrick, G. E. (1995). "Measurement of soil suction using the filter paper method." *Proceedings of the 1st International Conference on Unsaturated Soils*, 701-708.

Take, W. A., and Bolton, M. D. (2003). "Tensiometer saturation and the reliable measurement of soil suction." *Géotechnique*, 53(2), 159-172.

Thieu, N. T. M., Fredlund, M. D., Fredlund, D. G., and Vu, H. Q. (2001). "Seepage modelling in a saturated/unsaturated soil system." *Proceedings of the International Conference on Management of the Land and Water Resources, Hanoi, Vietnam*, 20-22.

Timlin, D., Ahuja, L. R., Pachepsky, Y., Williams, R. D., Gimenez, D., and Rawls, W. (1999). "Use of Brooks-Corey parameters to improve estimates of saturated conductivity from effective porosity." *Soil Science Society of America Journal*, 63(5), 1086-1092.

Tindall, J. A., Kunkel, J. R., and Anderson, D. E. (1999). "Unsaturated zone hydrology for scientists and engineers." Prentice Hall Upper Saddle River, NJ.

Tinjum, J. M., Benson, C. H., and Blotz, L. R. (1997). "Soil-water characteristic curves for compacted clays." *J Geotech Geoenviron*, 123(11), 1060-1069.

Toorman, A. F., Wierenga, P. J., and Hills, R. G. (1992). "Parameter estimation of hydraulic properties from one-step outflow data." *Water Resources Research*, 28(11), 3021-3028.

Topp, G. C., and Miller, E. E. (1966). "Hysteretic moisture characteristics and hydraulic conductivities for glass-bead media." *Soil Science Society of America Journal*, 30(2), 156-162.

Valiantzas, J. D., Kerkides, P. G., and Poulovassilis, A. (1988). "An improvement to the one-step outflow method for the determination of soil water diffusivities." *Water Resources Research*, 24(11), 1911-1920.

Van Dam, J. C., Stricker, J. N. M., and Droogers, P. (1990). "From one-step to multistep determination of soil hydraulic functions by outflow experiments." Report No. 7, Department of Hydrology, Soil Physics and Hydraulics, Wageningen Agricultural University, Wageningen, The Netherlands.

van Dam, J. C., Stricker, J. N. M., and Droogers, P. (1994). "Inverse method to determine soil hydraulic functions from multistep outflow experiments." *Soil Science Society of America Journal*, 58(3), 647-652.

van Genuchten, M. T. (1980). "A closed-form equation for predicting the hydraulic conductivity of unsaturated soils." *Soil Science Society of America journal*, 44(5), 892-898.

van Genuchten, M. T., Leij, F. J., and Yates, S. R. (1991). "The RETC code for quantifying the hydraulic functions of unsaturated soils." A. R. S. U.S. Department of Agriculture, ed.Riverside, CA.

van Genuchten, M. T., and Nielsen, D. R. (1985). "On describing and predicting the hydraulic properties of unsaturated soils." *Annales Geophysicae*, 3(5), 615-628.

van Genuchten, M. T., and Pachepsky, Y. (2011). "Hydraulic properties of unsaturated soils." J. Glinski, J. Horabik, and J. Lipiec, eds.Encyclopedia of Agrrophysics, Dordecht, Springer, 368-376.

Vanapalli, S. K. (1994). "Simple test procedures and their interpretation in evaluating the shear strength of an unsaturated soil." PhD thesis, University of Saskatchewan, Saskatoon, Canada.

Vanapalli, S. K., Fredlund, D. G., and Pufahl, D. E. (1999). "The influence of soil structure and stress history on the soil-water characteristics of a compacted till." *Getechnique*, 49(2), 143-159.

Vogel, T., and Cislerova, M. (1988). "On the reliability of unsaturated hydraulic conductivity calculated from the moisture retention curve." *Transport in porous media*, 3(1), 1-15.

Wayllace, A., and Lu, N. (2012). "A transient water release and imbibitions method for rapidly measuring wetting and drying soil water retention and hydraulic conductivity functions." *Geotechnical Testing Journal*, 5(1), 103-107.

White, W. A. (1949). "Atterberg plastic limits of clay minerals." *Report of Investigations*.

Wiederhold, P. R. (1997). *Water vapor measurement: methods and instrumentation*, CRC Press.

Wildenschild, D., Jensen, K. H., Hollenbeck, K.-J., Sonnenborg, T., Butts, M., Illangasekare, T., and Znidarcic, D. (1997). "A two-stage procedure for determining unsaturated hydraulic characteristics using a syringe pump and outflow observations." *Soil Science Society of America Journal*, 61(2), 347-359.

Williams, J., Prebble, R. E., Williams, W. T., and Hignett, C. T. (1983). "The influence of texture, structure and clay mineralogy on the soil moisture characteristic." *Soil Research*, 21(1), 15-32.

Wind, G. P. (1955). "Field experiment concerning capillary rise of moisture in heavy clay soil." *Netharlands Journal of Agriculture*, 3, 60-69.

Young, J. F. (1967). "Humidity control in the laboratory using salt solutions—a review." *Journal of Applied Chemistry*, 17(9), 241-245.

Yuster, S. T. (1951). "Theoretical considerations of multiphase flow in idealized capillary systems." *Proceedings of the 3rd World Petroleum Congress, Section II, The Hague*, 437-445.

Zapata, C. E., Houston, W. N., Houston, S. L., and Walsh, K. D. (2000). "Soil-water characteristic curve variability." *Geotechnical Special Publication*(99), 84-124.

Zhou, J., and Yu, J.-l. (2005). "Influences affecting the soil-water characteristic curve." *Journal-Zhejiang University Science*, 6(8), 797.

Zurmühl, T., and Durner, W. (1996). "Modeling transient water and solute transport in a biporous soil." *Water Resources Research*, 32(4), 819-829.

Zurmühl, T., and Durner, W. (1998). "Determination of parameters for bimodal hydraulic functions by inverse modeling." *Soil Science Society of America Journal*, 62(4), 874-880.

APPENDIX A – TRIM TEST RESULTS

Test No.: 28

Test Ref.: TRIMSC07

Test Soil: Stroubles Creek

Molding Water Content: 19.60% (w_{opt}-3)

Property	Before Saturation	After Saturation
Void Ratio, e	0.818	0.926
Porosity, n (%)	45.00	48.09
Std. Proctor Relative Compaction, RC (%)	91.90	86.78
Dry Density, γ_d (g/cm^3)	1.42	1.35

Unsaturated Hydraulic Soil Parameters	Drying	Wetting
Saturated Volumetric Water Content, θ_s	0.481	0.440
Residual Volumetric Water Content, θ_r	0.126	0.126
Air-Entry Pressure Parameter, α (1/kPa)	0.133	0.217
Pore-Size Distribution Parameter, n	1.638	1.605
Saturated Hydraulic Conductivity, k_{sat} (cm/s)	1.30E-05	9.50E-06

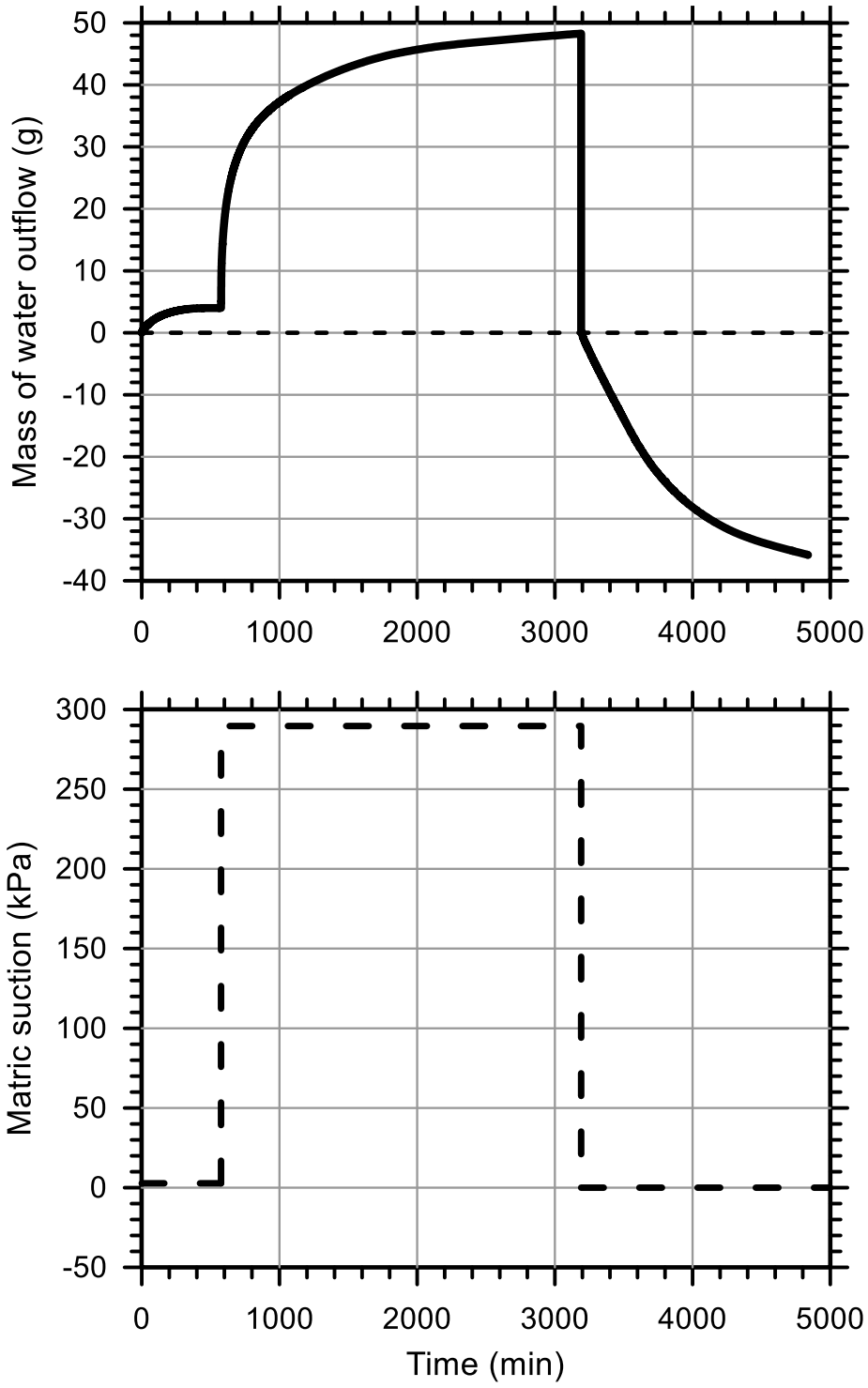
Mass of water outflow (g)
50
40
30
20
10
0
-10
-20
-30
-40
0
1000
2000
3000
4000
5000
Matric suction (kPa)
300
250
200
150
100
50
0
-50
0
1000
2000
3000
4000
5000
Time (min)

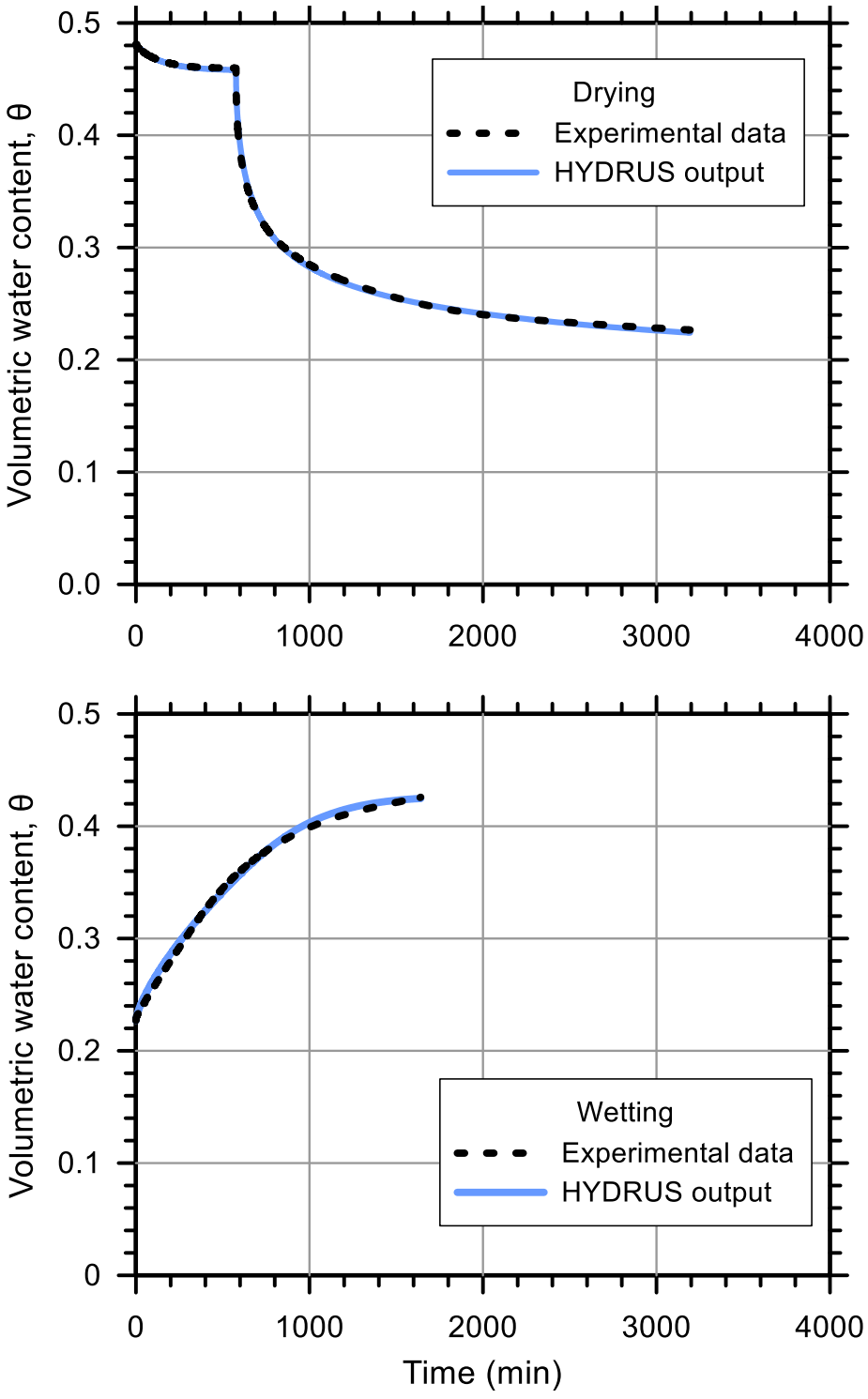
Drying
Experimental data
HYDRUS output
Volumetric water content, θ
0.5
0.4
0.3
0.2
0.1
0.0
0
1000
2000
3000
4000
Wetting
Experimental data
HYDRUS output
Volumetric water content, θ
0.5
0.4
0.3
0.2
0.1
0
0
1000
2000
3000
4000
Time (min)

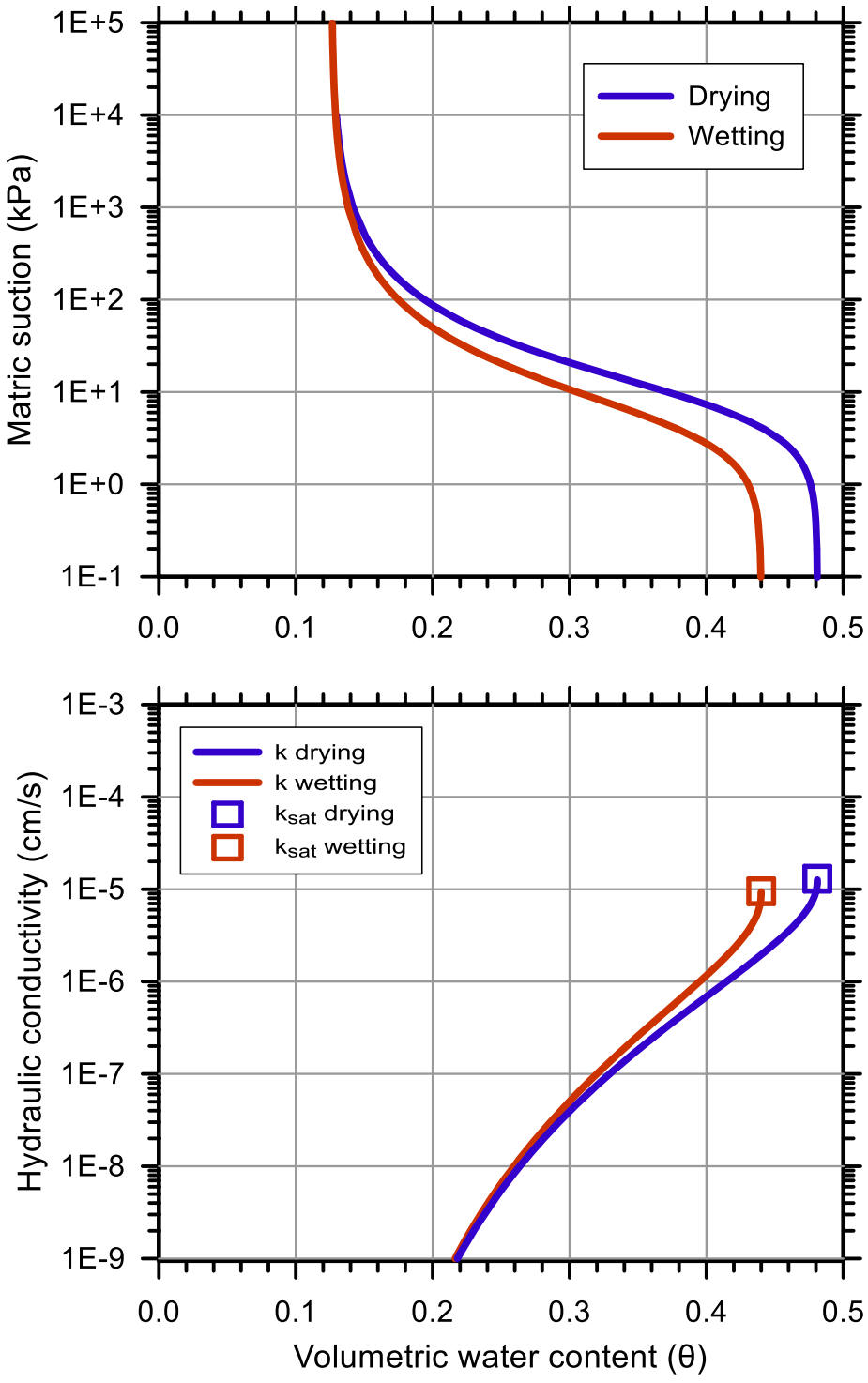
Matric suction (kPa)
1E+5
1E+4
1E+3
1E+2
1E+1
1E+0
1E-1
0.0
0.1
0.2
0.3
0.4
0.5
Drying
Wetting
Hydraulic conductivity (cm/s)
1E-3
1E-4
1E-5
1E-6
1E-7
1E-8
1E-9
k drying
k wetting
ksat drying
ksat wetting
Volumetric water content (θ)

Test No.: 4

Test Ref.: TRIMSC03

Test Soil: Stroubles Creek

Molding Water Content: 19.60% (w_{opt}-3)

Property	Before Saturation	After Saturation
Void Ratio, e	0.920	0.990
Porosity, n (%)	47.91	49.76
Std. Proctor Relative Compaction, RC (%)	87.04	83.96
Dry Density, γ_d (g/cm^3)	1.35	1.30

Unsaturated Hydraulic Soil Parameters	Drying	Wetting
Saturated Volumetric Water Content, θ_s	0.498	0.432
Residual Volumetric Water Content, θ_r	0.096	0.096
Air-Entry Pressure Parameter, α (1/kPa)	0.151	0.226
Pore-Size Distribution Parameter, n	1.522	1.480
Saturated Hydraulic Conductivity, k_{sat} (cm/s)	3.50E-05	1.50E-05

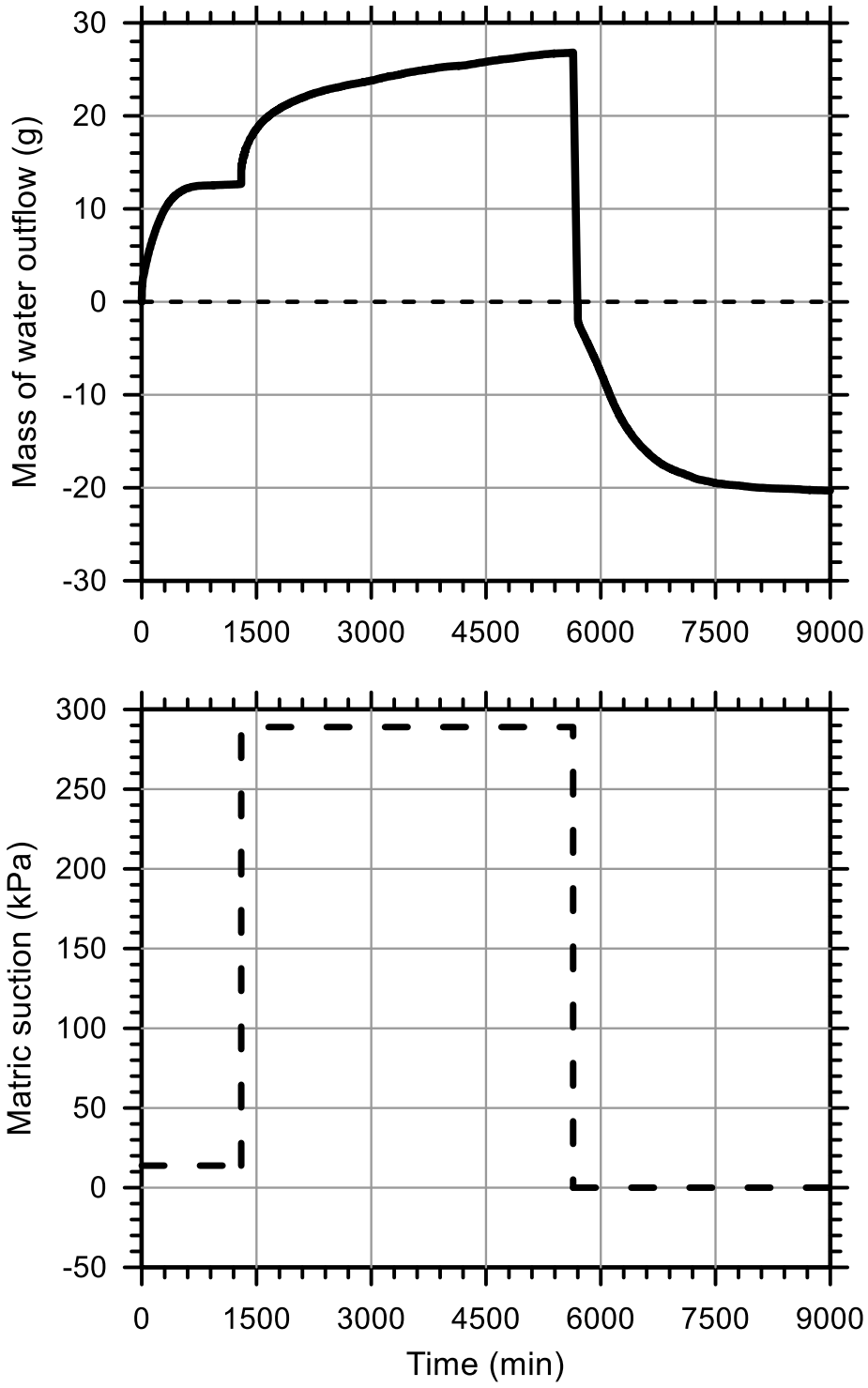
Mass of water outflow (g)
30
20
10
0
-10
-20
-30
0
1500
3000
4500
6000
7500
9000
Matric suction (kPa)
300
250
200
150
100
50
0
-50
0
1500
3000
4500
6000
7500
9000
Time (min)

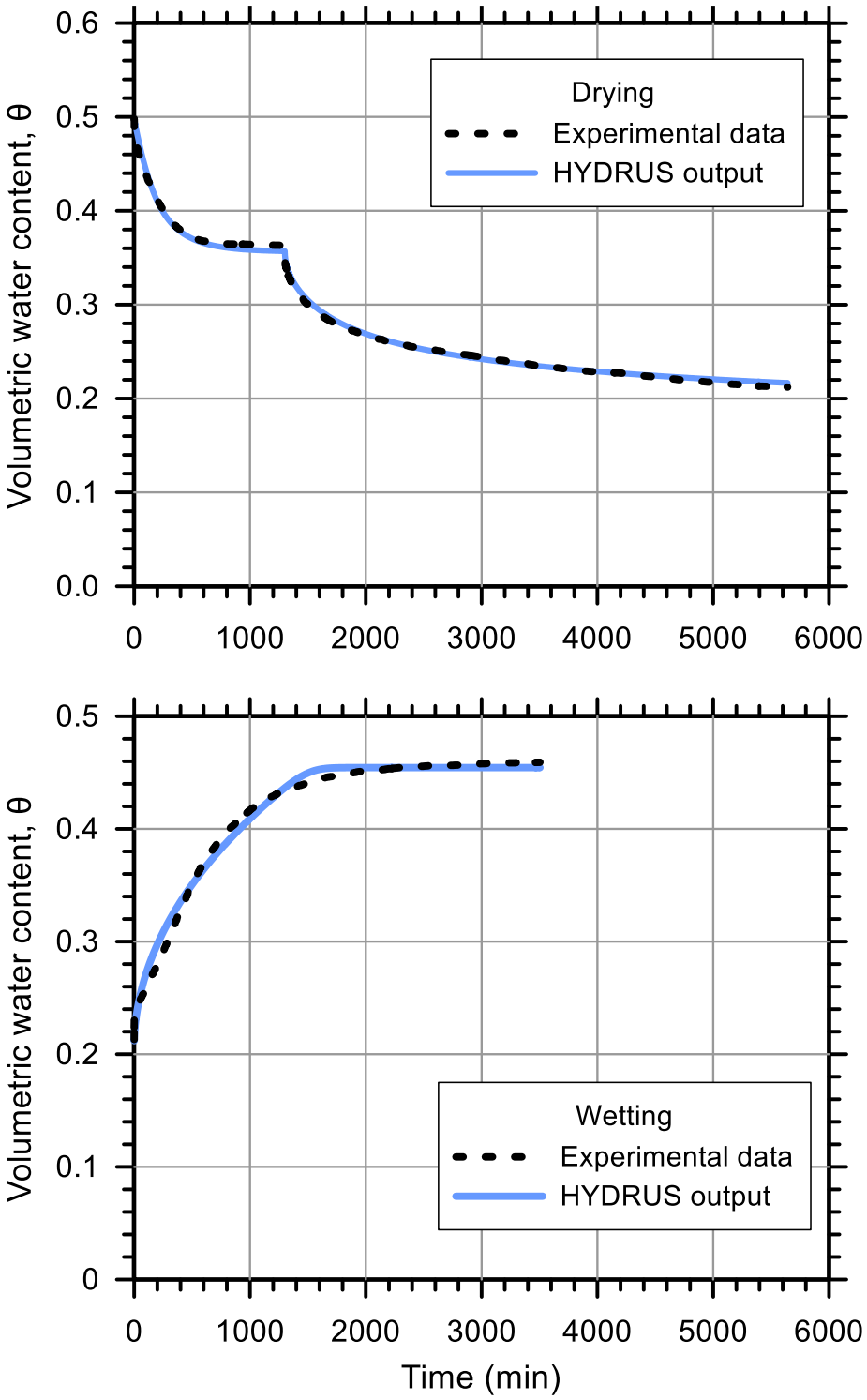
Drying
Experimental data
HYDRUS output
Volumetric water content, θ
0.6
0.5
0.4
0.3
0.2
0.1
0.0
0
1000
2000
3000
4000
5000
6000
Wetting
Experimental data
HYDRUS output
Volumetric water content, θ
0.5
0.4
0.3
0.2
0.1
0
Time (min)

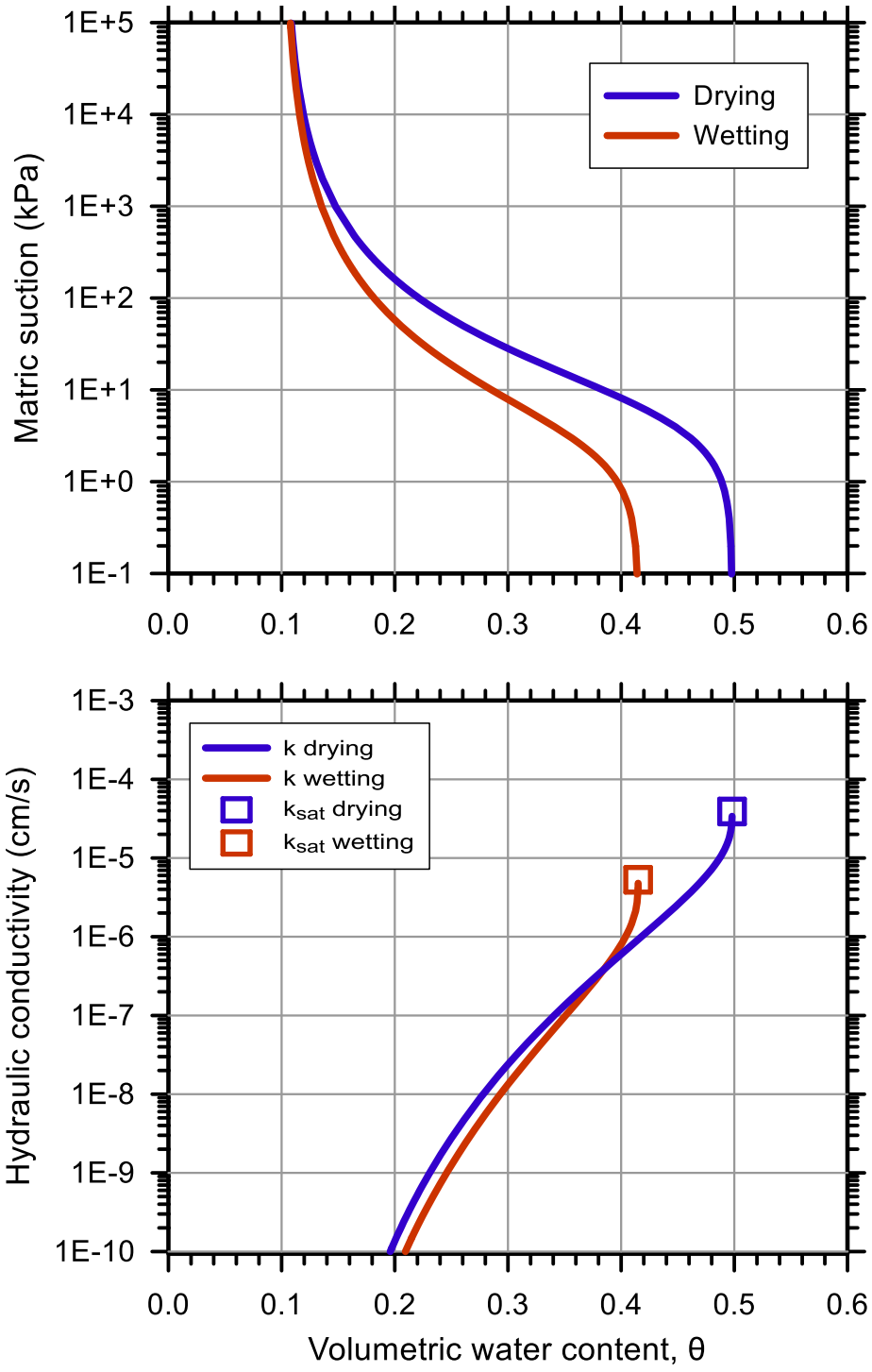
Matric suction (kPa)
1E+5
1E+4
1E+3
1E+2
1E+1
1E+0
1E-1
Drying
Wetting
0.0
0.1
0.2
0.3
0.4
0.5
0.6
Hydraulic conductivity (cm/s)
1E-3
1E-4
1E-5
1E-6
1E-7
1E-8
1E-9
1E-10
k drying
k wetting
ksat drying
ksat wetting
Volumetric water content, θ

Test No.: 5

Test Ref.: TRIMSC04

Test Soil: Stroubles Creek

Molding Water Content: 22.60% (w_{opt})

Property	Before Saturation	After Saturation
Void Ratio, e	0.839	0.888
Porosity, n (%)	45.63	47.03
Std. Proctor Relative Compaction, RC (%)	90.85	88.52
Dry Density, γ_d (g/cm^3)	1.41	1.37

Unsaturated Hydraulic Soil Parameters	Drying	Wetting
Saturated Volumetric Water Content, θ_s	0.470	0.444
Residual Volumetric Water Content, θ_r	0.145	0.145
Air-Entry Pressure Parameter, α (1/kPa)	0.172	0.204
Pore-Size Distribution Parameter, n	1.497	1.510
Saturated Hydraulic Conductivity, k_{sat} (cm/s)	9.66E-06	5.60E-06

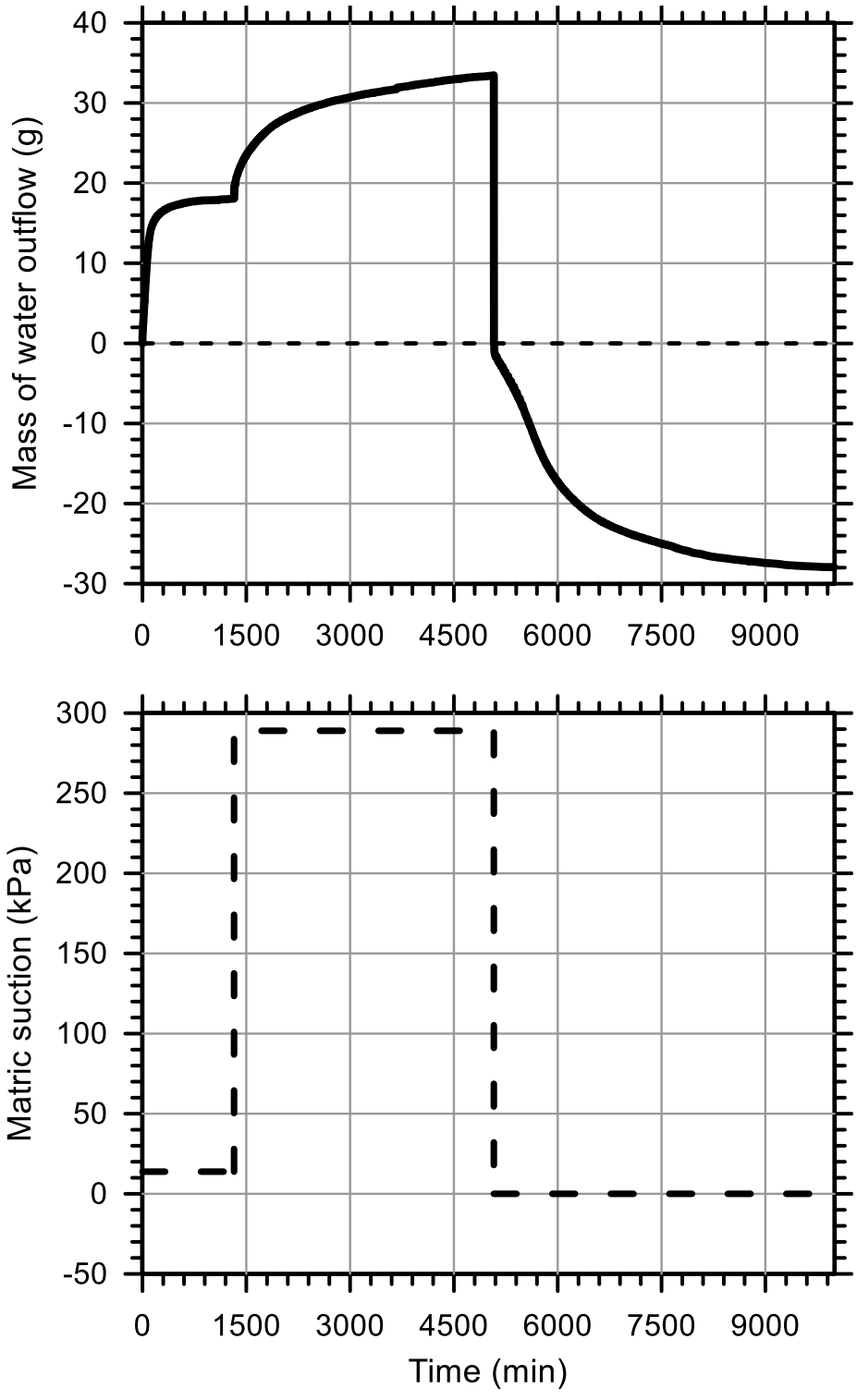
Mass of water outflow (g)
40
30
20
10
0
-10
-20
-30
0
1500
3000
4500
6000
7500
9000
Matric suction (kPa)
300
250
200
150
100
50
0
-50
0
1500
3000
4500
6000
7500
9000
Time (min)

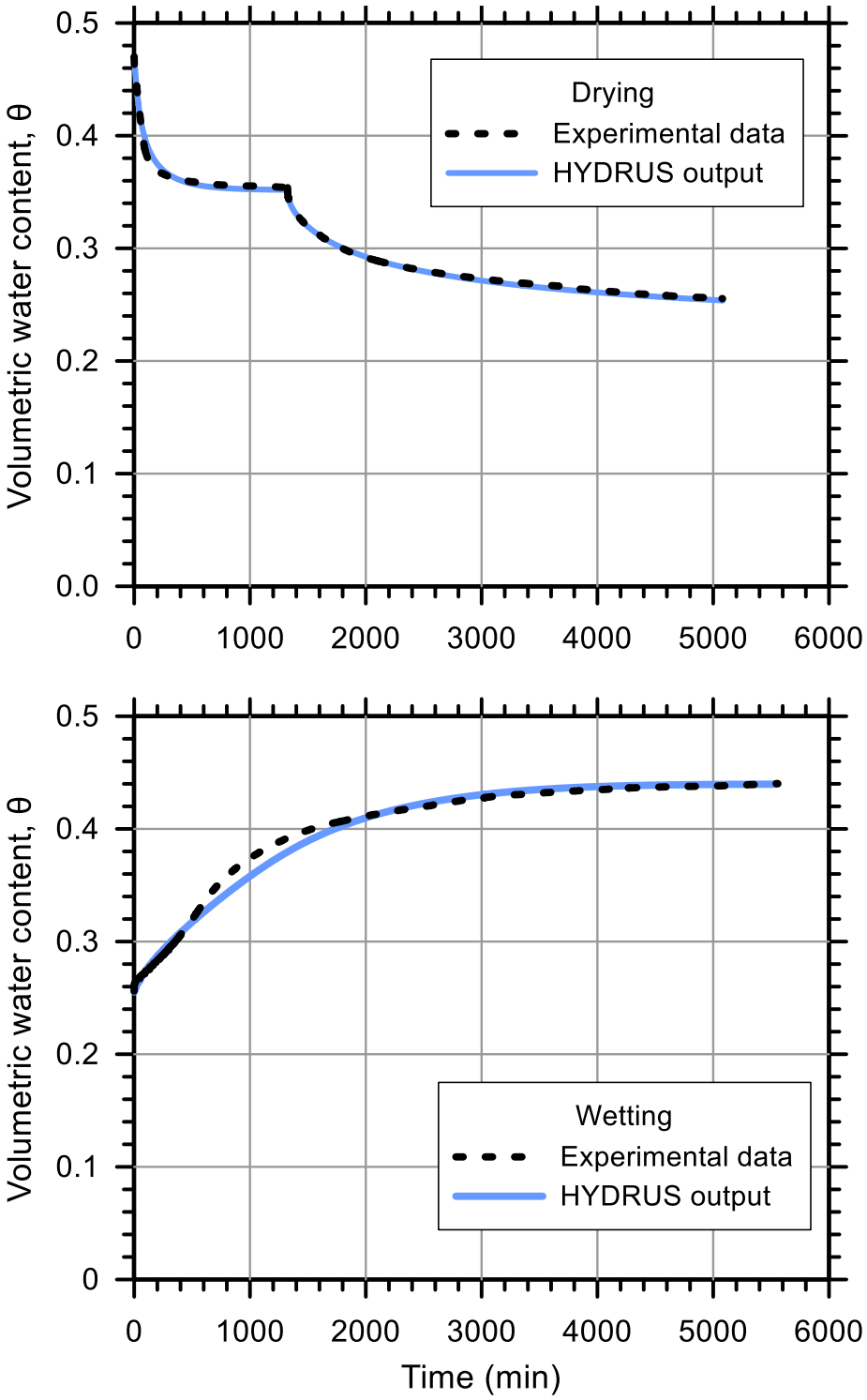
Drying
Experimental data
HYDRUS output
Volumetric water content, θ
0.5
0.4
0.3
0.2
0.1
0.0
0
1000
2000
3000
4000
5000
6000
Wetting
Experimental data
HYDRUS output
Volumetric water content, θ
0.5
0.4
0.3
0.2
0.1
0
0
1000
2000
3000
4000
5000
6000
Time (min)

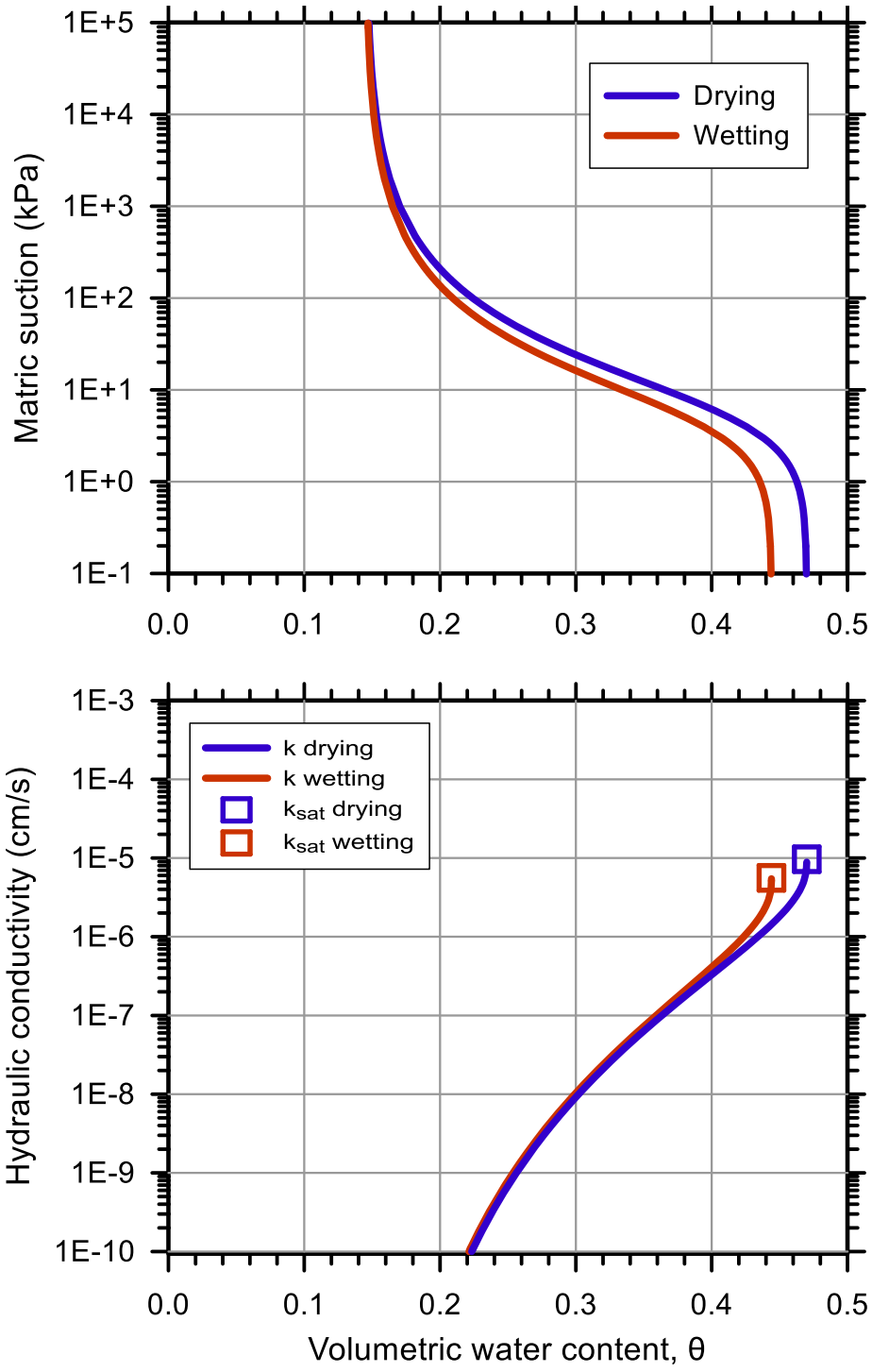
Matric suction (kPa)
1E+5
1E+4
1E+3
1E+2
1E+1
1E+0
1E-1
0.0
0.1
0.2
0.3
0.4
0.5
Drying
Wetting
Hydraulic conductivity (cm/s)
1E-3
1E-4
1E-5
1E-6
1E-7
1E-8
1E-9
1E-10
k drying
k wetting
ksat drying
ksat wetting
Volumetric water content, θ

Test No.: 3

Test Ref.: TRIMSC02

Test Soil: Stroubles Creek

Molding Water Content: 22.60% (w_{opt})

Property	Before Saturation	After Saturation
Void Ratio, e	1.081	1.109
Porosity, n (%)	51.94	52.59
Std. Proctor Relative Compaction, RC (%)	80.31	79.22
Dry Density, γ_d (g/cm^3)	1.24	1.23

Unsaturated Hydraulic Soil Parameters	Drying	Wetting
Saturated Volumetric Water Content, θ_s	0.526	0.425
Residual Volumetric Water Content, θ_r	0.085	0.085
Air-Entry Pressure Parameter, α (1/kPa)	0.278	0.428
Pore-Size Distribution Parameter, n	1.488	1.380
Saturated Hydraulic Conductivity, k_{sat} (cm/s)	9.94E-05	7.50E-05

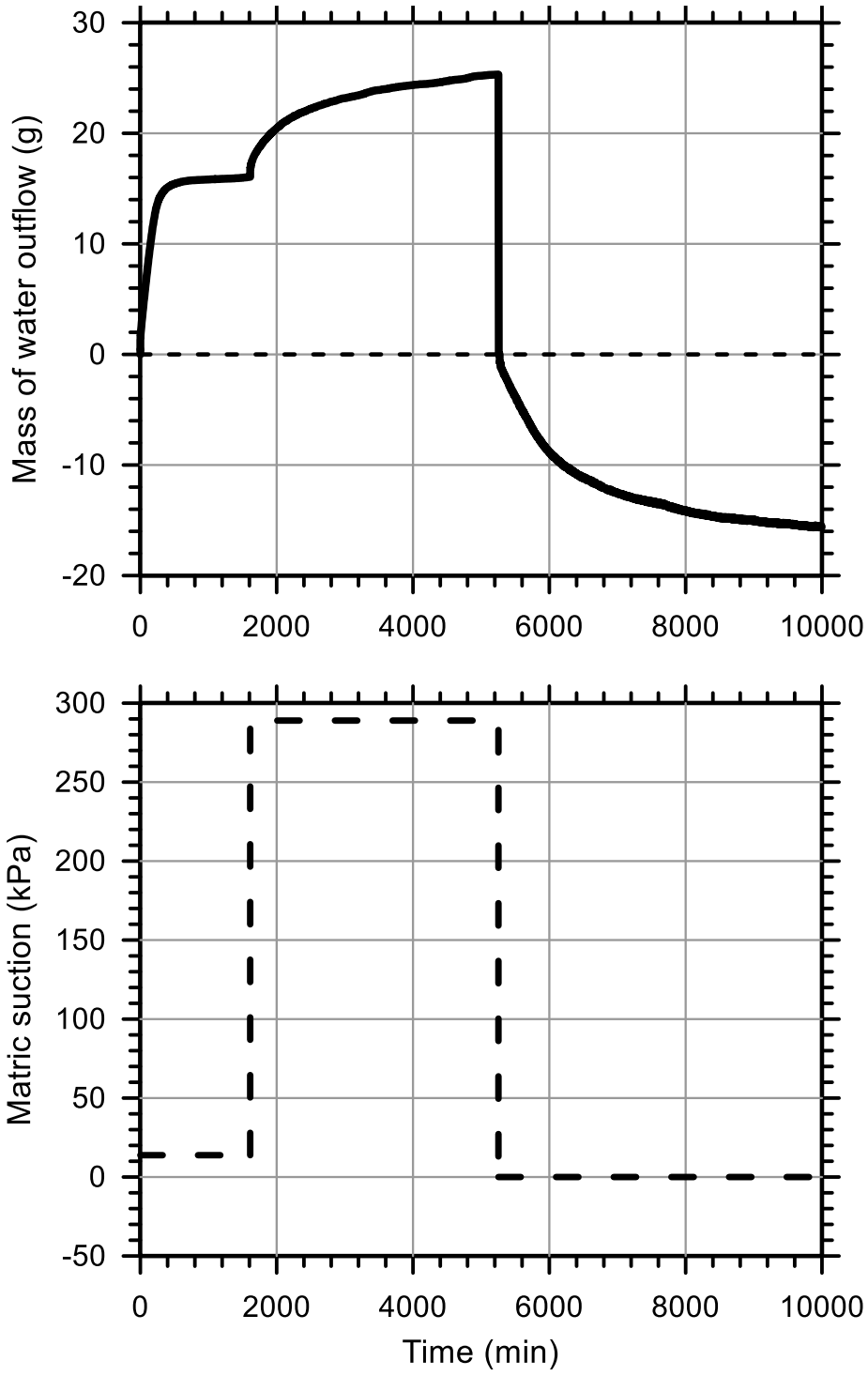
Mass of water outflow (g)
30
20
10
0
-10
-20
0
2000
4000
6000
8000
10000
Matric suction (kPa)
300
250
200
150
100
50
0
-50
0
2000
4000
6000
8000
10000
Time (min)

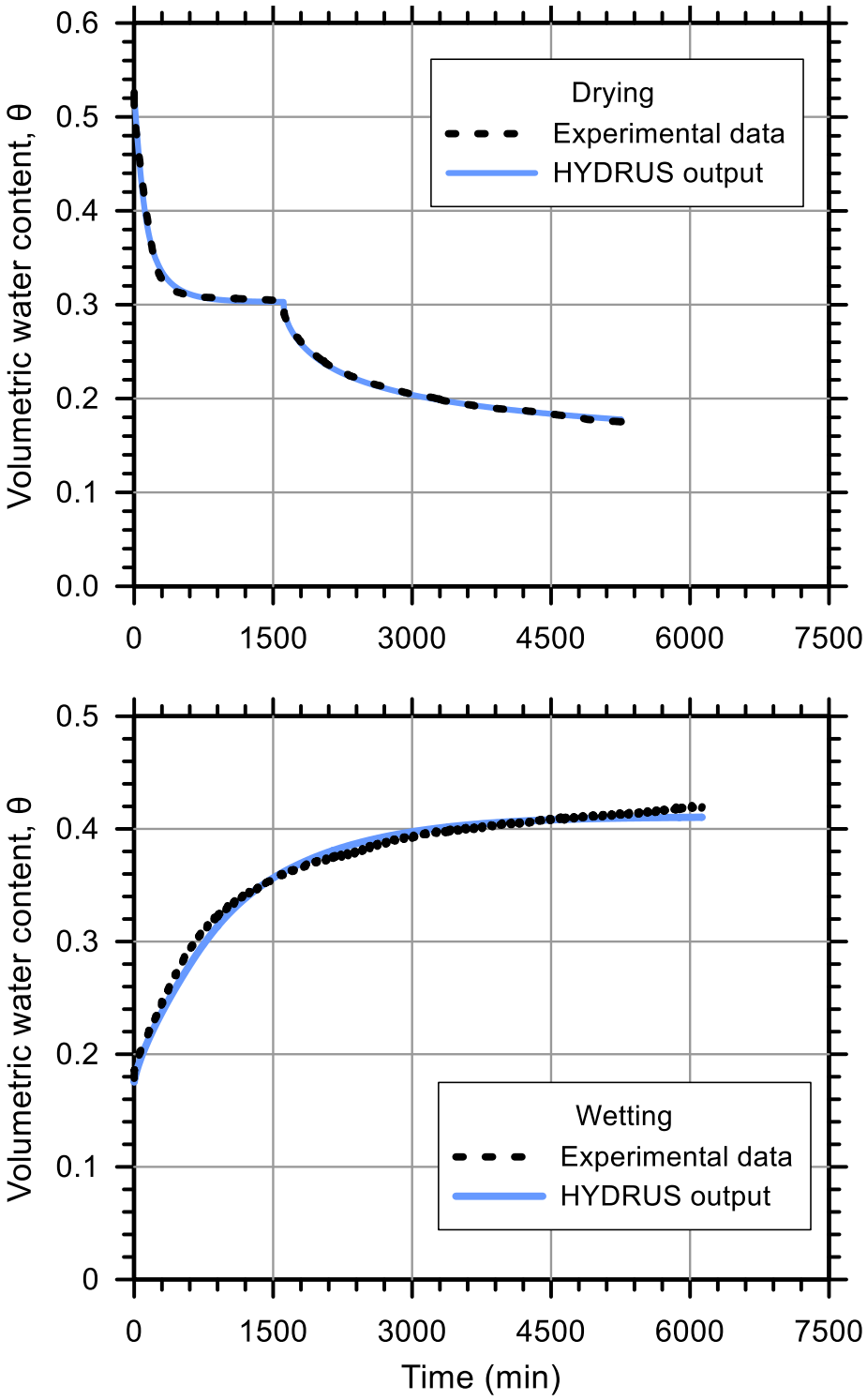
Drying
Experimental data
HYDRUS output
Volumetric water content, θ
0.6
0.5
0.4
0.3
0.2
0.1
0.0
0
1500
3000
4500
6000
7500
Wetting
Experimental data
HYDRUS output
Volumetric water content, θ
0.5
0.4
0.3
0.2
0.1
0
0
1500
3000
4500
6000
7500
Time (min)

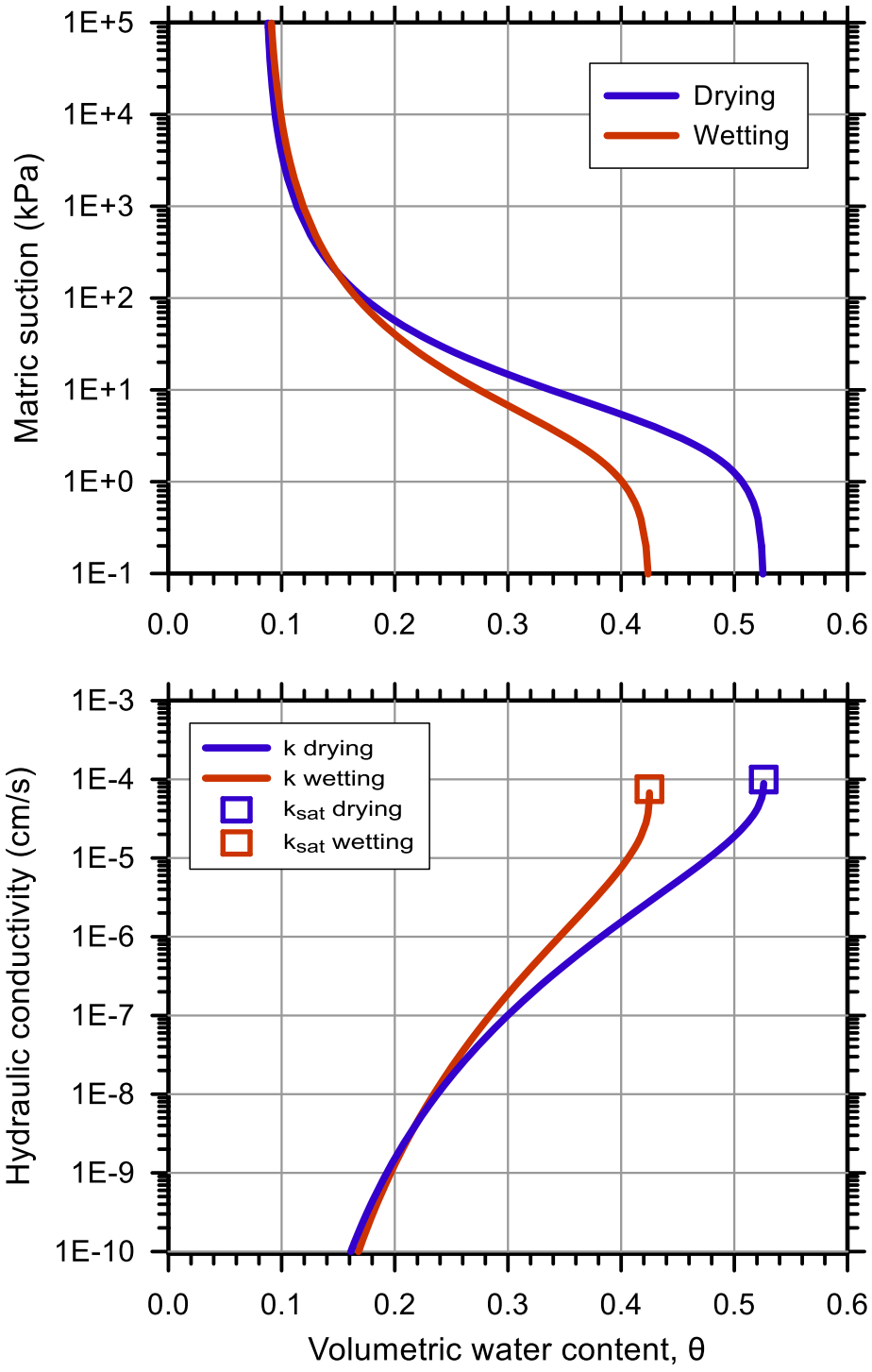
Matric suction (kPa)
1E+5
1E+4
1E+3
1E+2
1E+1
1E+0
1E-1
Drying
Wetting
0.0
0.1
0.2
0.3
0.4
0.5
0.6
Hydraulic conductivity (cm/s)
1E-3
1E-4
1E-5
1E-6
1E-7
1E-8
1E-9
1E-10
k drying
k wetting
ksat drying
ksat wetting
Volumetric water content, θ

Test No.: 15

Test Ref.: TRIMSC06

Test Soil: Stroubles Creek

Molding Water Content: 25.60% (w_{opt}+3)

Property	Before Saturation	After Saturation
Void Ratio, e	0.825	0.850
Porosity, n (%)	45.22	45.95
Std. Proctor Relative Compaction, RC (%)	91.54	90.32
Dry Density, γ_d (g/cm^3)	1.42	1.40

Unsaturated Hydraulic Soil Parameters	Drying	Wetting
Saturated Volumetric Water Content, θ_s	0.459	0.405
Residual Volumetric Water Content, θ_r	0.120	0.120
Air-Entry Pressure Parameter, α (1/kPa)	0.248	0.356
Pore-Size Distribution Parameter, n	1.885	1.760
Saturated Hydraulic Conductivity, k_{sat} (cm/s)	6.00E-06	3.29E-06

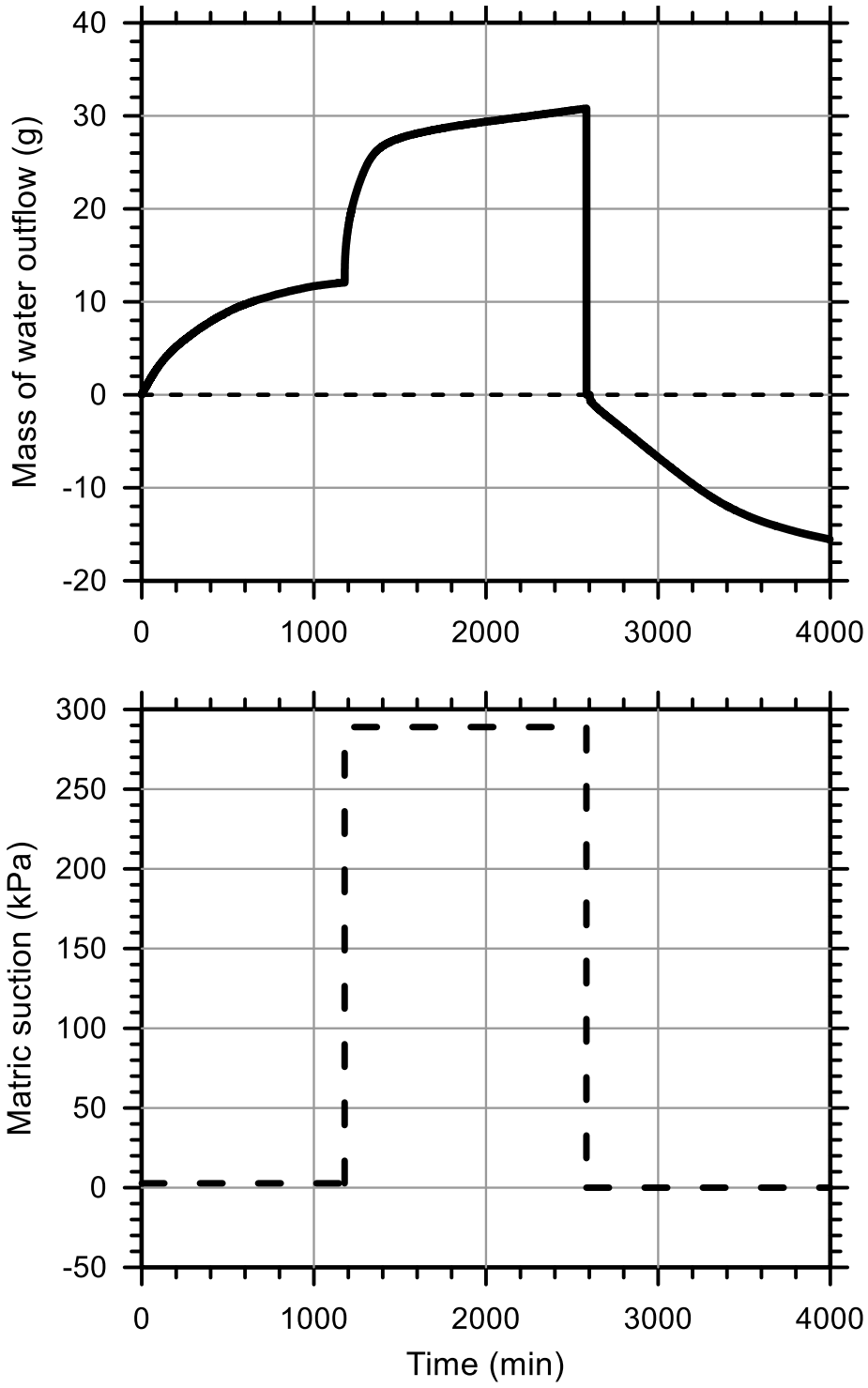
Mass of water outflow (g)
40
30
20
10
0
-10
-20
0
1000
2000
3000
4000
Matric suction (kPa)
300
250
200
150
100
50
0
-50
0
1000
2000
3000
4000
Time (min)

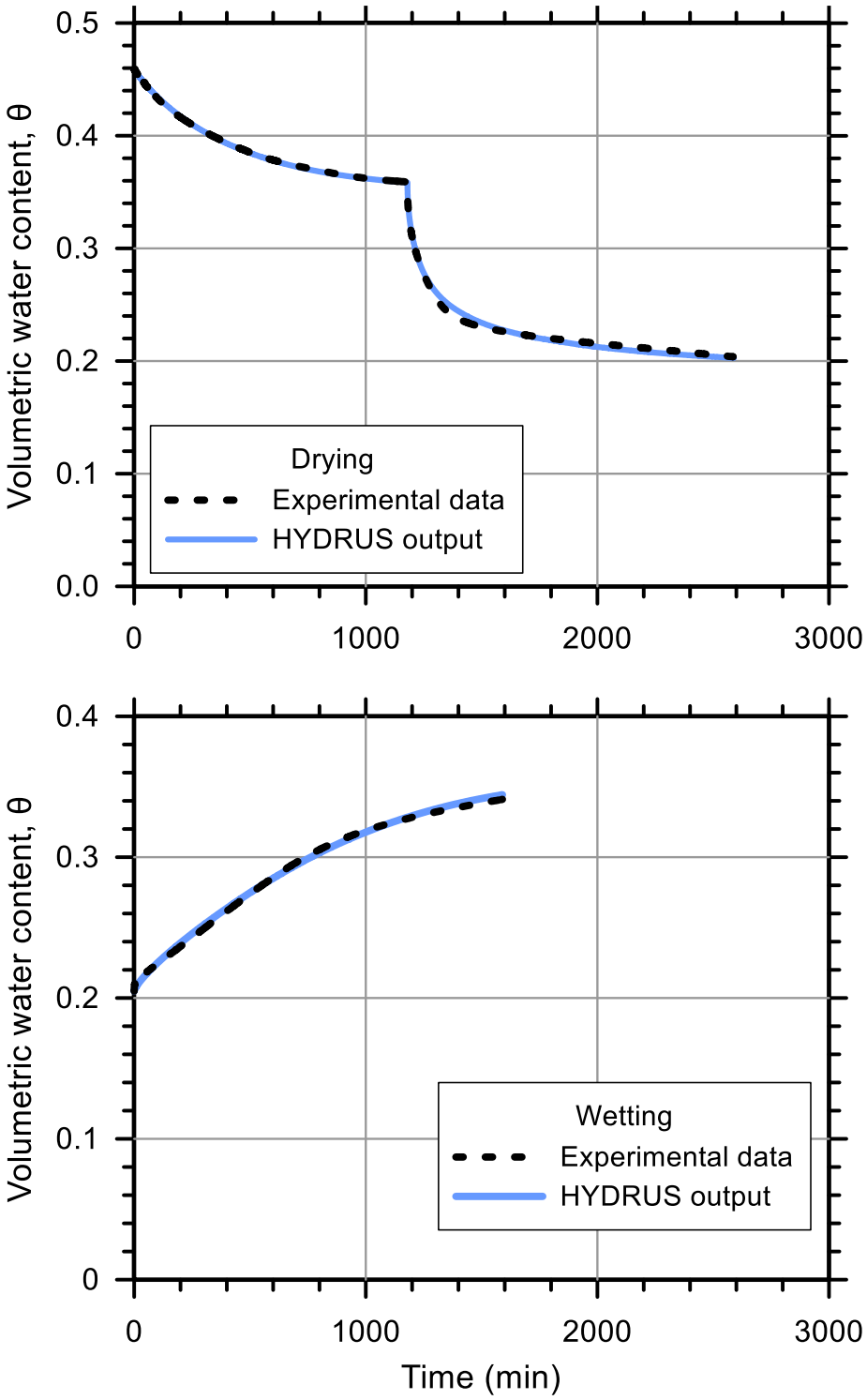
0.5
0.4
0.3
0.2
0.1
0.0
Volumetric water content, θ
Drying
Experimental data
HYDRUS output
0
1000
2000
3000
0.4
0.3
0.2
0.1
0
Volumetric water content, θ
Wetting
Experimental data
HYDRUS output
0
1000
2000
3000
Time (min)

Test No.: 7

Test Ref.: TRIMSC05

Test Soil: Stroubles Creek

Molding Water Content: 25.60% (w_{opt}+3)

Property	Before Saturation	After Saturation
Void Ratio, e	0.950	0.962
Porosity, n (%)	48.73	49.02
Std. Proctor Relative Compaction, RC (%)	85.67	85.15
Dry Density, γ_d (g/cm^3)	1.33	1.32

Unsaturated Hydraulic Soil Parameters	Drying	Wetting
Saturated Volumetric Water Content, θ_s	0.490	0.435
Residual Volumetric Water Content, θ_r	0.116	0.116
Air-Entry Pressure Parameter, α (1/kPa)	0.191	0.224
Pore-Size Distribution Parameter, n	1.580	1.550
Saturated Hydraulic Conductivity, k_{sat} (cm/s)	2.70E-05	1.40E-05

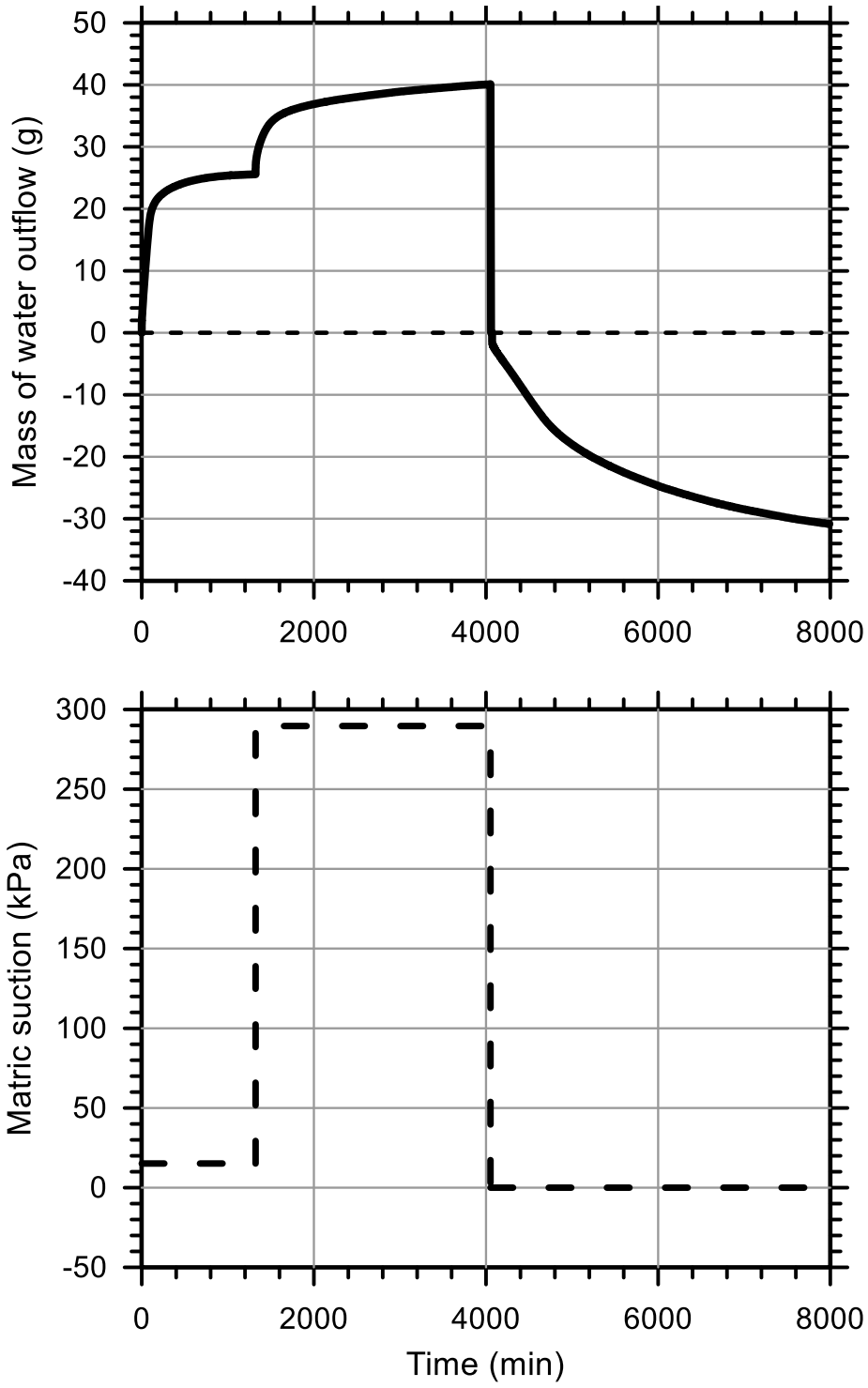
Mass of water outflow (g)
50
40
30
20
10
0
-10
-20
-30
-40
0
2000
4000
6000
8000
Matric suction (kPa)
300
250
200
150
100
50
0
-50
0
2000
4000
6000
8000
Time (min)

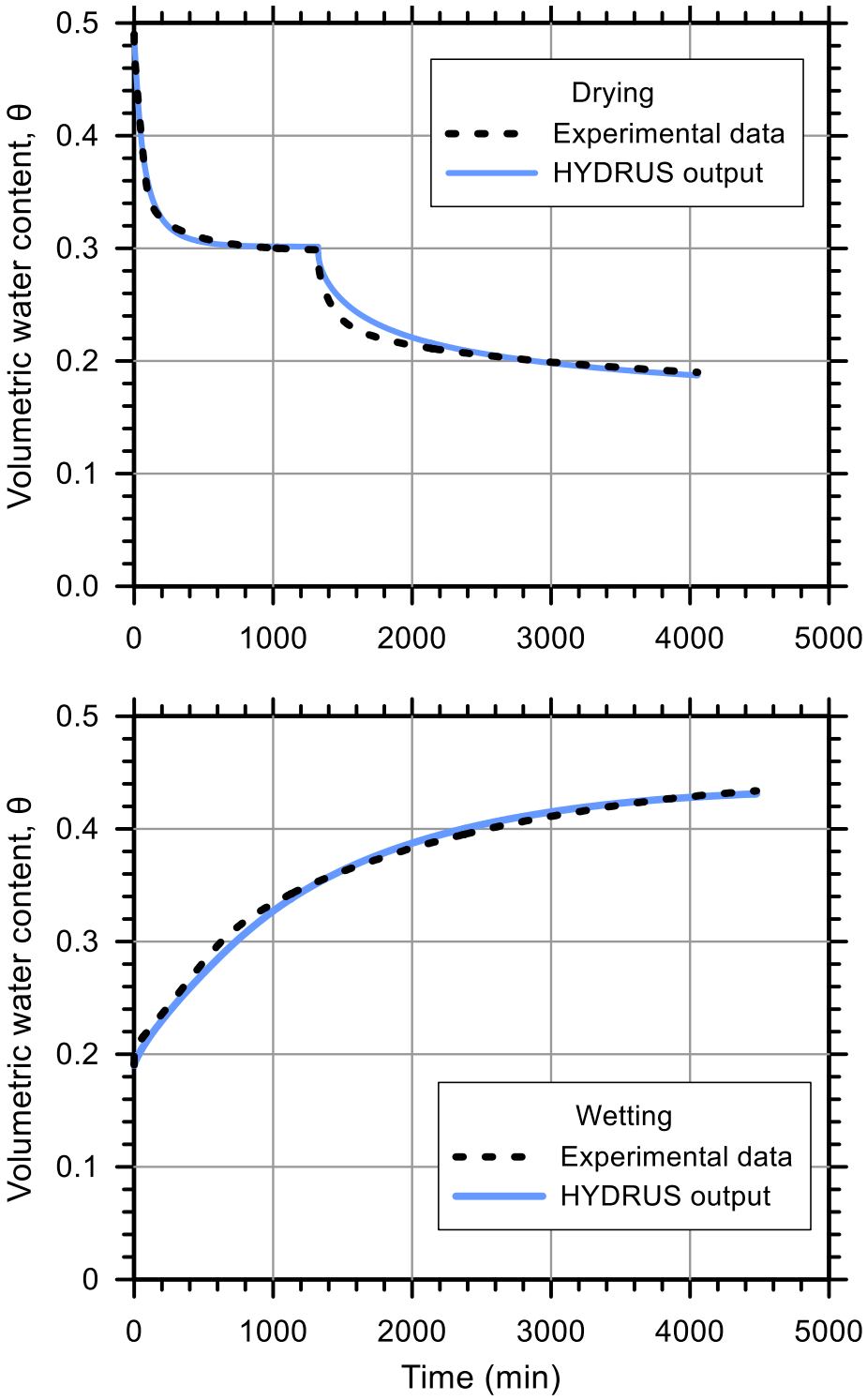
Drying
Experimental data
HYDRUS output
Volumetric water content, θ
0.5
0.4
0.3
0.2
0.1
0.0
0
1000
2000
3000
4000
5000
Wetting
Experimental data
HYDRUS output
Volumetric water content, θ
0.5
0.4
0.3
0.2
0.1
0
0
1000
2000
3000
4000
5000
Time (min)

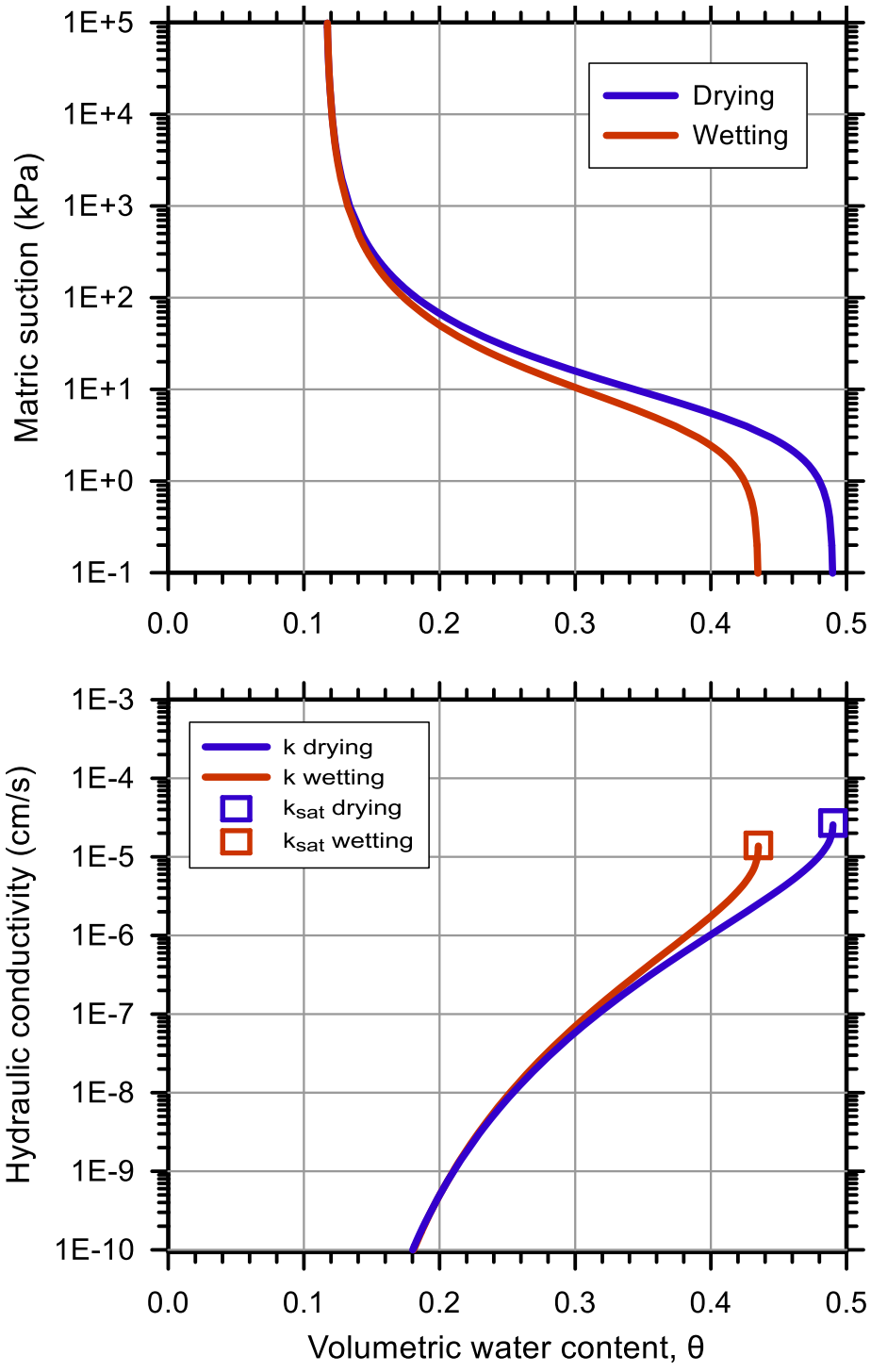
Matric suction (kPa)
1E+5
1E+4
1E+3
1E+2
1E+1
1E+0
1E-1
0.0
0.1
0.2
0.3
0.4
0.5
Drying
Wetting
Hydraulic conductivity (cm/s)
1E-3
1E-4
1E-5
1E-6
1E-7
1E-8
1E-9
1E-10
k drying
k wetting
ksat drying
ksat wetting
Volumetric water content, θ

Test No.: 27

Test Ref.: TRIMWH11

Test Soil: Whithorne

Molding Water Content: 27.70% (w_{opt}-2)

Property	Before Saturation	After Saturation
Void Ratio, e	0.984	1.028
Porosity, n (%)	49.60	50.70
Std. Proctor Relative Compaction, RC (%)	98.24	96.09
Dry Density, γ_d (g/cm^3)	1.35	1.32

Unsaturated Hydraulic Soil Parameters	Drying	Wetting
Saturated Volumetric Water Content, θ_s	0.507	0.450
Residual Volumetric Water Content, θ_r	0.173	0.173
Air-Entry Pressure Parameter, α (1/kPa)	0.143	0.357
Pore-Size Distribution Parameter, n	1.850	1.940
Saturated Hydraulic Conductivity, k_{sat} (cm/s)	1.50E-05	3.93E-06

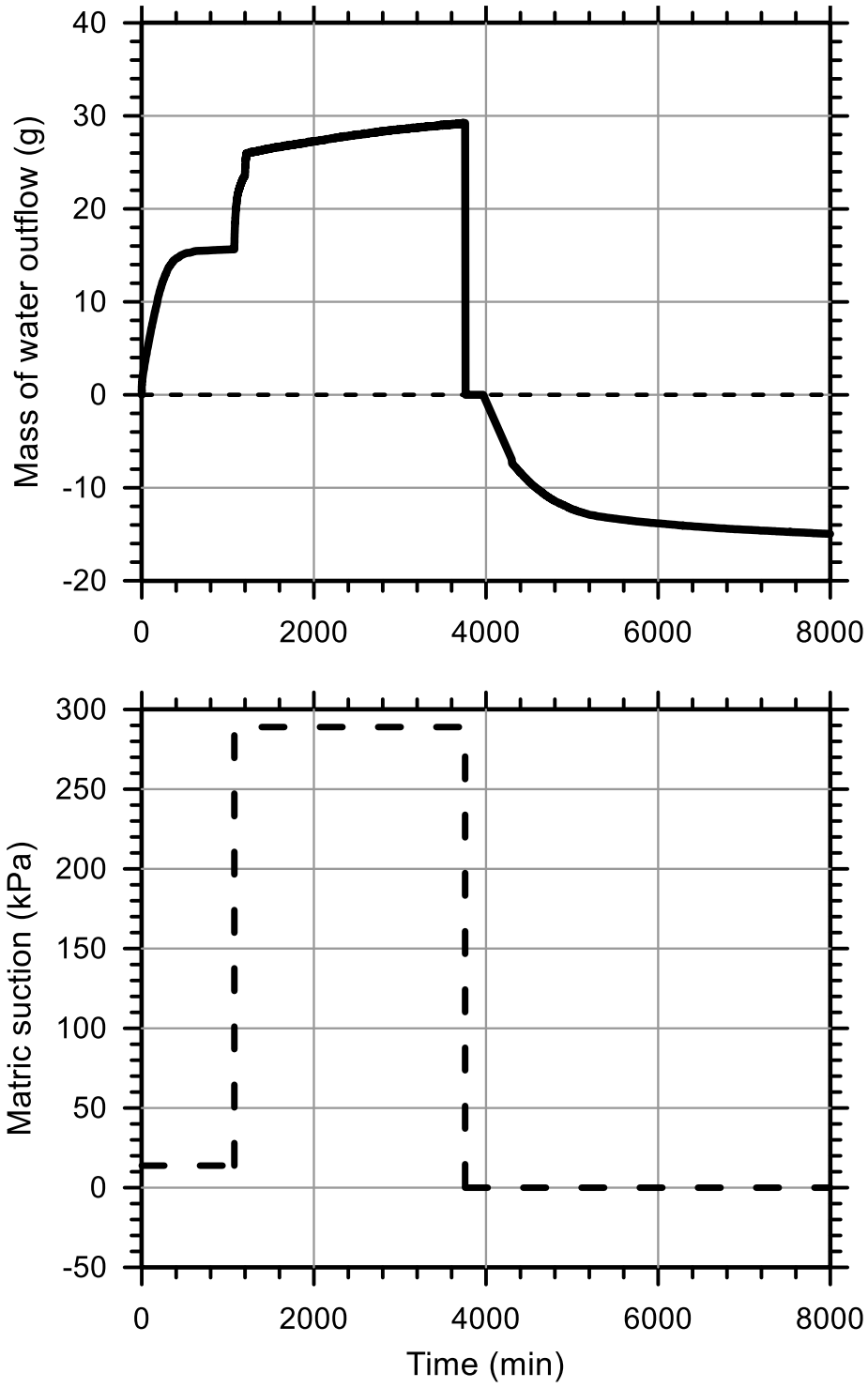
Mass of water outflow (g)
40
30
20
10
0
-10
-20
0
2000
4000
6000
8000
Matric suction (kPa)
300
250
200
150
100
50
0
-50
0
2000
4000
6000
8000
Time (min)

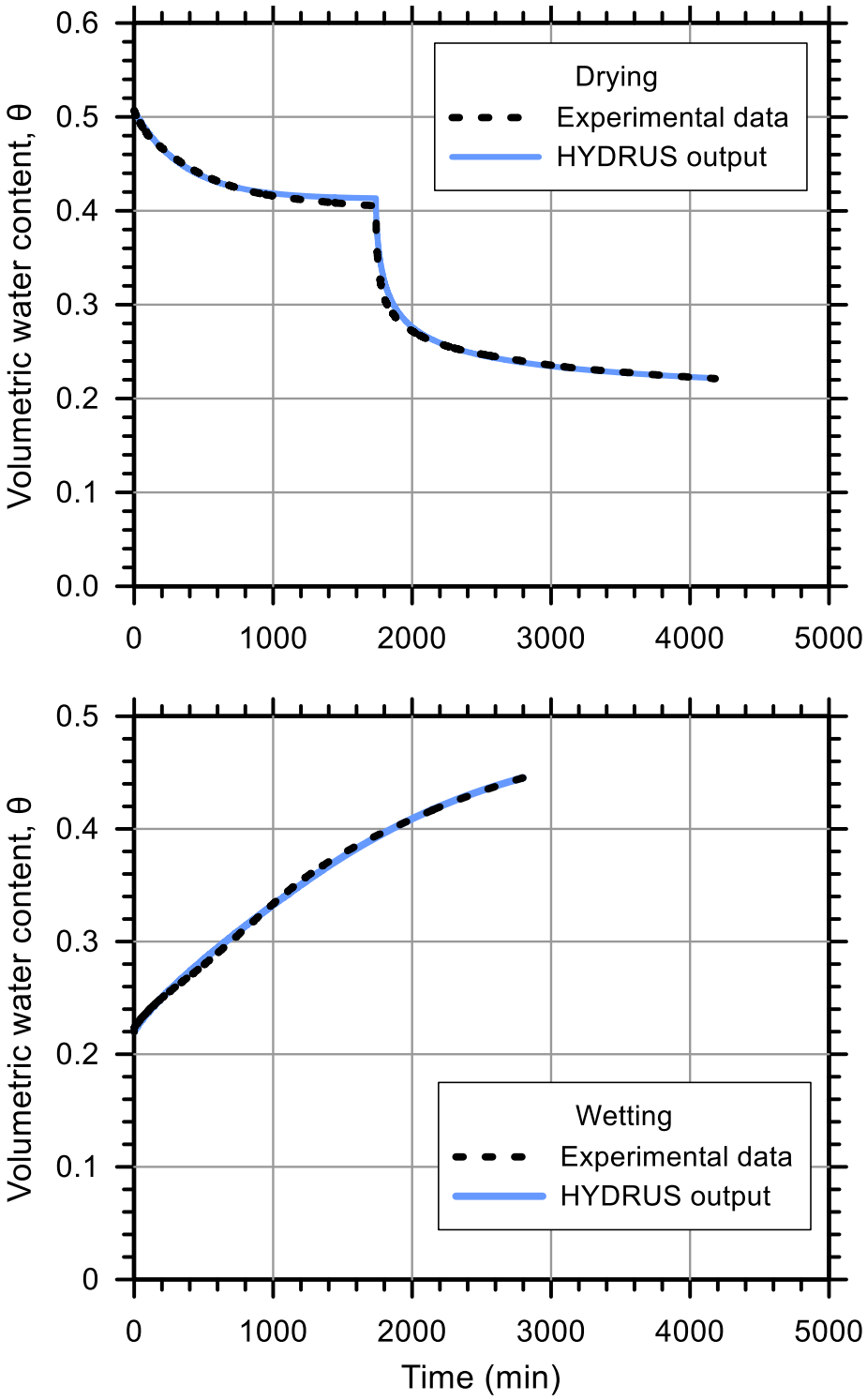
Drying
Experimental data
HYDRUS output
Volumetric water content, θ
0.6
0.5
0.4
0.3
0.2
0.1
0.0
0
1000
2000
3000
4000
5000
Wetting
Experimental data
HYDRUS output
Volumetric water content, θ
0.5
0.4
0.3
0.2
0.1
0
0
1000
2000
3000
4000
5000
Time (min)

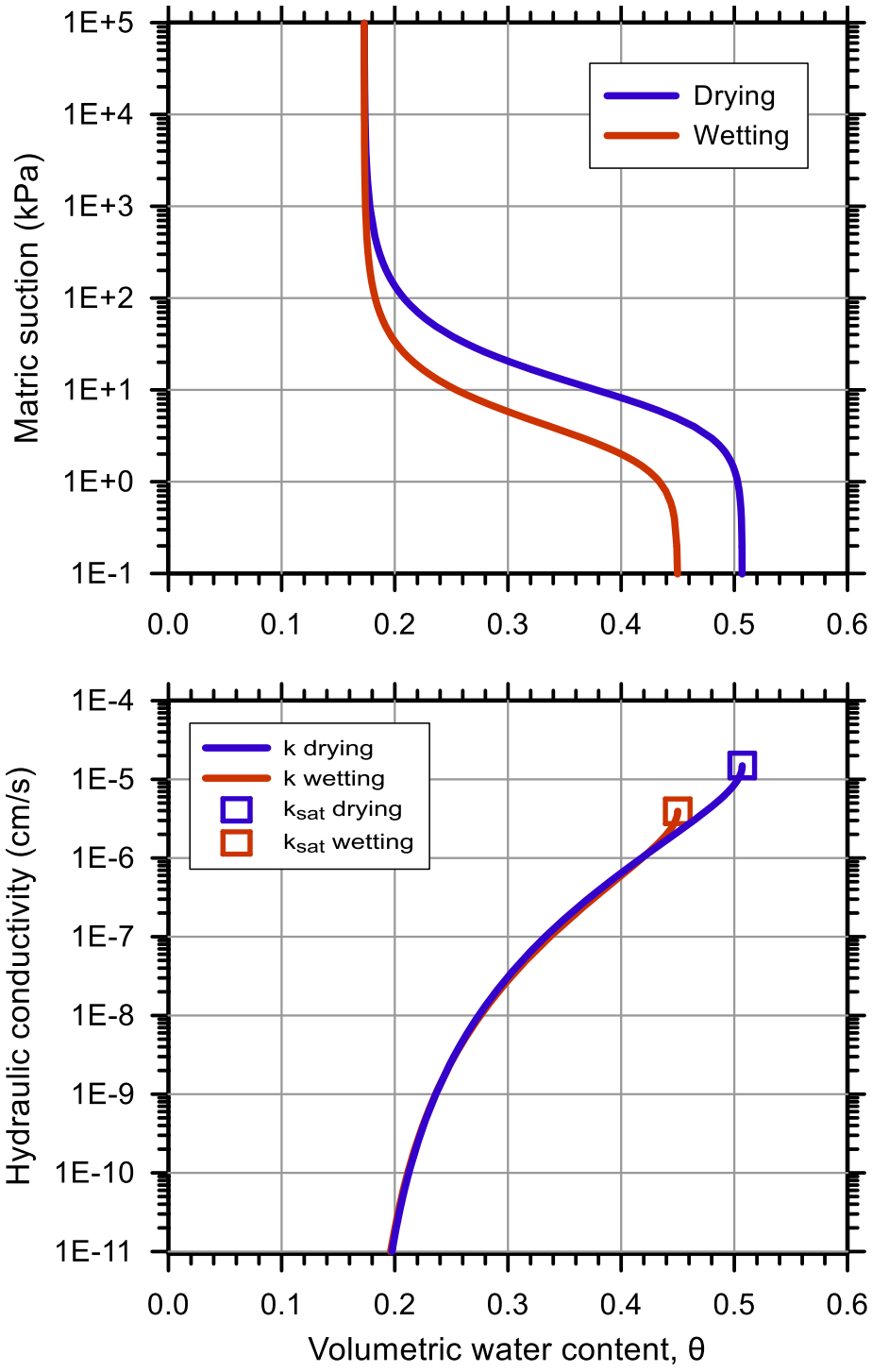
Matric suction (kPa)
1E+5
1E+4
1E+3
1E+2
1E+1
1E+0
1E-1
0.0
0.1
0.2
0.3
0.4
0.5
0.6
Drying
Wetting
Hydraulic conductivity (cm/s)
1E-4
1E-5
1E-6
1E-7
1E-8
1E-9
1E-10
1E-11
k drying
k wetting
ksat drying
ksat wetting
Volumetric water content, θ

Test No.: 9

Test Ref.: TRIMWH10

Test Soil: Whithorne

Molding Water Content: 27.70% (w_{opt}-2)

Property	Before Saturation	After Saturation
Void Ratio, e	1.393	1.336
Porosity, n (%)	58.21	57.20
Std. Proctor Relative Compaction, RC (%)	81.45	83.43
Dry Density, γ_d (g/cm^3)	1.12	1.15

Unsaturated Hydraulic Soil Parameters	Drying	Wetting
Saturated Volumetric Water Content, θ_s	0.572	0.459
Residual Volumetric Water Content, θ_r	0.145	0.145
Air-Entry Pressure Parameter, α (1/kPa)	0.151	0.194
Pore-Size Distribution Parameter, n	1.950	1.850
Saturated Hydraulic Conductivity, k_{sat} (cm/s)	2.15E-04	8.51E-05

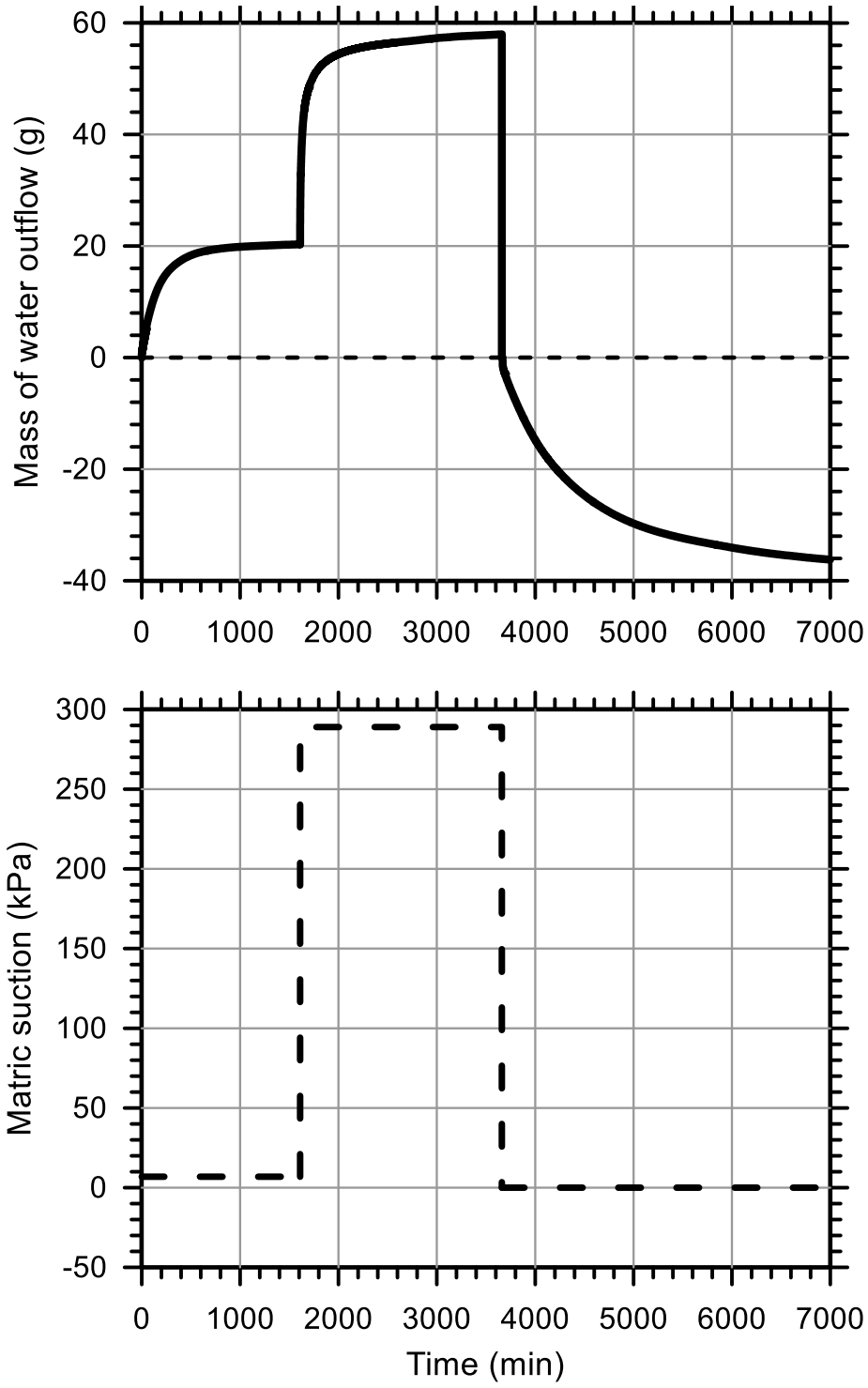
Mass of water outflow (g)
60
40
20
0
-20
-40
0
1000
2000
3000
4000
5000
6000
7000
Matric suction (kPa)
300
250
200
150
100
50
0
-50
0
1000
2000
3000
4000
5000
6000
7000
Time (min)

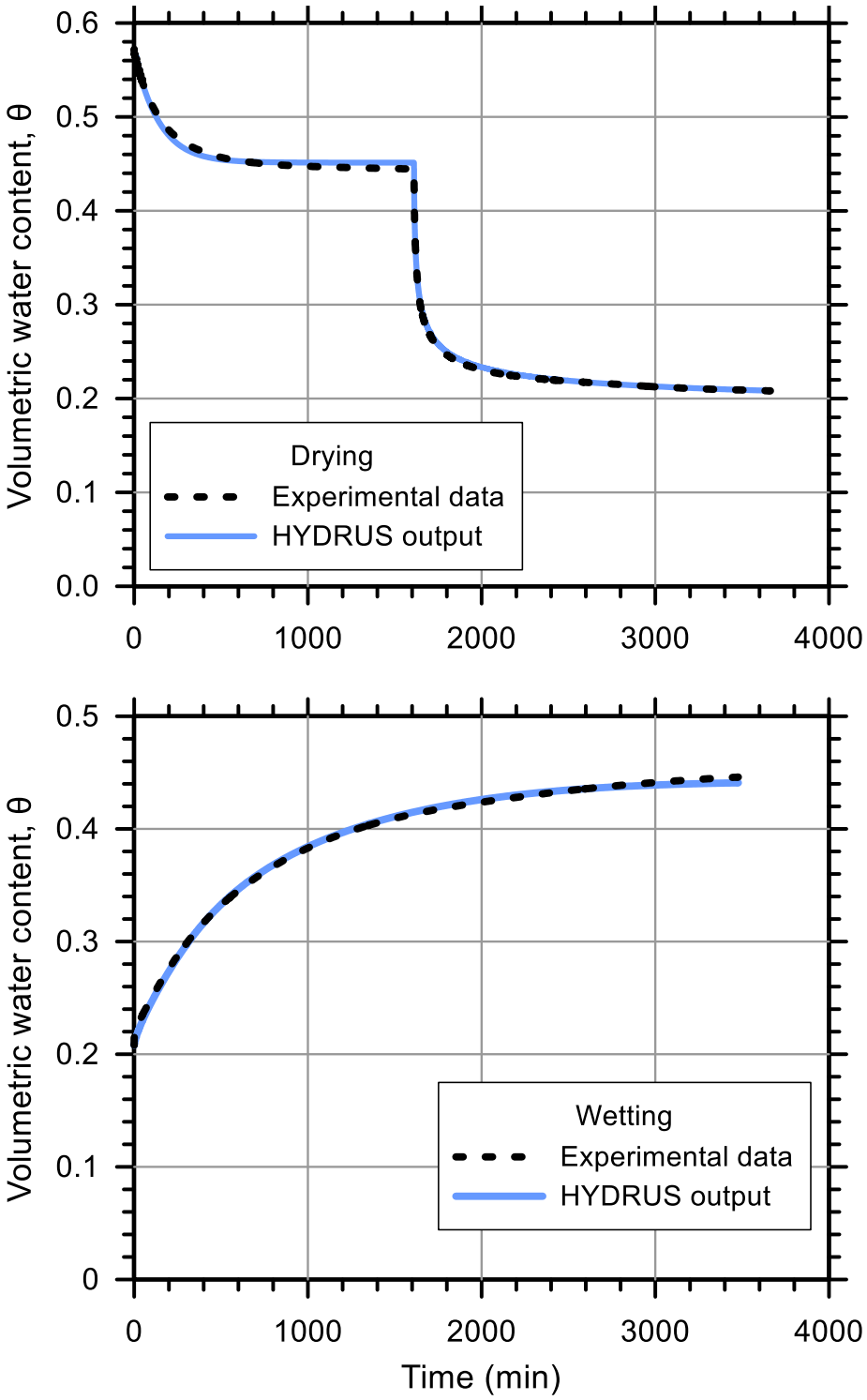
Volumetric water content, θ
0.6
0.5
0.4
0.3
0.2
0.1
0.0
0
1000
2000
3000
4000
Drying
Experimental data
HYDRUS output
Volumetric water content, θ
0.5
0.4
0.3
0.2
0.1
0
0
1000
2000
3000
4000
Time (min)
Wetting
Experimental data
HYDRUS output

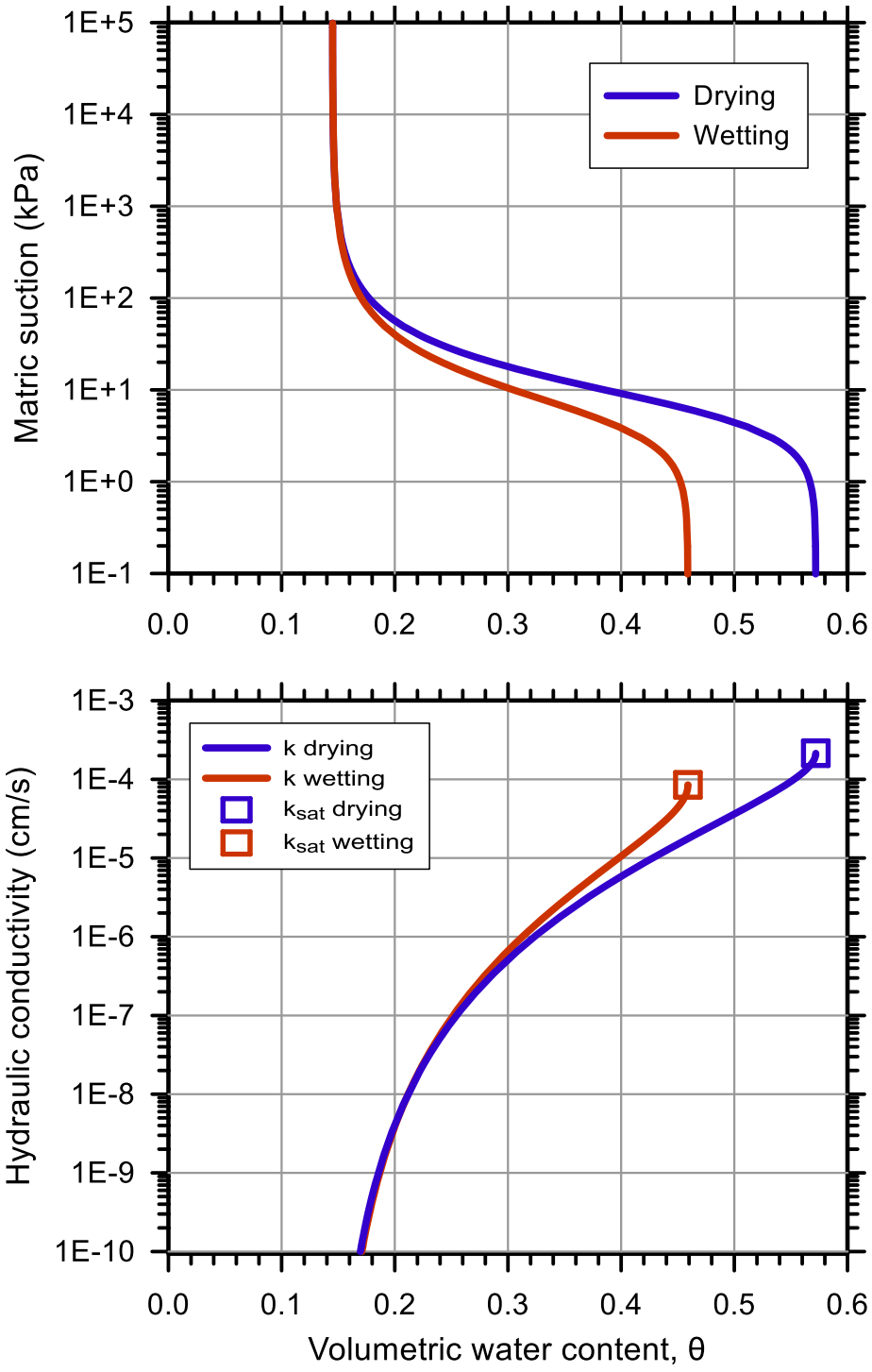
Matric suction (kPa)
1E+5
1E+4
1E+3
1E+2
1E+1
1E+0
1E-1
0.0
0.1
0.2
0.3
0.4
0.5
0.6
Drying
Wetting
Hydraulic conductivity (cm/s)
1E-3
1E-4
1E-5
1E-6
1E-7
1E-8
1E-9
1E-10
k drying
k wetting
ksat drying
ksat wetting
Volumetric water content, θ

Test No.: R1

Test Ref.: TRIMWH01

Test Soil: Whithorne

Molding Water Content: 27.70% (w_{opt}-2)

Property	Before Saturation	After Saturation
Void Ratio, e	1.548	1.548
Porosity, n (%)	60.76	60.75
Std. Proctor Relative Compaction, RC (%)	76.49	76.50
Dry Density, γ_d (g/cm^3)	1.05	1.05

Unsaturated Hydraulic Soil Parameters	Drying	Wetting
Saturated Volumetric Water Content, θ_s	0.608	0.492
Residual Volumetric Water Content, θ_r	0.114	0.114
Air-Entry Pressure Parameter, α (1/kPa)	0.170	0.415
Pore-Size Distribution Parameter, n	1.609	1.570
Saturated Hydraulic Conductivity, k_{sat} (cm/s)	7.95E-04	4.50E-04

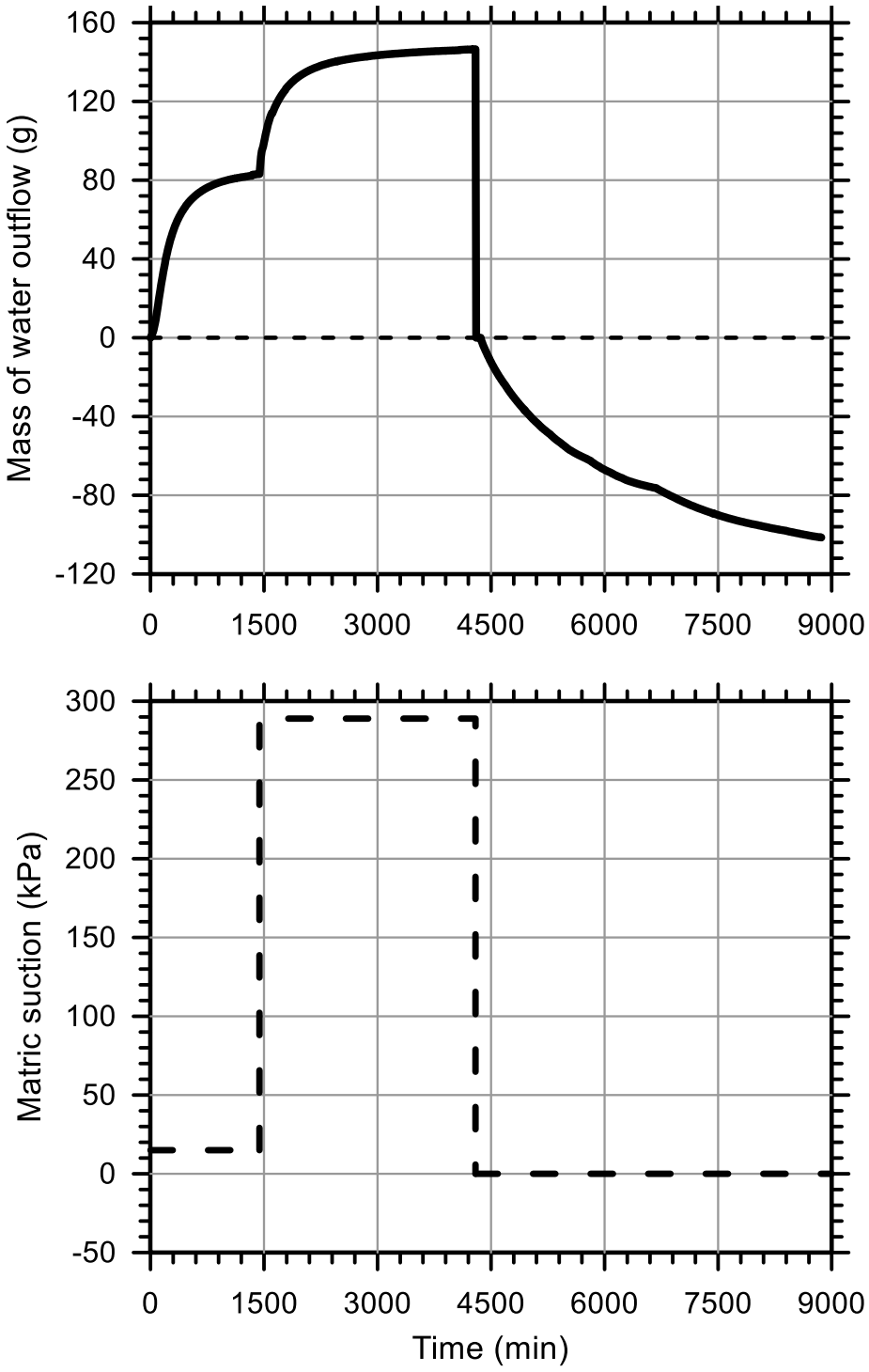
Mass of water outflow (g)
160
120
80
40
0
-40
-80
-120
0
1500
3000
4500
6000
7500
9000
Matric suction (kPa)
300
250
200
150
100
50
0
-50
0
1500
3000
4500
6000
7500
9000
Time (min)

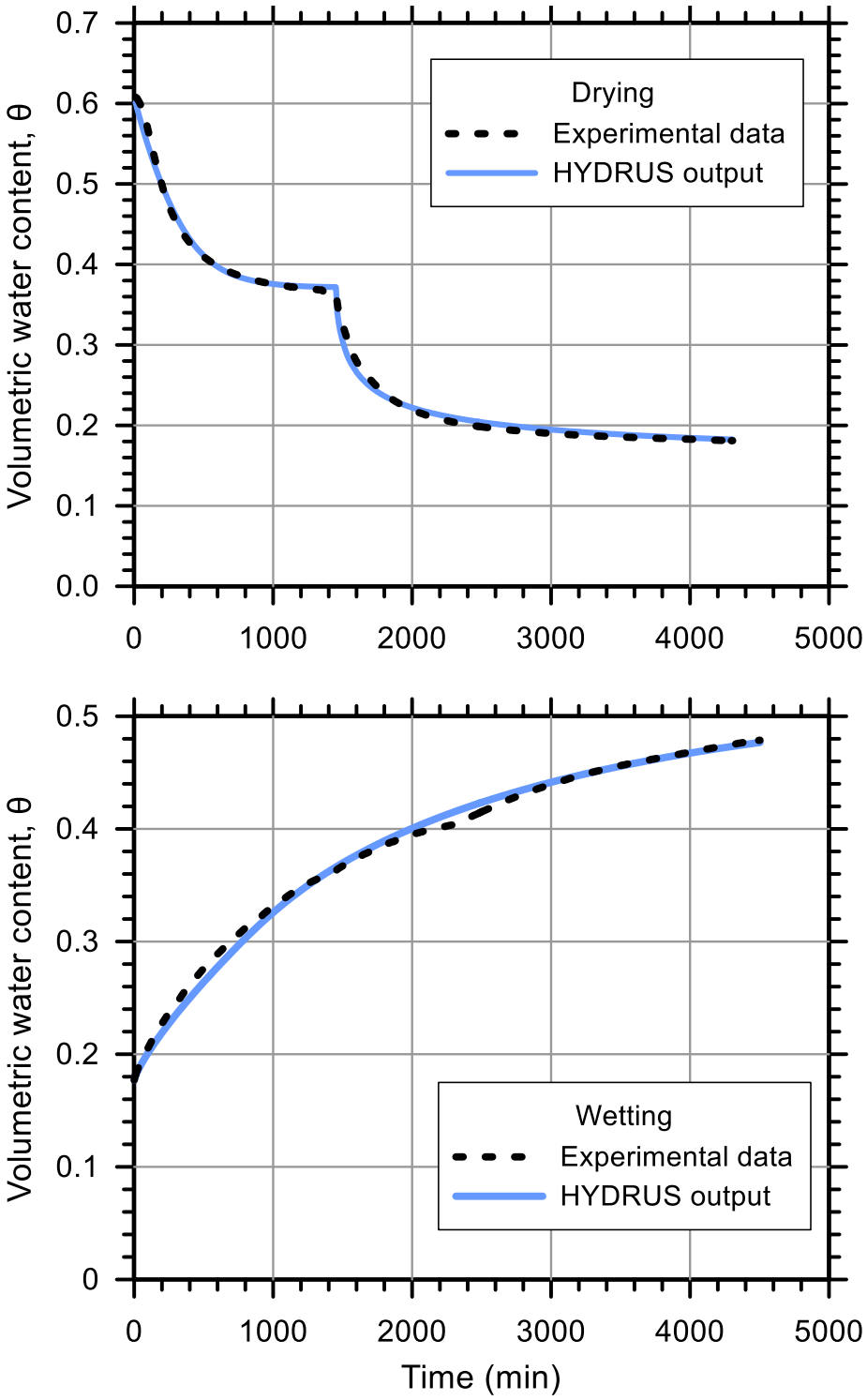
Drying
Experimental data
HYDRUS output
Volumetric water content, θ
0.7
0.6
0.5
0.4
0.3
0.2
0.1
0.0
0
1000
2000
3000
4000
5000
Wetting
Experimental data
HYDRUS output
Volumetric water content, θ
0.5
0.4
0.3
0.2
0.1
0
0
1000
2000
3000
4000
5000
Time (min)

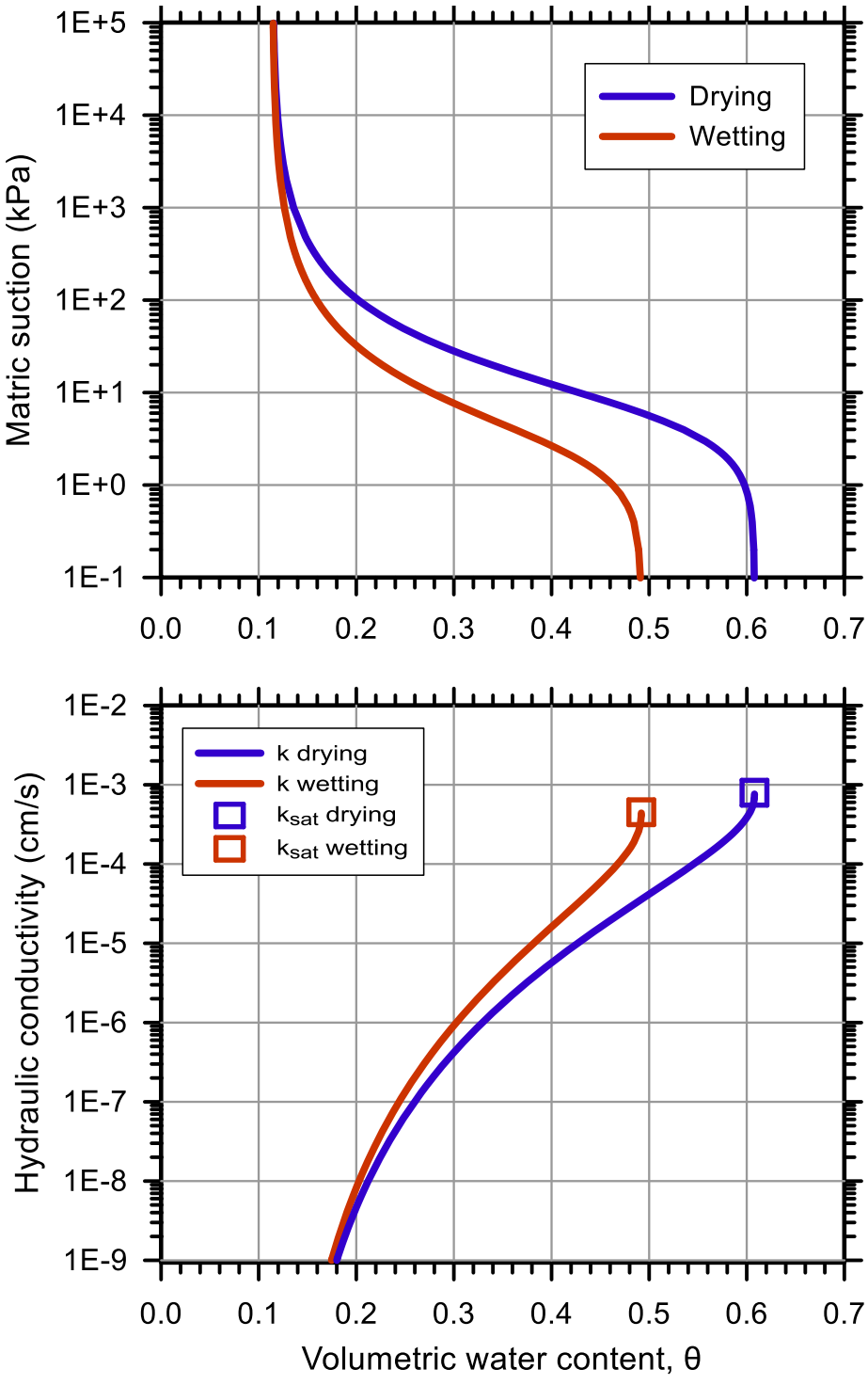
Matric suction (kPa)
1E+5
1E+4
1E+3
1E+2
1E+1
1E+0
1E-1
Drying
Wetting
0.0
0.1
0.2
0.3
0.4
0.5
0.6
0.7
Hydraulic conductivity (cm/s)
1E-2
1E-3
1E-4
1E-5
1E-6
1E-7
1E-8
1E-9
k drying
k wetting
ksat drying
ksat wetting
Volumetric water content, θ

Test No.: R2

Test Ref.: TRIMWH04

Test Soil: Whithorne

Molding Water Content: 29.70% (w_{opt})

Property	Before Saturation	After Saturation
Void Ratio, e	1.169	1.168
Porosity, n (%)	53.90	53.87
Std. Proctor Relative Compaction, RC (%)	89.85	89.91
Dry Density, γ_d (g/cm^3)	1.24	1.24

Unsaturated Hydraulic Soil Parameters	Drying	Wetting
Saturated Volumetric Water Content, θ_s	0.539	0.452
Residual Volumetric Water Content, θ_r	0.166	0.166
Air-Entry Pressure Parameter, α (1/kPa)	0.124	0.363
Pore-Size Distribution Parameter, n	1.760	1.576
Saturated Hydraulic Conductivity, k_{sat} (cm/s)	5.63E-05	2.95E-05

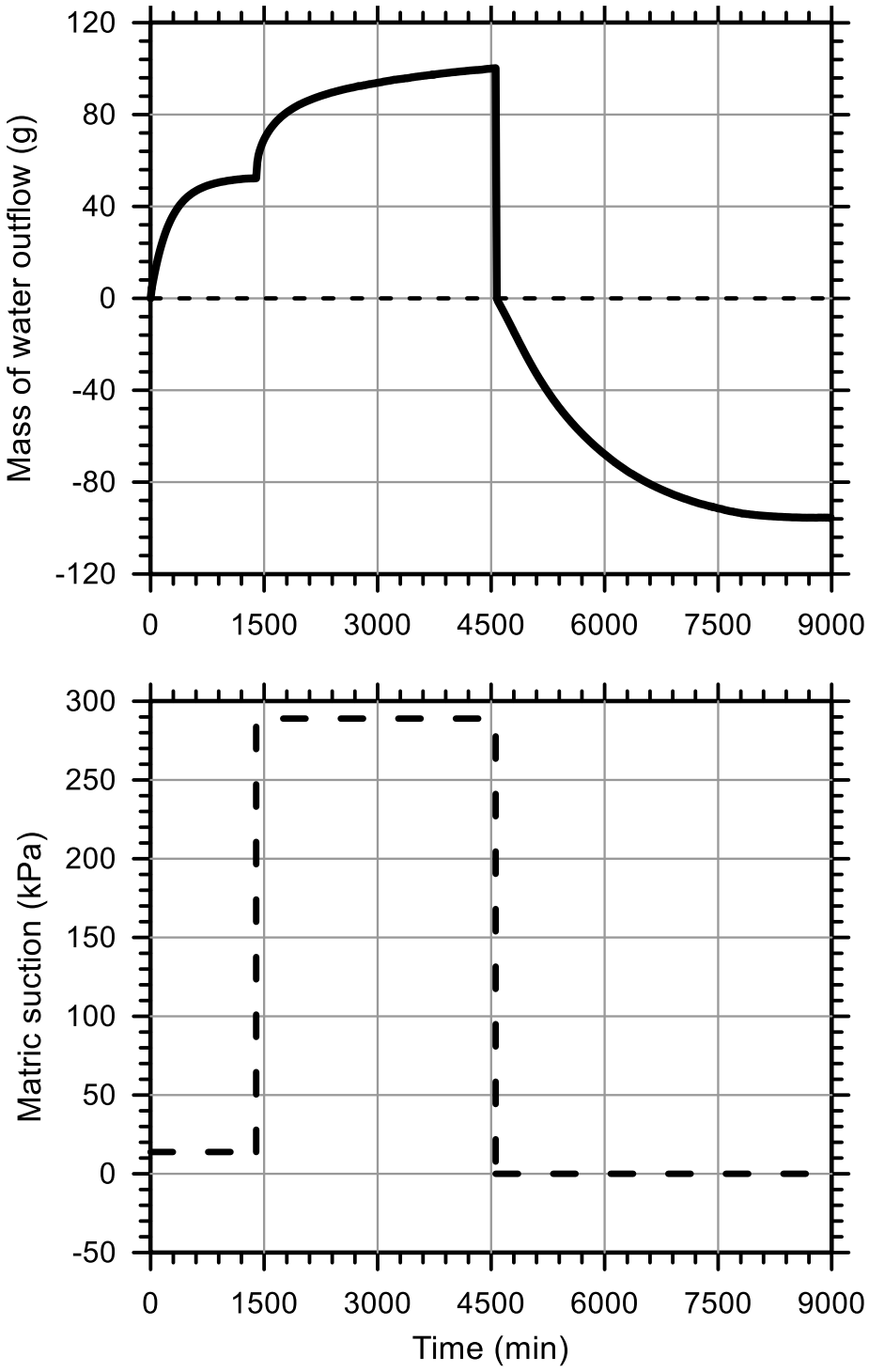
120
80
40
0
-40
-80
-120
Mass of water outflow (g)
0
1500
3000
4500
6000
7500
9000
300
250
200
150
100
50
0
-50
Matric suction (kPa)
0
1500
3000
4500
6000
7500
9000
Time (min)

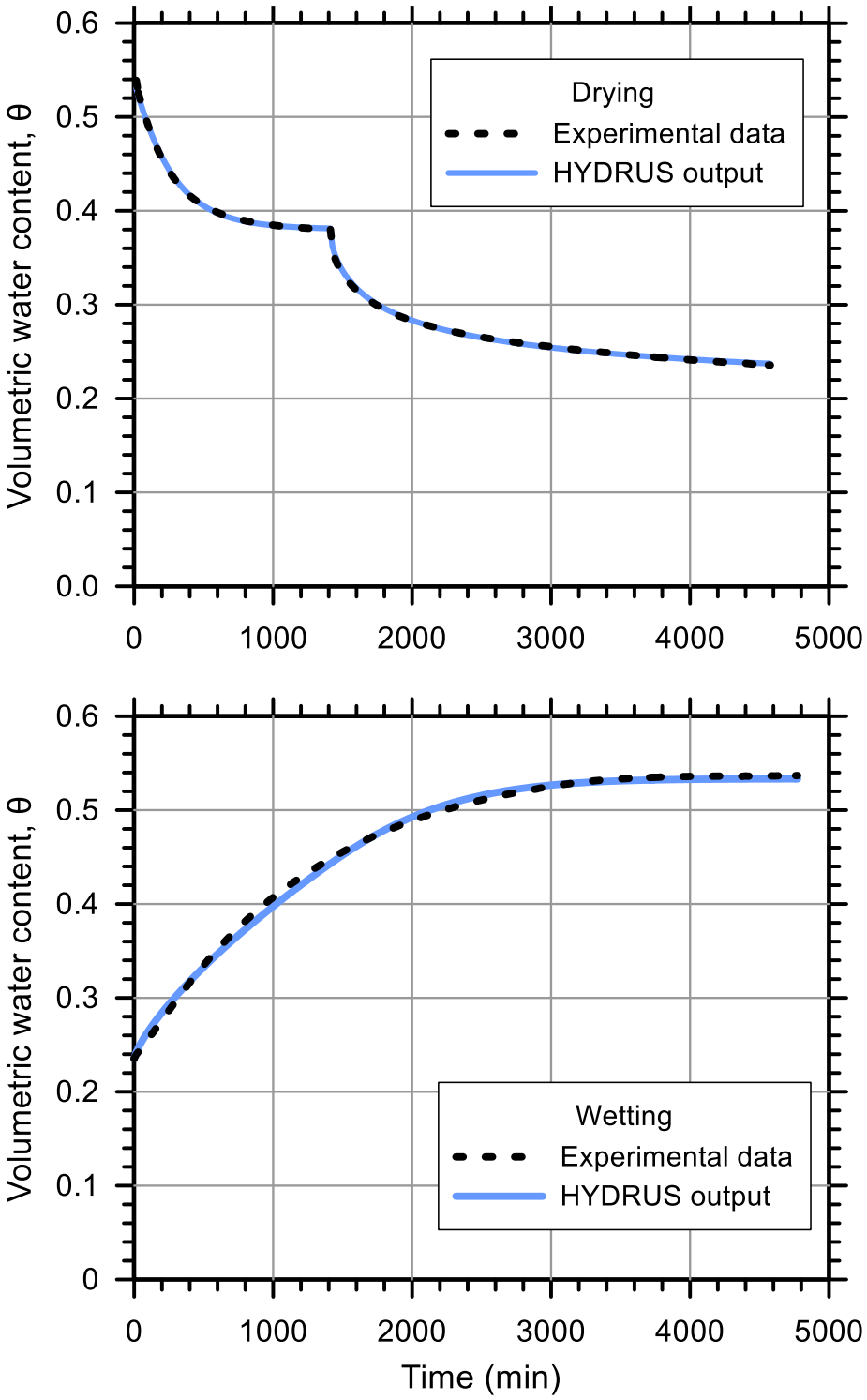
Drying
Experimental data
HYDRUS output
Volumetric water content, θ
0.6
0.5
0.4
0.3
0.2
0.1
0.0
0
1000
2000
3000
4000
5000
Wetting
Experimental data
HYDRUS output
Volumetric water content, θ
0.6
0.5
0.4
0.3
0.2
0.1
0
0
1000
2000
3000
4000
5000
Time (min)

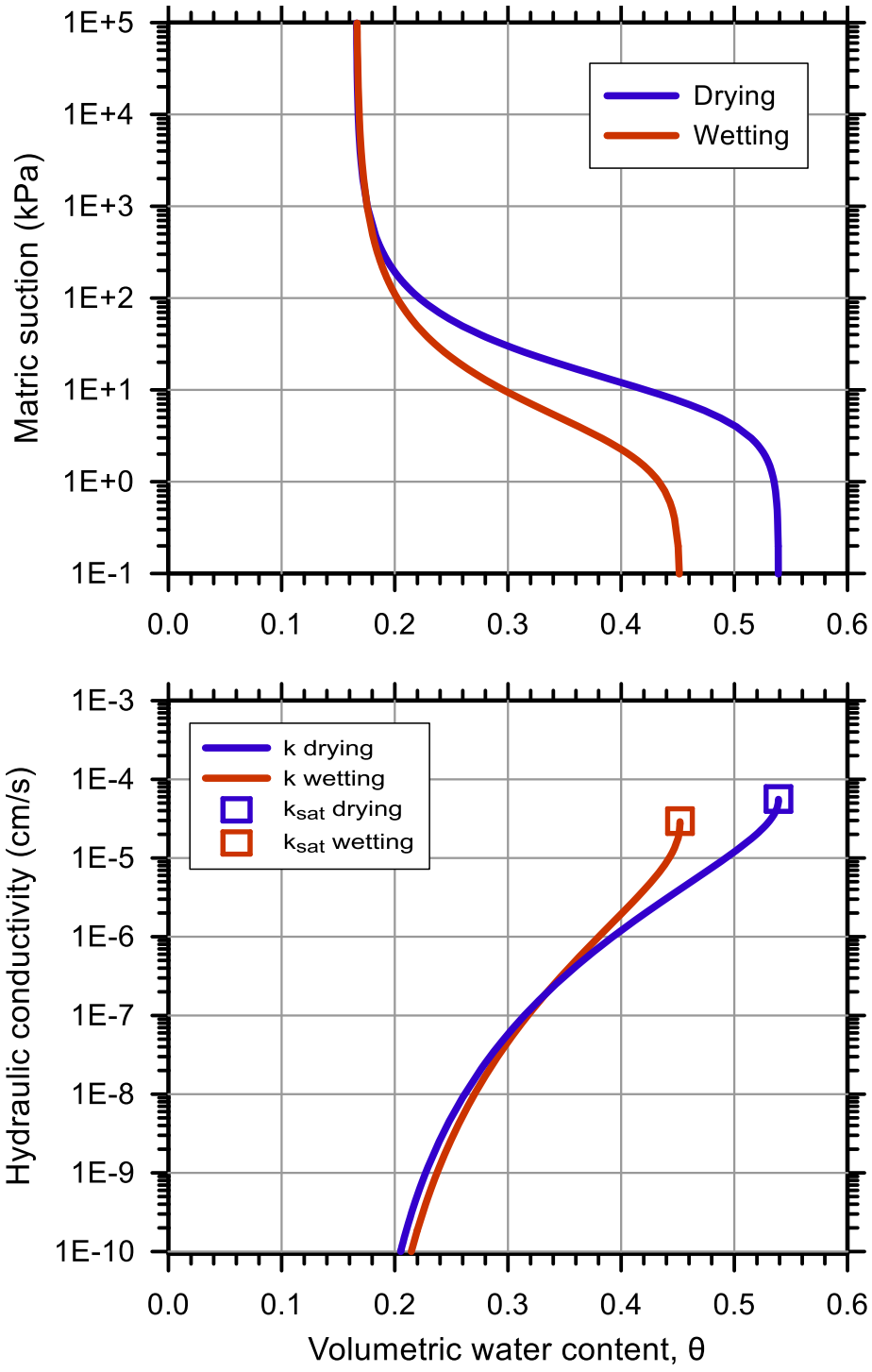
Matric suction (kPa)
1E+5
1E+4
1E+3
1E+2
1E+1
1E+0
1E-1
0.0
0.1
0.2
0.3
0.4
0.5
0.6
Drying
Wetting
Hydraulic conductivity (cm/s)
1E-3
1E-4
1E-5
1E-6
1E-7
1E-8
1E-9
1E-10
k drying
k wetting
ksat drying
ksat wetting
Volumetric water content, θ

Test No.: 1

Test Ref.: TRIMWH06

Test Soil: Whithorne

Molding Water Content: 29.70% (w_{opt})

Property	Before Saturation	After Saturation
Void Ratio, e	1.169	1.168
Porosity, n (%)	60.23	60.66
Std. Proctor Relative Compaction, RC (%)	77.52	76.68
Dry Density, γ_d (g/cm^3)	1.07	1.05

Unsaturated Hydraulic Soil Parameters	Drying	Wetting
Saturated Volumetric Water Content, θ_s	0.607	0.488
Residual Volumetric Water Content, θ_r	0.122	0.122
Air-Entry Pressure Parameter, α (1/kPa)	0.198	0.418
Pore-Size Distribution Parameter, n	1.699	1.580
Saturated Hydraulic Conductivity, k_{sat} (cm/s)	7.50E-04	3.50E-04

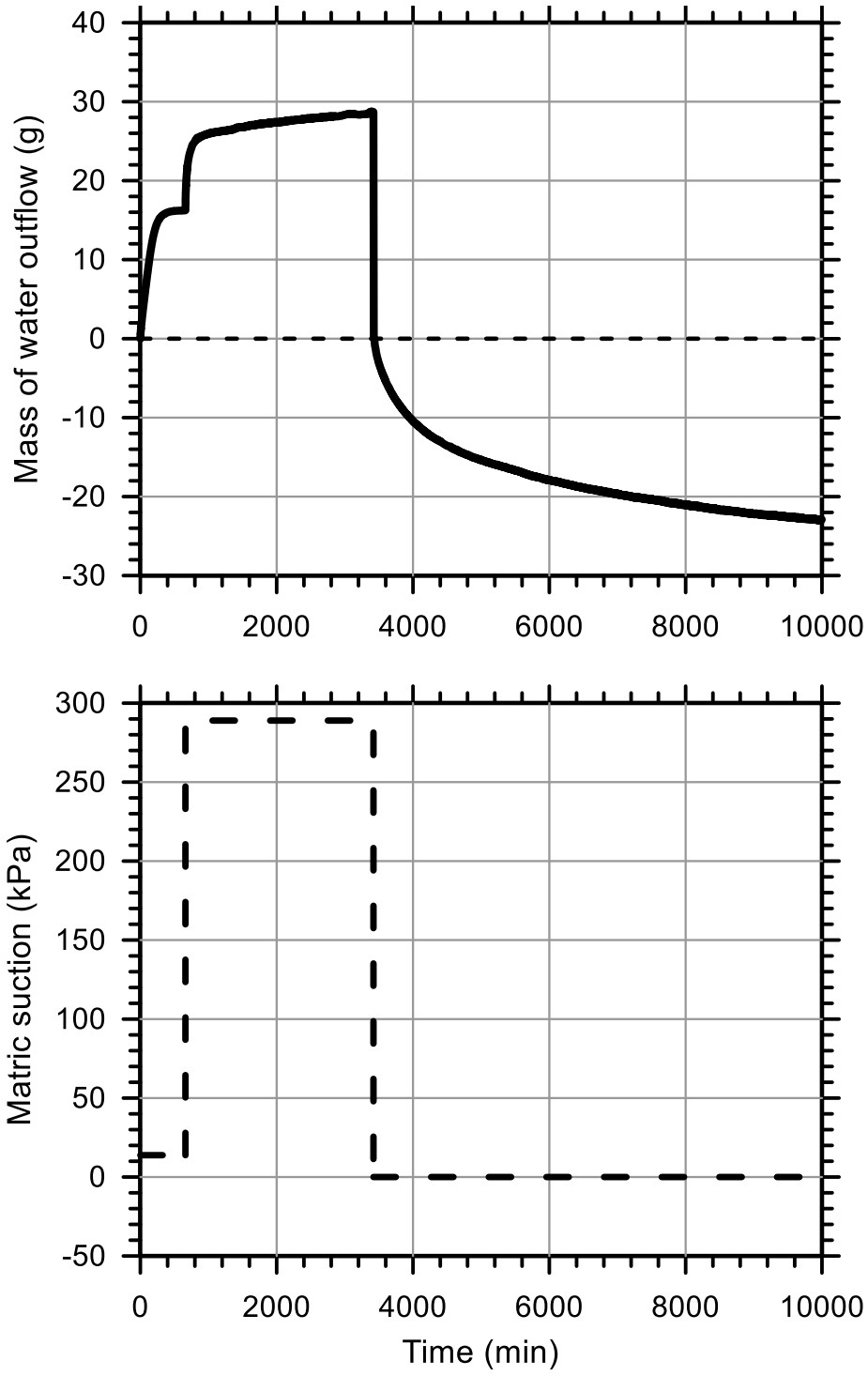
Mass of water outflow (g)
40
30
20
10
0
-10
-20
-30
0
2000
4000
6000
8000
10000
Matric suction (kPa)
300
250
200
150
100
50
0
-50
0
2000
4000
6000
8000
10000
Time (min)

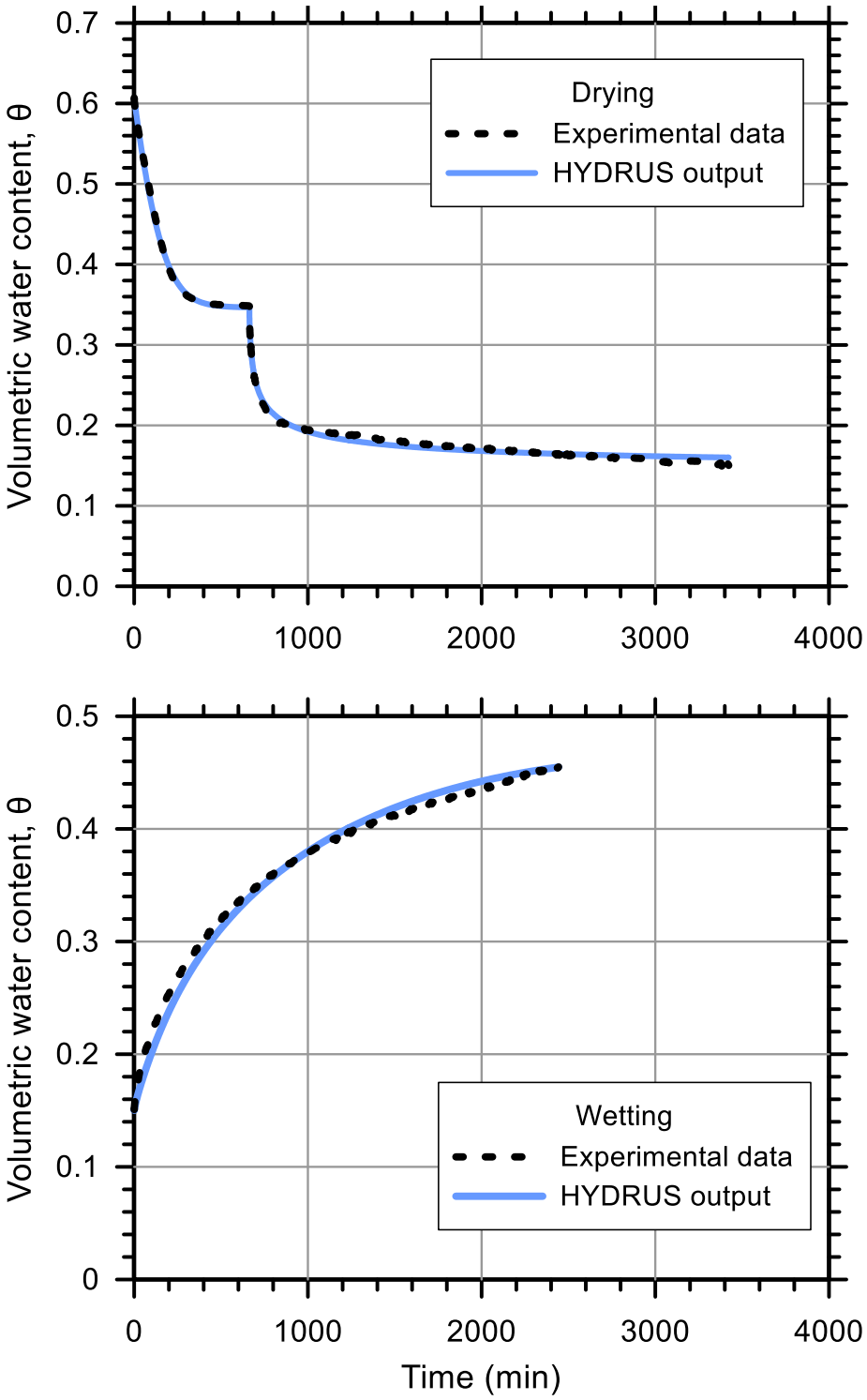
Drying
Experimental data
HYDRUS output
Volumetric water content, θ
0.7
0.6
0.5
0.4
0.3
0.2
0.1
0.0
0
1000
2000
3000
4000
Wetting
Experimental data
HYDRUS output
Volumetric water content, θ
0.5
0.4
0.3
0.2
0.1
0
0
1000
2000
3000
4000
Time (min)

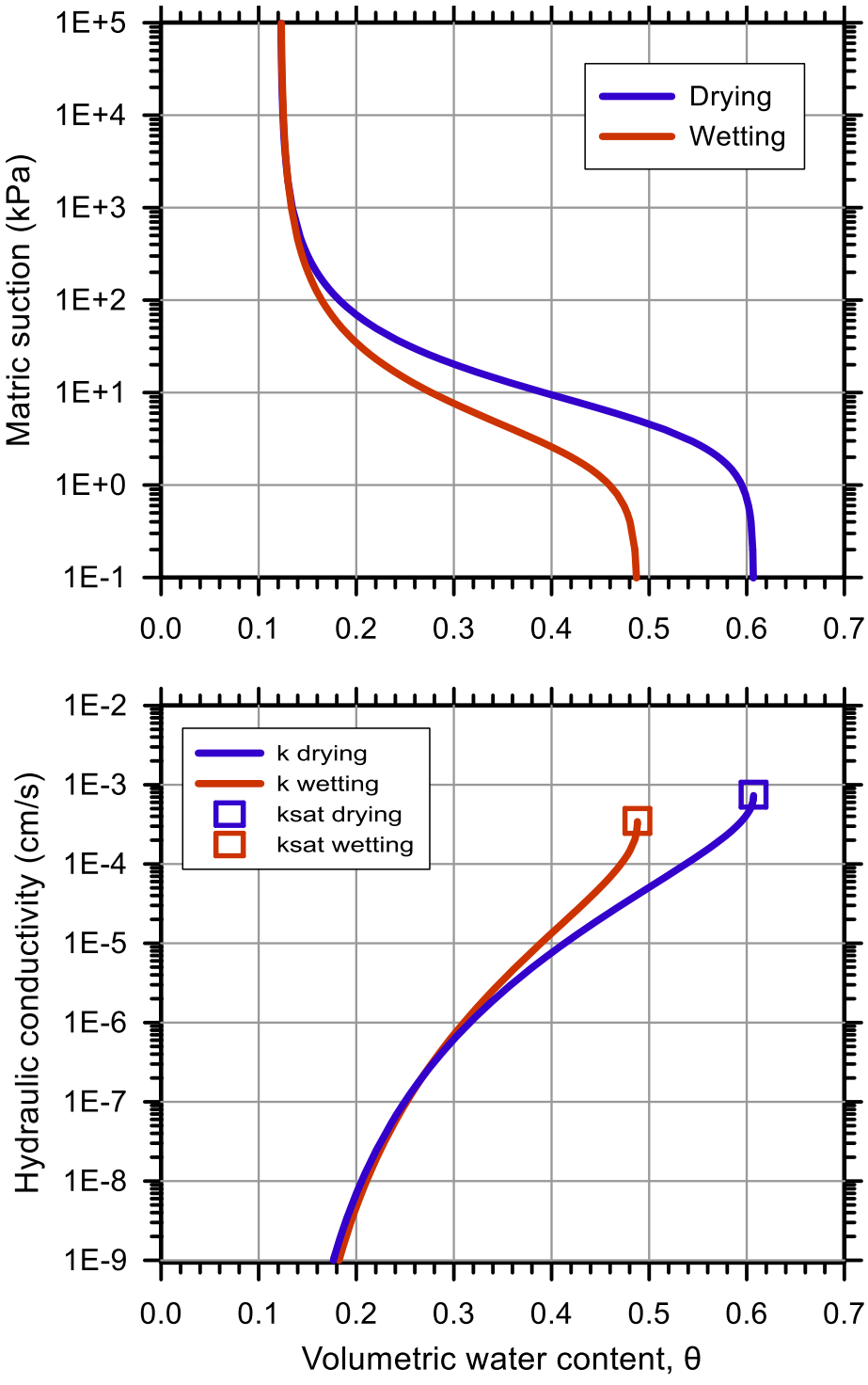
Matric suction (kPa)
1E+5
1E+4
1E+3
1E+2
1E+1
1E+0
1E-1
Drying
Wetting
0.0
0.1
0.2
0.3
0.4
0.5
0.6
0.7
Hydraulic conductivity (cm/s)
1E-2
1E-3
1E-4
1E-5
1E-6
1E-7
1E-8
1E-9
k drying
k wetting
ksat drying
ksat wetting
Volumetric water content, θ

Test No.: 6

Test Ref.: TRIMWH09

Test Soil: Whithorne

Molding Water Content: 31.70% (w_{opt}+2)

Property	Before Saturation	After Saturation
Void Ratio, e	1.003	1.021
Porosity, n (%)	50.07	50.53
Std. Proctor Relative Compaction, RC (%)	97.32	96.43
Dry Density, γ_d (g/cm^3)	1.34	1.33

Unsaturated Hydraulic Soil Parameters	Drying	Wetting
Saturated Volumetric Water Content, θ_s	0.505	0.541
Residual Volumetric Water Content, θ_r	0.184	0.184
Air-Entry Pressure Parameter, α (1/kPa)	0.117	0.319
Pore-Size Distribution Parameter, n	1.800	1.700
Saturated Hydraulic Conductivity, k_{sat} (cm/s)	2.21E-06	8.38E-07

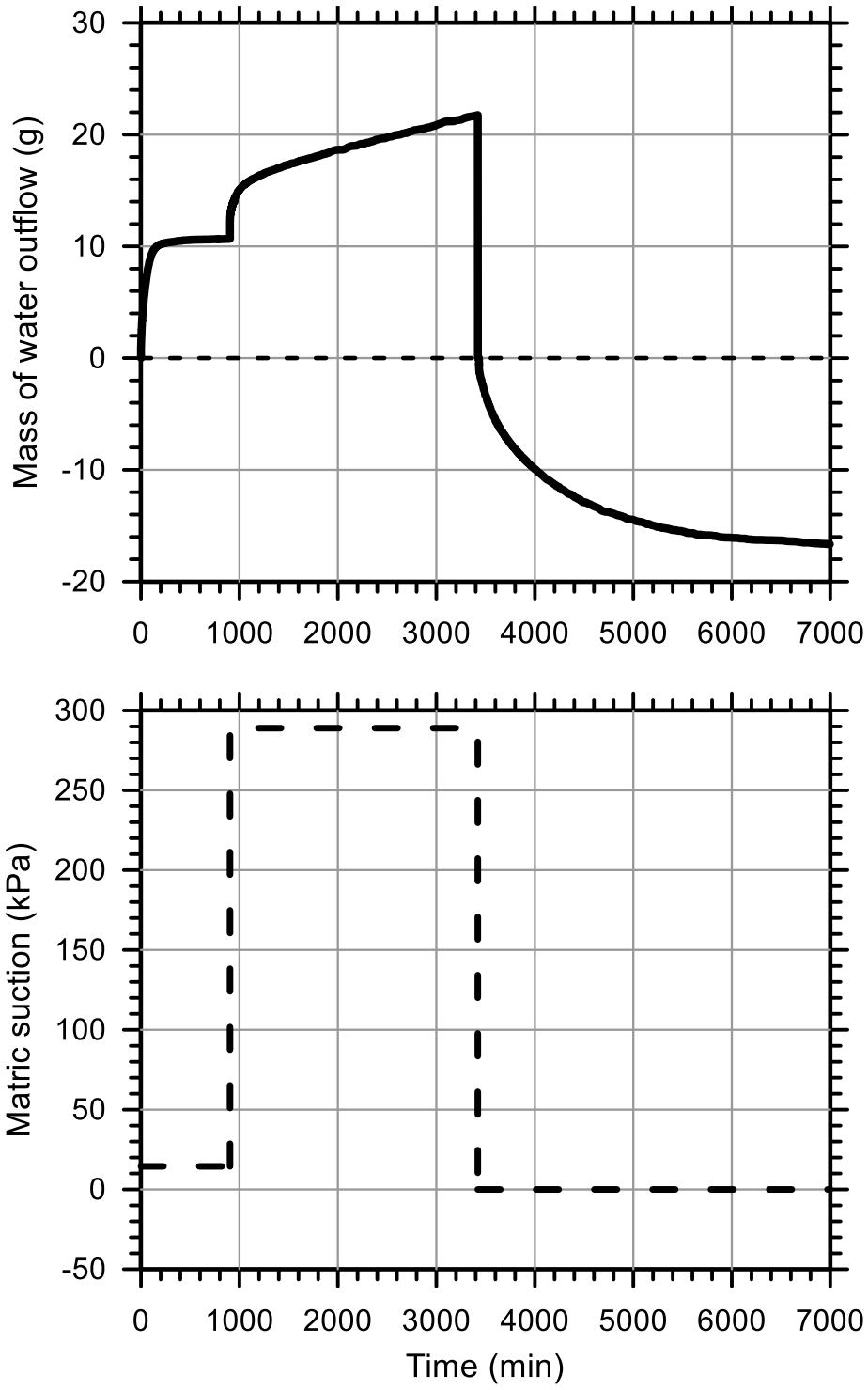
Mass of water outflow (g)
30
20
10
0
-10
-20
0
1000
2000
3000
4000
5000
6000
7000
Matric suction (kPa)
300
250
200
150
100
50
0
-50
0
1000
2000
3000
4000
5000
6000
7000
Time (min)

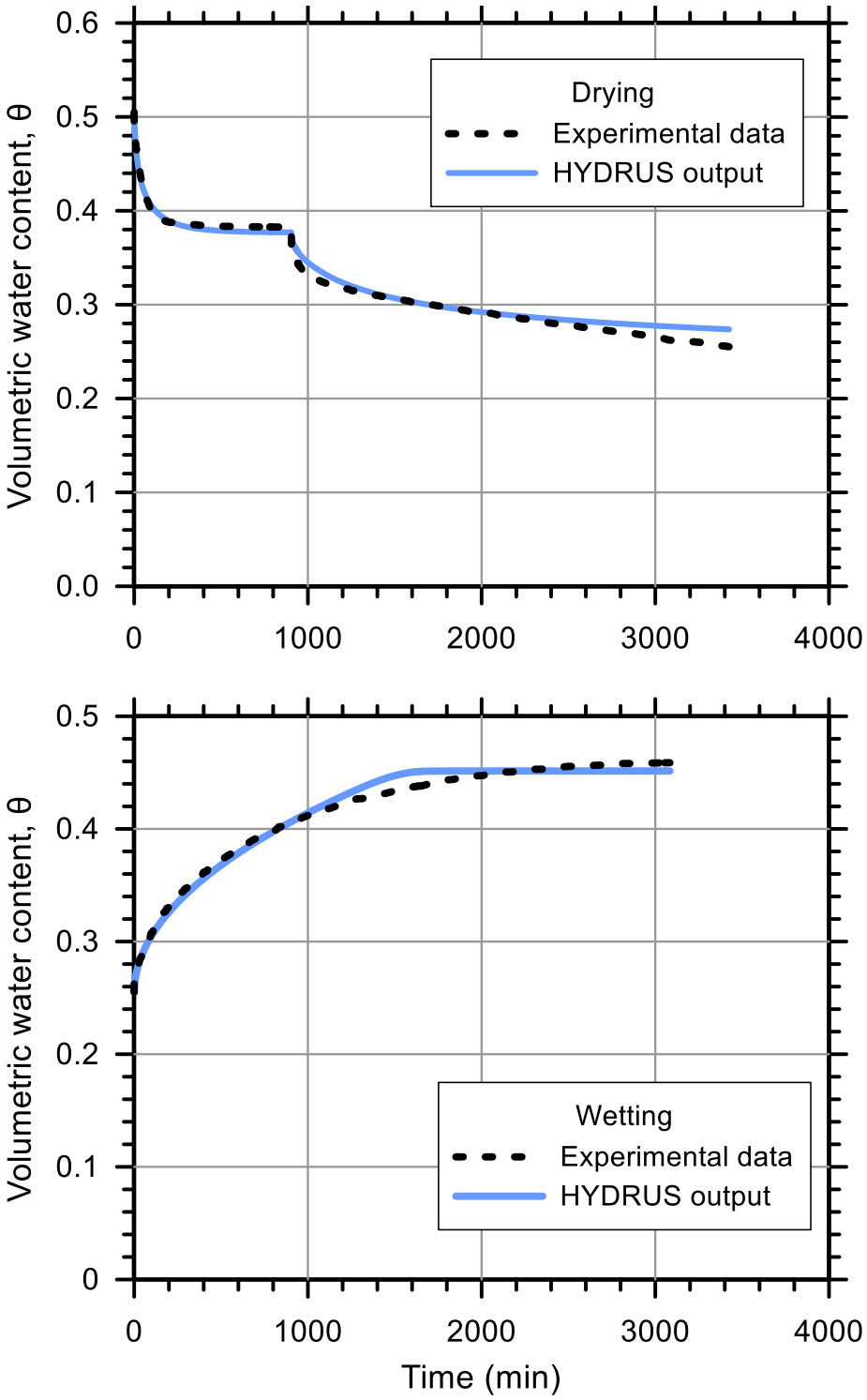
Drying
Experimental data
HYDRUS output
Volumetric water content, θ
0.6
0.5
0.4
0.3
0.2
0.1
0.0
0
1000
2000
3000
4000
Wetting
Experimental data
HYDRUS output
Volumetric water content, θ
0.5
0.4
0.3
0.2
0.1
0
0
1000
2000
3000
4000
Time (min)

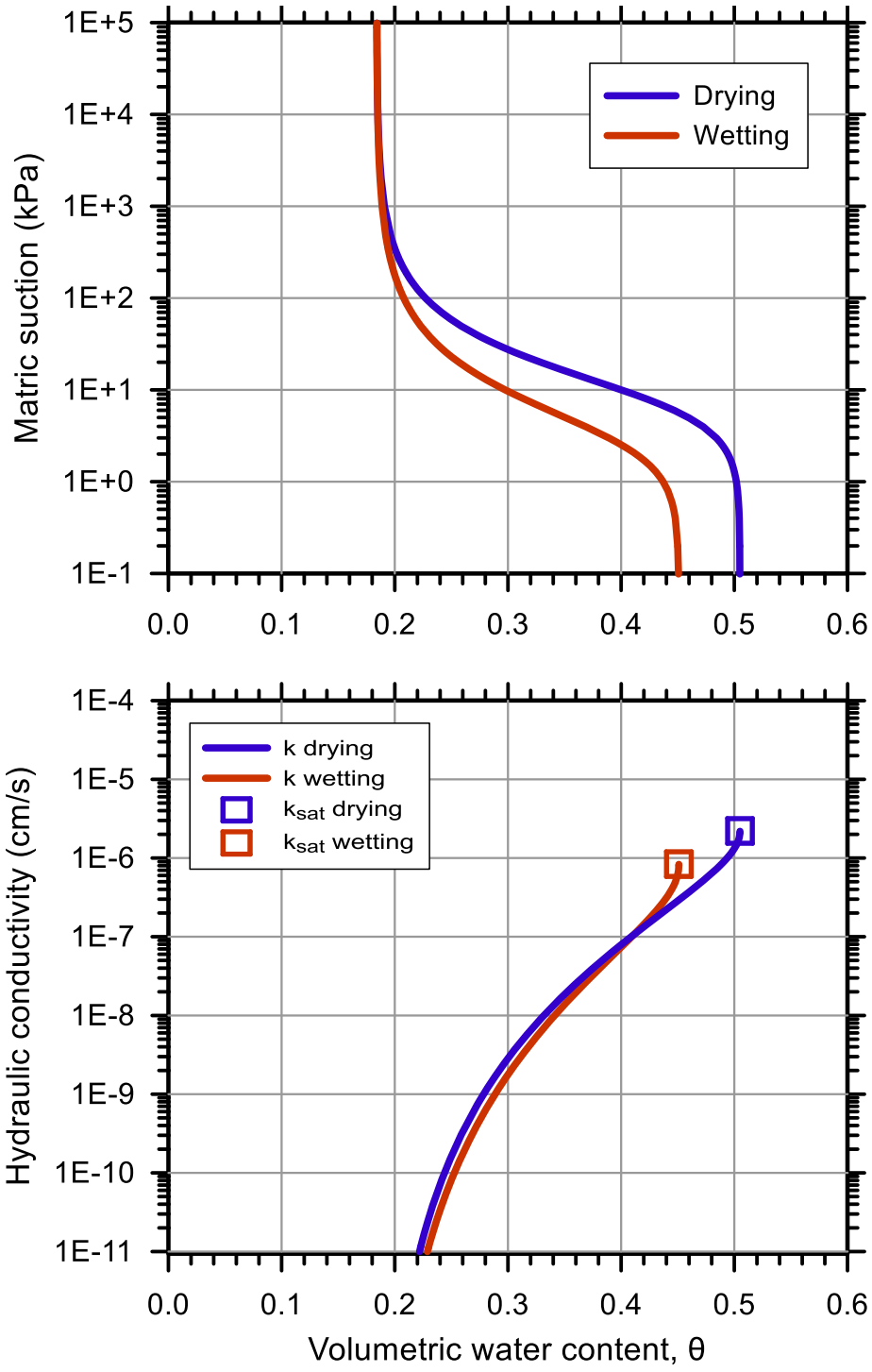
Matric suction (kPa)
1E+5
1E+4
1E+3
1E+2
1E+1
1E+0
1E-1
0.0
0.1
0.2
0.3
0.4
0.5
0.6
Drying
Wetting
Hydraulic conductivity (cm/s)
1E-4
1E-5
1E-6
1E-7
1E-8
1E-9
1E-10
1E-11
k drying
k wetting
ksat drying
ksat wetting
Volumetric water content, θ

Test No.: 2

Test Ref.: TRIMWH07

Test Soil: Whithorne

Molding Water Content: 31.70% (w_{opt}+2)

Property	Before Saturation	After Saturation
Void Ratio, e	1.498	1.500
Porosity, n (%)	59.97	60.01
Std. Proctor Relative Compaction, RC (%)	78.03	77.95
Dry Density, γ_d (g/cm^3)	1.07	1.07

Unsaturated Hydraulic Soil Parameters	Drying	Wetting
Saturated Volumetric Water Content, θ_s	0.600	0.478
Residual Volumetric Water Content, θ_r	0.115	0.115
Air-Entry Pressure Parameter, α (1/kPa)	0.191	0.410
Pore-Size Distribution Parameter, n	1.623	1.500
Saturated Hydraulic Conductivity, k_{sat} (cm/s)	6.30E-04	2.90E-04

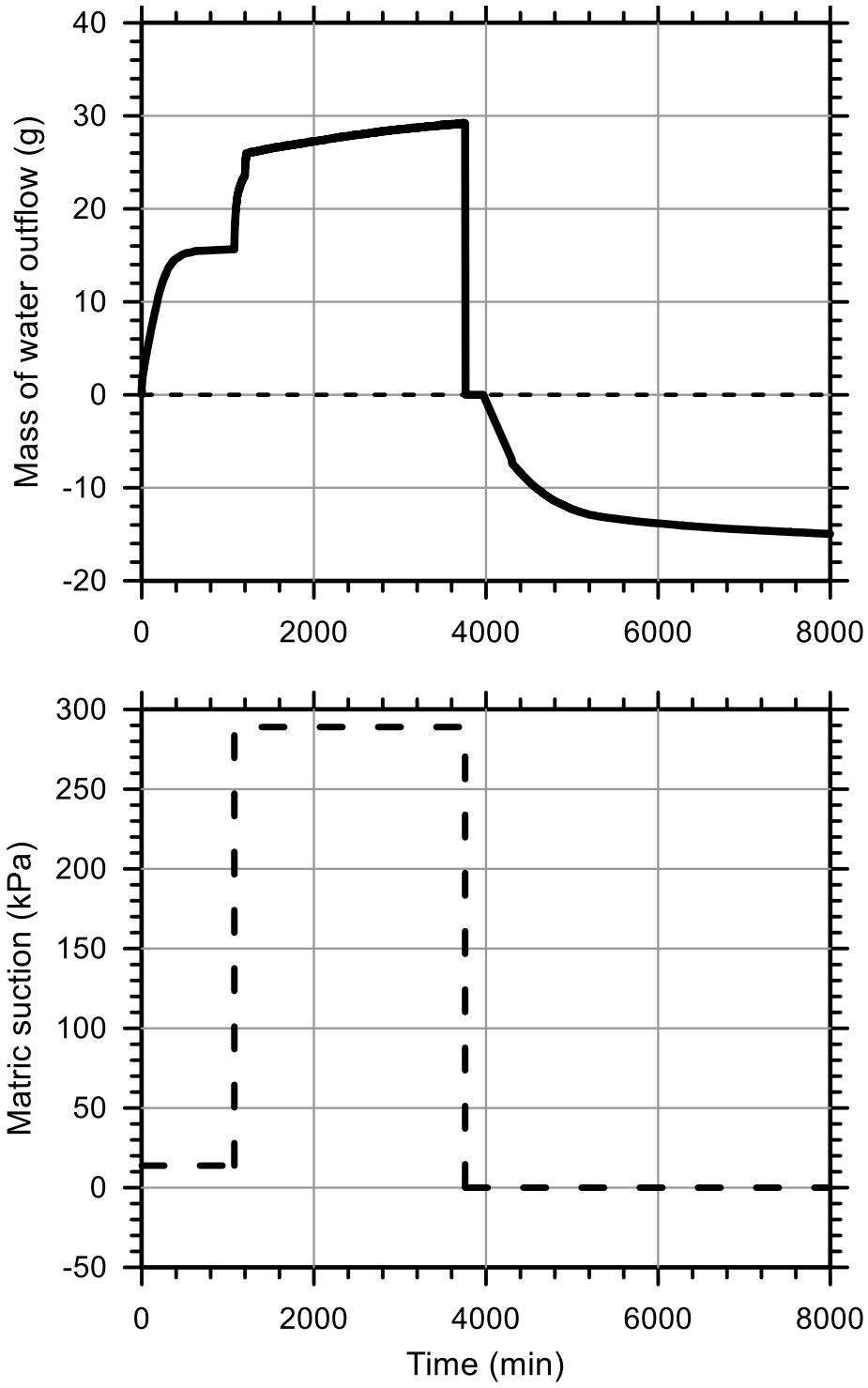
Mass of water outflow (g)
40
30
20
10
0
-10
-20
0
2000
4000
6000
8000
Matric suction (kPa)
300
250
200
150
100
50
0
-50
0
2000
4000
6000
8000
Time (min)

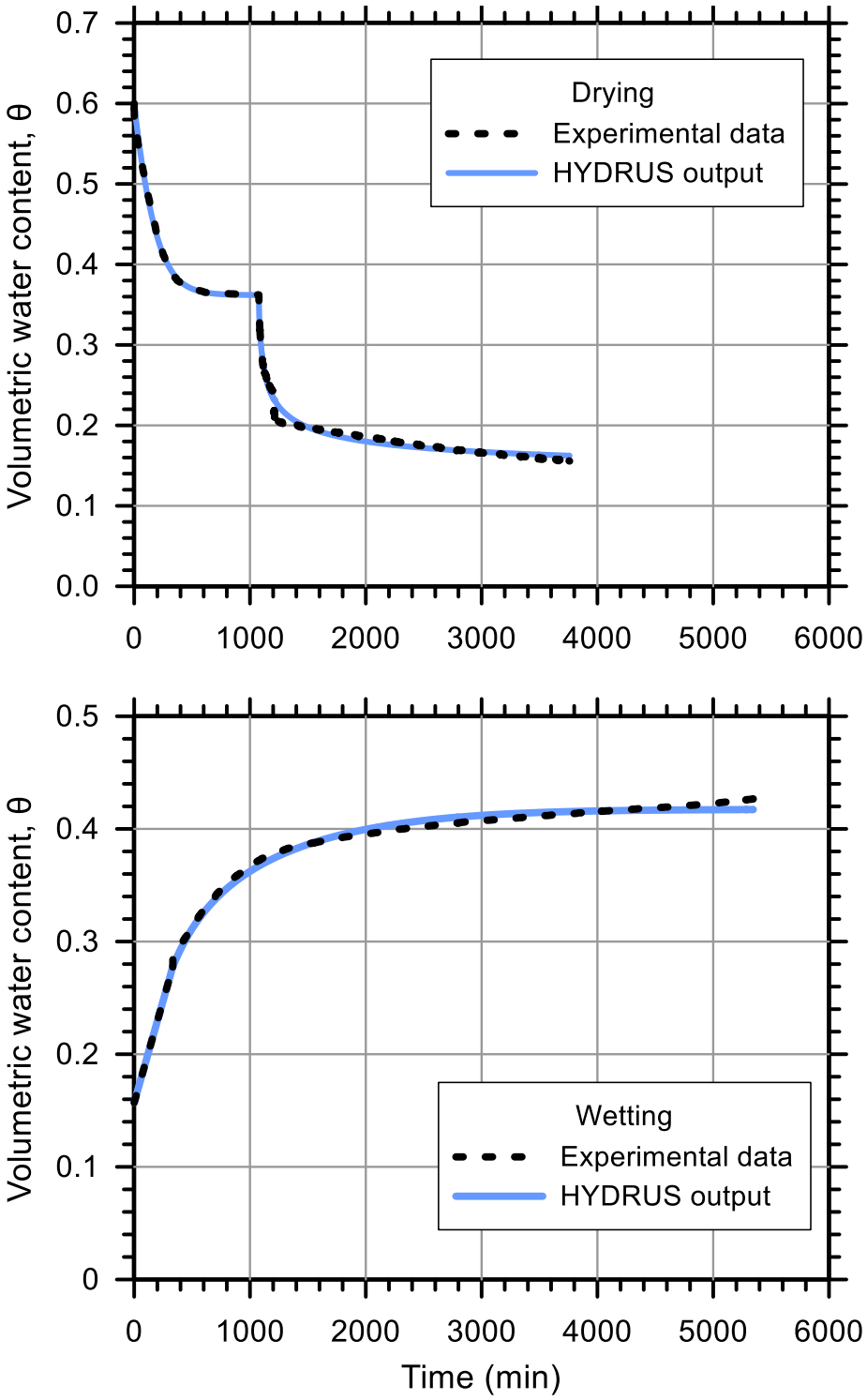
Drying
Experimental data
HYDRUS output
Volumetric water content, θ
0.7
0.6
0.5
0.4
0.3
0.2
0.1
0.0
0
1000
2000
3000
4000
5000
6000
Wetting
Experimental data
HYDRUS output
Volumetric water content, θ
0.5
0.4
0.3
0.2
0.1
0
Time (min)

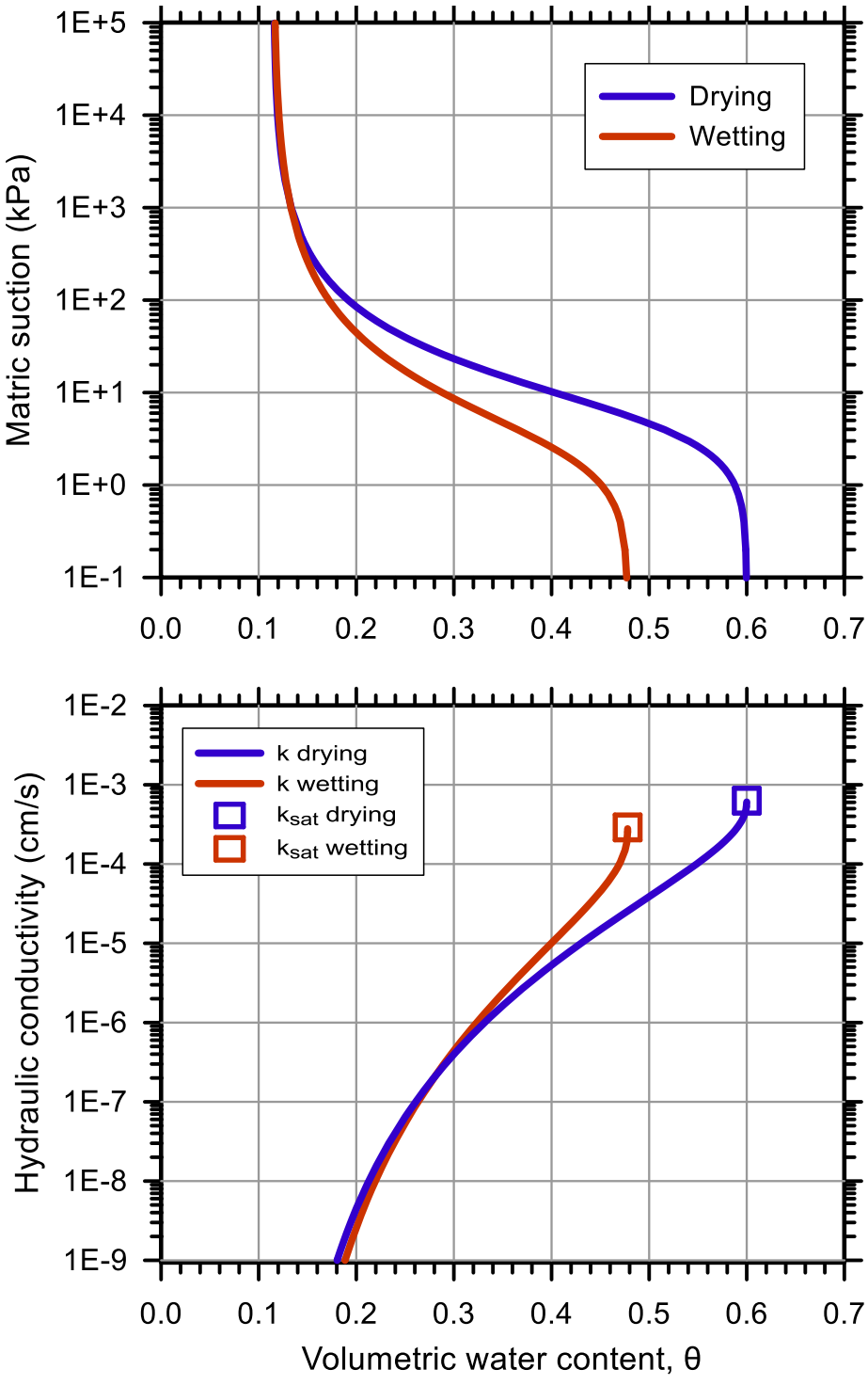
Matric suction (kPa)
1E+5
1E+4
1E+3
1E+2
1E+1
1E+0
1E-1
Drying
Wetting
0.0
0.1
0.2
0.3
0.4
0.5
0.6
0.7
Hydraulic conductivity (cm/s)
1E-2
1E-3
1E-4
1E-5
1E-6
1E-7
1E-8
1E-9
k drying
k wetting
ksat drying
ksat wetting
Volumetric water content, θ

Test No.: 8

Test Ref.: TRIMTC06

Test Soil: Tom's Creek

Molding Water Content: 15.70% (w_{opt}-2.5)

Property	Before Saturation	After Saturation
Void Ratio, e	0.582	0.630
Porosity, n (%)	36.77	38.63
Std. Proctor Relative Compaction, RC (%)	97.08	94.21
Dry Density, γ_d (g/cm^3)	1.65	1.60

Unsaturated Hydraulic Soil Parameters	Drying	Wetting
Saturated Volumetric Water Content, θ_s	0.386	0.309
Residual Volumetric Water Content, θ_r	0.125	0.125
Air-Entry Pressure Parameter, α (1/kPa)	0.140	0.252
Pore-Size Distribution Parameter, n	1.600	1.600
Saturated Hydraulic Conductivity, k_{sat} (cm/s)	7.50E-05	2.83E-05

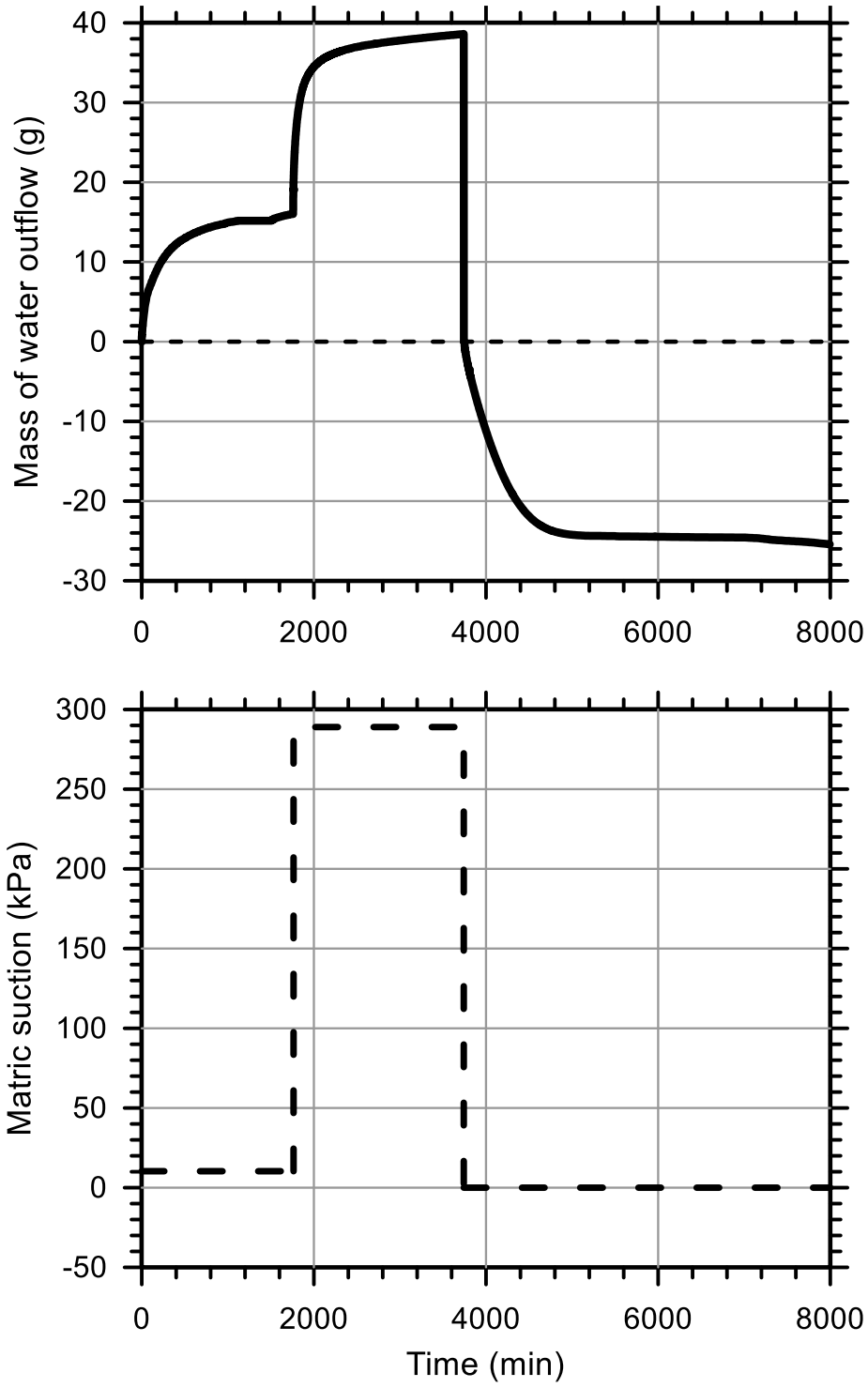
Mass of water outflow (g)
40
30
20
10
0
-10
-20
-30
0
2000
4000
6000
8000
Matric suction (kPa)
300
250
200
150
100
50
0
-50
0
2000
4000
6000
8000
Time (min)

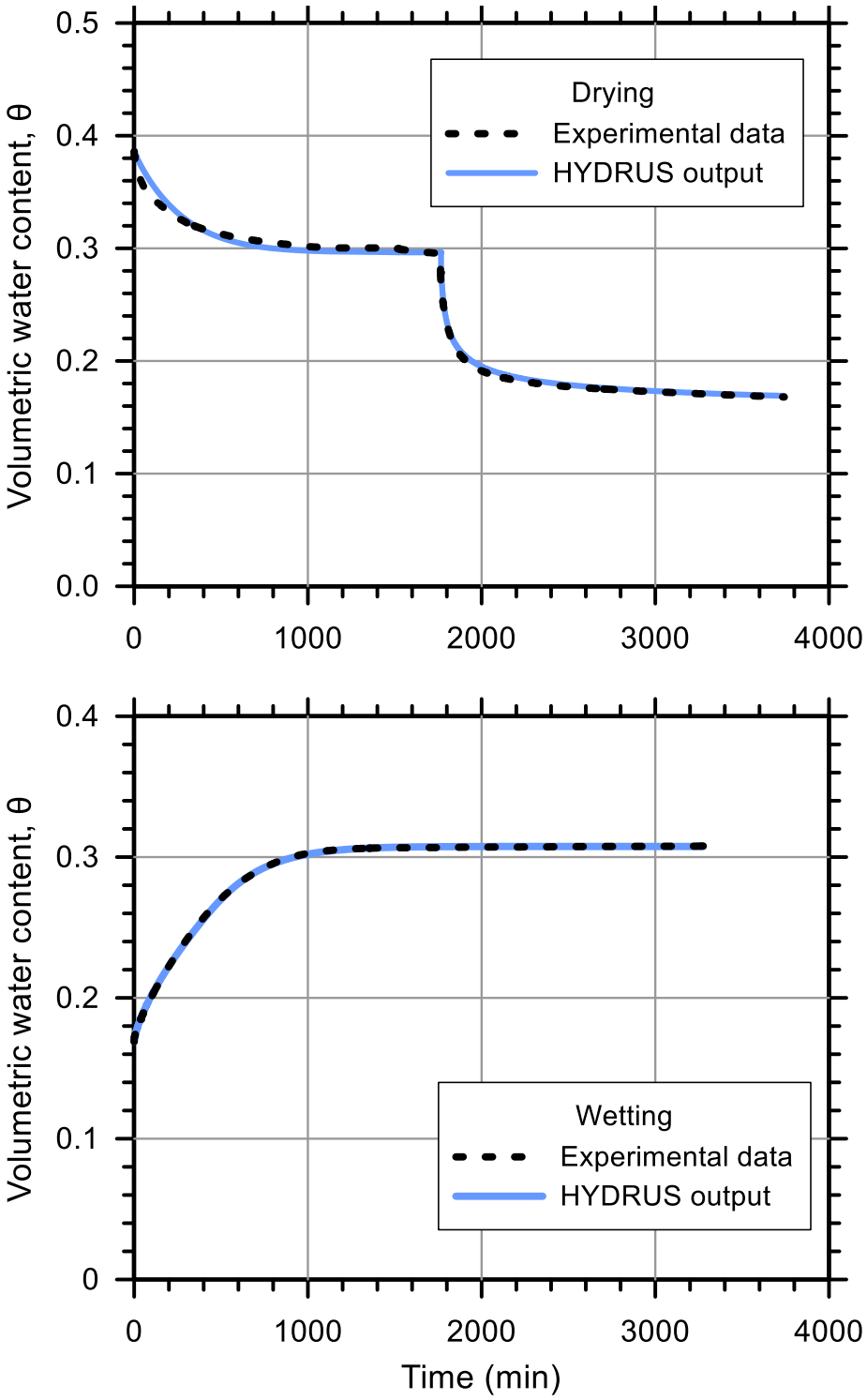
Drying
Experimental data
HYDRUS output
Volumetric water content, θ
0.5
0.4
0.3
0.2
0.1
0.0
0
1000
2000
3000
4000
Wetting
Experimental data
HYDRUS output
Volumetric water content, θ
0.4
0.3
0.2
0.1
0
0
1000
2000
3000
4000
Time (min)

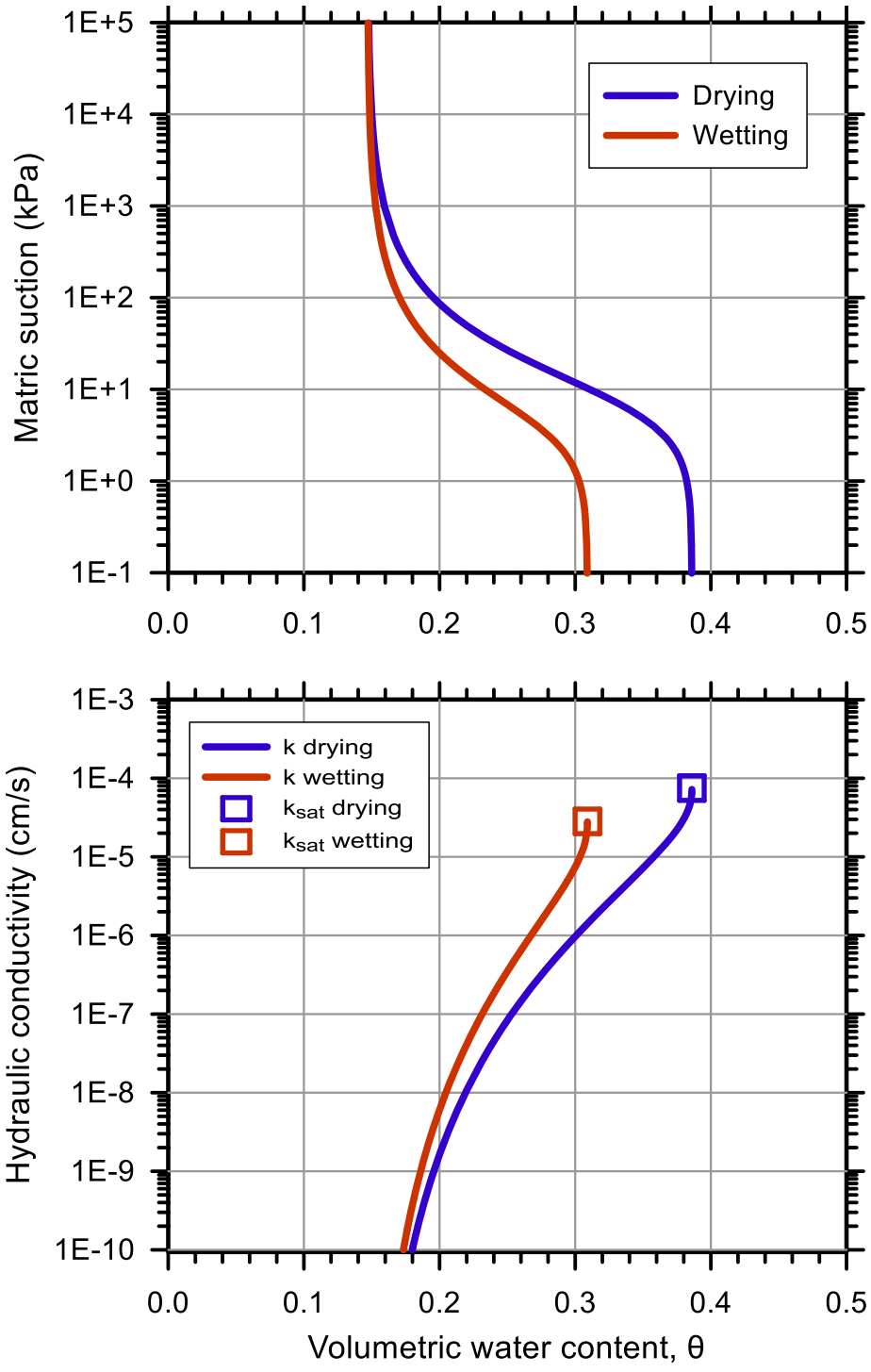
Matric suction (kPa)
1E+5
1E+4
1E+3
1E+2
1E+1
1E+0
1E-1
0.0
0.1
0.2
0.3
0.4
0.5
Drying
Wetting
Hydraulic conductivity (cm/s)
1E-3
1E-4
1E-5
1E-6
1E-7
1E-8
1E-9
1E-10
k drying
k wetting
ksat drying
ksat wetting
Volumetric water content, θ

Test No.: 17

Test Ref.: TRIMTC09

Test Soil: Tom's Creek

Molding Water Content: 15.70% (w_{opt}-2.5)

Property	Before Saturation	After Saturation
Void Ratio, e	0.715	0.736
Porosity, n (%)	41.69	42.38
Std. Proctor Relative Compaction, RC (%)	89.53	88.46
Dry Density, γ_d (g/cm^3)	1.52	1.50

Unsaturated Hydraulic Soil Parameters	Drying	Wetting
Saturated Volumetric Water Content, θ_s	0.424	0.320
Residual Volumetric Water Content, θ_r	0.120	0.120
Air-Entry Pressure Parameter, α (1/kPa)	0.154	0.173
Pore-Size Distribution Parameter, n	1.675	1.620
Saturated Hydraulic Conductivity, k_{sat} (cm/s)	2.11E-04	1.00E-04

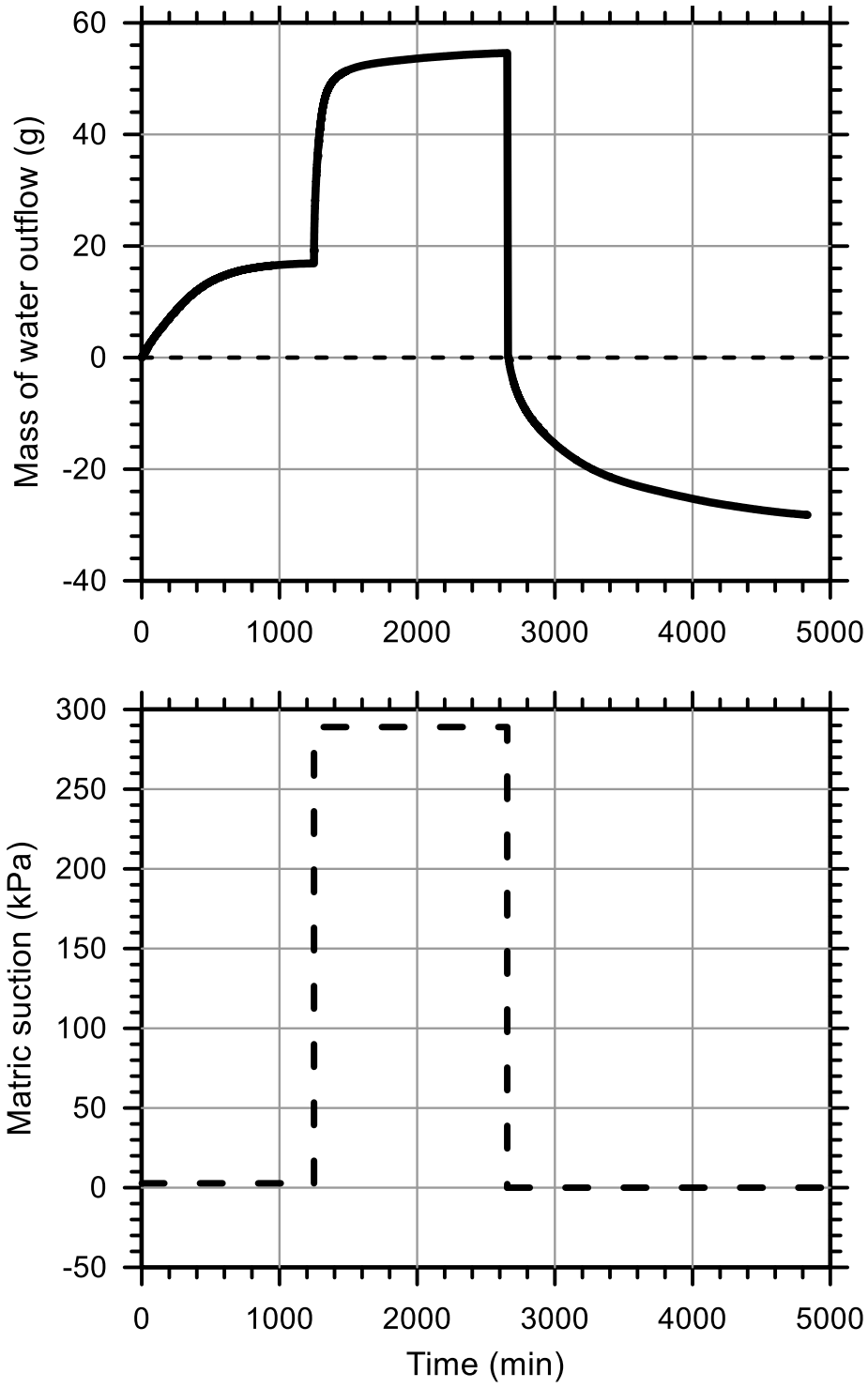
Mass of water outflow (g)
60
40
20
0
-20
-40
0
1000
2000
3000
4000
5000
Matric suction (kPa)
300
250
200
150
100
50
0
-50
0
1000
2000
3000
4000
5000
Time (min)

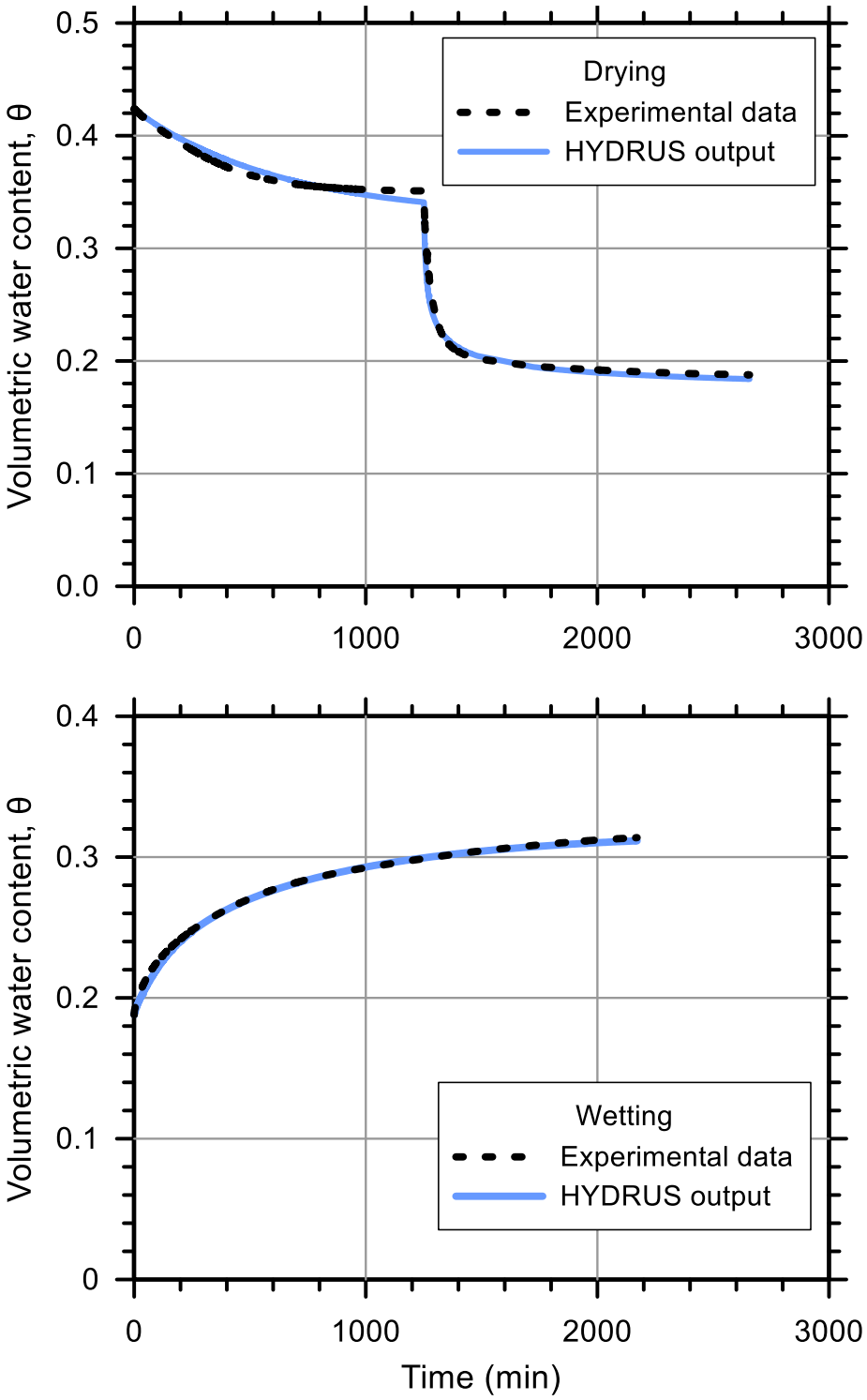
Drying
Experimental data
HYDRUS output
Volumetric water content, θ
0.5
0.4
0.3
0.2
0.1
0.0
0
1000
2000
3000
Wetting
Experimental data
HYDRUS output
Volumetric water content, θ
0.4
0.3
0.2
0.1
0
0
1000
2000
3000
Time (min)

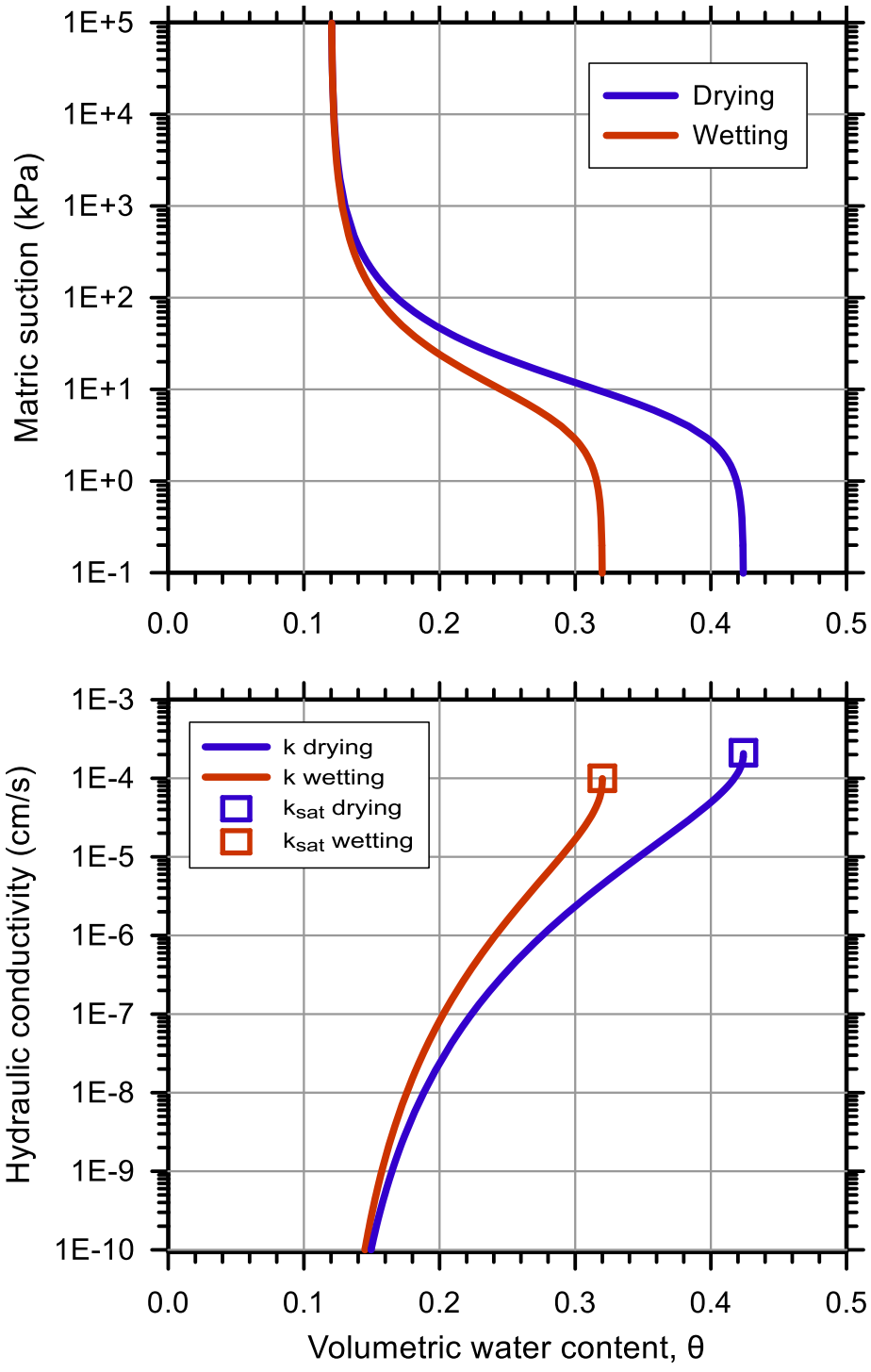
Matric suction (kPa)
1E+5
1E+4
1E+3
1E+2
1E+1
1E+0
1E-1
Drying
Wetting
0.0
0.1
0.2
0.3
0.4
0.5
Hydraulic conductivity (cm/s)
1E-3
1E-4
1E-5
1E-6
1E-7
1E-8
1E-9
1E-10
k drying
k wetting
ksat drying
ksat wetting
Volumetric water content, θ

Test No.: 13

Test Ref.: TRIMTC08

Test Soil: Tom's Creek

Molding Water Content: 15.70% (w_{opt}-2.5)

Property	Before Saturation	After Saturation
Void Ratio, e	0.715	0.736
Porosity, n (%)	41.69	42.38
Std. Proctor Relative Compaction, RC (%)	89.53	88.46
Dry Density, γ_d (g/cm^3)	1.52	1.50

Unsaturated Hydraulic Soil Parameters	Drying	Wetting
Saturated Volumetric Water Content, θ_s	0.463	0.369
Residual Volumetric Water Content, θ_r	0.115	0.115
Air-Entry Pressure Parameter, α (1/kPa)	0.390	0.805
Pore-Size Distribution Parameter, n	1.601	1.300
Saturated Hydraulic Conductivity, k_{sat} (cm/s)	6.10E-04	1.82E-04

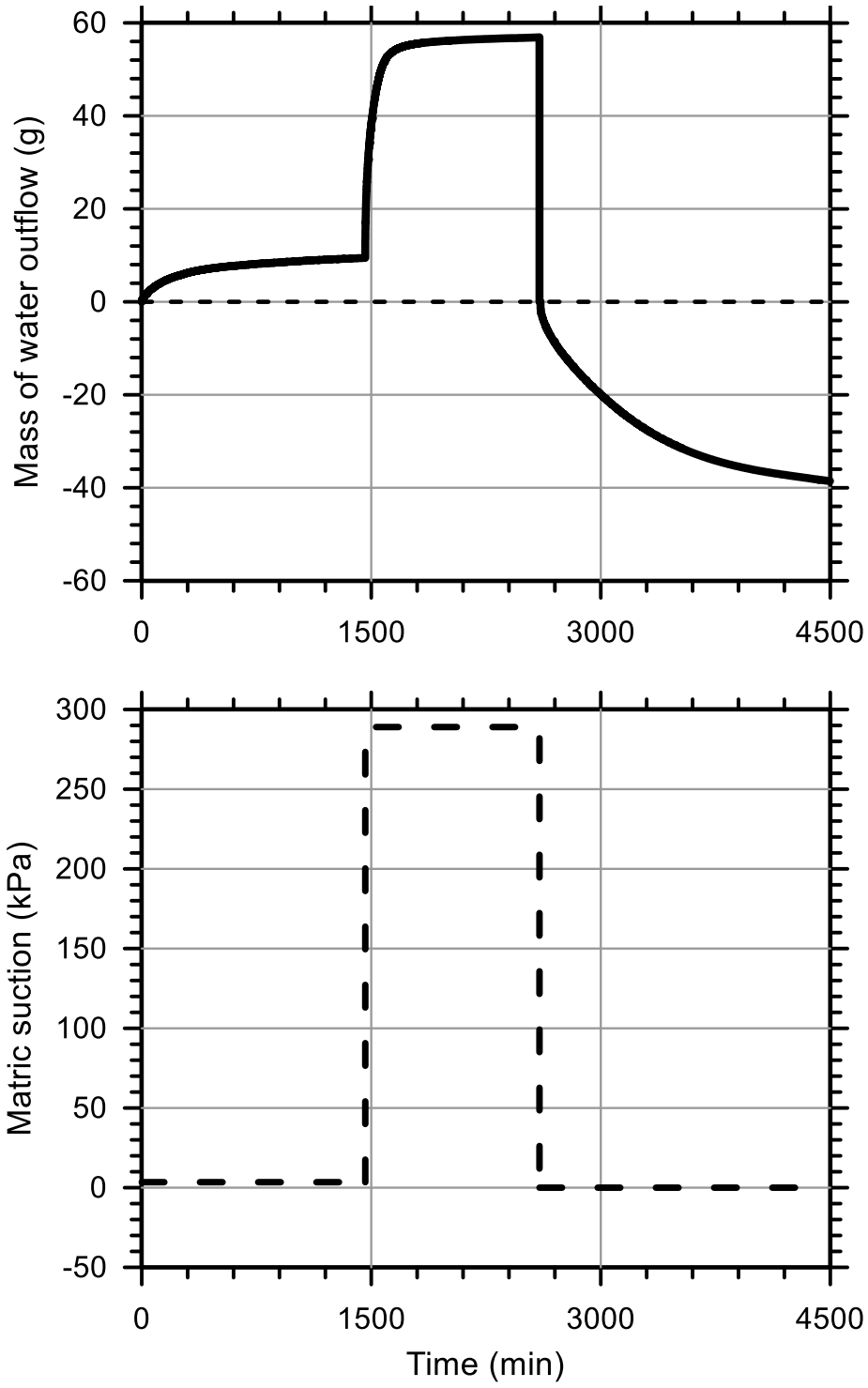
60
40
20
0
-20
-40
-60
Mass of water outflow (g)
0
1500
3000
4500
300
250
200
150
100
50
0
-50
Matric suction (kPa)
0
1500
3000
4500
Time (min)

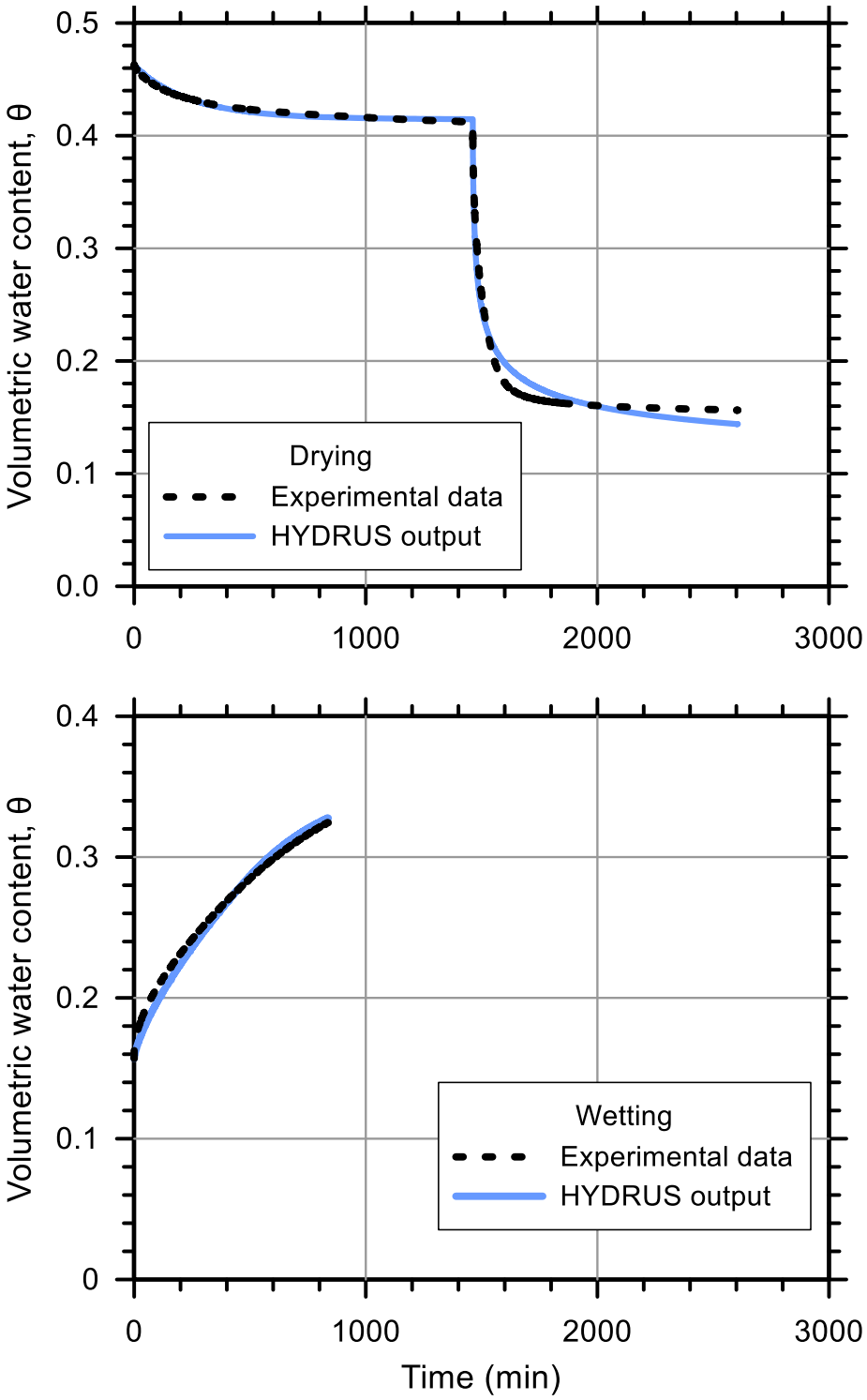
0.5
0.4
0.3
0.2
0.1
0.0
Volumetric water content, θ
Drying
Experimental data
HYDRUS output
0
1000
2000
3000
0.4
0.3
0.2
0.1
0
Volumetric water content, θ
Wetting
Experimental data
HYDRUS output
0
1000
2000
3000
Time (min)

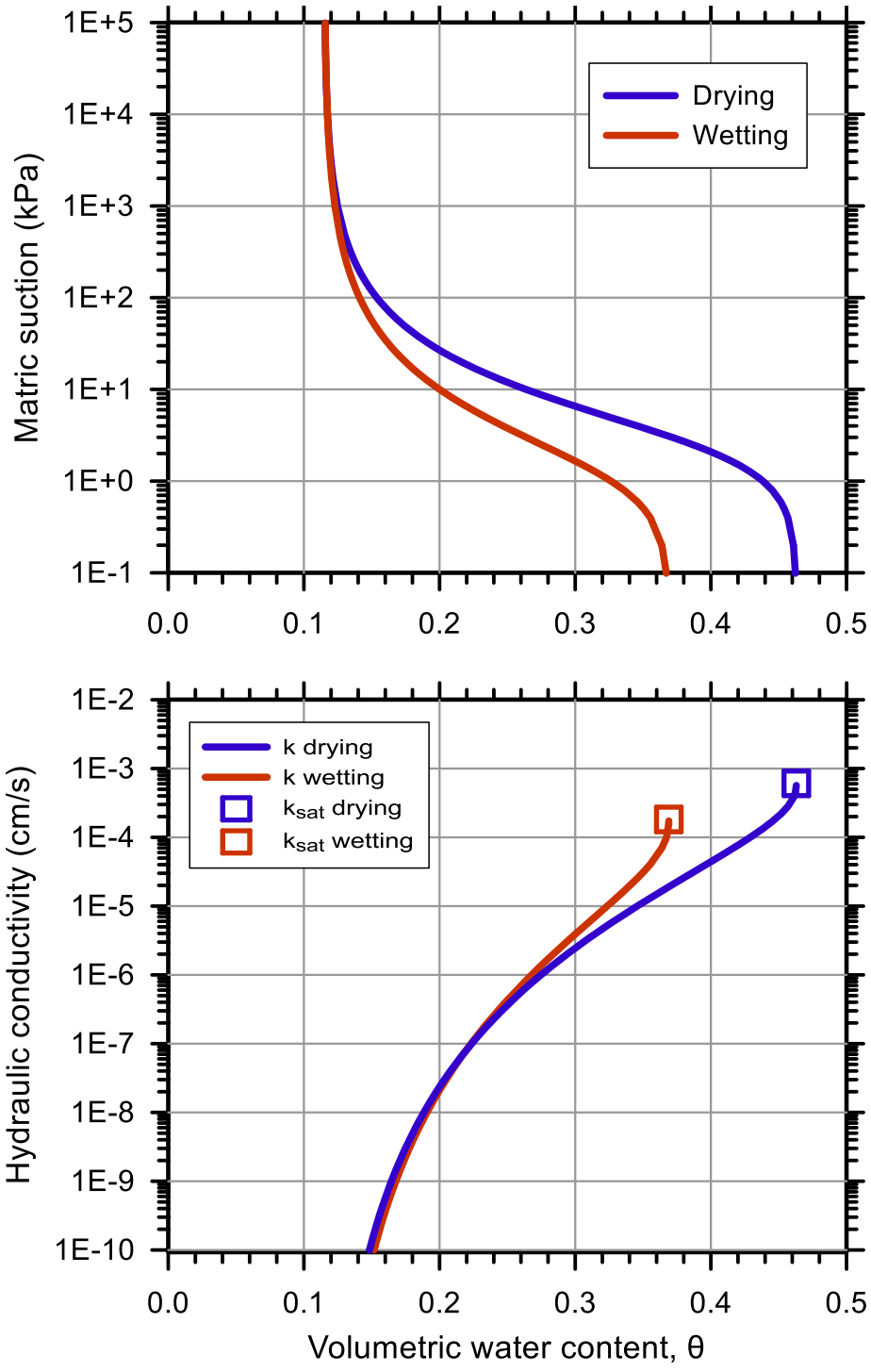
Matric suction (kPa)
1E+5
1E+4
1E+3
1E+2
1E+1
1E+0
1E-1
0.0
0.1
0.2
0.3
0.4
0.5
Drying
Wetting
Hydraulic conductivity (cm/s)
1E-2
1E-3
1E-4
1E-5
1E-6
1E-7
1E-8
1E-9
1E-10
k drying
k wetting
ksat drying
ksat wetting
Volumetric water content, θ

Test No.: 10

Test Ref.: TRIMTC07

Test Soil: Tom's Creek

Molding Water Content: 15.70% (w_{opt}+0.5)

Property	Before Saturation	After Saturation
Void Ratio, e	0.631	0.648
Porosity, n (%)	38.67	39.32
Std. Proctor Relative Compaction, RC (%)	94.16	93.16
Dry Density, γ_d (g/cm^3)	1.60	1.58

Unsaturated Hydraulic Soil Parameters	Drying	Wetting
Saturated Volumetric Water Content, θ_s	0.393	0.325
Residual Volumetric Water Content, θ_r	0.133	0.133
Air-Entry Pressure Parameter, α (1/kPa)	0.347	0.408
Pore-Size Distribution Parameter, n	1.580	1.520
Saturated Hydraulic Conductivity, k_{sat} (cm/s)	6.82E-05	3.96E-05

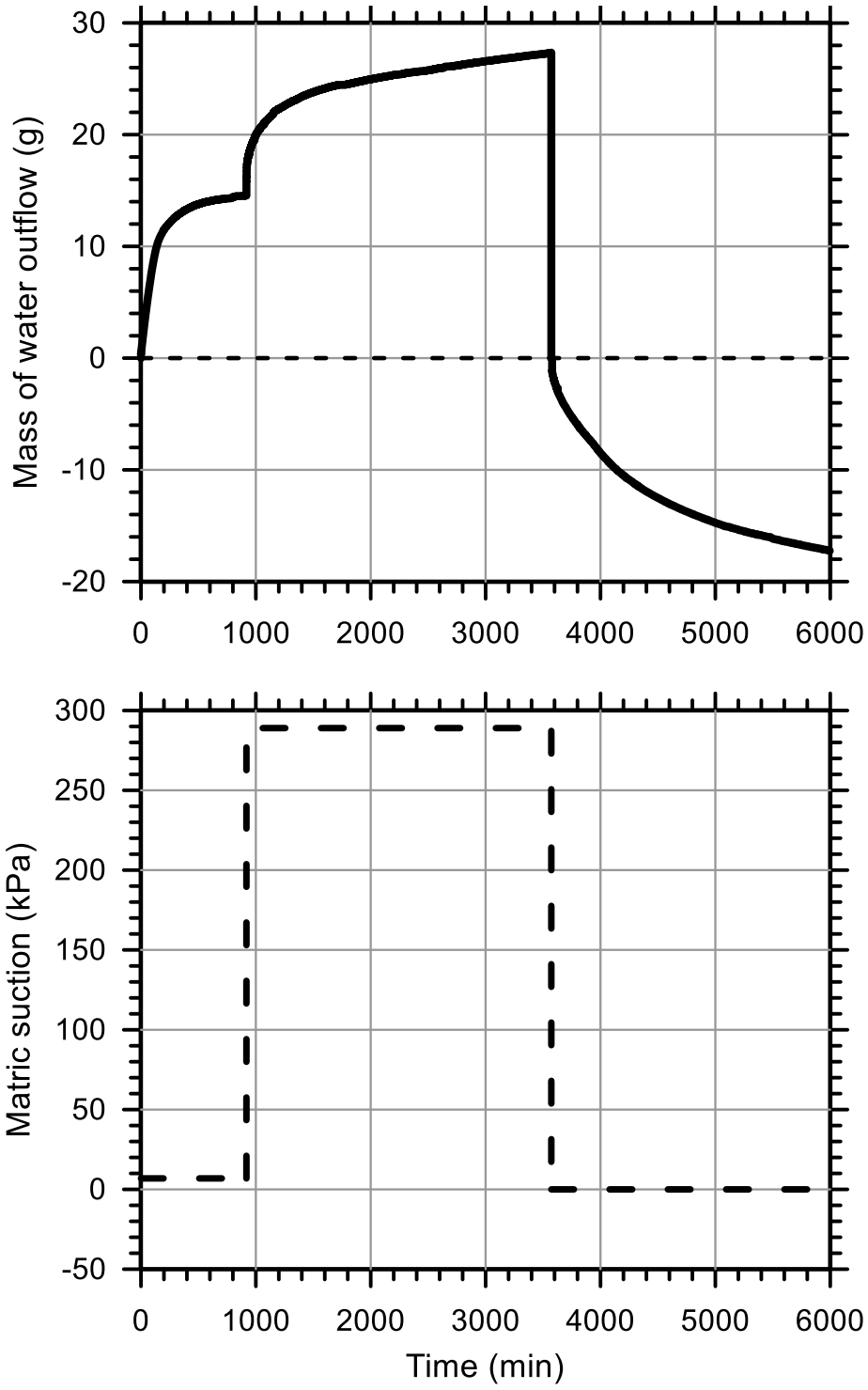
Mass of water outflow (g)
30
20
10
0
-10
-20
0
1000
2000
3000
4000
5000
6000
Matric suction (kPa)
300
250
200
150
100
50
0
-50
0
1000
2000
3000
4000
5000
6000
Time (min)

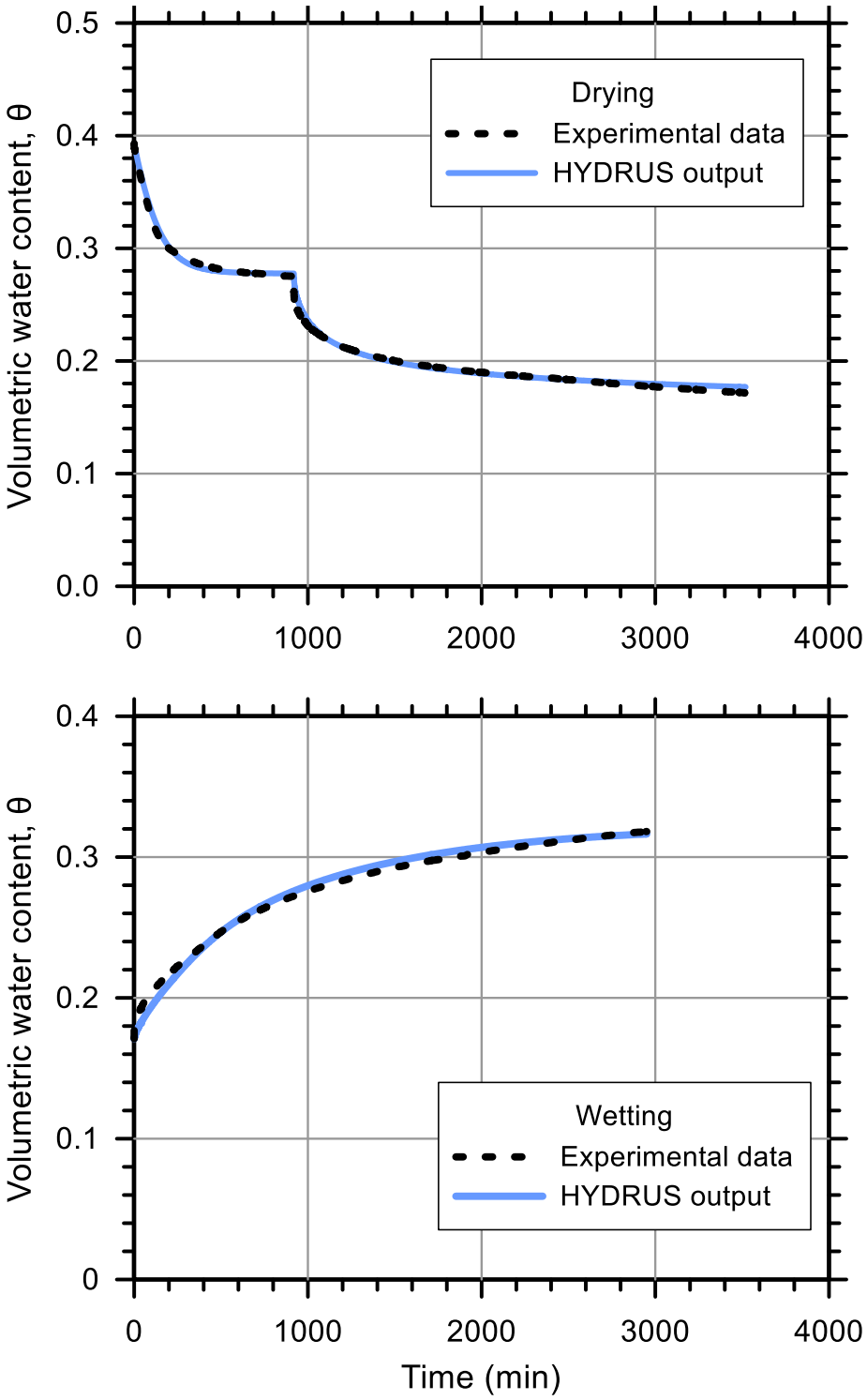
Drying
Experimental data
HYDRUS output
Volumetric water content, θ
0.5
0.4
0.3
0.2
0.1
0.0
0
1000
2000
3000
4000
Wetting
Experimental data
HYDRUS output
Volumetric water content, θ
0.4
0.3
0.2
0.1
0
0
1000
2000
3000
4000
Time (min)

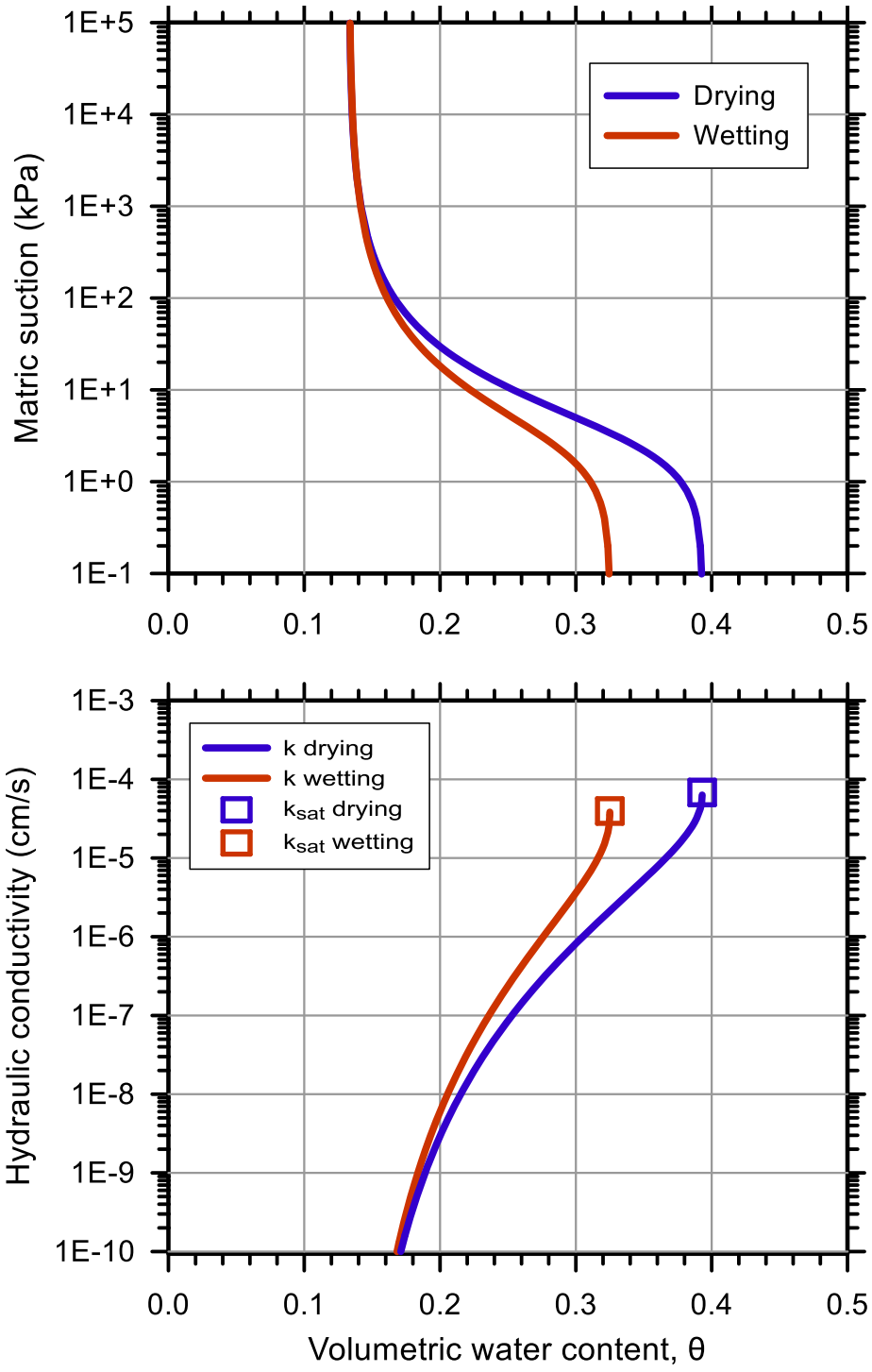
Matric suction (kPa)
1E+5
1E+4
1E+3
1E+2
1E+1
1E+0
1E-1
Drying
Wetting
0.0
0.1
0.2
0.3
0.4
0.5
Hydraulic conductivity (cm/s)
1E-3
1E-4
1E-5
1E-6
1E-7
1E-8
1E-9
1E-10
k drying
k wetting
ksat drying
ksat wetting
Volumetric water content, θ

Test No.: 22

Test Ref.: TRIMTC10

Test Soil: Tom's Creek

Molding Water Content: 18.70% (w_{opt}+0.5)

Property	Before Saturation	After Saturation
Void Ratio, e	0.707	0.694
Porosity, n (%)	41.43	40.97
Std. Proctor Relative Compaction, RC (%)	89.92	90.63
Dry Density, γ_d (g/cm^3)	1.53	1.54

Unsaturated Hydraulic Soil Parameters	Drying	Wetting
Saturated Volumetric Water Content, θ_s	0.410	0.325
Residual Volumetric Water Content, θ_r	0.125	0.125
Air-Entry Pressure Parameter, α (1/kPa)	0.487	0.560
Pore-Size Distribution Parameter, n	1.619	1.500
Saturated Hydraulic Conductivity, k_{sat} (cm/s)	1.09E-04	8.27E-05

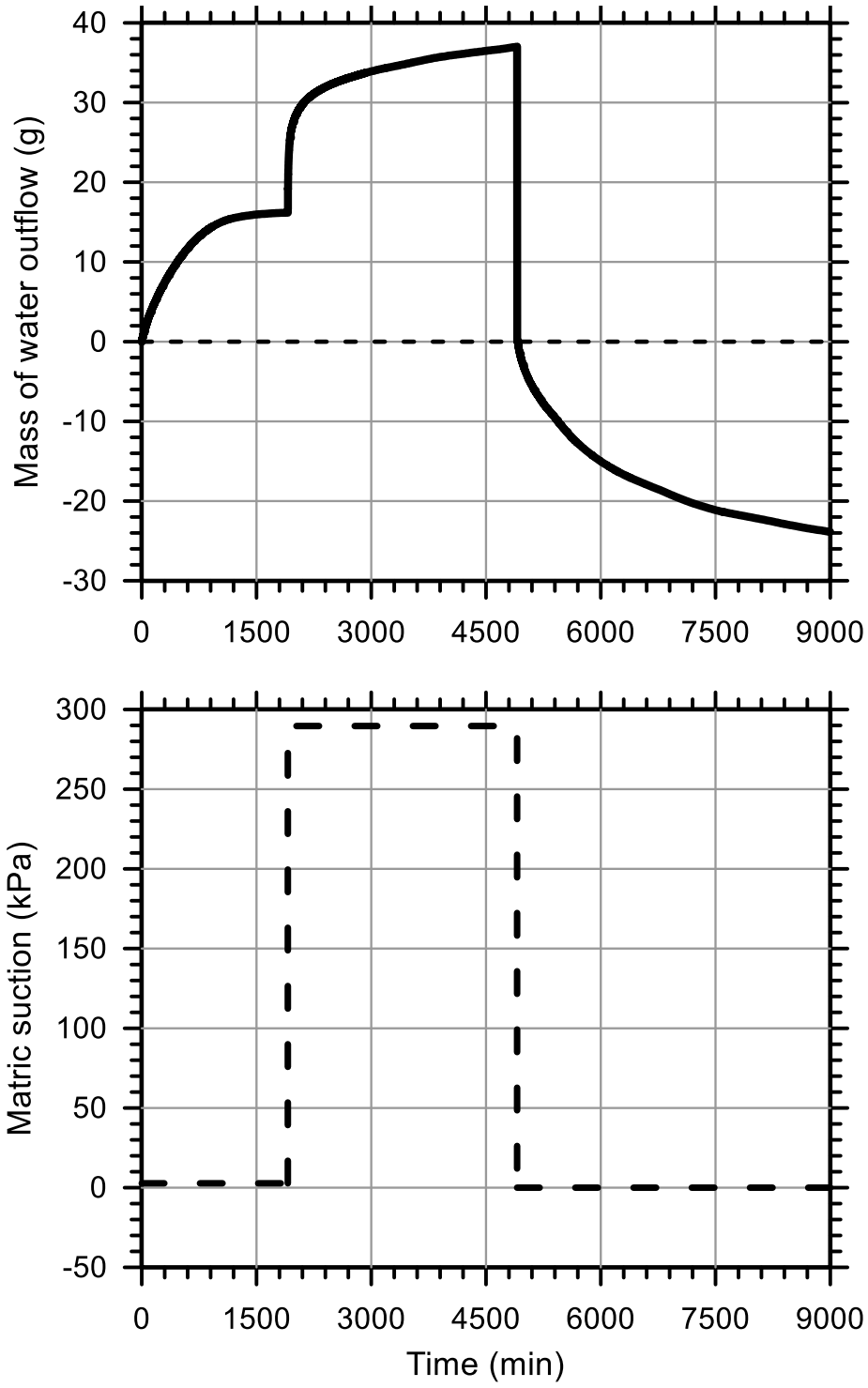
Mass of water outflow (g)
40
30
20
10
0
-10
-20
-30
0
1500
3000
4500
6000
7500
9000
Matric suction (kPa)
300
250
200
150
100
50
0
-50
0
1500
3000
4500
6000
7500
9000
Time (min)

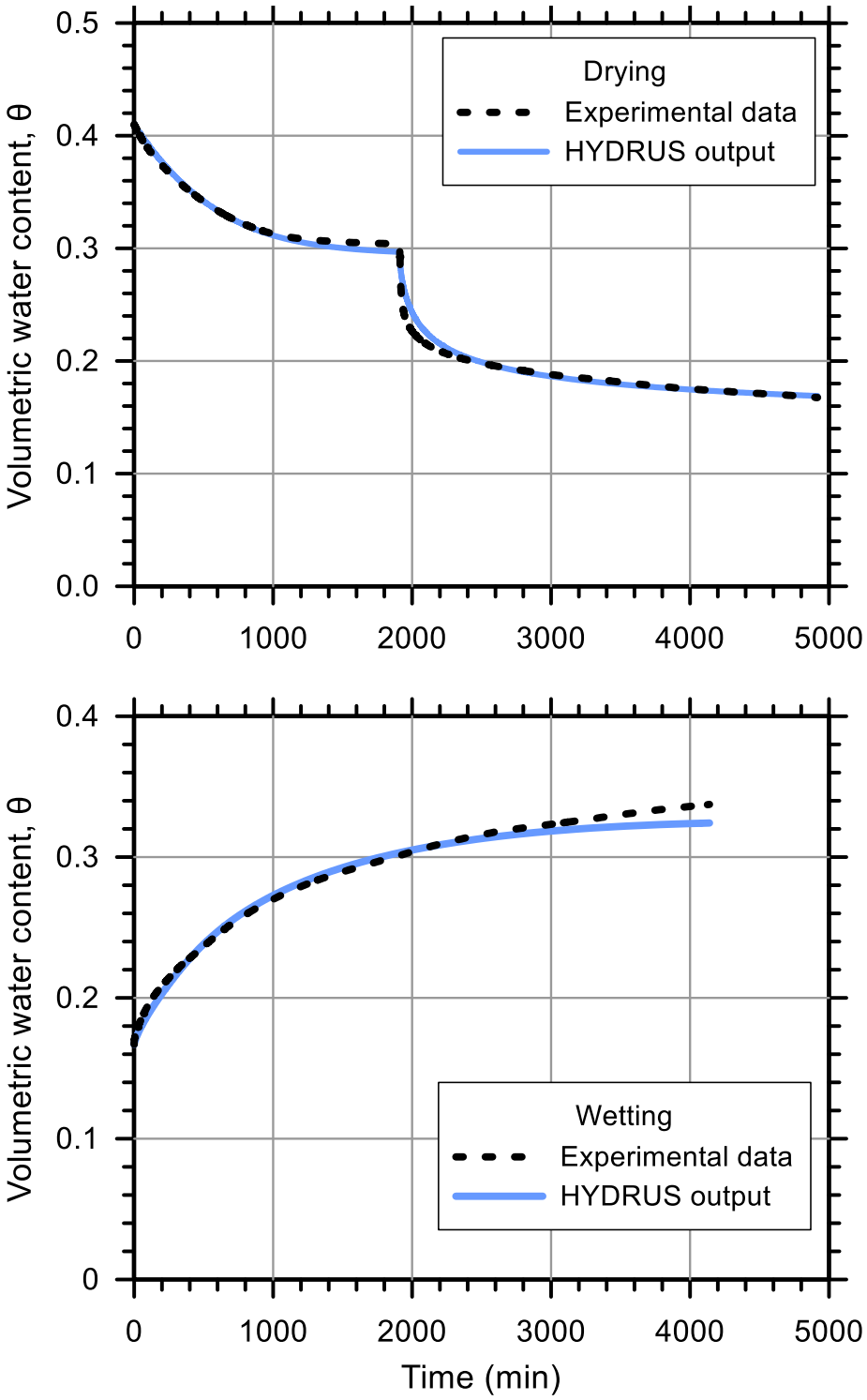
Drying
Experimental data
HYDRUS output
Volumetric water content, θ
0.5
0.4
0.3
0.2
0.1
0.0
0
1000
2000
3000
4000
5000
Wetting
Experimental data
HYDRUS output
Volumetric water content, θ
0.4
0.3
0.2
0.1
0
0
1000
2000
3000
4000
5000
Time (min)

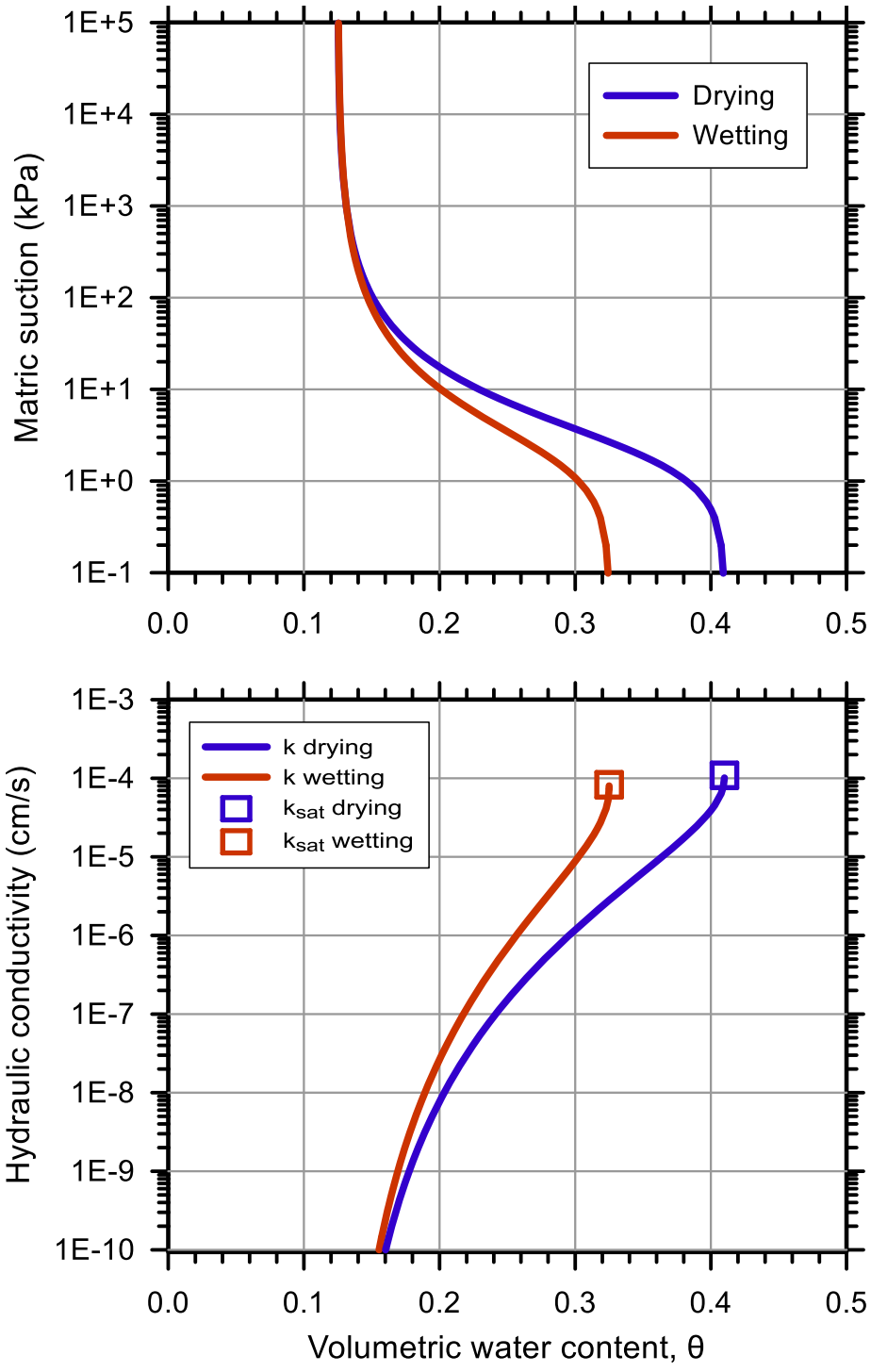
Matric suction (kPa)
1E+5
1E+4
1E+3
1E+2
1E+1
1E+0
1E-1
Drying
Wetting
0.0
0.1
0.2
0.3
0.4
0.5
Hydraulic conductivity (cm/s)
1E-3
1E-4
1E-5
1E-6
1E-7
1E-8
1E-9
1E-10
k drying
k wetting
ksat drying
ksat wetting
Volumetric water content, θ

Test No.: 24

Test Ref.: TRIMTC11

Test Soil: Tom's Creek

Molding Water Content: 18.70% (w_{opt}+0.5)

Property	Before Saturation	After Saturation
Void Ratio, e	0.864	0.858
Porosity, n (%)	46.36	46.18
Std. Proctor Relative Compaction, RC (%)	82.36	82.63
Dry Density, γ_d (g/cm^3)	1.40	1.40

Unsaturated Hydraulic Soil Parameters	Drying	Wetting
Saturated Volumetric Water Content, θ_s	0.462	0.375
Residual Volumetric Water Content, θ_r	0.118	0.118
Air-Entry Pressure Parameter, α (1/kPa)	0.510	0.703
Pore-Size Distribution Parameter, n	1.789	1.528
Saturated Hydraulic Conductivity, k_{sat} (cm/s)	6.21E-04	3.32E-04

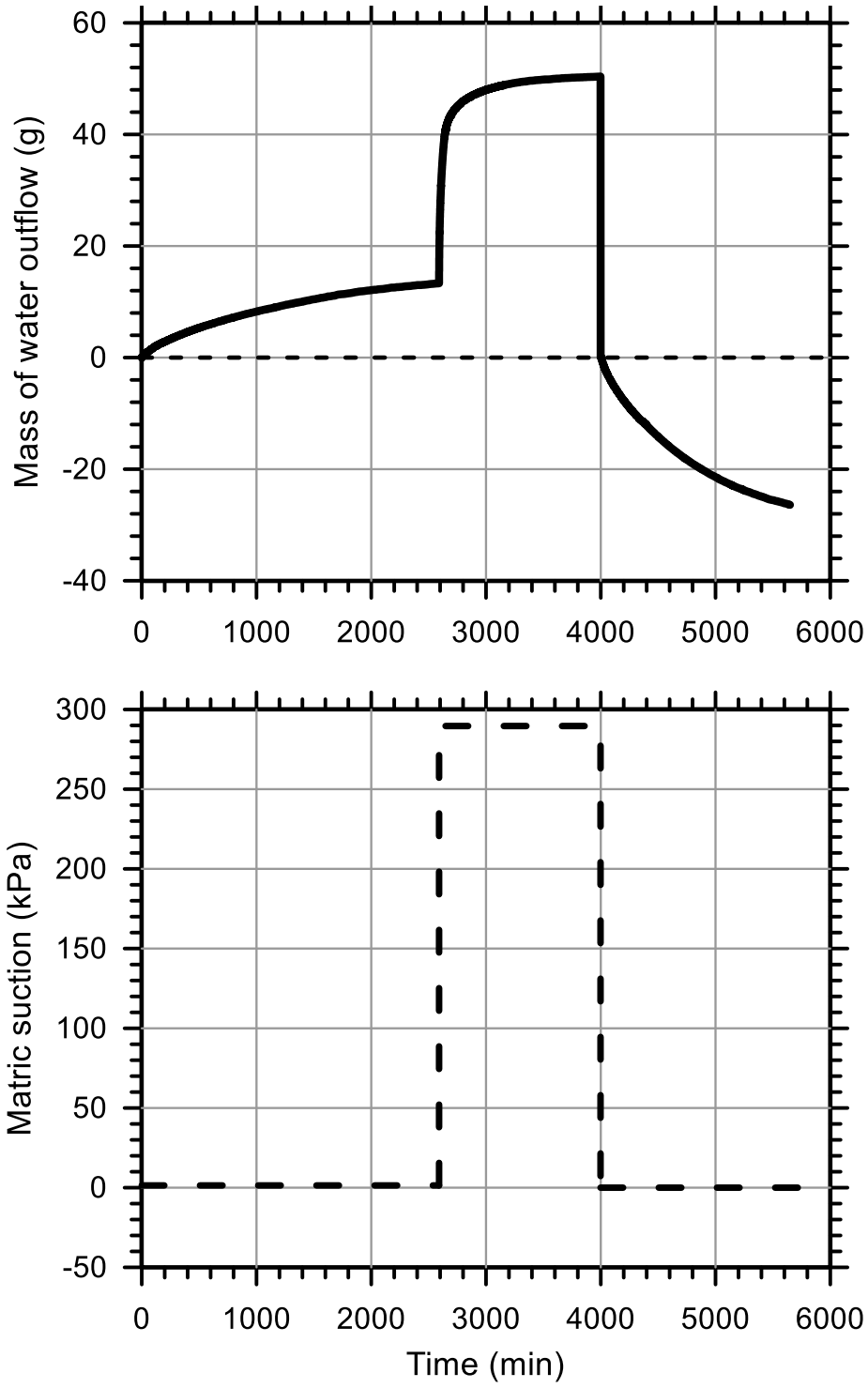
Mass of water outflow (g)
60
40
20
0
-20
-40
0
1000
2000
3000
4000
5000
6000
Matric suction (kPa)
300
250
200
150
100
50
0
-50
0
1000
2000
3000
4000
5000
6000
Time (min)

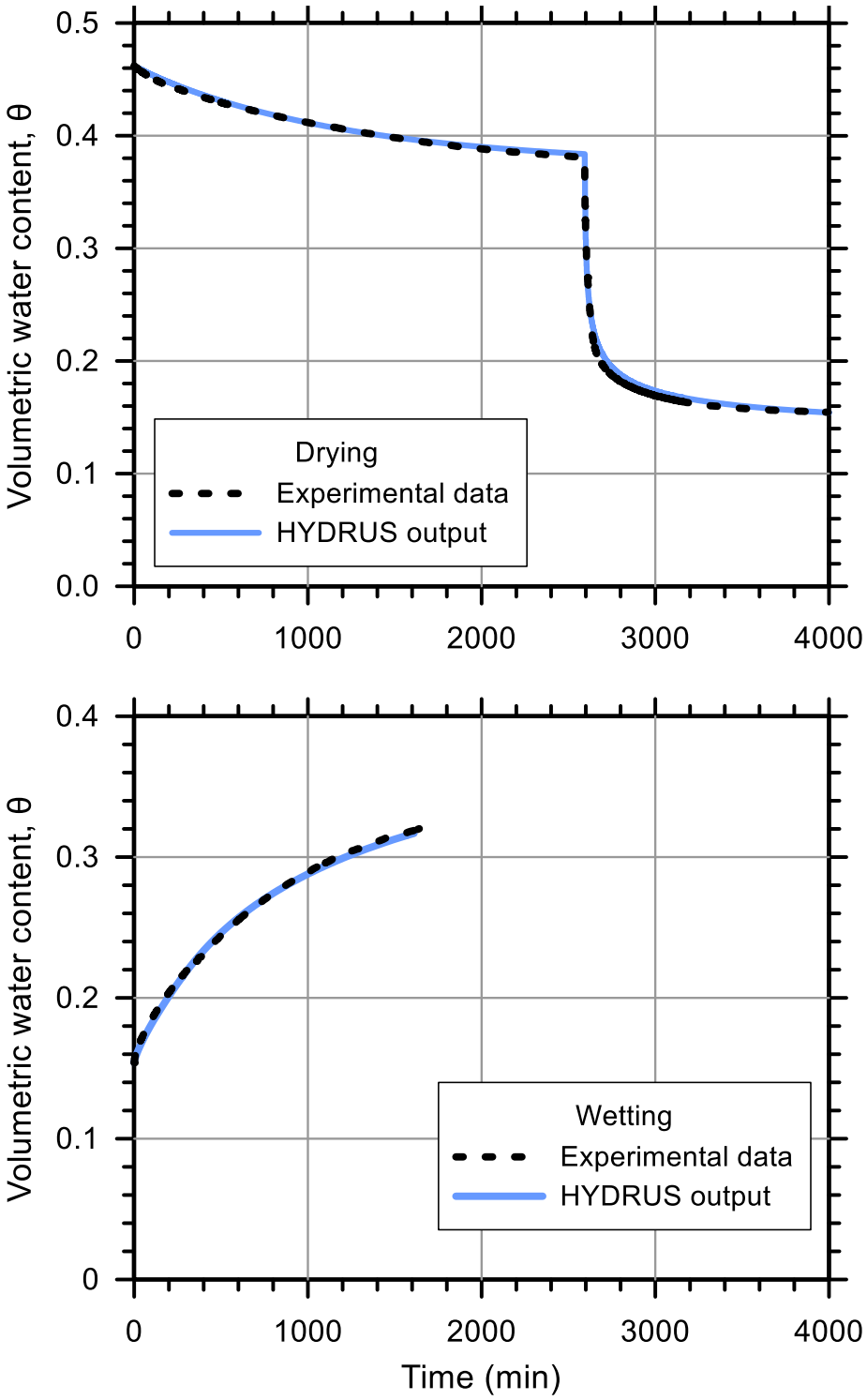
0.5
0.4
0.3
0.2
0.1
0.0
Volumetric water content, θ
Drying
Experimental data
HYDRUS output
0
1000
2000
3000
4000
0.4
0.3
0.2
0.1
0
Volumetric water content, θ
Wetting
Experimental data
HYDRUS output
0
1000
2000
3000
4000
Time (min)

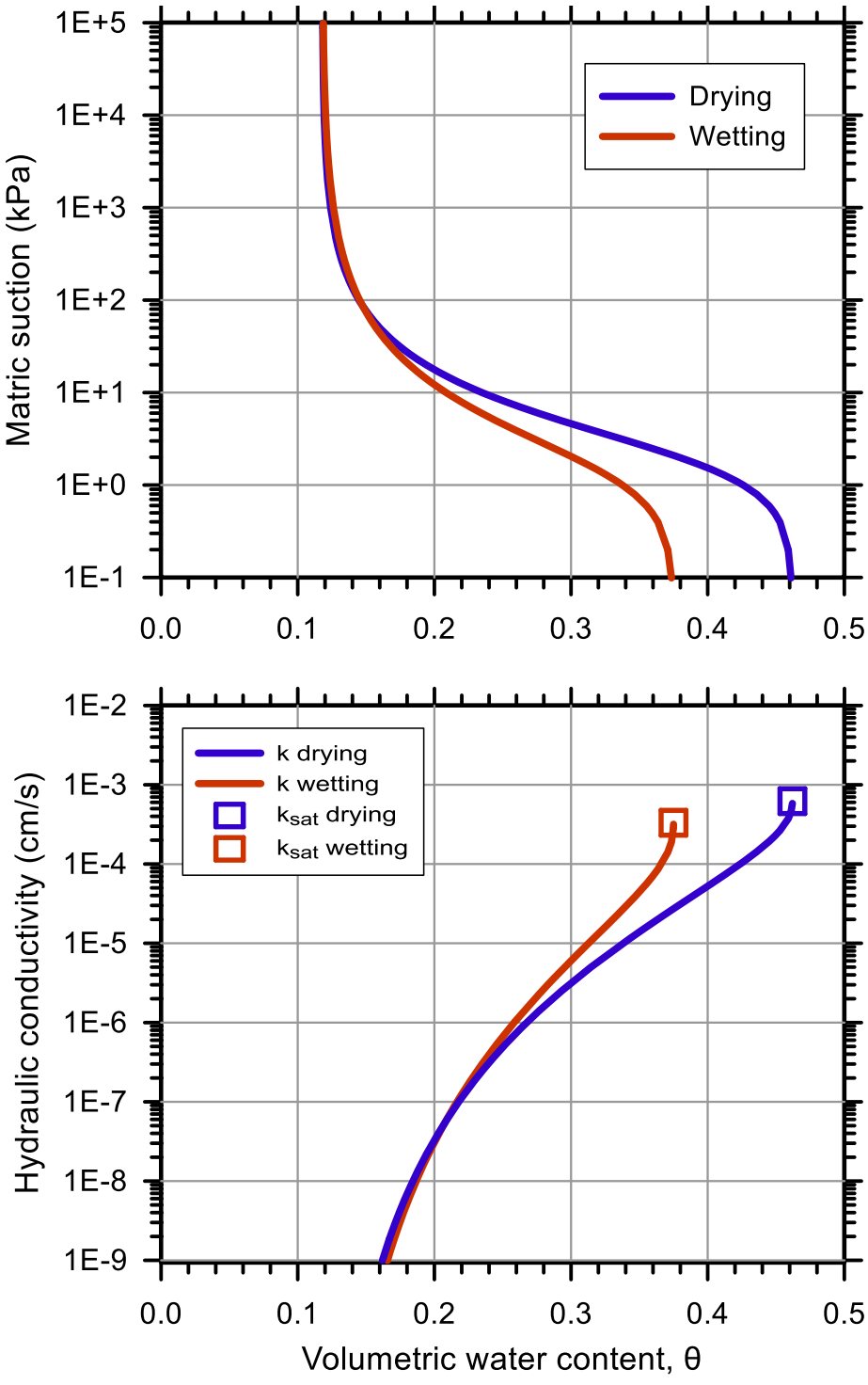
Matric suction (kPa)
1E+5
1E+4
1E+3
1E+2
1E+1
1E+0
1E-1
0.0
0.1
0.2
0.3
0.4
0.5
Drying
Wetting
Hydraulic conductivity (cm/s)
1E-2
1E-3
1E-4
1E-5
1E-6
1E-7
1E-8
1E-9
k drying
k wetting
ksat drying
ksat wetting
Volumetric water content, θ

Test No.: 20

Test Ref.: TRIMM7X03

Test Soil: Sand-Clay (75%-25%)

Molding Water Content: 8.40% (w_{opt}-2)

Property	Before Saturation	After Saturation
Void Ratio, e	0.404	0.399
Porosity, n (%)	28.76	28.51
Std. Proctor Relative Compaction, RC (%)	94.30	94.64
Dry Density, γ_d (g/cm^3)	1.89	1.89

Unsaturated Hydraulic Soil Parameters	Drying	Wetting
Saturated Volumetric Water Content, θ_s	0.285	0.210
Residual Volumetric Water Content, θ_r	0.137	0.137
Air-Entry Pressure Parameter, α (1/kPa)	0.231	0.316
Pore-Size Distribution Parameter, n	1.921	1.883
Saturated Hydraulic Conductivity, k_{sat} (cm/s)	2.18E-04	5.84E-05

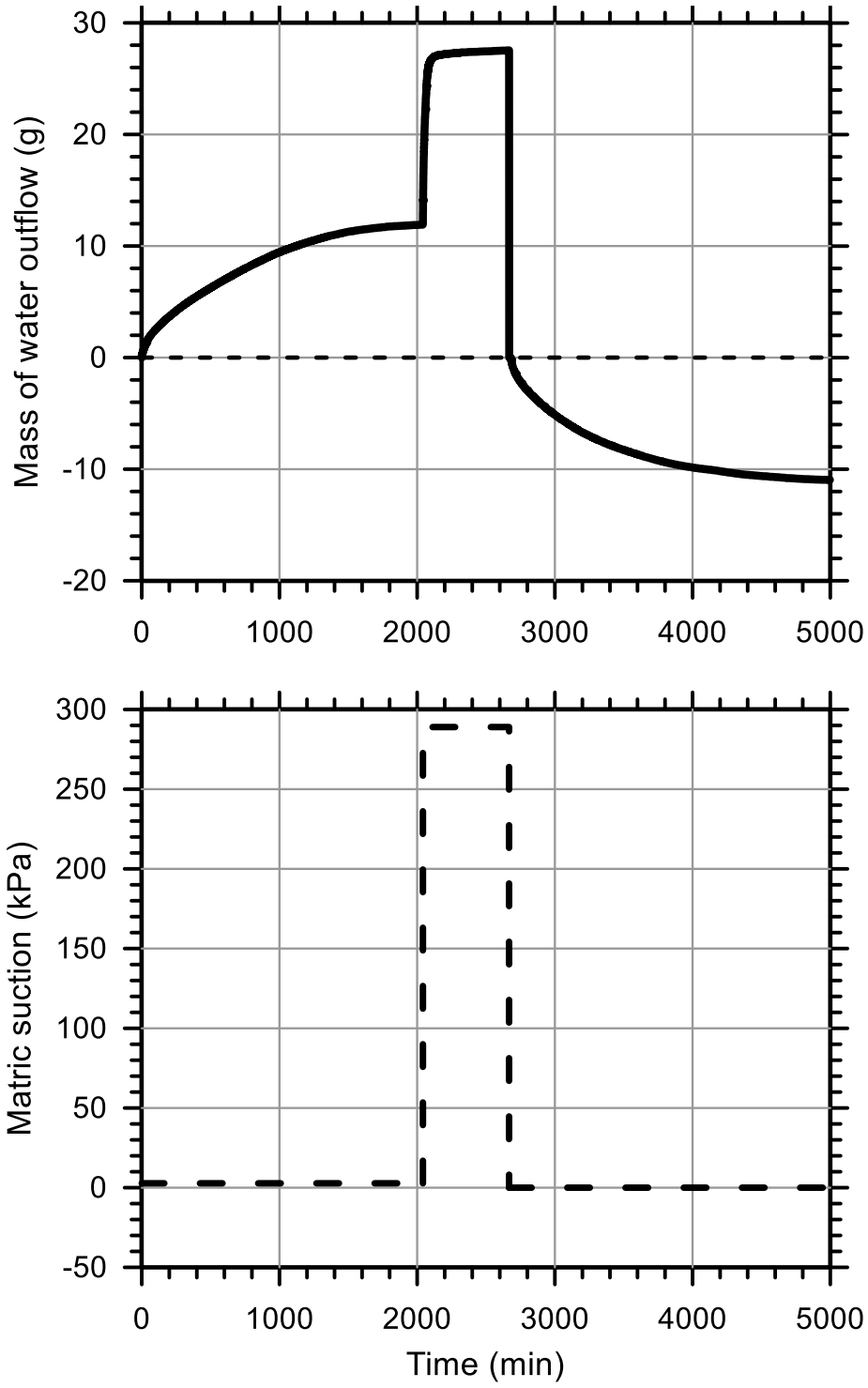
Mass of water outflow (g)
30
20
10
0
-10
-20
0
1000
2000
3000
4000
5000
Matric suction (kPa)
300
250
200
150
100
50
0
-50
0
1000
2000
3000
4000
5000
Time (min)

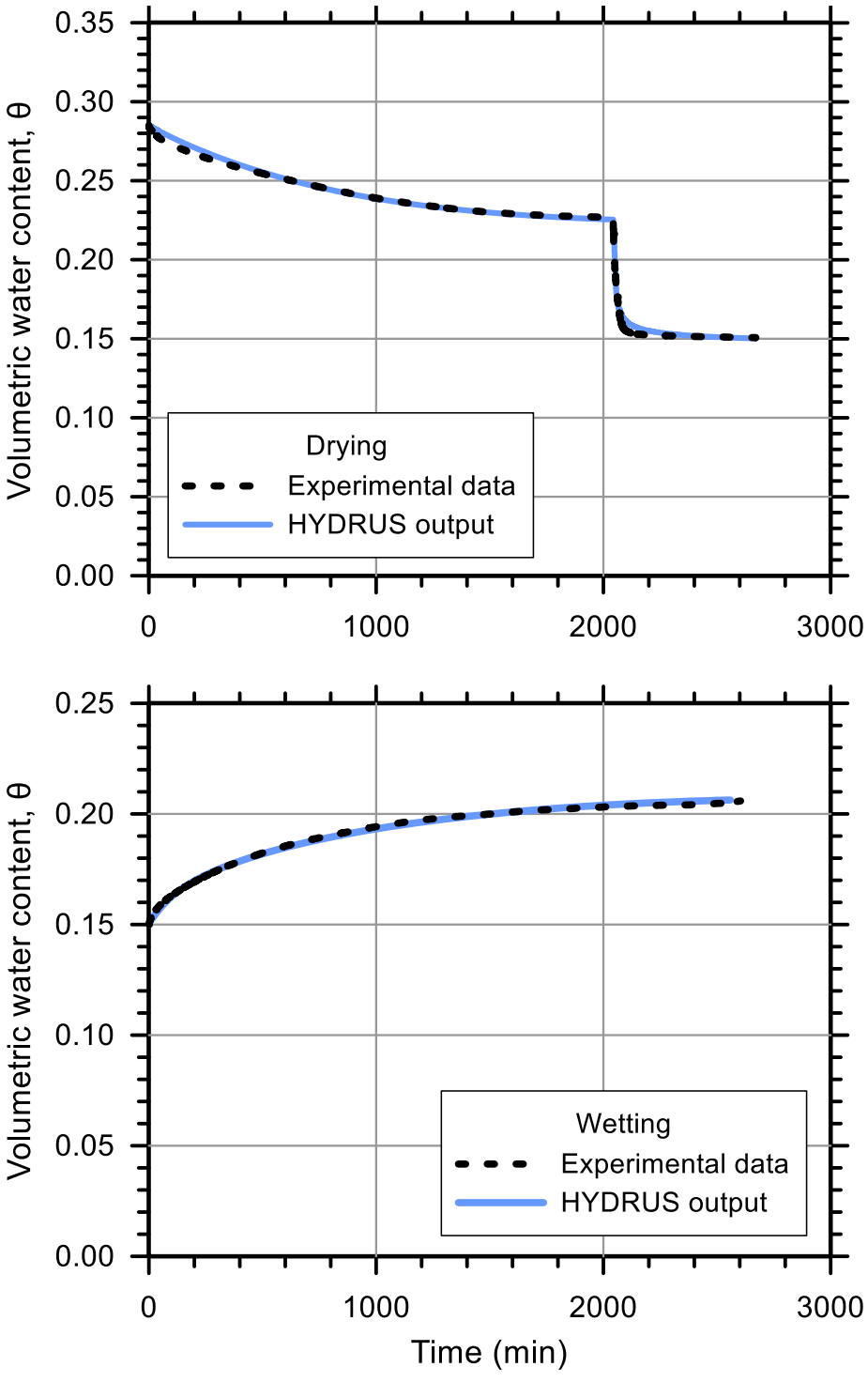
0.35
0.30
0.25
0.20
0.15
0.10
0.05
0.00
Volumetric water content, θ
Drying
Experimental data
HYDRUS output
0
1000
2000
3000
0.25
0.20
0.15
0.10
0.05
0.00
Volumetric water content, θ
Wetting
Experimental data
HYDRUS output
0
1000
2000
3000
Time (min)

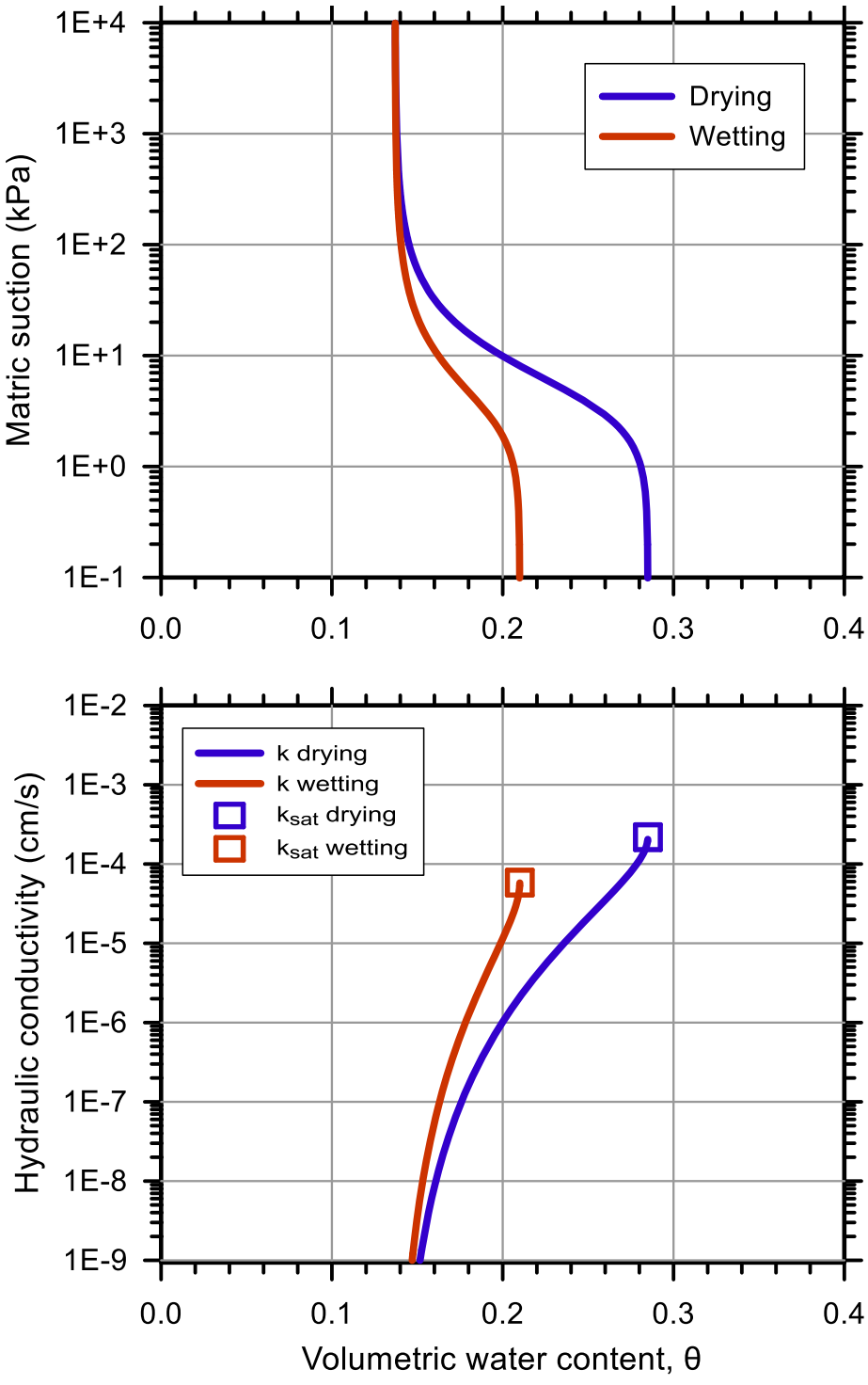
1E+4
1E+3
1E+2
1E+1
1E+0
1E-1
Matric suction (kPa)
Drying
Wetting
0.0
0.1
0.2
0.3
0.4
1E-2
1E-3
1E-4
1E-5
1E-6
1E-7
1E-8
1E-9
Hydraulic conductivity (cm/s)
k drying
k wetting
ksat drying
ksat wetting
0.0
0.1
0.2
0.3
0.4
Volumetric water content, θ

Test No.: 12

Test Ref.: TRIMM7X01

Test Soil: Sand-Clay (75%-25%)

Molding Water Content: 8.40% (w_{opt}-2)

Property	Before Saturation	After Saturation
Void Ratio, e	0.484	0.456
Porosity, n (%)	32.60	31.30
Std. Proctor Relative Compaction, RC (%)	89.22	90.94
Dry Density, γ_d (g/cm^3)	1.79	1.82

Unsaturated Hydraulic Soil Parameters	Drying	Wetting
Saturated Volumetric Water Content, θ_s	0.313	0.243
Residual Volumetric Water Content, θ_r	0.108	0.108
Air-Entry Pressure Parameter, α (1/kPa)	0.430	0.724
Pore-Size Distribution Parameter, n	2.200	2.000
Saturated Hydraulic Conductivity, k_{sat} (cm/s)	4.00E-04	6.88E-05

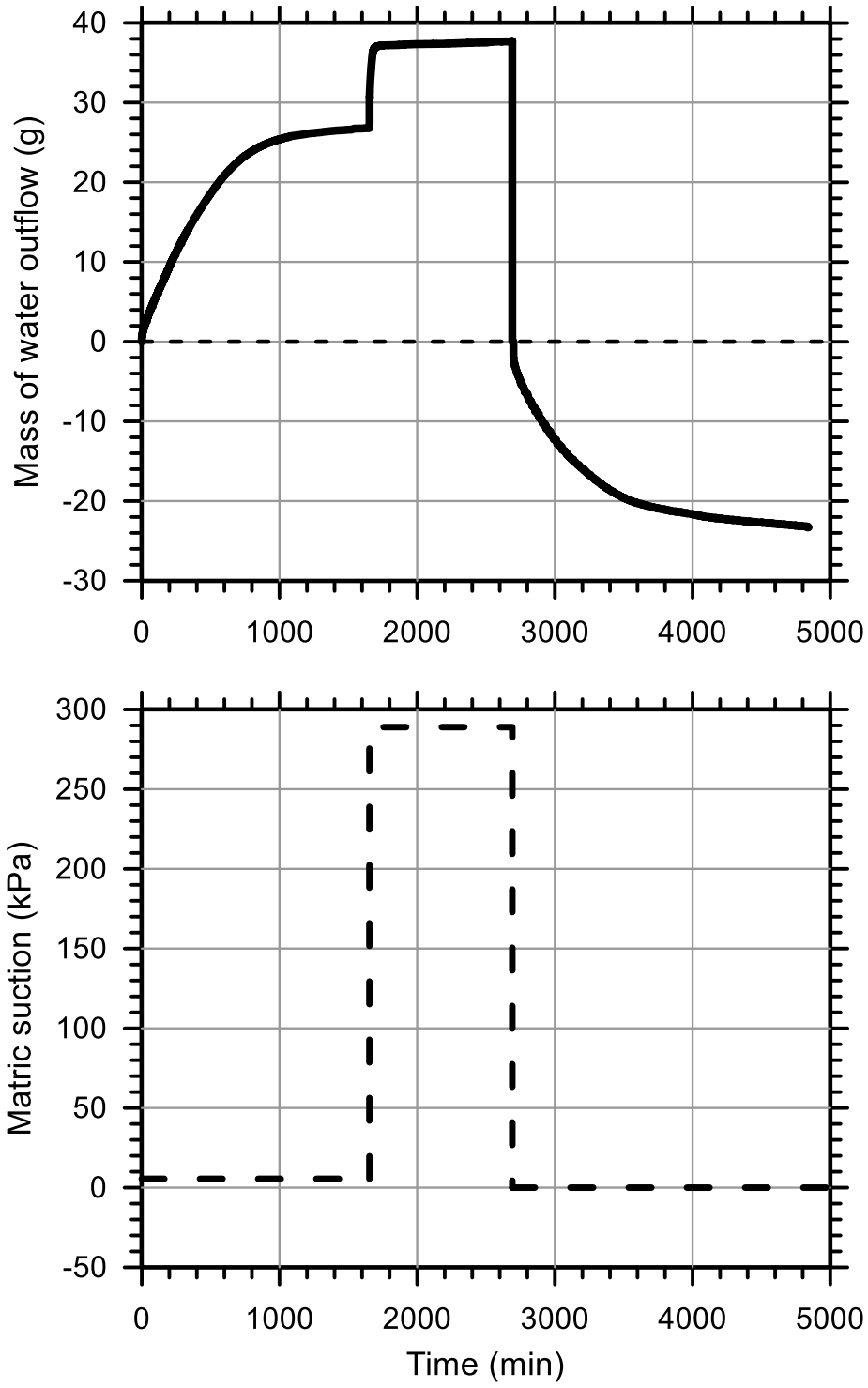
Mass of water outflow (g)
40
30
20
10
0
-10
-20
-30
0
1000
2000
3000
4000
5000
Matric suction (kPa)
300
250
200
150
100
50
0
-50
0
1000
2000
3000
4000
5000
Time (min)

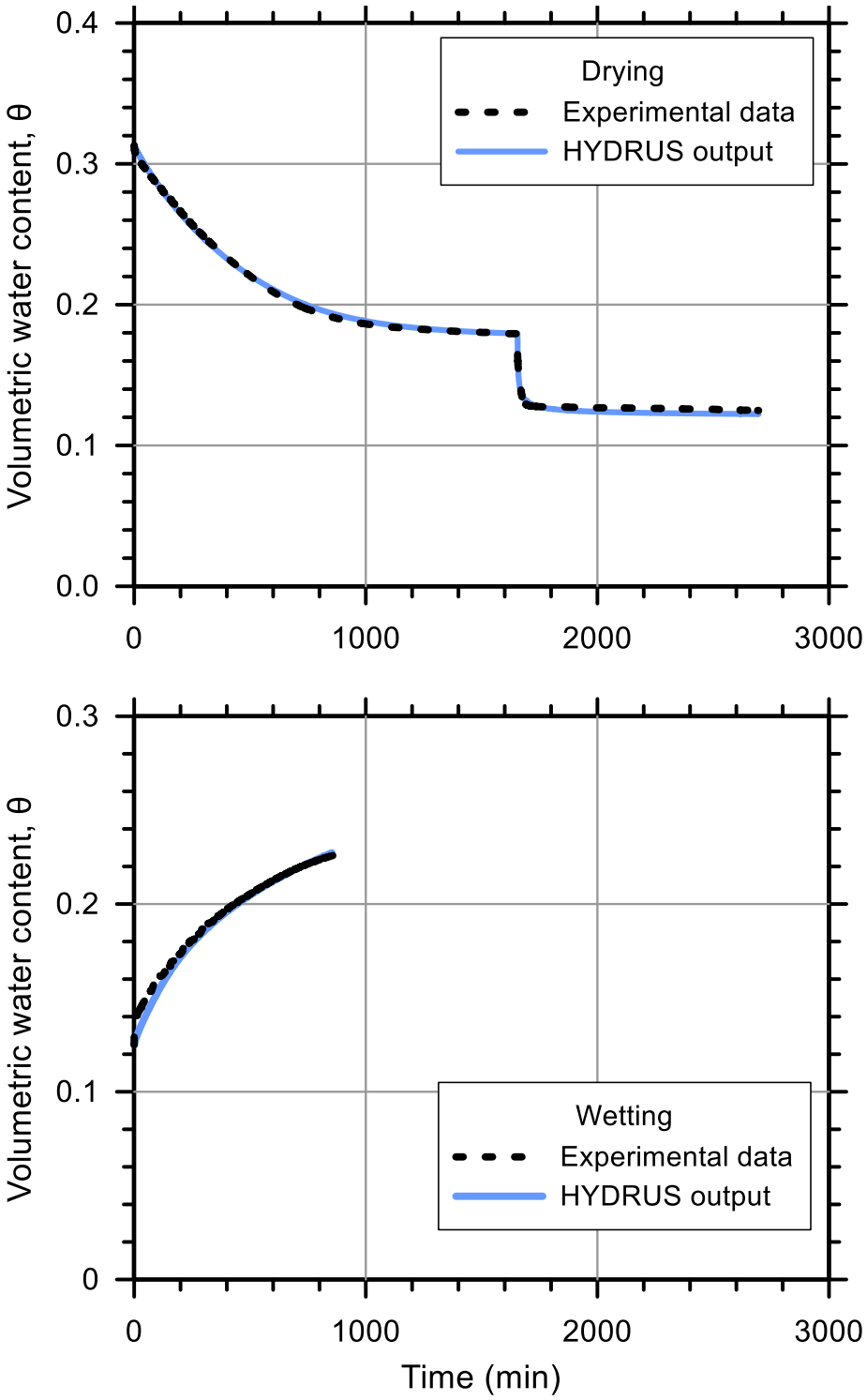
Drying
Experimental data
HYDRUS output
Volumetric water content, θ
0.4
0.3
0.2
0.1
0.0
0
1000
2000
3000
Wetting
Experimental data
HYDRUS output
Volumetric water content, θ
0.3
0.2
0.1
0
0
1000
2000
3000
Time (min)

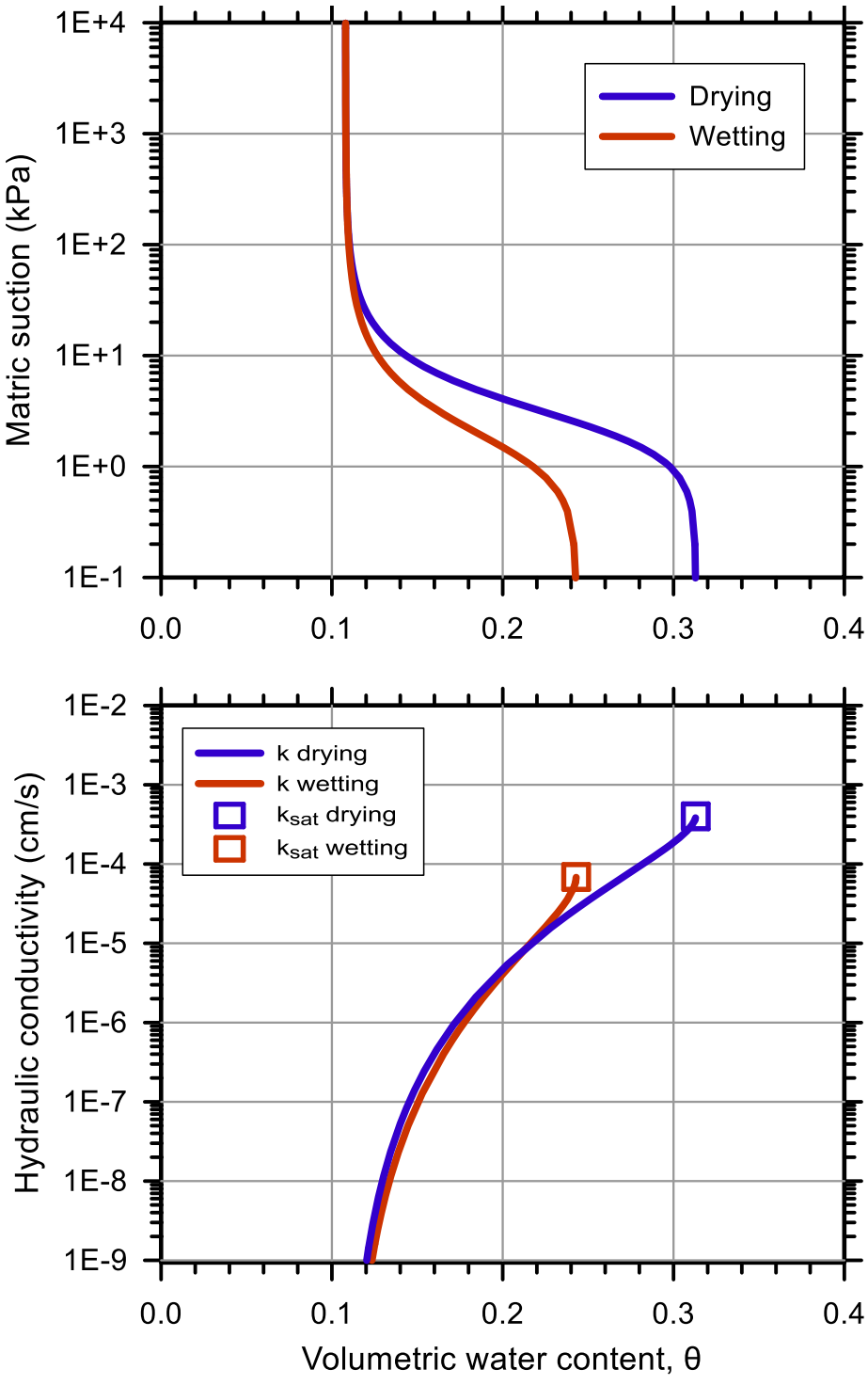
1E+4
1E+3
1E+2
1E+1
1E+0
1E-1
Matric suction (kPa)
Drying
Wetting
0.0
0.1
0.2
0.3
0.4
1E-2
1E-3
1E-4
1E-5
1E-6
1E-7
1E-8
1E-9
Hydraulic conductivity (cm/s)
k drying
k wetting
ksat drying
ksat wetting
0.0
0.1
0.2
0.3
0.4
Volumetric water content, θ

Test No.: 25

Test Ref.: TRIMM7X05

Test Soil: Sand-Clay (75%-25%)

Molding Water Content: 9.90% (w_{opt}-0.5)

Property	Before Saturation	After Saturation
Void Ratio, e	0.445	0.436
Porosity, n (%)	30.79	30.35
Std. Proctor Relative Compaction, RC (%)	91.62	92.20
Dry Density, γ_d (g/cm^3)	1.83	1.85

Unsaturated Hydraulic Soil Parameters	Drying	Wetting
Saturated Volumetric Water Content, θ_s	0.304	0.245
Residual Volumetric Water Content, θ_r	0.121	0.121
Air-Entry Pressure Parameter, α (1/kPa)	0.280	0.459
Pore-Size Distribution Parameter, n	2.071	2.100
Saturated Hydraulic Conductivity, k_{sat} (cm/s)	3.70E-04	7.50E-05

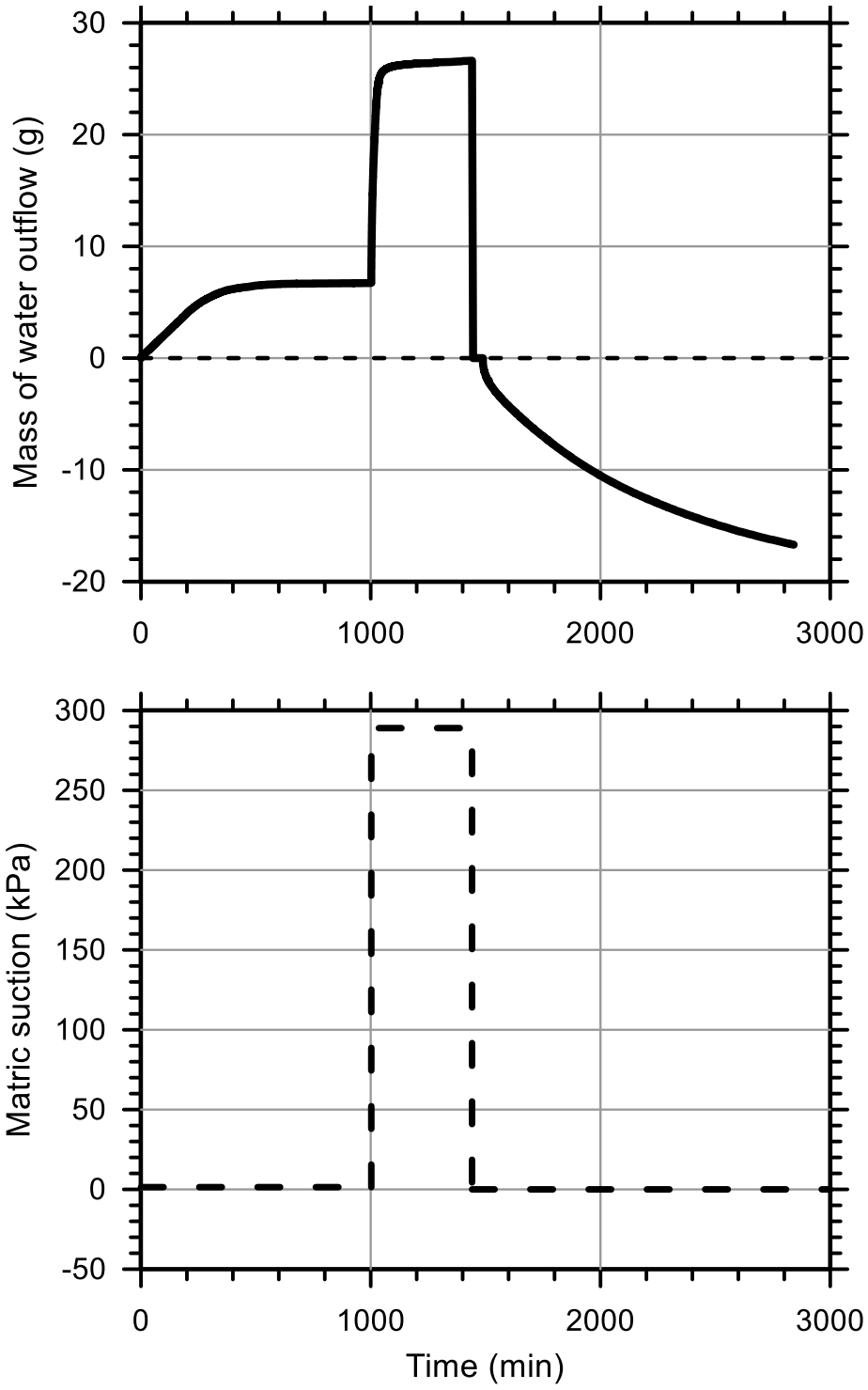
Mass of water outflow (g)
30
20
10
0
-10
-20
0
1000
2000
3000
Matric suction (kPa)
300
250
200
150
100
50
0
-50
0
1000
2000
3000
Time (min)

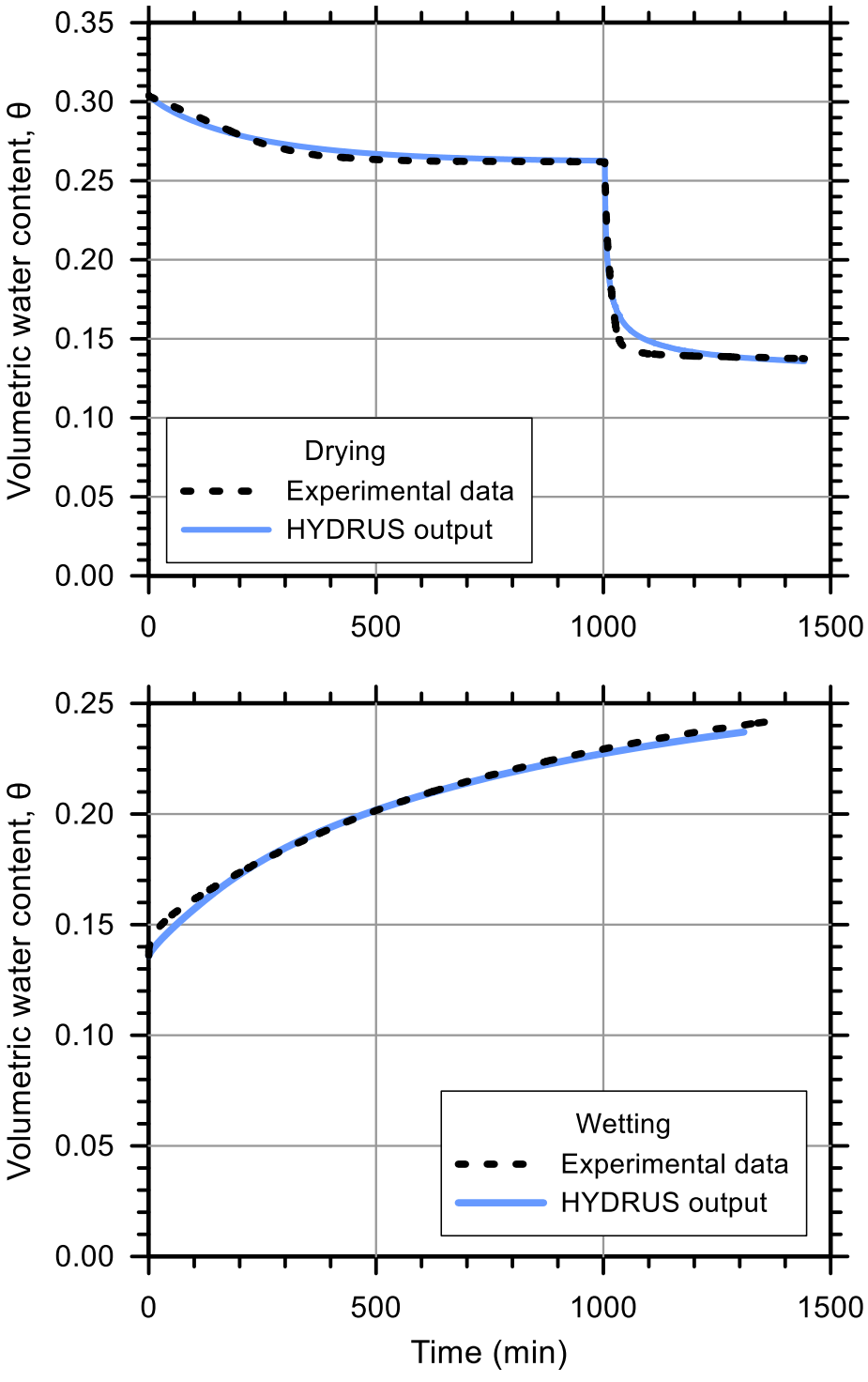
0.35
0.30
0.25
0.20
0.15
0.10
0.05
0.00
Volumetric water content, θ
Drying
Experimental data
HYDRUS output
0
500
1000
1500
0.25
0.20
0.15
0.10
0.05
0.00
Volumetric water content, θ
Wetting
Experimental data
HYDRUS output
0
500
1000
1500
Time (min)

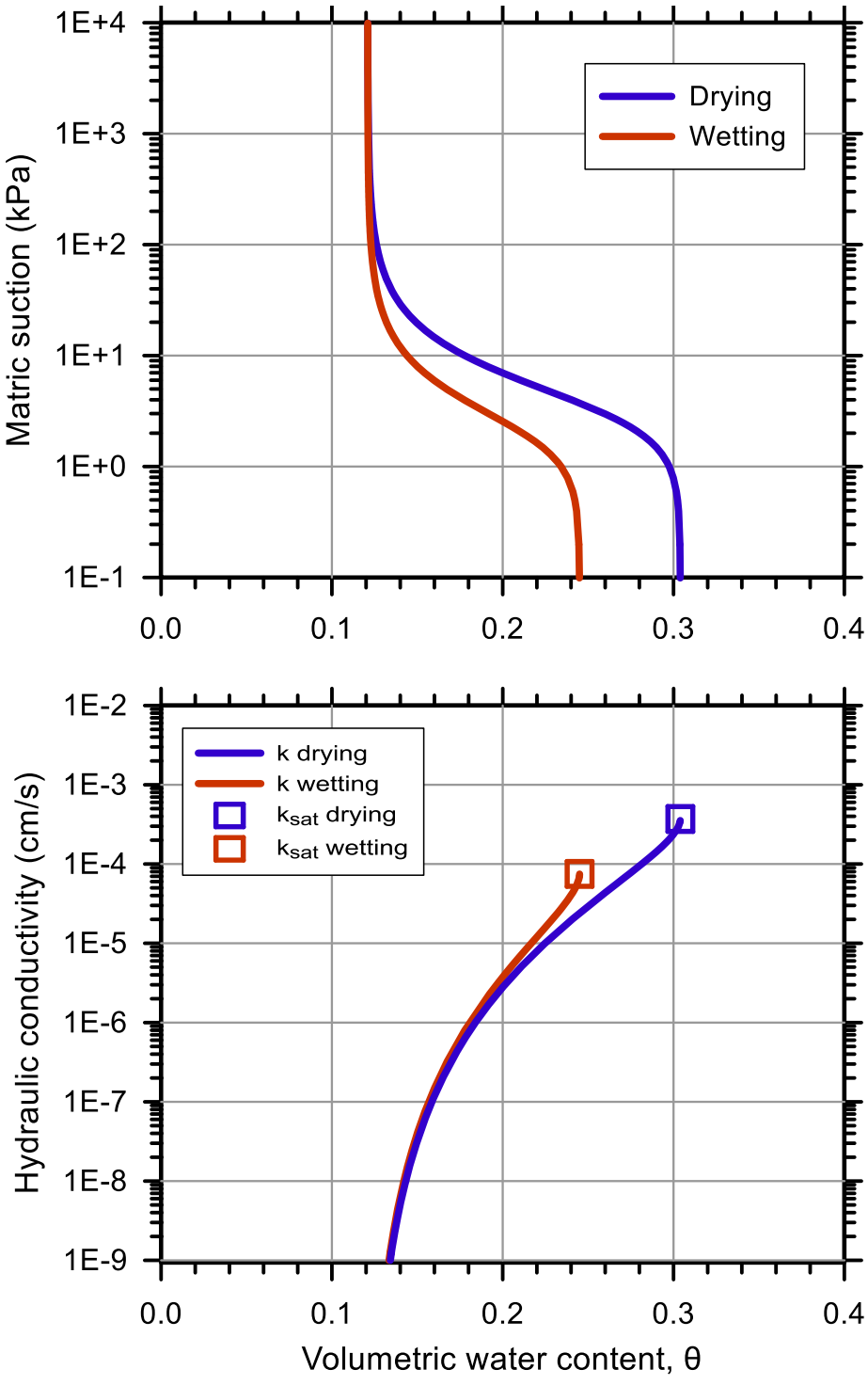
1E+4
1E+3
1E+2
1E+1
1E+0
1E-1
Matric suction (kPa)
Drying
Wetting
0.0
0.1
0.2
0.3
0.4
1E-2
1E-3
1E-4
1E-5
1E-6
1E-7
1E-8
1E-9
Hydraulic conductivity (cm/s)
k drying
k wetting
ksat drying
ksat wetting
0.0
0.1
0.2
0.3
0.4
Volumetric water content, θ

Test No.: 29

Test Ref.: TRIMM7X06

Test Soil: Sand-Clay (75%-25%)

Molding Water Content: 9.90% (w_{opt}-0.5)

Property	Before Saturation	After Saturation
Void Ratio, e	0.553	0.565
Porosity, n (%)	35.59	36.12
Std. Proctor Relative Compaction, RC (%)	85.26	84.56
Dry Density, γ_d (g/cm^3)	1.71	1.69

Unsaturated Hydraulic Soil Parameters	Drying	Wetting
Saturated Volumetric Water Content, θ_s	0.361	0.265
Residual Volumetric Water Content, θ_r	0.084	0.084
Air-Entry Pressure Parameter, α (1/kPa)	0.499	0.978
Pore-Size Distribution Parameter, n	2.252	2.138
Saturated Hydraulic Conductivity, k_{sat} (cm/s)	8.04E-04	4.00E-04

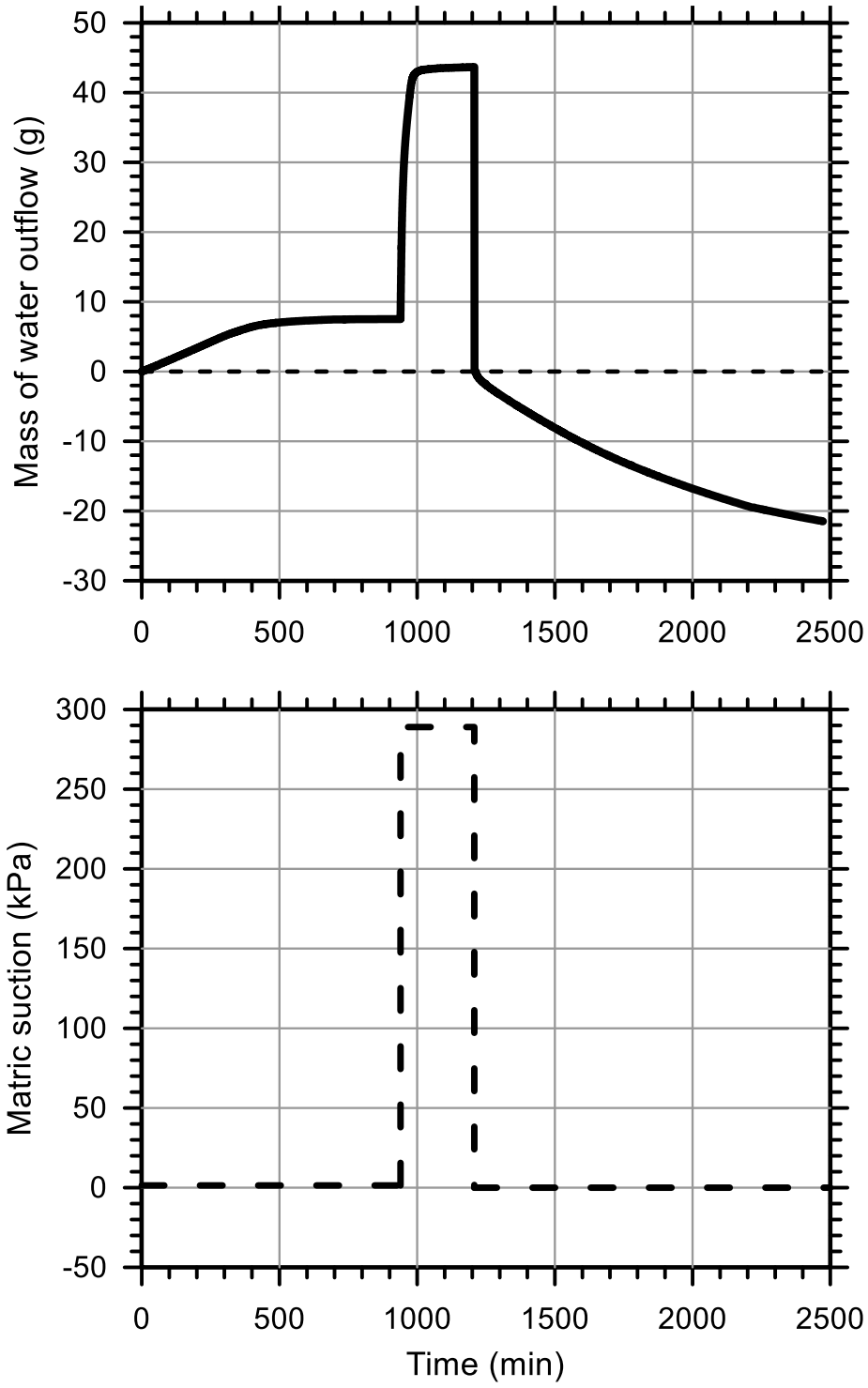
Mass of water outflow (g)
50
40
30
20
10
0
-10
-20
-30
0
500
1000
1500
2000
2500
Matric suction (kPa)
300
250
200
150
100
50
0
-50
0
500
1000
1500
2000
2500
Time (min)

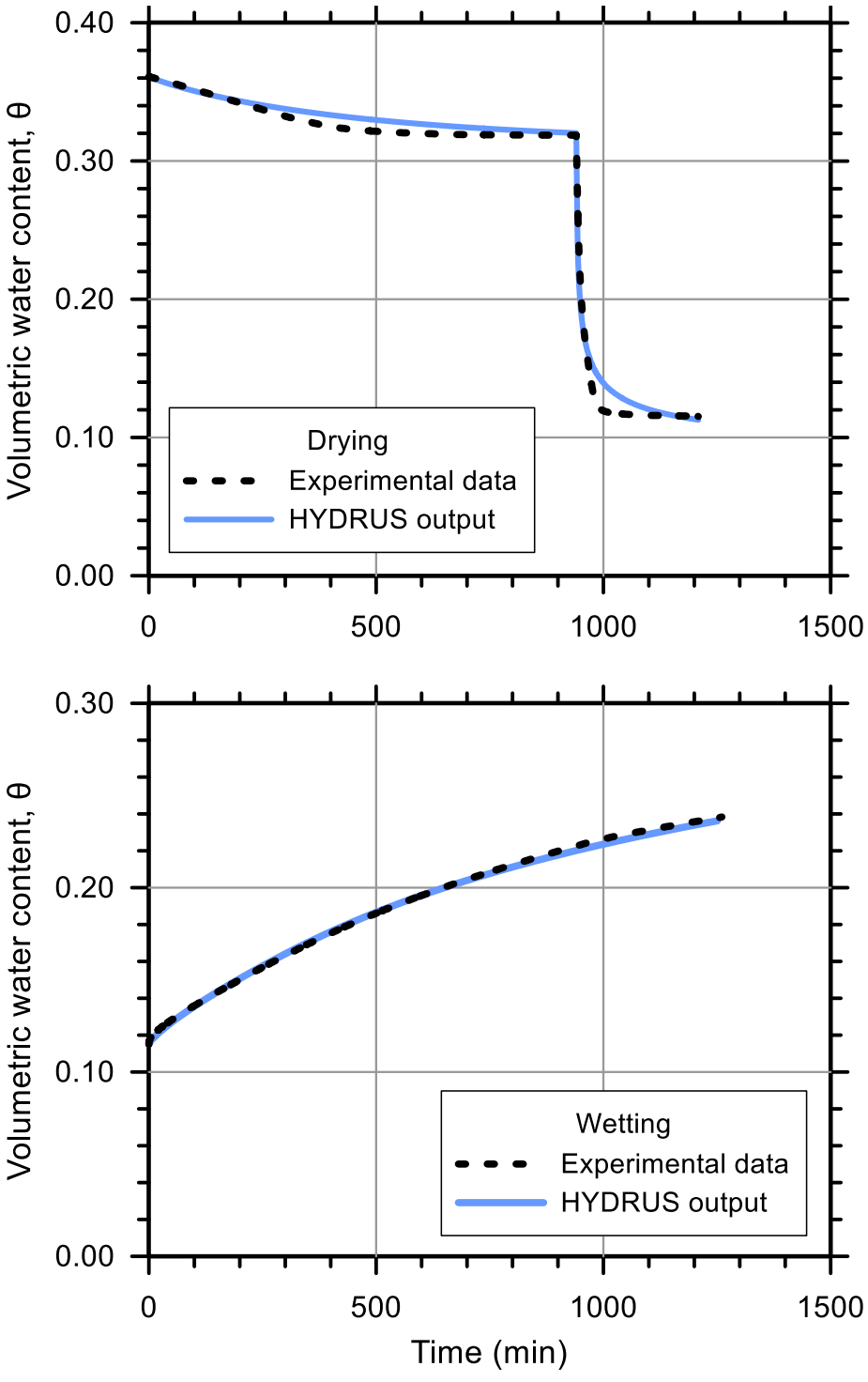
0.40
0.30
0.20
0.10
0.00
Volumetric water content, θ
Drying
Experimental data
HYDRUS output
0
500
1000
1500
0.30
0.20
0.10
0.00
Volumetric water content, θ
Wetting
Experimental data
HYDRUS output
0
500
1000
1500
Time (min)

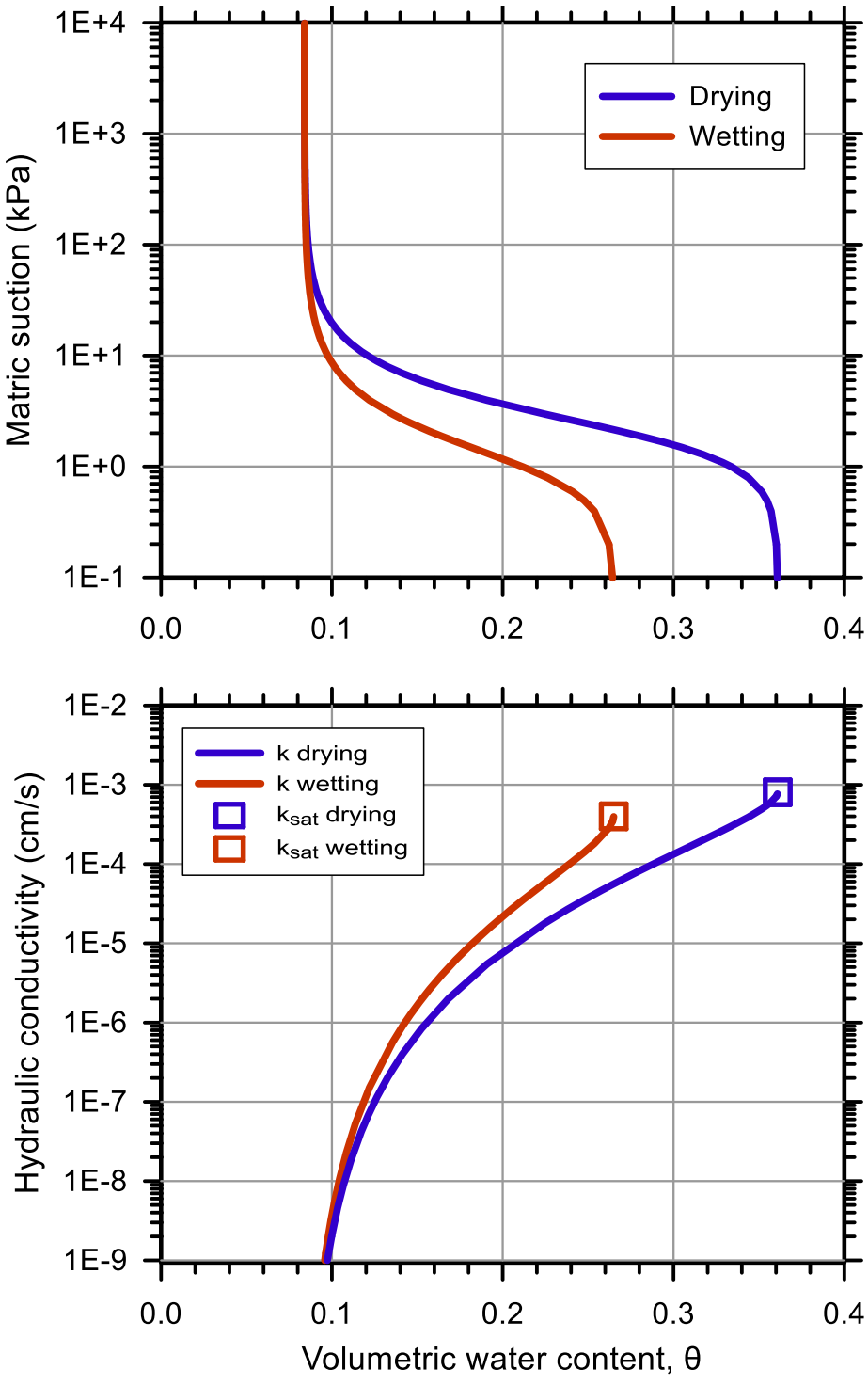
1E+4
1E+3
1E+2
1E+1
1E+0
1E-1
Matric suction (kPa)
Drying
Wetting
0.0
0.1
0.2
0.3
0.4
1E-2
1E-3
1E-4
1E-5
1E-6
1E-7
1E-8
1E-9
Hydraulic conductivity (cm/s)
k drying
k wetting
ksat drying
ksat wetting
0.0
0.1
0.2
0.3
0.4
Volumetric water content, θ

Test No.: 21

Test Ref.: TRIMM7X04

Test Soil: Sand-Clay (75%-25%)

Molding Water Content: 11.40% (w_{opt}+1)

Property	Before Saturation	After Saturation
Void Ratio, e	0.401	0.419
Porosity, n (%)	28.65	29.55
Std. Proctor Relative Compaction, RC (%)	94.45	93.25
Dry Density, γ_d (g/cm^3)	1.89	1.87

Unsaturated Hydraulic Soil Parameters	Drying	Wetting
Saturated Volumetric Water Content, θ_s	0.296	0.219
Residual Volumetric Water Content, θ_r	0.130	0.130
Air-Entry Pressure Parameter, α (1/kPa)	0.234	0.307
Pore-Size Distribution Parameter, n	1.800	1.800
Saturated Hydraulic Conductivity, k_{sat} (cm/s)	2.50E-04	8.98E-05

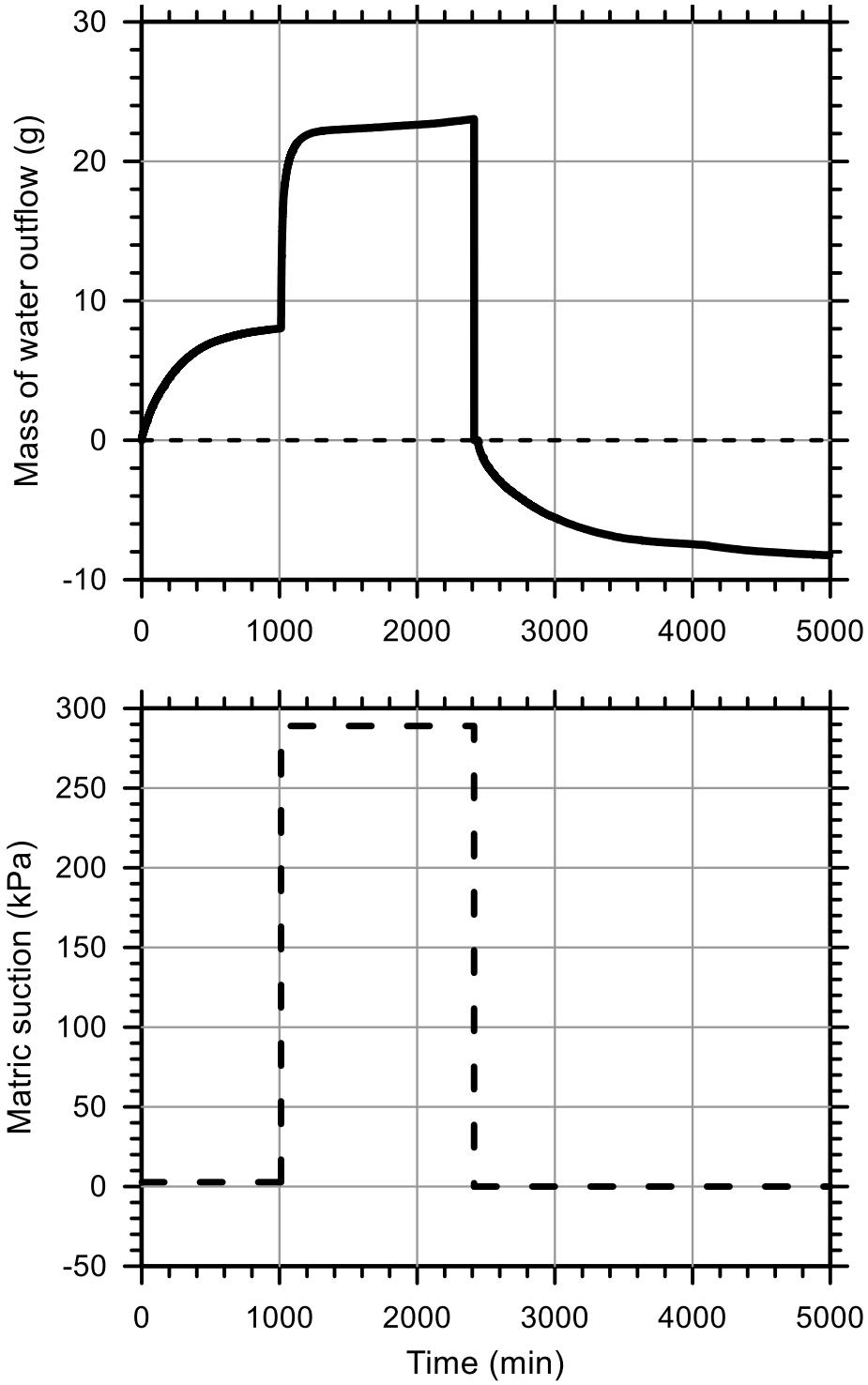
Mass of water outflow (g)
30
20
10
0
-10
0
1000
2000
3000
4000
5000
Matric suction (kPa)
300
250
200
150
100
50
0
-50
0
1000
2000
3000
4000
5000
Time (min)

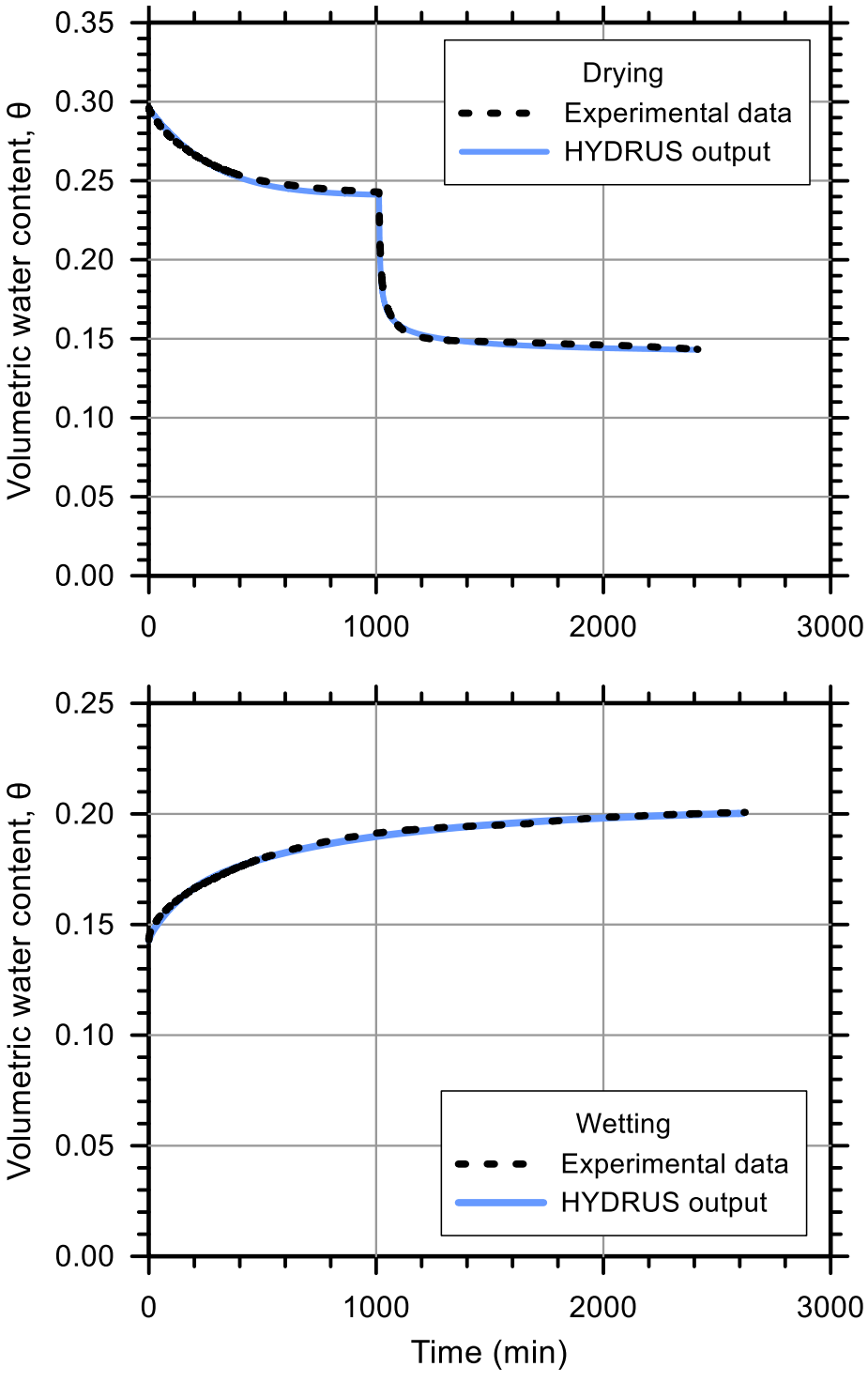
Drying
Experimental data
HYDRUS output
Volumetric water content, θ
0.35
0.30
0.25
0.20
0.15
0.10
0.05
0.00
0
1000
2000
3000
Wetting
Experimental data
HYDRUS output
Volumetric water content, θ
0.25
0.20
0.15
0.10
0.05
0.00
0
1000
2000
3000
Time (min)

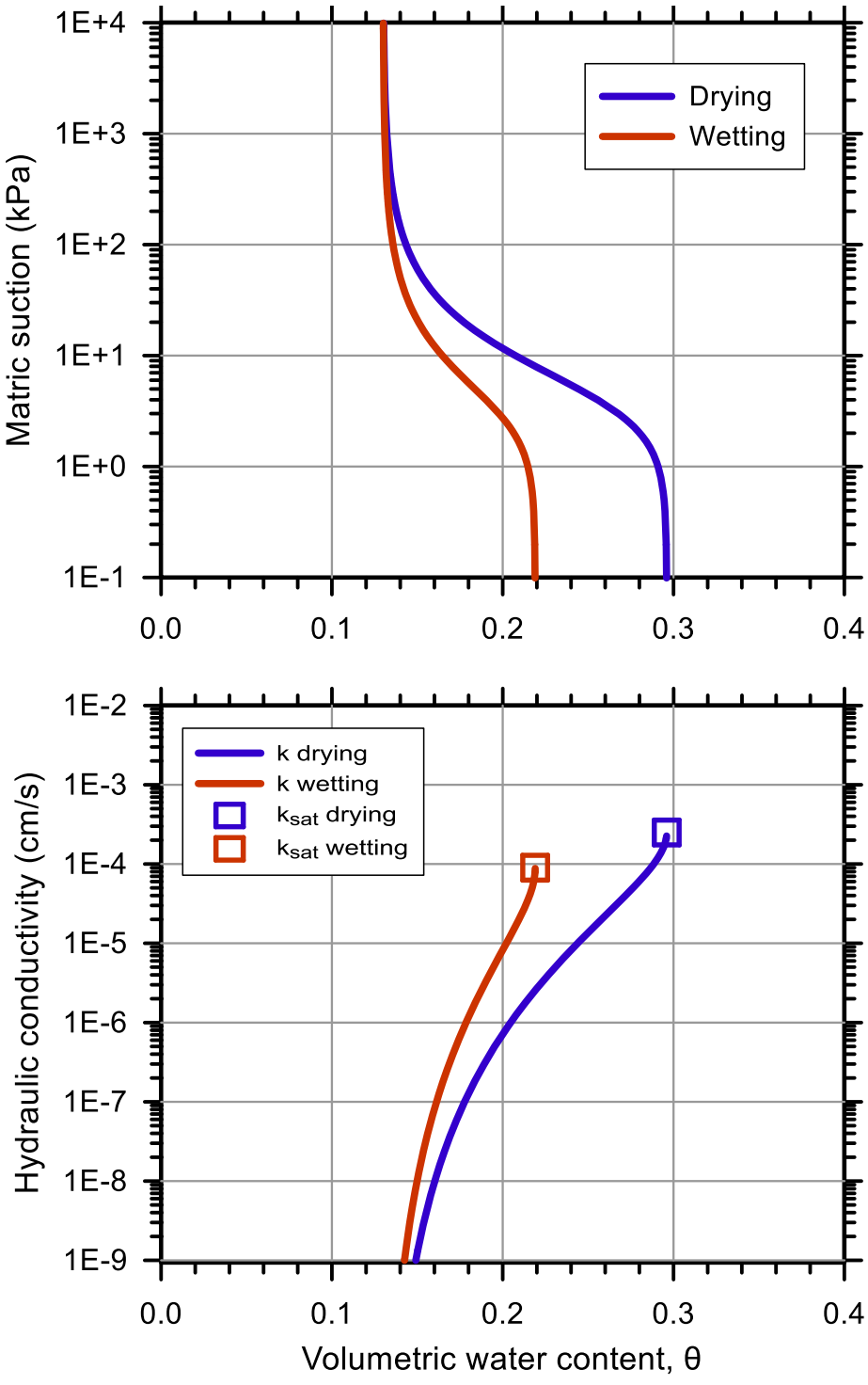
1E+4
1E+3
1E+2
1E+1
1E+0
1E-1
Matric suction (kPa)
Drying
Wetting
0.0
0.1
0.2
0.3
0.4
1E-2
1E-3
1E-4
1E-5
1E-6
1E-7
1E-8
1E-9
Hydraulic conductivity (cm/s)
k drying
k wetting
ksat drying
ksat wetting
0.0
0.1
0.2
0.3
0.4
Volumetric water content, θ

Test No.: 16

Test Ref.: TRIMM7X02

Test Soil: Sand-Clay (75%-25%)

Molding Water Content: 11.40% (w_{opt}+1)

Property	Before Saturation	After Saturation
Void Ratio, e	0.464	0.450
Porosity, n (%)	31.70	31.05
Std. Proctor Relative Compaction, RC (%)	90.41	91.27
Dry Density, γ_d (g/cm^3)	1.81	1.83

Unsaturated Hydraulic Soil Parameters	Drying	Wetting
Saturated Volumetric Water Content, θ_s	0.311	0.240
Residual Volumetric Water Content, θ_r	0.111	0.111
Air-Entry Pressure Parameter, α (1/kPa)	0.423	0.513
Pore-Size Distribution Parameter, n	2.484	2.350
Saturated Hydraulic Conductivity, k_{sat} (cm/s)	4.19E-04	8.05E-05

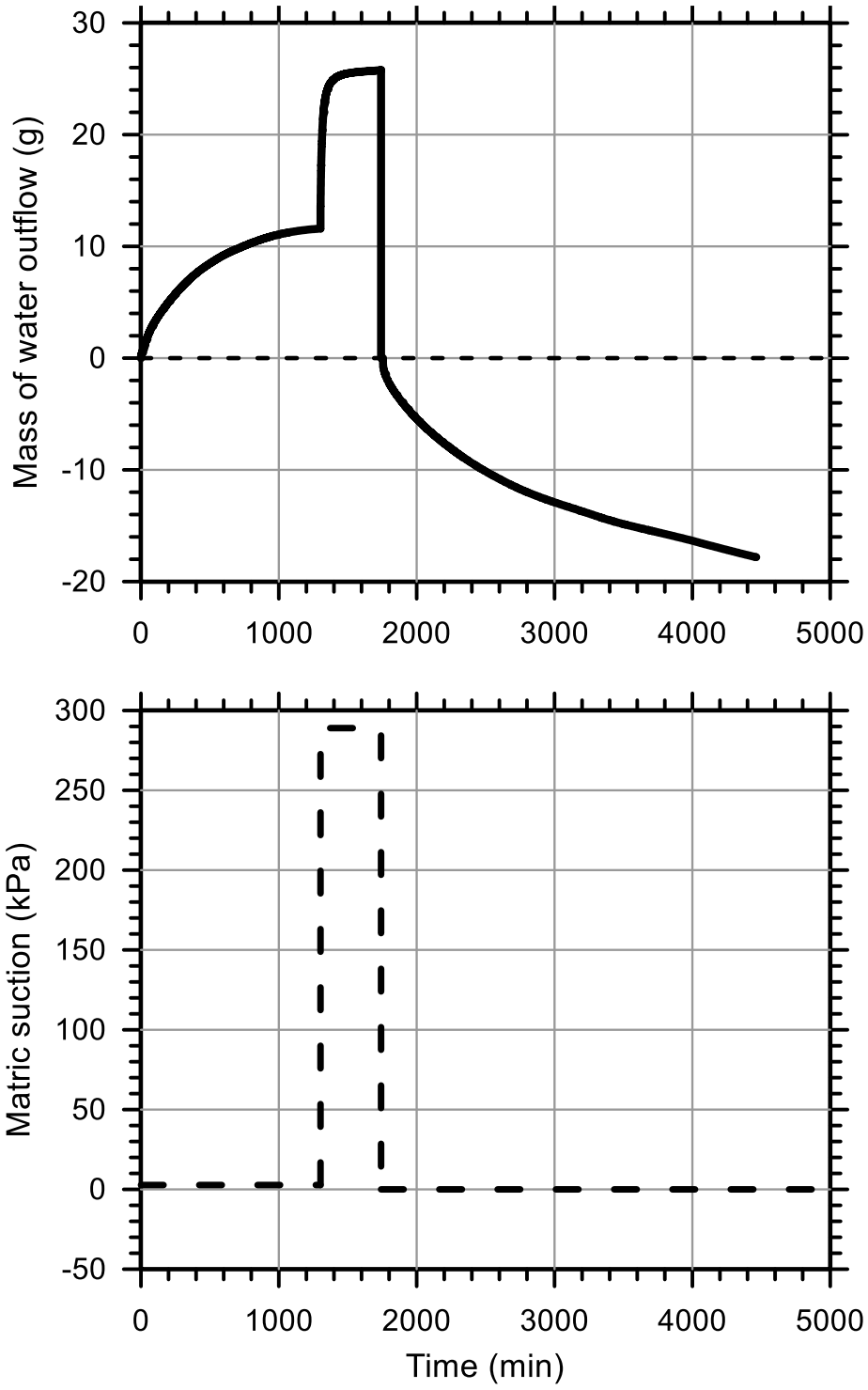
Mass of water outflow (g)
30
20
10
0
-10
-20
0
1000
2000
3000
4000
5000
Matric suction (kPa)
300
250
200
150
100
50
0
-50
0
1000
2000
3000
4000
5000
Time (min)

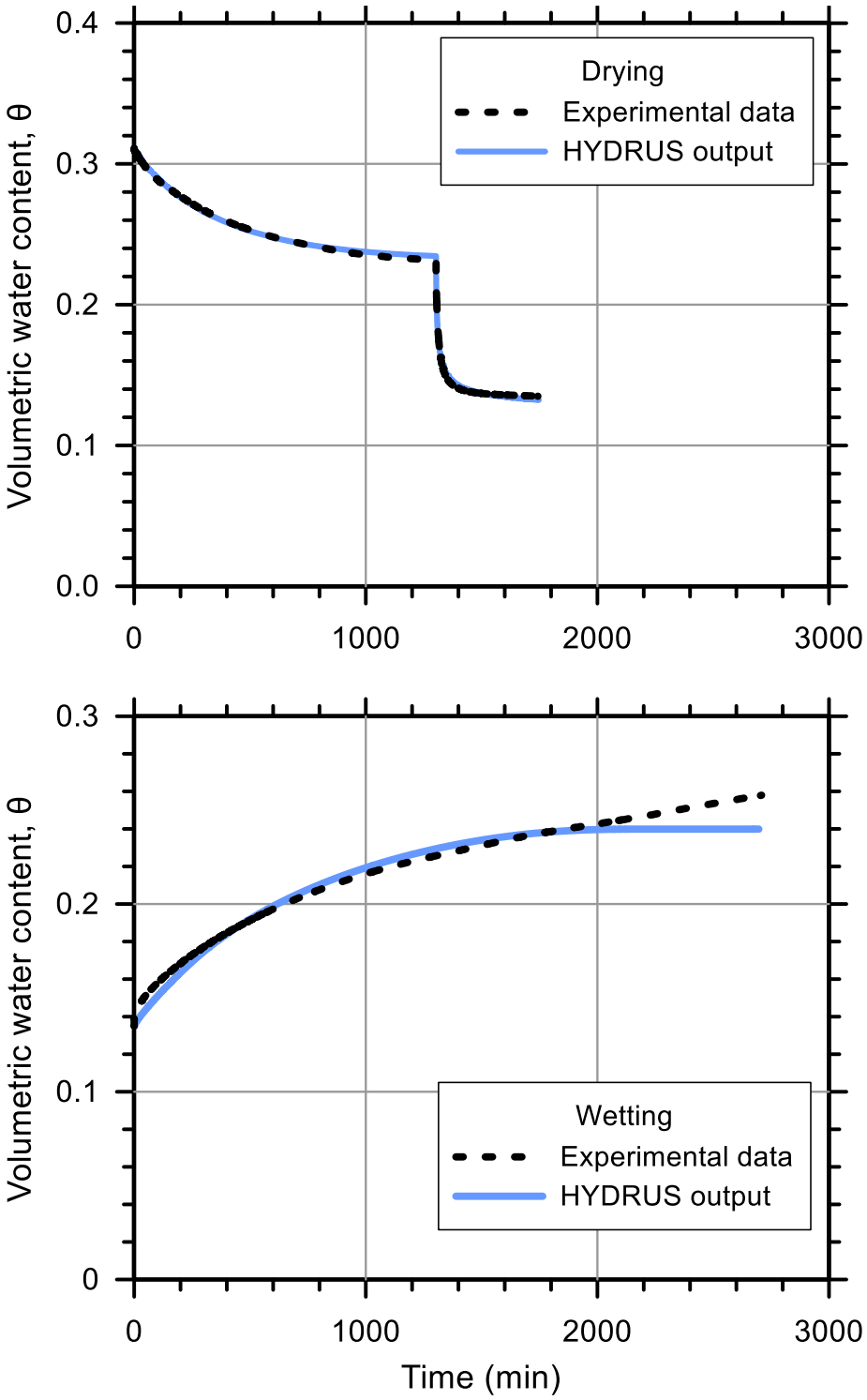
Drying
Experimental data
HYDRUS output
Volumetric water content, θ
0.4
0.3
0.2
0.1
0.0
0
1000
2000
3000
Wetting
Experimental data
HYDRUS output
Volumetric water content, θ
0.3
0.2
0.1
0
0
1000
2000
3000
Time (min)

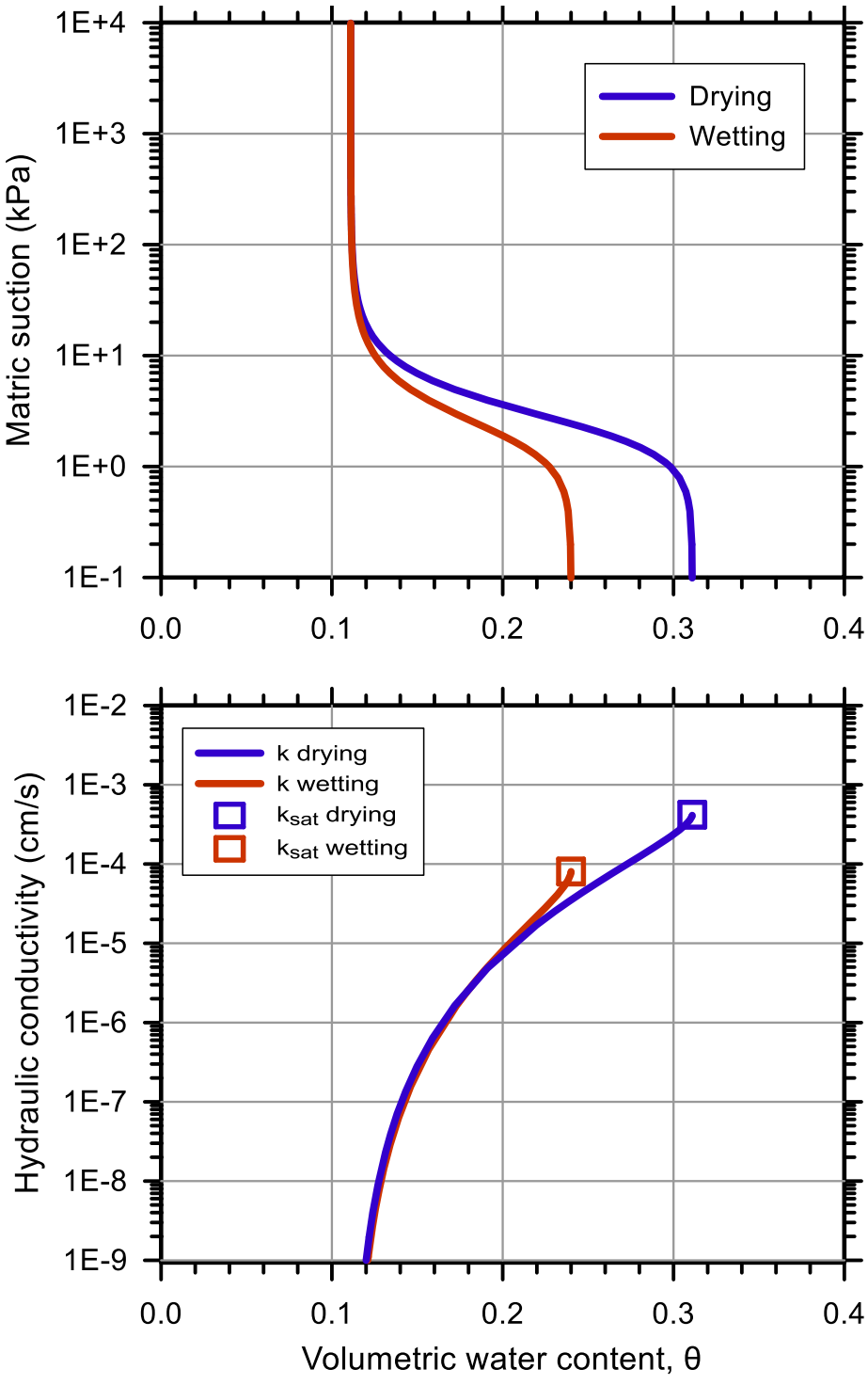
1E+4
1E+3
1E+2
1E+1
1E+0
1E-1
Matric suction (kPa)
Drying
Wetting
0.0
0.1
0.2
0.3
0.4
1E-2
1E-3
1E-4
1E-5
1E-6
1E-7
1E-8
1E-9
Hydraulic conductivity (cm/s)
k drying
k wetting
ksat drying
ksat wetting
0.0
0.1
0.2
0.3
0.4
Volumetric water content, θ

Test No.: 19

Test Ref.: TRIMM8X04

Test Soil: Sand-Clay (85%-15%)

Molding Water Content: 8.10% (w_{opt}-1.3)

Property	Before Saturation	After Saturation
Void Ratio, e	0.426	0.450
Porosity, n (%)	29.89	31.04
Std. Proctor Relative Compaction, RC (%)	95.91	94.34
Dry Density, γ_d (g/cm^3)	1.86	1.83

Unsaturated Hydraulic Soil Parameters	Drying	Wetting
Saturated Volumetric Water Content, θ_s	0.310	0.265
Residual Volumetric Water Content, θ_r	0.086	0.086
Air-Entry Pressure Parameter, α (1/kPa)	0.422	0.605
Pore-Size Distribution Parameter, n	2.197	2.123
Saturated Hydraulic Conductivity, k_{sat} (cm/s)	4.83E-04	2.18E-04

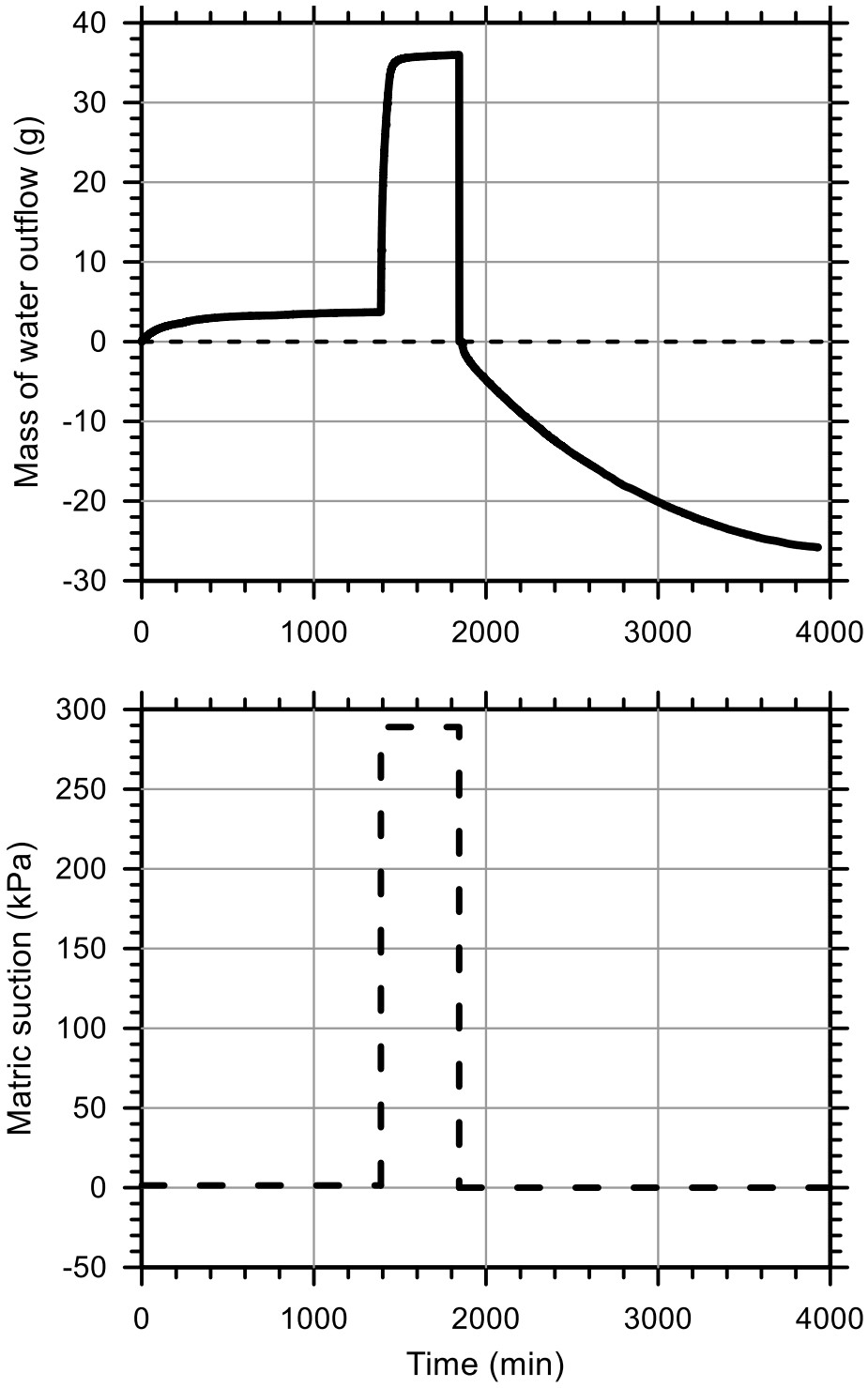
Mass of water outflow (g)
40
30
20
10
0
-10
-20
-30
0
1000
2000
3000
4000
Matric suction (kPa)
300
250
200
150
100
50
0
-50
0
1000
2000
3000
4000
Time (min)

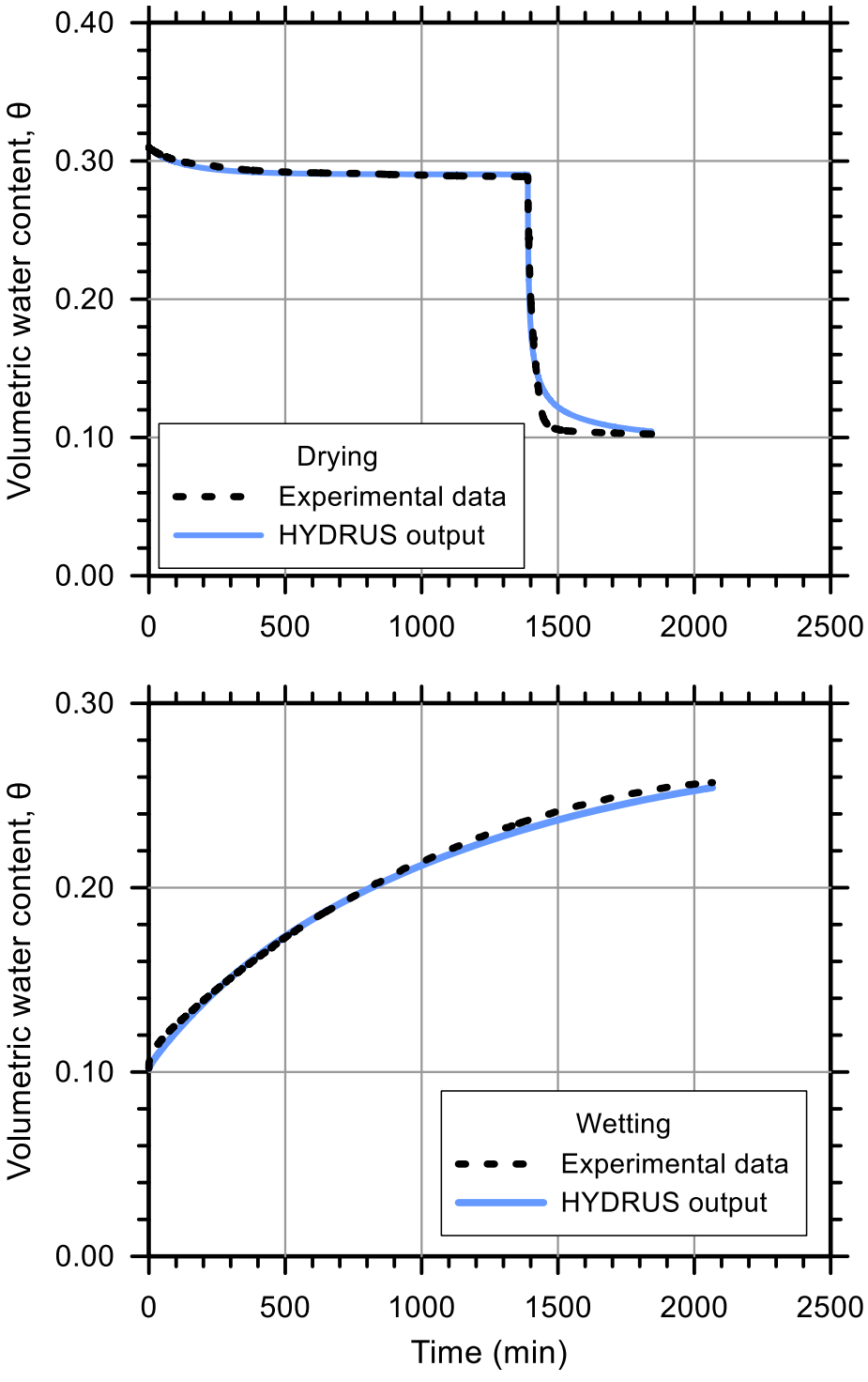
0.40
0.30
0.20
0.10
0.00
Volumetric water content, θ
Drying
Experimental data
HYDRUS output
0
500
1000
1500
2000
2500
0.30
0.20
0.10
0.00
Volumetric water content, θ
Wetting
Experimental data
HYDRUS output
0
500
1000
1500
2000
2500
Time (min)

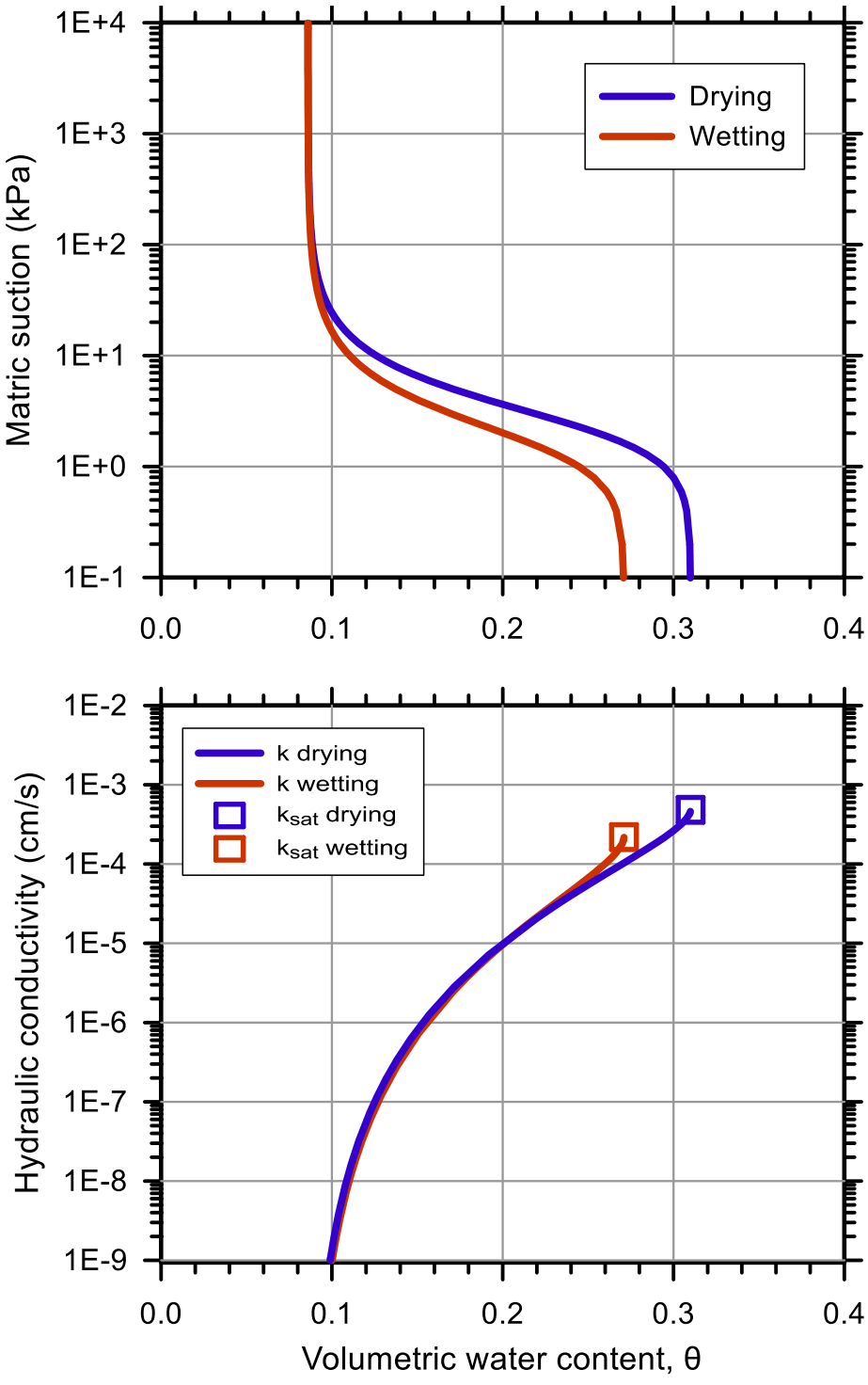
1E+4
1E+3
1E+2
1E+1
1E+0
1E-1
Matric suction (kPa)
Drying
Wetting
0.0
0.1
0.2
0.3
0.4
1E-2
1E-3
1E-4
1E-5
1E-6
1E-7
1E-8
1E-9
Hydraulic conductivity (cm/s)
k drying
k wetting
ksat drying
ksat wetting
0.0
0.1
0.2
0.3
0.4
Volumetric water content, θ

Test No.: 11

Test Ref.: TRIMM8X01

Test Soil: Sand-Clay (85%-15%)

Molding Water Content: 8.10% (w_{opt}-1.3)

Property	Before Saturation	After Saturation
Void Ratio, e	0.561	0.525
Porosity, n (%)	35.93	34.42
Std. Proctor Relative Compaction, RC (%)	87.65	89.72
Dry Density, γ_d (g/cm^3)	1.70	1.74

Unsaturated Hydraulic Soil Parameters	Drying	Wetting
Saturated Volumetric Water Content, θ_s	0.344	0.257
Residual Volumetric Water Content, θ_r	0.073	0.073
Air-Entry Pressure Parameter, α (1/kPa)	0.418	0.612
Pore-Size Distribution Parameter, n	2.337	2.243
Saturated Hydraulic Conductivity, k_{sat} (cm/s)	9.00E-04	7.00E-04

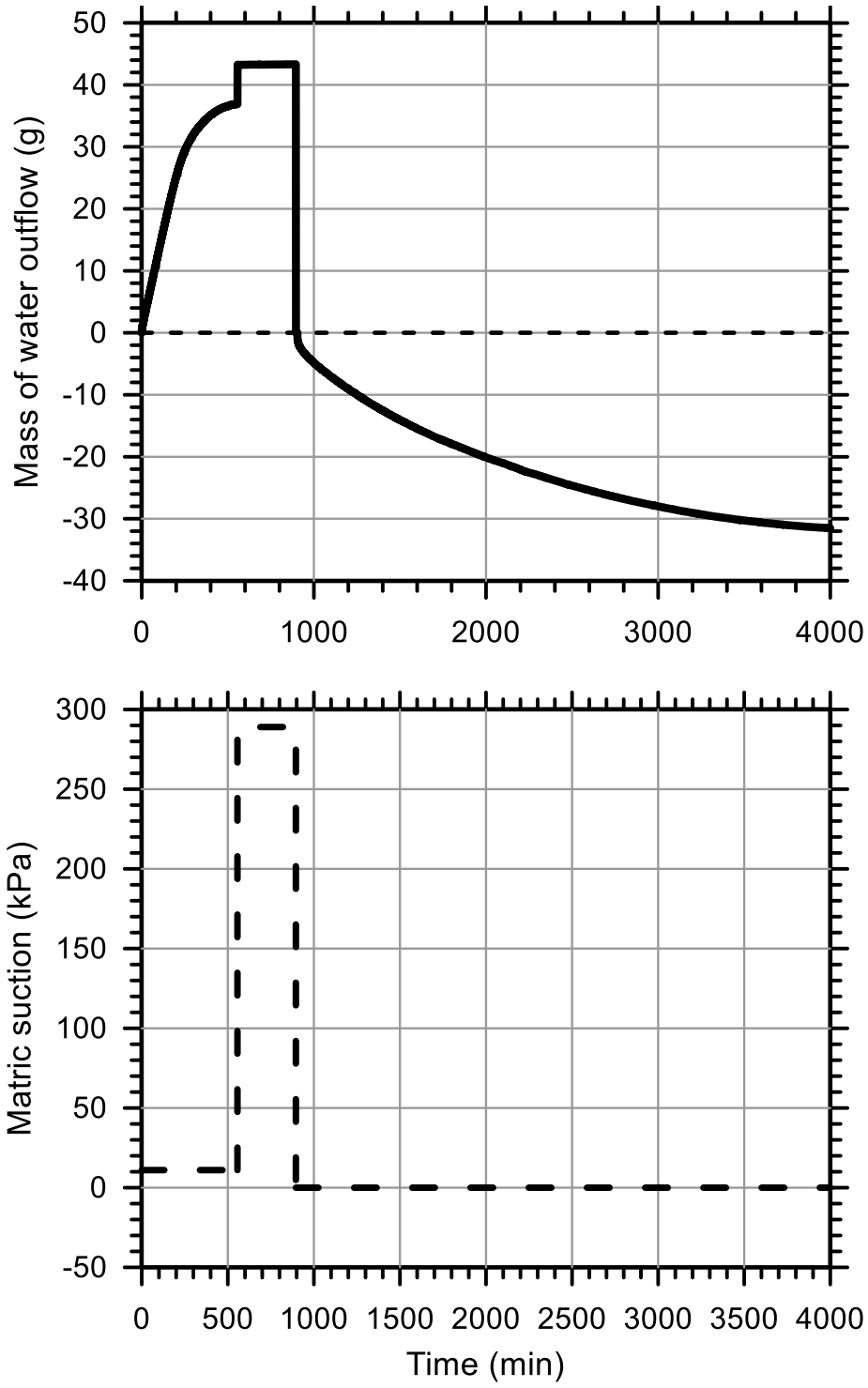
Mass of water outflow (g)
50
40
30
20
10
0
-10
-20
-30
-40
0
1000
2000
3000
4000
Matric suction (kPa)
300
250
200
150
100
50
0
-50
0
500
1000
1500
2000
2500
3000
3500
4000
Time (min)

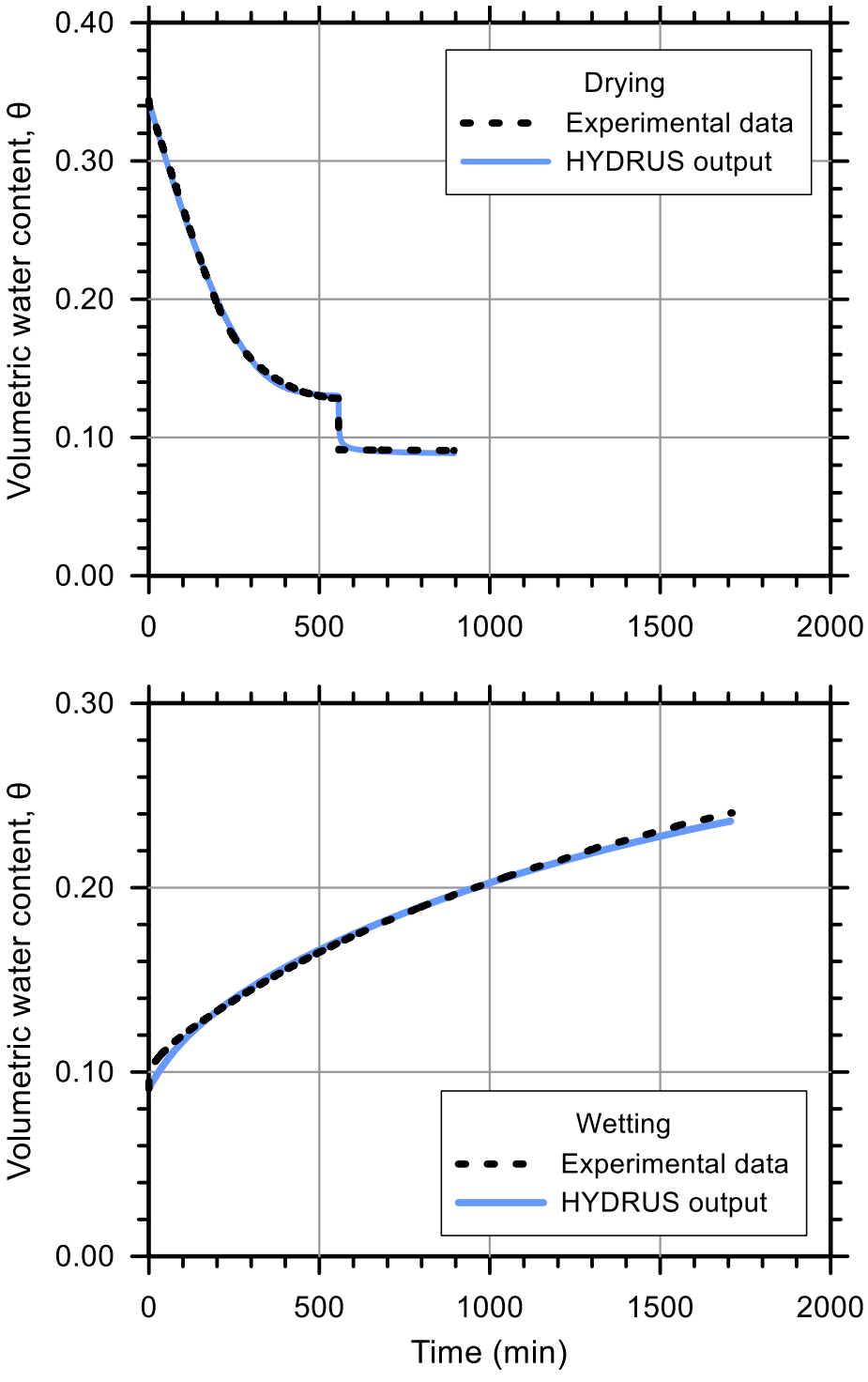
0.40
0.30
0.20
0.10
0.00
Volumetric water content, θ
Drying
Experimental data
HYDRUS output
0
500
1000
1500
2000
0.30
0.20
0.10
0.00
Volumetric water content, θ
Wetting
Experimental data
HYDRUS output
0
500
1000
1500
2000
Time (min)

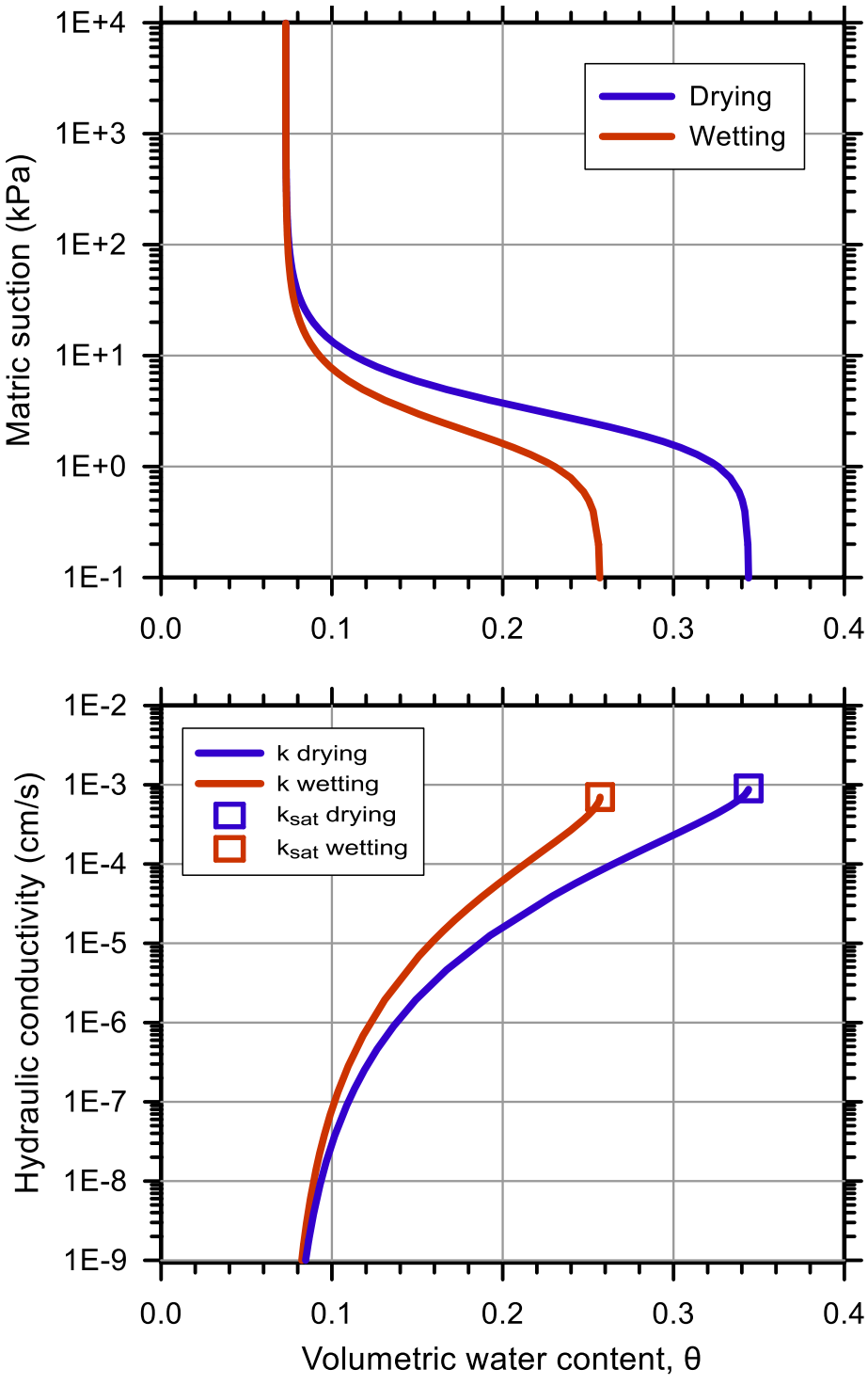
1E+4
1E+3
1E+2
1E+1
1E+0
1E-1
Matric suction (kPa)
Drying
Wetting
0.0
0.1
0.2
0.3
0.4
1E-2
1E-3
1E-4
1E-5
1E-6
1E-7
1E-8
1E-9
Hydraulic conductivity (cm/s)
k drying
k wetting
ksat drying
ksat wetting
0.0
0.1
0.2
0.3
0.4
Volumetric water content, θ

Test No.: 26

Test Ref.: TRIMM8X05

Test Soil: Sand-Clay (85%-15%)

Molding Water Content: 9.40% (w_{opt})

Property	Before Saturation	After Saturation
Void Ratio, e	0.448	0.461
Porosity, n (%)	30.94	31.56
Std. Proctor Relative Compaction, RC (%)	94.47	93.63
Dry Density, γ_d (g/cm^3)	1.83	1.81

Unsaturated Hydraulic Soil Parameters	Drying	Wetting
Saturated Volumetric Water Content, θ_s	0.316	0.245
Residual Volumetric Water Content, θ_r	0.085	0.085
Air-Entry Pressure Parameter, α (1/kPa)	0.438	0.703
Pore-Size Distribution Parameter, n	2.200	2.050
Saturated Hydraulic Conductivity, k_{sat} (cm/s)	5.50E-04	4.50E-04

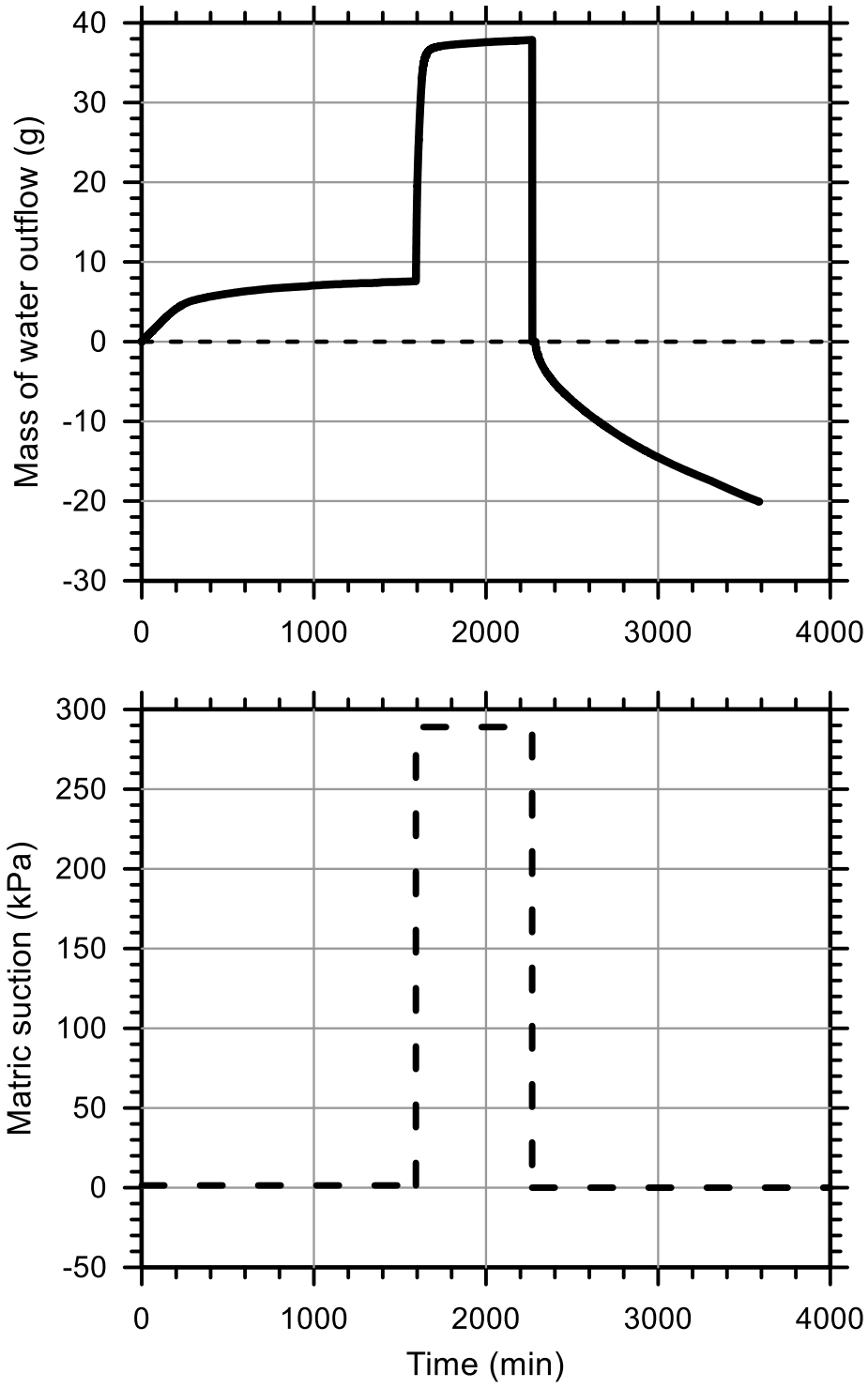
Mass of water outflow (g)
40
30
20
10
0
-10
-20
-30
0
1000
2000
3000
4000
Matric suction (kPa)
300
250
200
150
100
50
0
-50
0
1000
2000
3000
4000
Time (min)

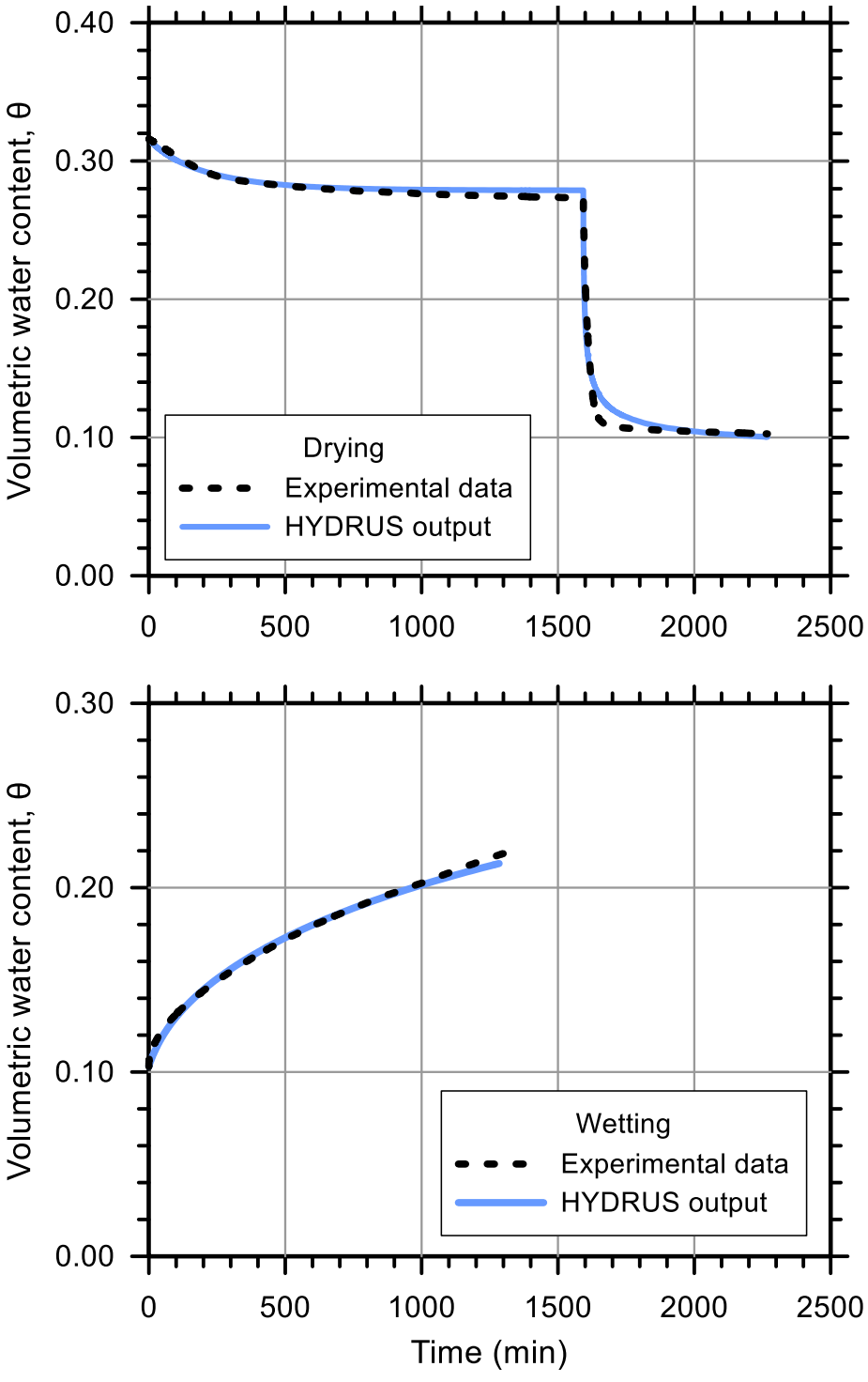
0.40
0.30
0.20
0.10
0.00
Volumetric water content, θ
Drying
Experimental data
HYDRUS output
0
500
1000
1500
2000
2500
0.30
0.20
0.10
0.00
Volumetric water content, θ
Wetting
Experimental data
HYDRUS output
0
500
1000
1500
2000
2500
Time (min)

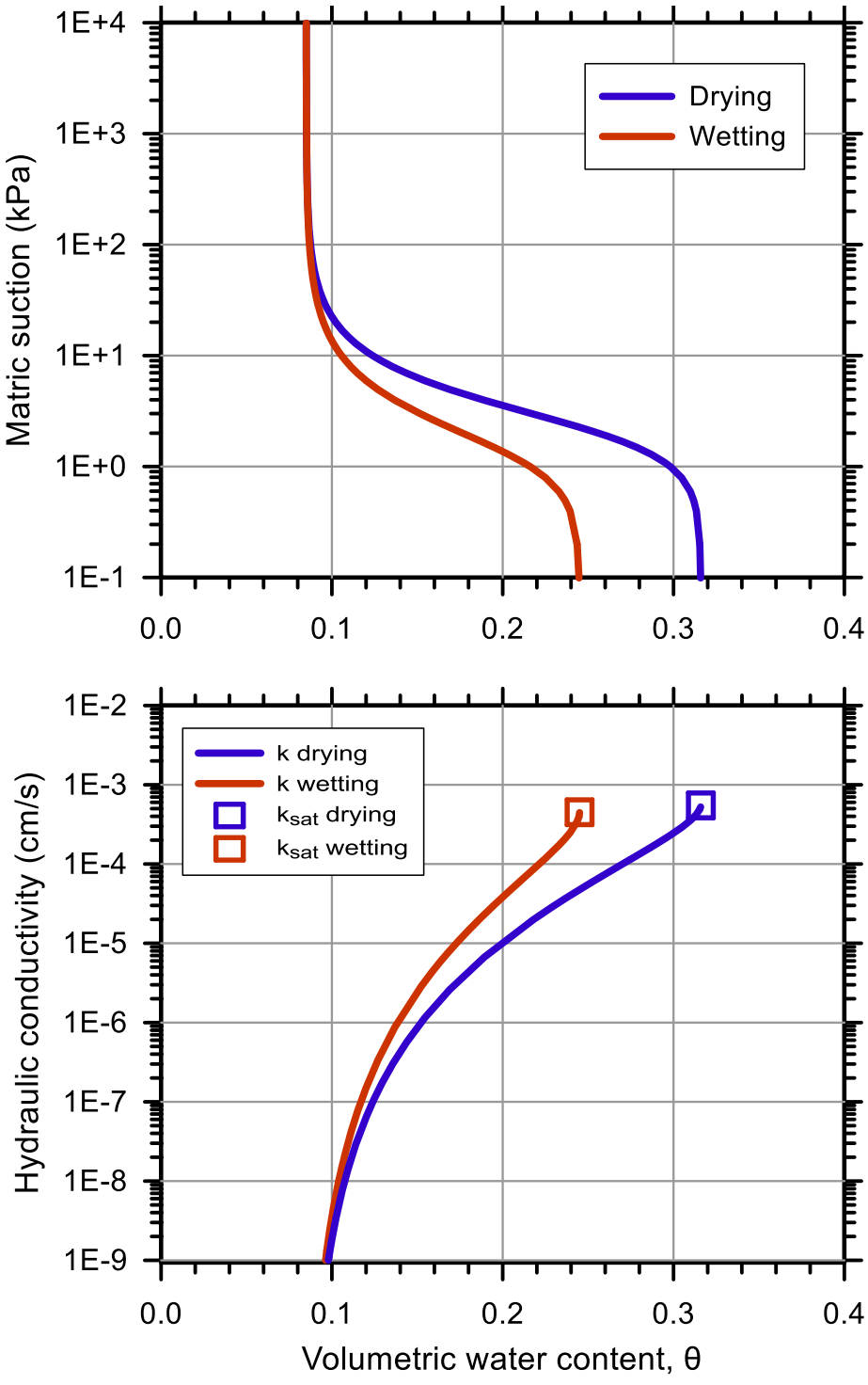
1E+4
1E+3
1E+2
1E+1
1E+0
1E-1
Matric suction (kPa)
Drying
Wetting
0.0
0.1
0.2
0.3
0.4
1E-2
1E-3
1E-4
1E-5
1E-6
1E-7
1E-8
1E-9
Hydraulic conductivity (cm/s)
k drying
k wetting
ksat drying
ksat wetting
0.0
0.1
0.2
0.3
0.4
Volumetric water content, θ

Test No.: 30

Test Ref.: TRIMM8X06

Test Soil: Sand-Clay (85%-15%)

Molding Water Content: 9.40% (w_{opt})

Property	Before Saturation	After Saturation
Void Ratio, e	0.551	0.568
Porosity, n (%)	35.51	36.23
Std. Proctor Relative Compaction, RC (%)	88.22	87.24
Dry Density, γ_d (g/cm^3)	1.71	1.69

Unsaturated Hydraulic Soil Parameters	Drying	Wetting
Saturated Volumetric Water Content, θ_s	0.362	0.277
Residual Volumetric Water Content, θ_r	0.072	0.072
Air-Entry Pressure Parameter, α (1/kPa)	0.509	0.598
Pore-Size Distribution Parameter, n	2.350	2.277
Saturated Hydraulic Conductivity, k_{sat} (cm/s)	2.19E-03	8.00E-04

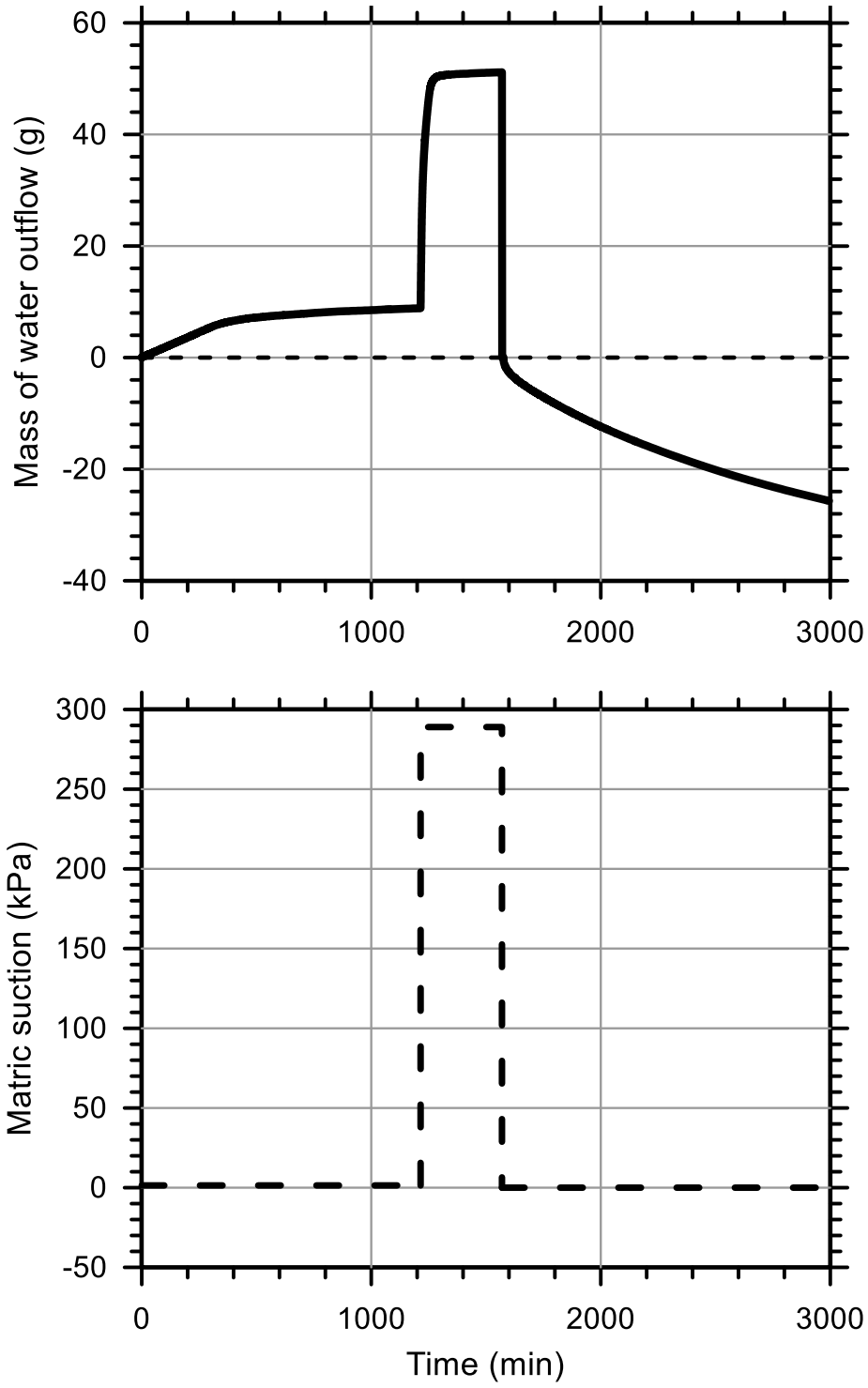
60
40
20
0
-20
-40
Mass of water outflow (g)
0
1000
2000
3000
300
250
200
150
100
50
0
-50
Matric suction (kPa)
0
1000
2000
3000
Time (min)

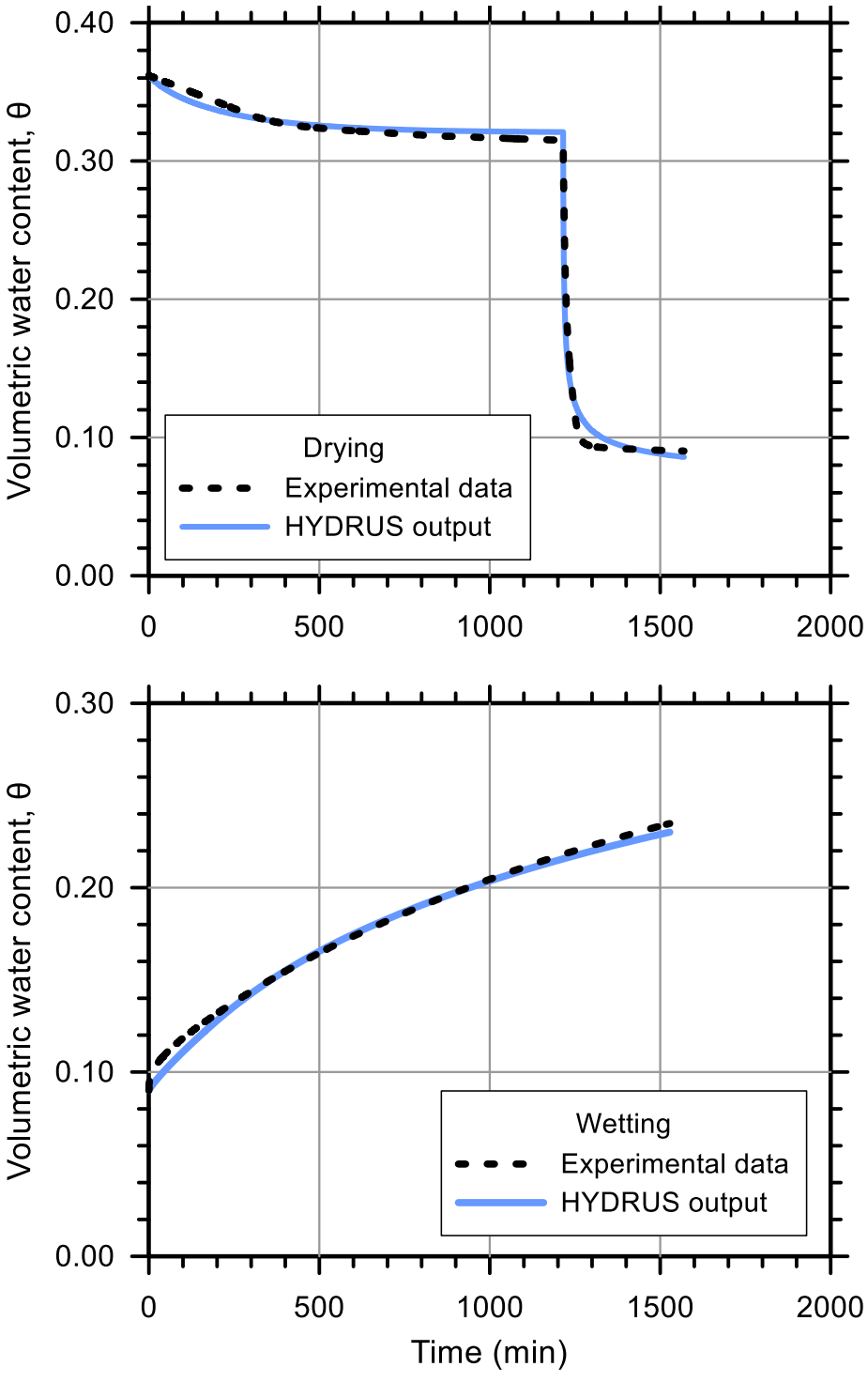
0.40
0.30
0.20
0.10
0.00
Volumetric water content, θ
Drying
Experimental data
HYDRUS output
0
500
1000
1500
2000
0.30
0.20
0.10
0.00
Volumetric water content, θ
Wetting
Experimental data
HYDRUS output
0
500
1000
1500
2000
Time (min)

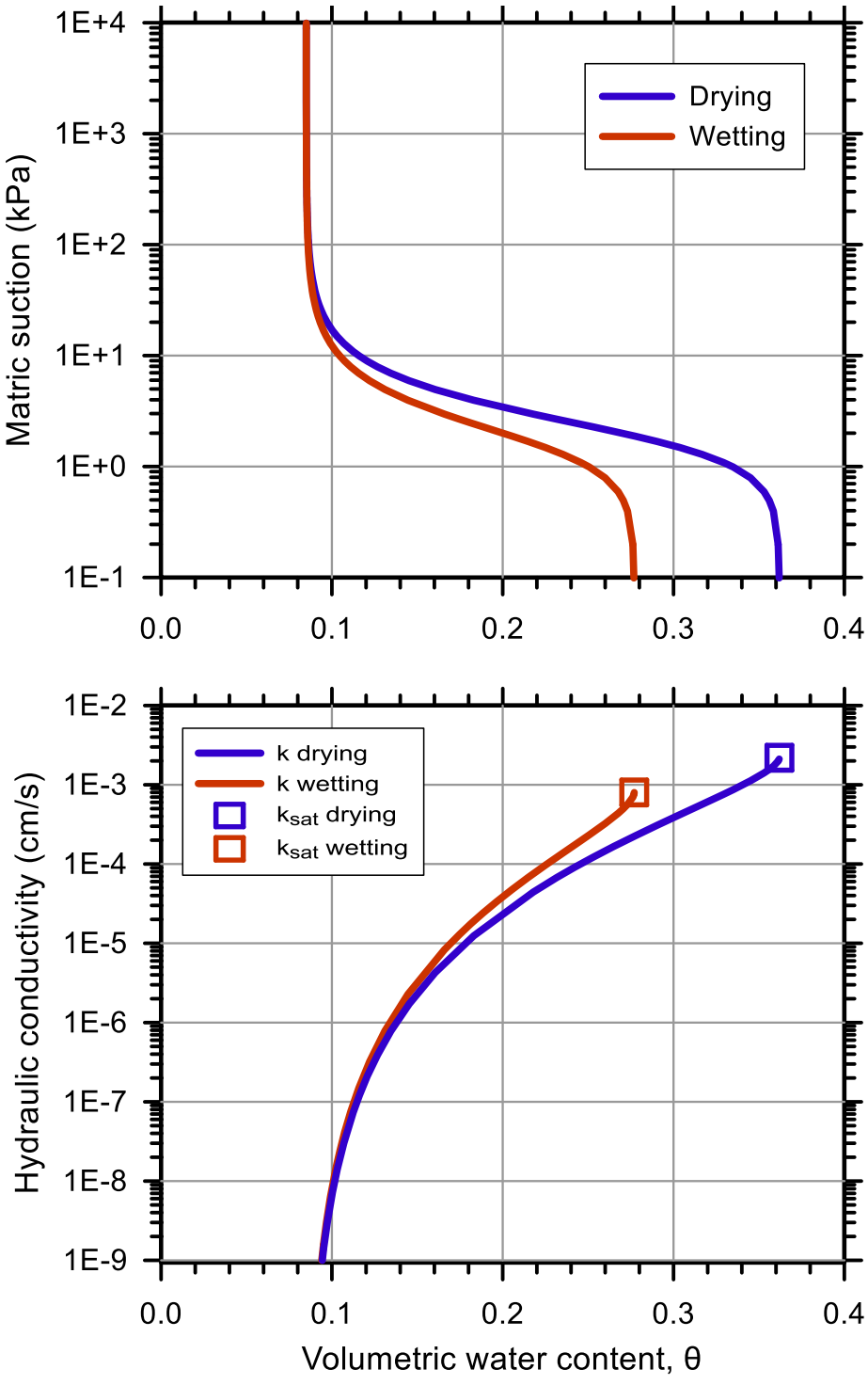
1E+4
1E+3
1E+2
1E+1
1E+0
1E-1
Matric suction (kPa)
Drying
Wetting
0.0
0.1
0.2
0.3
0.4
1E-2
1E-3
1E-4
1E-5
1E-6
1E-7
1E-8
1E-9
Hydraulic conductivity (cm/s)
k drying
k wetting
ksat drying
ksat wetting
0.0
0.1
0.2
0.3
0.4
Volumetric water content, θ

Test No.: 18

Test Ref.: TRIMM8X03

Test Soil: Sand-Clay (85%-15%)

Molding Water Content: 11.10% (w_{opt}+1.7)

Property	Before Saturation	After Saturation
Void Ratio, e	0.420	0.455
Porosity, n (%)	29.58	31.28
Std. Proctor Relative Compaction, RC (%)	96.34	94.02
Dry Density, γ_d (g/cm^3)	1.87	1.82

Unsaturated Hydraulic Soil Parameters	Drying	Wetting
Saturated Volumetric Water Content, θ_s	0.313	0.263
Residual Volumetric Water Content, θ_r	0.087	0.087
Air-Entry Pressure Parameter, α (1/kPa)	0.301	0.642
Pore-Size Distribution Parameter, n	2.390	2.100
Saturated Hydraulic Conductivity, k_{sat} (cm/s)	2.31E-04	1.00E-04

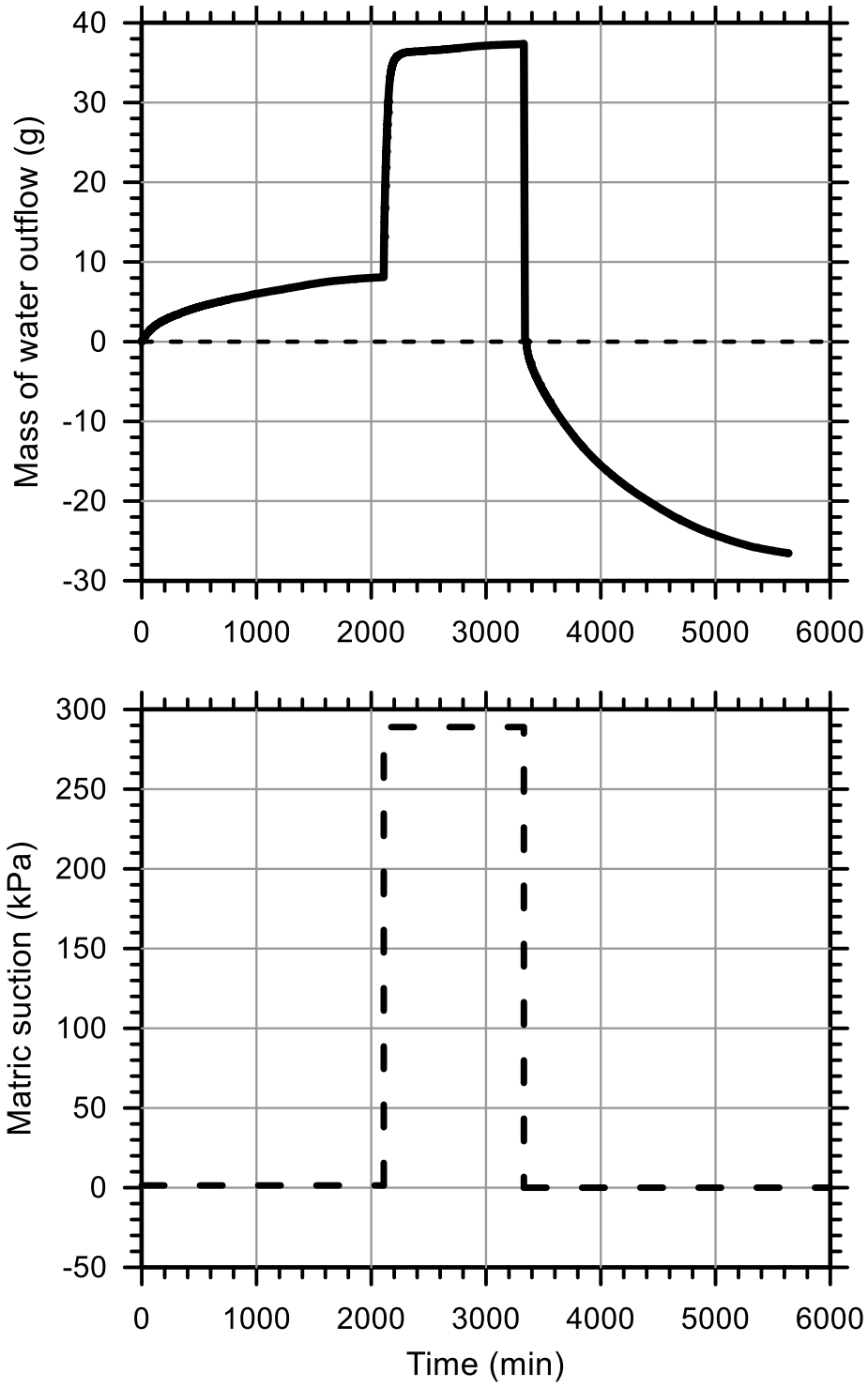
Mass of water outflow (g)
40
30
20
10
0
-10
-20
-30
0
1000
2000
3000
4000
5000
6000
Matric suction (kPa)
300
250
200
150
100
50
0
-50
0
1000
2000
3000
4000
5000
6000
Time (min)

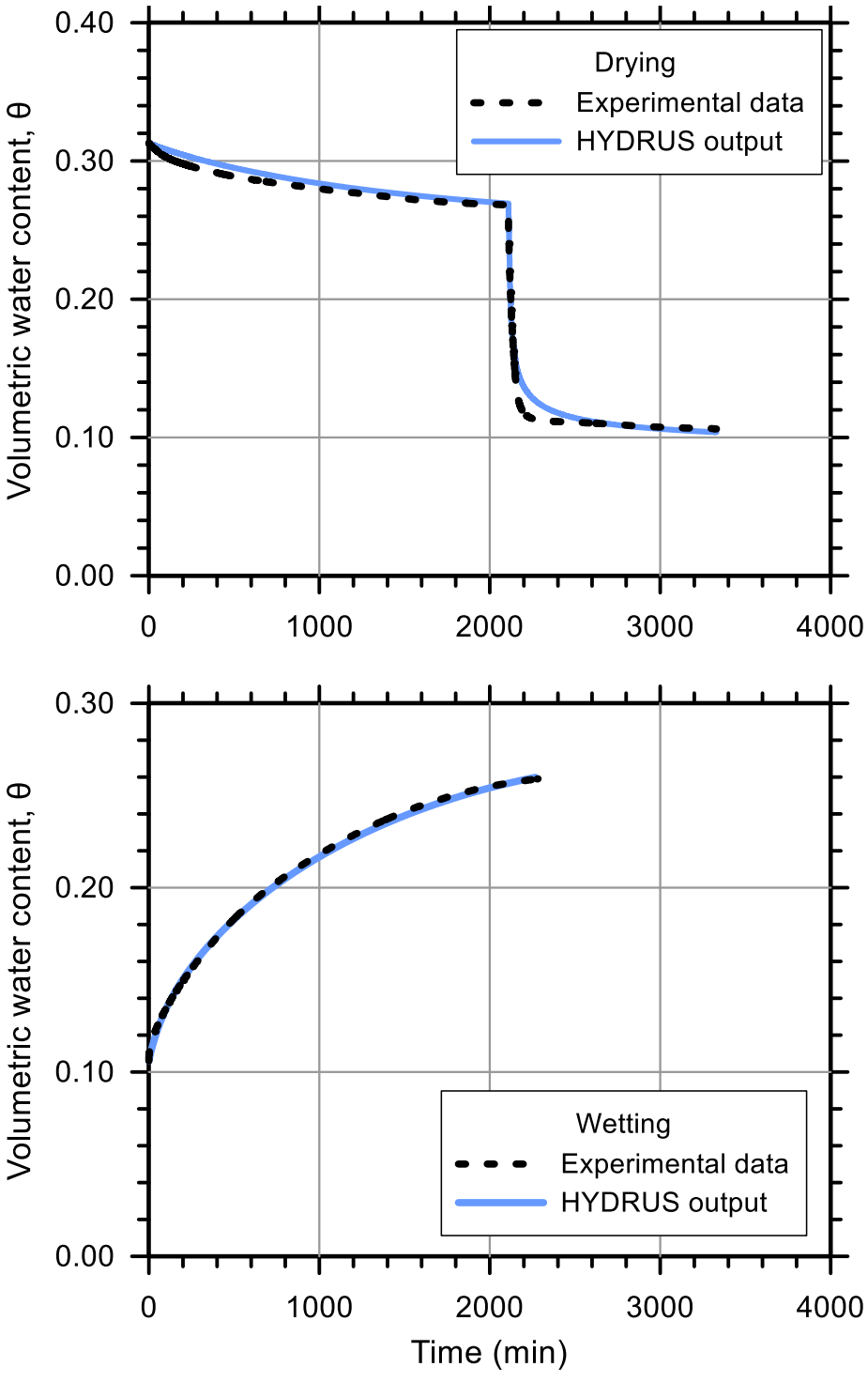
Drying
Experimental data
HYDRUS output
Volumetric water content, θ
0.40
0.30
0.20
0.10
0.00
0
1000
2000
3000
4000
Wetting
Experimental data
HYDRUS output
Volumetric water content, θ
0.30
0.20
0.10
0.00
0
1000
2000
3000
4000
Time (min)

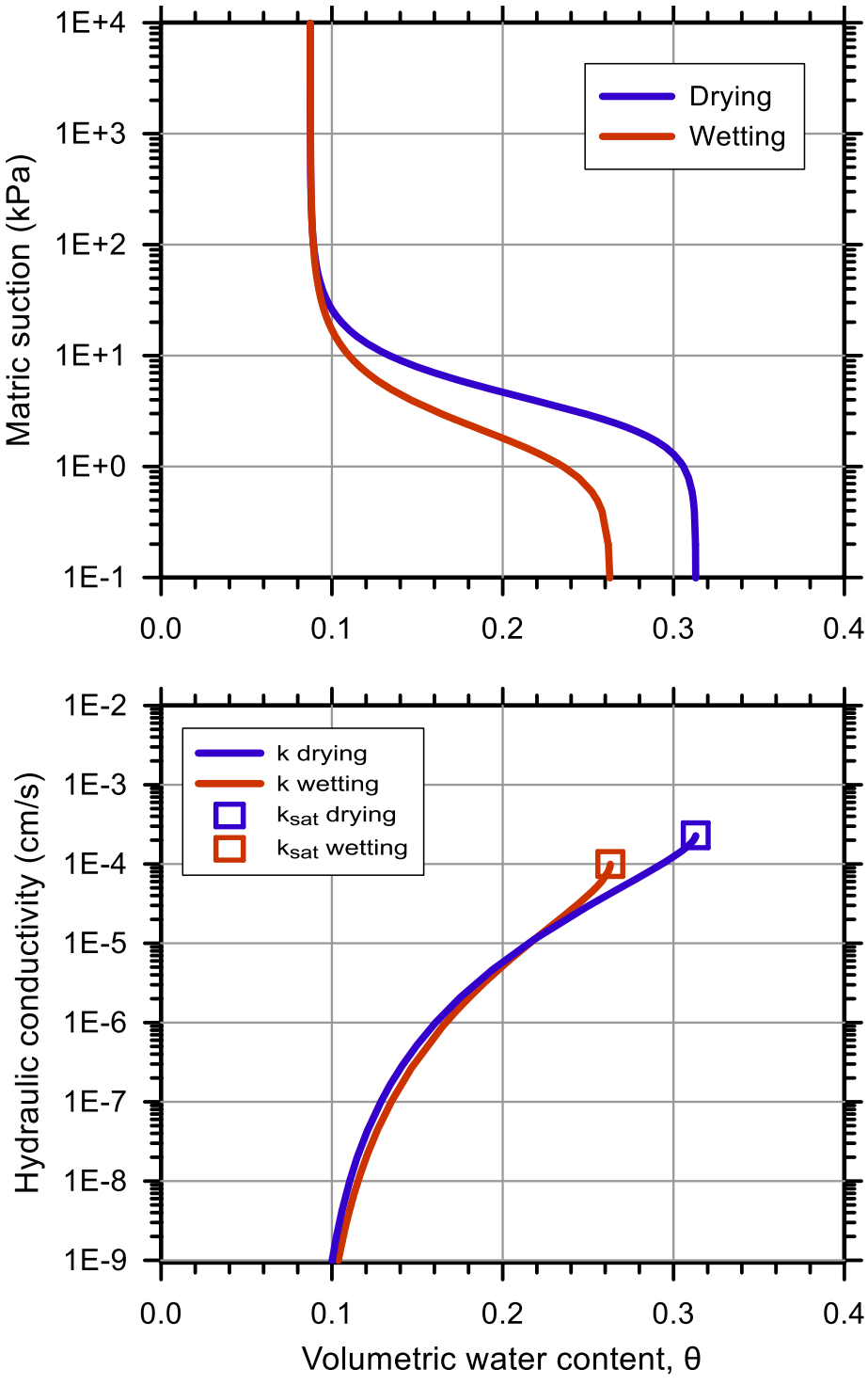
1E+4
1E+3
1E+2
1E+1
1E+0
1E-1
Matric suction (kPa)
Drying
Wetting
0.0
0.1
0.2
0.3
0.4
1E-2
1E-3
1E-4
1E-5
1E-6
1E-7
1E-8
1E-9
Hydraulic conductivity (cm/s)
k drying
k wetting
ksat drying
ksat wetting
0.0
0.1
0.2
0.3
0.4
Volumetric water content, θ

Test No.: 14

Test Ref.: TRIMM8X02

Test Soil: Sand-Clay (85%-15%)

Molding Water Content: 11.10% (w_{opt}+1.7)

Property	Before Saturation	After Saturation
Void Ratio, e	0.540	0.588
Porosity, n (%)	35.08	37.03
Std. Proctor Relative Compaction, RC (%)	88.81	86.15
Dry Density, γ_d (g/cm^3)	1.72	1.67

Unsaturated Hydraulic Soil Parameters	Drying	Wetting
Saturated Volumetric Water Content, θ_s	0.371	0.290
Residual Volumetric Water Content, θ_r	0.066	0.066
Air-Entry Pressure Parameter, α (1/kPa)	0.709	1.317
Pore-Size Distribution Parameter, n	2.500	2.338
Saturated Hydraulic Conductivity, k_{sat} (cm/s)	2.27E-03	9.00E-04

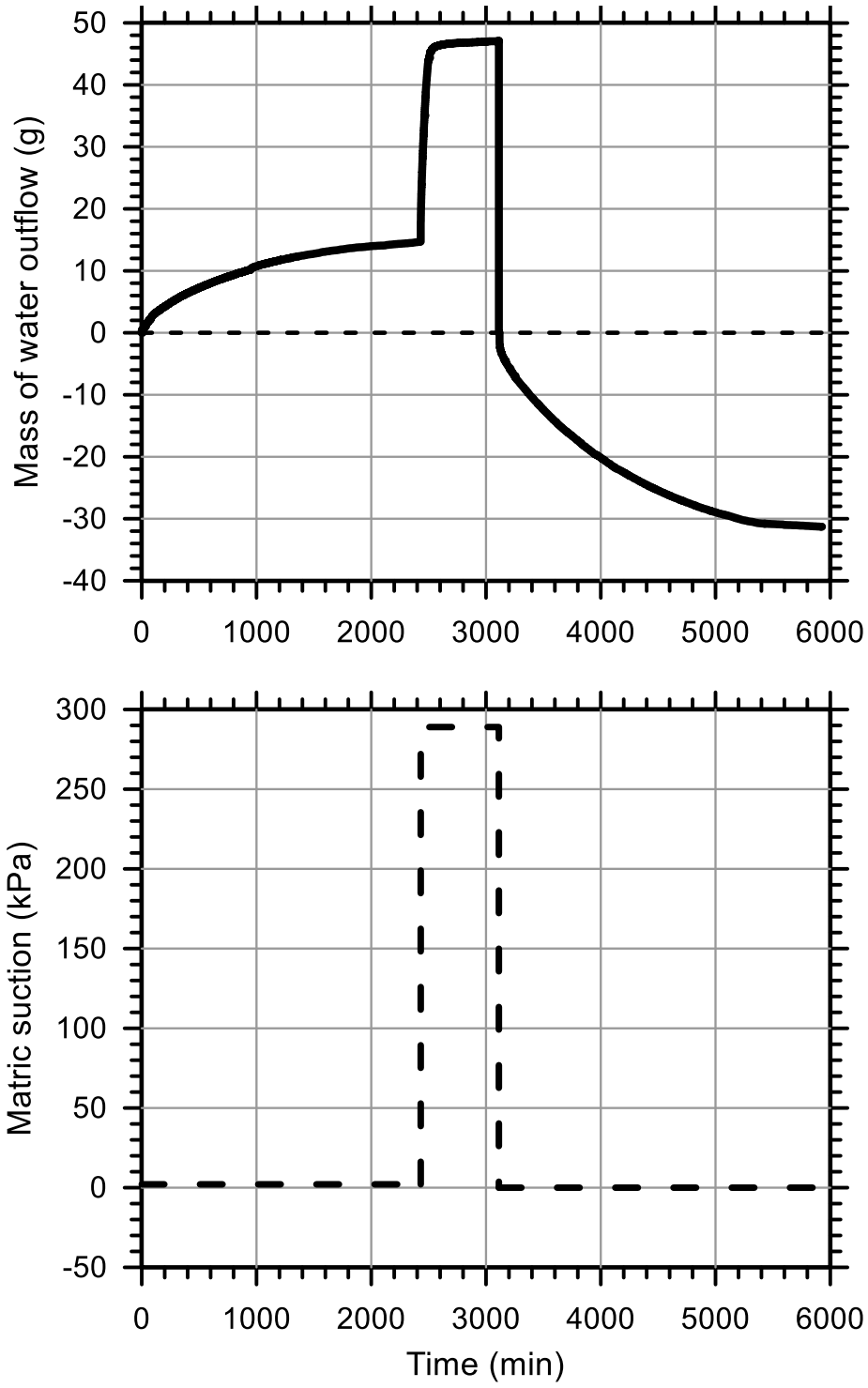
Mass of water outflow (g)
50
40
30
20
10
0
-10
-20
-30
-40
0
1000
2000
3000
4000
5000
6000
Matric suction (kPa)
300
250
200
150
100
50
0
-50
0
1000
2000
3000
4000
5000
6000
Time (min)

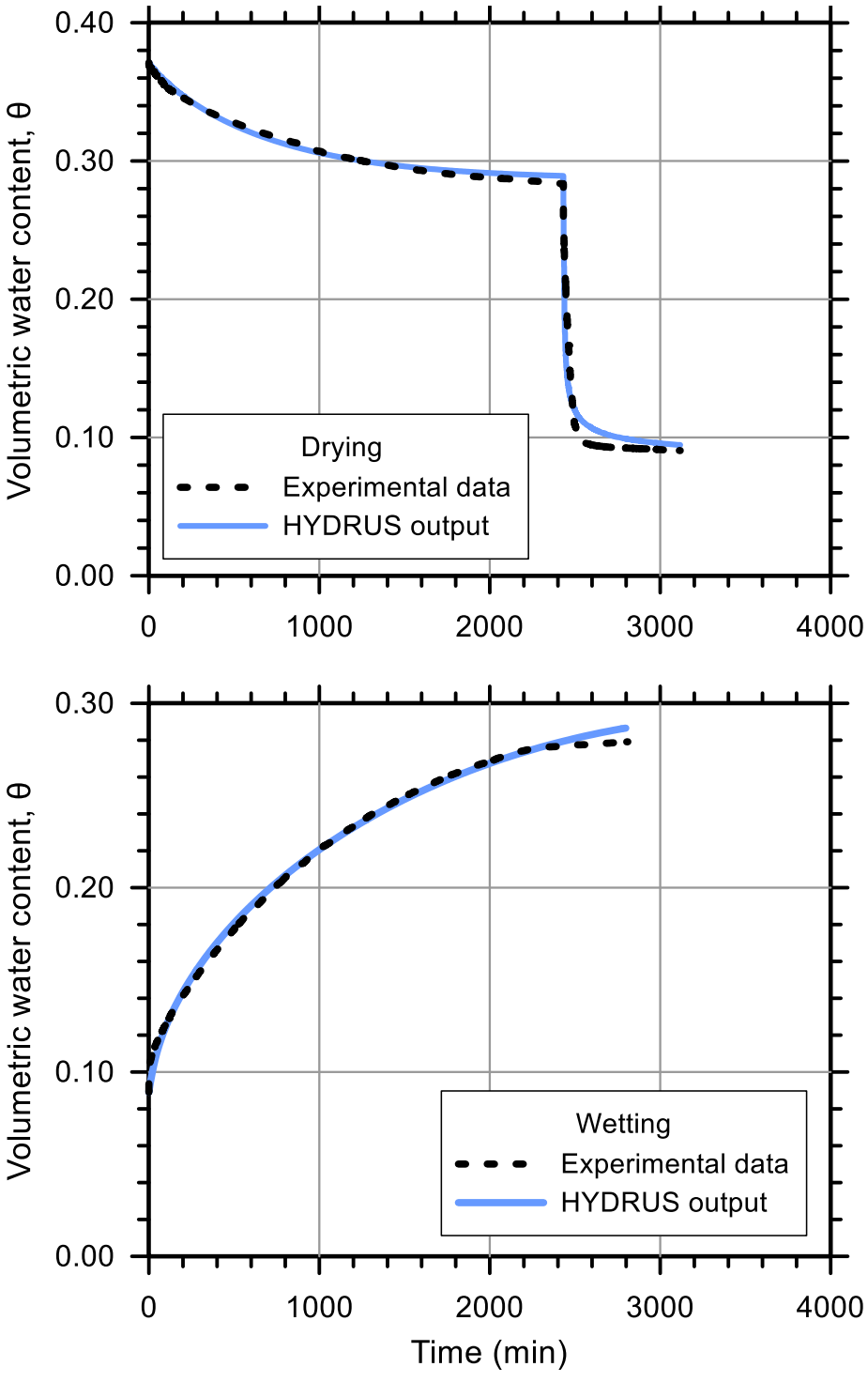
0.40
0.30
0.20
0.10
0.00
Volumetric water content, θ
Drying
Experimental data
HYDRUS output
0
1000
2000
3000
4000
0.30
0.20
0.10
0.00
Volumetric water content, θ
Wetting
Experimental data
HYDRUS output
0
1000
2000
3000
4000
Time (min)

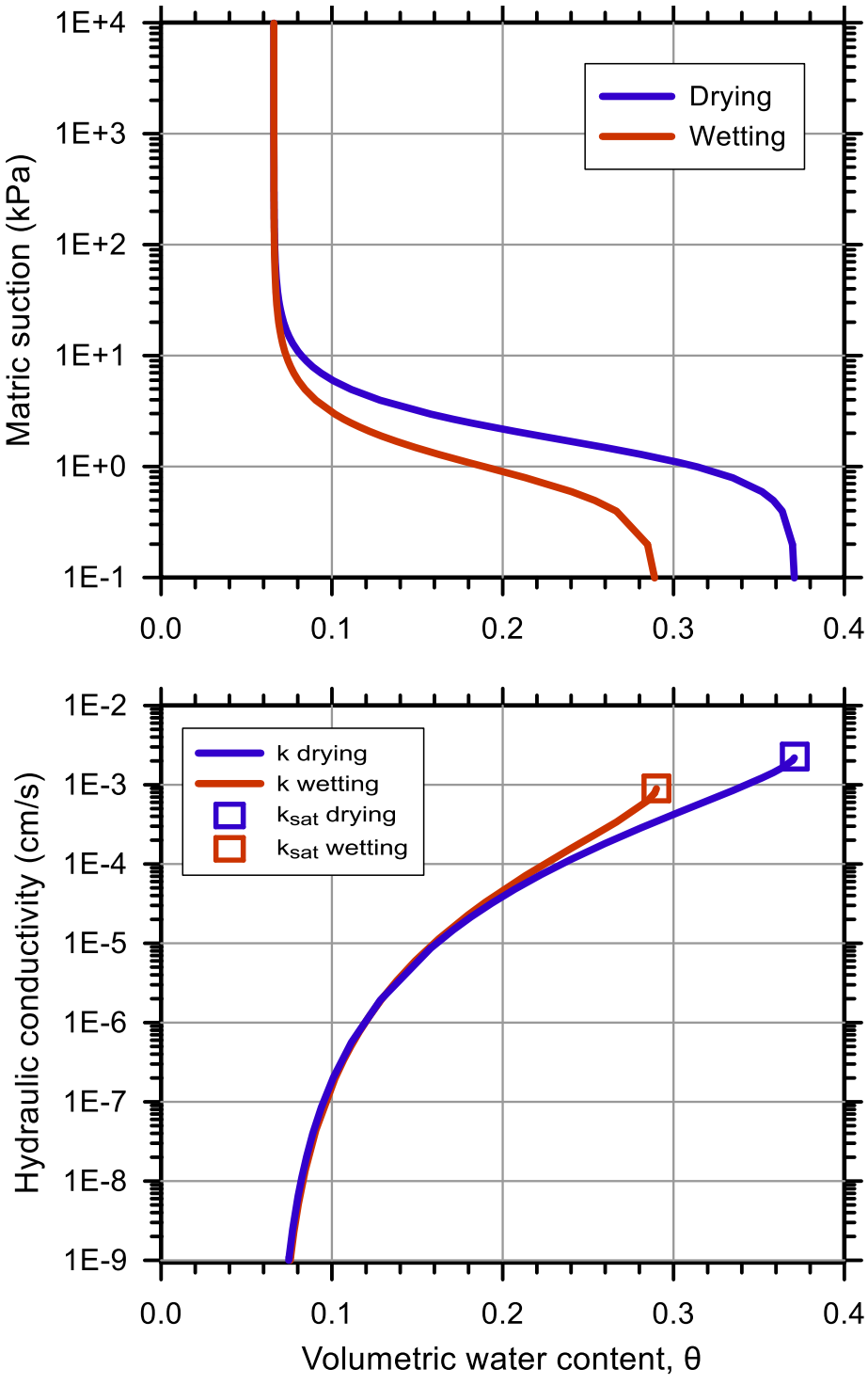
1E+4
1E+3
1E+2
1E+1
1E+0
1E-1
Matric suction (kPa)
Drying
Wetting
0.0
0.1
0.2
0.3
0.4
1E-2
1E-3
1E-4
1E-5
1E-6
1E-7
1E-8
1E-9
Hydraulic conductivity (cm/s)
k drying
k wetting
ksat drying
ksat wetting
0.0
0.1
0.2
0.3
0.4
Volumetric water content, θ

Test No.: 31

Test Ref.: TRIMPS01

Test Soil: Play Sand

Molding Water Content: 0%

Property	Before Saturation	After Saturation
Void Ratio, e	0.658	0.671
Porosity, n (%)	39.70	40.15
Std. Proctor Relative Compaction, RC (%)	92.53	91.84
Dry Density, γ_d (g/cm^3)	1.60	1.59

Unsaturated Hydraulic Soil Parameters	Drying	Wetting
Saturated Volumetric Water Content, θ_s	0.401	0.298
Residual Volumetric Water Content, θ_r	0.019	0.019
Air-Entry Pressure Parameter, α (1/kPa)	0.489	1.019
Pore-Size Distribution Parameter, n	3.081	3.160
Saturated Hydraulic Conductivity, k_{sat} (cm/s)	9.00E-03	3.00E-03

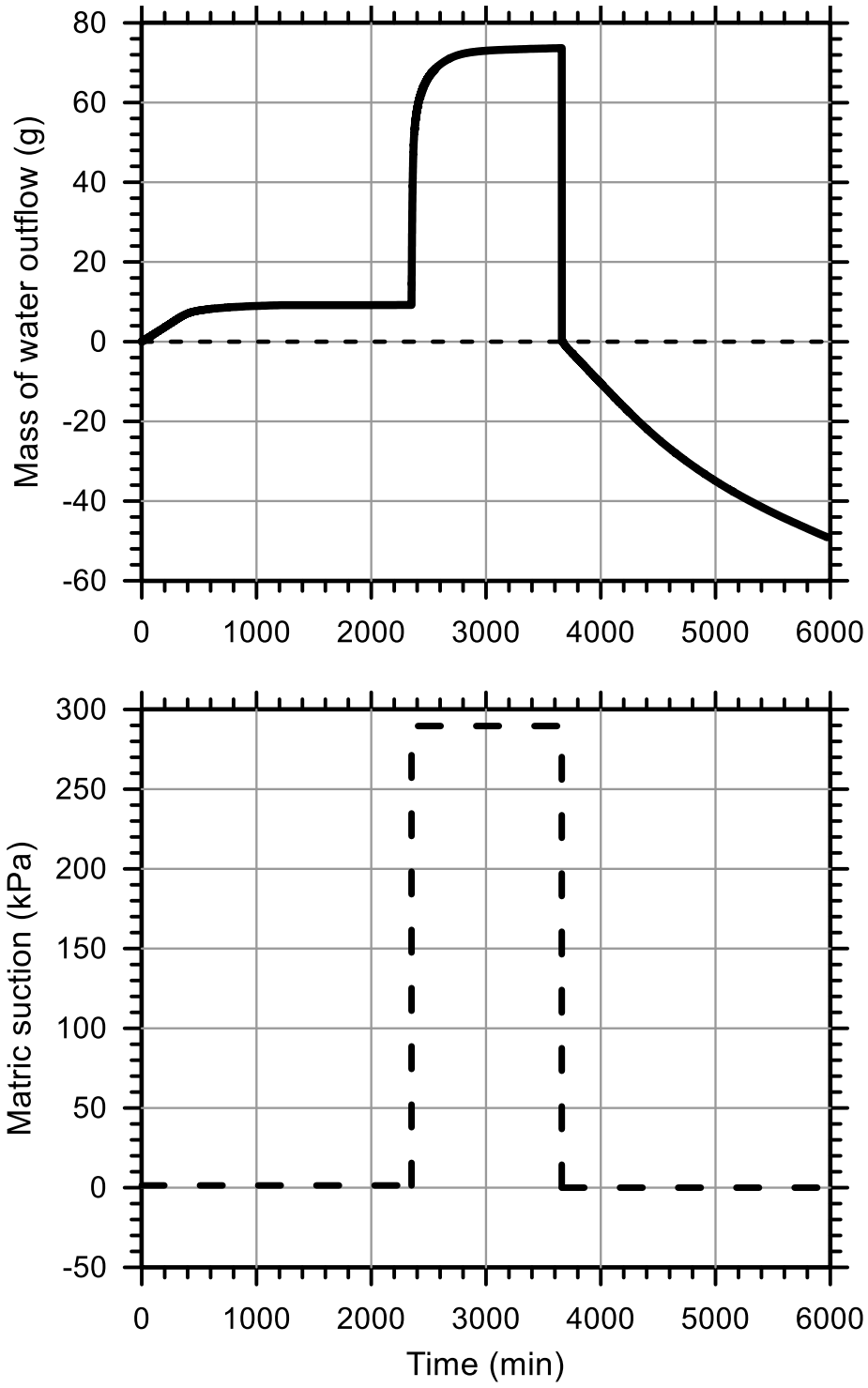
Mass of water outflow (g)
80
60
40
20
0
-20
-40
-60
0
1000
2000
3000
4000
5000
6000
Matric suction (kPa)
300
250
200
150
100
50
0
-50
0
1000
2000
3000
4000
5000
6000
Time (min)

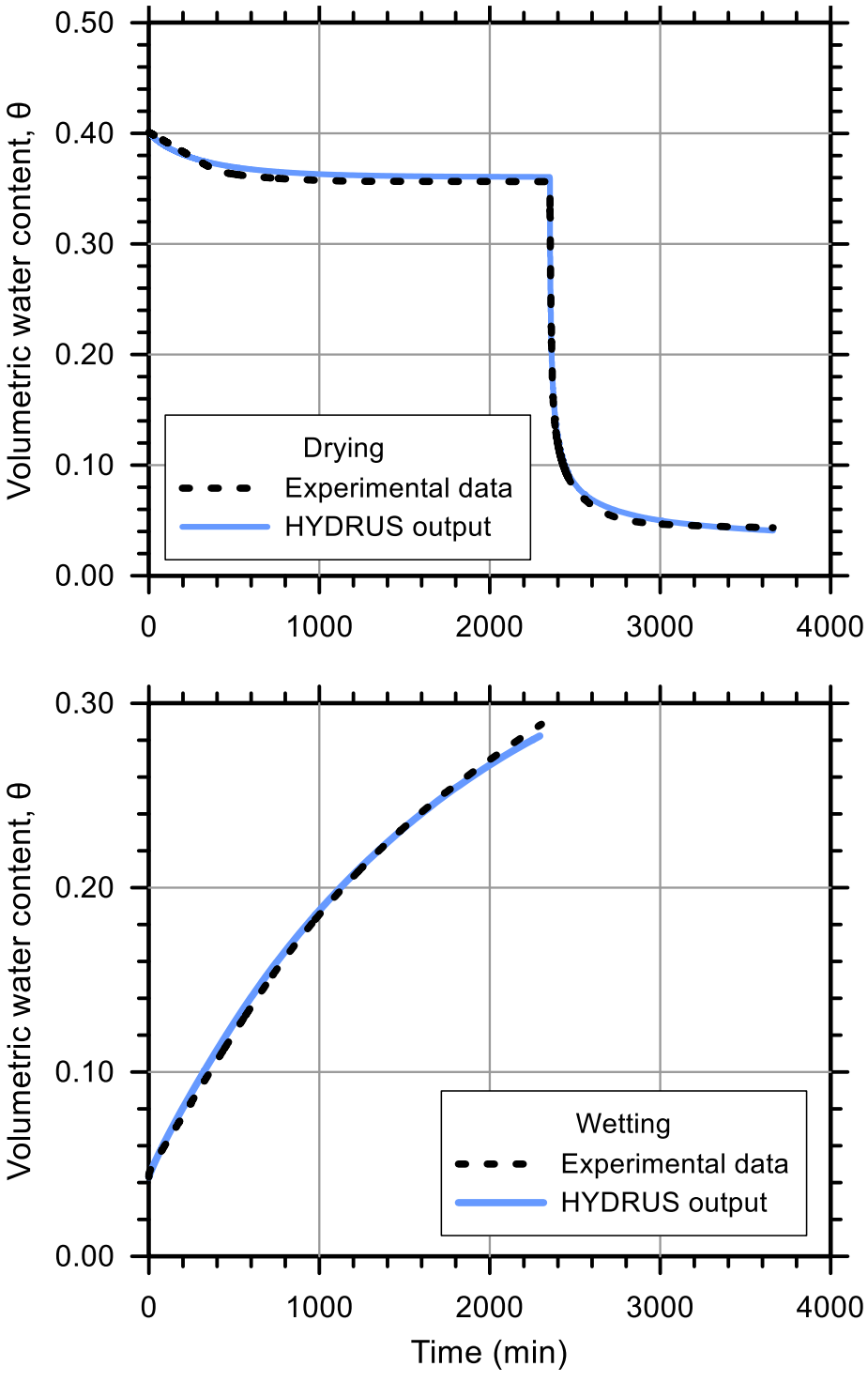
0.50
0.40
0.30
0.20
0.10
0.00
Volumetric water content, θ
Drying
Experimental data
HYDRUS output
0
1000
2000
3000
4000
0.30
0.20
0.10
0.00
Volumetric water content, θ
Wetting
Experimental data
HYDRUS output
0
1000
2000
3000
4000
Time (min)

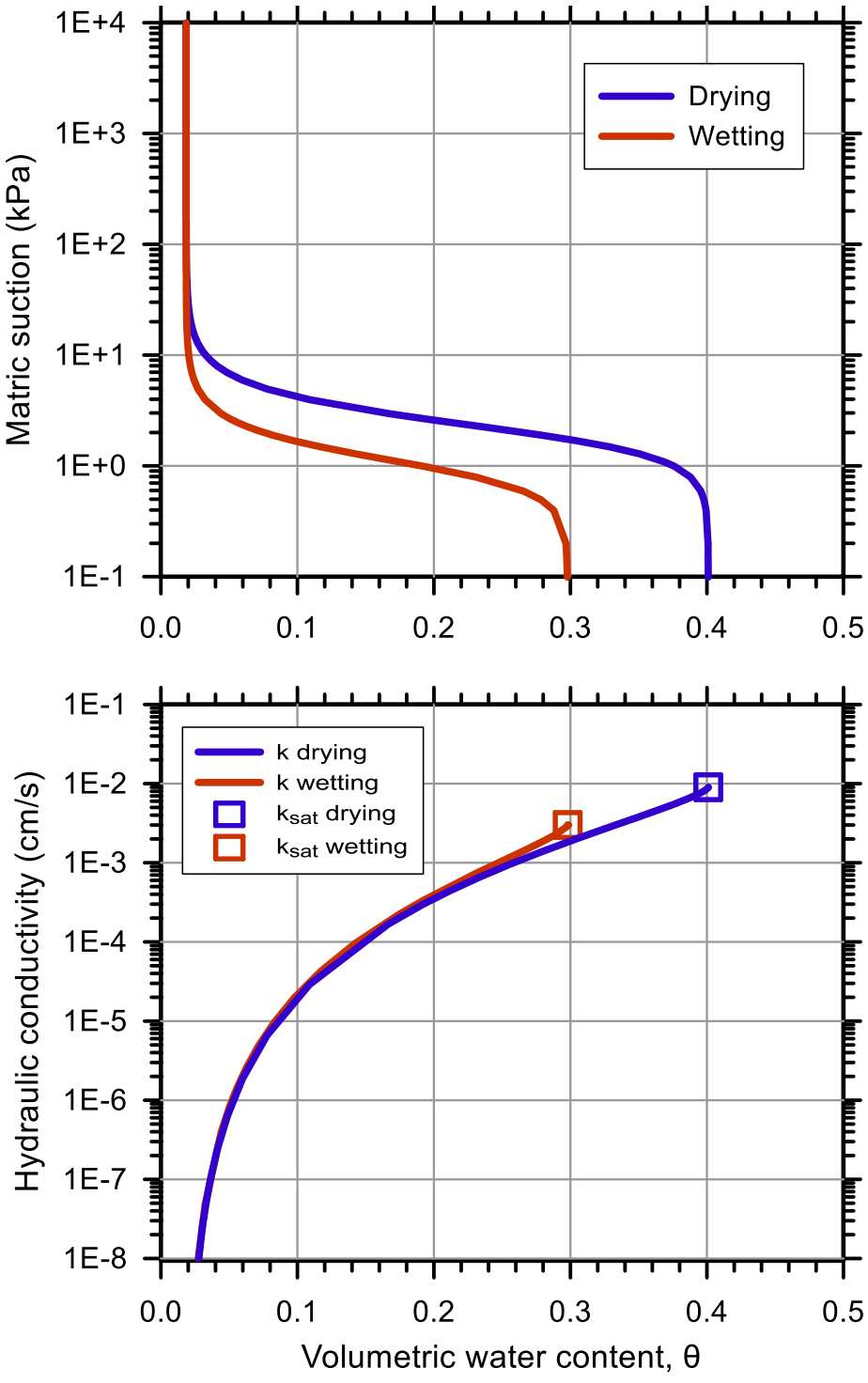
Matric suction (kPa)
1E+4
1E+3
1E+2
1E+1
1E+0
1E-1
0.0
0.1
0.2
0.3
0.4
0.5
Drying
Wetting
Hydraulic conductivity (cm/s)
1E-1
1E-2
1E-3
1E-4
1E-5
1E-6
1E-7
1E-8
k drying
k wetting
ksat drying
ksat wetting
Volumetric water content, θ

Test No.: 32

Test Ref.: TRIMKC01

Test Soil: Wilco LPC Kaolin Clay

Molding Water Content: 23.50% (PL)

Property	Before Saturation	After Saturation
Void Ratio, e	1.027	1.098
Porosity, n (%)	50.67	52.35
Std. Proctor Relative Compaction, RC (%)	-	-
Dry Density, γ_d (g/cm^3)	1.31	1.26

Unsaturated Hydraulic Soil Parameters	Drying	Wetting
Saturated Volumetric Water Content, θ_s	0.523	0.439
Residual Volumetric Water Content, θ_r	0.202	0.202
Air-Entry Pressure Parameter, α (1/kPa)	0.107	0.137
Pore-Size Distribution Parameter, n	1.206	1.208
Saturated Hydraulic Conductivity, k_{sat} (cm/s)	1.49E-03	1.00E-03

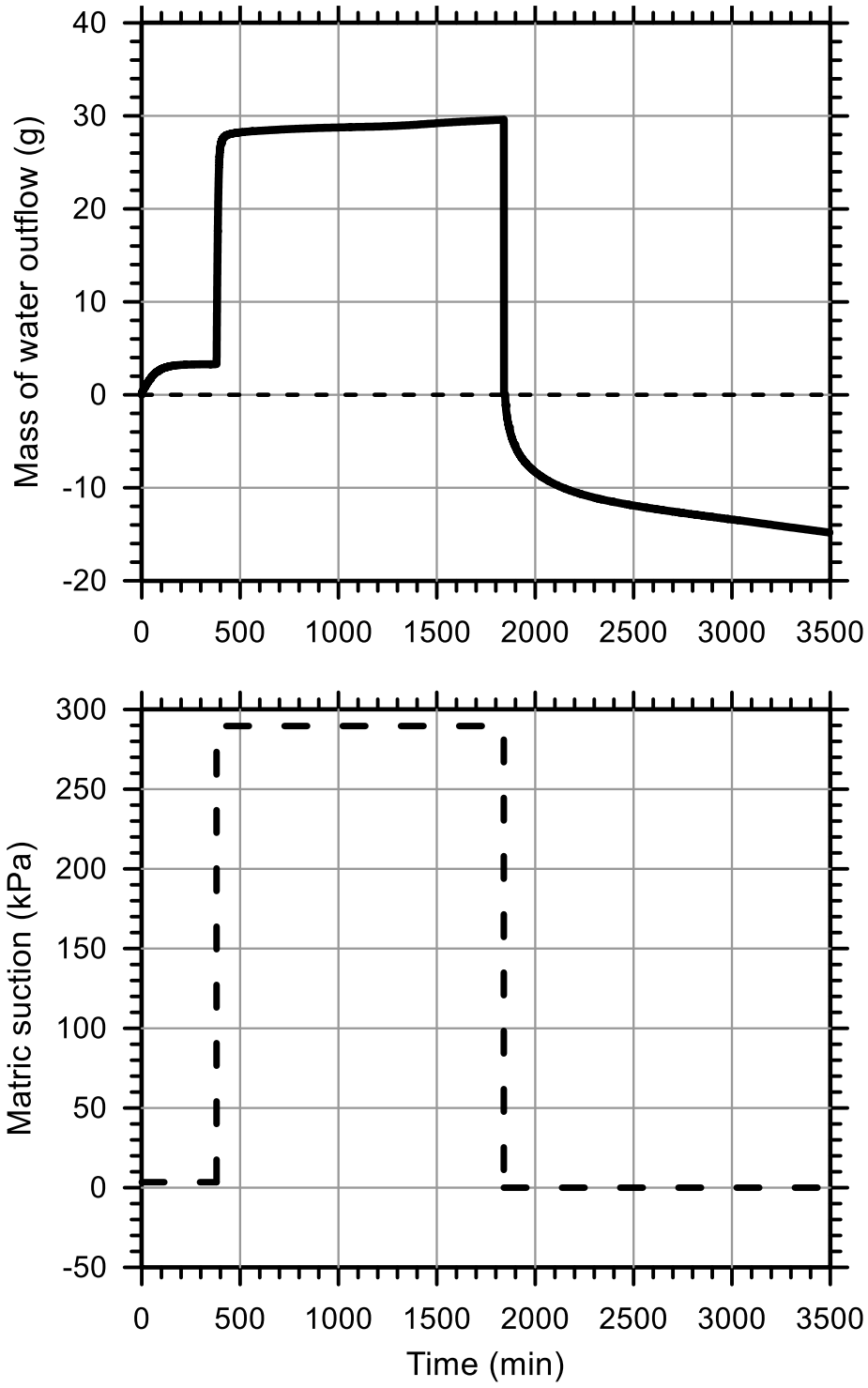
Mass of water outflow (g)
40
30
20
10
0
-10
-20
0
500
1000
1500
2000
2500
3000
3500
Matric suction (kPa)
300
250
200
150
100
50
0
-50
0
500
1000
1500
2000
2500
3000
3500
Time (min)

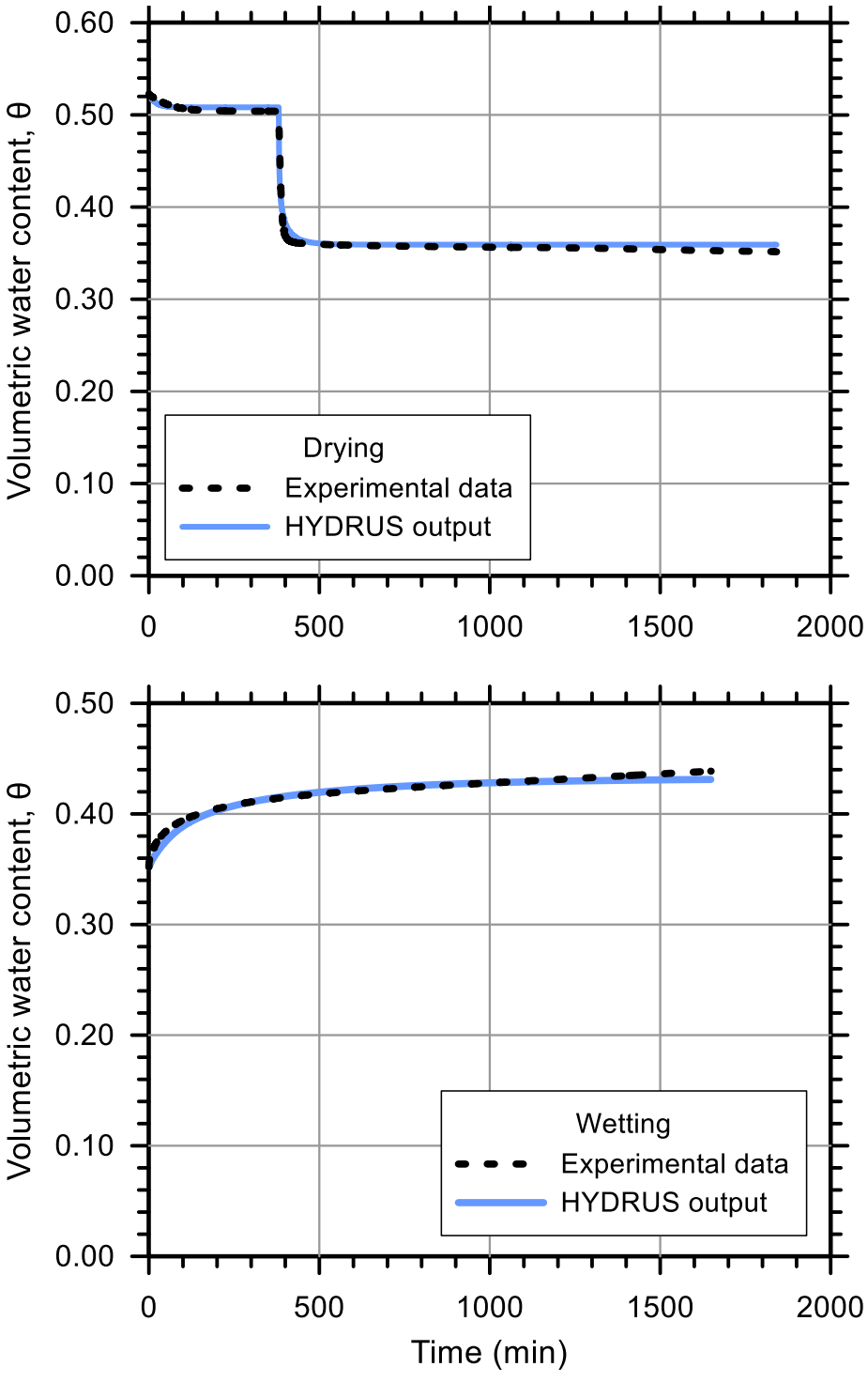
0.60
0.50
0.40
0.30
0.20
0.10
0.00
Volumetric water content, θ
Drying
Experimental data
HYDRUS output
0
500
1000
1500
2000
0.50
0.40
0.30
0.20
0.10
0.00
Volumetric water content, θ
Wetting
Experimental data
HYDRUS output
0
500
1000
1500
2000
Time (min)

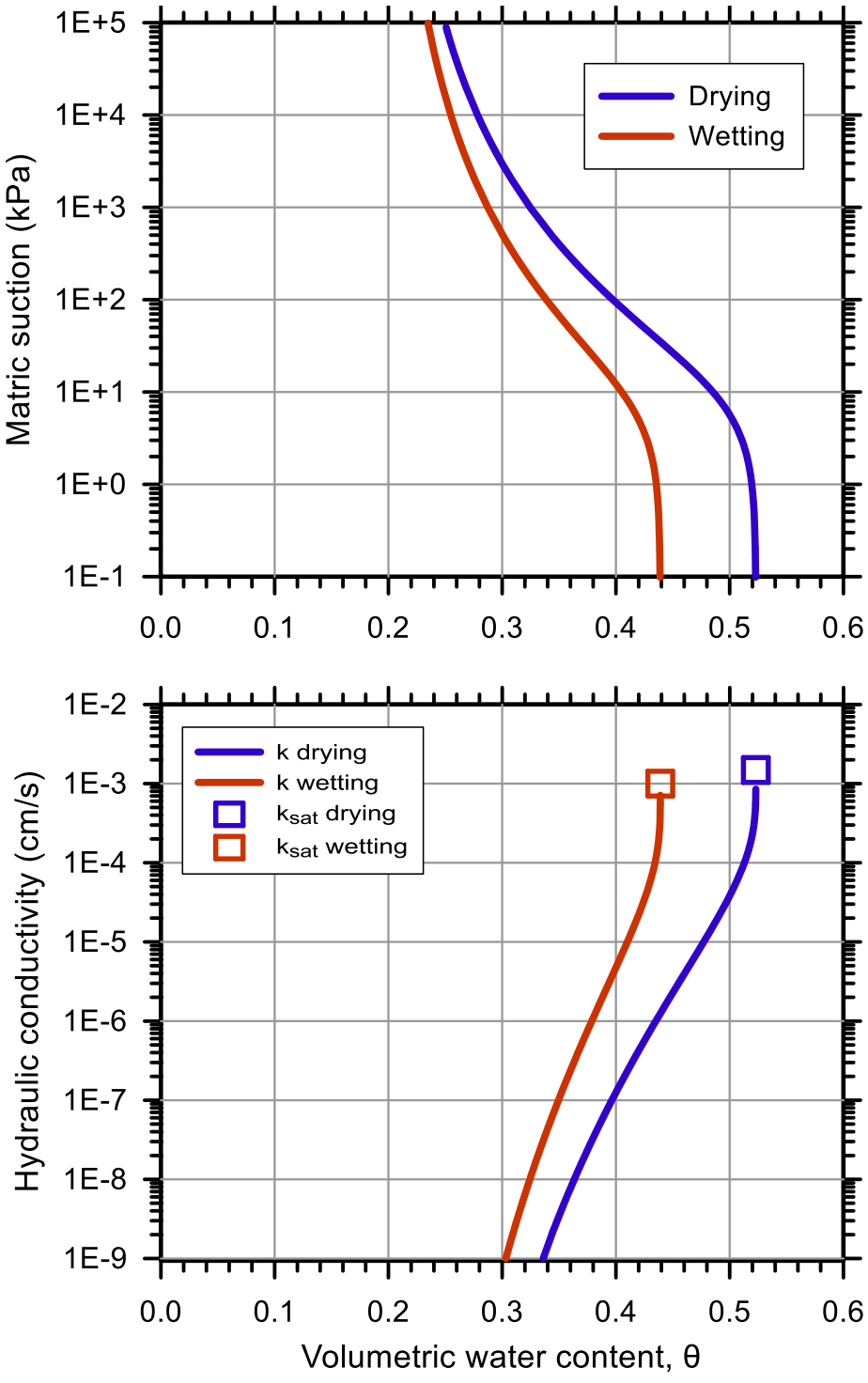
Matric suction (kPa)
1E+5
1E+4
1E+3
1E+2
1E+1
1E+0
1E-1
Drying
Wetting
0.0
0.1
0.2
0.3
0.4
0.5
0.6
Hydraulic conductivity (cm/s)
1E-2
1E-3
1E-4
1E-5
1E-6
1E-7
1E-8
1E-9
k drying
k wetting
ksat drying
ksat wetting
Volumetric water content, θ

Test No.: 35

Test Ref.: TRIMKC02

Test Soil: Wilco LPC Kaolin Clay

Molding Water Content: 23.50% (PL)

Property	Before Saturation	After Saturation
Void Ratio, e	1.245	1.308
Porosity, n (%)	55.45	56.66
Std. Proctor Relative Compaction, RC (%)	-	-
Dry Density, γ_d (g/cm^3)	1.18	1.15

Unsaturated Hydraulic Soil Parameters	Drying	Wetting
Saturated Volumetric Water Content, θ_s	0.567	0.429
Residual Volumetric Water Content, θ_r	0.178	0.178
Air-Entry Pressure Parameter, α (1/kPa)	0.265	0.275
Pore-Size Distribution Parameter, n	1.215	1.205
Saturated Hydraulic Conductivity, k_{sat} (cm/s)	2.21E-02	9.74E-03

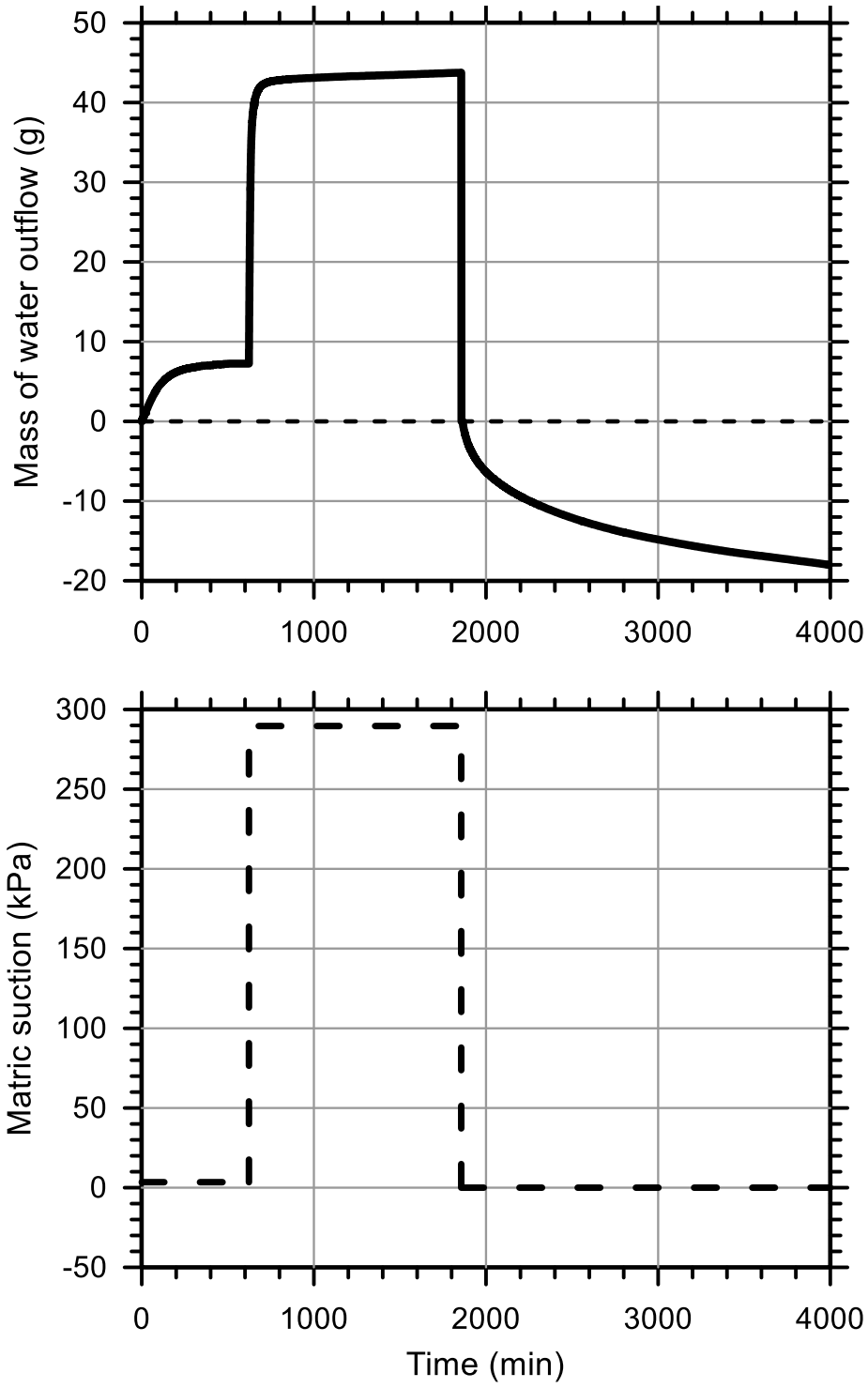
Mass of water outflow (g)
50
40
30
20
10
0
-10
-20
0
1000
2000
3000
4000
Matric suction (kPa)
300
250
200
150
100
50
0
-50
0
1000
2000
3000
4000
Time (min)

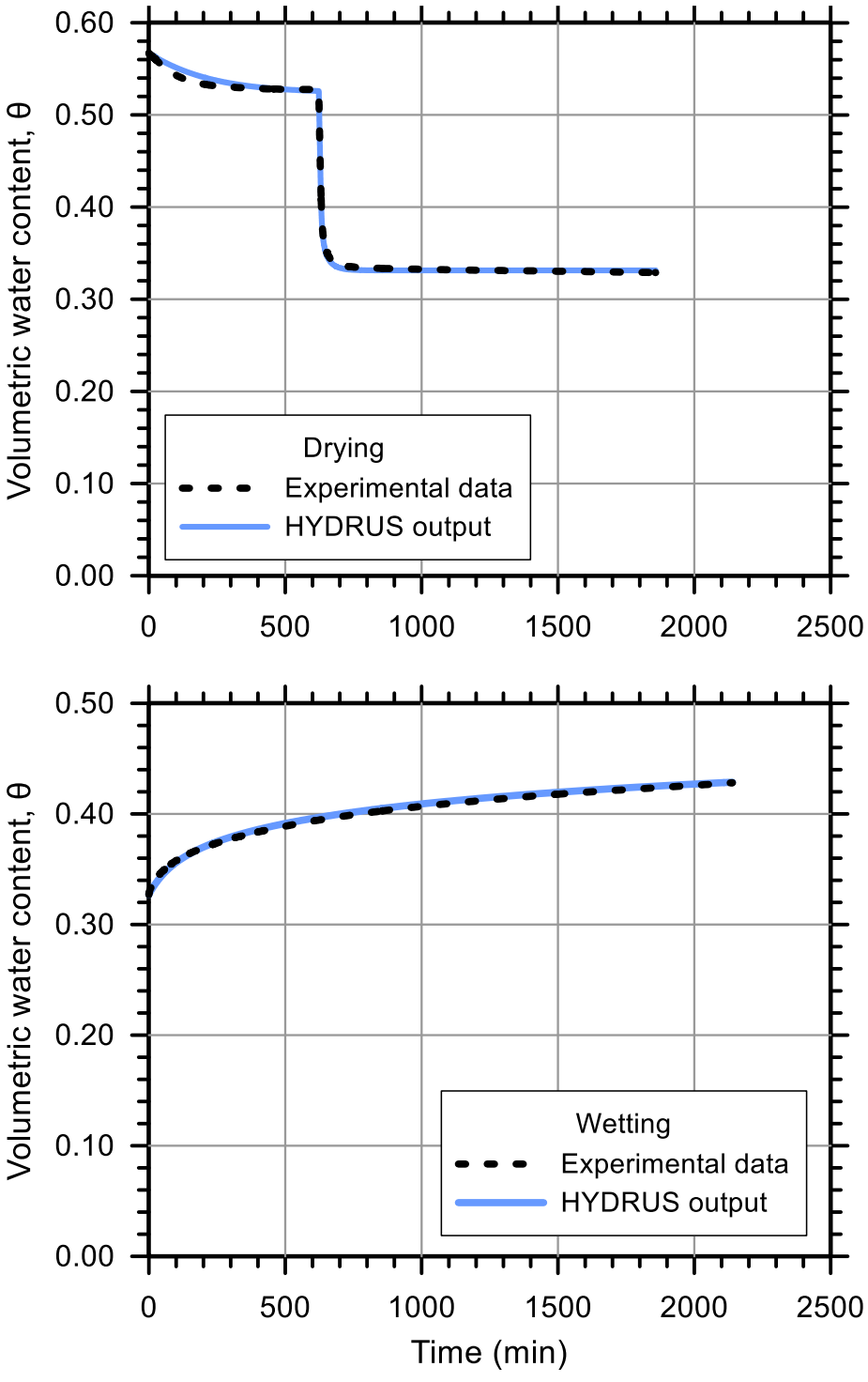
0.60
0.50
0.40
0.30
0.20
0.10
0.00
Volumetric water content, θ
Drying
Experimental data
HYDRUS output
0
500
1000
1500
2000
2500
0.50
0.40
0.30
0.20
0.10
0.00
Volumetric water content, θ
Wetting
Experimental data
HYDRUS output
0
500
1000
1500
2000
2500
Time (min)

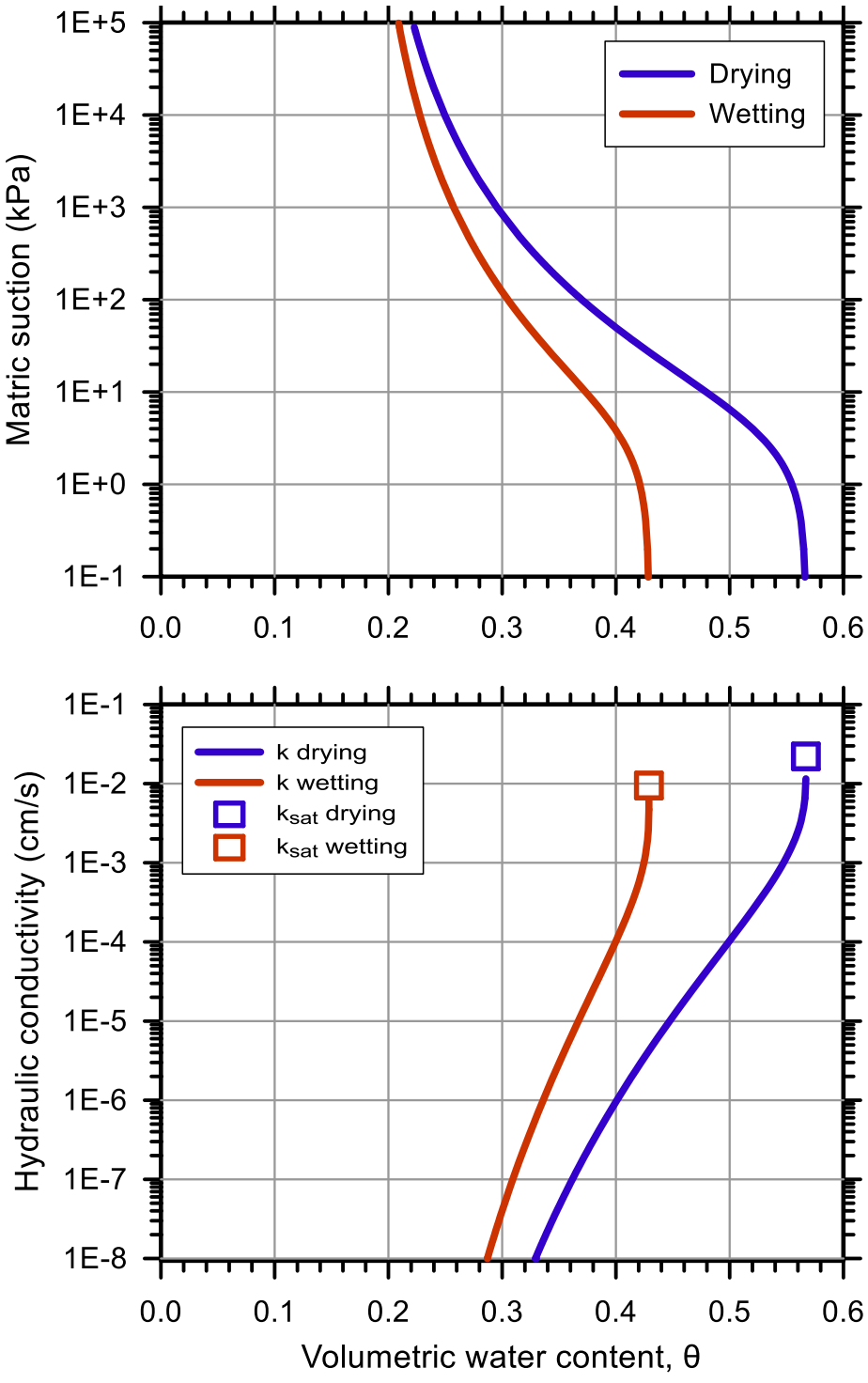
Matric suction (kPa)
1E+5
1E+4
1E+3
1E+2
1E+1
1E+0
1E-1
0.0
0.1
0.2
0.3
0.4
0.5
0.6
Drying
Wetting
Hydraulic conductivity (cm/s)
1E-1
1E-2
1E-3
1E-4
1E-5
1E-6
1E-7
1E-8
k drying
k wetting
ksat drying
ksat wetting
Volumetric water content, θ

APPENDIX B – FLEXIBLE WALL SATURATED HYDRAULIC CONDUCTIVITY TEST RESULTS

Test No.: 35

Test Ref.: FXSC35

Test Soil: Stroubles Creek

Molding Water Content: 19.60% (w_{opt}-3)

Property	Before Test	After Test
Total Mass (g)	342.00	372.10
Mass of Solids (g)	285.95	285.94
Mass of Water (g)	56.05	86.16
Total Volume (cm^3)	200.80	197.29
Volume of Solids (cm^3)	110.83	110.83
Volume of Water (cm^3)	56.05	86.16
Volume of Air (cm^3)	33.92	0.30
Water Content (%)	19.60	30.13
Volume of Voids (cm^3)	89.96	86.46
Void Ratio, e	0.812	0.780
Porosity, n (%)	0.448	0.438
Std. Proctor Relative Compaction, RC (%)	91.88	93.51
Moist Density, γ_m (g/cm^3)	1.70	1.89
Dry Density, γ_d (g/cm^3)	1.42	1.45
Degree of Saturation, S (%)	62.30	99.65
Consolidation Cell Pressure (kPa)	482.7	
Consolidation Back Pressure (kPa)	413.7	
Effective Consolidation Pressure (kPa)	69.0	

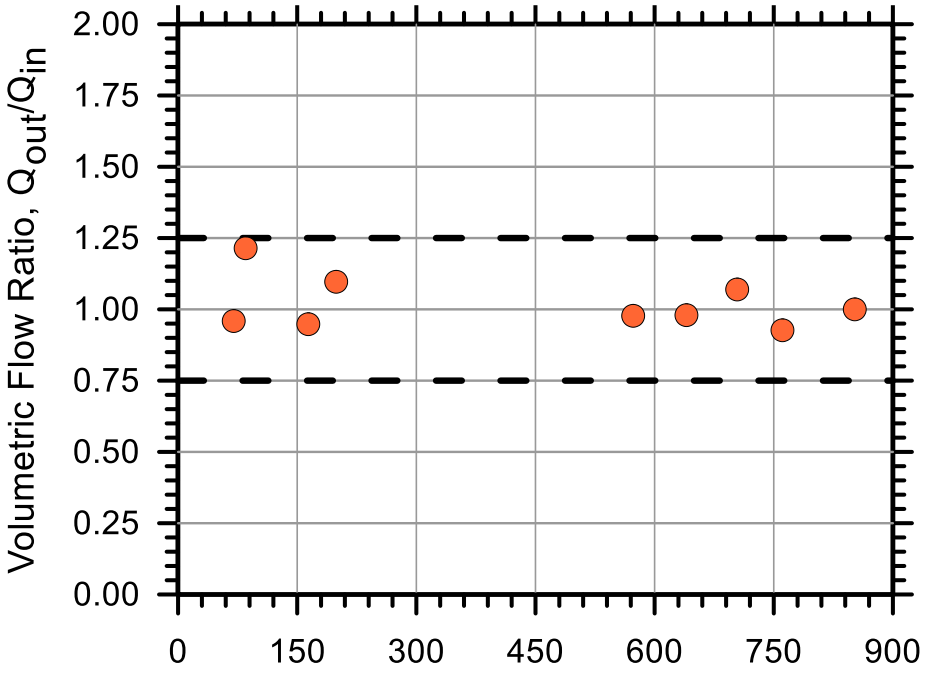
Volumetric Flow Ratio, Q_{out}/Q_{in}
2.00
1.75
1.50
1.25
1.00
0.75
0.50
0.25
0.00
0
150
300
450
600
750
900

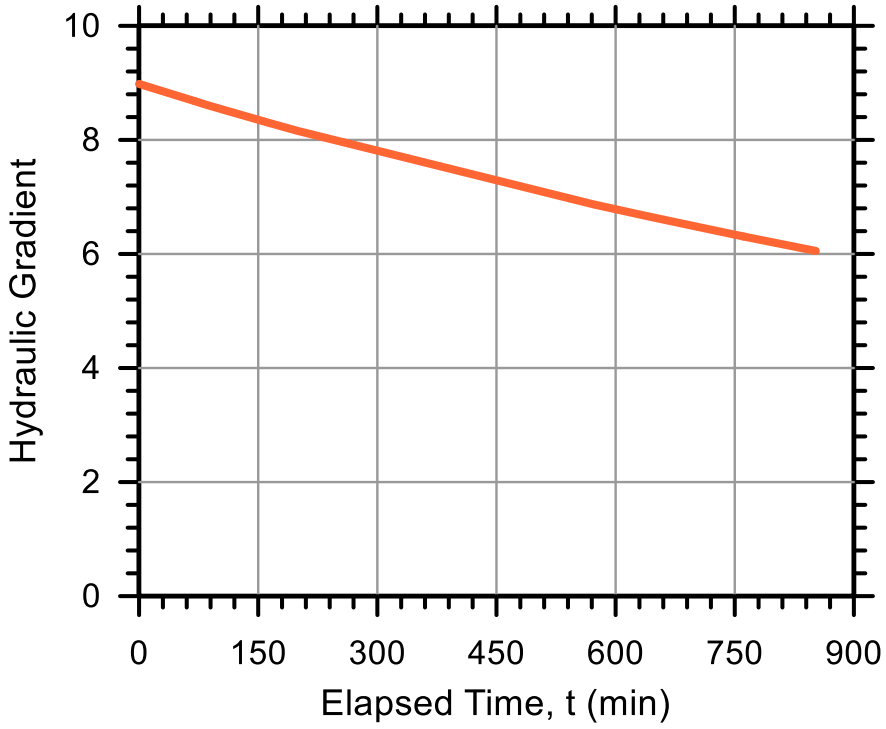
Hydraulic Gradient
10
8
6
4
2
0
0
150
300
450
600
750
900
Elapsed Time, t (min)

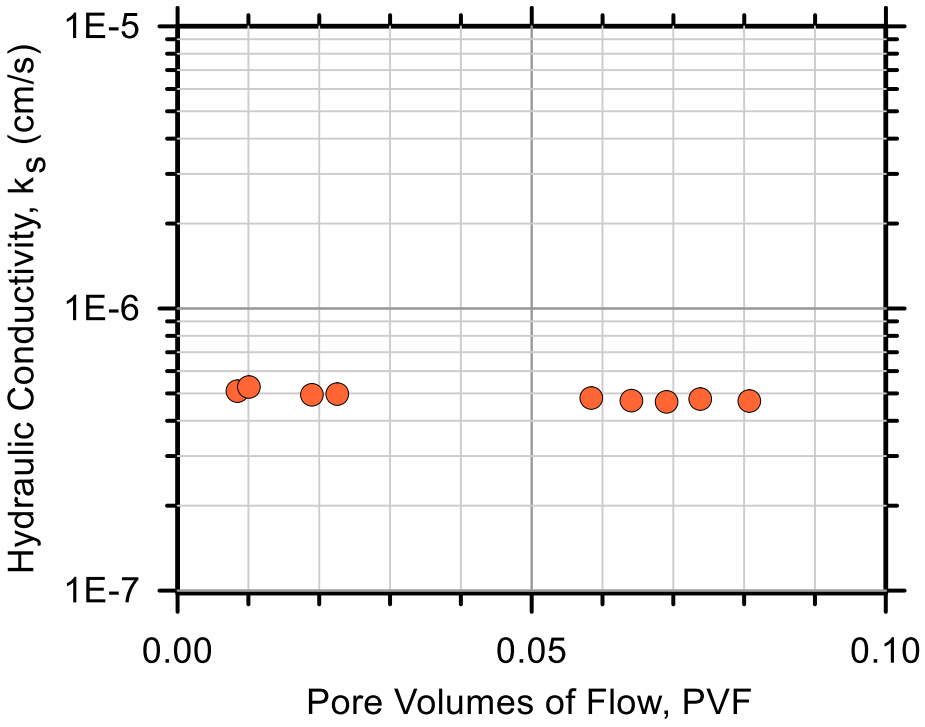
1E-5
1E-6
1E-7
Hydraulic Conductivity, k_s (cm/s)
0.00
0.05
0.10
Pore Volumes of Flow, PVF

Test No.: 40

Test Ref.: FXSC40

Test Soil: Stroubles Creek

Molding Water Content: 19.60% (w_{opt}-3)

Property	Before Test	After Test
Total Mass (g)	310.00	348.19
Mass of Solids (g)	259.20	259.15
Mass of Water (g)	50.80	89.04
Total Volume (cm^3)	201.81	189.73
Volume of Solids (cm^3)	100.46	100.44
Volume of Water (cm^3)	50.80	89.04
Volume of Air (cm^3)	50.54	0.24
Water Content (%)	19.60	34.36
Volume of Voids (cm^3)	101.34	89.28
Void Ratio, e	1.009	0.889
Porosity, n (%)	0.502	0.471
Std. Proctor Relative Compaction, RC (%)	82.86	88.12
Moist Density, γ_m (g/cm^3)	1.54	1.84
Dry Density, γ_d (g/cm^3)	1.28	1.37
Degree of Saturation, S (%)	50.13	99.73
Consolidation Cell Pressure (kPa)	441.3	
Consolidation Back Pressure (kPa)	413.7	
Effective Consolidation Pressure (kPa)	27.6	

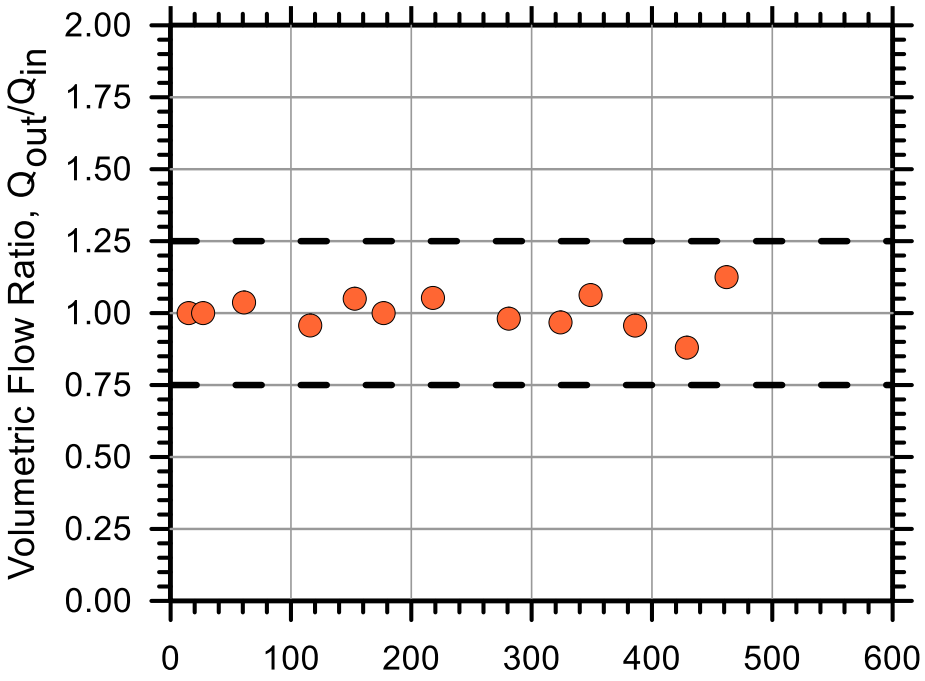
Volumetric Flow Ratio, Q_{out}/Q_{in}
2.00
1.75
1.50
1.25
1.00
0.75
0.50
0.25
0.00
0
100
200
300
400
500
600

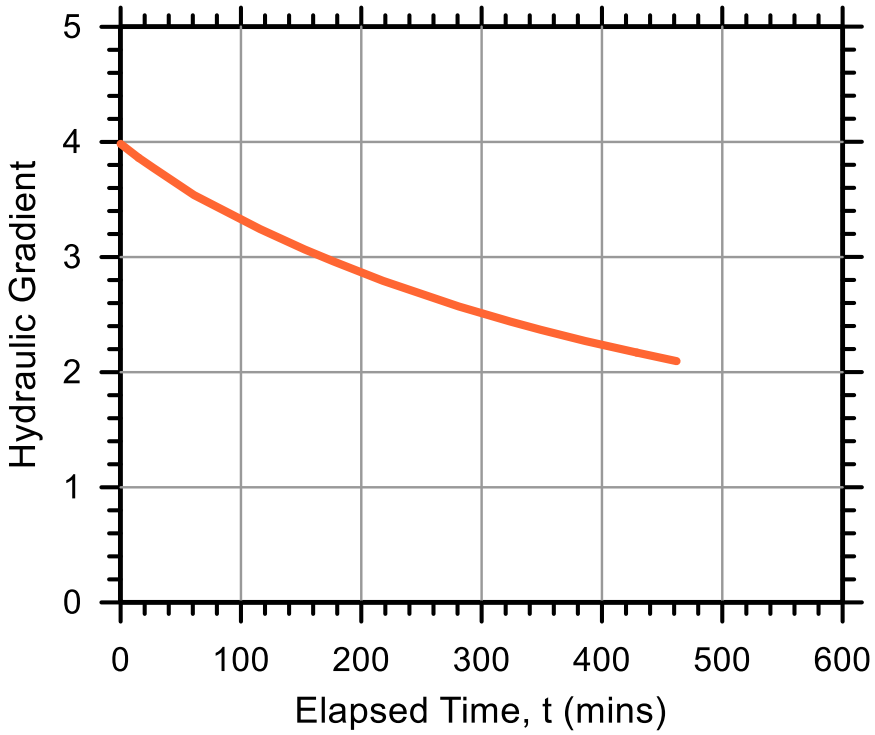
Hydraulic Gradient
5
4
3
2
1
0
0
100
200
300
400
500
600
Elapsed Time, t (mins)

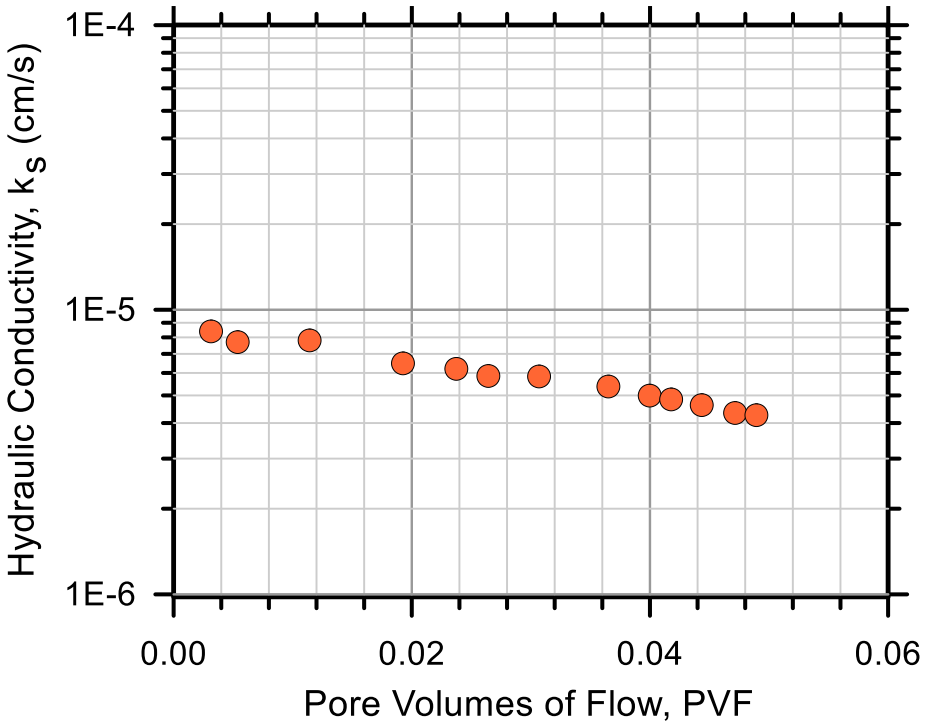
1E-4
1E-5
1E-6
Hydraulic Conductivity, k_S (cm/s)
0.00
0.02
0.04
0.06
Pore Volumes of Flow, PVF

Test No.: 10

Test Ref.: FXSC10

Test Soil: Stroubles Creek

Molding Water Content: 19.60% (w_{opt}-3)

Property	Before Test	After Test
Total Mass (g)	158.00	178.50
Mass of Solids (g)	132.11	131.10
Mass of Water (g)	25.89	47.40
Total Volume (cm^3)	100.90	98.58
Volume of Solids (cm^3)	51.20	50.81
Volume of Water (cm^3)	25.89	47.40
Volume of Air (cm^3)	23.81	0.36
Water Content (%)	19.60	36.16
Volume of Voids (cm^3)	49.70	47.77
Void Ratio, e	0.971	0.940
Porosity, n (%)	0.493	0.485
Std. Proctor Relative Compaction, RC (%)	84.47	85.80
Moist Density, γ_m (g/cm^3)	1.57	1.81
Dry Density, γ_d (g/cm^3)	1.31	1.33
Degree of Saturation, S (%)	52.10	99.24
Consolidation Cell Pressure (kPa)	420.6	
Consolidation Back Pressure (kPa)	413.7	
Effective Consolidation Pressure (kPa)	6.9	

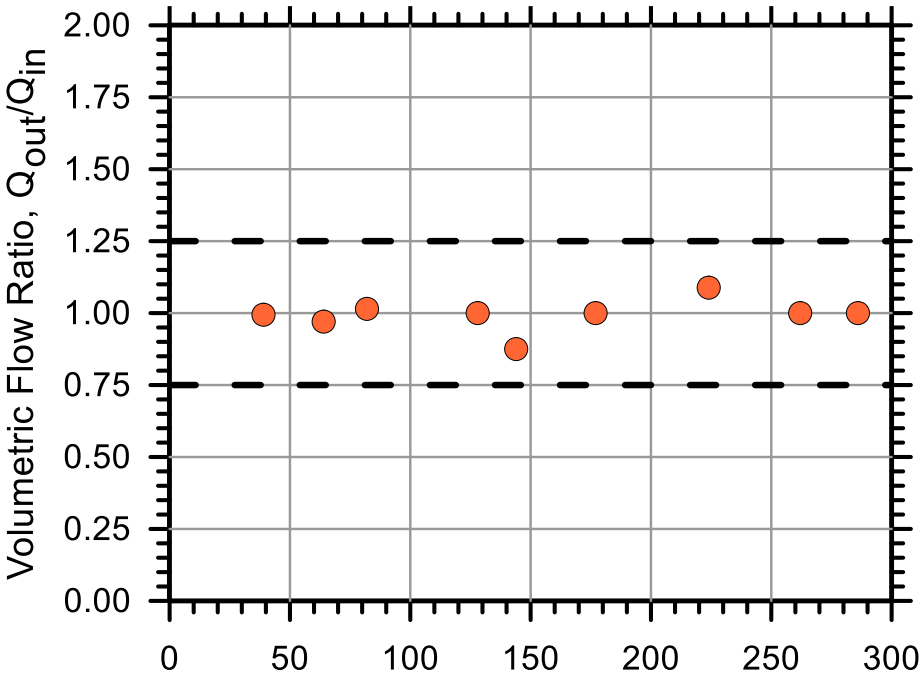
Volumetric Flow Ratio, Q_{out}/Q_{in}
2.00
1.75
1.50
1.25
1.00
0.75
0.50
0.25
0.00
0
50
100
150
200
250
300

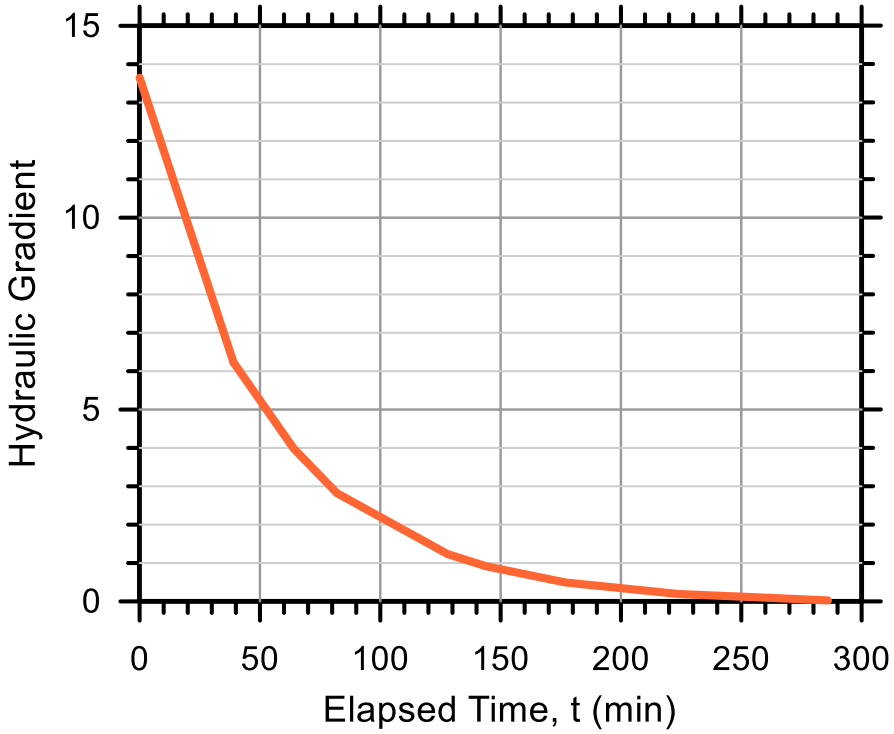
Hydraulic Gradient
15
10
5
0
0
50
100
150
200
250
300
Elapsed Time, t (min)

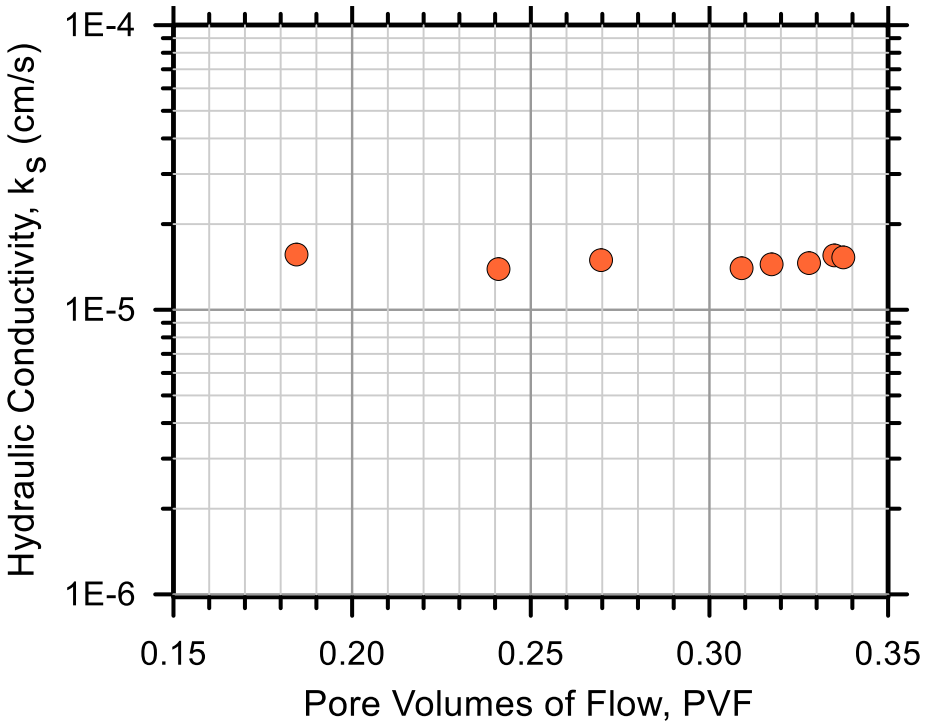
1E-4
1E-5
1E-6
Hydraulic Conductivity, k_S (cm/s)
0.15
0.20
0.25
0.30
0.35
Pore Volumes of Flow, PVF

Test No.: 36

Test Ref.: FXSC36

Test Soil: Stroubles Creek

Molding Water Content: 22.60% (w_{opt})

Property	Before Test	After Test
Total Mass (g)	347.00	366.88
Mass of Solids (g)	283.03	282.54
Mass of Water (g)	63.97	84.34
Total Volume (cm^3)	201.81	193.86
Volume of Solids (cm^3)	109.70	109.51
Volume of Water (cm^3)	63.97	84.34
Volume of Air (cm^3)	28.14	0.01
Water Content (%)	22.60	29.85
Volume of Voids (cm^3)	92.10	84.35
Void Ratio, e	0.840	0.770
Porosity, n (%)	0.456	0.435
Std. Proctor Relative Compaction, RC (%)	90.48	94.03
Moist Density, γ_m (g/cm^3)	1.72	1.89
Dry Density, γ_d (g/cm^3)	1.40	1.46
Degree of Saturation, S (%)	69.45	99.99
Consolidation Cell Pressure (kPa)	482.7	
Consolidation Back Pressure (kPa)	413.7	
Effective Consolidation Pressure (kPa)	69.0	

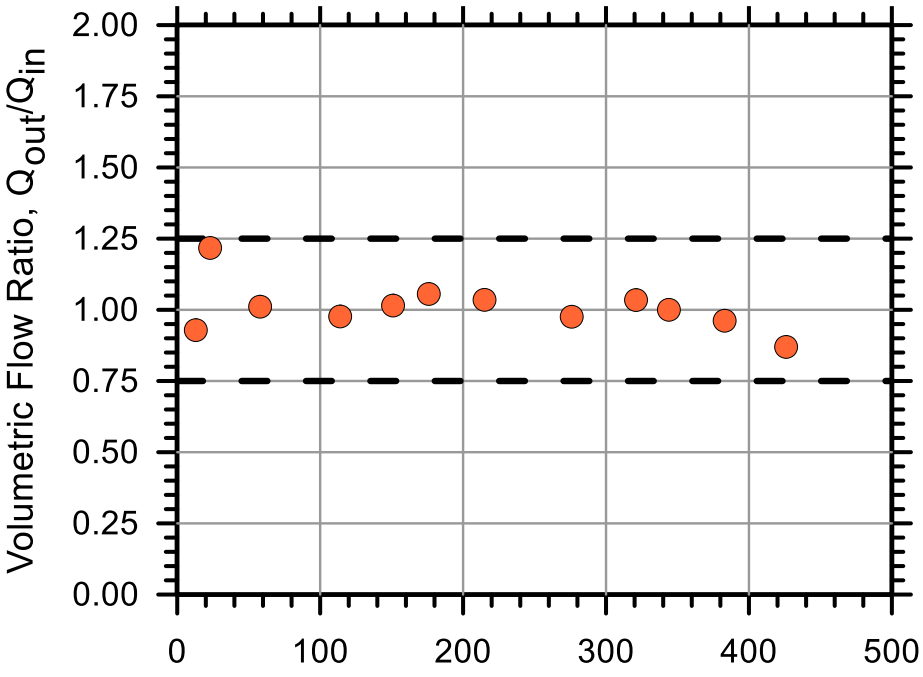
Volumetric Flow Ratio, Q_{out}/Q_{in}
2.00
1.75
1.50
1.25
1.00
0.75
0.50
0.25
0.00
0
100
200
300
400
500

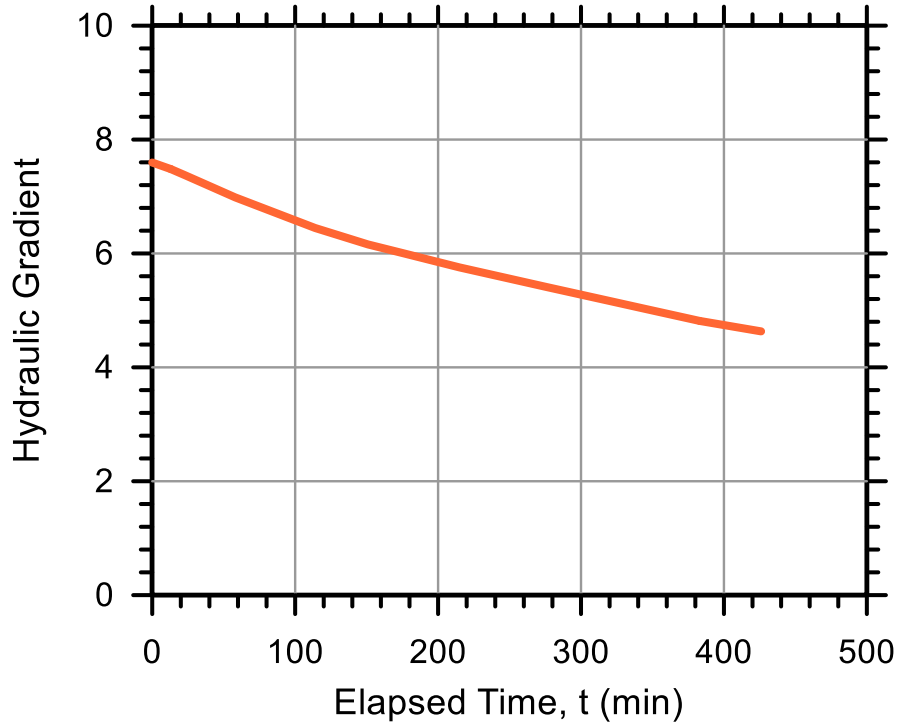
Hydraulic Gradient
10
8
6
4
2
0
0
100
200
300
400
500
Elapsed Time, t (min)

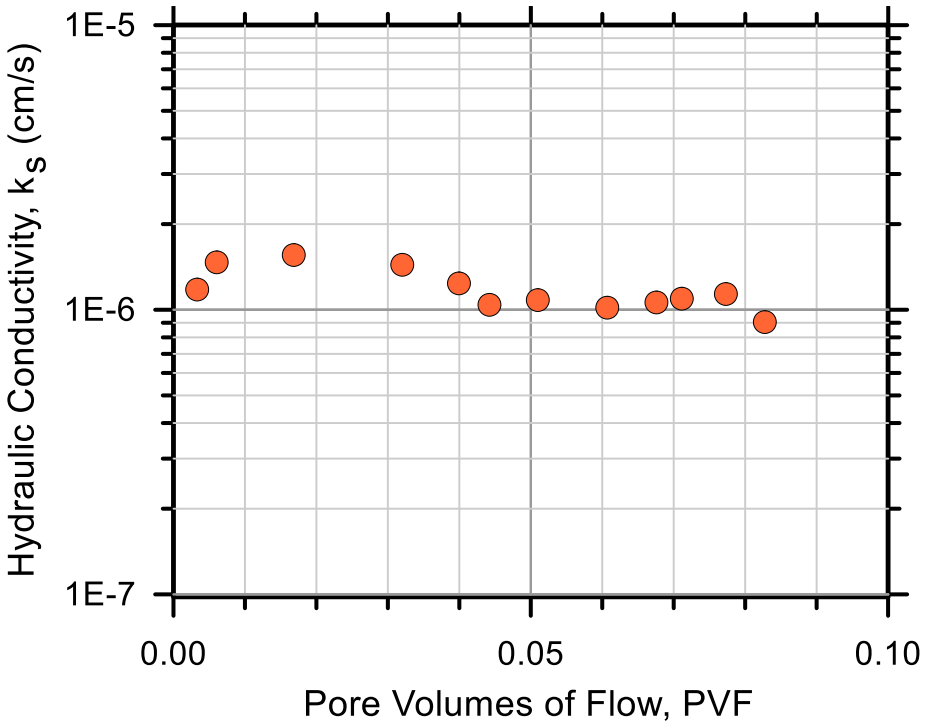
1E-5
1E-6
1E-7
Hydraulic Conductivity, k_S (cm/s)
0.00
0.05
0.10
Pore Volumes of Flow, PVF

Test No.: 31

Test Ref.: FXSC31

Test Soil: Stroubles Creek

Molding Water Content: 22.60% (w_{opt})

Property	Before Test	After Test
Total Mass (g)	326.00	359.99
Mass of Solids (g)	265.91	264.99
Mass of Water (g)	60.09	95.00
Total Volume (cm^3)	201.81	197.72
Volume of Solids (cm^3)	103.06	102.71
Volume of Water (cm^3)	60.09	95.00
Volume of Air (cm^3)	38.65	0.01
Water Content (%)	22.60	35.85
Volume of Voids (cm^3)	98.74	95.01
Void Ratio, e	0.958	0.925
Porosity, n (%)	0.489	0.481
Std. Proctor Relative Compaction, RC (%)	85.01	86.47
Moist Density, γ_m (g/cm^3)	1.62	1.82
Dry Density, γ_d (g/cm^3)	1.32	1.34
Degree of Saturation, S (%)	60.86	99.99
Consolidation Cell Pressure (kPa)	434.4	
Consolidation Back Pressure (kPa)	413.7	
Effective Consolidation Pressure (kPa)	20.7	

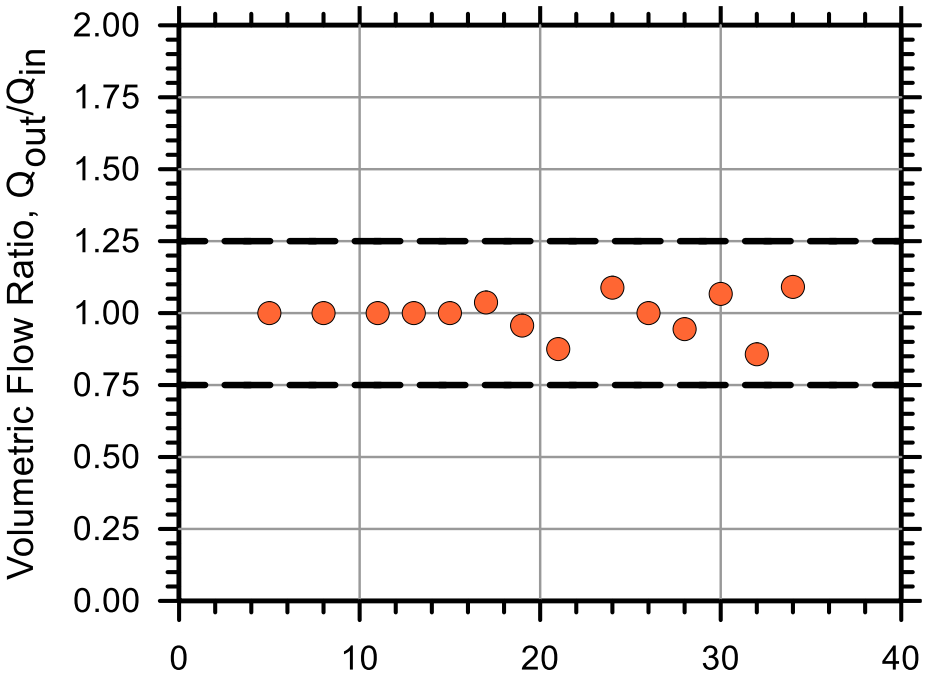
Volumetric Flow Ratio, Q_{out}/Q_{in}
2.00
1.75
1.50
1.25
1.00
0.75
0.50
0.25
0.00
0
10
20
30
40

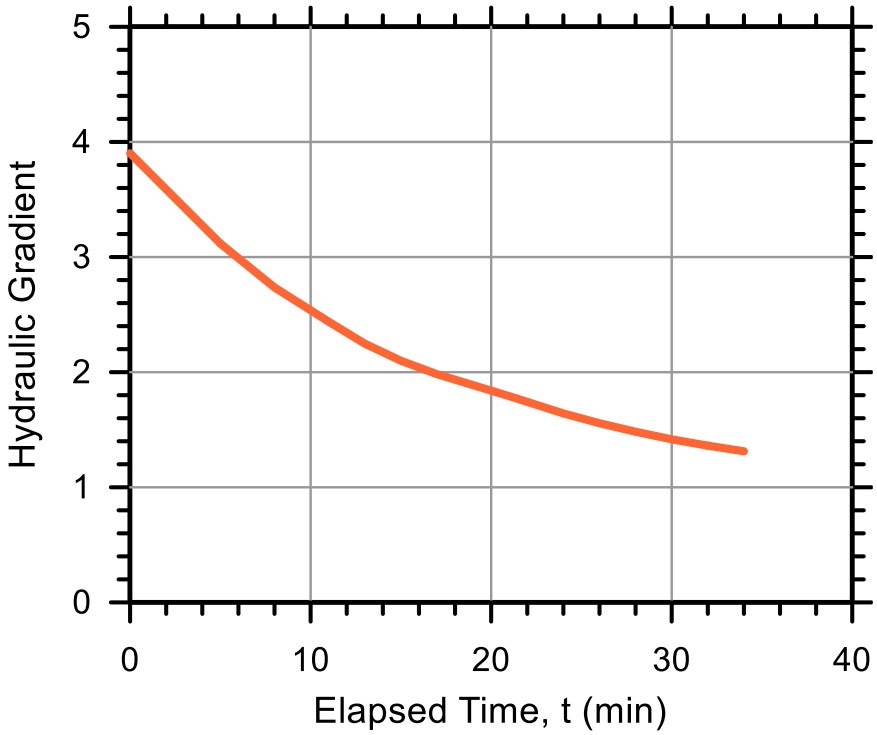
Hydraulic Gradient
5
4
3
2
1
0
0
10
20
30
40
Elapsed Time, t (min)

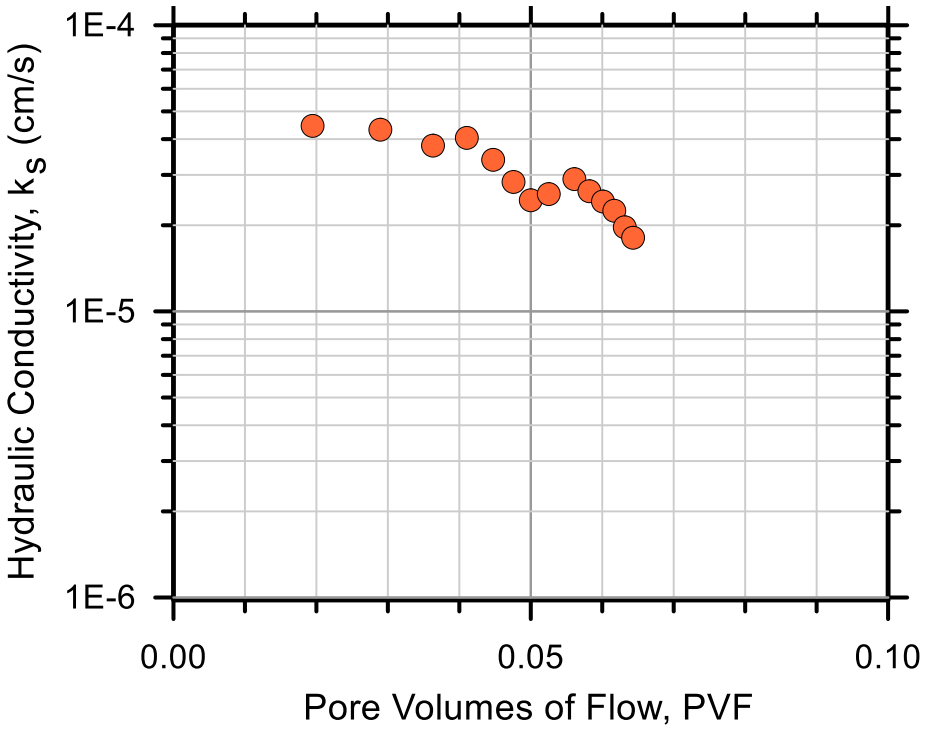
1E-4
1E-5
1E-6
Hydraulic Conductivity, k_s (cm/s)
0.00
0.05
0.10
Pore Volumes of Flow, PVF

Test No.: 32

Test Ref.: FXSC32

Test Soil: Stroubles Creek

Molding Water Content: 22.60% (w_{opt})

Property	Before Test	After Test
Total Mass (g)	298.00	333.94
Mass of Solids (g)	243.07	242.60
Mass of Water (g)	54.93	91.34
Total Volume (cm^3)	201.81	187.44
Volume of Solids (cm^3)	94.21	94.03
Volume of Water (cm^3)	54.93	91.34
Volume of Air (cm^3)	52.66	2.07
Water Content (%)	22.60	37.65
Volume of Voids (cm^3)	107.60	93.41
Void Ratio, e	1.142	0.993
Porosity, n (%)	0.533	0.498
Std. Proctor Relative Compaction, RC (%)	77.71	83.66
Moist Density, γ_m (g/cm^3)	1.48	1.78
Dry Density, γ_d (g/cm^3)	1.20	1.30
Degree of Saturation, S (%)	51.06	97.78
Consolidation Cell Pressure (kPa)	419.2	
Consolidation Back Pressure (kPa)	413.7	
Effective Consolidation Pressure (kPa)	5.5	

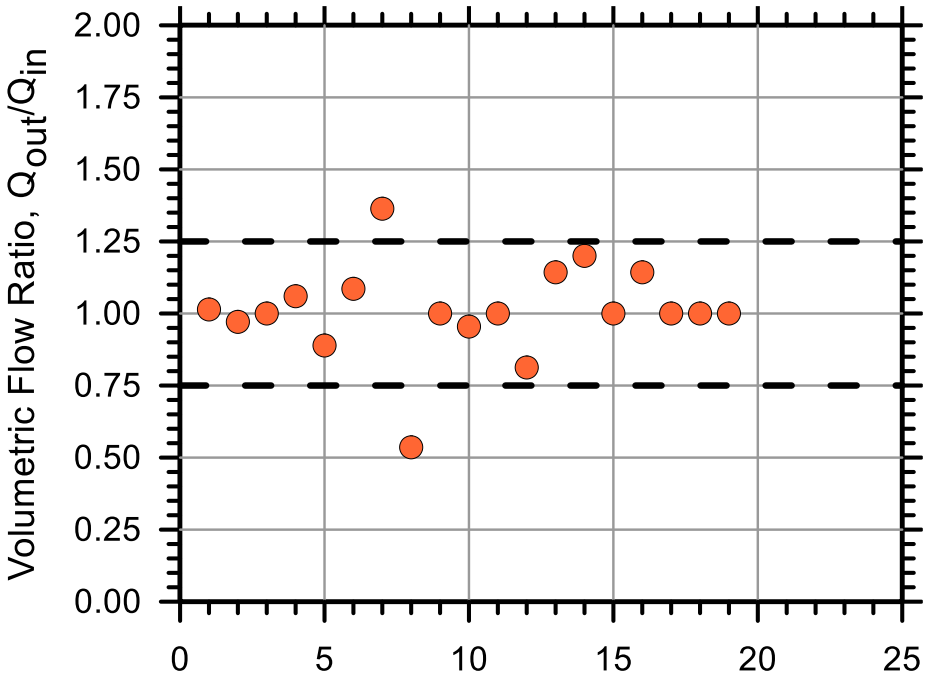
Volumetric Flow Ratio, Q_{out}/Q_{in}
2.00
1.75
1.50
1.25
1.00
0.75
0.50
0.25
0.00
0
5
10
15
20
25

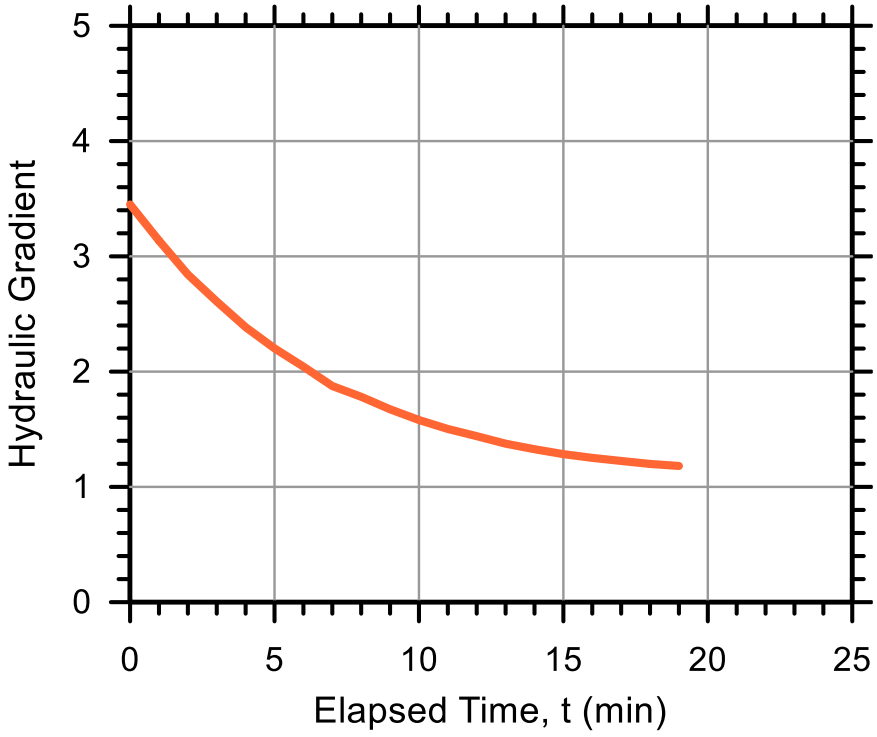
Hydraulic Gradient
5
4
3
2
1
0
0
5
10
15
20
25
Elapsed Time, t (min)

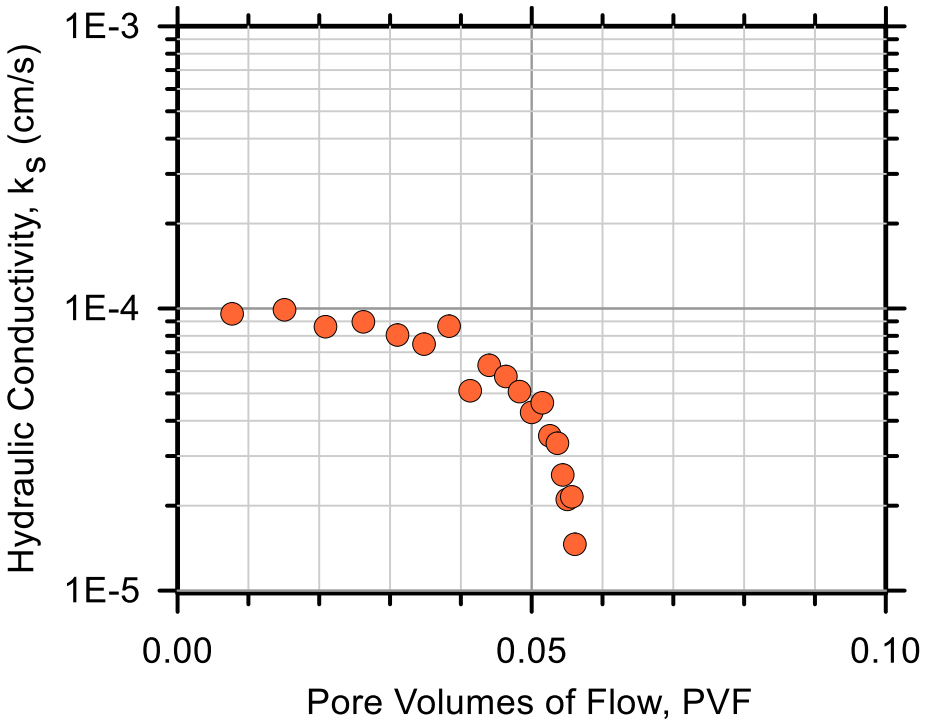
1E-3
1E-4
1E-5
Hydraulic Conductivity, k_S (cm/s)
0.00
0.05
0.10
Pore Volumes of Flow, PVF

Test No.: 50

Test Ref.: FXSC50

Test Soil: Stroubles Creek

Molding Water Content: 25.60% (w_{opt}+3)

Property	Before Test	After Test
Total Mass (g)	361.00	370.71
Mass of Solids (g)	287.42	287.17
Mass of Water (g)	73.58	83.54
Total Volume (cm^3)	201.81	194.88
Volume of Solids (cm^3)	111.40	111.31
Volume of Water (cm^3)	73.58	83.54
Volume of Air (cm^3)	16.82	0.03
Water Content (%)	25.60	29.09
Volume of Voids (cm^3)	90.40	83.57
Void Ratio, e	0.812	0.751
Porosity, n (%)	0.448	0.429
Std. Proctor Relative Compaction, RC (%)	91.89	95.07
Moist Density, γ_m (g/cm^3)	1.79	1.90
Dry Density, γ_d (g/cm^3)	1.42	1.47
Degree of Saturation, S (%)	81.39	99.96
Consolidation Cell Pressure (kPa)	482.7	
Consolidation Back Pressure (kPa)	413.7	
Effective Consolidation Pressure (kPa)	69.0	

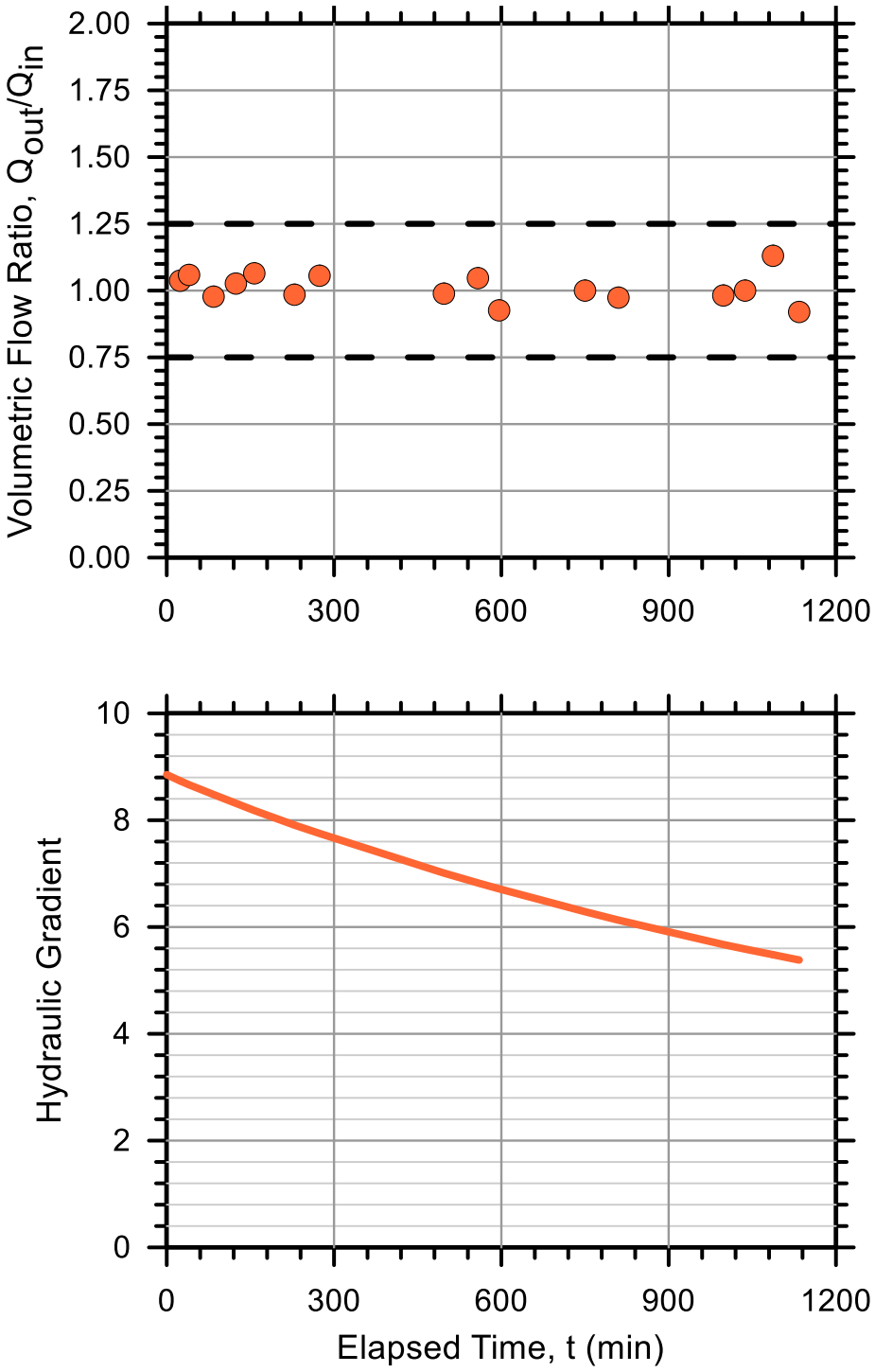
Volumetric Flow Ratio, Q_{out}/Q_{in}
2.00
1.75
1.50
1.25
1.00
0.75
0.50
0.25
0.00
0
300
600
900
1200
Hydraulic Gradient
10
8
6
4
2
0
0
300
600
900
1200
Elapsed Time, t (min)

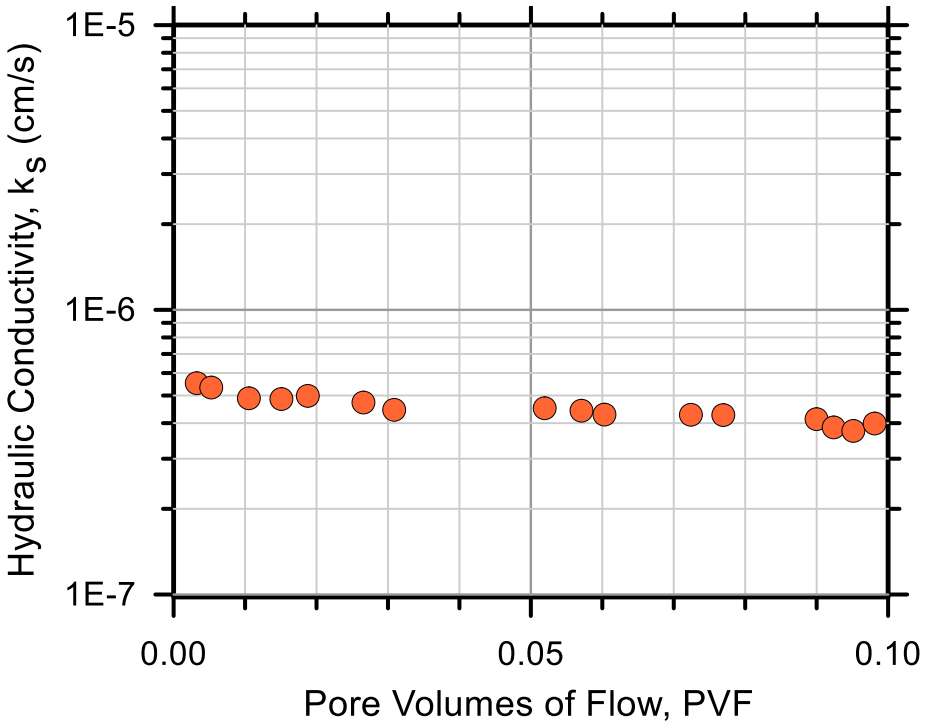
1E-5
1E-6
1E-7
Hydraulic Conductivity, k_S (cm/s)
0.00
0.05
0.10
Pore Volumes of Flow, PVF

Test No.: 19

Test Ref.: FXSC19

Test Soil: Stroubles Creek

Molding Water Content: 25.60% (w_{opt}+3)

Property	Before Test	After Test
Total Mass (g)	361.00	376.40
Mass of Solids (g)	287.42	287.33
Mass of Water (g)	73.58	89.07
Total Volume (cm^3)	201.81	200.53
Volume of Solids (cm^3)	111.40	111.37
Volume of Water (cm^3)	73.58	89.07
Volume of Air (cm^3)	16.82	0.09
Water Content (%)	25.60	31.00
Volume of Voids (cm^3)	90.40	89.16
Void Ratio, e	0.812	0.801
Porosity, n (%)	0.448	0.445
Std. Proctor Relative Compaction, RC (%)	91.89	92.44
Moist Density, γ_m (g/cm^3)	1.79	1.88
Dry Density, γ_d (g/cm^3)	1.42	1.43
Degree of Saturation, S (%)	81.39	99.90
Consolidation Cell Pressure (kPa)	379.2	
Consolidation Back Pressure (kPa)	344.8	
Effective Consolidation Pressure (kPa)	34.5	

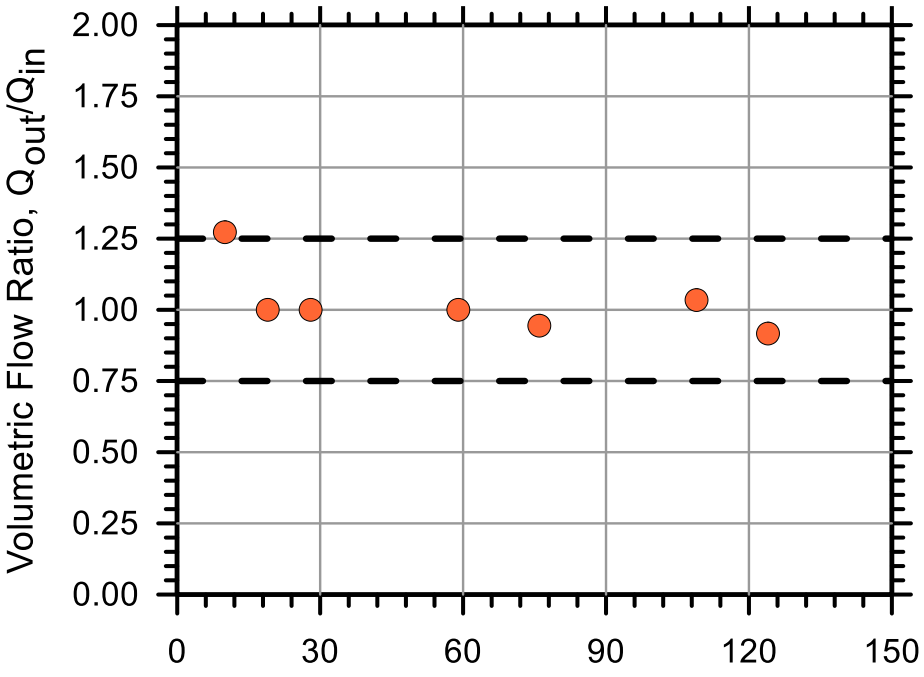
Volumetric Flow Ratio, Q_{out}/Q_{in}
2.00
1.75
1.50
1.25
1.00
0.75
0.50
0.25
0.00
0
30
60
90
120
150

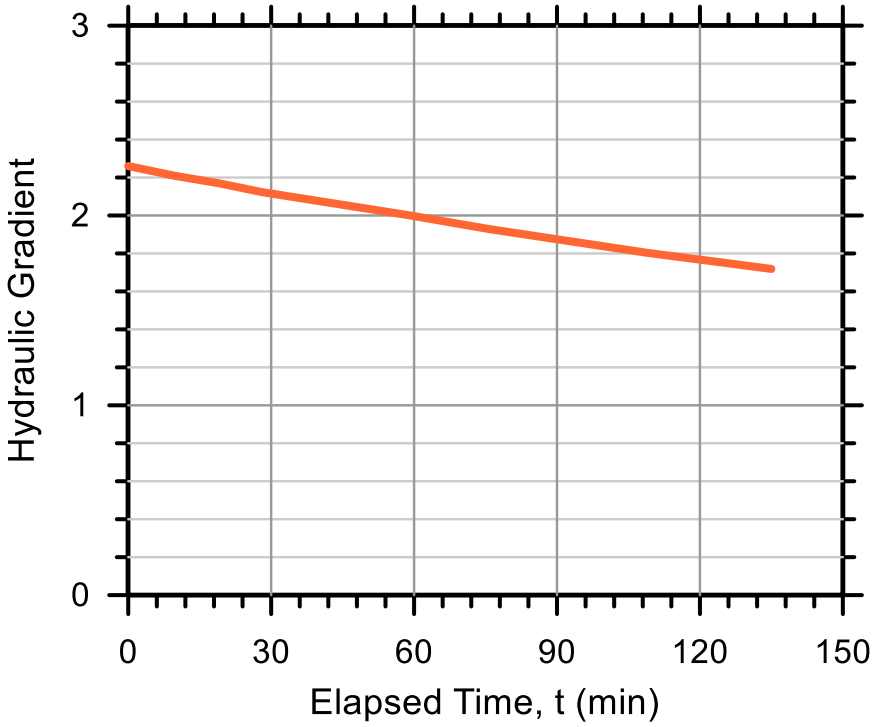
Hydraulic Gradient
3
2
1
0
0
30
60
90
120
150
Elapsed Time, t (min)

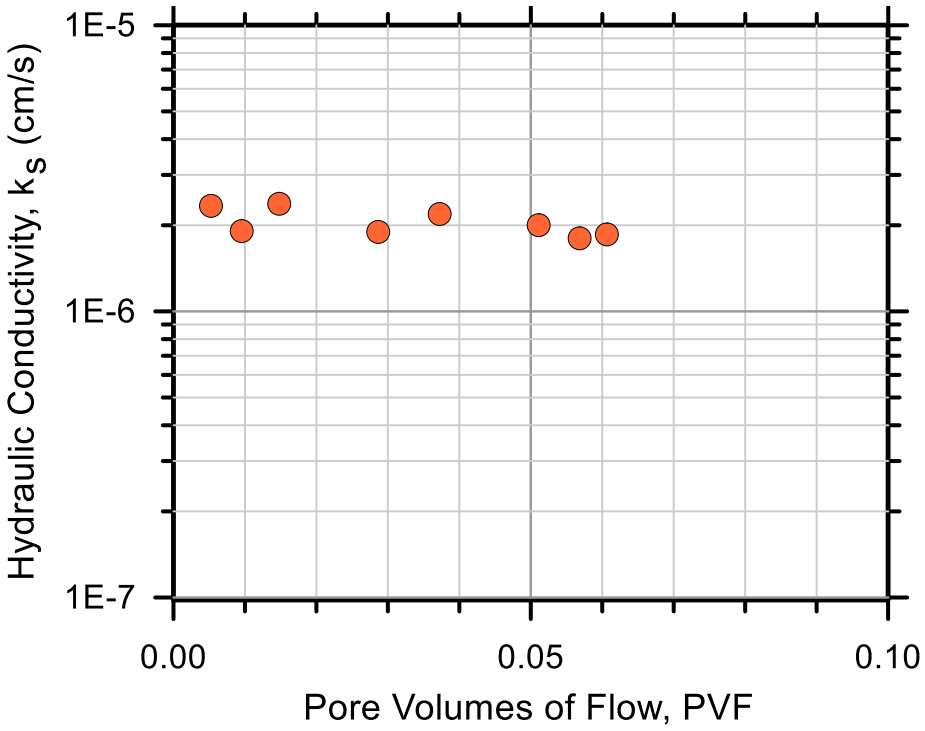
1E-5
1E-6
1E-7
Hydraulic Conductivity, k_S (cm/s)
0.00
0.05
0.10
Pore Volumes of Flow, PVF

Test No.: 20

Test Ref.: FXSC20

Test Soil: Stroubles Creek

Molding Water Content: 25.60% (w_{opt}+3)

Property	Before Test	After Test
Total Mass (g)	333.00	355.15
Mass of Solids (g)	265.13	265.02
Mass of Water (g)	67.87	90.13
Total Volume (cm^3)	201.81	192.92
Volume of Solids (cm^3)	102.76	102.72
Volume of Water (cm^3)	67.87	90.13
Volume of Air (cm^3)	31.17	0.07
Water Content (%)	25.60	34.01
Volume of Voids (cm^3)	99.04	90.20
Void Ratio, e	0.964	0.878
Porosity, n (%)	0.491	0.468
Std. Proctor Relative Compaction, RC (%)	84.76	88.63
Moist Density, γ_m (g/cm^3)	1.65	1.84
Dry Density, γ_d (g/cm^3)	1.31	1.37
Degree of Saturation, S (%)	68.53	99.92
Consolidation Cell Pressure (kPa)	406.8	
Consolidation Back Pressure (kPa)	379.2	
Effective Consolidation Pressure (kPa)	27.6	

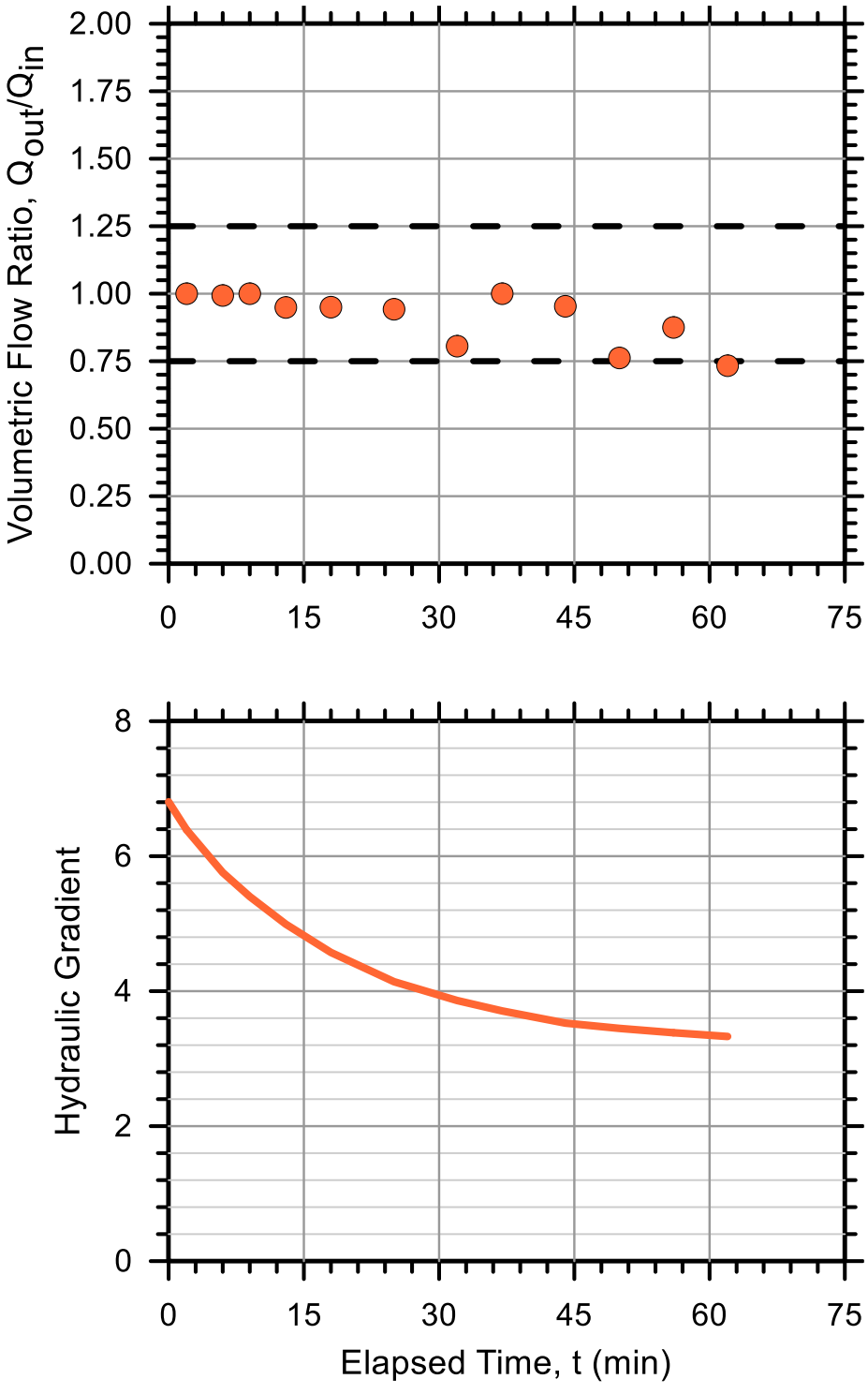
Volumetric Flow Ratio, Q_{out}/Q_{in}
2.00
1.75
1.50
1.25
1.00
0.75
0.50
0.25
0.00
0
15
30
45
60
75
Hydraulic Gradient
8
6
4
2
0
0
15
30
45
60
75
Elapsed Time, t (min)

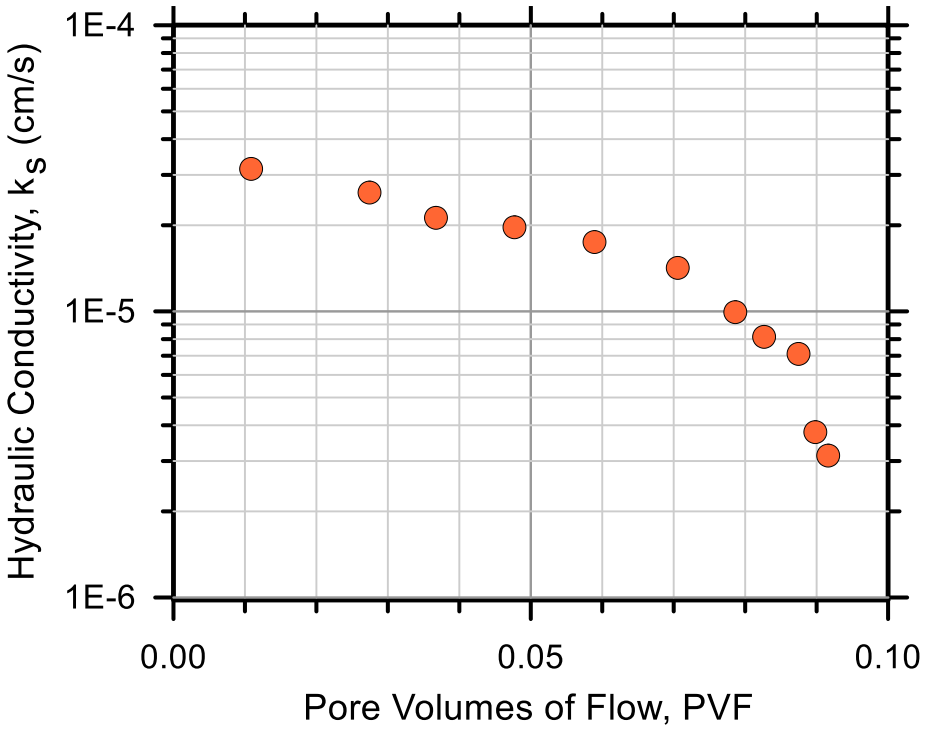
1E-4
1E-5
1E-6
Hydraulic Conductivity, k_S (cm/s)
0.00
0.05
0.10
Pore Volumes of Flow, PVF

Test No.: 39

Test Ref.: FXSC39

Test Soil: Stroubles Creek

Molding Water Content: 25.60% (w_{opt}+3)

Property	Before Test	After Test
Total Mass (g)	330.00	356.10
Mass of Solids (g)	262.74	262.65
Mass of Water (g)	67.26	93.45
Total Volume (cm^3)	201.81	196.55
Volume of Solids (cm^3)	101.84	101.80
Volume of Water (cm^3)	67.26	93.45
Volume of Air (cm^3)	32.71	1.29
Water Content (%)	25.60	35.58
Volume of Voids (cm^3)	99.97	94.74
Void Ratio, e	0.982	0.931
Porosity, n (%)	0.495	0.482
Std. Proctor Relative Compaction, RC (%)	84.00	86.21
Moist Density, γ_m (g/cm^3)	1.64	1.81
Dry Density, γ_d (g/cm^3)	1.30	1.34
Degree of Saturation, S (%)	67.28	98.63
Consolidation Cell Pressure (kPa)	427.5	
Consolidation Back Pressure (kPa)	413.7	
Effective Consolidation Pressure (kPa)	13.8	

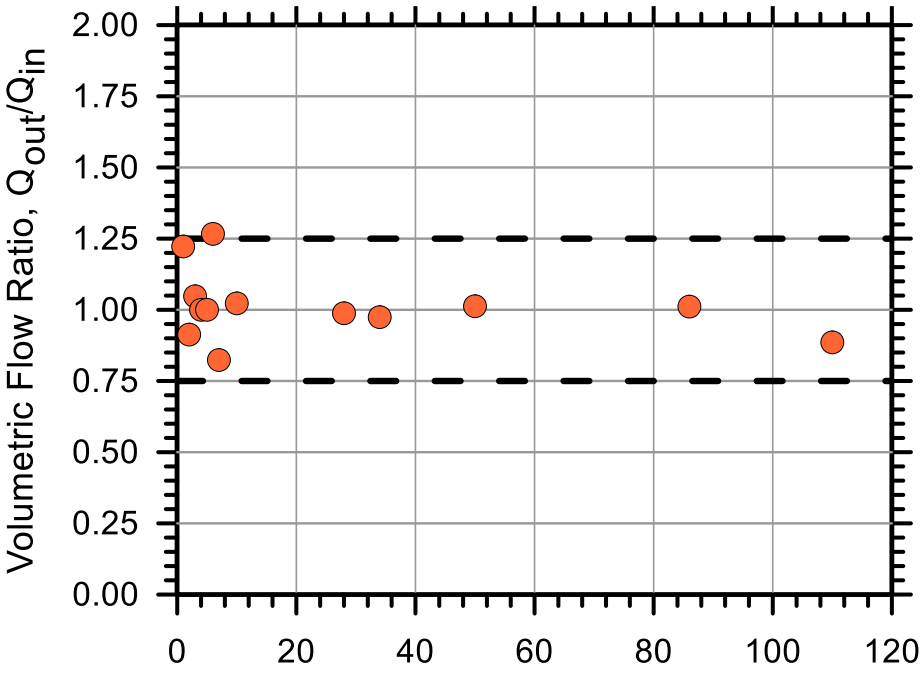
Volumetric Flow Ratio, Q_{out}/Q_{in}
2.00
1.75
1.50
1.25
1.00
0.75
0.50
0.25
0.00
0
20
40
60
80
100
120

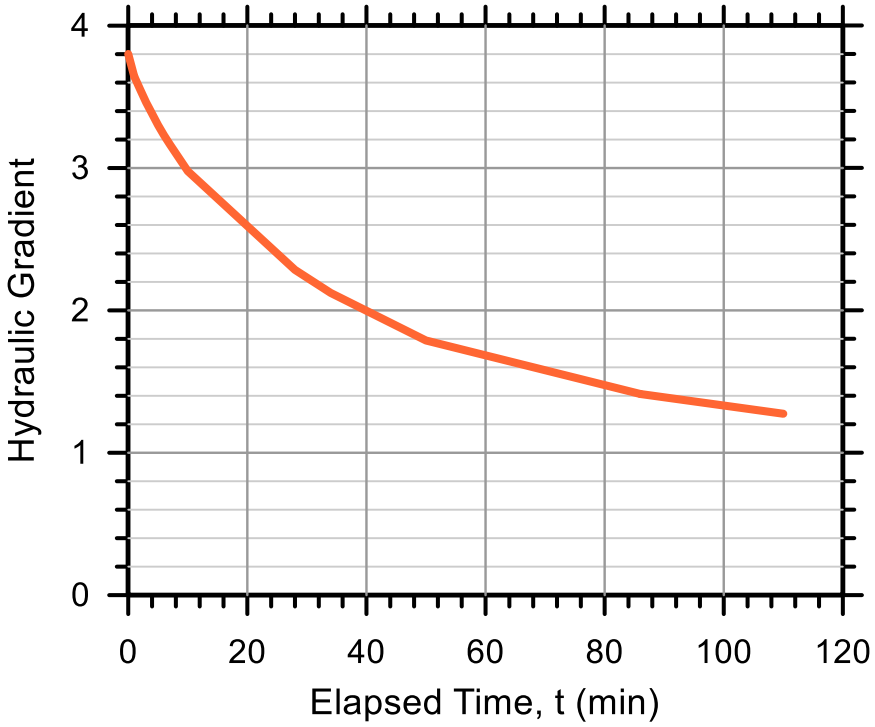
Hydraulic Gradient
4
3
2
1
0
0
20
40
60
80
100
120
Elapsed Time, t (min)

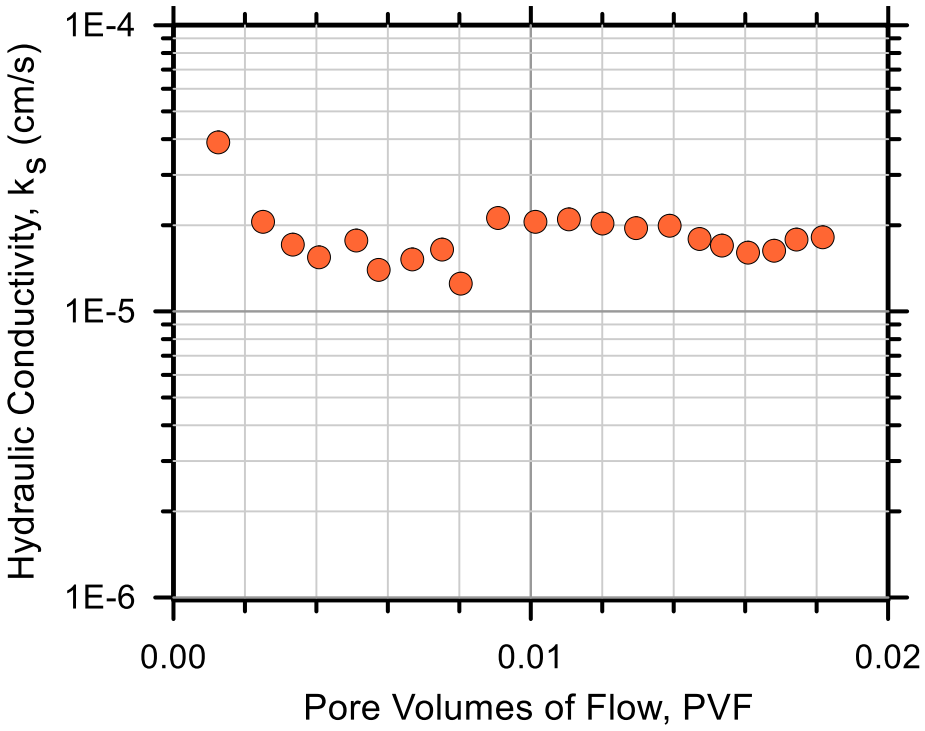
1E-4
1E-5
1E-6
Hydraulic Conductivity, k_S (cm/s)
0.00
0.01
0.02
Pore Volumes of Flow, PVF

Test No.: 27

Test Ref.: FXWH27

Test Soil: Whitehorne

Molding Water Content: 27.70% (w_{opt}-2)

Property	Before Test	After Test
Total Mass (g)	341.00	357.31
Mass of Solids (g)	267.03	267.01
Mass of Water (g)	73.97	90.30
Total Volume (cm^3)	201.81	190.63
Volume of Solids (cm^3)	99.64	99.63
Volume of Water (cm^3)	73.97	90.30
Volume of Air (cm^3)	28.20	0.70
Water Content (%)	27.70	33.82
Volume of Voids (cm^3)	102.17	91.00
Void Ratio, e	1.025	0.913
Porosity, n (%)	50.6	47.7
Std. Proctor Relative Compaction, RC (%)	96.23	101.86
Moist Density, γ_m (g/cm^3)	1.69	1.87
Dry Density, γ_d (g/cm^3)	1.32	1.40
Degree of Saturation, S (%)	72.40	99.23
Consolidation Cell Pressure (kPa)	482.7	
Consolidation Back Pressure (kPa)	413.7	
Effective Consolidation Pressure (kPa)	69.0	

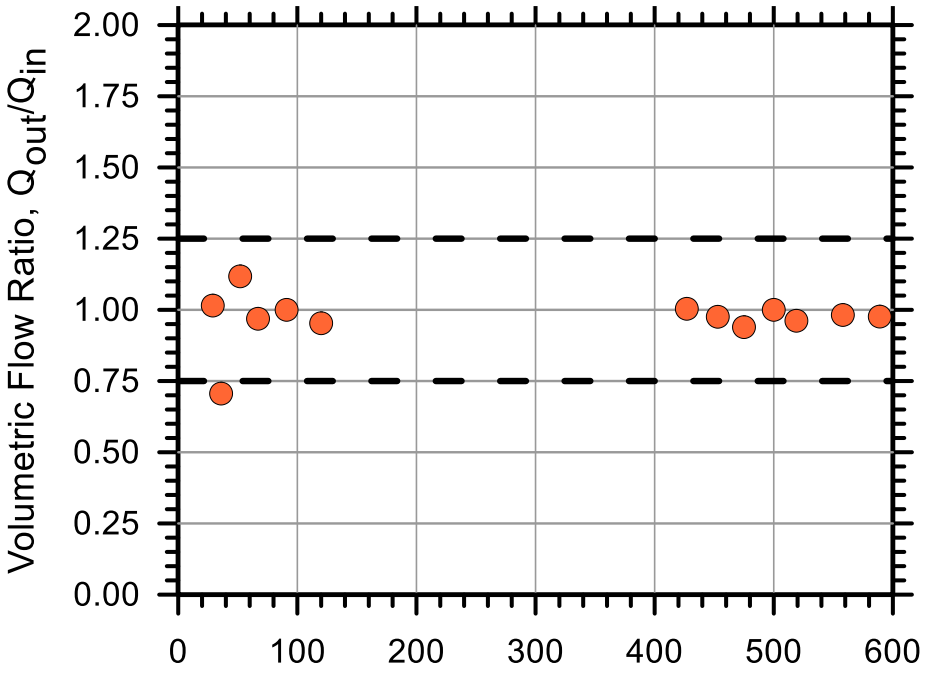
Volumetric Flow Ratio, Q_{out}/Q_{in}
2.00
1.75
1.50
1.25
1.00
0.75
0.50
0.25
0.00
0
100
200
300
400
500
600

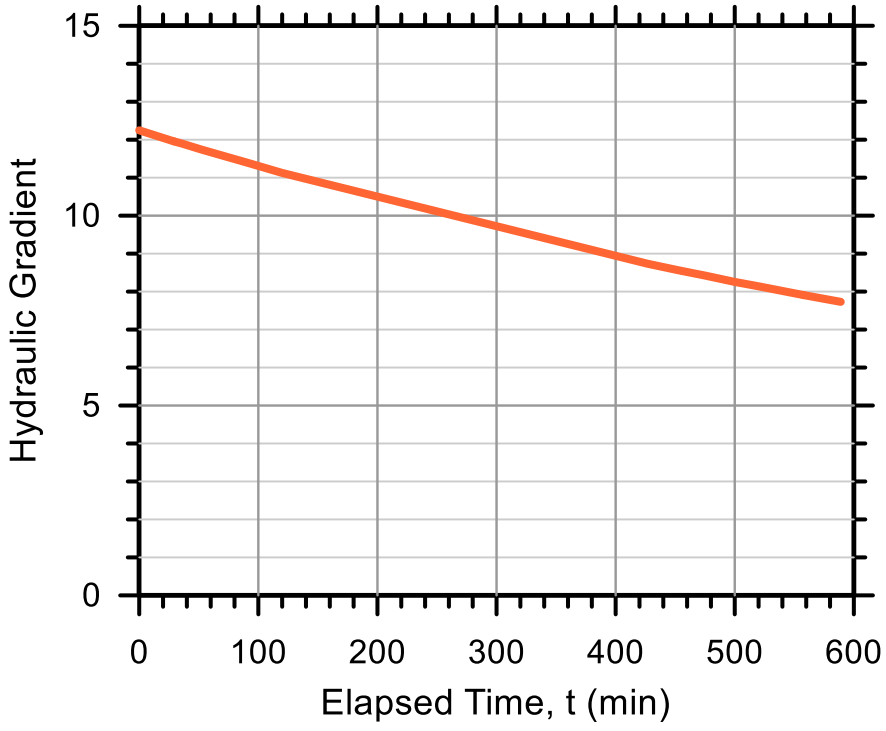
Hydraulic Gradient
15
10
5
0
0
100
200
300
400
500
600
Elapsed Time, t (min)

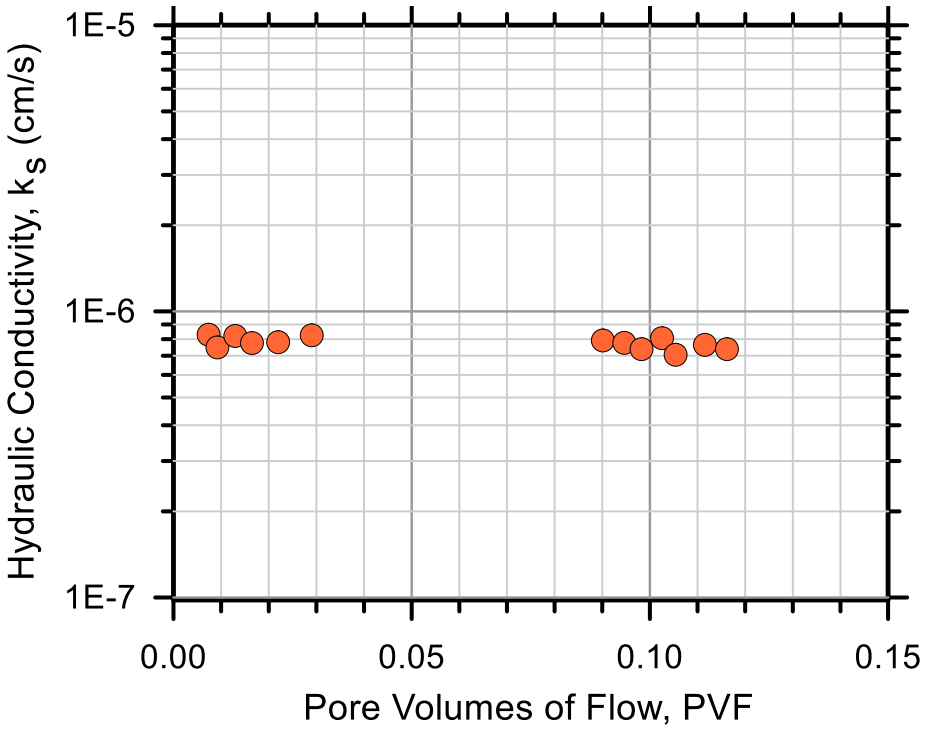
1E-5
1E-6
1E-7
Hydraulic Conductivity, k_S (cm/s)
0.00
0.05
0.10
0.15
Pore Volumes of Flow, PVF

Test No.: 9

Test Ref.: FXWH09

Test Soil: Whitehorne

Molding Water Content: 27.70% (w_{opt}-2)

Property	Before Test	After Test
Total Mass (g)	157.00	174.60
Mass of Solids (g)	122.94	122.88
Mass of Water (g)	34.06	51.72
Total Volume (cm^3)	100.90	97.58
Volume of Solids (cm^3)	45.87	45.85
Volume of Water (cm^3)	34.06	51.72
Volume of Air (cm^3)	20.97	0.00
Water Content (%)	27.70	42.09
Volume of Voids (cm^3)	55.03	51.72
Void Ratio, e	1.200	1.128
Porosity, n (%)	54.5	53.0
Std. Proctor Relative Compaction, RC (%)	88.61	91.59
Moist Density, γ_m (g/cm^3)	1.56	1.79
Dry Density, γ_d (g/cm^3)	1.22	1.26
Degree of Saturation, S (%)	61.89	99.99
Consolidation Cell Pressure (kPa)	372.3	
Consolidation Back Pressure (kPa)	344.8	
Effective Consolidation Pressure (kPa)	27.6	

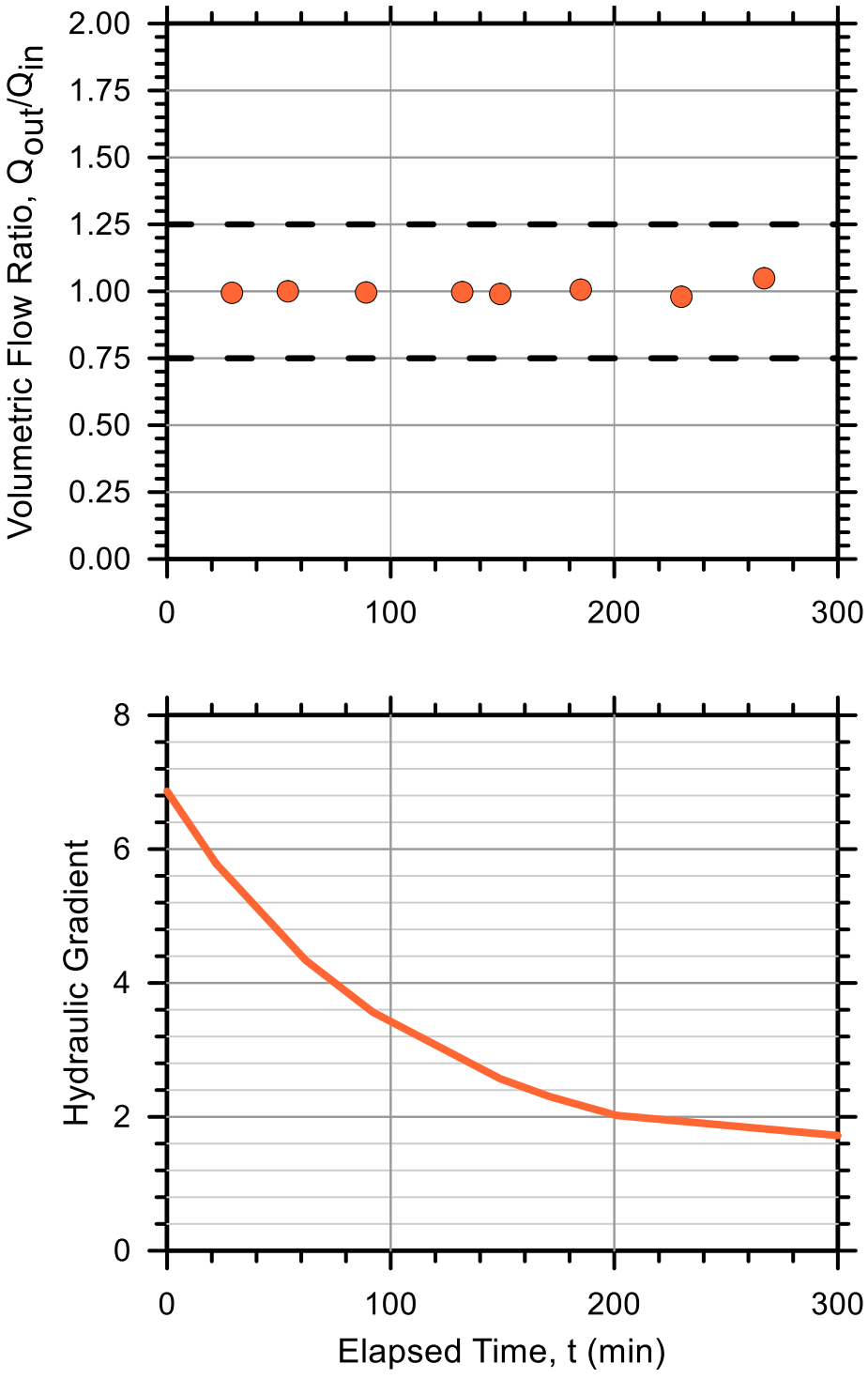
Volumetric Flow Ratio, Q_{out}/Q_{in}
2.00
1.75
1.50
1.25
1.00
0.75
0.50
0.25
0.00
0
100
200
300
Hydraulic Gradient
8
6
4
2
0
0
100
200
300
Elapsed Time, t (min)

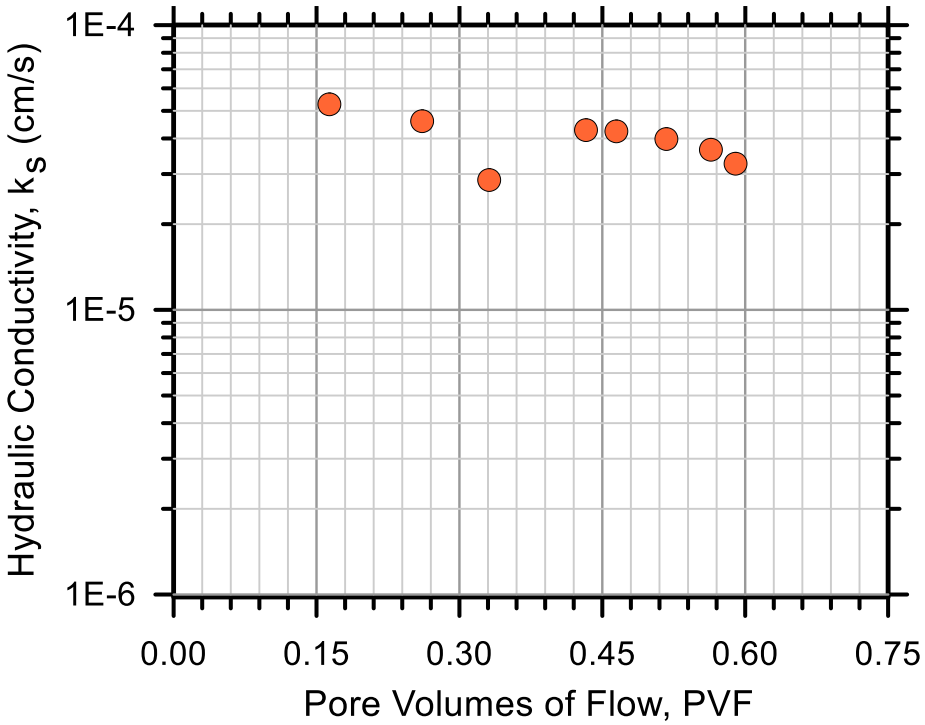
1E-4
1E-5
1E-6
Hydraulic Conductivity, k_S (cm/s)
0.00
0.15
0.30
0.45
0.60
0.75
Pore Volumes of Flow, PVF

Test No.: 26

Test Ref.: FXWH26

Test Soil: Whitehorne

Molding Water Content: 27.70% (w_{opt}-2)

Property	Before Test	After Test
Total Mass (g)	279.00	311.10
Mass of Solids (g)	218.48	218.29
Mass of Water (g)	60.52	92.81
Total Volume (cm^3)	201.81	174.28
Volume of Solids (cm^3)	81.52	81.45
Volume of Water (cm^3)	60.52	92.81
Volume of Air (cm^3)	59.77	0.02
Water Content (%)	27.70	42.52
Volume of Voids (cm^3)	120.28	92.83
Void Ratio, e	1.475	1.140
Porosity, n (%)	59.6	53.3
Std. Proctor Relative Compaction, RC (%)	78.74	91.09
Moist Density, γ_m (g/cm^3)	1.38	1.79
Dry Density, γ_d (g/cm^3)	1.08	1.25
Degree of Saturation, S (%)	50.31	99.98
Consolidation Cell Pressure (kPa)	448.2	
Consolidation Back Pressure (kPa)	413.7	
Effective Consolidation Pressure (kPa)	448.2	

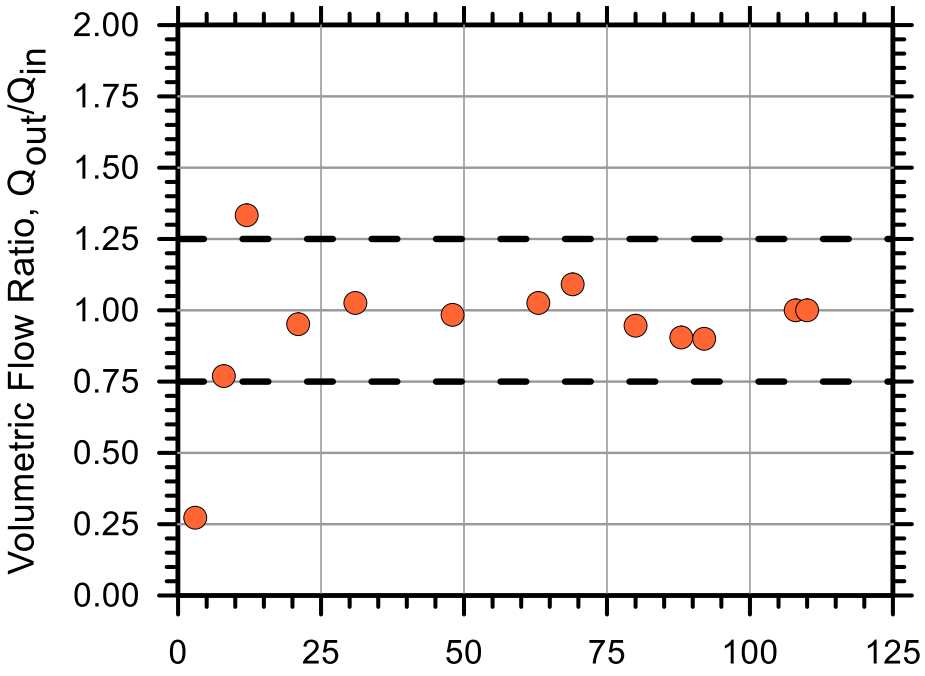
Volumetric Flow Ratio, Q_{out}/Q_{in}
2.00
1.75
1.50
1.25
1.00
0.75
0.50
0.25
0.00
0
25
50
75
100
125

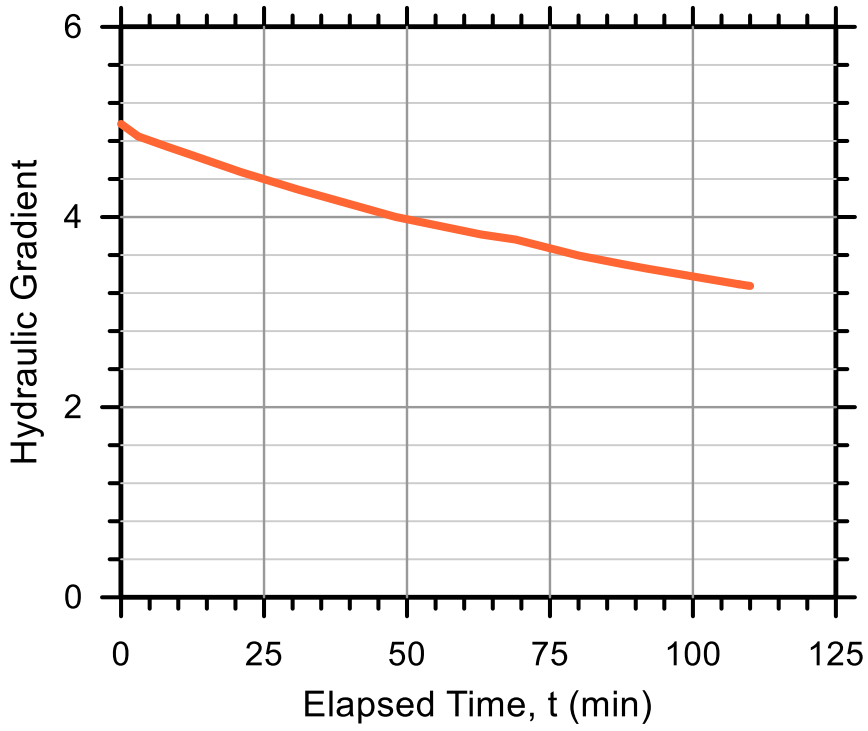
Hydraulic Gradient
6
4
2
0
0
25
50
75
100
125
Elapsed Time, t (min)

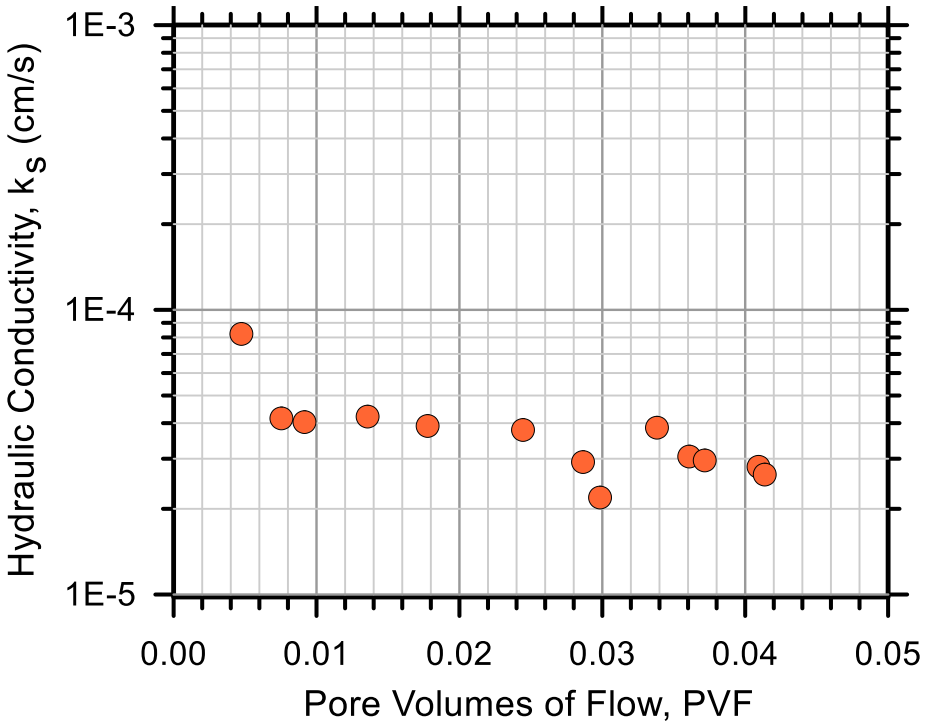
1E-3
1E-4
1E-5
Hydraulic Conductivity, k_S (cm/s)
0.00
0.01
0.02
0.03
0.04
0.05
Pore Volumes of Flow, PVF

Test No.: 18

Test Ref.: FXWH18

Test Soil: Whitehorne

Molding Water Content: 27.70% (w_{opt}-2)

Property	Before Test	After Test
Total Mass (g)	314.00	359.00
Mass of Solids (g)	245.89	245.47
Mass of Water (g)	68.11	113.53
Total Volume (cm^3)	201.81	205.30
Volume of Solids (cm^3)	91.75	91.59
Volume of Water (cm^3)	68.11	113.53
Volume of Air (cm^3)	41.95	0.17
Water Content (%)	27.70	46.25
Volume of Voids (cm^3)	110.06	113.70
Void Ratio, e	1.200	1.241
Porosity, n (%)	54.5	55.4
Std. Proctor Relative Compaction, RC (%)	88.61	87.11
Moist Density, γ_m (g/cm^3)	1.56	1.75
Dry Density, γ_d (g/cm^3)	1.22	1.20
Degree of Saturation, S (%)	61.89	99.85
Consolidation Cell Pressure (kPa)	348.2	
Consolidation Back Pressure (kPa)	344.8	
Effective Consolidation Pressure (kPa)	3.4	

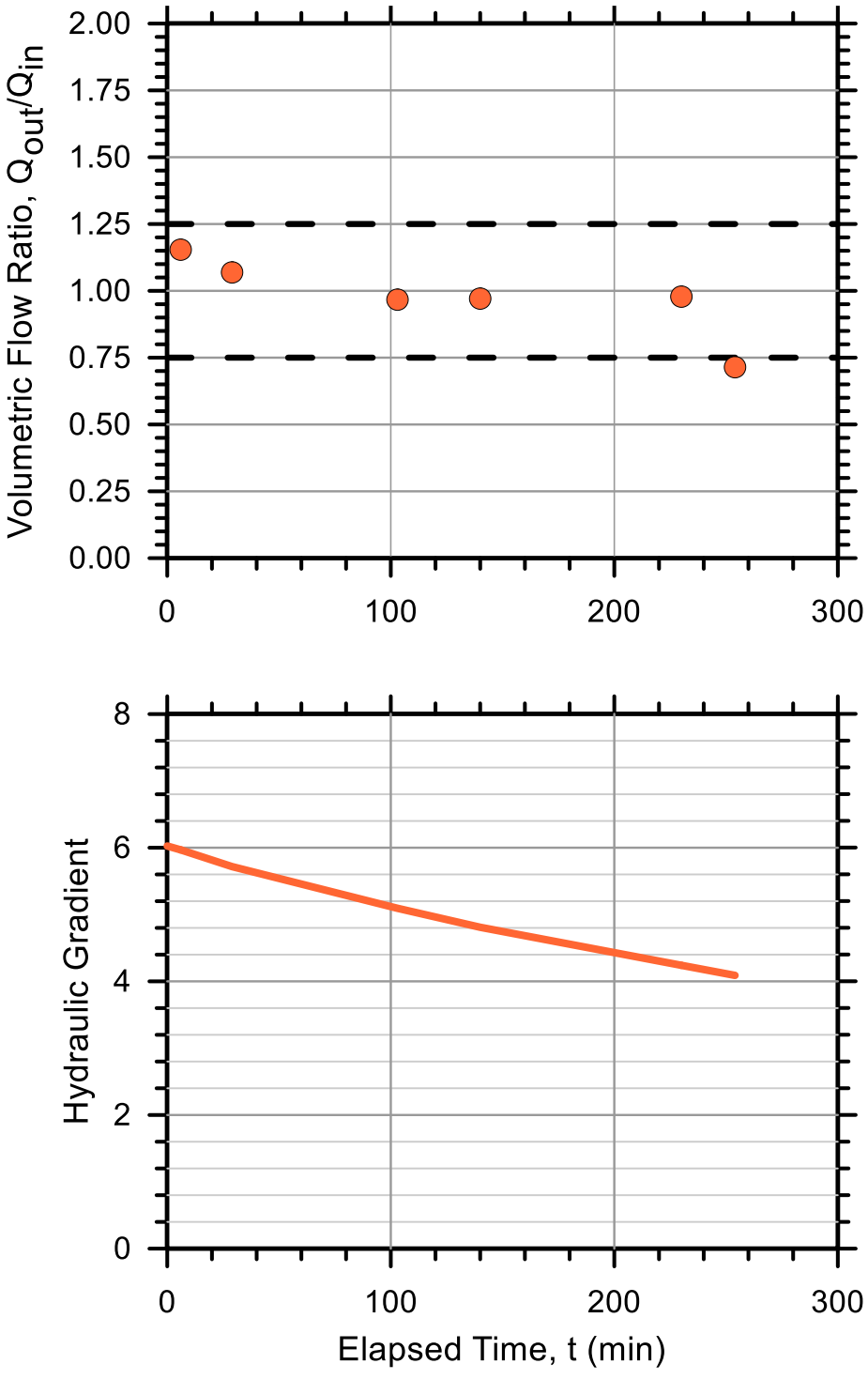
Volumetric Flow Ratio, Q_{out}/Q_{in}
2.00
1.75
1.50
1.25
1.00
0.75
0.50
0.25
0.00
0
100
200
300
Hydraulic Gradient
8
6
4
2
0
0
100
200
300
Elapsed Time, t (min)

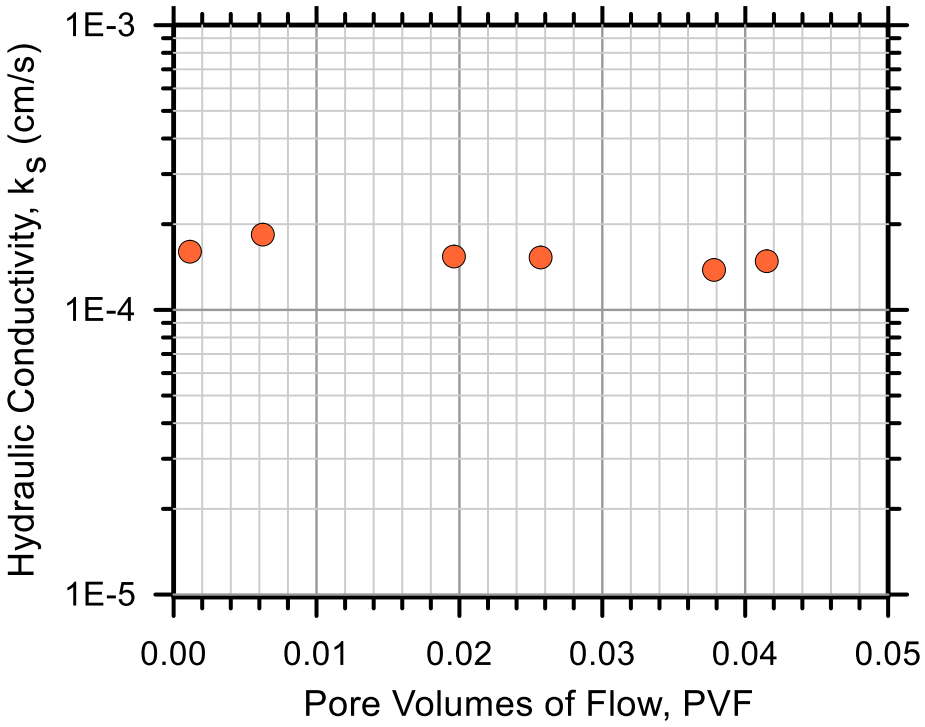
1E-3
1E-4
1E-5
Hydraulic Conductivity, k_s (cm/s)
0.00
0.01
0.02
0.03
0.04
0.05
Pore Volumes of Flow, PVF

Test No.: 49

Test Ref.: FXWH49

Test Soil: Whitehorne

Molding Water Content: 29.70% (w_{opt})

Property	Before Test	After Test
Total Mass (g)	346.00	358.42
Mass of Solids (g)	266.77	266.38
Mass of Water (g)	79.23	92.04
Total Volume (cm^3)	201.81	192.54
Volume of Solids (cm^3)	99.54	99.40
Volume of Water (cm^3)	79.23	92.04
Volume of Air (cm^3)	23.04	1.10
Water Content (%)	29.70	34.55
Volume of Voids (cm^3)	102.27	93.14
Void Ratio, e	1.027	0.937
Porosity, n (%)	50.7	48.4
Std. Proctor Relative Compaction, RC (%)	96.14	100.62
Moist Density, γ_m (g/cm^3)	1.71	1.86
Dry Density, γ_d (g/cm^3)	1.32	1.38
Degree of Saturation, S (%)	77.47	98.82
Consolidation Cell Pressure (kPa)	482.7	
Consolidation Back Pressure (kPa)	413.7	
Effective Consolidation Pressure (kPa)	69.0	

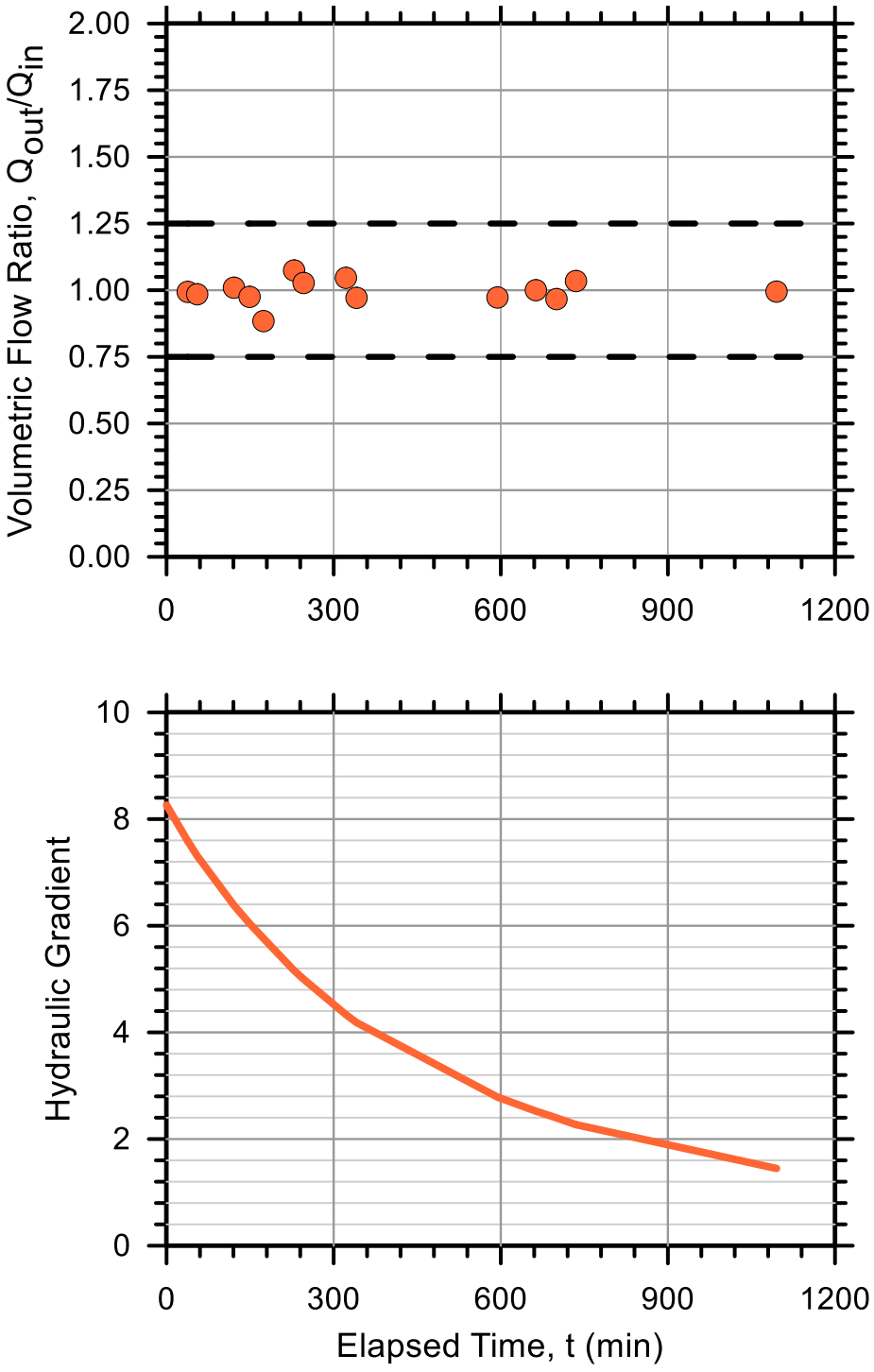
Volumetric Flow Ratio, Q_{out}/Q_{in}
2.00
1.75
1.50
1.25
1.00
0.75
0.50
0.25
0.00
0
300
600
900
1200
Hydraulic Gradient
10
8
6
4
2
0
0
300
600
900
1200
Elapsed Time, t (min)

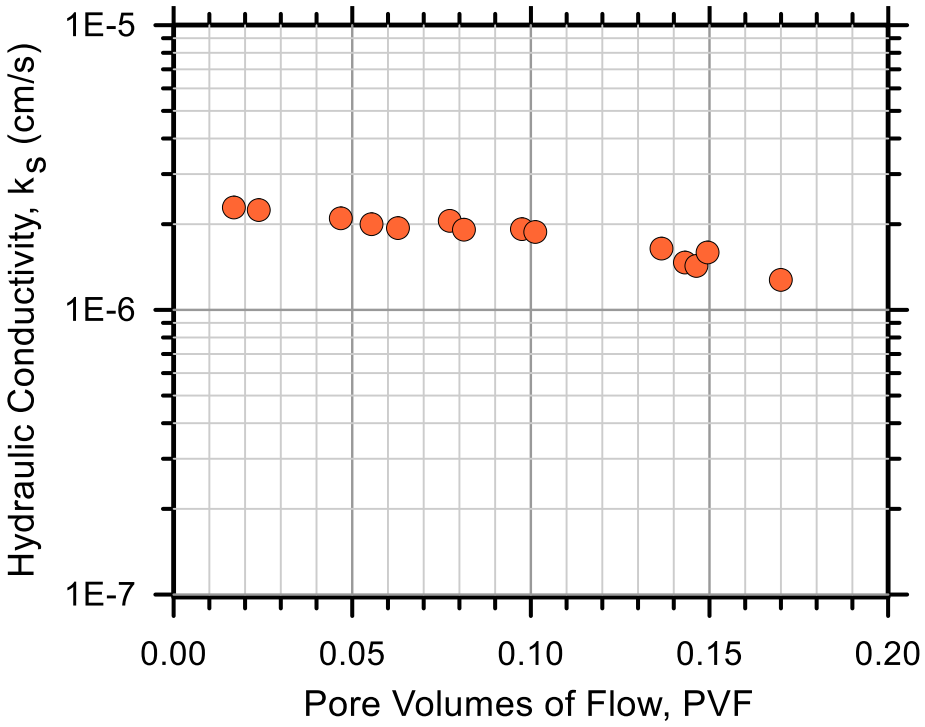
1E-5
1E-6
1E-7
Hydraulic Conductivity, k_S (cm/s)
0.00
0.05
0.10
0.15
0.20
Pore Volumes of Flow, PVF

Test No.: 17

Test Ref.: FXWH17

Test Soil: Whitehorne

Molding Water Content: 29.70% (w_{opt})

Property	Before Test	After Test
Total Mass (g)	346.00	367.44
Mass of Solids (g)	266.77	266.72
Mass of Water (g)	79.23	100.72
Total Volume (cm^3)	201.81	200.35
Volume of Solids (cm^3)	99.54	99.52
Volume of Water (cm^3)	79.23	100.72
Volume of Air (cm^3)	23.04	0.11
Water Content (%)	29.70	37.76
Volume of Voids (cm^3)	102.27	100.83
Void Ratio, e	1.027	1.013
Porosity, n (%)	50.7	50.3
Std. Proctor Relative Compaction, RC (%)	96.14	96.82
Moist Density, γ_m (g/cm^3)	1.71	1.83
Dry Density, γ_d (g/cm^3)	1.32	1.33
Degree of Saturation, S (%)	77.47	99.89
Consolidation Cell Pressure (kPa)	379.2	
Consolidation Back Pressure (kPa)	344.8	
Effective Consolidation Pressure (kPa)	34.5	

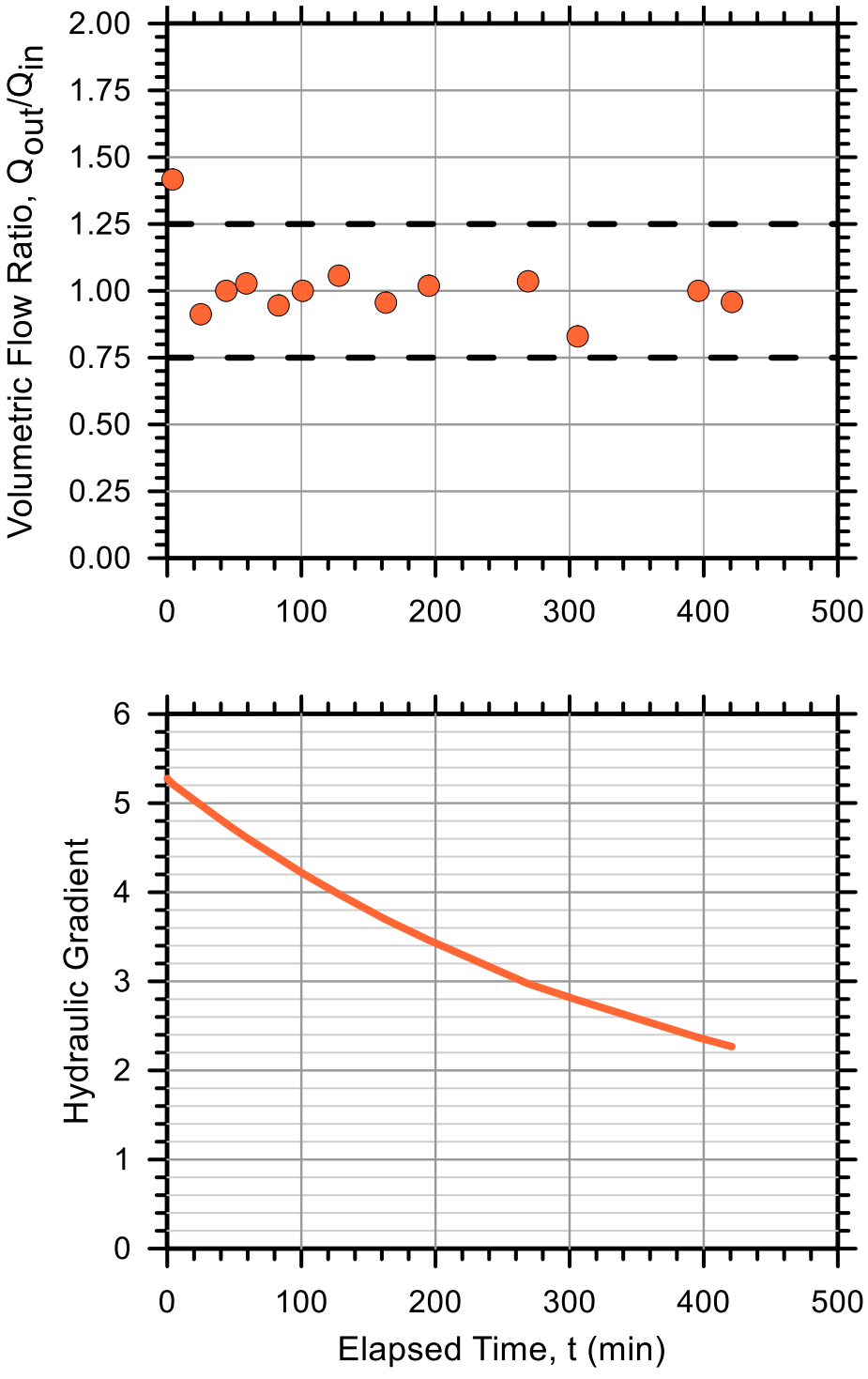
Volumetric Flow Ratio, Q_{out}/Q_{in}
2.00
1.75
1.50
1.25
1.00
0.75
0.50
0.25
0.00
0
100
200
300
400
500
Hydraulic Gradient
6
5
4
3
2
1
0
0
100
200
300
400
500
Elapsed Time, t (min)

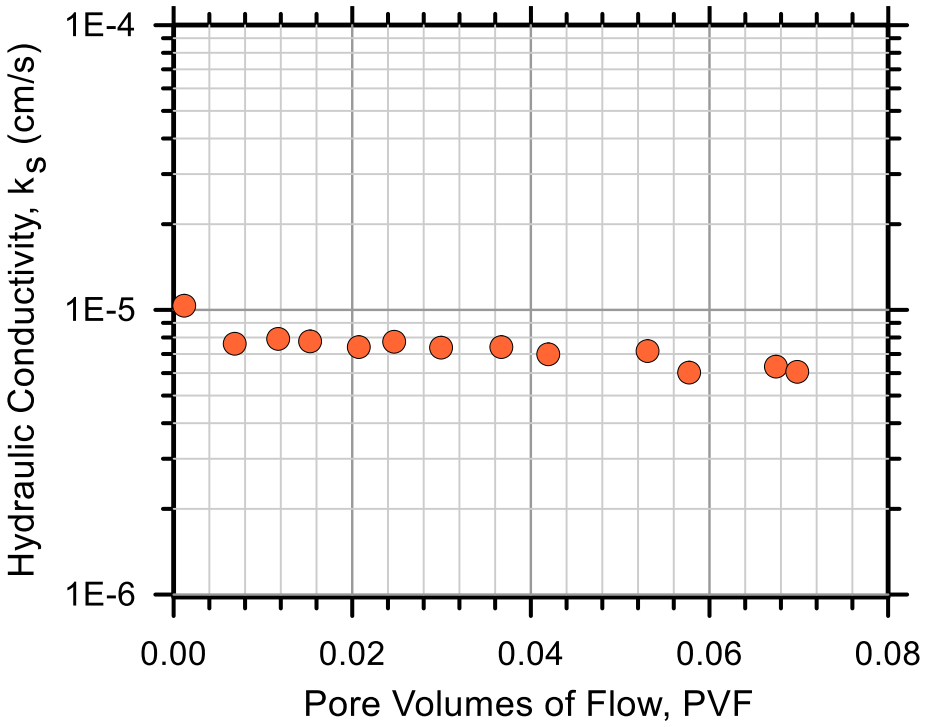
1E-4
1E-5
1E-6
Hydraulic Conductivity, k_S (cm/s)
0.00
0.02
0.04
0.06
0.08
Pore Volumes of Flow, PVF

Test No.: 25

Test Ref.: FXWH25

Test Soil: Whitehorne

Molding Water Content: 29.70% (w_{opt})

Property	Before Test	After Test
Total Mass (g)	315.00	343.87
Mass of Solids (g)	242.87	242.83
Mass of Water (g)	72.13	101.04
Total Volume (cm^3)	201.81	191.64
Volume of Solids (cm^3)	90.62	90.61
Volume of Water (cm^3)	72.13	101.04
Volume of Air (cm^3)	39.05	-0.01
Water Content (%)	29.70	41.61
Volume of Voids (cm^3)	111.18	101.03
Void Ratio, e	1.227	1.115
Porosity, n (%)	55.1	52.7
Std. Proctor Relative Compaction, RC (%)	87.52	92.15
Moist Density, γ_m (g/cm^3)	1.56	1.79
Dry Density, γ_d (g/cm^3)	1.20	1.27
Degree of Saturation, S (%)	64.88	100.01
Consolidation Cell Pressure (kPa)	430.9	
Consolidation Back Pressure (kPa)	413.7	
Effective Consolidation Pressure (kPa)	17.2	

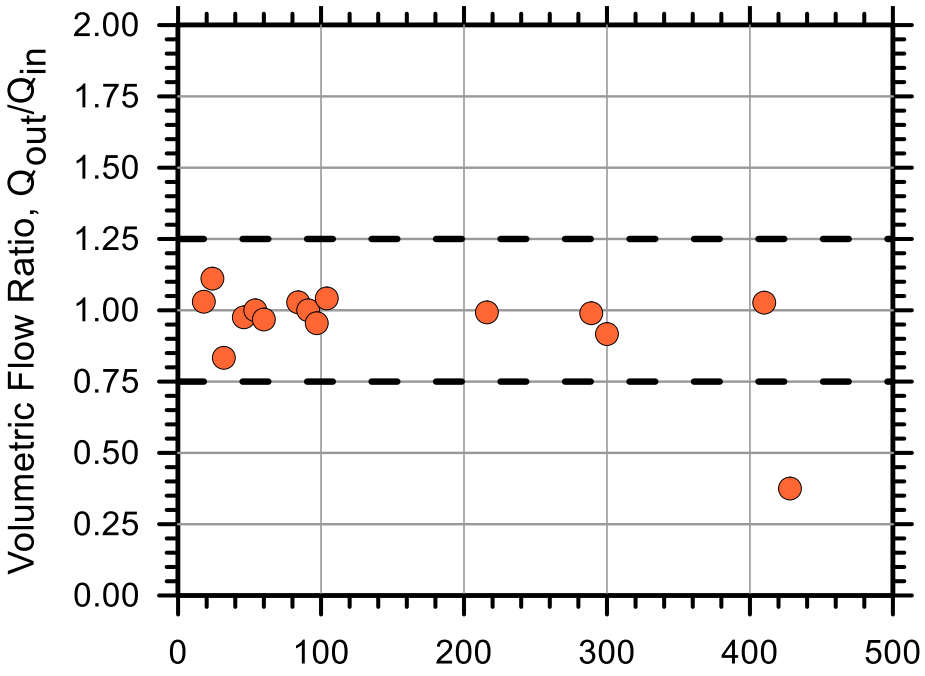
Volumetric Flow Ratio, Q_{out}/Q_{in}
2.00
1.75
1.50
1.25
1.00
0.75
0.50
0.25
0.00
0
100
200
300
400
500

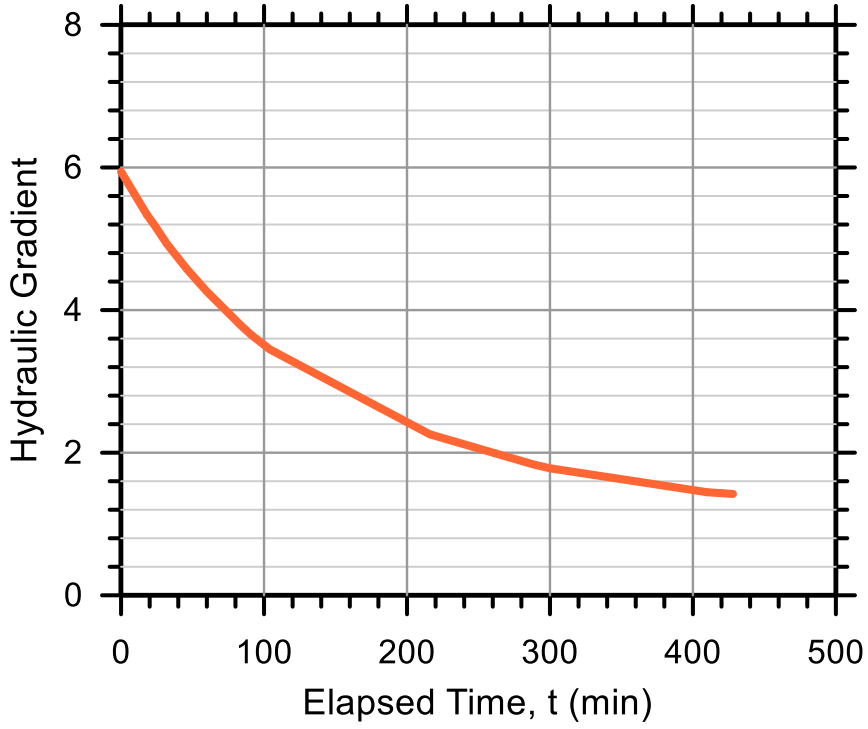
Hydraulic Gradient
8
6
4
2
0
0
100
200
300
400
500
Elapsed Time, t (min)

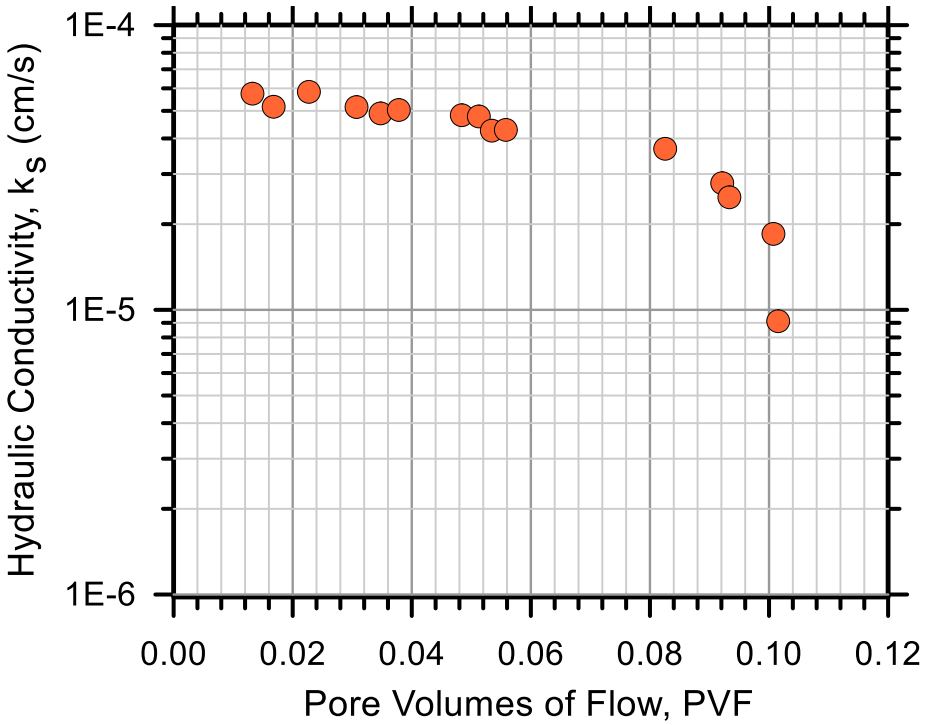
1E-4
1E-5
1E-6
Hydraulic Conductivity, k_S (cm/s)
0.00
0.02
0.04
0.06
0.08
0.10
0.12
Pore Volumes of Flow, PVF

Test No.: 46

Test Ref.: FXWH46

Test Soil: Whitehorne

Molding Water Content: 31.70% (w_{opt}+2)

Property	Before Test	After Test
Total Mass (g)	352.00	361.75
Mass of Solids (g)	267.27	267.21
Mass of Water (g)	84.73	94.54
Total Volume (cm^3)	201.81	195.85
Volume of Solids (cm^3)	99.73	99.71
Volume of Water (cm^3)	84.73	94.54
Volume of Air (cm^3)	17.35	1.61
Water Content (%)	31.70	35.38
Volume of Voids (cm^3)	102.08	96.15
Void Ratio, e	1.024	0.964
Porosity, n (%)	50.6	49.1
Std. Proctor Relative Compaction, RC (%)	96.32	99.22
Moist Density, γ_m (g/cm^3)	1.74	1.85
Dry Density, γ_d (g/cm^3)	1.32	1.36
Degree of Saturation, S (%)	83.00	98.33
Consolidation Cell Pressure (kPa)	482.7	
Consolidation Back Pressure (kPa)	413.7	
Effective Consolidation Pressure (kPa)	69.0	

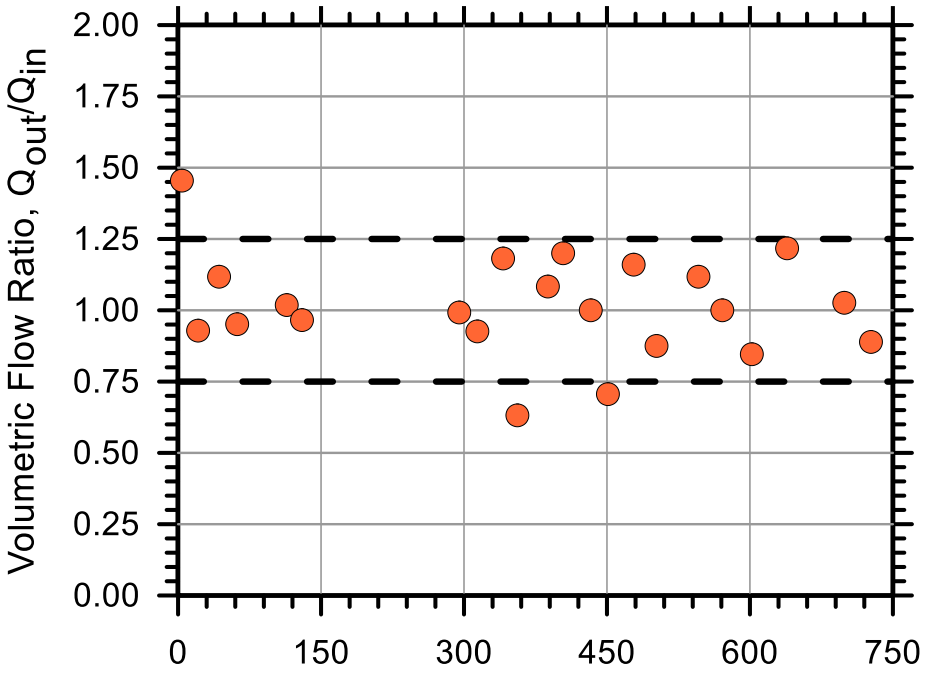
Volumetric Flow Ratio, Q_{out}/Q_{in}
2.00
1.75
1.50
1.25
1.00
0.75
0.50
0.25
0.00
0
150
300
450
600
750

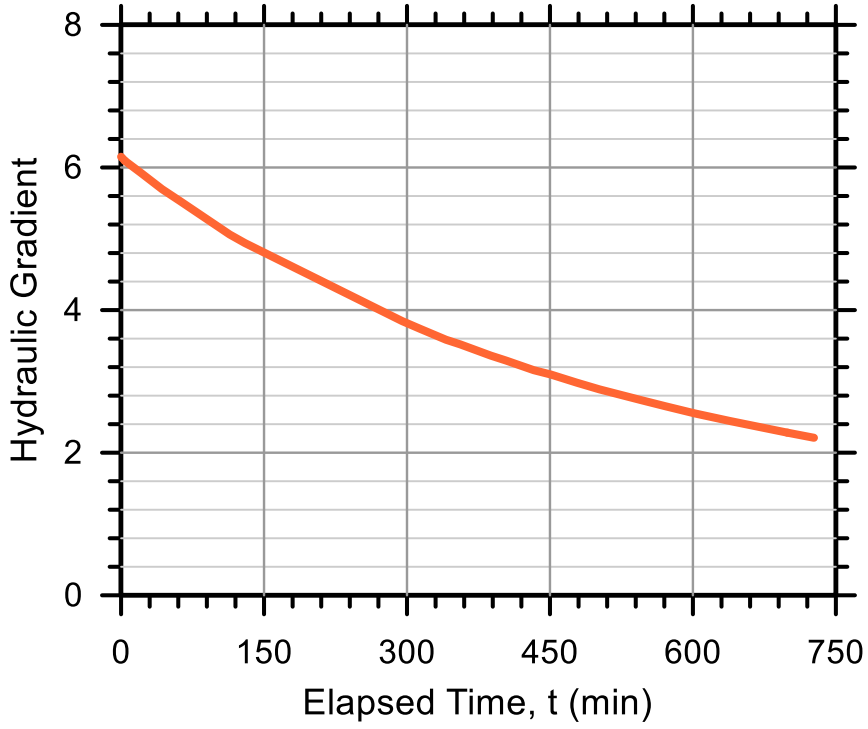
Hydraulic Gradient
8
6
4
2
0
0
150
300
450
600
750
Elapsed Time, t (min)

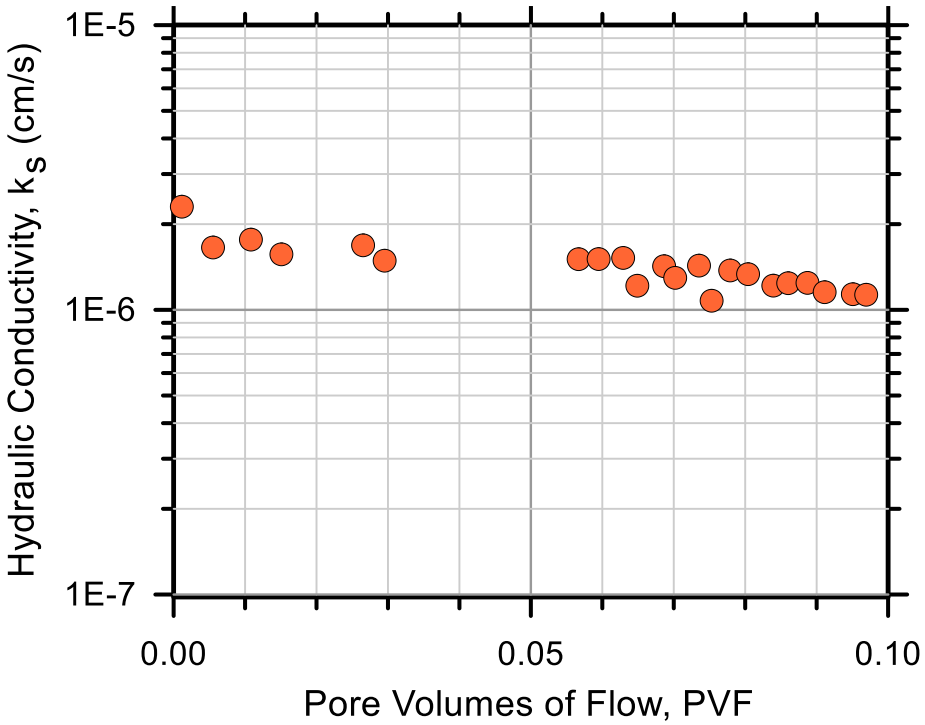
1E-5
1E-6
1E-7
Hydraulic Conductivity, k_S (cm/s)
0.00
0.05
0.10
Pore Volumes of Flow, PVF

Test No.: 11

Test Ref.: FXWH11

Test Soil: Whitehorne

Molding Water Content: 31.70% (w_{opt}+2)

Property	Before Test	After Test
Total Mass (g)	138.00	144.89
Mass of Solids (g)	104.78	104.81
Mass of Water (g)	33.22	40.08
Total Volume (cm^3)	100.90	79.22
Volume of Solids (cm^3)	39.10	39.11
Volume of Water (cm^3)	33.22	40.08
Volume of Air (cm^3)	28.59	0.03
Water Content (%)	31.70	38.24
Volume of Voids (cm^3)	61.81	40.11
Void Ratio, e	1.581	1.026
Porosity, n (%)	61.3	50.6
Std. Proctor Relative Compaction, RC (%)	75.52	96.22
Moist Density, γ_m (g/cm^3)	1.37	1.83
Dry Density, γ_d (g/cm^3)	1.04	1.32
Degree of Saturation, S (%)	53.74	99.92
Consolidation Cell Pressure (kPa)	448.2	
Consolidation Back Pressure (kPa)	413.7	
Effective Consolidation Pressure (kPa)	34.5	

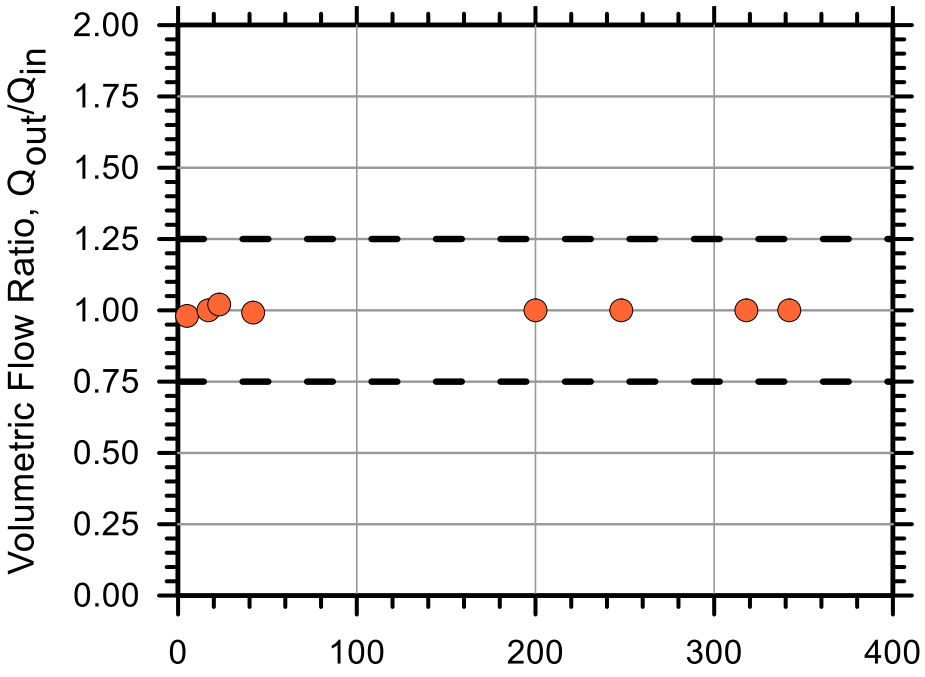
Volumetric Flow Ratio, Q_{out}/Q_{in}
2.00
1.75
1.50
1.25
1.00
0.75
0.50
0.25
0.00
0
100
200
300
400

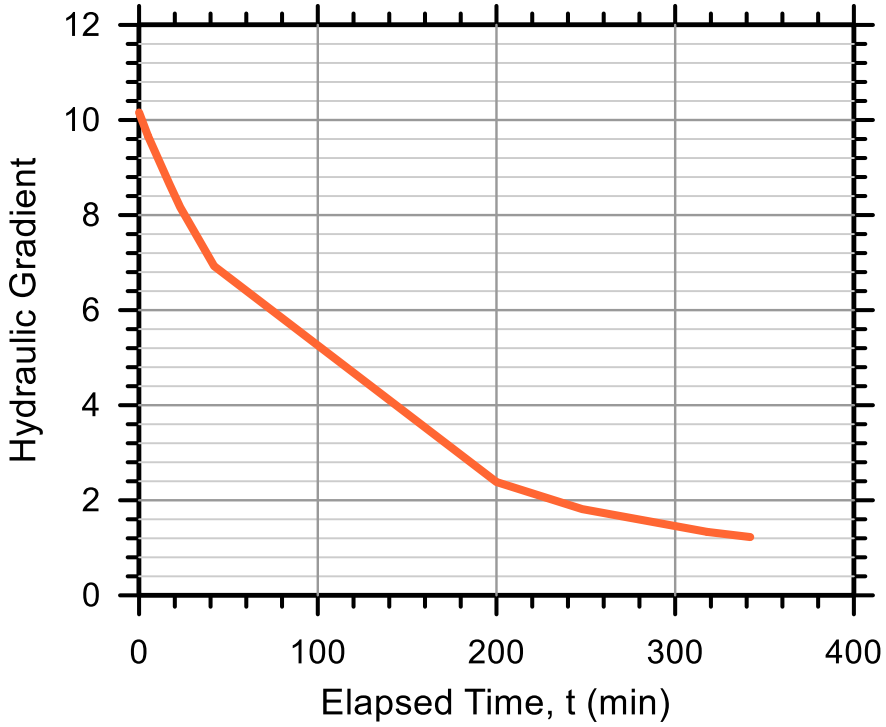
Hydraulic Gradient
12
10
8
6
4
2
0
0
100
200
300
400
Elapsed Time, t (min)

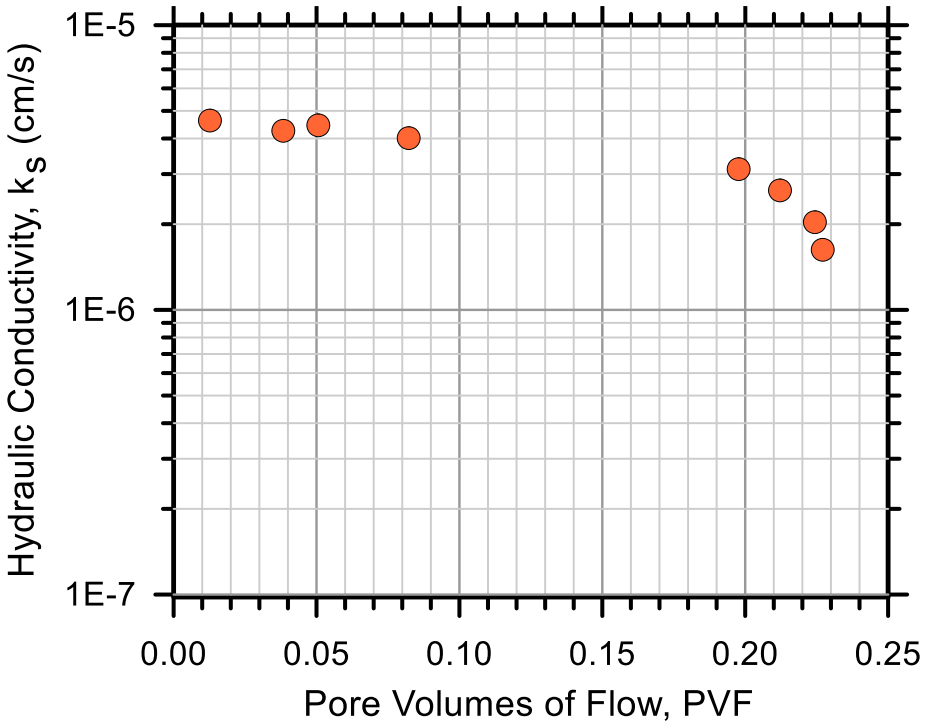
1E-5
1E-6
1E-7
Hydraulic Conductivity, k_S (cm/s)
0.00
0.05
0.10
0.15
0.20
0.25
Pore Volumes of Flow, PVF

Test No.: 3

Test Ref.: FXWH03

Test Soil: Whitehorne

Molding Water Content: 31.70% (w_{opt}+2)

Property	Before Test	After Test
Total Mass (g)	162.00	176.80
Mass of Solids (g)	123.01	122.97
Mass of Water (g)	38.99	53.83
Total Volume (cm^3)	100.90	99.74
Volume of Solids (cm^3)	45.90	45.89
Volume of Water (cm^3)	38.99	53.83
Volume of Air (cm^3)	16.01	0.03
Water Content (%)	31.70	43.77
Volume of Voids (cm^3)	55.01	53.86
Void Ratio, e	1.198	1.174
Porosity, n (%)	54.5	54.0
Std. Proctor Relative Compaction, RC (%)	88.66	89.67
Moist Density, γ_m (g/cm^3)	1.61	1.77
Dry Density, γ_d (g/cm^3)	1.22	1.23
Degree of Saturation, S (%)	70.89	99.94
Consolidation Cell Pressure (kPa)	427.5	
Consolidation Back Pressure (kPa)	413.7	
Effective Consolidation Pressure (kPa)	13.8	

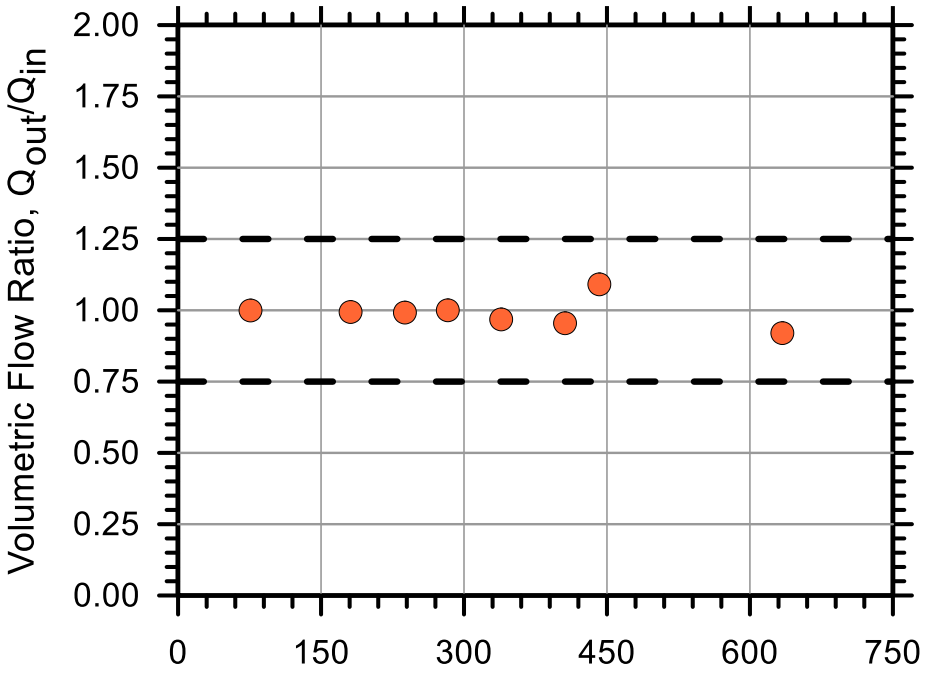
Volumetric Flow Ratio, Q_{out}/Q_{in}
2.00
1.75
1.50
1.25
1.00
0.75
0.50
0.25
0.00
0
150
300
450
600
750

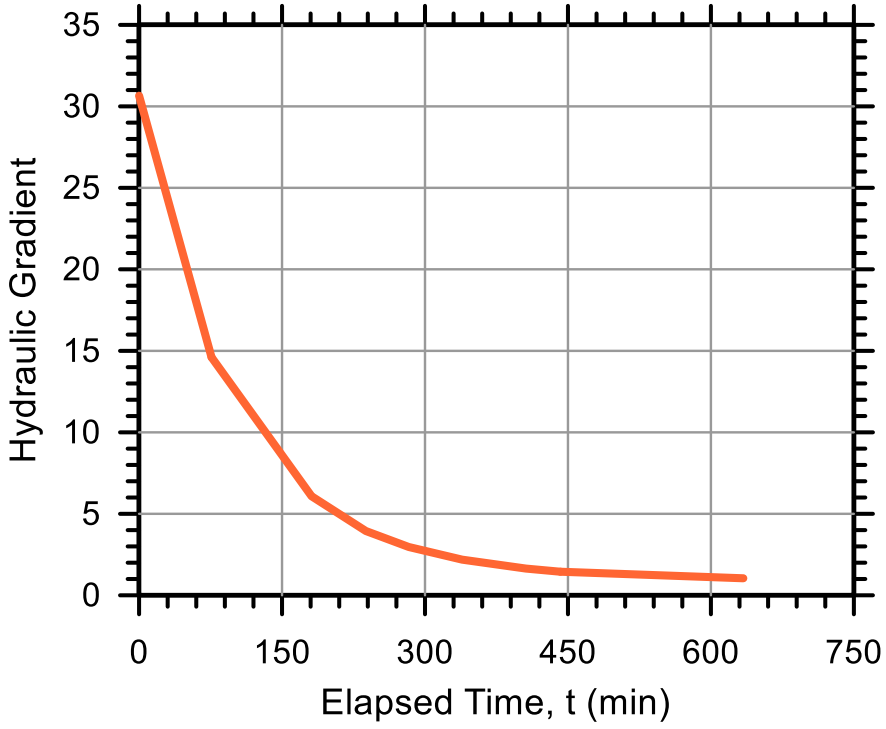
Hydraulic Gradient
35
30
25
20
15
10
5
0
0
150
300
450
600
750
Elapsed Time, t (min)

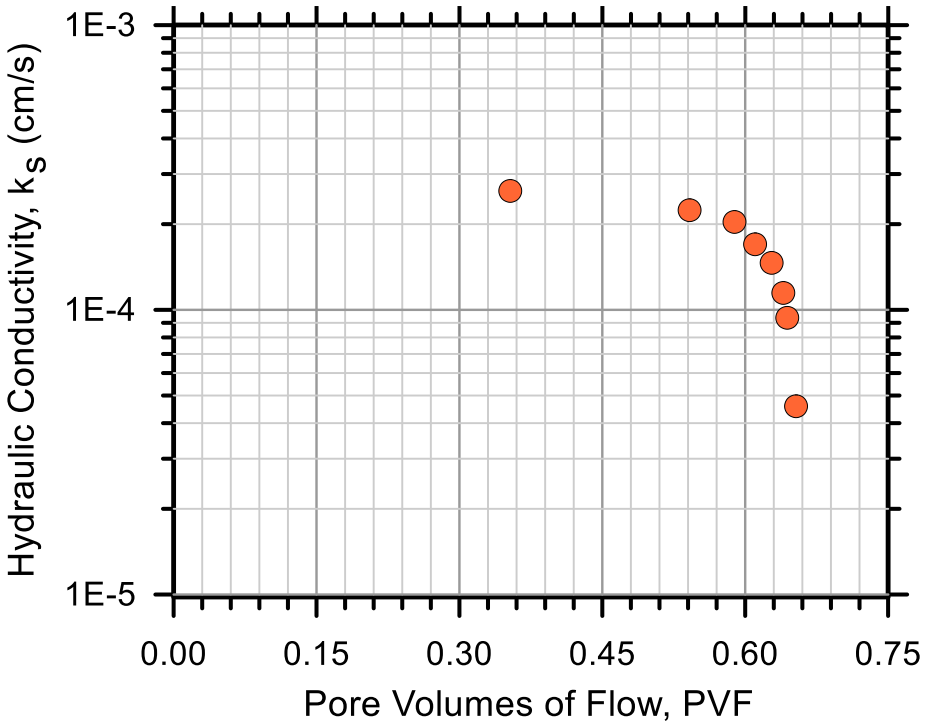
1E-3
1E-4
1E-5
Hydraulic Conductivity, k_S (cm/s)
0.00
0.15
0.30
0.45
0.60
0.75
Pore Volumes of Flow, PVF

Test No.: 28

Test Ref.: FXWH28

Test Soil: Whitehorne

Molding Water Content: 31.70% (w_{opt}+2)

Property	Before Test	After Test
Total Mass (g)	305.00	338.14
Mass of Solids (g)	231.59	231.54
Mass of Water (g)	73.41	106.60
Total Volume (cm^3)	201.81	193.04
Volume of Solids (cm^3)	86.41	86.40
Volume of Water (cm^3)	73.41	106.60
Volume of Air (cm^3)	41.98	0.04
Water Content (%)	31.70	46.04
Volume of Voids (cm^3)	115.39	106.64
Void Ratio, e	1.335	1.234
Porosity, n (%)	57.2	55.2
Std. Proctor Relative Compaction, RC (%)	83.46	87.23
Moist Density, γ_m (g/cm^3)	1.51	1.75
Dry Density, γ_d (g/cm^3)	1.15	1.20
Degree of Saturation, S (%)	63.62	99.96
Consolidation Cell Pressure (kPa)	417.1	
Consolidation Back Pressure (kPa)	413.7	
Effective Consolidation Pressure (kPa)	3.4	

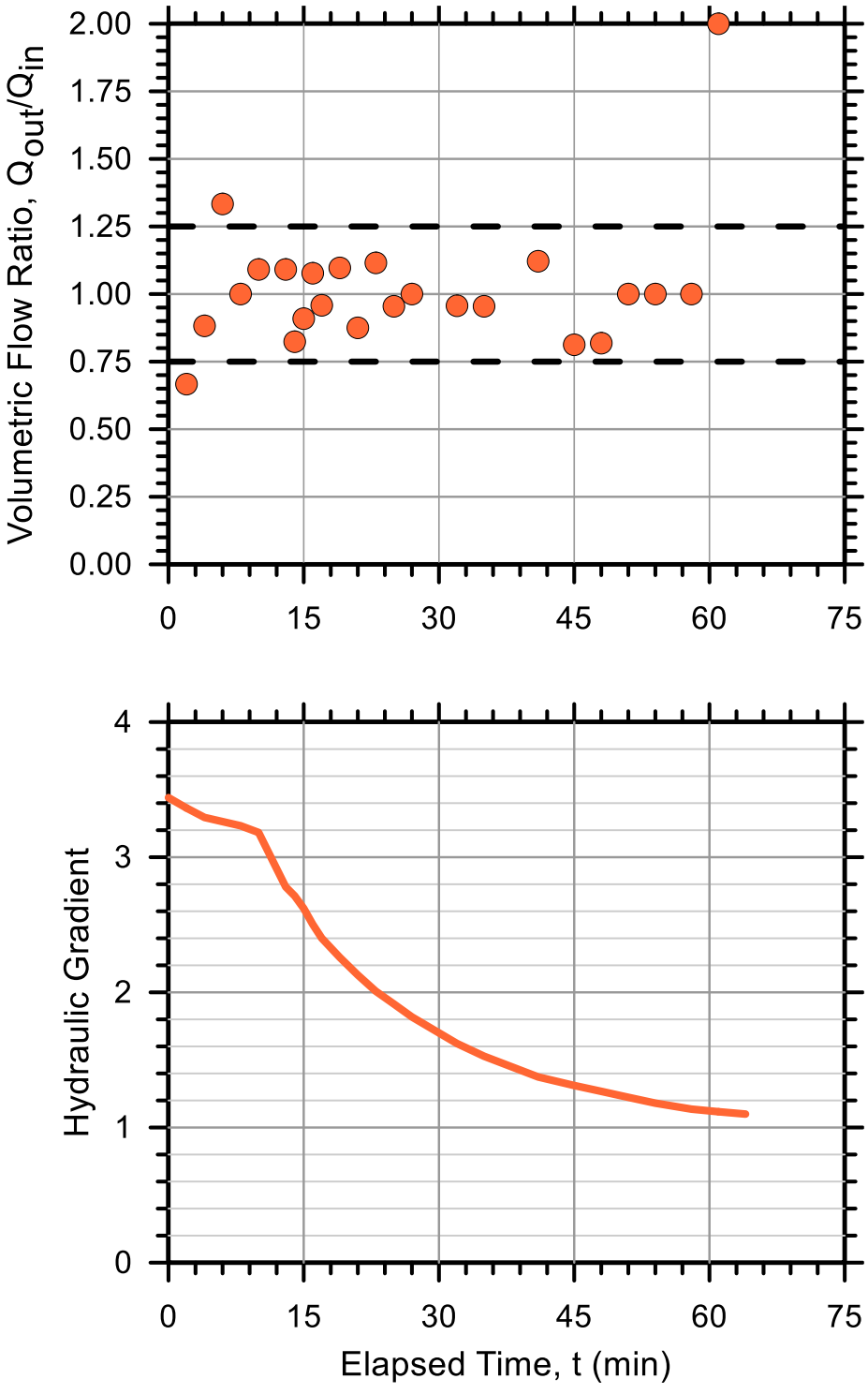
Volumetric Flow Ratio, Q_{out}/Q_{in}
2.00
1.75
1.50
1.25
1.00
0.75
0.50
0.25
0.00
0
15
30
45
60
75
Hydraulic Gradient
4
3
2
1
0
0
15
30
45
60
75
Elapsed Time, t (min)

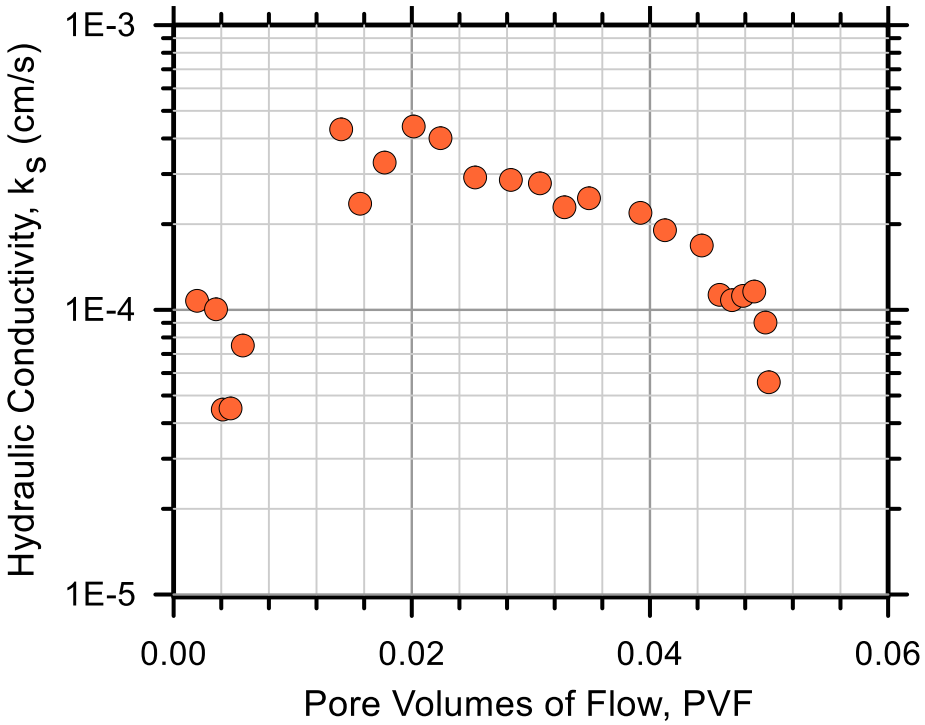
1E-3
1E-4
1E-5
Hydraulic Conductivity, k_S (cm/s)
0.00
0.02
0.04
0.06
Pore Volumes of Flow, PVF

Test No.: 47

Test Ref.: FXTC47

Test Soil: Tom's Creek

Molding Water Content: 15.70% (w_{opt}-2.5)

Property	Before Test	After Test
Total Mass (g)	374.00	395.13
Mass of Solids (g)	323.25	323.21
Mass of Water (g)	50.75	71.92
Total Volume (cm^3)	201.81	196.65
Volume of Solids (cm^3)	123.85	123.84
Volume of Water (cm^3)	50.75	71.92
Volume of Air (cm^3)	27.21	0.90
Water Content (%)	15.70	22.25
Volume of Voids (cm^3)	77.96	72.81
Void Ratio, e	0.629	0.588
Porosity, n (%)	0.386	0.370
Std. Proctor Relative Compaction, RC (%)	94.22	96.68
Moist Density, γ_m (g/cm^3)	1.85	2.01
Dry Density, γ_d (g/cm^3)	1.60	1.64
Degree of Saturation, S (%)	65.10	98.76
Consolidation Cell Pressure (kPa)	448.2	
Consolidation Back Pressure (kPa)	413.7	
Effective Consolidation Pressure (kPa)	34.5	

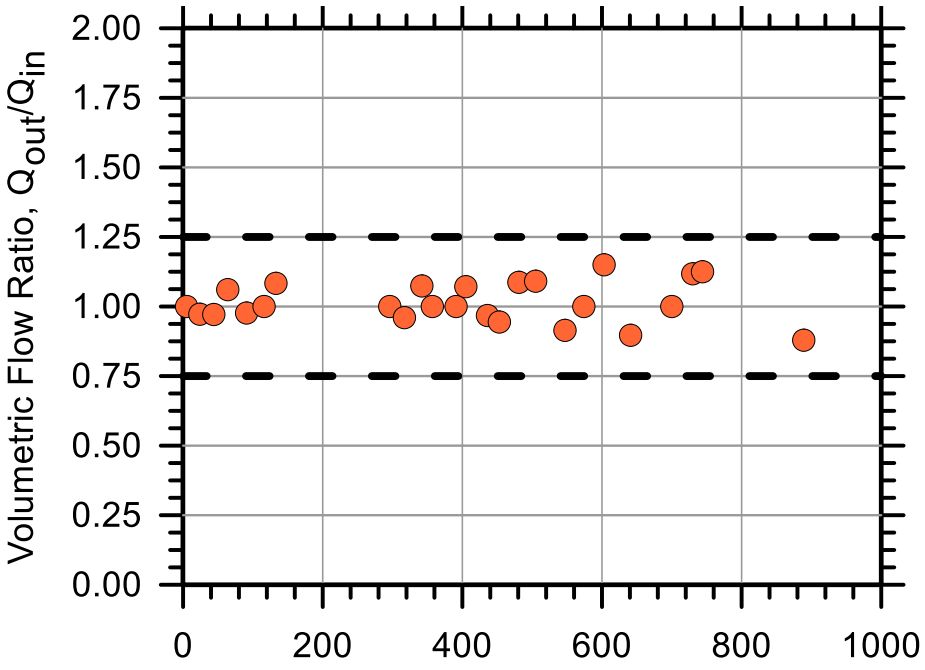
Volumetric Flow Ratio, Q_{out}/Q_{in}
2.00
1.75
1.50
1.25
1.00
0.75
0.50
0.25
0.00
0
200
400
600
800
1000

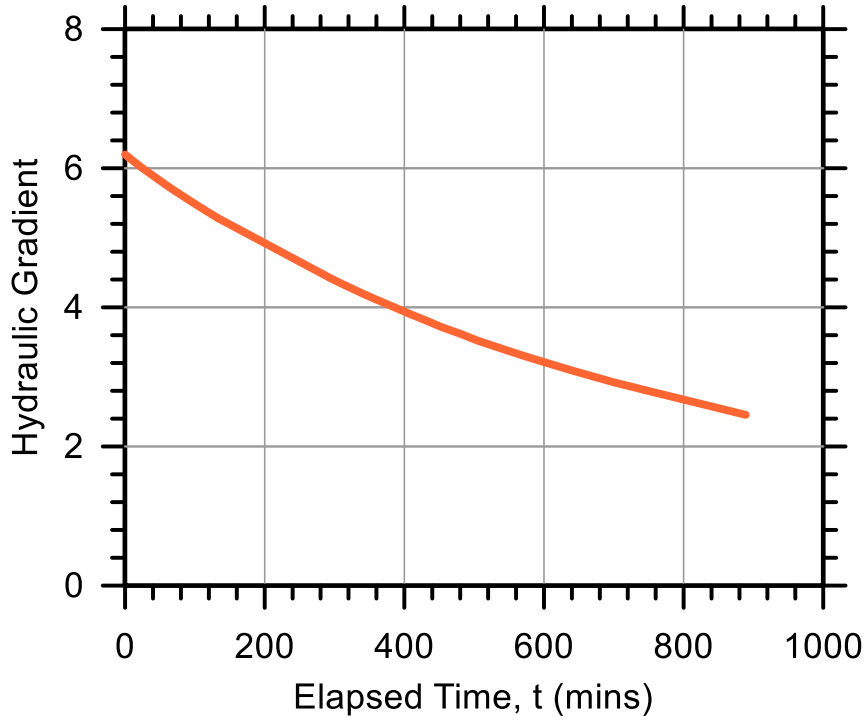
Hydraulic Gradient
8
6
4
2
0
0
200
400
600
800
1000
Elapsed Time, t (mins)

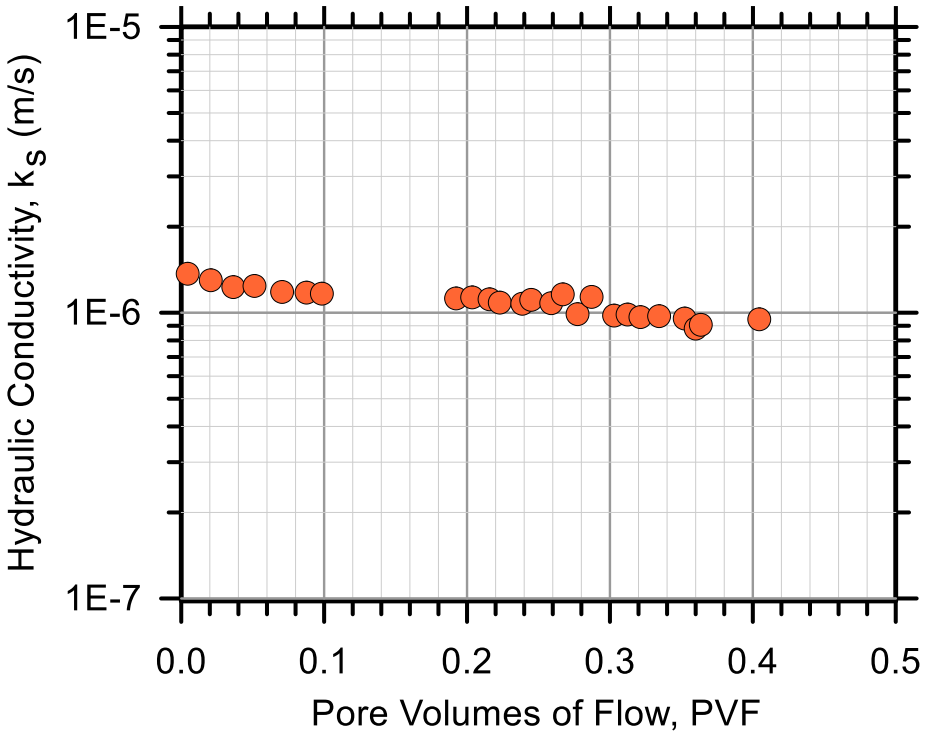
1E-5
1E-6
1E-7
Hydraulic Conductivity, k_S (m/s)
0.0
0.1
0.2
0.3
0.4
0.5
Pore Volumes of Flow, PVF

Test No.: 7

Test Ref.: FXTC07

Test Soil: Tom's Creek

Molding Water Content: 15.70% (w_{opt}-2.5)

Property	Before Test	After Test
Total Mass (g)	187.00	199.88
Mass of Solids (g)	161.62	161.56
Mass of Water (g)	25.38	38.32
Total Volume (cm^3)	100.90	100.26
Volume of Solids (cm^3)	61.93	61.90
Volume of Water (cm^3)	25.38	38.32
Volume of Air (cm^3)	13.60	0.04
Water Content (%)	15.70	23.72
Volume of Voids (cm^3)	38.98	38.36
Void Ratio, e	0.629	0.620
Porosity, n (%)	0.386	0.383
Std. Proctor Relative Compaction, RC (%)	94.22	94.78
Moist Density, γ_m (g/cm^3)	1.85	1.99
Dry Density, γ_d (g/cm^3)	1.60	1.61
Degree of Saturation, S (%)	65.10	99.89
Consolidation Cell Pressure (kPa)	434.4	
Consolidation Back Pressure (kPa)	413.7	
Effective Consolidation Pressure (kPa)	20.7	

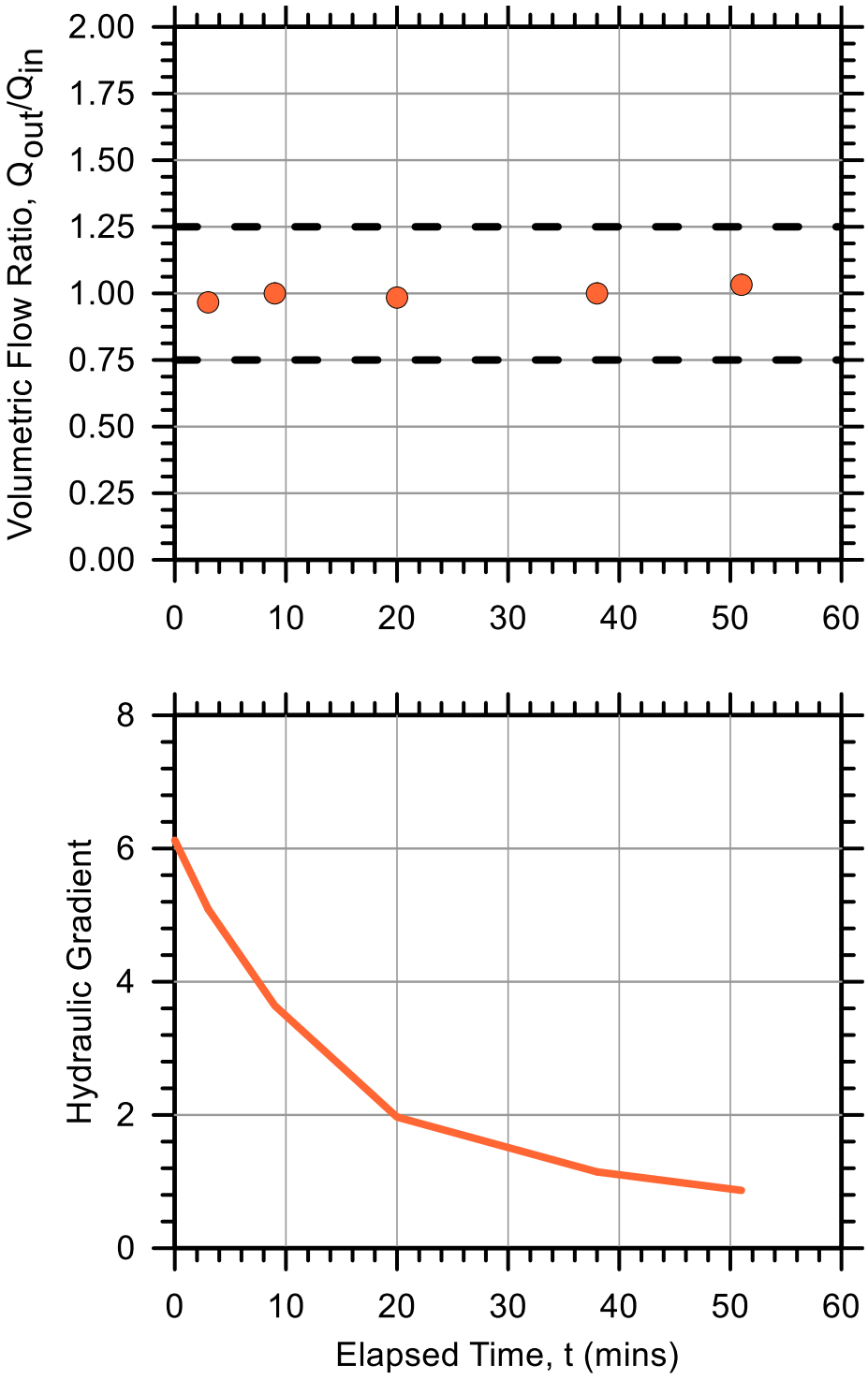
Volumetric Flow Ratio, Q_{out}/Q_{in}
2.00
1.75
1.50
1.25
1.00
0.75
0.50
0.25
0.00
0
10
20
30
40
50
60
Hydraulic Gradient
8
6
4
2
0
0
10
20
30
40
50
60
Elapsed Time, t (mins)

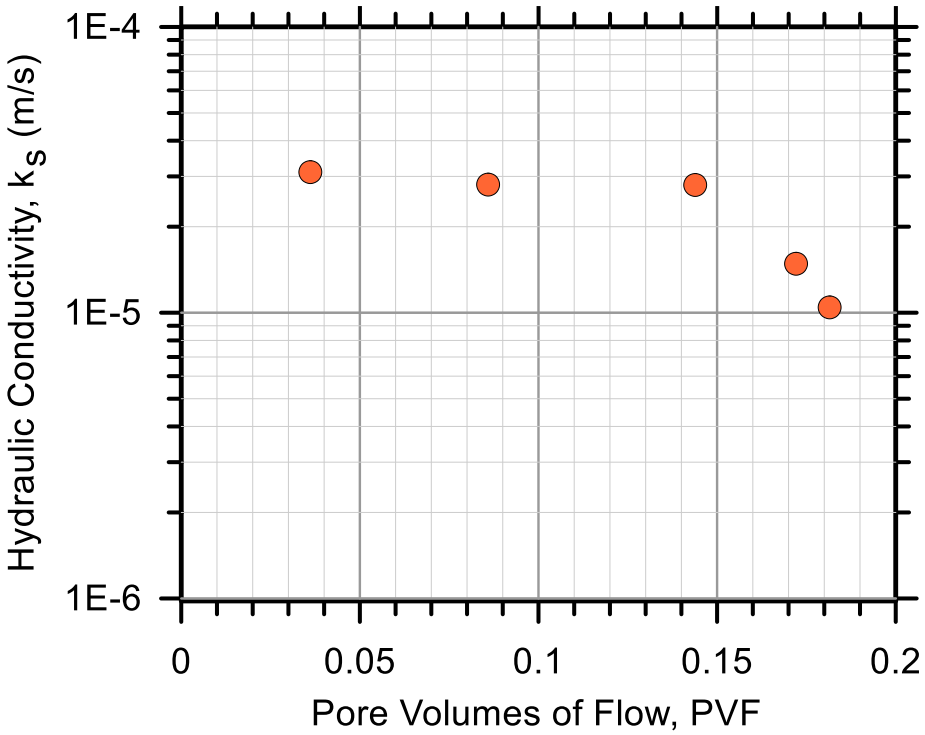
1E-4
1E-5
1E-6
Hydraulic Conductivity, k_S (m/s)
0
0.05
0.1
0.15
0.2
Pore Volumes of Flow, PVF

Test No.: 48

Test Ref.: FXTC48

Test Soil: Tom's Creek

Molding Water Content: 15.70% (w_{opt}-2.5)

Property	Before Test	After Test
Total Mass (g)	327.00	357.06
Mass of Solids (g)	282.63	282.57
Mass of Water (g)	44.37	74.49
Total Volume (cm^3)	201.81	182.77
Volume of Solids (cm^3)	108.29	108.27
Volume of Water (cm^3)	44.37	74.49
Volume of Air (cm^3)	49.15	0.02
Water Content (%)	15.70	26.36
Volume of Voids (cm^3)	93.52	74.50
Void Ratio, e	0.864	0.688
Porosity, n (%)	0.463	0.408
Std. Proctor Relative Compaction, RC (%)	82.38	90.95
Moist Density, γ_m (g/cm^3)	1.62	1.95
Dry Density, γ_d (g/cm^3)	1.40	1.55
Degree of Saturation, S (%)	47.45	99.98
Consolidation Cell Pressure (kPa)	420.6	
Consolidation Back Pressure (kPa)	413.7	
Effective Consolidation Pressure (kPa)	6.9	

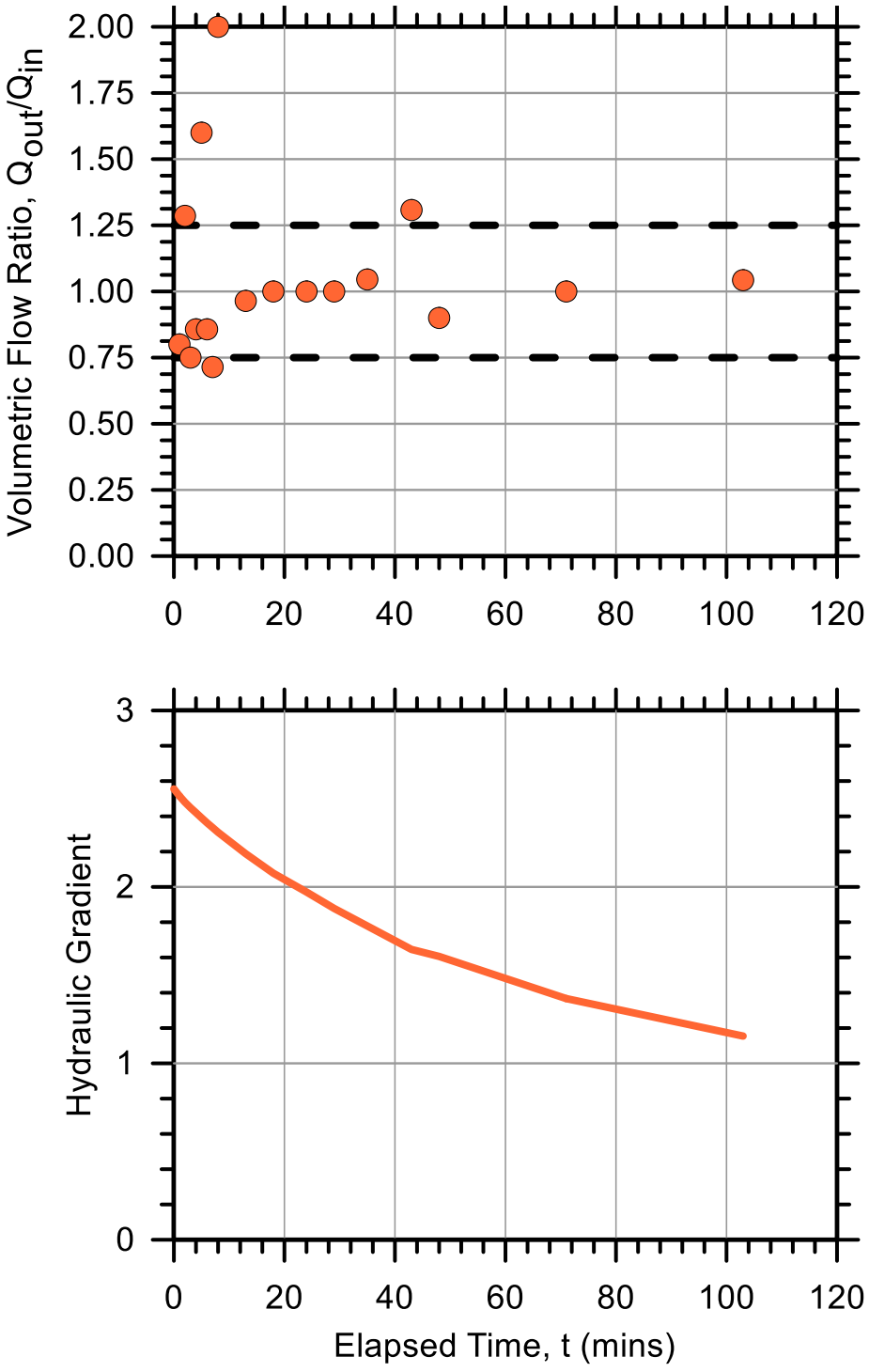
Volumetric Flow Ratio, Q_{out}/Q_{in}
2.00
1.75
1.50
1.25
1.00
0.75
0.50
0.25
0.00
0
20
40
60
80
100
120
Hydraulic Gradient
3
2
1
0
0
20
40
60
80
100
120
Elapsed Time, t (mins)

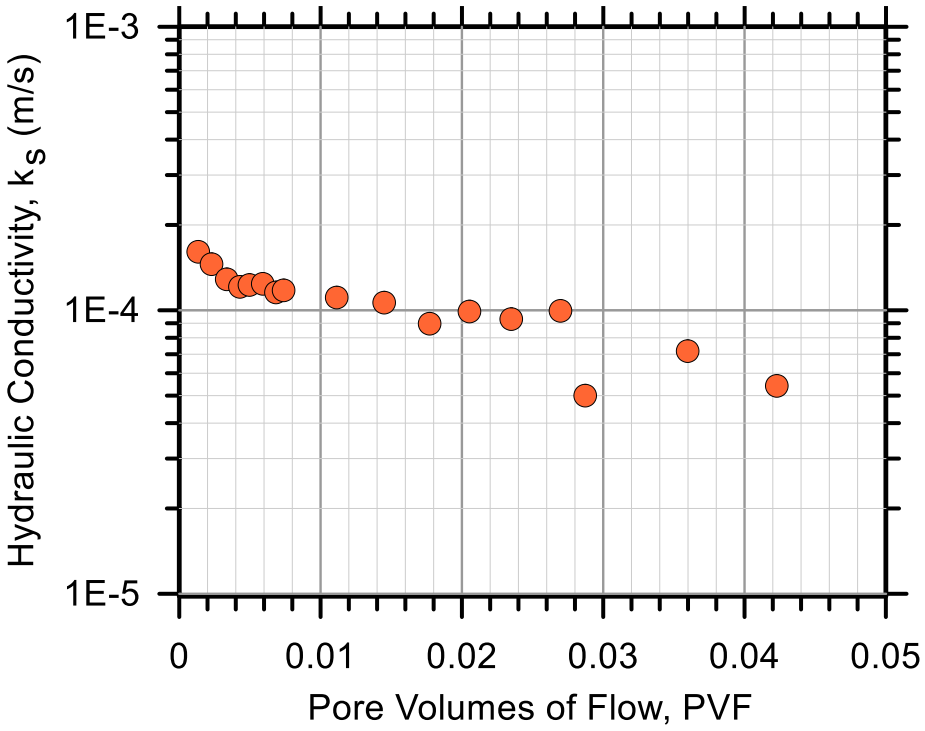
1E-3
1E-4
1E-5
Hydraulic Conductivity, k_S (m/s)
0
0.01
0.02
0.03
0.04
0.05
Pore Volumes of Flow, PVF

Test No.: 51

Test Ref.: FXTC51

Test Soil: Tom's Creek

Molding Water Content: 18.70% (w_{opt}+0.5)

Property	Before Test	After Test
Total Mass (g)	387.00	393.44
Mass of Solids (g)	326.03	326.05
Mass of Water (g)	60.97	67.39
Total Volume (cm^3)	201.81	192.59
Volume of Solids (cm^3)	124.92	124.92
Volume of Water (cm^3)	60.97	67.39
Volume of Air (cm^3)	15.92	0.27
Water Content (%)	18.70	20.67
Volume of Voids (cm^3)	76.89	67.66
Void Ratio, e	0.616	0.542
Porosity, n (%)	38.1	35.1
Std. Proctor Relative Compaction, RC (%)	95.03	99.59
Moist Density, γ_m (g/cm^3)	1.92	2.04
Dry Density, γ_d (g/cm^3)	1.62	1.69
Degree of Saturation, S (%)	79.29	99.60
Consolidation Cell Pressure (kPa)	482.7	
Consolidation Back Pressure (kPa)	413.7	
Effective Consolidation Pressure (kPa)	69.0	

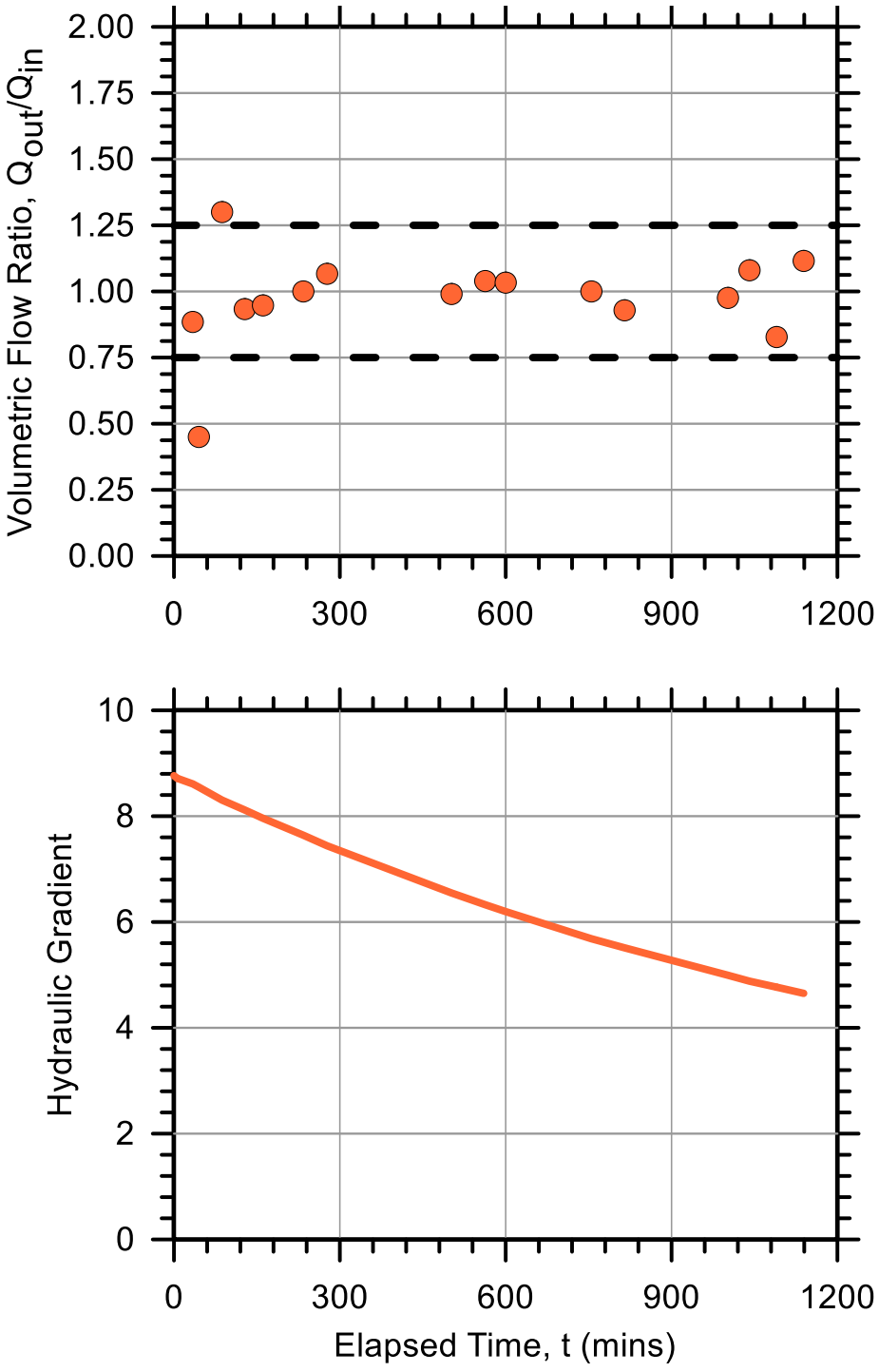
Volumetric Flow Ratio, Q_{out}/Q_{in}
2.00
1.75
1.50
1.25
1.00
0.75
0.50
0.25
0.00
0
300
600
900
1200
Hydraulic Gradient
10
8
6
4
2
0
0
300
600
900
1200
Elapsed Time, t (mins)

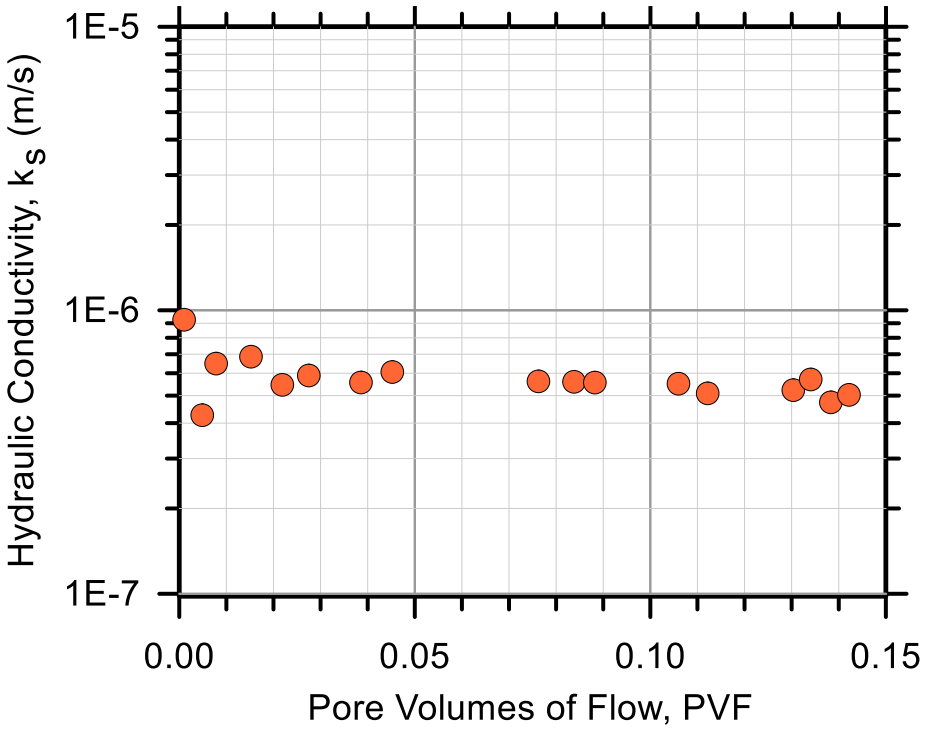
1E-5
1E-6
1E-7
Hydraulic Conductivity, k_S (m/s)
0.00
0.05
0.10
0.15
Pore Volumes of Flow, PVF

Test No.: 44

Test Ref.: FXTC44

Test Soil: Tom's Creek

Molding Water Content: 18.70% (w_{opt}+0.5)

Property	Before Test	After Test
Total Mass (g)	383.00	390.87
Mass of Solids (g)	322.66	322.23
Mass of Water (g)	60.34	68.64
Total Volume (cm^3)	201.81	193.07
Volume of Solids (cm^3)	123.63	123.46
Volume of Water (cm^3)	60.34	68.64
Volume of Air (cm^3)	17.84	0.98
Water Content (%)	18.70	21.30
Volume of Voids (cm^3)	78.18	69.61
Void Ratio, e	0.632	0.564
Porosity, n (%)	38.7	36.1
Std. Proctor Relative Compaction, RC (%)	94.05	98.18
Moist Density, γ_m (g/cm^3)	1.90	2.02
Dry Density, γ_d (g/cm^3)	1.60	1.67
Degree of Saturation, S (%)	77.18	98.60
Consolidation Cell Pressure (kPa)	448.2	
Consolidation Back Pressure (kPa)	413.7	
Effective Consolidation Pressure (kPa)	34.5	

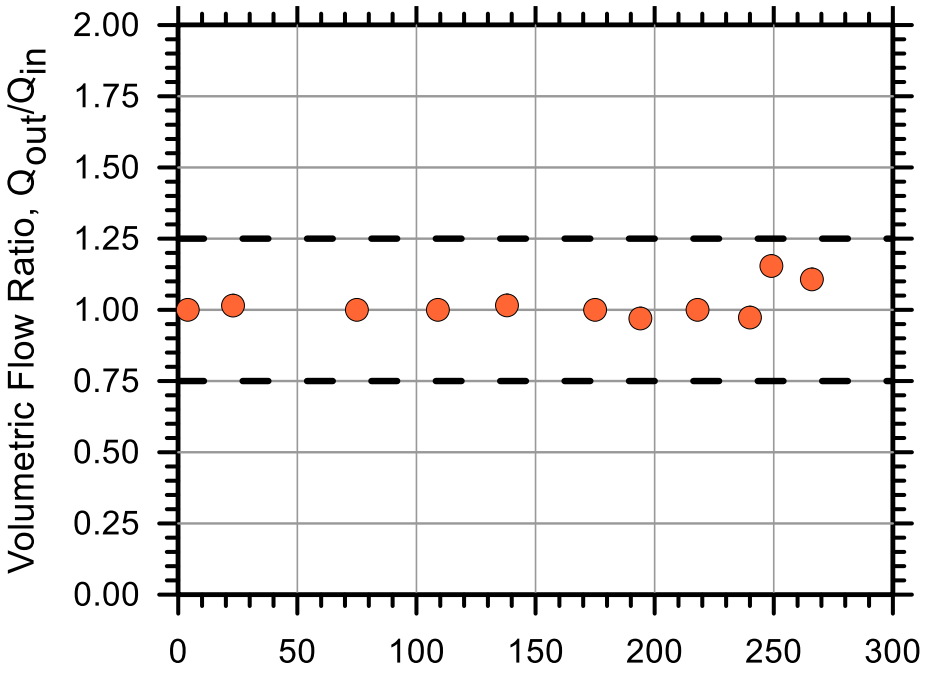
Volumetric Flow Ratio, Q_{out}/Q_{in}
2.00
1.75
1.50
1.25
1.00
0.75
0.50
0.25
0.00
0
50
100
150
200
250
300

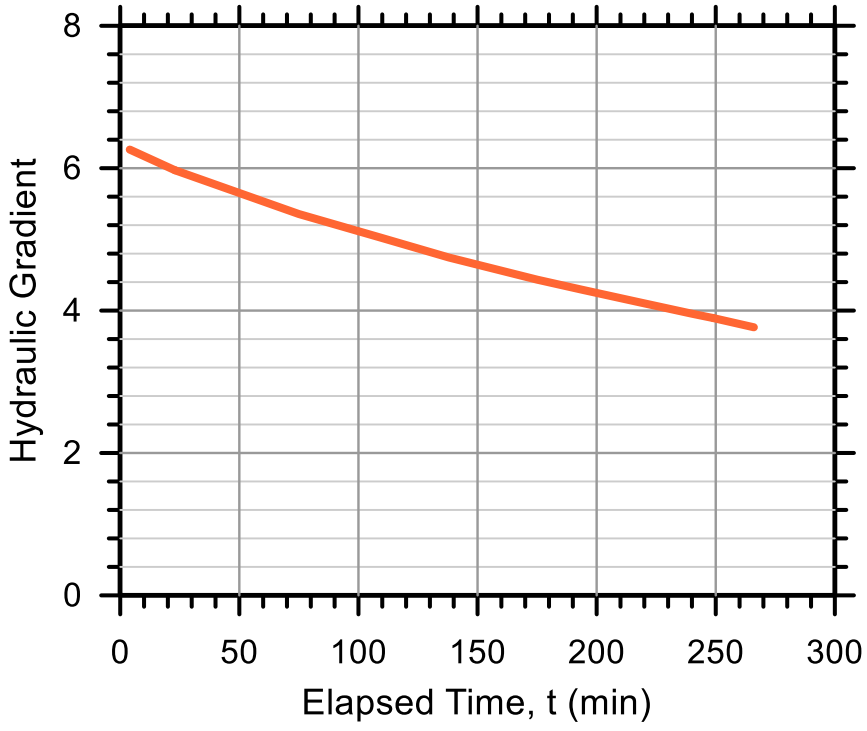
Hydraulic Gradient
8
6
4
2
0
0
50
100
150
200
250
300
Elapsed Time, t (min)

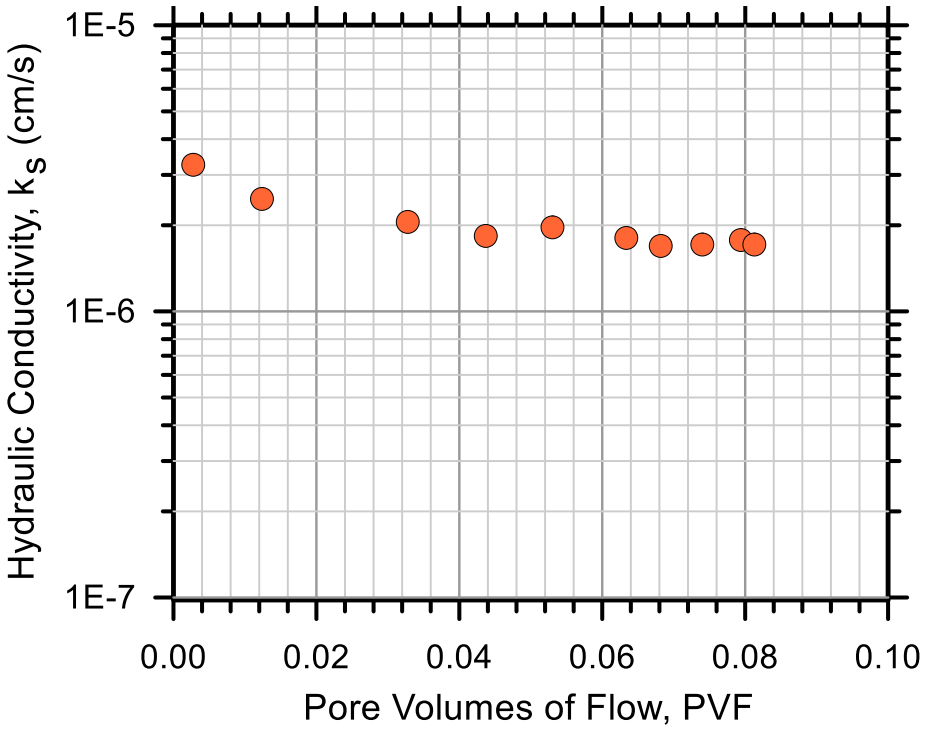
1E-5
1E-6
1E-7
Hydraulic Conductivity, k_s (cm/s)
0.00
0.02
0.04
0.06
0.08
0.10
Pore Volumes of Flow, PVF

Test No.: 24

Test Ref.: FXTC24

Test Soil: Tom's Creek

Molding Water Content: 18.70% (w_{opt}+0.5)

Property	Before Test	After Test
Total Mass (g)	348.00	367.10
Mass of Solids (g)	293.18	292.98
Mass of Water (g)	54.82	74.12
Total Volume (cm^3)	201.81	186.80
Volume of Solids (cm^3)	112.33	112.25
Volume of Water (cm^3)	54.82	74.12
Volume of Air (cm^3)	34.66	0.42
Water Content (%)	18.70	25.30
Volume of Voids (cm^3)	89.48	74.54
Void Ratio, e	0.797	0.664
Porosity, n (%)	44.3	39.9
Std. Proctor Relative Compaction, RC (%)	85.46	92.26
Moist Density, γ_m (g/cm^3)	1.72	1.97
Dry Density, γ_d (g/cm^3)	1.45	1.57
Degree of Saturation, S (%)	61.27	99.44
Consolidation Cell Pressure (kPa)	420.6	
Consolidation Back Pressure (kPa)	413.7	
Effective Consolidation Pressure (kPa)	420.6	

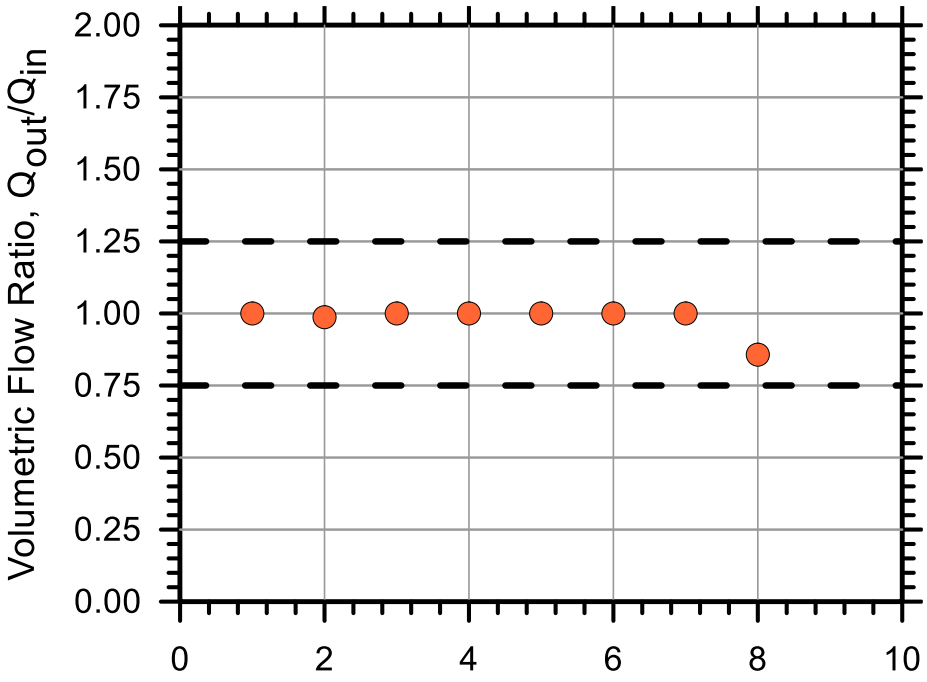
Volumetric Flow Ratio, Q_{out}/Q_{in}
2.00
1.75
1.50
1.25
1.00
0.75
0.50
0.25
0.00
0
2
4
6
8
10

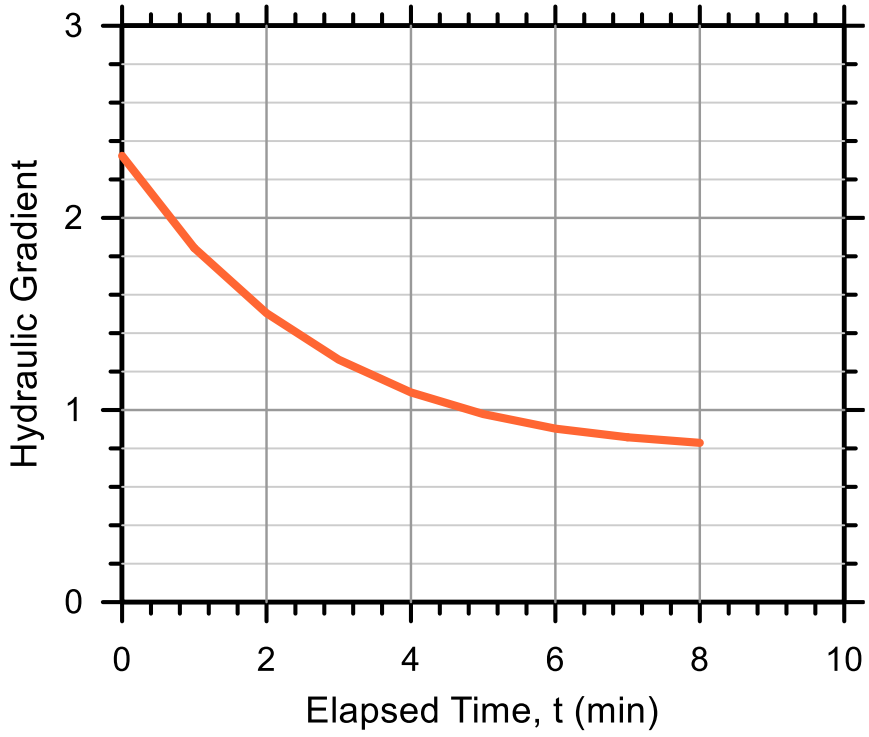
Hydraulic Gradient
3
2
1
0
0
2
4
6
8
10
Elapsed Time, t (min)

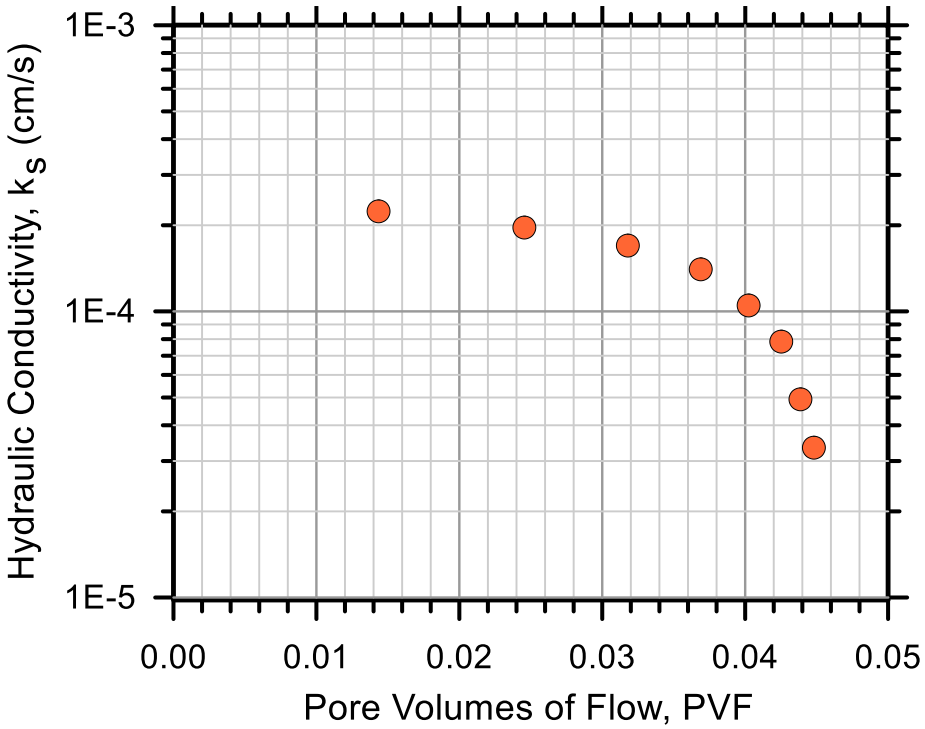
1E-3
1E-4
1E-5
Hydraulic Conductivity, k_s (cm/s)
0.00
0.01
0.02
0.03
0.04
0.05
Pore Volumes of Flow, PVF

Test No.: 45

Test Ref.: FXM7X45

Test Soil: Sand-Clay (75%-25%)

Molding Water Content: 8.40% (w_{opt}-2)

Property	Before Test	After Test
Total Mass (g)	410.00	432.75
Mass of Solids (g)	378.23	378.28
Mass of Water (g)	31.77	54.47
Total Volume (cm^3)	201.81	197.58
Volume of Solids (cm^3)	142.73	142.75
Volume of Water (cm^3)	31.77	54.47
Volume of Air (cm^3)	27.31	0.36
Water Content (%)	8.40	14.40
Volume of Voids (cm^3)	59.08	54.84
Void Ratio, e	0.414	0.384
Porosity, n (%)	0.293	0.278
Std. Proctor Relative Compaction, RC (%)	93.62	95.63
Moist Density, γ_m (g/cm^3)	2.03	2.19
Dry Density, γ_d (g/cm^3)	1.87	1.91
Degree of Saturation, S (%)	53.78	99.34
Consolidation Cell Pressure (kPa)	441.3	
Consolidation Back Pressure (kPa)	413.7	
Effective Consolidation Pressure (kPa)	27.6	

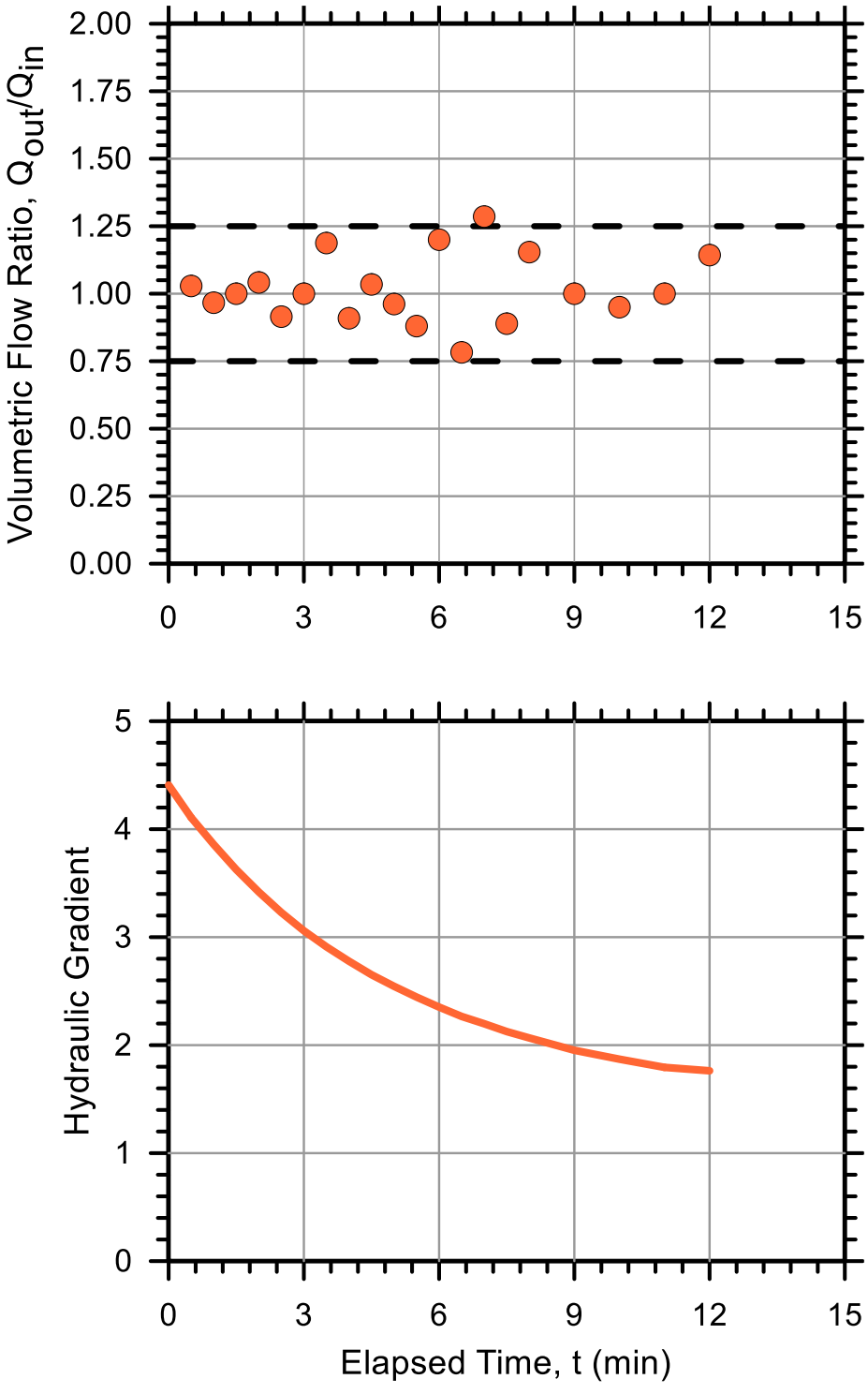
Volumetric Flow Ratio, Q_{out}/Q_{in}
2.00
1.75
1.50
1.25
1.00
0.75
0.50
0.25
0.00
0
3
6
9
12
15
Hydraulic Gradient
5
4
3
2
1
0
0
3
6
9
12
15
Elapsed Time, t (min)

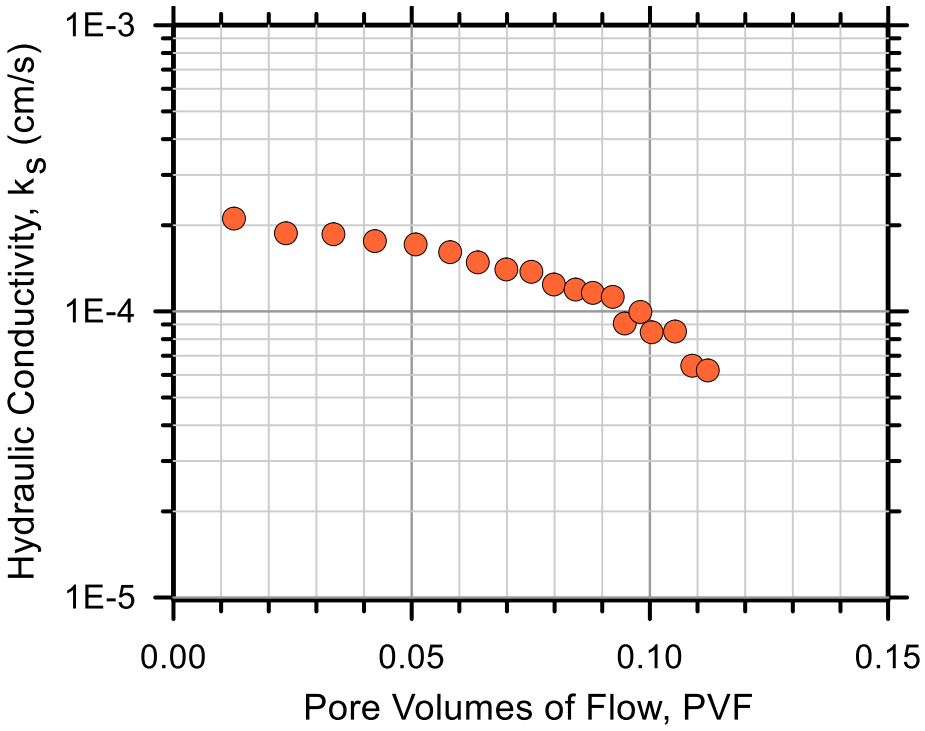
1E-3
1E-4
1E-5
Hydraulic Conductivity, k_S (cm/s)
0.00
0.05
0.10
0.15
Pore Volumes of Flow, PVF

Test No.: 33

Test Ref.: FXM7X33

Test Soil: Sand-Clay (75%-25%)

Molding Water Content: 8.40% (w_{opt}-2)

Property	Before Test	After Test
Total Mass (g)	390.00	420.67
Mass of Solids (g)	359.78	359.42
Mass of Water (g)	30.22	61.25
Total Volume (cm^3)	201.81	198.18
Volume of Solids (cm^3)	135.77	135.63
Volume of Water (cm^3)	30.22	61.25
Volume of Air (cm^3)	35.82	1.30
Water Content (%)	8.40	17.04
Volume of Voids (cm^3)	66.04	62.55
Void Ratio, e	0.486	0.461
Porosity, n (%)	32.7	31.6
Std. Proctor Relative Compaction, RC (%)	89.05	90.59
Moist Density, γ_m (g/cm^3)	1.93	2.12
Dry Density, γ_d (g/cm^3)	1.78	1.81
Degree of Saturation, S (%)	390.00	420.67
Consolidation Cell Pressure (kPa)	434.4	
Consolidation Back Pressure (kPa)	413.7	
Effective Consolidation Pressure (kPa)	20.7	

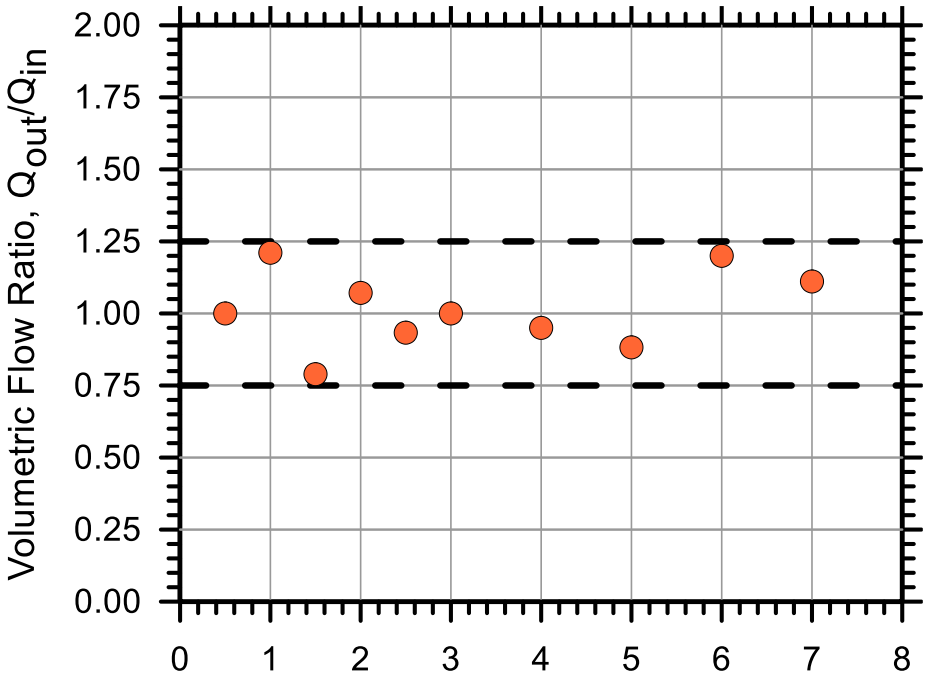
Volumetric Flow Ratio, Q_{out}/Q_{in}
2.00
1.75
1.50
1.25
1.00
0.75
0.50
0.25
0.00
0
1
2
3
4
5
6
7
8

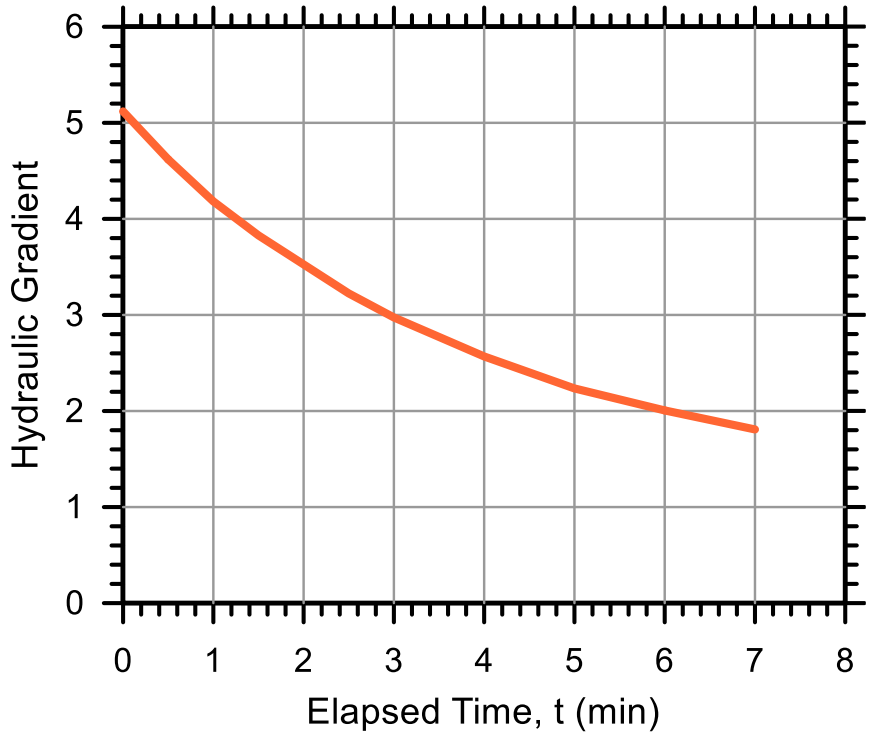
Hydraulic Gradient
6
5
4
3
2
1
0
0
1
2
3
4
5
6
7
8
Elapsed Time, t (min)

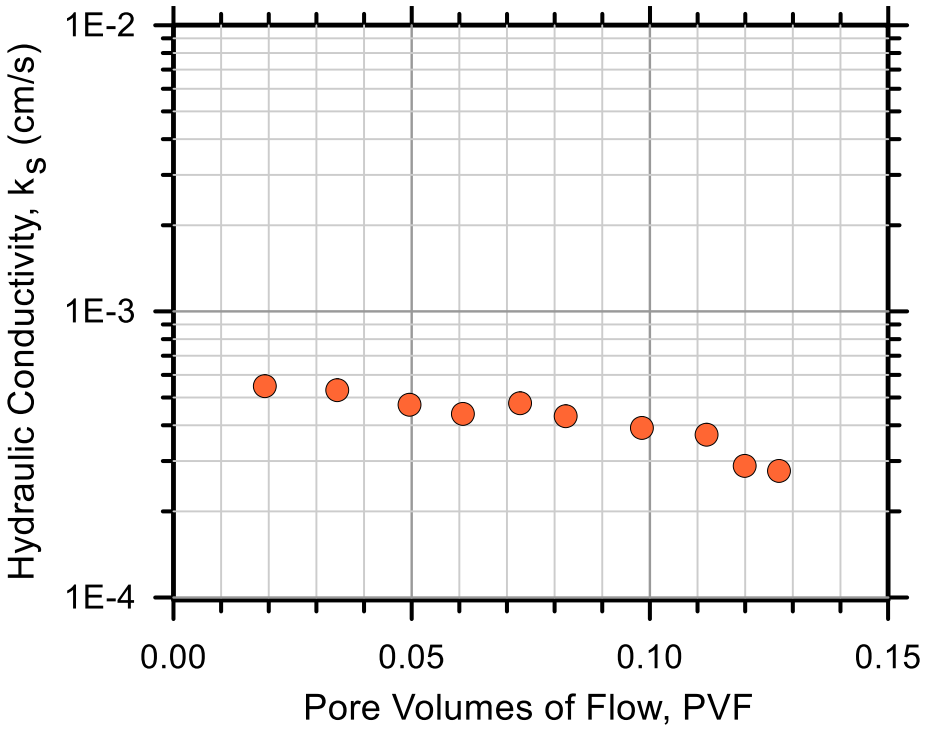
1E-2
1E-3
1E-4
Hydraulic Conductivity, k_S (cm/s)
0.00
0.05
0.10
0.15
Pore Volumes of Flow, PVF

Test No.: 38

Test Ref.: FXM7X38

Test Soil: Sand-Clay (75%-25%)

Molding Water Content: 8.40% (w_{opt}-2)

Property	Before Test	After Test
Total Mass (g)	367.00	400.30
Mass of Solids (g)	338.56	338.52
Mass of Water (g)	28.44	61.78
Total Volume (cm^3)	201.81	192.66
Volume of Solids (cm^3)	127.76	127.74
Volume of Water (cm^3)	28.44	61.78
Volume of Air (cm^3)	45.61	3.14
Water Content (%)	8.40	18.25
Volume of Voids (cm^3)	74.05	64.92
Void Ratio, e	0.580	0.508
Porosity, n (%)	36.7	33.7
Std. Proctor Relative Compaction, RC (%)	83.80	87.76
Moist Density, γ_m (g/cm^3)	1.82	2.08
Dry Density, γ_d (g/cm^3)	1.68	1.76
Degree of Saturation, S (%)	38.41	95.16
Consolidation Cell Pressure (kPa)	427.5	
Consolidation Back Pressure (kPa)	413.7	
Effective Consolidation Pressure (kPa)	13.8	

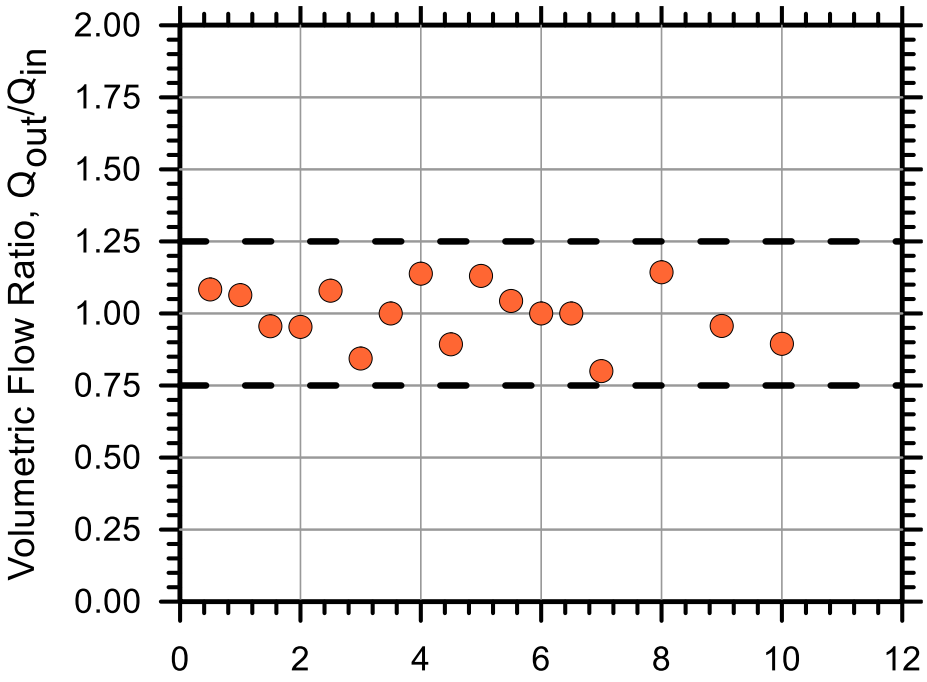
Volumetric Flow Ratio, Q_{out}/Q_{in}
2.00
1.75
1.50
1.25
1.00
0.75
0.50
0.25
0.00
0
2
4
6
8
10
12

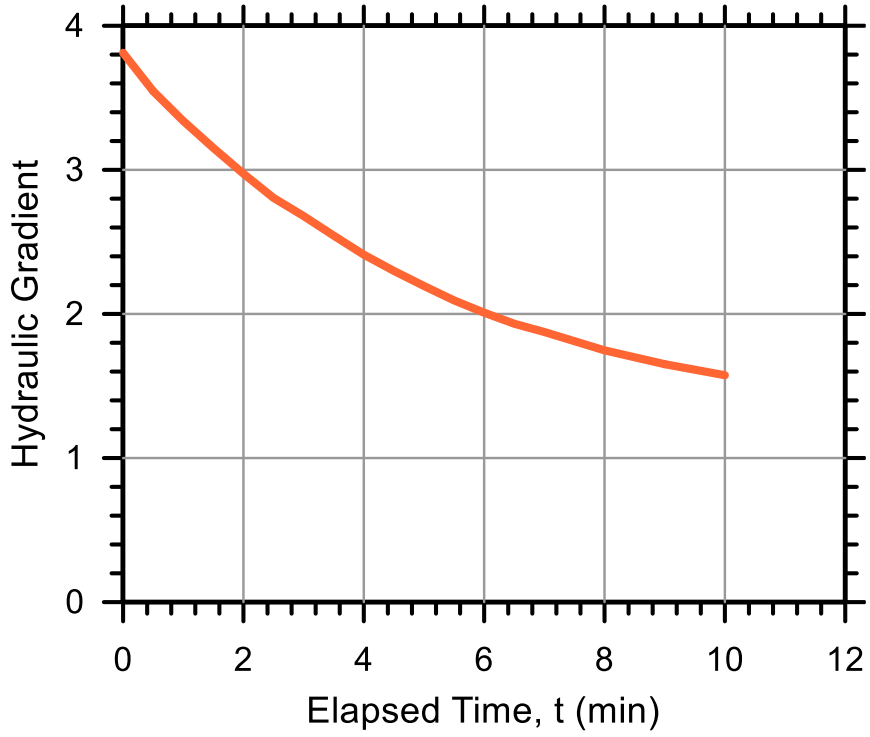
Hydraulic Gradient
4
3
2
1
0
0
2
4
6
8
10
12
Elapsed Time, t (min)

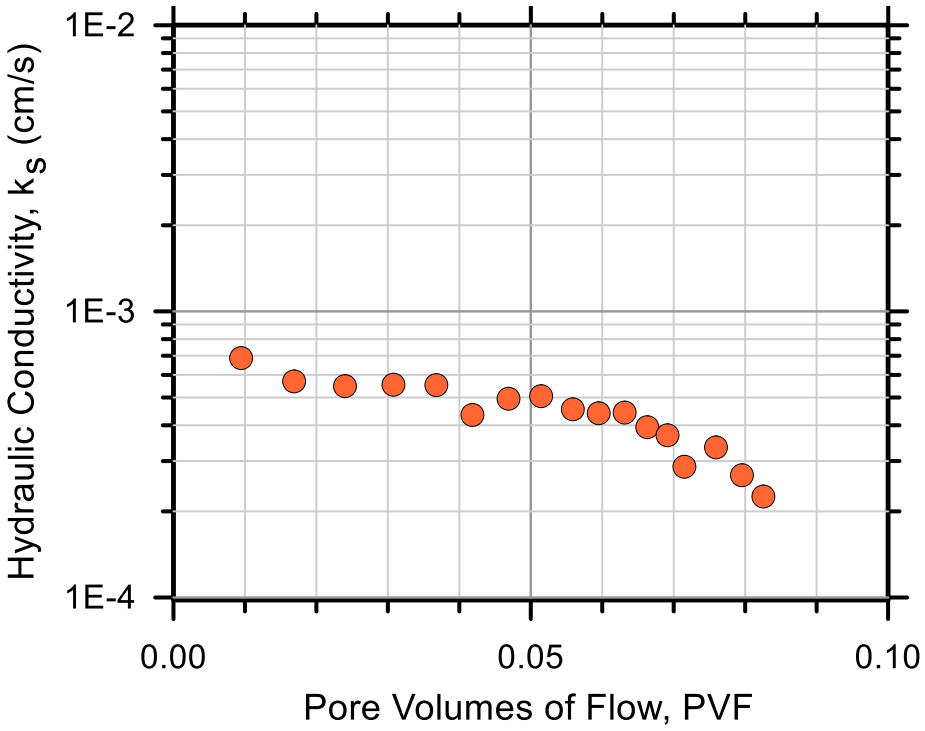
1E-2
1E-3
1E-4
Hydraulic Conductivity, k_S (cm/s)
0.00
0.05
0.10
Pore Volumes of Flow, PVF

Test No.: 43

Test Ref.: FXM7X43

Test Soil: Sand-Clay (75%-25%)

Molding Water Content: 11.40% (w_{opt}+1)

Property	Before Test	After Test
Total Mass (g)	428.00	433.88
Mass of Solids (g)	384.20	384.34
Mass of Water (g)	43.80	49.54
Total Volume (cm^3)	201.81	198.13
Volume of Solids (cm^3)	144.98	145.03
Volume of Water (cm^3)	43.80	49.54
Volume of Air (cm^3)	13.03	3.56
Water Content (%)	11.40	12.89
Volume of Voids (cm^3)	56.83	53.10
Void Ratio, e	0.392	0.366
Porosity, n (%)	28.2	26.8
Std. Proctor Relative Compaction, RC (%)	95.09	96.89
Moist Density, γ_m (g/cm^3)	2.12	2.19
Dry Density, γ_d (g/cm^3)	1.90	1.94
Degree of Saturation, S (%)	77.08	93.30
Consolidation Cell Pressure (kPa)	455.1	
Consolidation Back Pressure (kPa)	413.7	
Effective Consolidation Pressure (kPa)	41.4	

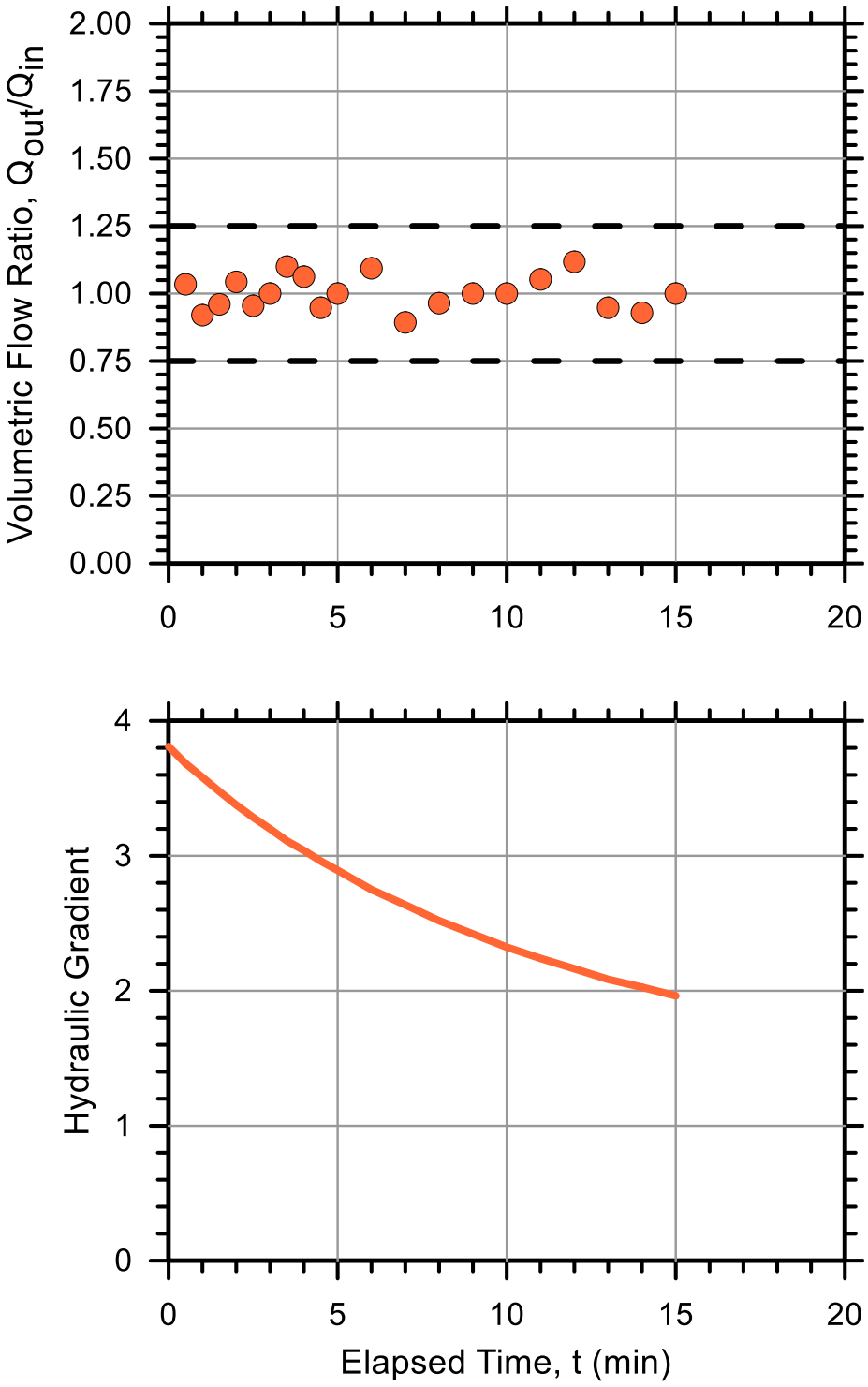
Volumetric Flow Ratio, Q_{out}/Q_{in}
2.00
1.75
1.50
1.25
1.00
0.75
0.50
0.25
0.00
0
5
10
15
20
Hydraulic Gradient
4
3
2
1
0
0
5
10
15
20
Elapsed Time, t (min)

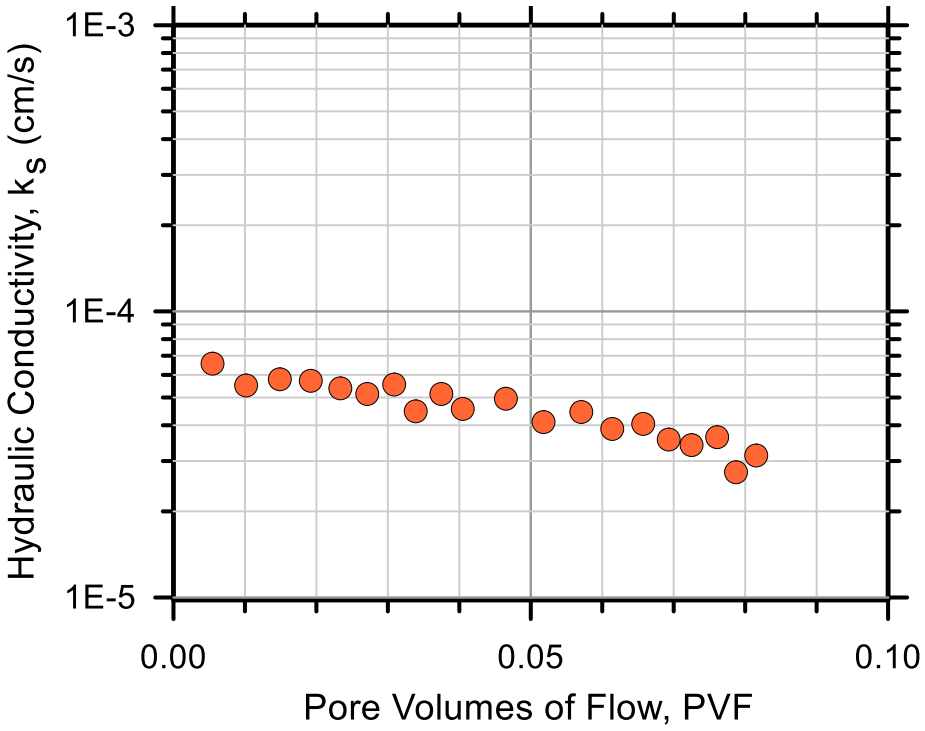
1E-3
1E-4
1E-5
Hydraulic Conductivity, k_s (cm/s)
0.00
0.05
0.10
Pore Volumes of Flow, PVF

Test No.: 42

Test Ref.: FXM8X42

Test Soil: Sand-Clay (85%-15%)

Molding Water Content: 8.10% (w_{opt}-1.3)

Property	Before Test	After Test
Total Mass (g)	400.00	424.91
Mass of Solids (g)	370.03	368.88
Mass of Water (g)	29.97	56.03
Total Volume (cm^3)	201.81	198.98
Volume of Solids (cm^3)	139.63	139.20
Volume of Water (cm^3)	29.97	56.03
Volume of Air (cm^3)	32.20	3.75
Water Content (%)	8.10	15.19
Volume of Voids (cm^3)	62.17	59.78
Void Ratio, e	0.445	0.429
Porosity, n (%)	30.8	30.0
Std. Proctor Relative Compaction, RC (%)	94.66	95.71
Moist Density, γ_m (g/cm^3)	1.98	2.14
Dry Density, γ_d (g/cm^3)	1.83	1.85
Degree of Saturation, S (%)	48.21	93.73
Consolidation Cell Pressure (kPa)	448.2	
Consolidation Back Pressure (kPa)	413.7	
Effective Consolidation Pressure (kPa)	34.5	

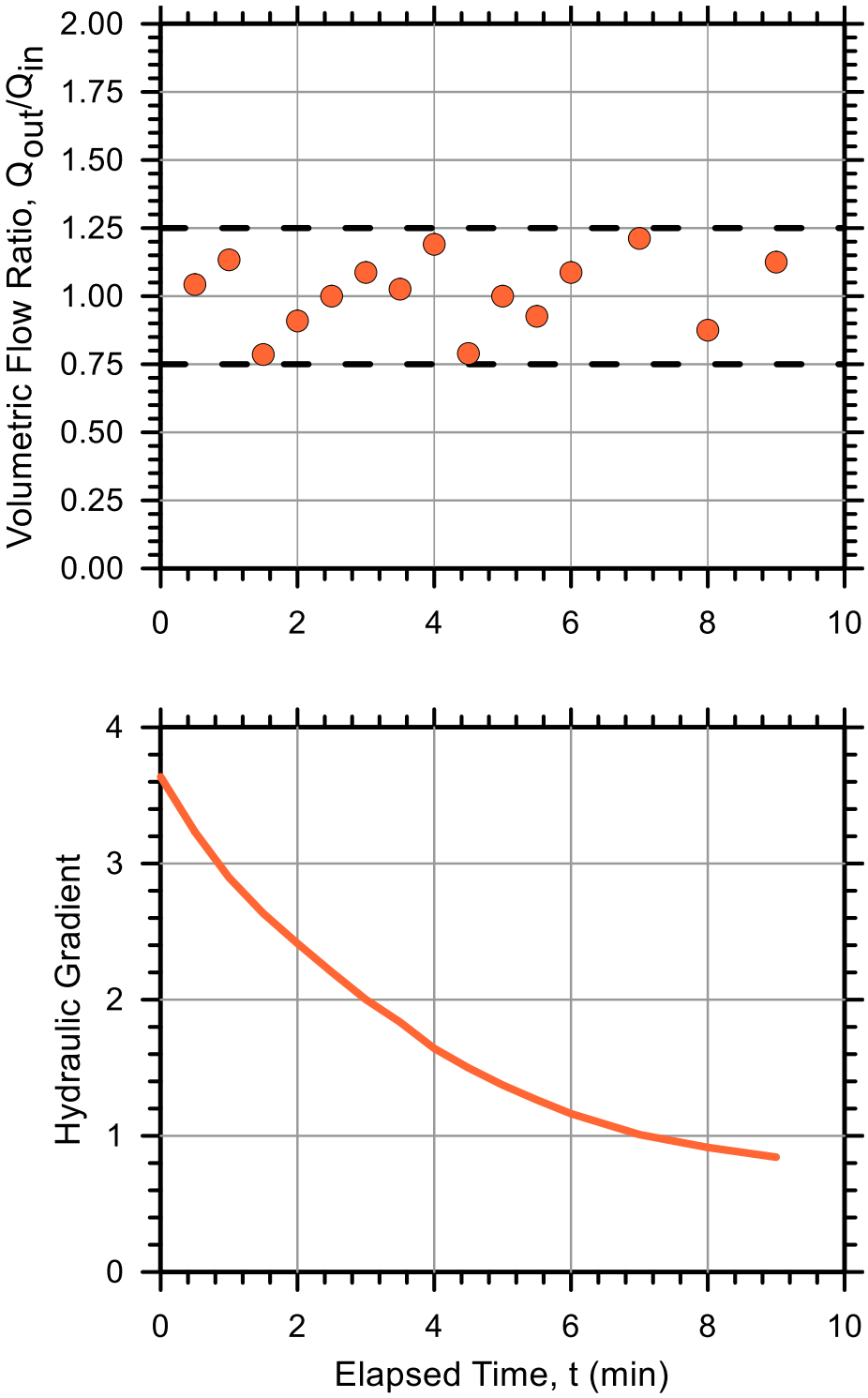
Volumetric Flow Ratio, Q_{out}/Q_{in}
2.00
1.75
1.50
1.25
1.00
0.75
0.50
0.25
0.00
0
2
4
6
8
10
Hydraulic Gradient
4
3
2
1
0
0
2
4
6
8
10
Elapsed Time, t (min)

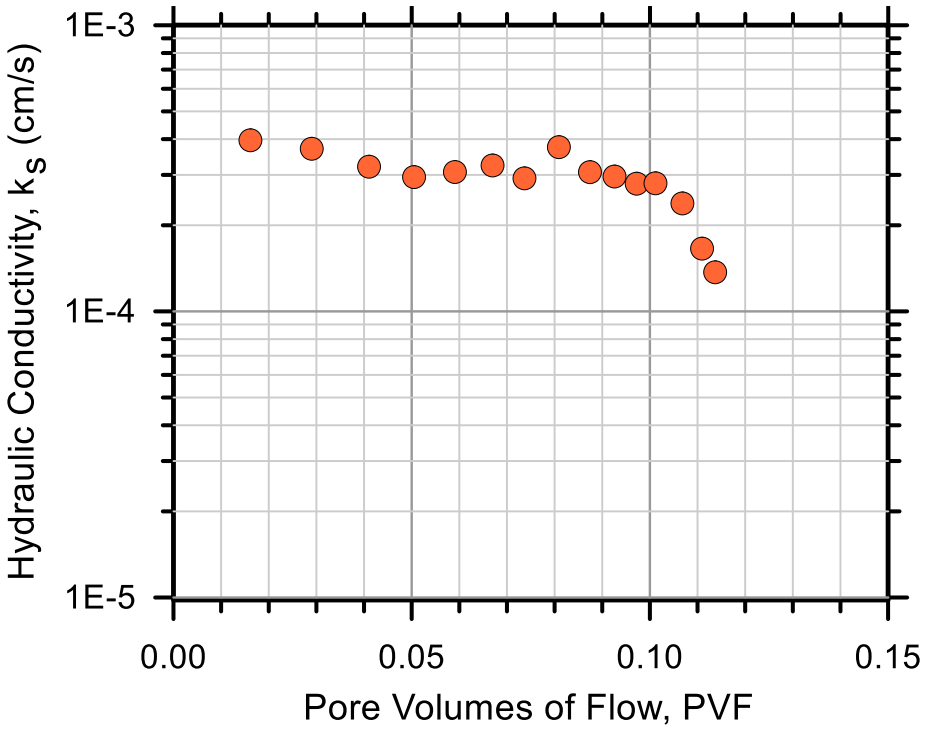
1E-3
1E-4
1E-5
Hydraulic Conductivity, k_S (cm/s)
0.00
0.05
0.10
0.15
Pore Volumes of Flow, PVF

Test No.: 34

Test Ref.: FXM8X34

Test Soil: Sand-Clay (85%-15%)

Molding Water Content: 8.10% (w_{opt}-1.3)

Property	Before Test	After Test
Total Mass (g)	378.00	411.34
Mass of Solids (g)	349.68	349.54
Mass of Water (g)	28.32	61.80
Total Volume (cm^3)	201.81	196.13
Volume of Solids (cm^3)	131.95	131.90
Volume of Water (cm^3)	28.32	61.80
Volume of Air (cm^3)	41.53	2.43
Water Content (%)	8.10	17.68
Volume of Voids (cm^3)	69.85	64.23
Void Ratio, e	0.529	0.487
Porosity, n (%)	34.6	32.7
Std. Proctor Relative Compaction, RC (%)	89.45	92.01
Moist Density, γ_m (g/cm^3)	1.87	2.10
Dry Density, γ_d (g/cm^3)	1.73	1.78
Degree of Saturation, S (%)	40.55	96.22
Consolidation Cell Pressure (kPa)	434.4	
Consolidation Back Pressure (kPa)	413.7	
Effective Consolidation Pressure (kPa)	20.7	

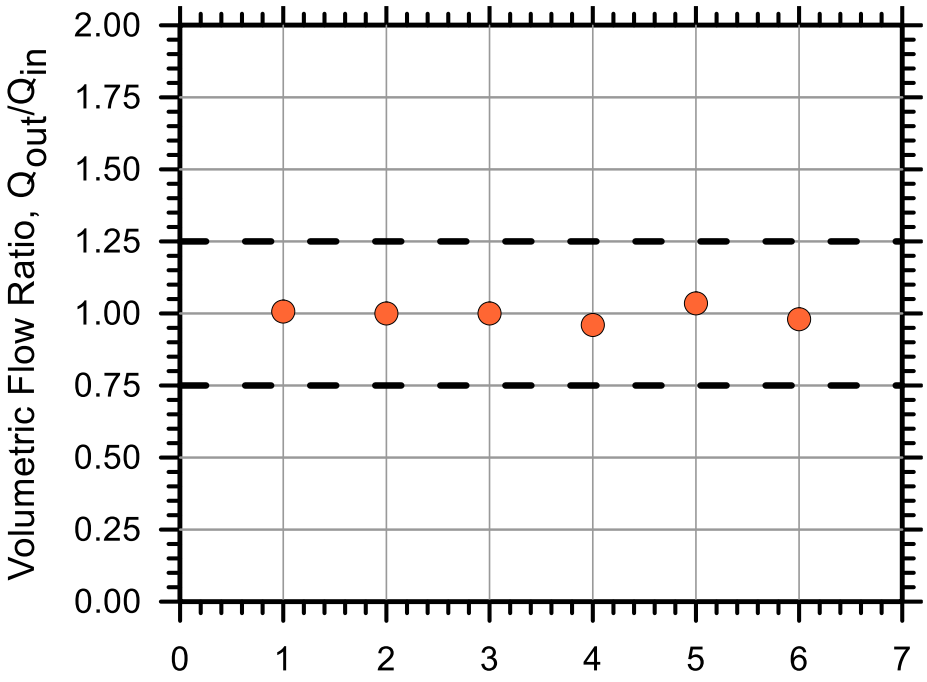
Volumetric Flow Ratio, Q_{out}/Q_{in}
2.00
1.75
1.50
1.25
1.00
0.75
0.50
0.25
0.00
0
1
2
3
4
5
6
7

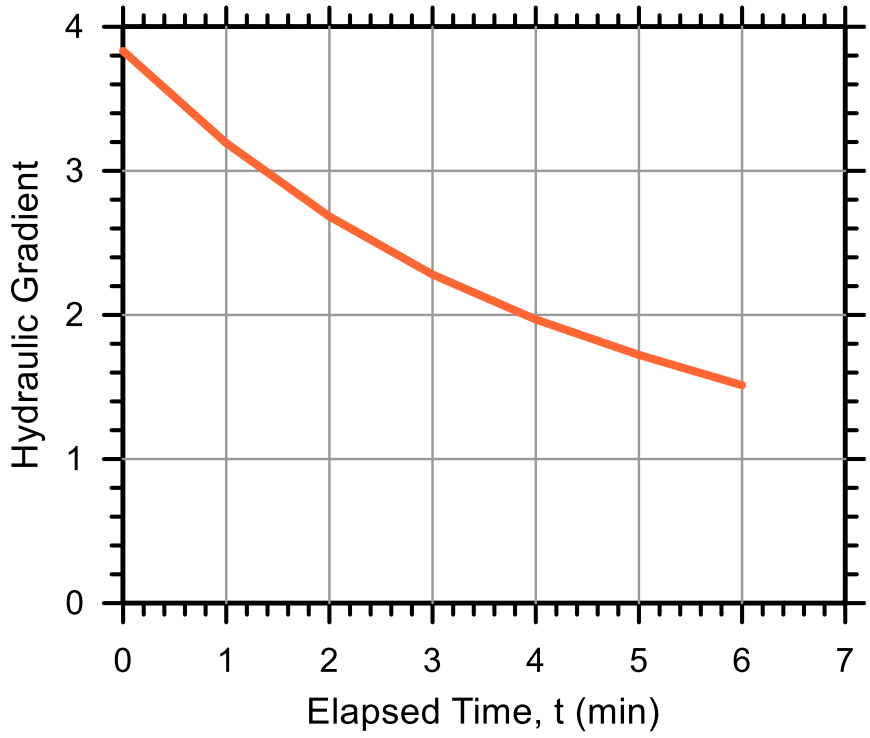
Hydraulic Gradient
4
3
2
1
0
0
1
2
3
4
5
6
7
Elapsed Time, t (min)

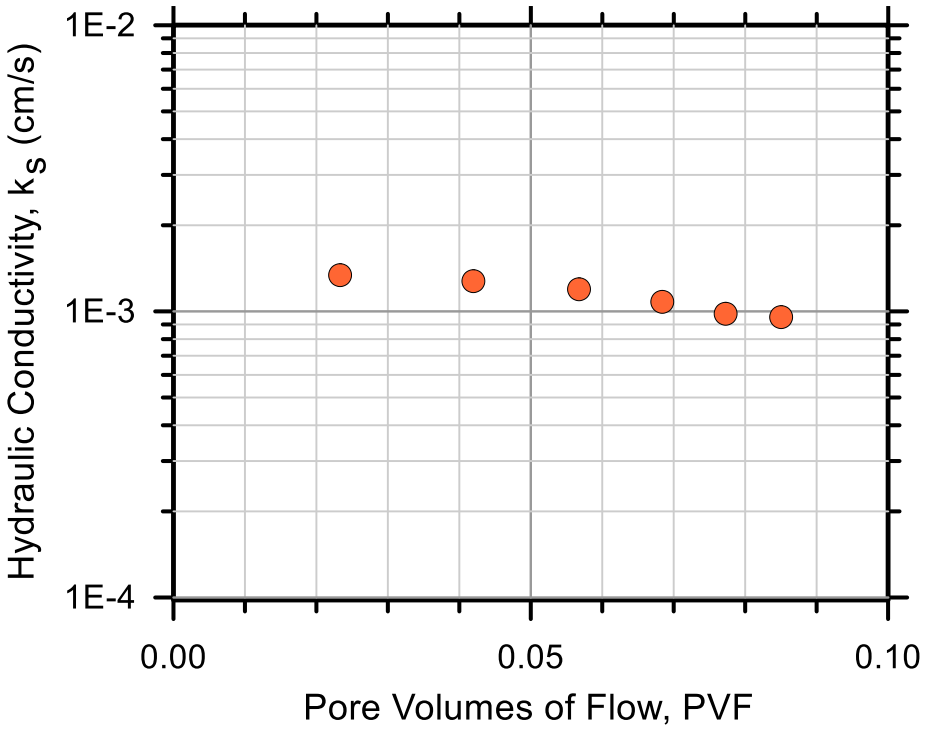
1E-2
1E-3
1E-4
Hydraulic Conductivity, k_s (cm/s)
0.00
0.05
0.10
Pore Volumes of Flow, PVF

Test No.: 41

Test Ref.: FXM8X41

Test Soil: Sand-Clay (85%-15%)

Molding Water Content: 11.10% (w_{opt}+1.7)

Property	Before Test	After Test
Total Mass (g)	411.00	425.85
Mass of Solids (g)	369.94	369.92
Mass of Water (g)	41.06	55.93
Total Volume (cm^3)	201.81	199.65
Volume of Solids (cm^3)	139.60	139.59
Volume of Water (cm^3)	41.06	55.93
Volume of Air (cm^3)	21.15	4.13
Water Content (%)	11.10	15.12
Volume of Voids (cm^3)	62.21	60.06
Void Ratio, e	0.446	0.430
Porosity, n (%)	30.8	30.1
Std. Proctor Relative Compaction, RC (%)	94.64	95.65
Moist Density, γ_m (g/cm^3)	2.04	2.13
Dry Density, γ_d (g/cm^3)	1.83	1.85
Degree of Saturation, S (%)	66.01	93.12
Consolidation Cell Pressure (kPa)	448.2	
Consolidation Back Pressure (kPa)	413.7	
Effective Consolidation Pressure (kPa)	34.5	

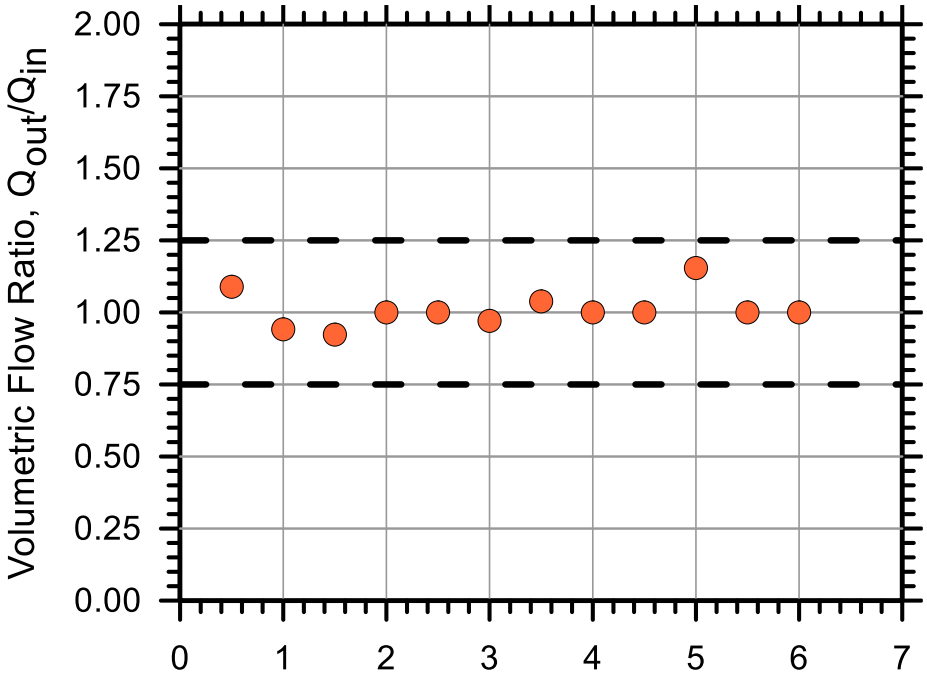
Volumetric Flow Ratio, Q_{out}/Q_{in}
2.00
1.75
1.50
1.25
1.00
0.75
0.50
0.25
0.00
0
1
2
3
4
5
6
7

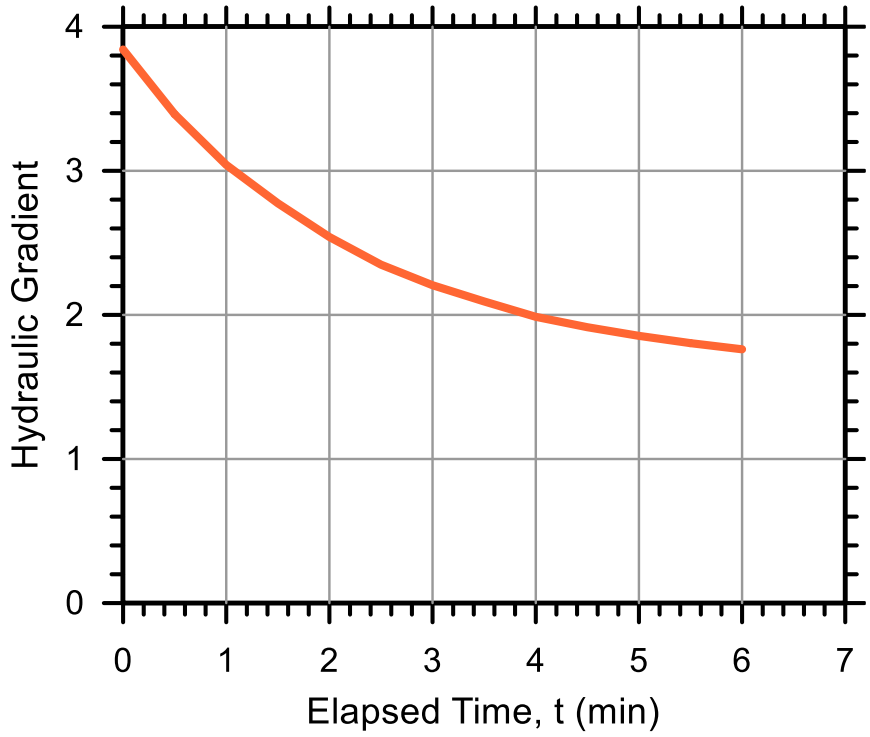
Hydraulic Gradient
4
3
2
1
0
0
1
2
3
4
5
6
7
Elapsed Time, t (min)

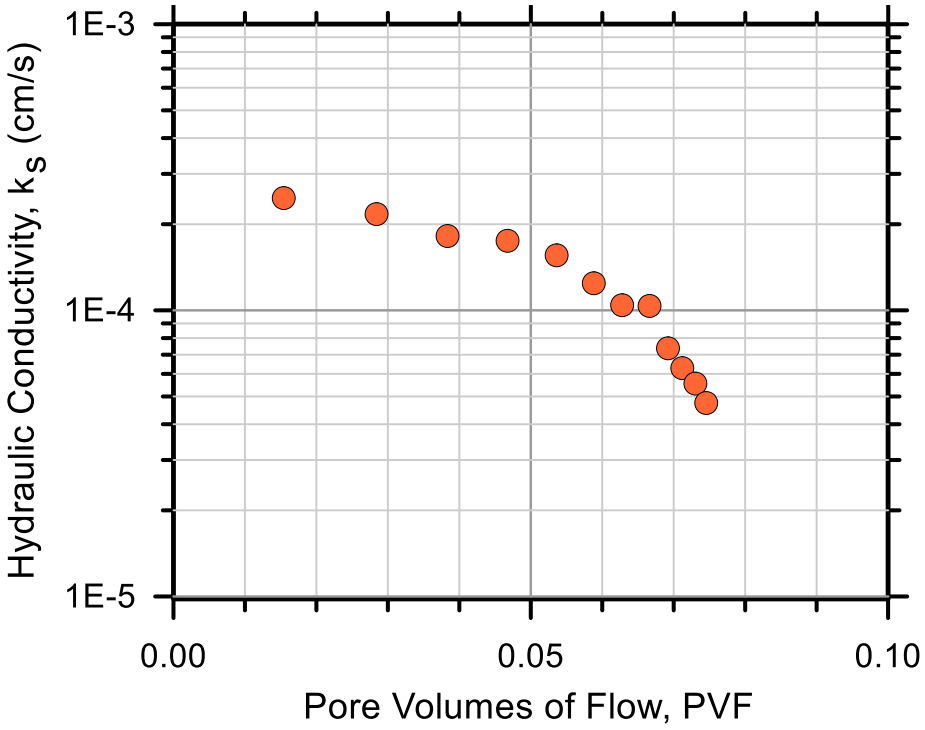
1E-3
1E-4
1E-5
Hydraulic Conductivity, k_s (cm/s)
0.00
0.05
0.10
Pore Volumes of Flow, PVF

Test No.: 37

Test Ref.: FXM8X37

Test Soil: Sand-Clay (85%-15%)

Molding Water Content: 11.10% (w_{opt}+1.7)

Property	Before Test	After Test
Total Mass (g)	384.00	410.17
Mass of Solids (g)	345.63	345.46
Mass of Water (g)	38.37	64.71
Total Volume (cm^3)	201.81	195.82
Volume of Solids (cm^3)	130.43	130.36
Volume of Water (cm^3)	38.37	64.71
Volume of Air (cm^3)	33.01	0.75
Water Content (%)	11.10	18.73
Volume of Voids (cm^3)	71.38	65.46
Void Ratio, e	0.547	0.502
Porosity, n (%)	35.4	33.4
Std. Proctor Relative Compaction, RC (%)	88.42	91.08
Moist Density, γ_m (g/cm^3)	1.90	2.09
Dry Density, γ_d (g/cm^3)	1.71	1.76
Degree of Saturation, S (%)	53.75	98.85
Consolidation Cell Pressure (kPa)	430.9	
Consolidation Back Pressure (kPa)	413.7	
Effective Consolidation Pressure (kPa)	17.2	

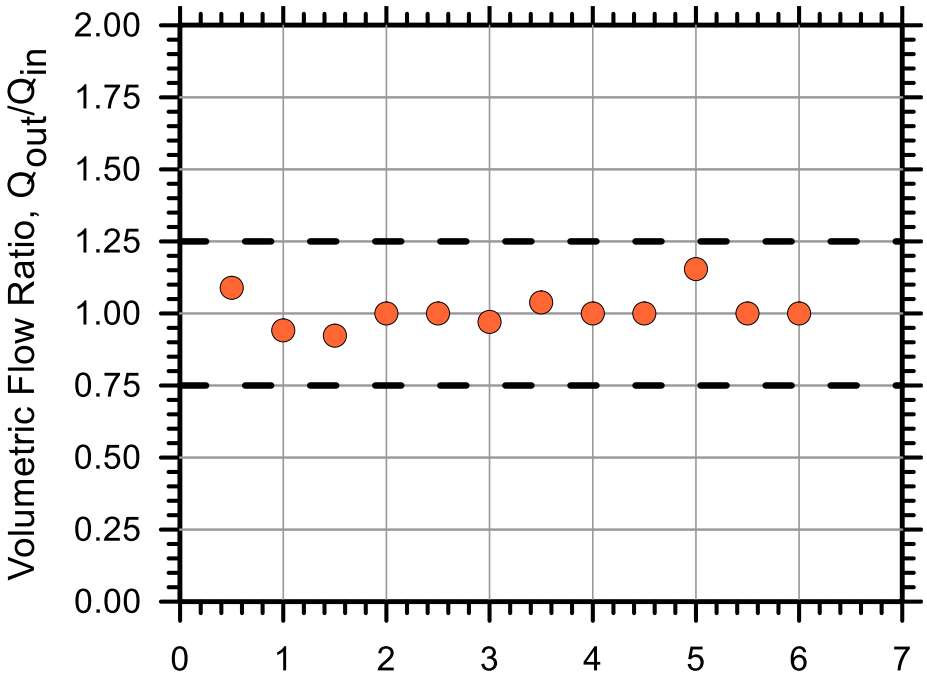
Volumetric Flow Ratio, Q_{out}/Q_{in}
2.00
1.75
1.50
1.25
1.00
0.75
0.50
0.25
0.00
0
1
2
3
4
5
6
7

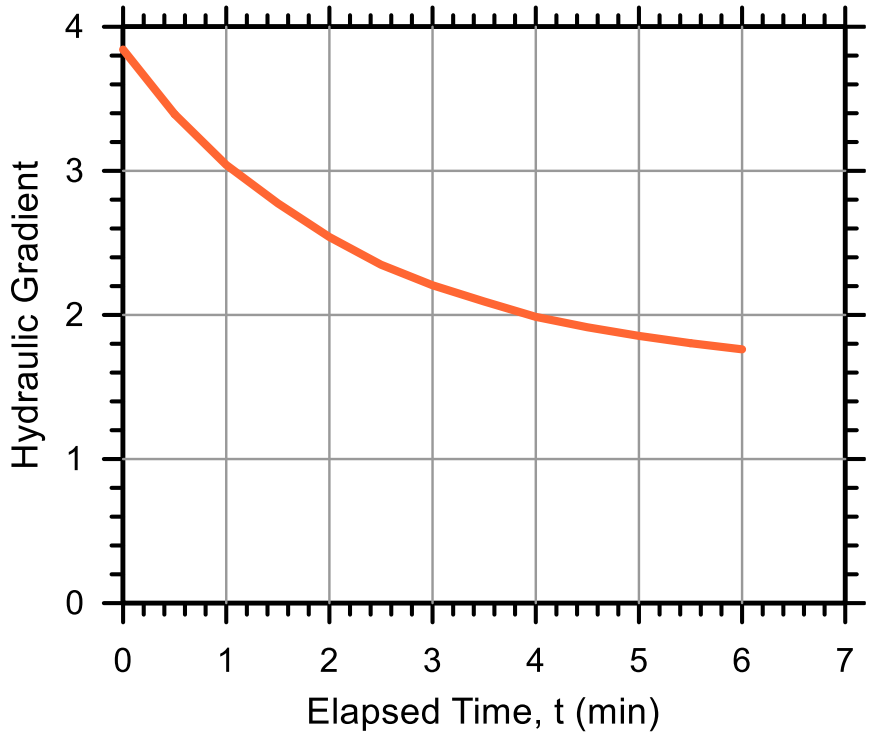
Hydraulic Gradient
4
3
2
1
0
0
1
2
3
4
5
6
7
Elapsed Time, t (min)

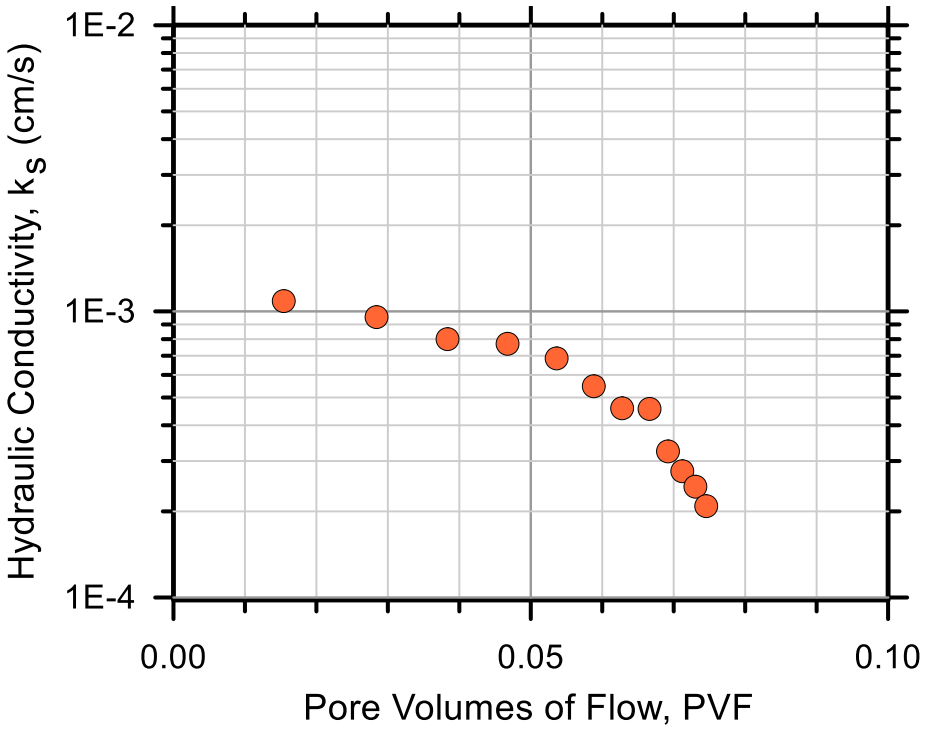
1E-2
1E-3
1E-4
Hydraulic Conductivity, k_s (cm/s)
0.00
0.05
0.10
Pore Volumes of Flow, PVF

Test No.: 52

Test Ref.: FXKC52

Test Soil: Wilco LPC Kaolin Clay

Molding Water Content: 23.50% (PL)

Property	Before Test	After Test
Total Mass (g)	338.00	369.26
Mass of Solids (g)	274.80	274.75
Mass of Water (g)	63.20	94.51
Total Volume (cm^3)	201.81	200.42
Volume of Solids (cm^3)	103.70	103.68
Volume of Water (cm^3)	63.20	94.51
Volume of Air (cm^3)	34.91	2.23
Water Content (%)	23.00	34.40
Volume of Voids (cm^3)	98.11	96.74
Void Ratio, e	0.946	0.933
Porosity, n (%)	48.6	48.3
Std. Proctor Relative Compaction, RC (%)	-	-
Moist Density, γ_m (g/cm^3)	1.67	1.84
Dry Density, γ_d (g/cm^3)	1.36	1.37
Degree of Saturation, S (%)	64.42	97.69
Consolidation Cell Pressure (kPa)	482.7	
Consolidation Back Pressure (kPa)	413.7	
Effective Consolidation Pressure (kPa)	69.0	

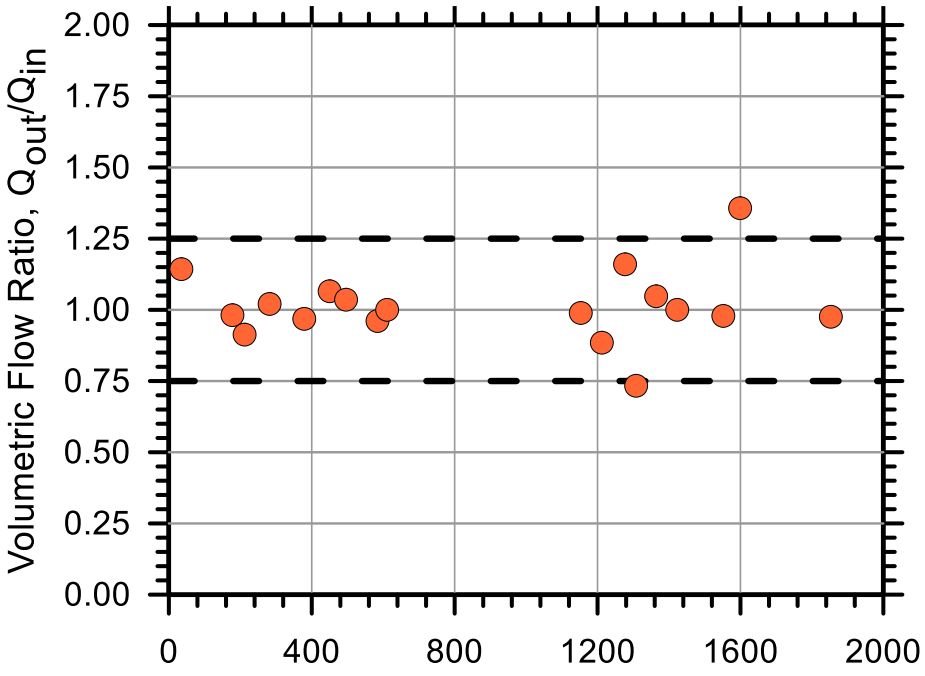
Volumetric Flow Ratio, Q_{out}/Q_{in}
2.00
1.75
1.50
1.25
1.00
0.75
0.50
0.25
0.00
0
400
800
1200
1600
2000

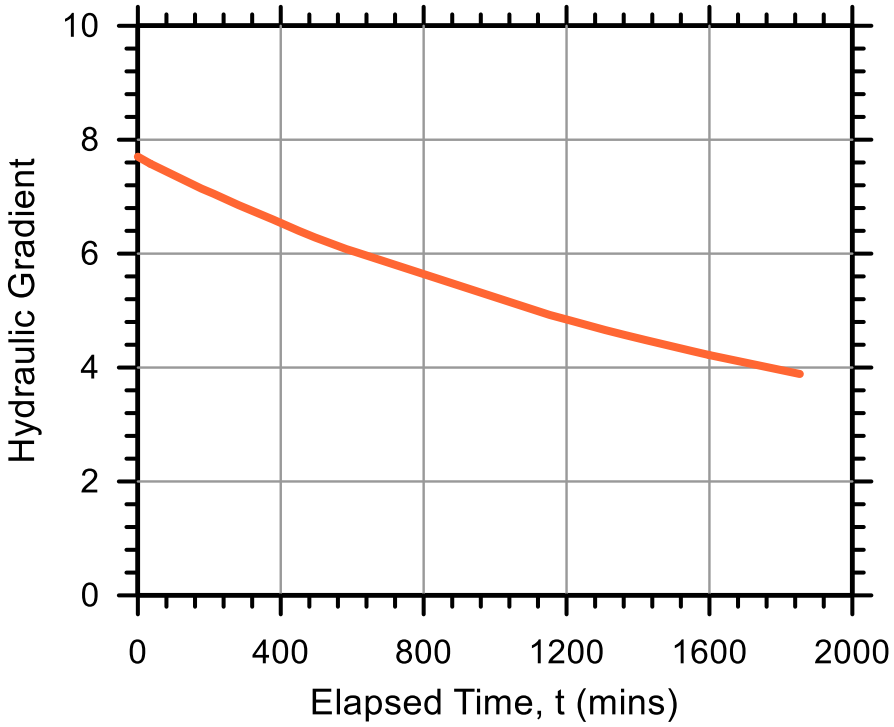
Hydraulic Gradient
10
8
6
4
2
0
0
400
800
1200
1600
2000
Elapsed Time, t (mins)

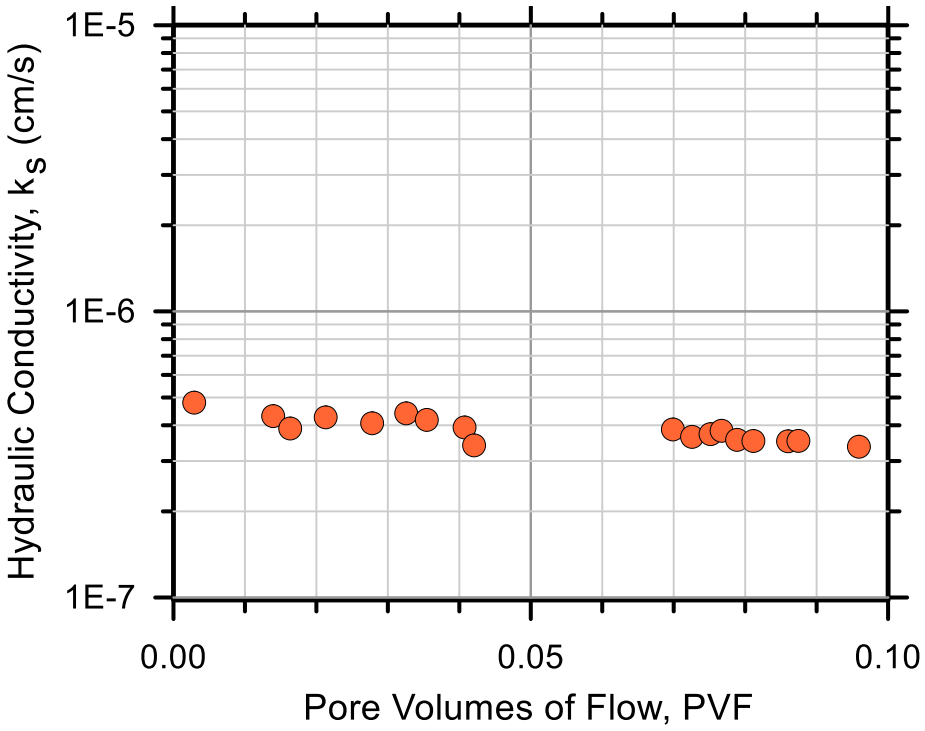
1E-5
1E-6
1E-7
Hydraulic Conductivity, k_S (cm/s)
0.00
0.05
0.10
Pore Volumes of Flow, PVF

Test No.: 53

Test Ref.: FXKC53

Test Soil: Wilco LPC Kaolin Clay

Molding Water Content: 23.50% (PL)

Property	Before Test	After Test
Total Mass (g)	300.00	343.87
Mass of Solids (g)	243.90	250.82
Mass of Water (g)	56.10	93.05
Total Volume (cm^3)	201.81	187.75
Volume of Solids (cm^3)	92.04	94.65
Volume of Water (cm^3)	56.10	93.05
Volume of Air (cm^3)	53.67	0.05
Water Content (%)	23.00	37.10
Volume of Voids (cm^3)	109.77	93.11
Void Ratio, e	1.193	0.984
Porosity, n (%)	54.4	49.6
Std. Proctor Relative Compaction, RC (%)	-	-
Moist Density, γ_m (g/cm^3)	1.49	1.83
Dry Density, γ_d (g/cm^3)	1.21	1.34
Degree of Saturation, S (%)	51.11	99.94
Consolidation Cell Pressure (kPa)	434.4	
Consolidation Back Pressure (kPa)	413.7	
Effective Consolidation Pressure (kPa)	20.7	

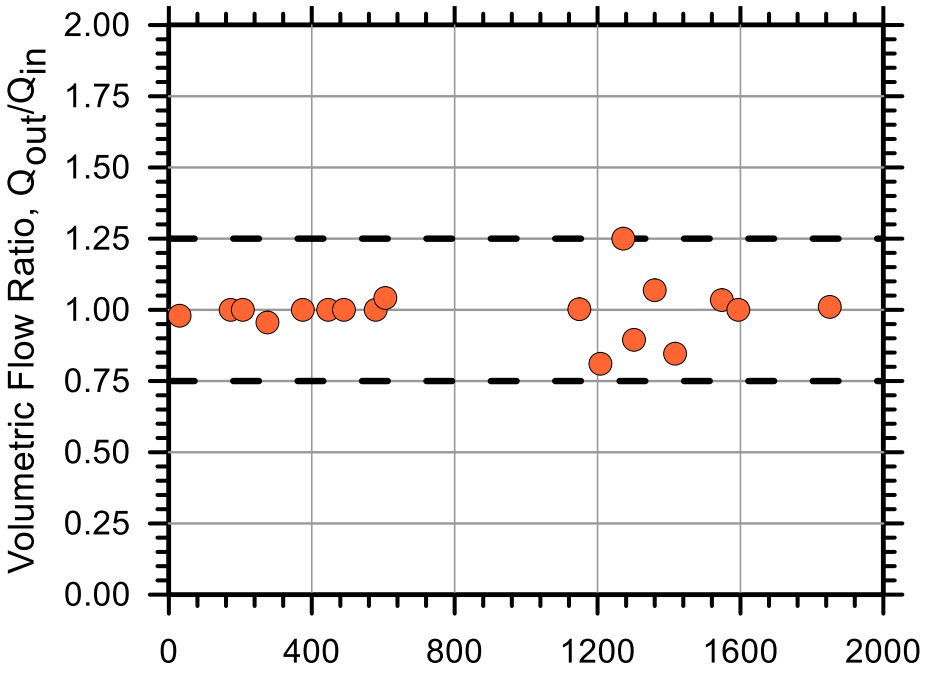
Volumetric Flow Ratio, Q_{out}/Q_{in}
2.00
1.75
1.50
1.25
1.00
0.75
0.50
0.25
0.00
0
400
800
1200
1600
2000

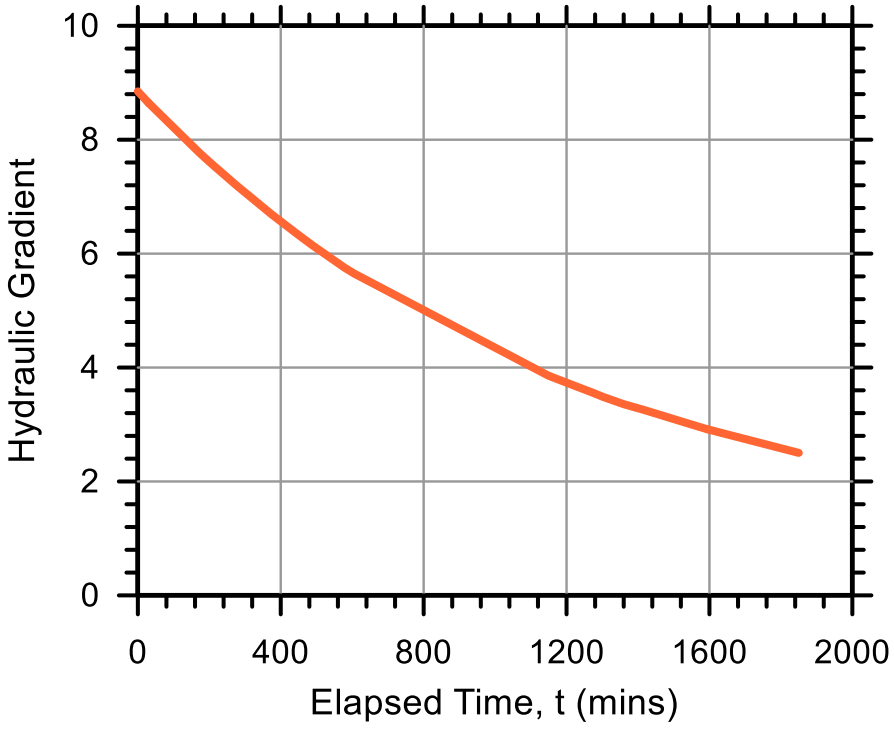
Hydraulic Gradient
10
8
6
4
2
0
0
400
800
1200
1600
2000
Elapsed Time, t (mins)

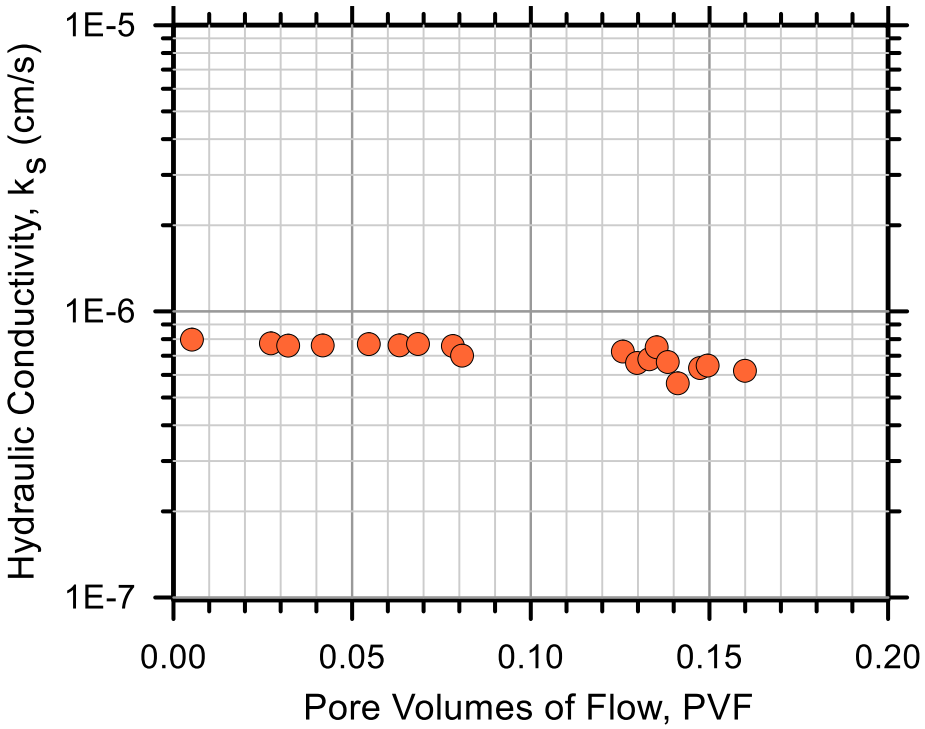
1E-5
1E-6
1E-7
Hydraulic Conductivity, k_s (cm/s)
0.00
0.05
0.10
0.15
0.20
Pore Volumes of Flow, PVF

Test No.: 54

Test Ref.: FXKC54

Test Soil: Wilco LPC Kaolin Clay

Molding Water Content: 23.50% (PL)

Property	Before Test	After Test
Total Mass (g)	297.50	338.17
Mass of Solids (g)	240.95	241.03
Mass of Water (g)	56.55	97.14
Total Volume (cm^3)	201.81	190.85
Volume of Solids (cm^3)	90.92	90.96
Volume of Water (cm^3)	56.55	97.14
Volume of Air (cm^3)	54.33	2.75
Water Content (%)	23.47	40.30
Volume of Voids (cm^3)	110.88	99.89
Void Ratio, e	1.220	1.098
Porosity, n (%)	54.9	52.3
Std. Proctor Relative Compaction, RC (%)	85.28	90.18
Moist Density, γ_m (g/cm^3)	1.47	1.77
Dry Density, γ_d (g/cm^3)	1.19	1.26
Degree of Saturation, S (%)	51.00	97.24
Consolidation Cell Pressure (kPa)	488.2	
Consolidation Back Pressure (kPa)	482.7	
Effective Consolidation Pressure (kPa)	5.5	

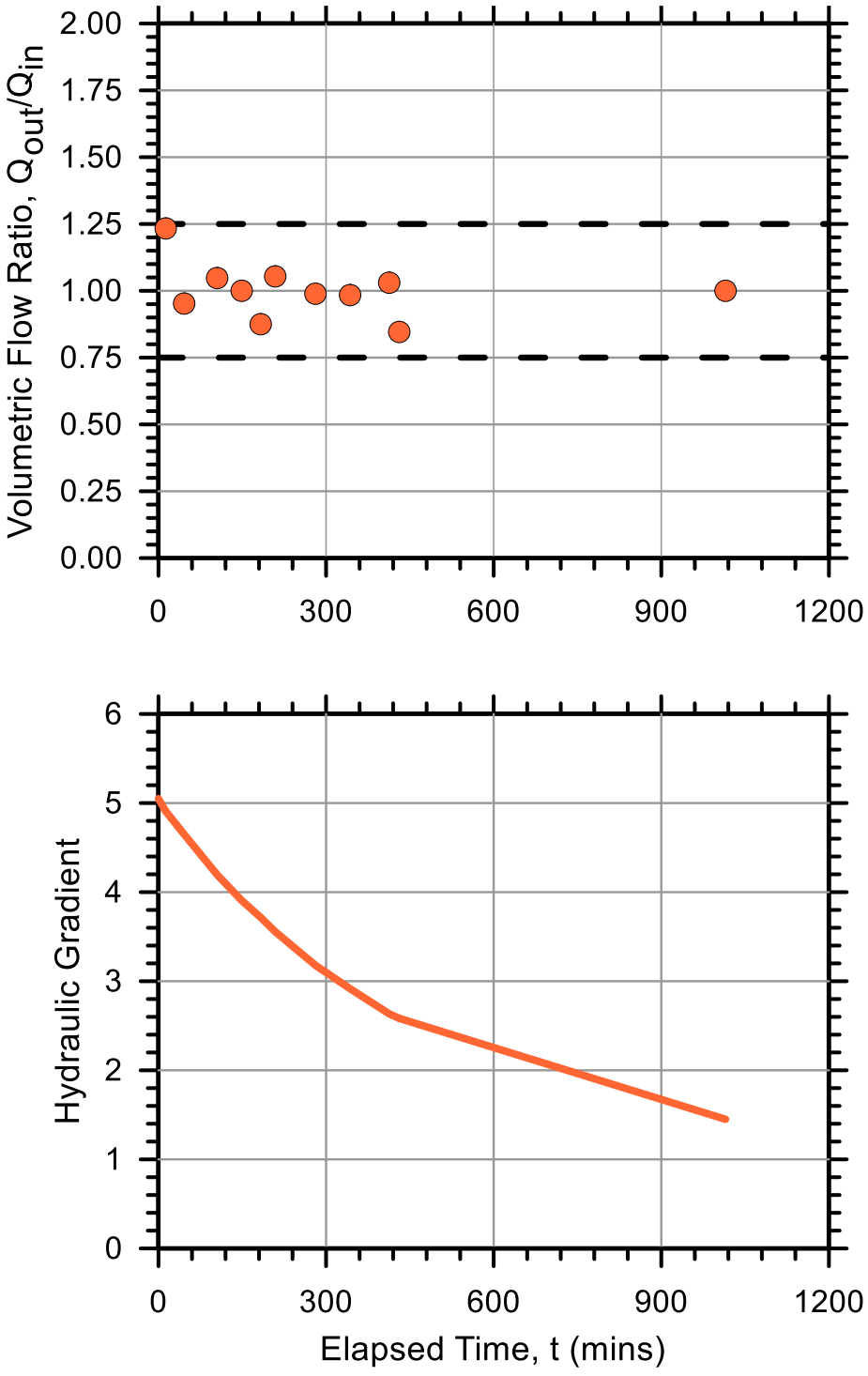
Volumetric Flow Ratio, Q_{out}/Q_{in}
2.00
1.75
1.50
1.25
1.00
0.75
0.50
0.25
0.00
0
300
600
900
1200
Hydraulic Gradient
6
5
4
3
2
1
0
0
300
600
900
1200
Elapsed Time, t (mins)

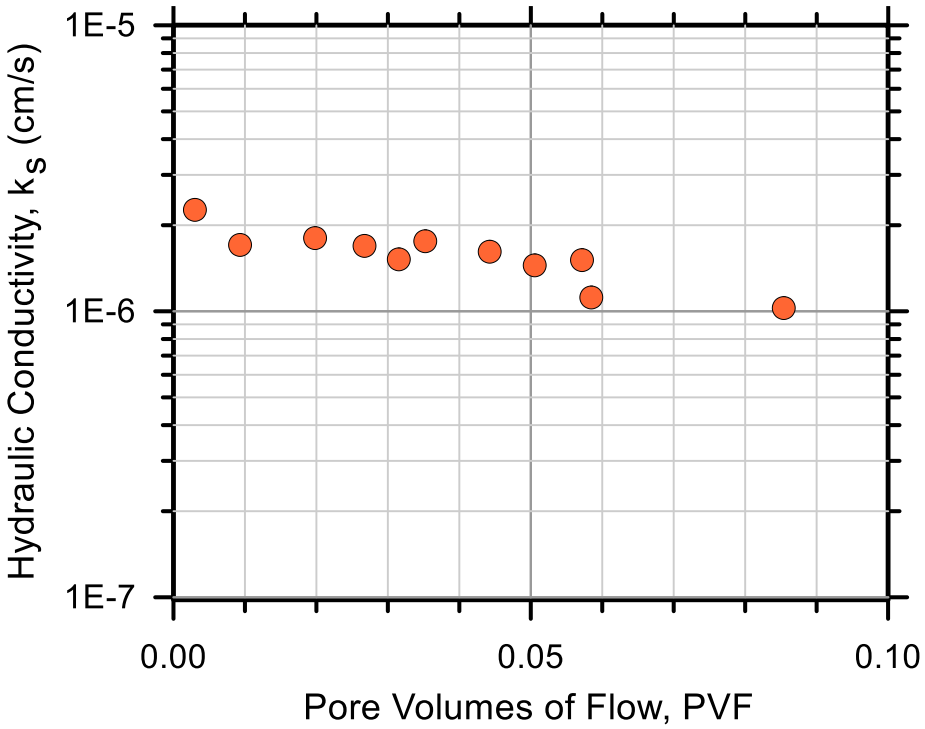
1E-5
1E-6
1E-7
Hydraulic Conductivity, k_s (cm/s)
0.00
0.05
0.10
Pore Volumes of Flow, PVF